The Meteorological Magazine

January 1992

Hoar-frost deposition
Angular momentum of the atmosphere

HMSO
Met.O.1004 Vol. 121 No. 1434

First published 1991

HMSO

HMSO publications are available

HMSO Publications Centre
(Mail and telephone only)
PO Box 276, London, SW8 5DT
Telephone orders 071-873 9090
General enquiries 071-873 0011
(queuing system in operation for

HMSO Bookshops
49 High Holborn, London, WC1
258 Broad Street, Birmingham, B
Southey House, 33 Wine Street, I
9–21 Princess Street, Manchester,
80 Chichester Street, Belfast, BT1
71 Lothian Road, Edinburgh, EH

HMSO's Accredited Agents
(see Yellow Pages)

and through good booksellers

The
Meteorological
Magazine

January 1992
Vol. 121 No. 1434

551.574.42:551.509.543:625.7

Hoar-frost deposition on roads

T.D. Hewson
Joint Centre for Mesoscale Meteorology, Department of Meteorology, University of Reading
N.J. Gait
Meteorological Office College, Shinfield Park, Reading

Summary

By combining physical reasoning with several case-studies it is shown that the most important factors in determining hoar-frost deposition on UK roads are moisture gradients in the atmosphere's lowest layers, wind speed, weather of recent days and time of year. The Meteorological Office road surface temperature model is shown to give useful guidance if fed with accurate input parameters, although on occasions its predictions of hoar frost accumulation are deficient because of an inability to handle the obstruction of direct sunshine. Two additional forecasting tools are proposed; one a checklist, the other based on a manual time-integral of the depression of road surface temperature below dew-point.

1. Introduction

In recent years much research has been devoted to road surface temperatures (RST, T_r), their measurement and their prediction. This has culminated in the development of one-dimensional numerical models of the 'road environment' (RST models) which are now used widely in forecasting. The main objective has been to improve the efficiency of road-salting operations during winter. Improved efficiency entails many economic, environmental and human benefits; notably safer roads, fewer wasted saltings*, less rust damage to cars and bridges and reduced waterway pollution (Soveri 1990). An overview of recent research and its applications can be found in Boselly *et al.* (1990).

There can be little doubt that substantial improvements have been made in our knowledge of the behaviour of RSTs (Bogren and Gustavsson (1989) give a wide-ranging summary). What is less clear, however, is whether the efficiency of road-salting has improved much as a result. A cost-benefit analysis by Thornes (1989) indicates that savings probably are being made. However, Mansell (1989) rightly points out that in the United Kingdom there is still a marked tendency to forecast ice too often and hence salt roads too often, most wasted saltings being on frosty nights when roads are dry. Such errors should show up in the verification of operational forecasts, as performed by Thornes (1989) and Thornes and Shao (1991a). Sadly they do not because the verification system is formulated such that a forecast of icy roads will be 'correct' irrespective of whether unsalted roads stay dry or turn icy, provided the RST falls to zero or below.

One reason a large number of wasted saltings occur is because recent theoretical and observational studies have tended to overemphasize RSTs, and pay scant attention to road surface conditions (RSCs; i.e. dry, wet or icy). One aim of this paper is to redress the balance.

It is convenient to subdivide occasions when ice forms on road surfaces into two categories, with nomenclature as shown:

* The cost of winter maintenance in the United Kingdom is about £100M for an average winter (Thornes 1989).

(a) 'Water freezing': when surface water freezes over (most commonly rainwater, but also snowmelt and seepage).

(b) 'Hoar frost deposition': when the source of the ice is direct sublimation and/or direct condensation from the atmosphere onto the road surface. This includes occasions when dew was deposited and then froze over.

When warned of water freezing, local authorities tend not to salt roads until they are wet. Thus the wasted saltings noted by Mansell to occur on 'frosty nights with dry roads' must have been initiated, in general, by incorrect forecasts of hoar-frost deposition. This suggests that of (a) and (b) it is hoar-frost deposition which is more difficult to forecast correctly, and less well understood. It is for these reasons that this study investigates hoar frost deposition. It will also be possible, however, to apply some of the results to cases of water freezing.

Hoar-frost deposition is influenced by factors as wide-ranging as air temperature and traffic speed. The main emphasis in this paper is on *meteorological* factors. The intention is to elucidate those which favour hoar-frost deposition by bringing together physical reasoning, case-studies and site-specific numerical predictions from the UK Meteorological Office RST model. Some verification of perfect prognosis predictions from this model will also be attempted.

In section 2 results of previous work directly relevant to hoar-frost deposition are summarized. The physics which govern the process are described in section 3. Section 4 provides a brief overview of the RST model, together with a discussion of ice thickness.

Section 5 covers in detail four occasions on which hoar-frost deposition occurred during a single night. The physical processes at work are discussed, and similarities between the cases noted.

In section 6 two aids for forecasting rapid hoar-frost deposition are proposed, and tested out on data from the 1990/91 UK winter. A simple calculation reveals the financial savings which might result from using these techniques.

Section 7 looks at a case where hoar-frost deposits probably accrued over several days. It is used to investigate the differences that can arise between road conditions in built-up areas and open countryside.

Conclusions are presented in section 8.

Excluded from this study are occasions when snow was lying on road surfaces, and also occasions of widespread fog.

2. Previous studies

There seem to be two main reasons for the lack of past research specifically into RSCs. The first is the shortage of verifying data. Icy roads are not at all easy to measure, and it has never been standard practice to report such phenomena from manned observing stations. The second reason is that ice formation is influenced by such a wide range of factors.

Takle (1990) tried to overcome both these problems, by using the experience of authorities responsible for salting roads. His investigation began by distributing questionnaires to 125 highway maintenance garages in the American state of Iowa (latitudes 40–44° N).

One question related to factors which determine why a particular stretch of road is more prone to hoar-frost. A majority (70%) of respondents felt that 'shelter/shading' of the road was important. This is supported by the observational study of Bogren (1991), which identified large systematic differences between RSTs on shaded and open roads in southern Sweden. Similarly Milloy and Humphreys (1969) noted differences in the 'duration of ice-forming conditions' between shaded and open roads in southern Scotland. Such results give a feasible explanation for localized hoar-frost deposition, and are discussed further in section 7.

Other factors covered in the above question, namely 'road material', 'road age', 'presence of rivers/lakes nearby', 'low lying' and 'hilly' were considered unimportant by most respondents. Despite not being of general importance, such factors could still be significant in certain meteorological situations. Examples in sections 5 and 6 show this to be true for factors 'hilly' and 'low lying'.

Another of Takle's questions was "does the volume of traffic affect the formation of frost?" — 70% thought it did not. This conflicts with the work of Farmer and Tonkinson (1989), who noted and discussed how rush-hour traffic affects the diurnal cycle of RSTs on different motorway lanes. A lower traffic density in Iowa may partly explain the discrepancy. However the fact that Farmer and Tonkinson used measurements suggests that their results are more reliable. Here the view is taken that higher traffic volumes generally increase RSTs. Occasional reference will be made, in a qualitative sense, to this effect.

Of past studies we are aware of that of Gustavsson and Bogren (1990) bears the greatest similarity to our work. They concentrated on spatial variations in the time of onset of hoar-frost deposition in southern Sweden. It seems that the wild swings in temperature experienced in this region can sometimes make substantial hoar-frost deposition a certainty, and thus the main forecasting problem is the time of onset. In the United Kingdom, temperature fluctuations are generally less severe; and the main difficulties in defining whether or not there will be any hoar-frost deposition, and whether any that does occur will be sufficent to cause dangerously icy roads.

Monteith (1957) showed that on calm nights the moisture which forms dew on grass comes from the underlying soil and not the atmosphere. This needs to be borne in mind when making comparisons between grass and road surface.

The local consequences of large amounts of deposition of atmospheric moisture are well illustrated in Davey (1982). In the case he studied, previously dry roads became covered in pools of water in just 7 hours, despite the absence of any rain. It is also noteworthy that during that period the surrounding grass remained completely dry. Evidently moisture deposition is not a trivial problem.

3. The physics of hoar-frost deposition

Hoar-frost deposition on road surfaces is essentially controlled by three factors; the RST, the moisture content of the air and the wind speed.

Equations presented in Rayer (1987) can be simplified to give an expression for the net flux of moisture onto the road surface, F;

$$F = K_1 U(e_s(T_d) - e_s(T_r)) \quad (1)$$

where K_1 (positive) is a constant given that the stability of the air is fixed, U is the 10-metre wind speed, $e_s(\,)$ is the saturated vapour pressure at a specific temperature, and T_d is the screen dew-point temperature. This equation is essentially Dalton's Law of evaporation.

Both deposition ($F>0$) and evaporation ($F<0$) from roads are controlled by equation (1). Whether F is positive or negative depends on whether T_r is, respectively, less than or greater than T_d. As an example of the use of equation (1) consider the single case where moisture is *known* to be condensing on a road surface. The *stronger* the wind the *greater* will be the rate of moisture accumulation. This fact is noted in order to dispell the notion that strong winds always dry off roads. In this respect it is noteworthy that the rapid condensation described by Davey (1982) occurred when mean wind speeds were a sizeable 15 knots.

Over small ranges of T_d and T_r a valid and useful approximation is that $e_s(T_d) - e_s(T_r)$ is proportional to $T_d - T_r$. For values likely to give rise to hoar-frost deposition on UK roads this approximation holds to about 75% accuracy. Thus from equation (1):

$$F \approx K_2 U(T_d - T_r) \quad (2)$$

where K_2 is a positive constant.

So for moisture to be deposited on the road surface T_r must be less than T_d, which necessarily means that T_r must also be less than T, the air temperature at screen level. Consideration of which physical mechanisms are likely to adjust the relative positions of T_r, T and T_d on a temperature scale can be very informative (a thorough discussion is given in section 5.3).

As implied above, K_2 remains constant if the stability remains constant. Were the stability of the air close to the road surface to increase, F would decrease slightly; whereas the opposite would happen if the air became more unstable. An indication of whether the lowest few metres of the atmosphere are stable or unstable is given by the the sign of $(T - T_r)$. Using this criterion means that any occurrence of moisture transfer to or from a road surface can be assigned to one of three regimes :

$T_r > T > T_d$, giving 'efficient' evaporation;
$T > T_r > T_d$, giving 'inefficient' evaporation;
$T > T_d > T_r$, giving 'inefficient' hoar-frost/moisture deposition.

So evaporation generally proceeds, *per se*, more rapidly than hoar-frost deposition. This partly explains why roads do, on occasions, dry out very rapidly.

As dew-points are critical to hoar-frost deposition it is important to consider the accuracy of standard dew-point measurements. Fig. 1(a) of Painter (1973) implies that given a real (psychrometer) dew-point depression of 2 °C, dew-points derived from standard screen measurements are on average 0.2 °C too high with winds up to 5 kn, and 0.1 °C too high with winds over 10 kn. These values are probably small enough to be discounted, although it is noteworthy that there was a large amount of variability in the errors. Measurement accuracy is dependent on a lot of factors — chapter 3 of the *Handbook of Meteorological Instruments* (Meteorological Office, 1981) gives a comprehensive discussion.

Does water on a road surface freeze at 0 °C? Ritchie (1976) analysed 27 cases and found that freezing of distilled water occurred with an average temperature of −0.4 °C just above the surface, and +0.7 °C just below. So the true RST is probably about 0 °C, given that the water is free from impurities (such as salt!).

The concept of cooling due to evaporation is widely understood. What is not so widely appreciated perhaps is that the converse is also true, whereby the deposition of moisture/hoar-frost onto a surface actually warms that surface. Evidence for this effect can be seen in Fig. 6 of Thornes (1972). This shows subzero road temperatures predicted by regression equations from which the effects of latent heat had been omitted to be quite accurate on nights with heavy rain, but systematically too cold on nights with hoar-frost on the road surface (for water/ice at 0 °C the latent heat of sublimation is about 8½ times greater than the latent heat of fusion).

These latent heat differences mean that ice formed by hoar-frost deposition will in general not be as cold as ice formed by water freezing. In turn this makes ice formed by hoar-frost deposition potentially more dangerous to the motorist, because the friction of ice increases as its temperature decreases (Moore (1975), chapter 6).

4. The RST model

4.1 Description

The UK Meteorological Office RST model, described in Rayer (1987), integrates physical equations in order to calculate RST and RSC at one site over a 24-hour period beginning at midday. The effects on the RST of latent heating and 'latent cooling' *are* included. (The thermodynamic constant used is the latent heat of condensation. No account is taken of the latent heat of fusion, but as this is almost an order of magnitude less, the resulting errors in RST should be negligible.) Boundary conditions for the equations are provided by the user, i.e. values of specific meteorological variables for specific times during the 24-hour period. The table in the top half of Fig. 1(d) shows what these input variables are and the times for which values are required.

4.2 Output

The bottom half of Fig. 1(d) contains an example of an output profile. The main part of this profile indicates how RST (vertical axis) varies through the forecast period (horizontal axis), the letter 'R' indicating the profile. Below this the line of dots and letters between 'REL' and 'ICE' indicate the predicted RSC. There is a key for these at the foot of the graph.

4.3 Ice thickness

Letters at the foot of an RST model output profile can be converted into the total depth of ice/water calculated to have accumulated on road surfaces at given times through the night; 'f' and 'd' represent 0.001 mm to 0.01 mm whilst 'I' and 'W' represent 0.01 mm or greater.

The lack of resolution can sometimes be misleading. For example the last in a long line of 'f's may still only represent 0.001 mm. When performing 'perfect prognosis' predictions for the case-studies this difficulty was overcome by extracting from the model the exact depths of condensated moisture/ice calculated for hourly intervals through the night.

Tiny fractions of a millimetre may *seem* trivially small. The results of Monteith (1957) indicate that they are not, however. He weighed dewfall* on short grass on a number of occasions and found a maximum deposition rate of 0.035 mm h^{-1}, and a maximum accumulation during one night of 0.15 mm. Before equating these values to hoar-frost deposition on roads the following points should be noted: (i) when the values were measured, on 1 September 1953, the moisture content of the air was greater than it is on typical winter nights in the United Kingdom (about 8 g kg^{-1}, compared to 4 g kg^{-1}), and (ii) on clear nights the depression of the grass temperature below air temperature is generally larger than the depression of the RST below the air temperature (typically 2–6 °C, compared to 1–3 °C). As deposition on a surface is proportional to both moisture content of the air, and temperature difference between the air and that surface, it therefore follows that Monteith's values should be multiplied by $(4/8)+(2/4)$ to give equivalent, albeit approximate, values for hoar-frost deposition on roads. This gives a potential maximum deposition rate of 0.01 mm h^{-1} and a potential maximum one-night accumulation of 0.04 mm.

* We have adopted Monteith's definition of dewfall, namely 'the turbulent transfer of water vapour from the atmosphere'. Dewfall does not, therefore, include the transfer of water vapour from soil to grass.

4.4 Verification

A satisfactory verification of model output clearly requires some idea of the minimum depth of hoar-frost likely to be dangerous to a motorist. This presents problems because such a value has never been accurately measured (to the authors' knowledge) and also depends, very probably, on the precise structure of the road surface (J.E. Thornes, personal communication). Field experiments utilizing a sensitive rain-gauge indicated that 0.01 mm of drizzle was quite sufficient to dampen roads. In addition, a simple laboratory experiment demonstrated that by spreading out a water droplet on a smooth surface it was quite easy to produce a visible layer of water only 0.002 mm thick. Thus tiny amounts do have the potential to make roads dangerously icy. We tentatively suggest that the average 'danger level' lies somewhere between 0.002 and 0.01 mm.

5. Hoar-frost case-studies

5.1 Selection

Evidence of hoar-frost deposition on the occasions to be described came from two sources: a weather diary, kept by N.J. Gait between 1972 and 1980 in Wallington, south London, and chance observations made by forecasters at weather centres in south-east England. For the most recent cases use was also made of measurements from roadside sensors in Kent and Berkshire*.

At the outset a random search for examples of hoar-frost deposition in winters prior to 1990/91 yielded six good cases. 'Good' means there was strong evidence to suggest the observed ice was *not* due to water freezing. Other cases could undoubtedly have been found had the temporal and spatial data coverage been better.

Five of the six cases were of short time-scale, meaning most if not all the hoar-frost deposition occurred during one night. These are described in section 5.2. Regional variations can arise during these short time-scale events. Sensor data which was available for case 4 is used to highlight these.

The sixth case was characterized by a long, clear, cold spell with light winds, in which the deposits appeared to have accumulated over several days — this is dealt with later, in section 7.

5.2 Description of cases

Two consecutive midday North Atlantic pressure patterns are shown for each of the four cases, the dates being those which straddled the night/morning when hoar-frost was observed (Figs 1(a), 2(a), 3(a) and 4(a)).

* Kent use Vaisala sensors whilst Berkshire use Scan sensors. Sensor measurements of the hoar-frost itself were discounted — the authors regard such measurements to be far too unreliable at present.

Thickness lines 1000–500 mb for 564, 546, 528 and 510 dam have been superimposed. Also shown are observations over south-east England at a relevant time (Figs 1(b), 2(b), 3(b) and 4(b)), all current weather included, and the lower part of a representative tephigram (Figs 1(c), 2(c), 3(c) and 4(c)) with its corresponding 900 m wind. The RST model was run for each case (as described below); Figs 1(d), 2(d), 3(d), 4(d) and 4(e) indicate the input values used, and the resulting output profiles.

On Figs 1(b), 2(b), 3(b) and 4(b) T denotes the location of the radiosonde ascents, P marks the sites which correspond to the RST model profiles, and F shows where hoar-frost was *observed* on road surfaces (it probably also *occurred* in many other locations).

For each case the figures should provide a comprehensive guide to synoptic micrometeorological developments during the night in question. Supplementary information is given under the heading 'synoptic background' in the case descriptions.

The RST model was in fact run for two consecutive 24-hour periods for each case (referred to as runs 1 and 2). Run 2 (shown) ended at the midday immediately after ice was observed. The purpose of run 1 (not shown) was to initialize the sub-surface temperature profile for run 2; this initialization procedure having been strongly recommended by Farmer and Tonkinson (1989), to allow for differences such as those illustrated in Fig. 5. The midday input values of RST and RDT (road depth temperature) used for run 2 were those predicted at the end of run 1. The corresponding inputs for run 1 were estimated using forecaster experience and analysis of the weather of the previous two or three days. Input values of the other variables were estimated using routine observations from the local area and, where available, observations from the weather diary and roadside sensors. In this way the model's performance under 'perfect prognosis' conditions could be assessed.

5.2.1 Case 1: morning of 3 December 1976

See Figs 1(a) to 1(d).

Evidence: Thick hoar-frost observed on suburban roads at Wallington, South London (from personal weather diary).

Synoptic background: A cold cyclonic north-westerly pattern covered the British Isles. The night of the 1st/2nd had been cloudy with temperatures around 5 °C. Cloud started to clear around midday on the 2nd.

RST model: Maximum depth of hoar-frost = 0.004 mm, 7 a.m. to 10 a.m. A prolonged period of hoar-frost is indicated, but the depth may well be insufficient.

Discussion: The Crawley ascent shows a plentiful supply of moisture at low levels, but dry air above 960 mb. The limited depth of moisture, together with light winds, prevented low cloud forming in Wallington. In East Anglia though (north-east corner of Fig. 1(b)), where winds were a little stronger, road temperatures probably rose above zero when a cover of stratus formed around midnight. Clearly there was a fine balance on this night between skies remaining clear and turning cloudy — wind speed was apparently the deciding factor. The source for the observed hoar-frost was undoubtedly the moisture shown on the ascent, it's deposition onto the road surface being aided by the gentle westerly wind.

The variation in dew-point depression on the ascent probably resulted from the long passage of essentially cold, dry arctic air across warm seas.

5.2.2 Case 2: night of 4–5 December 1977

See Figs 2(a) to 2(d).

Evidence: Extensive hoar-frost/ice was observed on most roads around Wallington at 2200 on the 4th. Road conditions were extremely dangerous, the frost mixed with water in places.

Synoptic background: A cold south-easterly flow had persisted for several days. Rain was last reported on the evening of the 1st. Skies had been clear since dawn on 2nd.

RST Model: Shows substantial accumulation of hoar-frost. Maximum depth = 0.022 mm at 0700. At 2200 depth = 0.006 mm. Profile considered reasonable, though hoar-frost underpredicted at 2200. Road conditions may well have deteriorated further through the night.

Discussion: 60 hours of clear skies and low temperatures must have left roads very cold through depth — note the low RDT. A rise in dew-point occurred right across south-east England on the afternoon of the 4th. This may have resulted from a change in the origin of the low-level air from north of the Alps to west of them, brought about by fronts pushing in from the west. The ascent again shows low-level moisture, the difference between the dew-point in the lowest 20 mb and the profile RST is unusually large. Strong winds certainly aided hoar-frost deposition.

5.2.3 Case 3: morning of 7 December 1988

See Figs 3(a) to 3(d).

Evidence: Some roads in south Oxfordshire, west Berkshire, north Hampshire and Bedfordshire were affected by extensive frost/ice. The observation from south Oxfordshire indicated that the ice there was confined to roads above 300 ft.

Synoptic background: A rather cold north to north-westerly flow covered the British Isles. On the night of the 5th/6th a cold pool had produced localized wintry showers, but there were also long clear periods. The 6th was dry and mostly sunny.

RST model: Shows some accumulation of hoar-frost after 2300. Maximum depth = 0.006 mm at 0900. Seems reasonable guidance, perhaps slightly deficient.

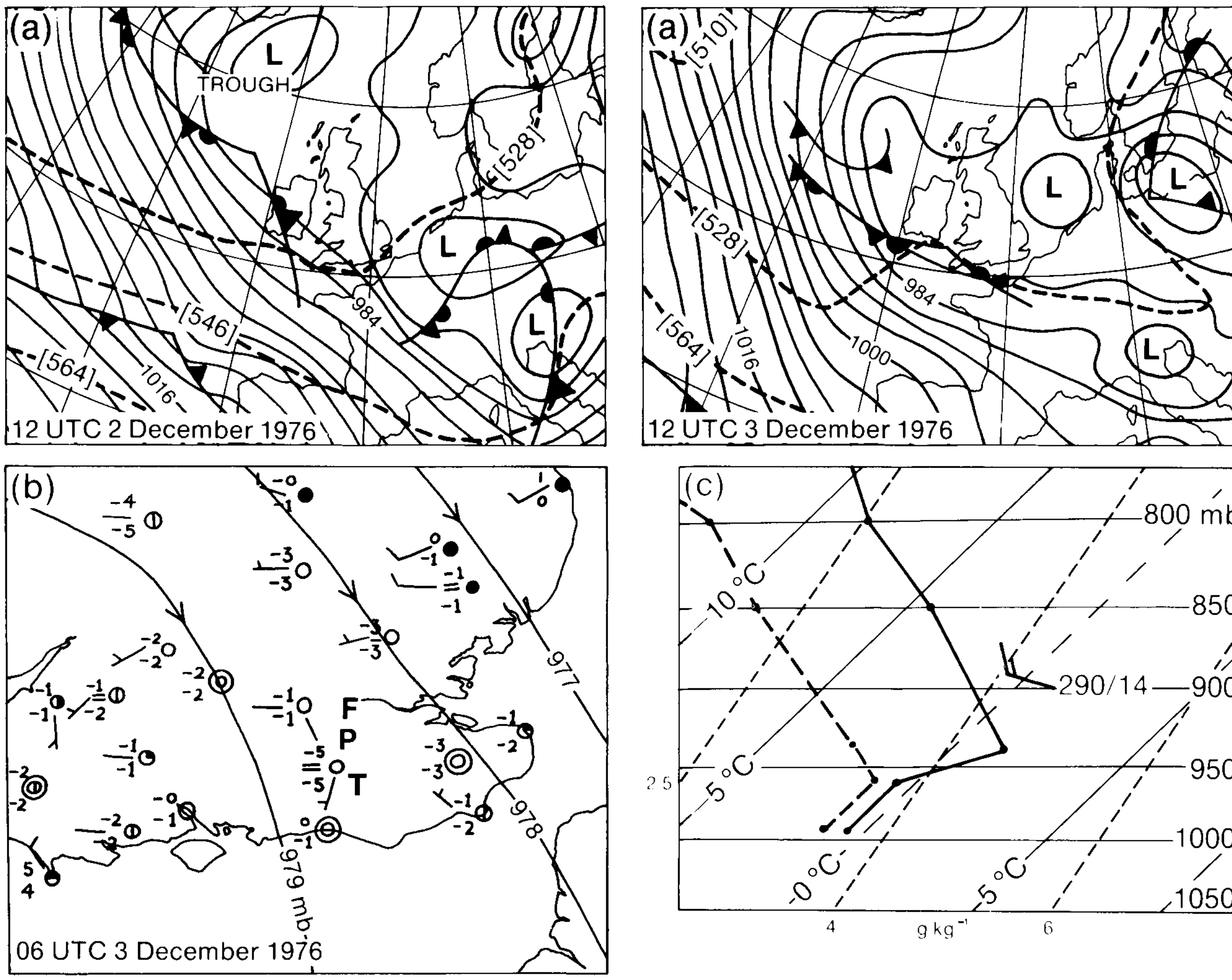

Figure 1. Data for case 1, 2/3 December 1976. (a) Synoptic charts for 12 UTC on the days in question, (b) plotted chart for south-east England at 06 UTC on 3 December 1976, (c) tephigram for Crawley at 00 UTC on 3 December 1976, and (d) input values and resulting output profiles for Wallington (Greater London). For further details see section 5.2.

Discussion: Cold, dry air moving on a long sea track produced the type of ascent favouring hoar-frost deposition, as in case 1. The Cheshire gap (near the north-west corner of Fig. 3(b)) may have allowed low-level moisture to penetrate well inland. Note on the ascent the strong wind and the negative hydrolapse in the lowest 15 mb. The very shallow depth of moisture precluded stratus — cloud near the east coast is convective stratocumulus, base about 2800 ft. Why low-level roads were wet rather than icy is not entirely clear. However, it is probable that air temperatures and RDTs at low levels were higher than at altitude. This combined with the heat generated by the morning's traffic may have been sufficient to just keep the water there from freezing.

5.2.4 Case 4: early morning of 14 January 1990

See Figs 4(a) to 4(e).

Evidence: White hoar-frost observed on the sides of roads near Mitcham, south London between 0800 and 0900. Roads nearby were wet. Minimum RSTs at the six roadside sites in Kent were all subzero. The wetness of the south London roads implies that at least some of these Kent roads were icy. Observations from three sites still showed subzero RSTs at 0800. Widespread hoar-frost also observed on Norfolk roads around dawn.

Synoptic background: Cloud and rain linked to a cold front cleared the south-east between midnight and 0600 on the 13th; with air temperatures dipping to 1 or 2 °C at dawn. A sunny day followed.

RST model: Two sets of model runs were performed, using roadside sensor measurements of air temperature, dew-point and wind from Coxett Wood, an exposed site in north Kent, and Stile Bridge, a very sheltered site in the Weald. The Coxett Wood profile shows substantial hoar-frost accumulation, reaching 0.011 mm at 0600. At Stile Bridge there was barely 0.001 mm at 0900. The RSTs predicted at both sites were quite accurate, measured minima being −1.2 °C and −3.3 °C, respectively.

Discussion: The ascent characteristics are very similar to case 3. The moisture came north from the English Channel in the developing southerly breeze. The

(d) SITE: WALLINGTON (GREATER LONDON) Date 2/3 Dec 76

Road Surface Temperature: 5.0} at midday, for start of profile
Road Depth Temperature: 4.0} at midday, for start of profile

Time (UTC)	1200	1500	1800	2100	2400	0300	0600	0900	1200	
Air Temp	5.5	4.5	1.0	-0.5	-1.0	-1.5	-2.0	-1.5	3.5	
Dew Point	1.0	0.5	-0.5	-1.0	-1.5	-2.0	-2.0	-2.0	0.5	
Avg Wind Speed		12	4	3	4	3	3	2	2	*
Avg L/Cld & C/Amt		44	22	11	00	00	00	00	00	+
Avg Cloud Type		1	1	1	0	0	0	0	0	$
Avg Rainfall		0	0	0	0	0	0	0	0	∴

'Air Temp' and 'Dew Point' are spot values for the stated times. The values for 'Avg Wind Speed', 'Avg L/Cld & C/Amt' 'Avg Cloud Type' and 'Avg Rainfall' are 'averages' over 3-hour periods.

* = at 10 m
+ = Average low cloud (oktas) and total cloud amount (oktas)
$ = '0' if no cloud, '1' if cloud mainly low cloud, '2' if cloud mainly medium cloud
∴ = '1' if precipitation during period and roads expected to be wet/icy at end of that period, '0' otherwise

FORECAST GRAPH FOR SITE: WALLINGTON

ROAD TEMPERATURE (DEGREES CELSIUS) AND ICE PREDICTION FROM 1200 2/12/76

```
+14|..|..|..|..|..|..|..|..|..|..|..|..+..|..|..|..|..|..|..|..|..|..|..|..|+14
+13|..|..|..|..|..|..|..|..|..|..|..|..+..|..|..|..|..|..|..|..|..|..|..|..|+13
+12|..|..|..|..|..|..|..|..|..|..|..|..+..|..|..|..|..|..|..|..|..|..|..|..|+12
+11|..|..|..|..|..|..|..|..|..|..|..|..+..|..|..|..|..|..|..|..|..|..|..|..|+11
+10|..|..|..|..|..|..|..|..|..|..|..|..+..|..|..|..|..|..|..|..|..|..|..|..|+10
+ 9|..|..|..|..|..|..|..|..|..|..|..|..+..|..|..|..|..|..|..|..|..|..|..|..|+ 9
+ 8|..|..|..|..|..|..|..|..|..|..|..|..+..|..|..|..|..|..|..|..|..|..|..|..|+ 8
+ 7|.RRRR|..|..|..|..|..|..|..|..|..|..+..|..|..|..|..|..|..|..|..|..|..|..|+ 7
+ 6|R.|..RRR|..|..|..|..|..|..|..|..|..+..|..|..|..|..|..|..|..|..|..|..|..|+ 6
+ 5R..|..|..R..|..|..|..|..|..|..|..|..+..|..|..|..|..|..|..|..|..|..|..|..R+ 5
+ 4|..|..|..|RR|..|..|..|..|..|..|..|..+..|..|..|..|..|..|..|..|..|..|..|.R|+ 4
+ 3|..|..|..|..RR.|..|..|..|..|..|..|..+..|..|..|..|..|..|..|..|..|..|..|R.|+ 3
+ 2|..|..|..|..|.RRR.|..|..|..|..|..|..+..|..|..|..|..|..|..|..|..|..|..R..|+ 2
+ 1|..|..|..|..|..|.RRRR|..|..|..|..|..+..|..|..|..|..|..|..|..|..|..|.R|..|+ 1
  0+--+--+--+--+--+--RRRRR-+--+--+--+--+--+--+--+--+--+--+--+--+--+--+R-+--+ 0
- 1|..|..|..|..|..|..|..|..|.RRRRR..|..+..|..|..|..|..|..|..|..|..R..|..|..|- 1
- 2|..|..|..|..|..|..|..|..|..|..|..|RRRRRRRR|..|..|..|..|..|..|..|.R|..|..|- 2
- 3|..|..|..|..|..|..|..|..|..|..|..|..+..RRRRRRRRR|..|..|..|..|..|R.|..|..|- 3
- 4|..|..|..|..|..|..|..|..|..|..|..|..+..|..|..|..|RRRRRRRRRRRR.RR..|..|..|- 4
- 5|..|..|..|..|..|..|..|..|..|..|..|..+..|..|..|..|..|..|..|..|R.|..|..|..|- 5
- 6|..|..|..|..|..|..|..|..|..|..|..|..+..|..|..|..|..|..|..|..|..|..|..|..|- 6
    +++++++++++++++++++++++++++++++++++++++++++++++++++++++++++++++++++++++++
    12 13 14 15 16 17 18 19 20 21 22 23 0  1  2  3  4  5  6  7  8  9  10 11 12
REL...............................fffffffffffffffffffffffffffffffffddddd ICE
```

PERIOD OF FREEZING ROAD TEMPERATURES: 1940-1020

MINIMUM ROAD TEMPERATURE : -4.5

KEY: ..dry (d)ew hoar (f)rost (P)recipitation (W)et (I)ce

Figure 1. Continued

differences between hoar-frost amounts on the two profiles are very probably not erroneous, but in fact a function of site exposure. The difference in wind speed appears to be the crucial factor — the effect of this (see equation 2) would be augmented by stability differences between the two sites. It is noteworthy that the iciest road is the *warmer* of the two.

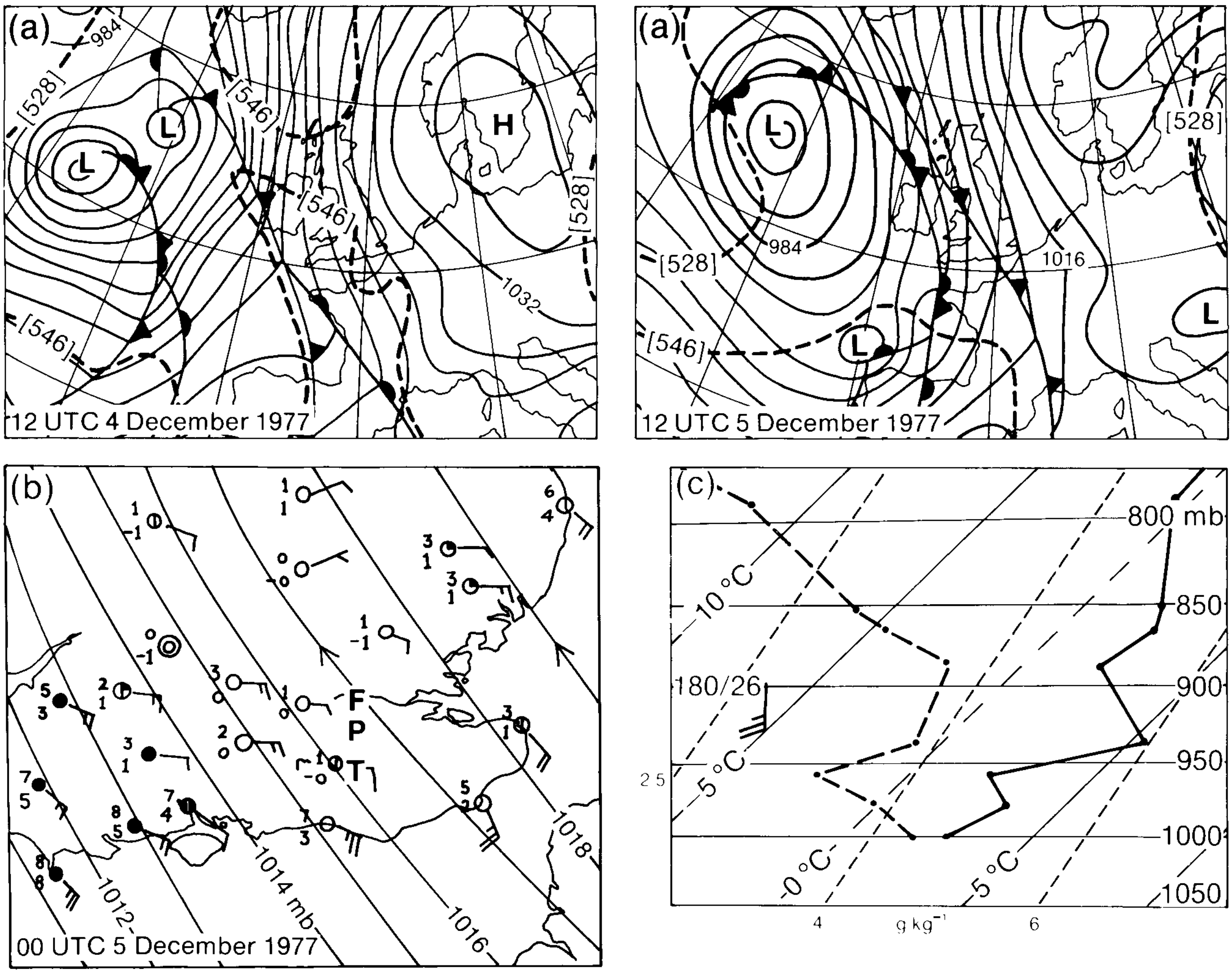

Figure 2. Data for case 2, 4/5 December 1977. (a) Synoptic charts for 12 UTC on the days in question, (b) plotted chart for south-east England at 00 UTC on 5 December 1977, (c) tephigram for Crawley at 00 UTC on 5 December 1977, and (d) input values and resulting output profiles for Wallington (Greater London). For further details see section 5.2.

5.2.5 Case 5: morning of 26 December 1979

Evidence: Thick hoar-frost observed on roads in Wallington.

RST model: produced a maximum of 0.027 mm of hoar-frost, the most seen in the five cases investigated. Deposition began at 2030.

Synoptic background: diagrams and detailed discussion have been omitted to avoid repetition. The synoptic set up was very similar to case 4 (except that the previous night had been mostly clear with a minimum of −3 °C). This 'developing southerly' synoptic situation can perhaps be considered the 'classic' one for hoar-frost deposition on roads in southern England, because the closest source of moisture is to the south.

5.3 Common features

In all the cases described, skies were clear yet there was a plentiful supply of moisture in the atmosphere's lowest layers. These two observations are almost contradictory — in that low-level moisture usually means low cloud or fog. What seems to have precluded cloud in most, if not all the cases, is that the layer of moisture was very shallow ($\approx$ 20 mb) and was capped by a deep layer of much drier air. The four tephigrams are strikingly similar in this respect.

Clear skies must be an important prerequisite for hoar-frost deposition. This is because far more long-wave radiation emanates from clouds than from clear skies. This radiation warms road surfaces, and hence reduces the chances both of T_r being below freezing point, and of T_r being below T_d (see equation 2). The sensitivity tests of Thornes and Shao (1991b) support this argument. They concluded 'cloud cover is the second most important factor governing the variation in RSTs'. There is, however, a subtle difference between the two investigations — they looked at the influence on T_r; we are effectively looking at the influence on $T_d - T_r$.

The low-level moisture evident on the tephigrams is similarly important, as its absence would also reduce the chances of T_d being above T_r. Thornes and Shao's (1991b) conclusion that 'dew-point seems to only have a minor influence on model output' is slightly misleading. What they mean is that dew-point has only a minor

(d)

SITE: WALLINGTON (GREATER LONDON) Date 4/5 Dec 77

Road Surface Temperature: 6.0
Road Depth Temperature: 3.0

Time (UTC)	1200	1500	1800	2100	2400	0300	0600	0900	1200
Air Temp	4.0	3.5	2.0	1.5	1.5	1.5	1.5	4.0	7.0
Dew Point	-1.0	-0.5	0.0	0.5	0.5	0.5	0.5	2.5	5.0
Avg Wind Speed	14	10	8	9	7	7	9	11	
Avg L/Cld & C/Amt	00	00	00	00	00	22	66	77	
Avg Cloud Type	0	0	0	0	0	1	1	1	
Avg Rainfall	0	0	0	0	0	0	0	1	

FORECAST GRAPH FOR SITE: WALLINGTON

```
ROAD TEMPERATURE (DEGREES CELSIUS) AND ICE PREDICTION FROM 1200  4/12/77
+17|..|..|..|..|..|..|..|..|..|..|..|..+..|..|..|..|..|..|..|..|..|..|..|+17
+16|..|..|..|..|..|..|..|..|..|..|..|..+..|..|..|..|..|..|..|..|..|..|..|+16
+15|..|..|..|..|..|..|..|..|..|..|..|..+..|..|..|..|..|..|..|..|..|..|..|+15
+14|..|..|..|..|..|..|..|..|..|..|..|..+..|..|..|..|..|..|..|..|..|..|..|+14
+13|..|..|..|..|..|..|..|..|..|..|..|..+..|..|..|..|..|..|..|..|..|..|..|+13
+12|..|..|..|..|..|..|..|..|..|..|..|..+..|..|..|..|..|..|..|..|..|..|..|+12
+11|..|..|..|..|..|..|..|..|..|..|..|..+..|..|..|..|..|..|..|..|..|..|..|+11
+10|..|..|..|..|..|..|..|..|..|..|..|..+..|..|..|..|..|..|..|..|..|..|..|+10
+ 9|..|..|..|..|..|..|..|..|..|..|..|..+..|..|..|..|..|..|..|..|..|..|..|+ 9
+ 8|..|..|..|..|..|..|..|..|..|..|..|..+..|..|..|..|..|..|..|..|..|..|..|+ 8
+ 7|..|..|..|..|..|..|..|..|..|..|..|..+..|..|..|..|..|..|..|..|..|..|..|+ 7
+ 6RRRRRRR..|..|..|..|..|..|..|..|..|..+..|..|..|..|..|..|..|..|..|..|..|+ 6
+ 5|..|..|R.|..|..|..|..|..|..|..|..|..+..|..|..|..|..|..|..|..|..|..|RRR+ 5
+ 4|..|..|.RR..|..|..|..|..|..|..|..|..+..|..|..|..|..|..|..|..|..|.RR..|+ 4
+ 3|..|..|..|R.|..|..|..|..|..|..|..|..+..|..|..|..|..|..|..|..|..RR.|..|+ 3
+ 2|..|..|..|.RR..|..|..|..|..|..|..|..+..|..|..|..|..|..|..|..|RR|..|..|+ 2
+ 1|..|..|..|..|RRR..|..|..|..|..|..|..+..|..|..|..|..|..|..|RRR..|..|..|+ 1
  0+--+--+--+--+--+RRRRRRR-+--+--+--+--+--+--+--+--+--+--RRRR--+--+--+--+  0
- 1|..|..|..|..|..|..|..|.RRRRRRRRRRRRRRRRR..|..|..|..RRRRRR|..|..|..|..|..|- 1
- 2|..|..|..|..|..|..|..|..|..|..|..|..+..|RRRRRRRRRRR|..|..|..|..|..|..|..|- 2
- 3|..|..|..|..|..|..|..|..|..|..|..|..+..|..|..|..|..|..|..|..|..|..|..|..|- 3
   +++++++++++++++++++++++++++++++++++++++++++++++++++++++++++++++++++++++++
   12 13 14 15 16 17 18 19 20 21 22 23 0  1  2  3  4  5  6  7  8  9  10 11 12
REL....................ffffffffffffffffffIIIIIIIIIIIIIIIIIIIIWWWWPPPPPPPP ICE
```

PERIOD OF FREEZING ROAD TEMPERATURES: 1810-0730
MINIMUM ROAD TEMPERATURE : -1.7

KEY: ..dry (d)ew hoar (f)rost (P)recipitation (W)et (I)ce

Figure 2. Continued

influence on RST, and that may only be in the absence of moisture fluxes to/from a road surface. Quite clearly dew-point has a very substantial impact on hoar-frost deposition!

It seems that on occasions the observed moisture distribution can be explained by the way in which the synoptic pattern is interacting with the physical geography of southern England and its surroundings. By physical geography is meant, primarily, the moisture sources (seas) and sinks (land, especially at altitude).

Inspection of the RST model data tables and also the thickness lines on the North Atlantic charts shows a notable abscence of very cold air from any of the cases. The fact that occasions when snow was lying on road surfaces were specifically excluded during case selection partly explains this. However, it is also physically reasonable because the capacity of air to hold water vapour (to be deposited) decreases as its temperature decreases. The depth of hoar-frost that can be deposited with a 1 °C difference between T_r and T_d at +1 °C is about 60% more than at −6 °C (1000 mb humidity mixing ratios at +1 °C and −6 °C are, respectively, 4 g kg^{-1} and 2.5 g kg^{-1} — calculating $((4-2.5)/2.5) \times 100\%$ gives 60%). This effect is not accounted for by equation (2). It should also be noted that T_d does not have to be below zero.

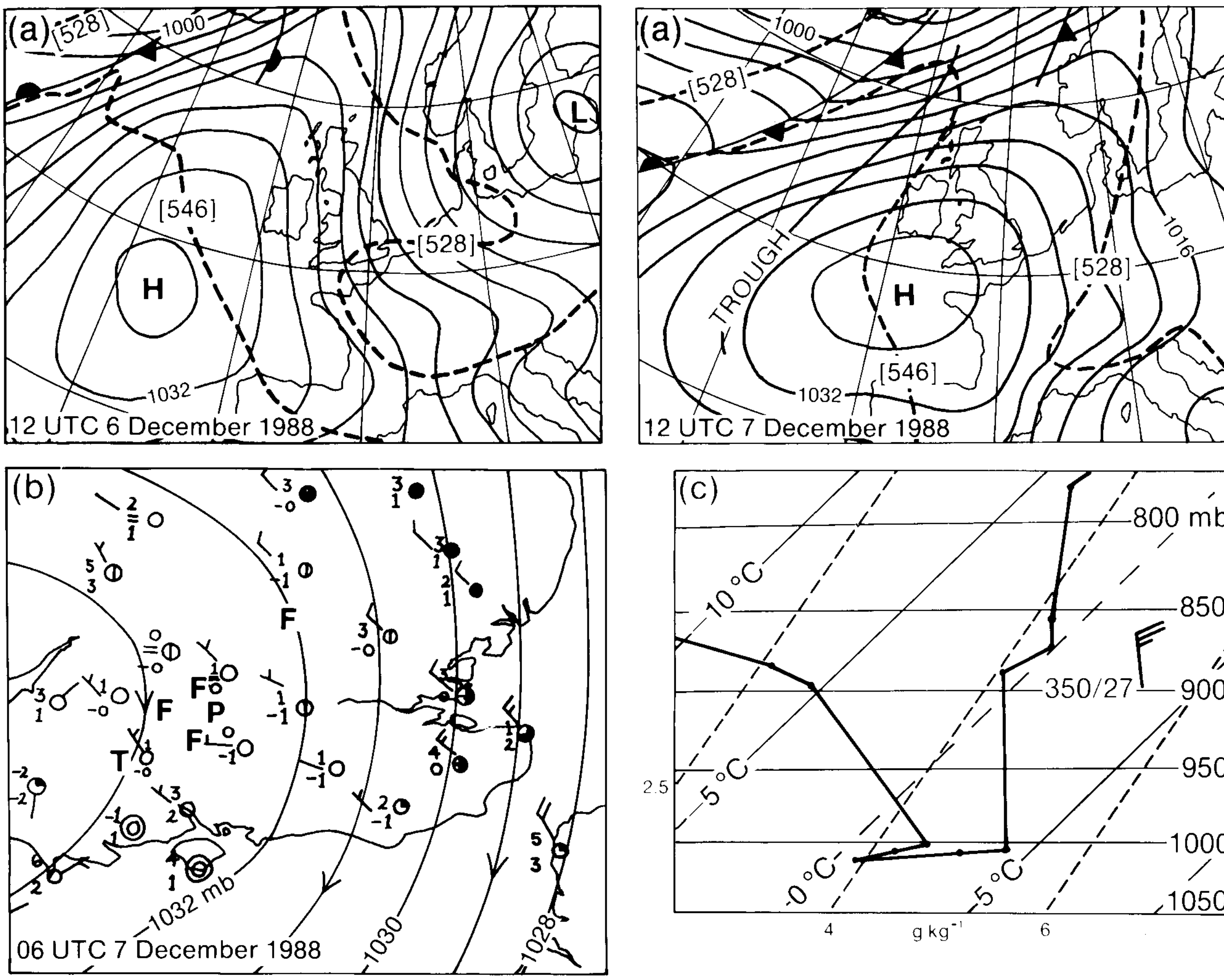

Figure 3. Data for case 3, 6/7 December 1988. (a) Synoptic charts for 12 UTC on the days in question, (b) plotted chart for south-east England at 06 UTC on 7 December 1988, (c) tephigram for Larkhill at 06 UTC on 7 December 1988, and (d) input values and resulting output profiles for the Berkshire Downs. For further details see section 5.2.

Another feature common to all cases is the steady breeze. Aside from aiding hoar-frost deposition through mechanical mixing, and hence vertical transport of moisture down onto the road surface (note U in equation (2)), this breeze was probably also mixing some dry air down onto the top of the shallow moist layer, helping preclude stratus development. The strength of the 900 m wind should in itself have been sufficient to make fog formation unlikely in case 4, and extremely unlikely in cases 2, 3 and 5 (Saunders (1973) concludes that radiation fog does not form with geostrophic wind speeds of above about 21 kn ($\approx$ 900 m wind speed)).

In cases 2, 3, 4 and 5 the night preceding the hoar-frost event had been cold and at least partly clear. It is physically sound to expect this to be a contributory factor. This is because at night the roadbed and underlying soil tend to act as a reservoir of heat, generating an upward heat flux, which effectively puts a brake on the fall of RST. One cold, clear night will reduce the amount of heat in the reservoir, thus making the 'brake' less effective the following night. This implies that on this second night T_r will be allowed to drop further below T than it would have had the first night not been cold and clear. Clearly this increases the chances of T_d being above T_r, and hence of hoar-frost deposition. The RDT gives one measure of the amount of heat stored below the road surface. Fig. 5 illustrates why the weather of the previous night is important in addition to this.

Any factor which increases the *general* risk of hoar-frost deposition will necessarily also increase the chances of hoar-frost deposition commencing *early* in the night-time period. However, this is *particularly* true for 'previous night's weather'. This is because the influence that a specific weather event has on subsequent RST must decrease with time. Thus any differences in RST profiles which can be attributed solely to the previous night's weather will be larger around dusk than around dawn. Inspection of the cases studies suggests that this effect is physically significant. Cases 2 and 5 were the only ones for which the RST model or observations indicated that the time of onset of hoar-frost deposition was before 2100. They were also the

(d)

```
SITE: BERKSHIRE DOWNS  Date 6/7 Dec 88

Road Surface Temperature:  6.0
Road Depth Temperature:    5.0
```

Time (UTC)	1200	1500	1800	2100	2400	0300	0600	0900	1200
Air Temp	6.0	5.5	4.0	2.0	1.0	0.3	0.3	0.5	4.5
Dew Point	2.0	1.5	1.0	0.0	0.0	-0.5	-0.5	-0.3	2.5
Avg Wind Speed	10	8	7	6	5	4	4	5	
Avg L/Cld & C/Amt	33	22	00	00	00	00	22	33	
Avg Cloud Type	1	1	0	0	0	0	1	1	
Avg Rainfall	0	0	0	0	0	0	0	0	

```
FORECAST GRAPH FOR   SITE: BERKSHIRE DOWNS

ROAD TEMPERATURE (DEGREES CELSIUS) AND ICE PREDICTION FROM 1200  6/12/88

+17|..|..|..|..|..|..|..|..|..|..|..|..+..|..|..|..|..|..|..|..|..|..|..|..|+17
+16|..|..|..|..|..|..|..|..|..|..|..|..+..|..|..|..|..|..|..|..|..|..|..|..|+16..
+15|..|..|..|..|..|..|..|..|..|..|..|..+..|..|..|..|..|..|..|..|..|..|..|..|+15..
+14|..|..|..|..|..|..|..|..|..|..|..|..+..|..|..|..|..|..|..|..|..|..|..|..|+14
+13|..|..|..|..|..|..|..|..|..|..|..|..+..|..|..|..|..|..|..|..|..|..|..|..|+13
+12|..|..|..|..|..|..|..|..|..|..|..|..+..|..|..|..|..|..|..|..|..|..|..|..|+12
+11|..|..|..|..|..|..|..|..|..|..|..|..+..|..|..|..|..|..|..|..|..|..|..|..|+11
+10|..|..|..|..|..|..|..|..|..|..|..|..+..|..|..|..|..|..|..|..|..|..|..|..|+10
+ 9|..|..|..|..|..|..|..|..|..|..|..|..+..|..|..|..|..|..|..|..|..|..|..|..|+ 9
+ 8|..|..|..|..|..|..|..|..|..|..|..|..+..|..|..|..|..|..|..|..|..|..|..|..|+ 8
+ 7|RRRRRRR.|..|..|..|..|..|..|..|..|..+..|..|..|..|..|..|..|..|..|..|..|..|+ 7
+ 6R..|..|.RR..|..|..|..|..|..|..|..+..|..|..|..|..|..|..|..|..|..|..|..|+ 6
+ 5|..|..|..|R.|..|..|..|..|..|..|..+..|..|..|..|..|..|..|..|..|..|..|..R+ 5
+ 4|..|..|..|.RRR.|..|..|..|..|..|..|..+..|..|..|..|..|..|..|..|..|..|..|RR|+ 4
+ 3|..|..|..|..|.RRRR|..|..|..|..|..|..+..|..|..|..|..|..|..|..|..|..|..R..|+ 3
+ 2|..|..|..|..|..|..RRRR..|..|..|..+..|..|..|..|..|..|..|..|..|RR|..|+ 2
+ 1|..|..|..|..|..|..|..|RRRRR|..|..|..+..|..|..|..|..|..|..|..|..R..|..|+ 1
   0+--+--+--+--+--+--+--+--RRRRRRRR-+--+--+--+--+--+--+--+--+--+-R+--+--+  0
- 1|..|..|..|..|..|..|..|..|..|..|..|..|.RRRRRRRRR.|..|..|..|..|..|..RR.|..|..|- 1
- 2|..|..|..|..|..|..|..|..|..|..|..|..+..|..|.RRRRRRRRRRRRRRRRRRR|..|..|..|- 2
- 3|..|..|..|..|..|..|..|..|..|..|..|..+..|..|..|..|..|..|..|..|..|..|..|..|- 3
   +++++++++++++++++++++++++++++++++++++++++++++++++++++++++++++++++++++++++++
   12 13 14 15 16 17 18 19 20 21 22 23 0  1  2  3  4  5  6  7  8  9  10 11 12
REL...............................ffffffffffffffffffffffffffffffdddddd ICE

PERIOD OF FREEZING ROAD TEMPERATURES:   2210-0950
MINIMUM ROAD TEMPERATURE            :   -2.2

KEY:  ..dry  (d)ew   hoar (f)rost   (P)recipitation   (W)et   (I)ce
```

Figure 3. Continued

only cases in which the previous night had had a minimum of 0 °C or below as well as largely clear skies.

The distribution by month for the five cases was December — 4, January — 1. There are two reasons for expecting the prevalence of cases in December to be no coincidence:

(a) it is in December that nights are longest, and hence road cooling greatest. Daytime warming is also least in this month, not only because of shorter days, but also because of the reduction in direct insolation caused by low solar elevation. Thus, on average, the depression of T_r below T is largest in December (as demonstrated by Parrey (1969)), and

(b) this reason is related directly to T_d. For a given wind direction over the British Isles T_d tends to be proportional to sea surface temperature upwind (T_{sea}). Therefore one would expect T_{min} (minimum air temperature) minus T_{sea} to be roughly proportional to the night-time dew-point depression, T minus T_d. Hence ($T_{min}-T_{sea}$) should give an indication of the risk of hoar-frost/dew deposition, whereby lower values imply greater risk. In Table I T_{min} at Heathrow

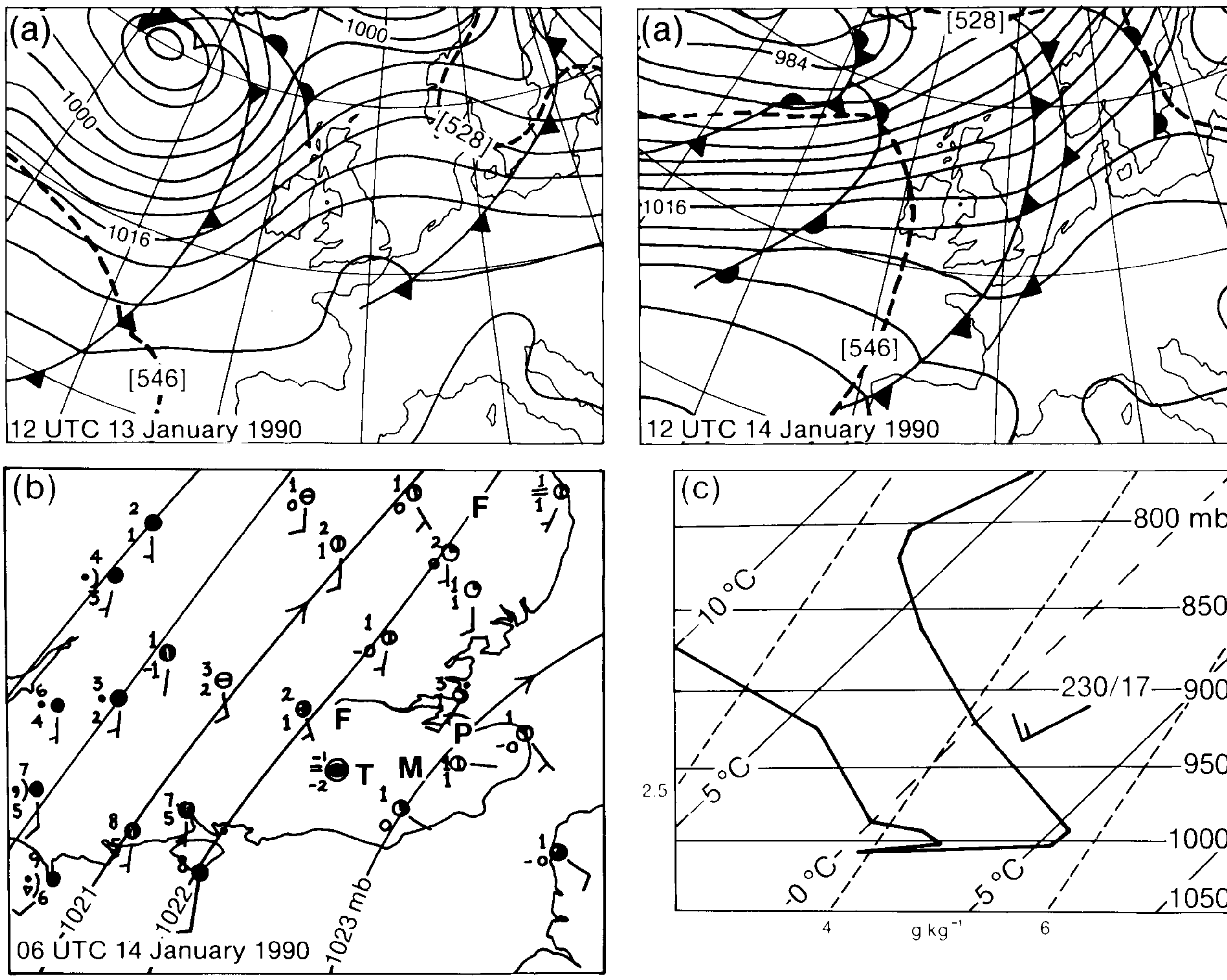

Figure 4. Data for case 4, 13/14 January 1990. (a) Synoptic charts for 12 UTC on the days in question, (b) plotted chart for south-east England at 06 UTC on 14 January 1990, (c) tephigram for Crawley at 00 UTC on 14 January 1990, and input values and resulting output profiles for (d) Stile Bridge (Kent) and (e) Coxett Wood (Kent). For further details see section 5.2.

airport is compared with T_{sea} in the English Channel, for November through to February. The difference column suggests hoar-frost/dew deposition is more likely early in the winter than later, and is consistent with the large number of December cases.

These arguments relating to 'time of year' are supported by the results of Takle (1990), who catalogued 1615 observations of hoar-frost deposition in Iowa. He found a frequency maximum split between December and January, but indicated that the way in which temperature and humidity during the analysis period had differed from climatology meant this probably gave an overestimate of January's true hoar-frost climatology.

The link between T_d and T_{sea}, and the dependence on temperature of the air's capacity to hold water vapour lead to another potentially useful result. This is that on a night when subzero RSTs are expected the risk of hoar-frost deposition will be greater if sea temperatures are anomalously high.

6. Forecasting hoar-frost deposition

6.1 Two new techniques

The main tool for a road condition forecaster in the UK Meteorological Office is the RST model. Comments in section 5.2 suggested that this model performs well if fed with accurate input parameters (albeit with perhaps a slight tendency to underestimate deposition). The forecaster's main difficulty then would seem to be getting these parameters right; particularly low cloud, dew-points and wind speeds*. In this sense it is a standard forecasting problem. Case 4 showed, however, that across a small region large differences in road conditions can sometimes arise. Given that a forecaster may have to cater for a large region by running the RST model for just one site, it is therefore important that they also appreciate the mechanisms which may lead to such differences. Only then can appropriate guidance be

* At London Weather Centre it has been found that on occasions forecast tephigrams taken from the UK limited-area model can be useful for obtaining accurate input parameters.

(d)

```
SITE: STILE BRIDGE, KENT        Date 13/14 Jan 90

Road Surface Temperature:  9.0
Road Depth Temperature:    6.0
```

Time (UTC)	1200	1500	1800	2100	2400	0300	0600	0900	1200
Air Temp	5.8	7.2	1.1	-0.9	-1.5	-2.5	-3.0	0.1	3.5
Dew Point	4.4	3.8	0.5	-1.3	-1.8	-2.9	-3.3	0.0	3.3
Avg Wind Speed	3	1	0	0	0	0	0	0	
Avg L/Cld & C/Amt	11	02	00	01	00	01	34	88	
Avg Cloud Type	1	2	0	2	0	2	1	1	
Avg Rainfall	0	0	0	0	0	0	0	1	

```
FORECAST GRAPH FOR   SITE: STILE BRIDGE, KENT

ROAD TEMPERATURE (DEGREES CELSIUS) AND ICE PREDICTION FROM 1200  13/1/90

+16|..|..|..|..|..|..|..|..|..|..|..|..+..|..|..|..|..|..|..|..|..|..|..|..|+16
+15|..|..|..|..|..|..|..|..|..|..|..|..+..|..|..|..|..|..|..|..|..|..|..|..|+15
+14|..|..|..|..|..|..|..|..|..|..|..|..+..|..|..|..|..|..|..|..|..|..|..|..|+14
+13|..|..|..|..|..|..|..|..|..|..|..|..+..|..|..|..|..|..|..|..|..|..|..|..|+13
+12|..|..|..|..|..|..|..|..|..|..|..|..+..|..|..|..|..|..|..|..|..|..|..|..|+12
+11|..|..|..|..|..|..|..|..|..|..|..|..+..|..|..|..|..|..|..|..|..|..|..|..|+11
+10|RRRRRR..|..|..|..|..|..|..|..|..|..+..|..|..|..|..|..|..|..|..|..|..|..|+10
+ 9R..|..|RR|..|..|..|..|..|..|..|..|..+..|..|..|..|..|..|..|..|..|..|..|..|+ 9
+ 8|..|..|..R..|..|..|..|..|..|..|..|..+..|..|..|..|..|..|..|..|..|..|..|..|+ 8
+ 7|..|..|..|R.|..|..|..|..|..|..|..|..+..|..|..|..|..|..|..|..|..|..|..|..|+ 7
+ 6|..|..|..|.R|..|..|..|..|..|..|..|..+..|..|..|..|..|..|..|..|..|..|..|..|+ 6
+ 5|..|..|..|..RR.|..|..|..|..|..|..|..+..|..|..|..|..|..|..|..|..|..|..|..|+ 5
+ 4|..|..|..|..|.RR..|..|..|..|..|..|..+..|..|..|..|..|..|..|..|..|..|..|..|+ 4
+ 3|..|..|..|..|..|RRR..|..|..|..|..|..+..|..|..|..|..|..|..|..|..|..|..|..R+ 3
+ 2|..|..|..|..|..|..|RRR..|..|..|..|..+..|..|..|..|..|..|..|..|..|..|..|RR|+ 2
+ 1|..|..|..|..|..|..|..|RRR..|..|..|..+..|..|..|..|..|..|..|..|..|..|.RR..|+ 1
  0+--+--+--+--+--+--+--+--+RRRRR+--+--+--+--+--+--+--+--+--+--+--+--RR-+--+  0
- 1|..|..|..|..|..|..|..|..|..|..|..RRRRRRR..|..|..|..|..|..|..|..|RR|..|..|- 1
- 2|..|..|..|..|..|..|..|..|..|..|..|..+RRRRRRRR|..|..|..|..|..|.RR..|..|..|- 2
- 3|..|..|..|..|..|..|..|..|..|..|..|..+..|..|..RRRRRRRRRRRRRRRRR.|..|..|..|- 3
- 4|..|..|..|..|..|..|..|..|..|..|..|..+..|..|..|..|..|..|..|..|..|..|..|..|- 4

   +++++++++++++++++++++++++++++++++++++++++++++++++++++++++++++++++++++++++

   12 13 14 15 16 17 18 19 20 21 22 23 0  1  2  3  4  5  6  7  8  9  10 11 12
REL..................................................ffffPPPPPPPP  ICE

PERIOD OF FREEZING ROAD TEMPERATURES:   2110-1010
MINIMUM ROAD TEMPERATURE            :   -3.3

KEY:  ..dry   (d)ew   hoar (f)rost   (P)recipitation   (W)et   (I)ce
```

Figure 4. Continued

given to the customer. A thorough understanding also enables the forecaster to attach a suitable confidence level to a prediction, or, equivalently, an 'ice probability'. The potential practical and economic advantages of probablistic type forecasts have been emphasized by Ayton (1988) and Takle (1990), to name but two.

It is with such benefits in mind that the following two aids to forecasting hoar-frost deposition are proposed.

6.1.1 Method 1

This method requires neither an RST model, nor sensor data. It comprises a check-list of factors which increase the risk of hoar-frost deposition (Table II). All have been discussed in section 5.3. It should be fairly quick and easy to see the extent to which they will be satisfied on a given night. To help with this values have been added alongside to suggest the level at which one might consider a particular criterion to have been met. All except (5) and (6) relate to the night in question. It is assumed that factor (6), the RDT, would be measured at midday just before the night in question.

In compiling this list factor (6) was seen to represent the weather of the previous few days and nights, whereas factor (5) represents, by definition, the weather of the

(e)

```
SITE: COXETT WOOD, KENT    Date 13/14 JAN 90

Road Surface Temperature:  9.0
Road Depth Temperature:    6.0
-------------------------------------------------------------------------

Time (UTC)             1200  1500  1800  2100  2400  0300  0600  0900  1200
Air Temp                6.6   7.0   3.1   2.2   2.2   2.2   2.0   4.2   6.5
Dew Point               4.4   3.8   2.0   1.2   1.2   1.2   1.3   3.5   5.5
Avg Wind Speed             5     5     4     5     5     8    12    13
Avg L/Cld & C/Amt         11    02    00    01    00    01    34    88
Avg Cloud Type             1     2     0     2     0     2     1     1
Avg Rainfall               0     0     0     0     0     0     0     1
-------------------------------------------------------------------------

FORECAST GRAPH FOR    SITE: COXETT WOOD, KENT

ROAD TEMPERATURE (DEGREES CELSIUS) AND ICE PREDICTION FROM 1200  13/1/90

+19|..|..|..|..|..|..|..|..|..|..|..|..+..|..|..|..|..|..|..|..|..|..|..|..|+19
+18|..|..|..|..|..|..|..|..|..|..|..|..+..|..|..|..|..|..|..|..|..|..|..|..|+18
+17|..|..|..|..|..|..|..|..|..|..|..|..+..|..|..|..|..|..|..|..|..|..|..|..|+17
+16|..|..|..|..|..|..|..|..|..|..|..|..+..|..|..|..|..|..|..|..|..|..|..|..|+16
+15|..|..|..|..|..|..|..|..|..|..|..|..+..|..|..|..|..|..|..|..|..|..|..|..|+15
+14|..|..|..|..|..|..|..|..|..|..|..|..+..|..|..|..|..|..|..|..|..|..|..|..|+14
+13|..|..|..|..|..|..|..|..|..|..|..|..+..|..|..|..|..|..|..|..|..|..|..|..|+13
+12|..|..|..|..|..|..|..|..|..|..|..|..+..|..|..|..|..|..|..|..|..|..|..|..|+12
+11|..|..|..|..|..|..|..|..|..|..|..|..+..|..|..|..|..|..|..|..|..|..|..|..|+11
+10|RRRRRR..|..|..|..|..|..|..|..|..|..+..|..|..|..|..|..|..|..|..|..|..|..|+10
+ 9R..|..|RR|..|..|..|..|..|..|..|..|..+..|..|..|..|..|..|..|..|..|..|..|..|+ 9
+ 8|..|..|..R..|..|..|..|..|..|..|..|..+..|..|..|..|..|..|..|..|..|..|..|..|+ 8
+ 7|..|..|..|R.|..|..|..|..|..|..|..|..+..|..|..|..|..|..|..|..|..|..|..|..|+ 7
+ 6|..|..|..|.R|..|..|..|..|..|..|..|..+..|..|..|..|..|..|..|..|..|..|..|.RR+ 6
+ 5|..|..|..|..RR.|..|..|..|..|..|..|..+..|..|..|..|..|..|..|..|..|..|.RRR.|+ 5
+ 4|..|..|..|..|.RRR.|..|..|..|..|..|..+..|..|..|..|..|..|..|..|..|..RR.|..|+ 4
+ 3|..|..|..|..|..|.RRR.|..|..|..|..|..+..|..|..|..|..|..|..|..|..|RR|..|..|+ 3
+ 2|..|..|..|..|..|..|.RRRRR..|..|..|..+..|..|..|..|..|..|..|..|.RR..|..|..|+ 2
+ 1|..|..|..|..|..|..|..|..|RRRRRRRRR..+..|..|..|..|..|..|..RRRRR.|..|..|..|+ 1
  0+--+--+--+--+--+--+--+--+--+--+--+RRRRRRRRRRRRRRRRRRRRRRR+--+--+--+--+--+  0
- 1|..|..|..|..|..|..|..|..|..|..|..|..+..|..|..|..|..|..|..|..|..|..|..|..|- 1
   +++++++++++++++++++++++++++++++++++++++++++++++++++++++++++++++++++++++++
   12 13 14 15 16 17 18 19 20 21 22 23 0  1  2  3  4  5  6  7  8  9  10 11 12
REL................................ddddddffffffffffffffIIWWWWWWWWPPPPPPPPP  ICE

PERIOD OF FREEZING ROAD TEMPERATURES:   0100-0600
MINIMUM ROAD TEMPERATURE            :   -0.3

KEY:   ..dry   (d)ew   hoar (f)rost   (P)recipitation   (W)et   (I)ce
```

Figure 4. Continued

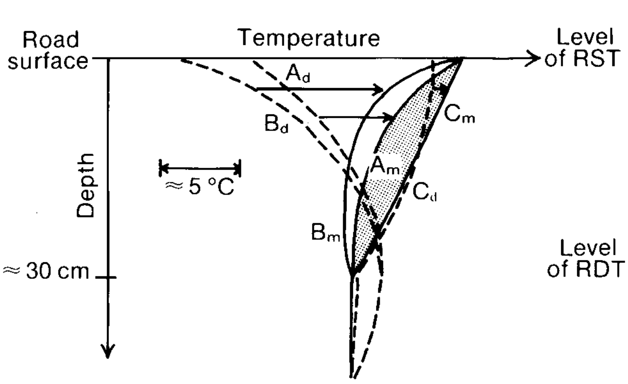

Figure 5. Schematic diagram of three midday subsurface temperature profiles (solid lines A_m, B_m and C_m) showing differences which can occur *for a given RST/RDT combination*. Corresponding dawn profiles are shown as dashed lines (A_d, B_d and C_d). A_m and B_m typically occur in clear weather. The curvature of the lines is due to the depth versus temperature profiles at dawn, A_d and B_d, having minima at the surface which effectively propogated downwards during the morning as sunshine increased the RST. The lower temperature on B_m reflects a lower RST on B_d, which in turn reflects a lower dawn air temperature. C_m typically occurs in cloudy conditions. The straighter line is symptomatic of a smaller diurnal range of RST. The area of shading is proportional to the difference in energy stored below the road surface between A_m and C_m.

Table I. Comparison of average minimum air temperature (°C) at London (Heathrow) Airport (T_{min}) with average sea temperatures in the English Channel (T_{sea})

	T_{min}	T_{sea}	Difference
November	4.5	12.9	−8.4
December	2.5	10.9	−8.4
January	1.4	9.4	−8.0
February	1.5	8.6	−7.1

previous night only. This is why both were included (see also Fig. 5) . Factor (7) is included to represent only solar elevation and duration, and not links with T_d discussed in section 5.3. T_d is catered for by other factors.

For each case-study in section 5 the number of criteria met was as follows:

(1):4 (2):7 (3):6 (4_{ex}):5 (5):7 (4_{sh}):3

('$_{ex}$' and '$_{sh}$' represent, respectively, the exposed and sheltered sites.)

First impressions from these figures are that higher numbers do indicate an increased risk of hoar-frost deposition.

6.1.2 Method 2

This technique is an extension, in graphical form, of equation (2). An allowance is made for some accumulation of hoar-frost over and above that implied by the equation, particularly on 'calm' nights, by putting $U = U + 1$ (kn). This seems justified because traffic causes extra stirring of the air which is unlikely to be reflected by the instruments on which the forecaster bases their estimates of wind speed (a measurement problem also noted in Boselly *et al.* (1990)). The '1' is, admittedly, a somewhat arbitrary figure. It is being assumed that the effect of extra stirring of the air is not being offset by traffic-induced increases in RST; caused by warm exhaust fumes, warm tyres and increased downward long-wave radiation. The assumption that traffic has minimal effect on RST seems to be inherent in all but the most recent RST models (Thornes and Shao 1991a).

The method assumes the forecaster has an RST model output profile to work with. Alternatively it could be used in conjunction with RSTs measured by sensors, to monitor hoar-frost accumulation through the night:

First plot dew-points onto the RST profile. Then estimate the area between tbe two lines where RST is less than dew-point (in °C hours, say). Finally, multiply this value by a number equal to 1 plus the average wind speed in knots. The resulting value is roughly proportional to the accumulated depth of hoar-frost.

Having performed such a calculation the forecaster can immediately get a feel for the likely error if winds were stronger than forecast, or dew-points higher, thus indicating forecast confidence (although RST is admittedly dependent on these factors).

The cases studied yielded the following values, when calculated up to the time RSTs rose to zero:

(1):50 (2):128 (3):55 (4_{ex}):66 (5):165 (4_{sh}):3
units: °C hour knots

First impressions again suggest that higher values indicate a greater risk of hoar-frost deposition.

There seems to be a very approximate relationship between these values and the depths of hoar-frost calculated by the RST model; the value *is* the depth, in ten-thousandths of a millimetre.

Equation (2) also applies when roads are drying out after rain, indicating that a similar technique could be used to assess 'drying time', provided the initial depth of water is known.

This method shows some similarity with the work of Gustavsson and Bogren (1990). They plotted RST and dew-point curves on the same graph and suggested that the area between the two indicated 'risk of slipperiness'. No mention was made of the importance of wind speed however.

6.1.3 Application in different climate regimes

Applying method 2 to one of the examples in Gustavsson and Bogren (1990) (station 20 on 18 January 1986) yields a massive total of 314 °C hour knots, and

Table II. Check list of factors which increase the risk of hoar-frost deposition

No.	Description	Definition
1	Clear sky	≤2/8 cloud cover
2	Small dew-point depression	≤1.5 °C
3	High dew-point	≥−1 °C
4	Wind	≥4 kn at 10 m
5	Cold and clear the preceeding night	Air minimum ≤0 °C and/or ≤2/8 cloud
6	Low RDT	≤4.5 °C
7	Long night	From 21 November to 20 January

A minimum $T_r \leq 0$ °C is obviously also a necessary condition.

that was during the daytime! This is consistent with our earlier suggestion (section 2) that hoar-frost is more of a problem in Sweden. Method 2 should be equally valid for any climate as it was based purely on physics. However, method 1, which was based partly on south-east England case-studies, and only gives a score of about 5 for the same Swedish case, is not so valid for climates which differ from that of south-east England.

6.2 Validation

In both the above methods it seemed that higher scores indicated a higher risk of hoar-frost deposition. This hypothesis is tested out below by applying the methods to new data for the winter of 1990/91. An attempt is also made to define scores which separate cases of icy roads from cases of dry roads. A separate investigation of the factors which make up method 1 is also performed.

6.2.1 Verifying data

The winter of 1990/91 differed from most of the case-study winters in that there was a large amount of RST sensor data available. This enabled the whole period from 1 November through to 30 April to be analysed. The area of interest comprised a broad band extending along the Thames valley, from the western edge of Berkshire to central London. In this area during the winter of 1990/91 there were 10 roadside sites at which RSTs and meteorological variables were measured.

The RST data was first scrutinized to find nights when RST fell to 0 °C at at least one site. From such cases were excluded occasions on which it was considered that one or more of the following criteria had been met: (i) any ice that occurred would have been due to water freezing, (ii) snow was lying on road surfaces, (iii) widespread fog occurred. This left 19 cases. Next, these cases were divided into two categories; 'icy' or 'non-icy'. 'Icy' nights were those on which ice had been observed by Meteorological Office employees and/or Berkshire County Council highway maintenance crews. 'Non-icy' were those for which there was no evidence of ice. These definitions yielded 6 'icy' and 13 'non-icy'.

Given that ice may have been missed by our circumstantial observations some other confirmation was required. The only routine observations which are of use here are 'concrete-slab minimum temperature' and 'state of concrete slab' (dry/moist/wet/icy), both measured once a day, at 0900 UTC, at climatological stations in the United Kingdom. Seven stations were close enough to the analysis area to be of use. It has to be assumed that the state of slab observation is representative of the 'worst' conditions which occurred during the night just ended. This is not unreasonable provided no major changes in the weather occurred, which for the vast majority of nights is true.

Regulations state that concrete slabs should be about 5 cm thick and mounted on a layer of sand over bare earth. As such they do behave differently from roads. For the 19 dates the average difference air minimum minus slab minimum at the climatological sites was +1.8 °C, whereas the average difference air minimum minus road minimum for the roadside sites was only +0.5 °C. Because a necessary condition for hoar-frost deposition is that air temperature is greater than RST (or slab temperature) it therefore follows that slabs are very probably wet or icy more often than are roads. So on occasions when the slabs were dry, roads were probably dry also.

For the 13 'non-icy' cases considered together 85% of all available slab reports indicated 'dry'; and when each case was considered separately there was only one for which less than two thirds of reports indicated dry. This suggests that roads *were* probably dry (free of ice) on the occasions classified as 'non-icy'. This conclusion is reinforced by the fact that reports for the 6 'icy' cases were markedly different; only 38% indicated 'dry'. Further investigation allayed a suspicion that the one apparently anomalous 'non-icy' case had been incorrectly categorized.

6.2.2 Results for method 1

Fig. 6 depicts the scores obtained with method 1. This provides clear evidence that higher scores do indicate a higher risk of hoar-frost deposition. It also suggests that **with a score of 3 or less, hoar-frost deposition will generally not be a problem; but with a score of 5 or more there is a high probability of icy roads.**

Table II shows various statistics relating to the seven factors which make up method 1. These were calculated on a data-set comprising both the 1990/91 cases and those from section 5. The following deductions can be made:

(a) For the proposed criteria the 'mean score per factor' is consistently greater for the icy cases.

(b) Mean *values* generally accord with (a), as would be expected.

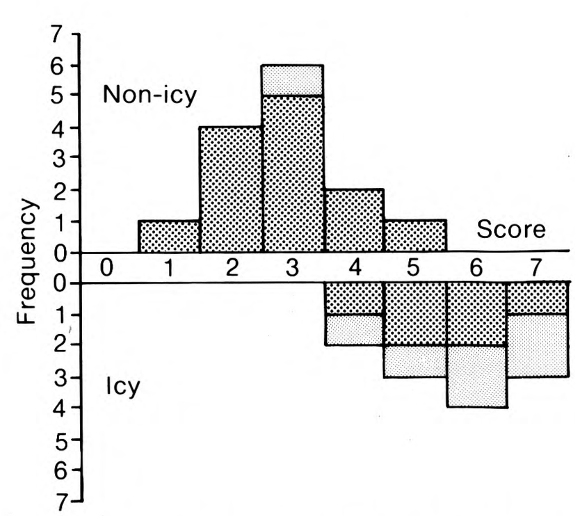

Figure 6. Histogram showing scores obtained using method 1 for cases in the winter of 1990/91 (dark shading) and cases described in section 5.2 (light shading).

(c) The mean wind-speed is virtually the same in both data sets. This is probably because stronger winds work in one of two ways — to increase the rate of deposition if RST is less than dew-point; or to increase the rate of evaporation if RST is greater than dew-point. Thus strong winds favour hoar-frost deposition *only* when other factors are also conducive to it.

(d) The differences between means are mostly not statistically significant. This is in part due to the relatively small data-set size. Recognizing that each factor is supported by physical argument, and noting (a) to (c) above, it is considered that all seven should be retained.

(e) Clear skies are probably *the* most important factor. This partly accords with a conclusion of Thornes and Shao (1991b) referred to earlier (in section 5.3). Every icy case considered here had a mean of ≤ 2/8 low + medium cloud between 1800 and 0600.

(f) There is significantly more variability in values in the non-icy cases. For factors 1, 2 and 7 this is partly because the data is not continuous.

(g) Differences in variability noted in (f) are particularly apparent for wind speed. In the icy cases wind speeds fall predominantly into the range from 4 to 7 kn.

The upper limit in (g) may well exist because stronger surface winds indicate increased mixing in the atmosphere's lowest layers, reducing the vertical moisture gradients seen to be so important on the tephigrams in section 5. Such mixing would lead, ultimately, to either the formation of cloud (note the discussion of case-study 1 in section 5.2.1) or a reduction in surface dew-point; both of which mollify hoar-frost deposition. A result in Bogren and Gustavsson (1991) seems to support this argument. This states that to completely destroy cold air pooling in valleys an ambient wind speed greater than 6 kn is required. In turn this suggests that mixing of the atmosphere's lowest layers is 'complete' for winds greater than 6 kn.

Monteith (1957) concluded that the optimal conditions for dewfall from the atmosphere onto short grass were clear skies, high relative humidity and a 2-metre wind of 1–3 $m\ s^{-1}$ (≈ 3–9 kn at 10 m). Although a grass surface is fundamentally different to a road surface, these conditions accord well with the results in Table III, and comments (e) and (g) above.

Quite clearly the factors comprising method 1 are not independent. On many nights the presence of one or two particular ones will preclude others. The skilful forecaster should be able to identify those few occasions when the synoptic set-up *is* conducive to the co-existence of many factors.

6.2.3 Results for method 2

Fig. 7 depicts the scores obtained with method 2. Calculations for this were generally based on *measured* RSTs. For only one case did lack of RST measurements

Table III. Statistical data for the factors which make up method 1 based on all cases from the winter of 1990/91 together with those discussed in section 5.2. The symbols *, ** and *** indicate differences between 'icy' and 'non-icy' cases to be significant at, respectively, the 90%, 95% and 99.5% levels (shown only for value mean and standard deviation).

	Factor 1	2	3	4	5	6	7
				Mean score per factor			
Icy	1.00	0.82	0.73	0.91	0.55	0.82	0.82
Non-icy	0.36	0.43	0.21	0.50	0.29	0.50	0.43
				Value mean			
Icy	0.6	1.2	−0.5	5.5	0.8	3.6	22
Non-icy	3.3	2.1	−2.1	5.6	0.5	4.5	37
	***	*	*				
				Value standard-deviation			
Icy	0.6	0.6	1.5	1.4	0.9	1.7	19
Non-icy	2.5	1.7	3.0	4.3	0.9	2.9	35
	***	***	**	***		*	*

For each factor, defined in section 6.1.1, the meaning of 'value' is as follows:
1. Mean number of oktas of low + medium cloud, 18–06 h
2. Mean dew-point depression (°C), 18–06 h
3. Mean dew-point (°C), 18–06 h
4. Mean 10 m wind speed (kn), 18–06 h
5. Number of criteria satisfied on previous night, the criteria being (i) air minumum ≦ 0 °C and (ii) ≦ oktas low + medium cloud
6. RDT at the midday just before the night in question.
7. Number of days from winter solstice.

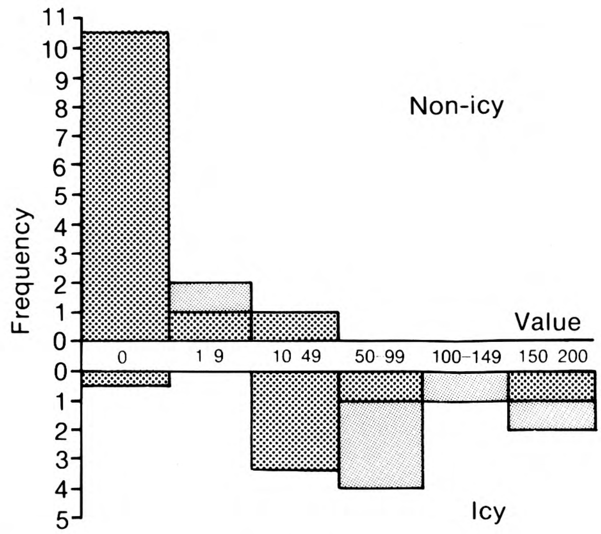

Figure 7. Histogram showing scores obtained using method 2. Shading as in Fig. 6.

necessitate a model run. For some cases two scores were evaluated, using data from two sites. In constructing Fig. 7 each such score had a frequency of one half.

Considering non-icy cases, the three scores which fell into the 1 to 9 category were almost negligible, being just 1, 1 and 3. The single score in the next category was 28. Although four out of six 'state of slab' reports for that occasion did indicate 'dry' it is possible that ice was present. Of all sensor sites in the Berkshire area only one reported subzero RSTs, and that was only for 2 hours. The probability of anyone having observed ice there and then must be small.

So it seems there is a fairly sharp division between icy and non-icy cases, around a score of about 10 ($\approx$ 0.001 mm). The fact that this division is close to zero means that the most difficult nights to forecast will generally be those where RST and dew-point are expected to be similar. On such nights the impact of a small dew-point underestimate has to be considered. This impact depends on wind speed. The stronger the wind the greater the impact, and the greater the potential for a forecast of dry roads to go badly wrong.

In compiling data for Fig. 7 another useful result emerged. When separate calculations were performed for two close sites, whose altitude differed by 300 ft, the scores for the higher site were, in general, significantly greater. This was because the site at greater altitude had similar RSTs, but somewhat higher dew-point and air temperatures. In turn this was probably due to it being more exposed. Exposed locations tend to experience higher night-time air temperatures in clear-sky/light-wind situations, due to cold air drainage away from them (for examples see Harrison (1971), Thornes (1989) and Gustavsson (1990)). They also experience lower daytime air temperatures, reducing the daytime heat input to the road, which helps to keep RST similar, at night, to a lower, less exposed site. It seems reasonable to infer that because of the higher scores obtained the higher site is generally more prone to rapid hoar-frost deposition. This result is similar to that highlighted in case study 4.

6.3 Economic implications

Thirteen non-icy cases from the 1990/91 winter were discussed in section 6.2. Berkshire County Council salted roads on eight of these. Each of the eight occasions were carefully analysed to see whether application of the two forecasting methods discussed above, backed up by an appreciation of the physics in section 3, could have changed the forecaster's advice in such a way that salting would not have proceeded. Whilst it is difficult to simulate both the conditions under which the forecaster had to prepare their forecasts, and the data available to them at the time, it does seem that two or three of the eight saltings could very reasonably have been avoided; on 17 December, 4 February and perhaps 22 January. These occasions scored, respectively, 3, 3 and 2 with method 1, and three zeros with method 2. Avoiding such saltings represents a saving for one county of about £25 000 on maintenance alone*. Were similar figures realized in all parts of the United Kingdom the savings, per winter, would be of the order of £3M†.

7. The urban effect

It is well known that air temperatures in cities average higher than in rural areas at the same altitude. The difference is particularly marked overnight. Oke and Hannel (1970) state that in Reading, Berkshire, the 10 m wind speed required to overcome this heat island effect is about 10 kn. Evidence is presented below to show that similar arguments do not always apply to road temperatures.

Figs 8(a) and 8(b) show sensor measurements from two road sites in Berkshire for 29–30 November 1989. The Reading sensor is on the very busy A329 about 1 mile west of the city centre, whilst the Shurlock Row sensor is on the fast westbound lane of the M4, 9 miles to the east.

Four of the five mornings prior to the 29th had produced sharp frosts. The 28th had been mostly cloudy, but the cloud cleared overnight, giving a slight frost on the morning of the 29th. Skies remained clear through the period shown. RDTs were about 5 °C at both sites on the 29th.

Fig. 8(a) shows the heat-island effect to be present for most of the period, consistent with observed wind speeds averaging about 3 kn. In spite of this RSTs at Reading are *lower* than at Shurlock Row for most of the time, the difference being particularly marked during daylight (Fig. 8(b)). The explanation lies in the exposure

* Source: Berkshire County Council. Total winter maintenance costs for Berkshire are about £900,000 for an average winter.
† Derived using data given in the footnotes on page 1 and above.

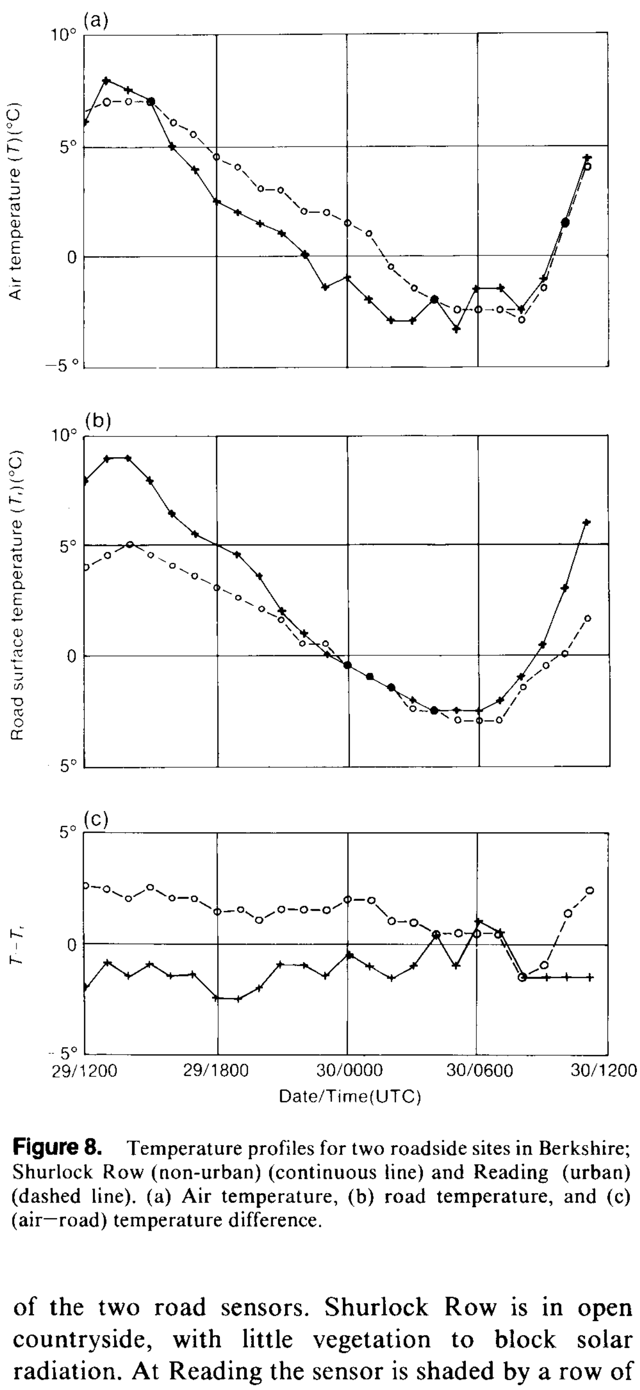

Figure 8. Temperature profiles for two roadside sites in Berkshire; Shurlock Row (non-urban) (continuous line) and Reading (urban) (dashed line). (a) Air temperature, (b) road temperature, and (c) (air—road) temperature difference.

of the two road sensors. Shurlock Row is in open countryside, with little vegetation to block solar radiation. At Reading the sensor is shaded by a row of two-storey buildings to the south, and so receives little or no direct sunshine during winter. It is ironic that buildings which are generally responsible for higher air temperatures in towns can at the same time cause, locally, lower RSTs. The implications of this are well illustrated in Fig. 8(c). Reference to equation (2) indicates that given suitable dew-points hoar-frost/dew could continue accumulating at Reading for almost all the period, but at Shurlock Row for a maximum of only 3 hours.

At 3 p.m. on the 30th side roads in a village about 20 miles south-east of Reading were observed still to be white with hoar-frost. So RSTs there had been subzero all day. Therefore the difference in RST maxima between this site and Shurlock Row must have been at least 9 °C (assuming the RST minimum at Shurlock Row was similar to the previous day). This may have been due, in part, to lower air temperatures. However, it is reasonable to expect the RSTs of such suburban roads to at least be comparable with those of the Reading road, because of similar shading by buildings, and in fact ultimately lower because of a much smaller traffic volume.

Bogren (1991) deduced that in clear weather the difference (°C) between daytime maximum RSTs at an open site ($T_{rmax(open)}$) and a site shaded from direct sunlight from sunrise ($T_{rmax(shaded)}$), is given by the equation

$$T_{rmax(open)} - T_{rmax(shaded)} = 0.47\,B_{max} - 1.5 \quad (3)$$

where B_{max} is the maximum solar elevation in degrees (the correlation coefficient of the regression was 0.94). For Reading on 29 November B_{max} is about 16°, giving a difference of +6 °C. This can be compared with +9 °C, referred to above. The slight discrepancy may have arisen as a result of the weather of previous days. Bogren shows, in addition, how RST differences also depend on 'recent' weather; during prolonged periods of clear skies there is a gradual increase, whereas the arrival of cloud causes a marked decrease.

Thus in prolonged spells of clear weather with very light winds it is probable that suburban roads are most susceptible to hoar-frost, urban roads are slightly less susceptible, and roads in flat, open countryside are least susceptible of all. A logical extension of the above arguments suggests that road stretches shaded by other objects, such as dense woodland or north facing hillsides, are probably as susceptible to hoar-frost as the suburban roads.

The magnitude of incident solar radiation (per unit area) depends strongly on solar elevation. Therefore to realize large RST differences, and hence local variations in hoar-frost deposition, it is most important that the road be shaded around the solar noon. Shading just after sunrise or just before sunset is relatively unimportant.

It is only when a period of clear weather with light winds is *prolonged* that tangible differences in road conditions between sites are likely to arise. Because of the light winds more than one night is probably needed for hoar-frost and dew to build up to dangerous levels. And similarly the RST differences increase in magnitude gradually, over a period of days.

At present the Meteorological Office RST model is unable to cope with the shading effect of obstacles — it assumes roads to be on a flat horizontal plane. This is appropriate for the Shurlock Row site, but not the Reading one. Thus under certain atmospheric conditions and at certain shaded sites the model will overestimate RSTs and underestimate hoar-frost deposition. Fig. 8 and equation (3) indicate that the discrepancies can be highly significant, a fact that the forecaster must take account of*. One quick (albeit imperfect) way to tackle this problem would be by generating a second RST profile appropriate to the shaded sites, by rerunning the model using a lower midday RST, this RST having been calculated using equation (3). As the model still includes solar insolation in the afternoon the profile may well not be cold enough. Nevertheless it could still provide useful guidance.

It is encouraging that a more recent RST model, the 'Icebreak' model, includes a 'sky view factor' (Thornes and Shao 1991a). This should reduce errors due to shading.

Not all shaded sites will have characteristics like those outlined above, because obstacles do also provide a negative feedback — both by reflecting back some of the road's outgoing long-wave radiation, and emitting towards the road surface some of their own. The example discussed was specifically selected to be one where this feedback was not apparent. The '−1.5' in equation (3) very probably reflects this negative feedback; in polar night conditions the shaded sites would probably be warmer.

In case 2 in section 5 the RST model appeared to underestimate the depth of hoar-frost. Bearing in mind that the model was being used for suburban roads, and that there had just been 60 hours of clear, cold weather, it is probable that many of the factors discussed in this section contributed to that underestimate. They may have also caused errors in the other cases.

8. Conclusions

A number of occasions when roads in south-east England became icy in the absence of precipitation have been carefully examined. By combining these case studies with physical reasoning, and testing out ideas on data from the 1990/91 winter, it was shown that the meteorological phenomena most conducive to rapid hoar-frost deposition are these: clear skies, a shallow layer of moist air in contact with the surface, high water vapour content in that layer, a gentle breeze (approximately 4 to 7 kn) and recent cold, clear weather. Short day-length is an important astronomical factor. RSTs must of course fall to 0 °C or below. Wind direction is also significant, because of a non-uniform distribution of moisture sources (seas) and sinks (land, especially at altitude) around south-east England.

Seas provide most moisture when sea surface temperatures are highest, i.e. early in the winter rather than later. This, together with the required low solar elevation, make December the most likely month for hoar-frost deposition to occur.

Evidence and physical argument suggest that the time of onset of any hoar-frost deposition will be earlier if the previous night was cold and clear.

* At the time of writing another problem the forecaster must take account of is that when the RST model is run it always begins with a dry road surface. Quite clearly the correct depth of ice/water will not be represented on the model output if it took more than one day for that depth to build up.

The rate of hoar-frost deposition was shown to be roughly proportional to both wind speed and depression of RST below dew-point.

Large local variations in hoar-frost deposition have been noted. The nature of these variations appears to depend on the current weather type. This is probably because the current weather type dictates which physical and meteorological factors are most important (as Gustavsson and Bogren (1990) found).

In spells of cold, clear, settled weather with very light winds the shading of a road surface appeared especially important. Hoar-frost deposition is favoured where the position and extent of this shading are such that there is both an obstruction of incoming short-wave (solar) radiation and a maintenance of relatively large net outgoing long-wave radiation. In theory these criteria are best satisfied by roads in open countryside on north facing hills. However, an example showed how roads bordered by buildings were susceptible too — particularly in suburban areas but notably also in a city centre.

In more mobile weather types, where there is only one night in which dangerous levels of hoar-frost can arise, the emphasis shifts towards other factors — notably wind speed. This puts exposed locations at greatest risk. In one example where the measured RST minima of two roads were −1 °C and −3 °C, it was shown that the warmer of the two probably became most icy, due to it being the most exposed. The 'best' situation for rapid hoar-frost deposition in south-east England appears to be in a developing southerly after the passage of a cold ridge.

During clear weather the UK Meteorological Office RST model tends to give poor guidance for areas where obstacles block out the sun, i.e. RSTs are too high and the road surface can be misleadingly dry. This is because sites are assumed to be on a flat plane. The model should perform much better in open countryside.

In the more mobile weather types the model seems to give reasonable predictions of hoar-frost accumulation, provided it is fed with accurate meteorological data. However, the forecaster must remember that it is site specific and that, on occasions, large differences can arise between exposed and sheltered sites.

There is some evidence to suggest that the minimum depth of hoar-frost likely to cause problems to the motorist is of the order of thousandths of a millimetre. Moore (1975) highlights many difficulties associated with ice-friction experiments, suggesting that a more accurate value may prove elusive.

Two hoar-frost forecasting tools have been proposed. One is valid worldwide; the other will work best in areas whose climate is similar to that of south-east England. They relate specifically to one-night events, but may also be used in settled weather provided an allowance is made for day-to-day accumulation of moisture. As well as supplementing guidance from the RST model these techniques can give insight into the physical processes at work, and also some idea of the appropriate confidence level to attach to a forecast. Hindcasts for the 1990/91 winter suggested that application of the techniques by forecasters might yield an annual saving on UK winter maintenance bills of the order of £3M.

Many questions raised in this paper warrant further research. One of the most important is the following. In what way does traffic modify wind speed close to a road surface, what are the simultaneous changes in RST, and how do moisture fluxes alter as a result?

Acknowledgements

The authors would like to thank Dr R.W. Riddaway for his constructive comments on earlier drafts of this paper.

References

Ayton, P., 1988: Perceptions of broadcast weather forecasts. *Weather*, **43**, 193–197.

Bogren, J., 1991: Screening effects on road surface temperature and road slipperiness. *Theor Appl Climatol*, **43**, 91–99.

Bogren, J. and Gustavsson, T., 1989: Modelling of local climate for prediction of road slipperiness. *Phys Geogr*, **10**, 147–164.

—, 1991: Nocturnal air and road surface temperature variations in complex terrain. *Int J Climatol*, **11**, 443–455.

Boselly III, S.E., Jonas, D.L. and Thornes, J.E., 1990: The strategic highway research program, addressing road weather information and applications in the U.S. *In* Int Conf Interact Inform Process Syst Met Oceanogr (6th, 1990, Anaheim, California).

Davey, B.A., 1982: Unusual road surface condensation. *Meteorol Mag*, **111**, 19–22.

Farmer, S.F.G. and Tonkinson, P.J., 1989: Road surface temperature model verification using input data from airfields, roadside sites and the mesoscale model. Bracknell, Meteorological Office, Special Investigations Technical Note No. 58. (Unpublished, copy available from National Meteorological Library, Bracknell.)

Gustavsson, T., 1990: Variation in road surface temperature due to topography and wind. *Theor Appl Climatol*, **41**, 227–236.

Gustavsson, T. and Bogren, J., 1990: Road slipperiness during warm-air advections. *Meteorol Mag*, **119**, 267–270.

Harrison, A.A., 1971: A discussion of the temperatures of inland Kent with particular reference to night minima in the lowlands. *Meteorol Mag*, **100**, 97–111.

Mansell, R., 1989: Icy roads (a sideways look at), *Weather*, **44**, 499–500.

Meteorological Office, 1981: Handbook of meteorological instruments, 2nd edition, Vol. 3, chapter 3. London, HMSO.

Milloy, M.H. and Humphreys, J.S., 1969: The influence of topography on the duration of ice-forming conditions on a road surface. Crowthorne, Transport and Road Research Laboratory, Report No. LR274.

Monteith, J.L., 1957: Dew. *Q J R Meteorol Soc*, **83**, 322–341.

Moore, D.F., 1975: The friction of pneumatic tyres. Amsterdam, Elsevier.

Oke, T.R. and Hannell, F.G., 1970: The form of the heat island in Hamilton, Canada. Geneva, WMO, Technical Note 108, 113–126.

Painter, H.E., 1973: The performance of wet-bulb thermometers in the large thermometer screen. *Meteorol Mag*, **102**, 212–215.

Parrey, G.E., 1969: Minimum road temperatures. *Meteorol Mag*, **98**, 286–290.

Rayer, P.J., 1987: The Meteorological Office forecast road surface temperature model. *Meteorol Mag*, **116**, 180–191.

Ritchie, W.G., 1976: A note on the readings of two differently exposed thermometers when water freezes on concrete. *Meteorol Mag*, **105**, 57–60.

Saunders, W.E., 1973: Radiation fog and stratus formation and fog clearance in terms of geostrophic wind — some applications of wind measurements on a high mast. *Meteorol Mag*, **102**, 140–146.

Soveri, J., 1990: Road salt is a danger to the groundwater. *Vaisala News*, **122**, 22.

Takle, E.S., 1990: Bridge and roadway frost: occurrence and prediction by use of an expert system. *J Appl Meteorol*, **29**, 727–734.

Thornes, J.E., 1972: An objective aid for estimating the night minimum temperature of a concrete road surface. *Meteorol Mag*, **101**, 13–24.

—, 1989: A preliminary performance and benefit analysis of the UK national ice-prediction system. *Meteorol Mag*, **118**, 93–99.

Thornes, J.E. and Shao, J., 1991a: A comparison of UK road ice prediction models. *Meteorol Mag*, **120**, 51–57.

—, 1991b: Spectral analysis and sensitivity tests for a numerical road surface temperature prediction model. *Meteorol Mag*, **120**, 117–124.

Analyses and forecasts of fluctuations in the angular momentum of the atmosphere and changes in the Earth's rotation

R. Hide
The Robert Hooke Institute (Meteorological Office Unit), The Observatory, Clarendon Laboratory, Parks Road, Oxford OX1 3PU, England
J.O. Dickey
Jet Propulsion Laboratory, California Institute of Technology, Pasadena, California 91109, USA

Summary

Fluctuations in all three components of the total atmospheric angular momentum (AAM) are evident from global meteorological data sets. The fluctuations are generated by dynamical interactions between the atmosphere and the underlying continental and oceanic regions of the surface of the planet, and they are intimately linked with baroclinic and barotropic energy conversion processes throughout the whole atmosphere. The correct representation of AAM fluctuations would constitute a most stringent test of the performance of a global numerical prediction model and the data sets used in its initialization. Research in this area exploits the facts that (a) the AAM fluctuations are accompanied by tiny but measurable irregular fluctuations in both the magnitude and direction of the Earth's rotation vector (so as to conserve angular momentum of the whole system), and (b), thanks to the introduction of a variety of new techniques, geodesists have achieved impressive refinements in their monitoring of Earth rotation fluctuations.

1. Atmospheric angular momentum fluctuations

The atmosphere super-rotates relative to the underlying planet at about 10 m s^{-1} on average. If transferred to the underlying planet, the angular momentum associated with this super-rotation would reduce the length of the day (LOD) by about 4 milliseconds (ms). Geodetic observations going back several decades reveal more or less irregular LOD fluctuations of up to about 1 ms on sub-seasonal, seasonal and interannual time-scales (Fig. 1), and detailed studies using modern meteorological and geodetic data have established that these fluctuations are largely of meteorological origin (Figs 2 and 3). Fluctuations in the equatorial components of atmospheric angular momentum (AAM) make a substantial contribution to the observed wobble of the rotation axis of the solid Earth with respect to geographical coordinates (Fig. 4).

2. Surface torques

The torques at the surface of the Earth (Fig. 5) that are implied by meteorologically induced fluctuations in the Earth's rotation are produced by (a) tangential stresses in turbulent boundary layers, and (b) normal (pressure) stresses acting on irregular topography and other departures from the spherical shape of the Earth (including the equatorial bulge). These stresses are transmitted directly to the solid Earth over continental regions and indirectly over the oceans. The investigation of the extent to which the stresses are represented satisfactorily in general circulation models of the atmosphere (and oceans) should be given high priority in any diagnostic schemes for assessing how well the models perform. Quite elementary reasoning shows that large errors in the treatment of energetic processes can be expected from models that fail to represent atmospheric angular momentum fluctuations satisfactorily.

3. Routine AAM determinations

Thanks to the First GARP Global Experiment (FGGE) of the Global Atmospheric Research Programme (GARP), in 1979 it was possible for the first time to obtain useful daily determinations of the total angular momentum of the atmosphere for comparison with geodetic data on the Earth's rotation. Manifold subsequent developments following this work done at the United Kingdom Meteorological Office (UKMO) include arrangements for producing and disseminating routine daily or twice-daily determinations of all three components of AAM. These are now made from analysis (and in some cases also from forecast) fields by several meteorological centres, namely the European Centre for Medium-range Weather Forecasts (ECMWF), the Japanese Meteorological Agency (JMA), UKMO and the United States National Meteorological Center

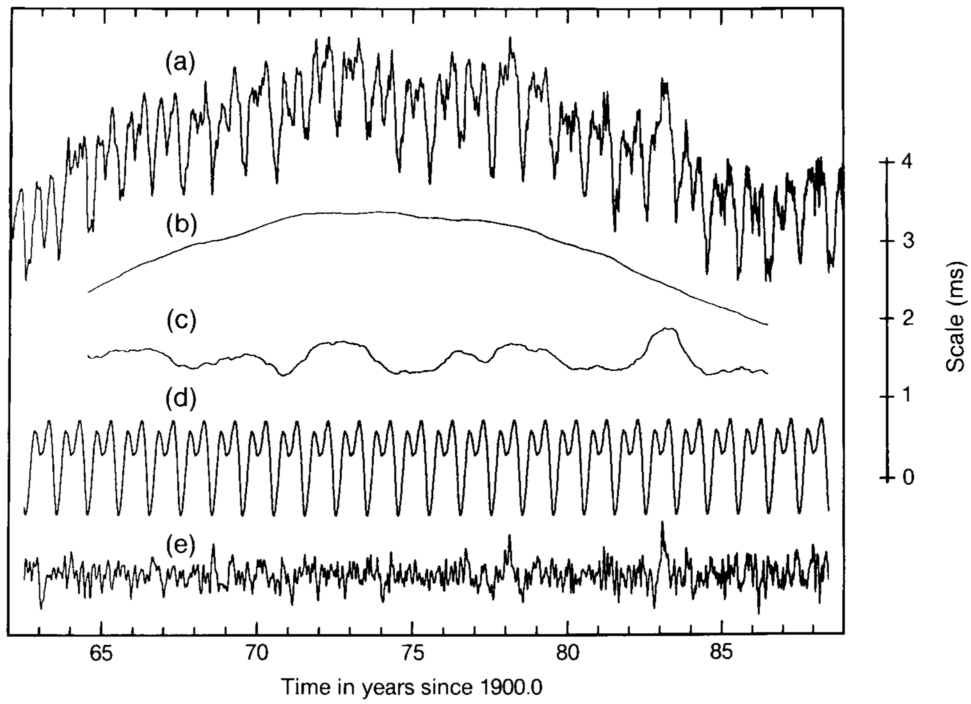

Figure 1. Irregular length of day fluctuations; (a) total, and on (b) decadal, (c) interannual, (d) seasonal and (e) intraseasonal time-scales (see Fig. 2 of Hide and Dickey (1991)).

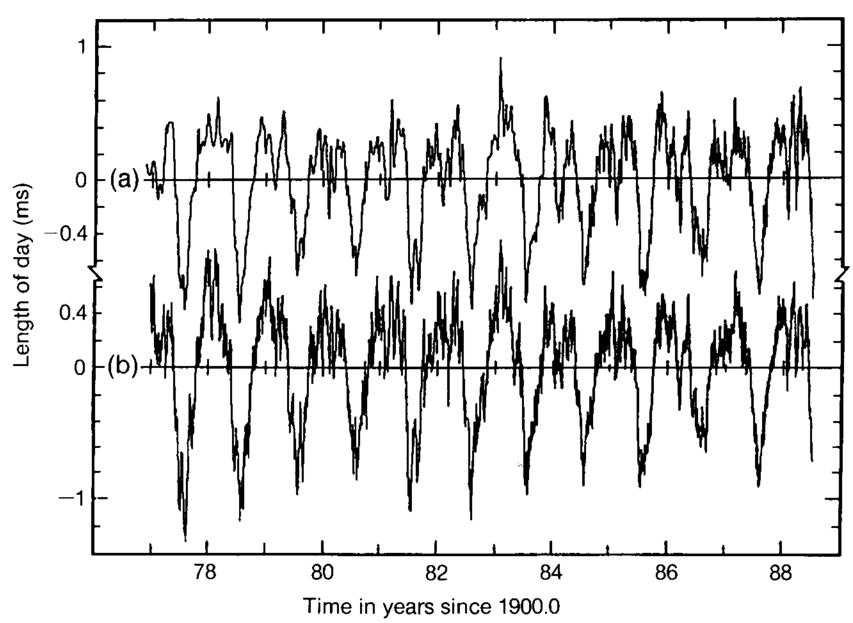

Figure 2. Irregular length of day fluctuations (a) measured by space geodetic techniques and (b) inferred from atmospheric angular momentum (see Fig. 7 of Hide and Dickey (1991)).

(USNMC). Plans have recently been initiated for producing routine determinations of torques from surface stresses, to supplement the AAM data and facilitate diagnostic studies bearing on their interpretation.

4. Earth rotation fluctuations; predictions of 'Universal Time'

Earth rotation determinations have greatly improved with the intensification of routine observations using Very Long Baseline Interferometry (VLBI) (see Fig. 4), Satellite Laser Ranging (SLR), and Lunar Laser Ranging (LLR). The International Earth Rotation Service (IERS) (based in Paris) of the International Astronomical Union (IAU) and International Union of Geodesy and Geophysics (IUGG) coordinates VLBI, SLR and LLR observations. The subcommission International Radio Interferometric Surveying (IRIS) of the International Association of Geodesy (IAG) of the IUGG and the joint commission on International Coordination of Space Techniques for Geodesy and Geophysics (CSTG) of the Committee on Space

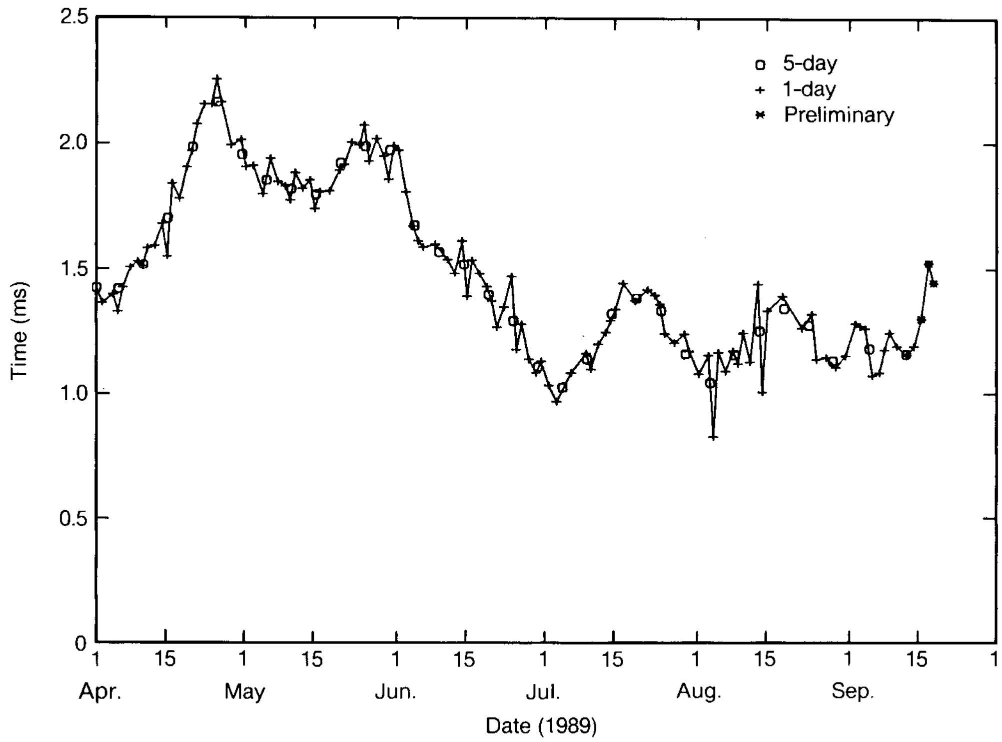

Figure 3. Excess length of day over a 6-month period as determined by very long baseline interferometry (from an IRIS Earth Orientation Bulletin (see section 4)).

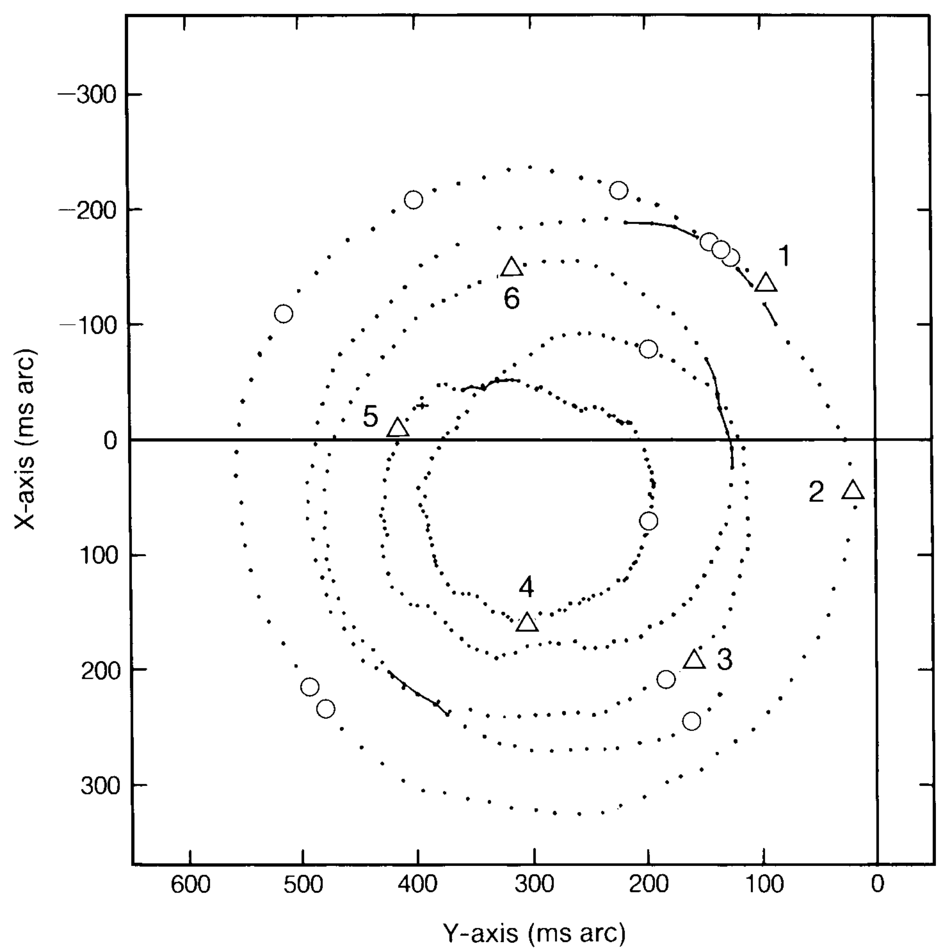

Figure 4. Variations in pole position at 5-day intervals from January 1984 to September 1989 with markers at (1) 3 January 1984, (2) 4 January 1985), (3) 4 January 1986, (4) 4 January 1987, (5) 4 January 1988 and (6) 3 January 1989 as determined by very long baseline interferometry (from an IRIS Earth Orientation Bulletin (see section 4)).

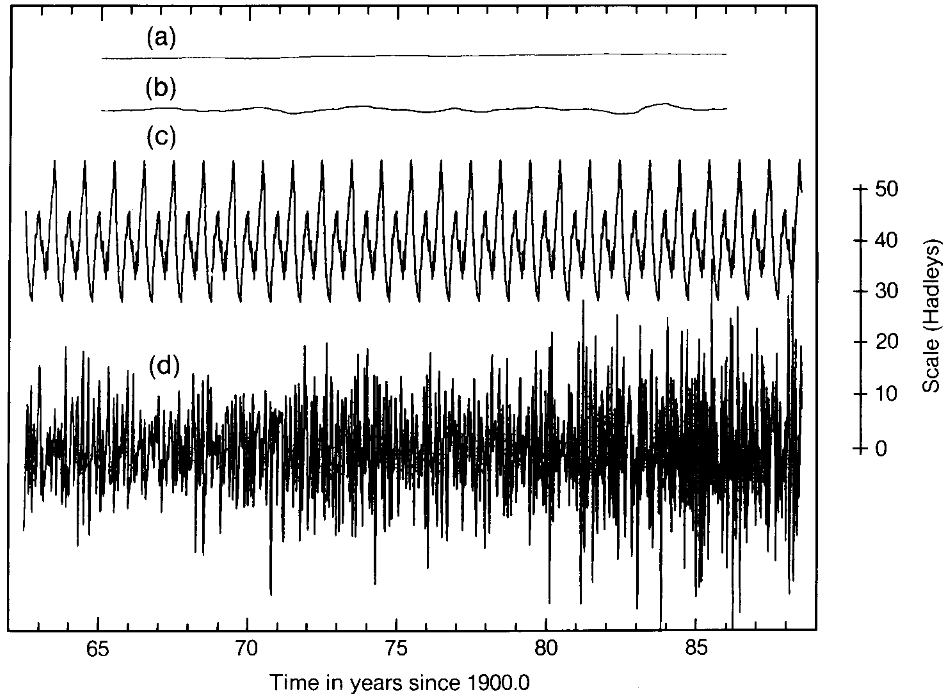

Figure 5. Fluctuations about zero of components of equivalent axial torque on (a) decadal, (b) interannual, (c) seasonal and (d) intraseasonal time-scales (see Fig. 4 of Hide and Dickey (1991)).

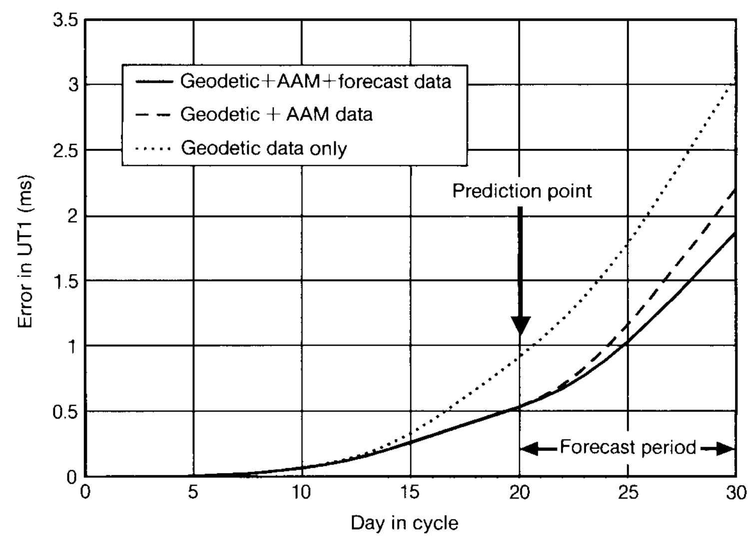

Figure 6. Root-mean-square errors in Universal Time (UT1) for three forecast series using 45 cycles of 30 days each from 1987.0 to 1990.7. These results indicate how forecasts of Universal Time can be improved by including atmospheric angular momentum analyses and forecasts from global numerical prediction models.

Research (COSPAR) publishes a monthly Earth Orientation Bulletin giving recent determinations of the length of the day and pole positions based largely on VLBI observations (see Figs 3 and 4). Liaison between the IERS and the various meteorological centres (ECMWF, JMA, UKMO, USNMC) producing routine AAM determinations is effected by the IERS Sub-Bureau for AAM based at the USNMC in Washington DC. It is noteworthy that AAM analyses and forecasts produced by meteorologists are now being used routinely to improve predictions of the Earth's rotation angle, that is 'Universal Time' (Fig. 6), which have various applications in astronomy and geodesy including the improvement of navigation schemes for current spacecraft missions, such as *Magellan* to the planet Venus and *Galileo* to the planet Jupiter.

5. Concluding remarks

In addition to its direct influence on research in meteorology and oceanography, recent work on AAM fluctuations is enabling geophysicists to refine their determinations of Earth rotation fluctuations produced by non-meteorological agencies, such as motions in the Earth's liquid core where the main geomagnetic field originates. Core motions evidently contribute little on sub-seasonal, seasonal and decadal time scales, but their effects are dominant on decadal time-scales, where irregular LOD changes of up to 5 ms are found. 'Spin-orbit' coupling in the Earth–Moon system increases the LOD steadily at about 1.4 ms per century and (to conserve total angular momentum) expands the mean radius of the Moon's orbit at about 4 cm per year. This coupling arises largely through tidal friction in the oceans, which produces a lag in the orientation of the tidal bulge relative to the line joining the centres of mass of the Earth and Moon, thereby enabling gravitational forces to exert a net torque. In the detailed interpretation of trends in the LOD observational record over the past century or so, allowance has to be made for contributions produced by a variety of processes, such as the moment of inertia changes associated with the melting of ice and any long-term variations that might have occurred in the distribution and strength of zonal winds, including any that might have been produced by increasing CO_2 content of the atmosphere.

The discussion of key dynamical processes in virtually all branches of the geophysical science is central to the task of interpreting fluctuations in the Earth's rotation, and herein lies the fascination of the subject. Meteorology is both contributing to and gaining from the findings of research in this area.

Bibliography

Extensive lists of references to the literature can be found in two recent articles 'Atmospheric angular momentum forecasts and analyses as novel tests of global numerical weather prediction models (M.J. Bell, R. Hide and G. Sakellarides, *Philos Trans R Soc London*, **A334**, 55–92, 1991) and 'Earth's variable rotation' (R. Hide and J.O. Dickey, *Science*, **253**, 629–637, 1991.

Contributions for 'Picture of the Month'

Topical satellite and/or radar pictures have been a regular back-page feature in the *Meteorological Magazine* for over 5 years. During this time, most articles have been prepared by Mike Bader's image-interpretation group. Now, however, an imminent reorganization of work within S-Division means that 'Picture of the Month' will no longer be coordinated by this group.

To remain a regular feature, articles are required from other contributors. It needn't take long to write — one page would suffice (including large picture!) and authors do receive a free copy of the magazine!

If anyone using images operationally or in research has any good examples and would like to contribute, please contact:

Meteorological Office,
Publications, Room 709,
London Road,
Bracknell,
Berkshire RG12 2SZ
Tel. 0344 856094

for further details.

Satellite and radar images — 12 November 1991

During the morning of 12 November 1991, a depresssion formed on a cold front stretching south from a primary low located to the north-west of Scotland; the secondary depression deepened during the day and moved north-east into central Scotland. The Meteosat water vapour image in Fig. 1 shows the system at 1500 UTC, during its rapidly deepening phase; a dry slot S–S–S separated the edge of the high cloud on the cold front from the cold and showery air mass behind. Comparing the image with the corresponding surface analysis (Fig. 2) reveals that the northern tip of the dry slot almost coincided with the centre of the depression; the most rapid falls in pressure were just ahead of this point. The surface front was just forward of the driest air, but the image also shows a band of much moister air ahead marking an upper frontal zone (labelled U–U).

As the frontal system moved across Wales into England during the afternoon it became very vigorous. The network composite radar image for 1500 UTC (Fig. 3) shows a wide band of rain associated with the upper front, and a squall line, with heavy thundery rain, on the surface front (labelled F–F).

The system moved eastwards at about 40 kn, and shortly before 1900 UTC a section of the squall line,

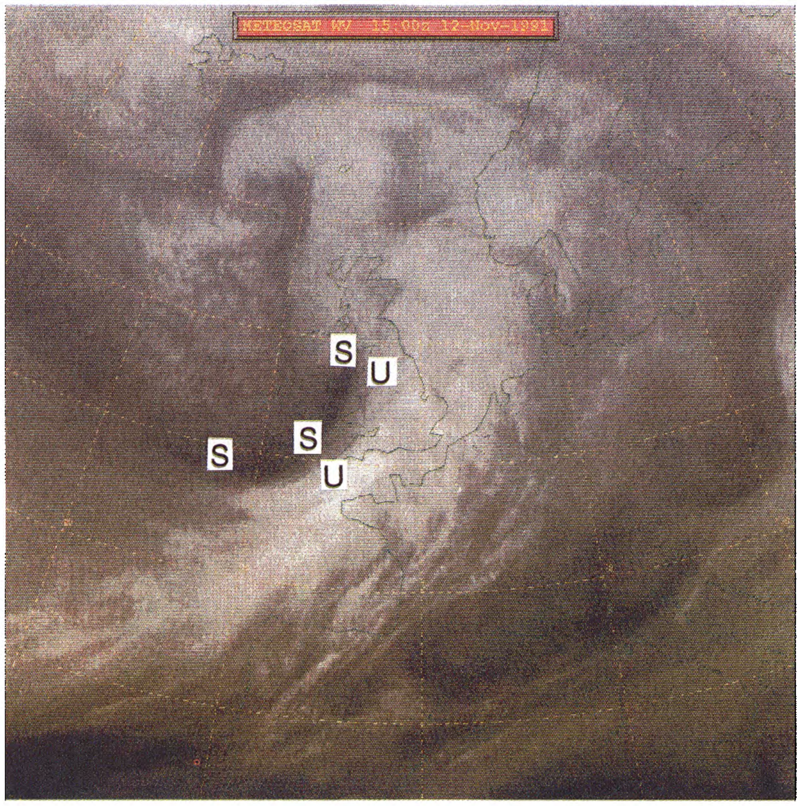

Figure 1. Meteosat water vapour image for 1500 UTC on 12 November 1991. S–S–S is the dry slot, U–U is the upper front. Black indicates dry air, and lighter shades of grey indicate increasing mid-level moisture.

approximately between The Wash and the Isle of Wight, intensified to give cells of very heavy rain and high winds. By 1930 UTC it was lying across East Anglia, and the radar image (Fig. 4) showed rainfall rates of over 32 mm h^{-1} in many places.

Just after 1930 UTC a tornado, which had formed on the squall line, approached the village of Dullingham in Cambridgeshire (D on Fig. 4). It moved north-east through the village, leaving a narrow trail of damage nearly a kilometre long; one house had its roof lifted off, two others lost substantial parts of their roofs, and a 200-year-old malt barn was demolished. Numerous trees were brought down, while others lost bark and branches, large branches being carried up to 200 m by the wind. The extent of the damage indicates that the tornado would be classed as T4 or T5 (strong or intense) on the international tornado intensity scale. According to this scale, the wind speed in the tornado must have been in the range 100–140 kn; the highest gusts measured on the squall line at official observing stations in East Anglia were 52 kn. Fig. 5 is a photograph taken the following day showing some of the tornado damage.

The squall line continued to move east through the evening, bringing torrential rain and high winds to most of East Anglia, but no further tornadoes were reported. By 2100 UTC it had reached the North Sea, where it eventually dissipated as the system drifted north-east overnight.

R.B.E. Lilley

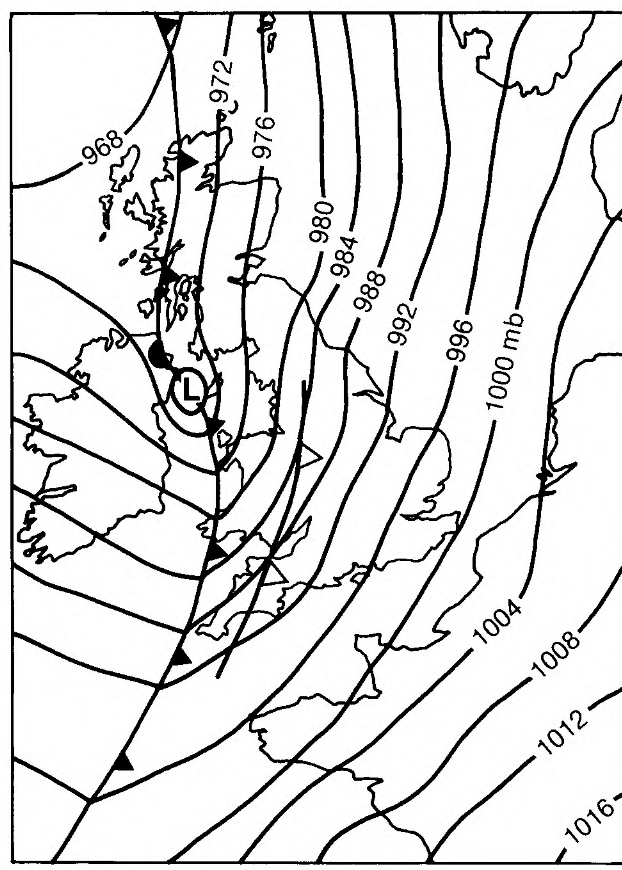

Figure 2. Surface analysis for 1500 UTC on 12 November 1991. Closed symbols indicate surface fronts, open triangles the upper frontal zone.

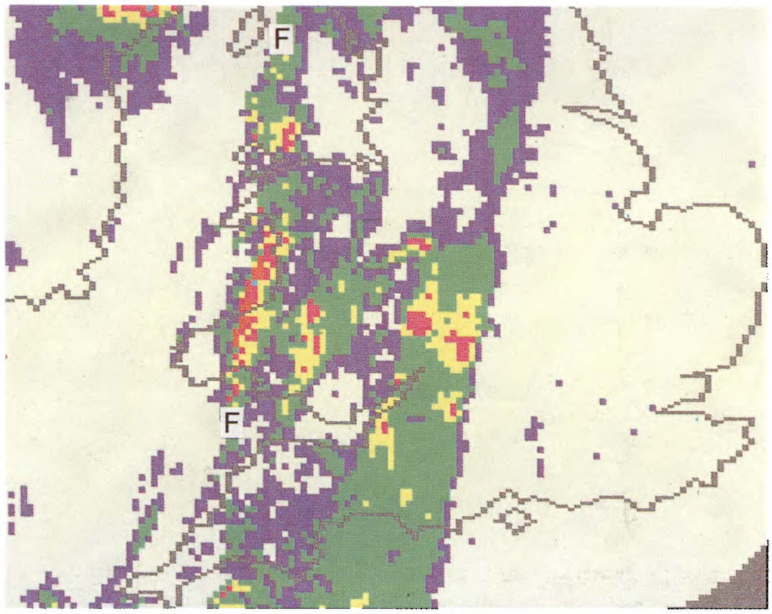

Figure 3. Network composite radar image for 1500 UTC on 12 November 1991. Rainfall rates (mm h^{-1}) shown are: purple 0.1–1, green 1–4, yellow 4–8, pink 8–16, red 16–32, and blue 32–64. F–F is the squall line on the surface cold front.

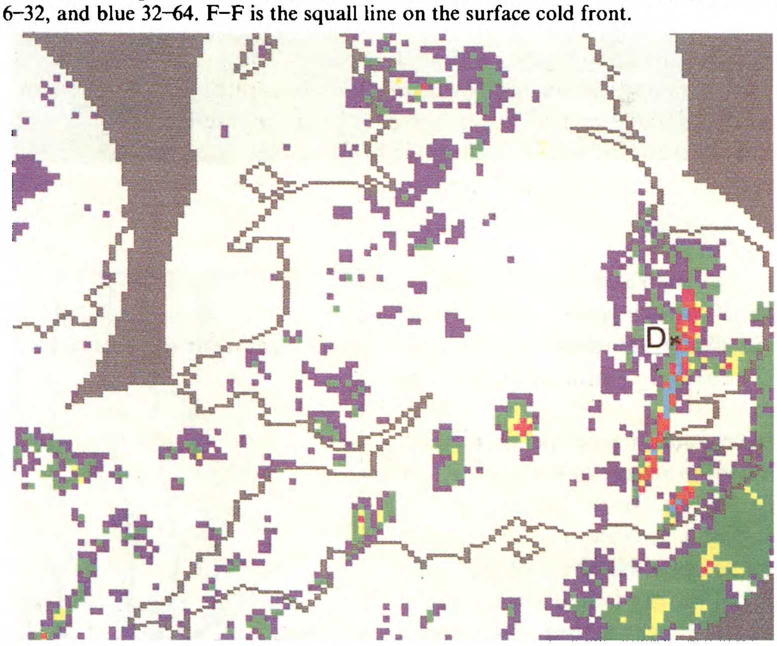

Figure 4. Network composite radar image for 1930 UTC on 12 November 1991. Rainfall rates as Fig. 3. D is the location of Dullingham.

Figure 5. Photograph showing some of the tornado damage, taken on 13 November 1991. (*Courtesy of W.S. Pike*)

GUIDE TO AUTHORS

Content

Articles on all aspects of meteorology are welcomed, particularly those which describe results of research in applied meteorology or the development of practical forecasting techniques.

Preparation and submission of articles

Articles, which must be in English, should be typed, double-spaced with wide margins, on one side only of A4-size paper. Tables, references and figure captions should be typed separately. Spelling should conform to the preferred spelling in the *Concise Oxford Dictionary* (latest edition). Articles prepared on floppy disk (IBM-compatible) can be labour-saving, but only a print-out should be submitted in the first instance.

References should be made using the Harvard system (author/date) and full details should be given at the end of the text. If a document is unpublished, details must be given of the library where it may be seen. Documents which are not available to enquirers must not be referred to, except by 'personal communication'.

Tables should be numbered consecutively using roman numerals and provided with headings.

Mathematical notation should be written with extreme care. Particular care should be taken to differentiate between Greek letters and Roman letters for which they could be mistaken. Double subscripts and superscripts should be avoided, as they are difficult to typeset and read. Notation should be kept as simple as possible. Guidance is given in BS 1991: Part 1: 1976, and *Quantities, Units and Symbols* published by the Royal Society. SI units, or units approved by the World Meteorological Organization, should be used.

Articles for publication and all other communications for the Editor should be addressed to: The Chief Executive, Meteorological Office, London Road, Bracknell, Berkshire RG12 2SZ and marked 'For Meteorological Magazine'.

Illustrations

Diagrams must be drawn clearly, preferably in ink, and should not contain any unnecessary or irrelevant details. Explanatory text should not appear on the diagram itself but in the caption. Captions should be typed on a separate sheet of paper and should, as far as possible, explain the meanings of the diagrams without the reader having to refer to the text. The sequential numbering should correspond with the sequential referrals in the text.

Sharp monochrome photographs on glossy paper are preferred; colour prints are acceptable but the use of colour is at the Editor's discretion.

Copyright

Authors should identify the holder of the copyright for their work when they first submit contributions.

Free copies

Three free copies of the magazine (one for a book review) are provided for authors of articles published in it. Separate offprints for each article are not provided.

Contributions: It is requested that all communications to the Editor and books for review be addressed to the Chief Executive, Meteorological Office, London Road, Bracknell, Berkshire RG12 2SZ, and marked 'For *Meteorological Magazine*'. Contributors are asked to comply with the guidelines given in the *Guide to authors* (above). The responsibility for facts and opinions expressed in the signed articles and letters published in *Meteorological Magazine* rests with their respective authors.

Subscriptions: Annual subscription £36.00 including postage; individual copies £3.25 including postage. Applications for postal subscriptions should be made to HMSO, PO Box 276, London SW8 5DT; subscription enquiries 071–873 8499.

Back numbers: Full-size reprints of Vols 1–75 (1866–1940) are available from Johnson Reprint Co. Ltd, 24–28 Oval Road, London NW1 7DX. Complete volumes of *Meteorological Magazine* commencing with volume 54 are available on microfilm from University Microfilms International, 18 Bedford Row, London WC1R 4EJ. Information on microfiche issues is available from Kraus Microfiche, Rte 100, Milwood, NY 10546, USA.

January 1992

Editor: R.M. Blackall
Vol. 121
No. 1434

Contents

ISSN 0026–1149

ISBN 0-11-728979-5

9 780117 289796

Printed in the United Kingdom for HMSO
Dd 291241 C13 1/92 12521

The Meteorological Magazine

February 1992

Retirement of Sir John Houghton
Models and images
Results from infrared and microwave experiments
Direction of gusts and lulls
Winter of 1990/91
Noctilucent clouds 1990

HMSO

Met.O.1004 Vol. 121 No. 1435

First published 1991

HMSO

HMSO publications are available from:

HMSO Publications Centre
(Mail and telephone only)
PO Box 276, London, SW8 5DT
Telephone orders 071-873 9090
General enquiries 071-873 0011
(queuing system in operation for both numbers)

HMSO Bookshops
49 High Holborn, London, WC1V 6HB   071-873 0011 (counter service only)
258 Broad Street, Birmingham, B1 2HE   021-643 3740
Southey House, 33 Wine Street, Bristol, BS1 2BQ   (0272) 264306
9–21 Princess Street, Manchester, M60 8AS   061-834 7201
80 Chichester Street, Belfast, BT1 4JY   (0232) 238451
71 Lothian Road, Edinburgh, EH3 9AZ   031-228 4181

HMSO's Accredited Agents
(see Yellow Pages)

and through good booksellers

The
Meteorological
Magazine

February 1992
Vol. 121 No. 1435

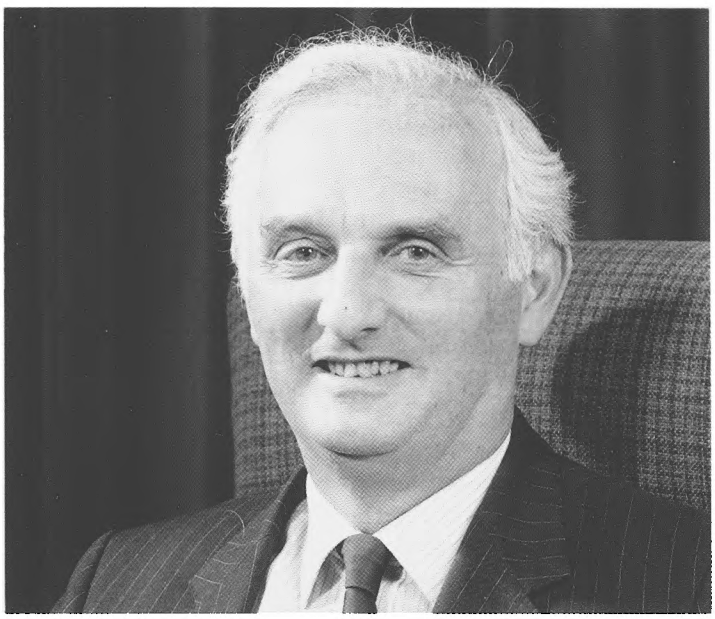

Retirement of Sir John Houghton

Sir John Houghton, CBE, FRS, took up his appointment as Director-General of the Meteorological Office on 1 October 1983, prior to which he was Deputy Director of the Rutherford Appleton Laboratory, SERC.

Born in 1931, Sir John was educated at Rhyl Grammar School and was a scholar at Jesus College, Oxford, where he took a double first in mathematics and physics. A Research Student in the Department of Meteorology, Clarendon Laboratory, from 1951–54, he took his D. Phil. in 1955. He was a Research Fellow at the Royal Aircraft Establishment, Farnborough, before returning to Oxford in 1958 as Lecturer in Atmospheric Physics. In 1962 he was appointed Reader and became Professor in 1976. Official Fellow and Tutor in Physics at Jesus from 1960–73, he became Professorial Fellow in 1973 and Honorary Fellow in 1983. He spent a term in 1969 as Visiting Professor at the University of California, Los Angeles. In 1979 Sir John was seconded from Oxford University to the Science and Engineering Research Council to be Director of the Appleton Laboratory during its move from Slough to Chilton to merge with the Rutherford Laboratory, adding to that laboratory a substantial expertise in space science and applications.

Elected Fellow of the Royal Society in 1972, Sir John is also Fellow of the Institute of Physics, Fellow of the Royal Meteorological Society (President 1976–78) and was awarded the Royal Meteorological Society's Darton Prize 1954, Buchan Prize 1966 and Symons Gold Medal 1991, the Charles Chree Medal of the Institute of Physics 1979, and the Glazebrook Medal 1990. He shared the Rank Prize for Opto-Electronics in 1988 with F.W. Taylor, C.D. Rogers and G.D. Peskett and in 1989 gave the Royal Society's Bakerian Prize Lecture. He is also a Fellow of the Optical Society of America and a Member of the American Meteorological Society and the American Geophysical Union. Between 1981 and early 1984 Sir John was Chairman of the Joint Scientific Committee for World Climate Research Programmes. Since 1983 he has been a member of the Executive Committee of the World Meteorological Organization (WMO) and from 1987 to 1991 was one of WMO's Vice-Presidents.

In 1988 Sir John was appointed as Chairman of the Scientific Assessment Working Group of the Intergovernmental Panel On Climate Change jointly set up by WMO and the UN Environment Programme. That Working Group produced a Report in September 1990 on the likely change in climate during the coming century due to the increasing release of greenhouse gases into the atmosphere. The Report has been very well received and as a result has had a substantial influence on the development of government policy in the United Kingdom and elsewhere concerning climate change.

In 1990 Sir John became the first Chief Executive of the Meteorological Office as it achieved Agency status within the Ministry of Defence. Under his guidance the year has been marked by commercial success and improvements in the range and quality of services.

Sir John has authored or co-authored several books — *Infra Red Physics* (with S.D. Smith) 1966, *The Physics of Atmospheres* 1977 (2nd edition 1986) and *Remote Sensing of Atmospheres* (with F.W. Taylor and C.D. Rogers) 1984 and *Does God Play Dice?* 1988.

Sir John is well known internationally for his outstanding research in remote sensing of the atmosphere from space. In co-operation with Professor Desmond Smith, he developed the Selective Chopper Radiometer for the Nimbus 4 and 5 satellites in the early 1970s — an instrument which sensed remotely the atmospheric temperature structure up to about 50 km altitude. Further developments by the group at Oxford led by Sir John, namely the Pressure Modulator Radiometer flown on Nimbus 6 in 1975 and the Stratospheric and Mesospheric Sounder flown on Nimbus 7 in 1978, enabled the temperature structure and the distribution of some minor constituents up to about 90 km altitude to be observed. These instruments provided, for the first time, global information of the structure of the stratosphere and mesosphere and have played a large part in enabling a detailed study of the radiation, dynamics and chemistry of the whole atmosphere to be pursued. Sir John also co-operated with Professor Fred Taylor, then at the Jet Propulsion Laboratory, in an instrument for the Pioneer Venus Orbiter in 1978. His interests in space activities continue — he is currently a member of the Board of the British National Space Centre.

In the Queen's Birthday Honours of 1991 Dr Houghton received the accolade of Knight Bachelor. In October 1991 he was appointed a member of the Royal Commission on Environmental Pollution.

Sir John is married, with two children and one grandchild. He lives in Begbroke, Oxon.

P. Ryder

The following articles are intended as a review of, and lead into, the main article. They represent an innovation which is part of the proposed expansion of the magazine.

Numerical weather prediction

Nina Morgan
Science writer

How is it possible to summarize the nature of weather systems, with all their quirks and complications, in a mathematical model? This is the problem those who work on numerical weather prediction (NWP) face daily – and not everyone views the problem in the same way.

1. Several models in use

There are a number of different NWP models currently in use around the world. For example, the

Meteorological Office in Bracknell, the European Centre for Medium-range Weather Forecasts in Shinfield, Reading in the United Kingdom, and the Japan Meteorological Agency all run different NWP models.

In the Bracknell Met. Office three models are run, a global area model, which covers the entire surface of the Earth and has a resolution of 20 levels and a grid spacing of 100 km; a limited area model covering Europe and the Atlantic, which has a resolution of 20 levels and grid points located 50 km apart; and the mesoscale model, covering only the United Kingdom and nearby areas on the continent, in which the grid points are 15 km apart and the resolution 32 levels.

The Japan Meteorological Agency run four models: a global model, with a resolution of 21 layers and a grid spacing of 110 km; an Asia model, with a resolution of 16 layers and a grid spacing of 75 km; a Japan model with a resolution of 19 layers and a grid spacing of 40 km; and a typhoon model, with a resolution of 8 layers and a grid spacing of 50 km.

All of the models are forced by the global model because they provide boundary and starting conditions for each of the higher-resolution models. Generally, the more localized the models, the higher the resolution. However, because higher-resolution models require a great deal of computer power to run, they are limited to a restricted area.

2. Navier–Stokes Equations

At the heart of each model are the Navier–Stokes equations, which describe the dynamics of fluid motion, and form the basis for describing flow in the atmosphere. Although the equations are the same, the models often differ in the approach taken to solving them.

There are two distinct methods in use — the grid-point method, used, for instance by the UK Met. Office in Bracknell, and the spectral model used, for example, by the Japan Meteorological Agency.

In the grid-point method the area being modelled is divided into a grid. The basic atmospheric variables are assigned values at each of the grid points, and values between the grid points are averaged.

In the spectral model, complex functions are used to describe the shape of flow in a given area. By applying a similar principle to the three-dimensional area of the model as that used in Fourier transforms for linear data, it is possible to describe conditions at any given point.

Although the spectral model is perhaps more difficult for outsiders to understand, it has some advantages. It more closely represents the wave nature of real atmospheric flow, preserving the speed and shape of individual components with different horizontal scales.

3. Physical parameters

Critical to all of the models are the physical process equations used to describe radiation, convection and turbulence in the atmosphere. These processes occur on scales which are smaller than can be resolved by the models.

The flexibility of the physics routines makes it possible to use the same model to predict weather in the tropics, where convection is very important, and at temperate latitudes, where cyclones and anticyclones dominate.

4. Keeping the models on track

The models are only able to predict a few days into the future with any degree of reliability — the current maximum limit is around 5 days. Errors in the initial variables and in the mathematical models mean that the predictions stray progressively from reality as time goes on.

To nudge the forecasts back into line, every observation which comes through the communications network is introduced into the model through an assimilation process. The model uses this information to continuously adjust its results. Usually the physics routines are the first to be altered because they contain more adjustable features. In general, the higher the resolution of the model being run, the greater the attempt made to incorporate information from satellites into the modelling process.

5. The future

NWP is central to any weather forecasting system, and its ultimate aims are to provide a more accurate representation of the weather than is presently possible. Improving the models and increasing the resolution by using bigger and better computers would go some way towards reaching this goal.

However, the greatest improvements will probably be due to improved observations collected from individual weather stations on the ground, geostationary satellites or aircraft. The human input into the models contributes as much to the accuracy of the predictions as do the supercomputers which run the models several times a day. By working together humans and computers can go along way towards untangling the complex weather maze and providing accurate forecasts.

(Information from Rick Rawlins and Akihide Segami)

Using satellite images

Nina Morgan
Science writer

1. Information from satellite images

Satellite imagery, which gives global coverage, has now surpassed point-data observations in the science of weather prediction. To trained interpreters, satellite and radar images give a useful picture of the dynamic and physical processes going on in the atmosphere, and provide helpful clues as to the likely evolution of atmospheric systems.

Satellites provide a global view of the weather. As they orbit the Earth they record weather data at regular intervals to supplement data gathered on the ground. They are also able to gather information from those parts that ground-based weather stations do not reach — for example over the oceans — or places, such as much of the southern hemisphere, where weather stations are relatively thin on the ground.

The first weather satellite was launched in 1960. Now an array of geostationary and polar-orbiting satellites provide a continuous flow of information to forecasters and a constant stream of data to verify and update numerical weather prediction models.

In nowcasting, the very-short-term forecasting of weather, satellite and radar images are an essential aid in predicting relatively short-lived phenomena such as thunderstorms which may easily be missed by other types of observations. The images also provide data for use in longer-term forecasts, including the monitoring, verification and adjustment guidance from numerical weather prediction (NWP) models.

2. Types of image

Images from geostationary and polar-orbiting satellites are obtained using radiometers which measure the amount of electromagnetic radiation emitted and scattered by the Earth and its atmosphere. Radiation intensity is recorded over specific ranges of wavelengths. The main types of satellite images currently used operationally include visible (VIS) images, recorded in the range 0.4–0.7 micrometres; infrared (IR) images derived from radiation in the 10–12 micrometre waveband; water vapour images from the 6–7 micrometre band and images from 3.7 micrometre wavelengths, which is on the boundary between the VIS and IR regions.

A visible image, only obtainable on a daylight pass, measures the amount of sunlight reflected from the Earth's surface or from cloud tops. Infrared images effectively provide information on the temperature of the Earth's surface, or the cloud above it. These can be recorded at anytime during the day or night.

3. Interpreting satellite images

Distinctive patterns of clouds seen on satellite images help forecasters to recognize and track weather systems. For example, mature depressions are recognized by their distinctive swirl of cloud. Frontal systems often appear as wishbone-shaped areas of cloud radiating from a depression. The images can also be interpreted to provide information about the composition of the atmosphere and the vertical temperature profile. By measuring the changing position of clouds on successive images, it is possible to get an indication of wind speed at the cloud levels. Future developments will obtain and interpret satellite images to give an idea of surface wind strengths by studying the characteristics of ocean waves, and measure rainfall.

Geostationary satellites provide new images every half hour. These can be displayed as an animated sequence to show the movement and breakup of cloud systems, as well as to provide insight into the dynamic evolution of weather patterns and help in their early recognition.

4. Visible, infrared and water vapour images

In the visible radiation spectrum images are reflected sunlight from the Earth's surface or from the clouds above it. In general, the cloud thickness determines the brightness of the image.

Infrared images measure the infrared radiation emitting from surfaces. and provide an indication of the temperature of the Earth's surface or, where there is cloud cover, of the cloud tops. The images are often displayed on a grey scale with the colder surfaces appearing lighter, and the warmer ones darker. Infrared images make it possible to distinguish between high cloud, which appears white on the images because it is cold, and low cloud, which looks dark on the images because it is warmer.

Combined study of visible and infrared images can often resolve uncertainty. For example, if both images are bright in a particular area, the cloud is likely to be high and thick. However, if the visible image shows areas of bright cloud, but the same area in the infrared image is dark, this indicates that the cloud is low, or that there is fog present.

Radiation from moisture in the cold upper troposphere will appear white, in the water vapour image spectrum, and radiation from water vapour at warmer, lower levels in the troposphere will appear dark. Water vapour radiation from these lower levels will only be picked up if the colder upper troposphere is dry.

5. Geostationary satellites

Geostationary satellites, orbiting at a height of 36 000 km over the equator, travel at the same speed as the Earth rotates, and thus stay over a particular location on the Earth's surface. Five geostationary satellites, the European Meteosat, two US satellites (Goes-E and Goes-W), the Soviet GOMS satellite and the Japanese GMS satellite, together would provide complete coverage of the globe. Each geostationary satellite views a full earth-disc and is able to collect good quality data, with a resolution of around 4–5 km, up to latitudes of around 65 degrees north and south.

Each of the geostationary satellites is capable of making images of the Earth's surface, every half hour, although the images are usually made available hourly.

The data received from the geostationary satellites are usually presented the form of images which resemble black and white or false colour pictures of the Earth from space. The images can be interpreted to provide cloud, water vapour, and sea surface temperature maps. Because new images are available hourly, they provide a convenient way to monitor the movement and development of weather systems. Wind speeds can be estimated by tracking the movement of clouds.

6. Polar-orbiting satellites

Two US polar-orbiting satellites are currently providing coverage of the Earth. They orbit at an altitude of roughly 870 km, in a fixed position relative to the Sun, which means they always cross the equator at the same local time. The polar orbiters take about 1 hour 42 minutes to pass round the Earth. During this time the rotating Earth has moved on by about 25 degrees, so the satellite views a different part of the Earth's surface on successive passes. Each satellite passes over any given point on the ground every 12 hours, so with two satellites in orbit, pictures of any particular area are available every 6 hours.

Because the polar orbiters view the Earth from a lower height than do the geostationary satellites they are capable of providing much higher spacial-resolution data. They are also able to provide vertical profiles, or soundings, of temperature or humidity data in the atmosphere by measuring over a wide range of wavebands. This provides much useful data input for numerical weather forecasts. The satellite soundings also complement the very detailed local measurements made using radiosondes sent up from the surface by providing a global view.

7. International co-operation

Keeping meteorological satellites in space is an expensive business and relies very much on international co-operation. The United Kingdom is one of the 16 European nations contributing to the European Eumetsat organization, which is responsible for operating the Meteosat geostationary satellite. Currently, two of the polar-orbiting satellites are provided by the United States, also two by USAF and two by USSR, but much of the instrumentation on board is contributed by other countries, including the United Kingdom. However, by around 1997–98, Eumetsat expects to be taking responsibility for one of the polar satellites, and the involvement of the Meteorological Office will increase, with a corresponding rise in their budget for space activities towards 15% of the total budget.

International collaboration also extends to lending a satellite when the need arises. During the summer of 1991 when one of the US geostationary satellites reached the end of its life and its replacement was delayed due to technical difficulties, Eumetsat moved one of their satellites to a new position in order to fill the gap in coverage. Meteosat-4 will continue to stand in until the US replacement satellite is operational.

8. Not just for forecasters

Satellite images also have their uses outside the weather forecasting field. Recent work by zoologists at Oxford University has shown that data from meteorological satellites can be used to map the distribution of tsetse flies, a series disease carrier in humans and animals in some parts of Africa. Because the flies are restricted to the moister parts of the continent, the zoologists believe that satellite data provides an inexpensive and effective way of estimating the tsetse fly distribution over vast areas where rain-gauges are few and far between. This could provide an effective means of deciding where insecticides are most needed. A similar process is already used to combat the desert locust.

Other satellite images are used to map the distribution of disease-causing organisms. This has important implications for the health of developing nations.

9. Looking ahead

Meteorological organizations are continuously working on new developments to ensure that even better data is available from satellites in the future. They have to look ahead to keep ahead, because development time-scales tend to be in the order of decades.

In the short term, plans for improvement include replacing temperature measurements made in the infrared, which can only be collected in cloud-free areas, with microwave measurements, which are not affected by clouds. Looking further ahead, new techniques to improve vertical temperature resolution are being studied. These will lead to improvements in forecasts and will provide better data for numerical weather prediction models.

Some of the instruments of the future are already in use. The recently launched Earth Resources Satellite is carrying the first generation of active microwave instrumentation, in the form of a radar scatterometer which can give indications of features such as sea surface winds. Once their value for meteorology has been demonstrated, active microwave instruments may eventually form part of the standard instrumentation on weather satellites.

Although satellite data is expensive to obtain many would argue that as the only available source of global information, it is cheap at the price. Satellite data provides essential information for accurate very-short-term nowcasting and is one of the factors behind the dramatic improvement in numerical weather prediction models capable of providing forecasts for up to 5 days in advance. As the numerical models continue to improve, they will need even better data to get the best performance, and satellite data will become even more critical. Forecasters of the future will wonder how anyone ever lived without it.

10. Not forgetting radar

Radar provides a valuable source of information about rainfall, echoes being produced as the emitted signals are scattered from raindrops.

Areas of rain cause interference on radar screens, a nuisance for air traffic controllers, but meteorologists now use radar to detect areas of rainfall, and provide information on the intensity. The British Isles radar network consists of 12 radar stations and is part of a larger European network.

Rainfall maps can be constructed from radar information to display areas of no rain, and rates of rainfall of different intensity using different colours or shades of grey on a 5 km grid. The images are recorded at 15-minute intervals These are animated by displaying them in sequence to track showers and monitor their development. It is left to the forecaster to decide the type of precipitation.

(Information from Dr Peter Curtis, Mike Bader, Ken Wright and the book *Weather Facts* by Dick File.)

551.501.777:551.501.795:551.507.362.2(52)

The application of satellite infrared and passive microwave rainfall estimation techniques to Japan: Results from the First GPCP Algorithm Intercomparison Project

E.C. Barrett and T.J. Bellerby
Remote Sensing Unit, Department of Geography, University of Bristol

Summary

The contribution of the University of Bristol Remote Sensing Unit (RSU) to the Global Precipitation Climatology Project (GPCP) Algorithm Intercomparison Project (AIP) is discussed. This contribution comprised the production of monthly, daily and hourly rainfall estimates using GMS infrared and SSM/I passive microwave data. A number of variations upon, and extensions to, the Bristol PERMIT infrared technique were implemented. Rainfall estimates were also produced from passive microwave data alone using a combined 37 GHz Polarization Corrected Temperature (PCT)/19 GHz Polarization Difference technique. The results of the algorithms described are evaluated against a composite radar/rain-gauge product. A second AIP is being organized by the GPCP and the UK Meteorological Office to cover parts of north-west Europe during 1991/92.

1. Introduction

Under the direction of Dr P. Arkin, the World Climate Research Programme's (WCRP) Global Precipitation Climatology Project (GPCP) has been organized to produce a 10-year archive of estimated monthly precipitation for all 2.5° latitude/longitude areas between 40° N and 40° S from 1986 to 1995. Statistics of IR imagery from the GOES, Meteosat, Insat and GMS geostationary satellites, and NOAA polar-orbiting satellites are being collected and used to compute estimates of accumulated rainfall.

At the 3rd Session of the GPCP International Working Group on Data Management (IWGDM) held at Darmstadt, Germany, in July 1988 it was agreed that a pilot project for GPCP algorithm validation and development should be organized as soon as possible. An Expert Meeting was held in Washington DC in April 1989 to lay detailed plans for the project for which a special data set would be prepared and in which it was hoped that several laboratories from different countries would participate. This meeting agreed that the general objectives for the Japanese GPCP project should be as follows:

(a) To assess the skills of existing algorithms in extracting rain information from satellite imagery.
(b) To help understand why different algorithms yield different results.
(c) To improve existing algorithms.
(d) To ensure that the GPCP algorithm performs adequately for needs of the WCRP.

The University of Bristol Remote Sensing Unit (RSU) participated in the resulting GPCP Japan Algorithm Intercomparison Project by producing outputs to the agreed project specification from satellite rainfall algorithms already implemented and tested for other areas of the world. A considerable measure of further algorithm calibration and development was necessary in order to apply the Bristol methods to the particular meteorological conditions prevalent in the study area over the study period. Throughout the course of the project it was the intention of the Bristol RSU to test several algorithms in sequence and generate a series of results which would elucidate the extents of the contributions made to rainfall estimates by different sources of satellite and collateral data.

The satellite methods to be used by the RSU were based on the objective Polar-Orbiter Effective Rainfall Monitoring Integrative Technique (PERMIT) infrared approach orginally developed for use with either NOAA or selected Meteosat imagery over Africa, and selected passive microwave methods already in the process of development at the RSU in conjunction with NASA, NOAA/NESDIS and the Meteorological Office.

1.1 The Intercomparison data set

The data for the First Algorithm Intercomparison Project were provided by the Japanese Meteorological Association in two parts. The first, containing satellite and meteorological model data for the study period, together with 9 years of precipitation climatology from ground stations, was to be used for the generation of rainfall estimates. The second, comprising rain-gauge and composite radar/rain-gauge data spanning the study period, was intended for verification purposes. Each data set spanned two month-long study periods: June 1989 (dominated by a persistent frontal regime, the 'Baiu') and 15 July–15 August 1989 (dominated by a tropical convective regime). The study area, and the included but much smaller region spanned by the validation data are shown in Fig. 1.

The following components of the initial data set were employed in this study:

(a) Hourly infrared GMS data for the study period. These images were stored on a latitude/longitude grid to a resolution of 0.05° × 0.625°.

(b) Passive microwave data. Data from the Special Sensor Microwave Imager on the Defense Meteorological Satellite Program (DMSP) Block 5D-2 Spacecraft were supplied for the study period. Data from this satellite should comprise dual-polarization measurements at 19.35, 37.0 and 85.5 GHz, plus vertical polarization observations at 22.235 GHz. In practice, the data for the intercomparison study were collected after partial failure of the 85.5 GHz vertical polarization sensor due to overheating. Data for the horizontal polarization at this frequency were available, but considered highly unreliable.

(c) Data from the Japanese Meteorological Association (JMA) Global Spectral Model. This comprised 12-hourly precipitation totals (to 0.01 mm) on a 1.25° grid together with daily values for sea level pressure, wind components, temperatures, heights and dewpoints for standard atmospheric levels.

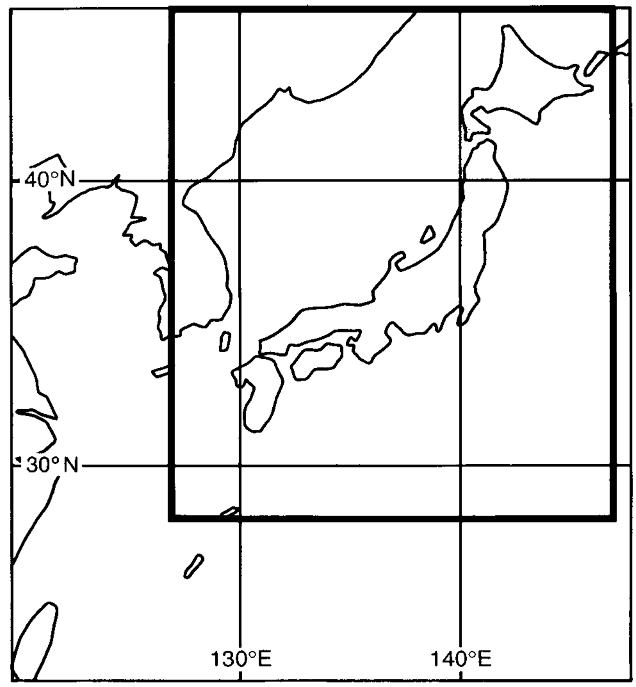

Figure 1. The area covered by the GPCP AIP dataset. The smaller area enclosing the composite radar/rain-gauge validation data set is also shown.

The validation data set, only supplied after the products derived from the initial data set had been supplied by participating laboratories including the RSU to the Algorithm Intercomparison Centre, comprised the following:

(a) Hourly Automated Meteorological Data Acquisition System (AMeDAS) radar/rain-gauge composite data to a resolution of 0.0625° longitude by 0.05° latitude covering a region bounded by 127° E and 147° E, 28° N and 46° N. The data comprised rain rates to a resolution of 1 mm h^{-1}.

(b) AMeDAS ground-station data comprising hourly and daily precipitation (mm), wind speed and direction, sunshine duration and temperature.

1.2 Intercomparison Project required products

The intercomparison study was based around the comparison of rainfall products produced by various participating groups using the first supplied data set only; as explained above, validation data was only supplied after the completed products had been submitted. The products required by the Algorithm Intercomparison Center (AIC) of the National Oceanographic and Atmospheric Administration (NOAA) consisted of the following:

For infrared algorithms:

(a) Fields of accumulated rainfall, to 0.1 mm, on a 1.25° grid covering the Japan study area, for each day during the two study periods.

(b) Time-series of accumulated rainfall for five specific areas, at the highest temporal resolution possible (up to hourly). The specified areas comprised four 1.25° × 1.25° latitude/longitude boxes and a further 2.5° latitude/longitude box.

For passive microwave algorithms:

(c) Fields of rain rates, to 0.01 mm h^{-1}, at the highest spatial resolution available for ten specified swaths.

For all algorithms:

(d) Fields of accumulated rainfall, to 0.1 mm, on a 1.25° grid for the two monthly periods.

2. Methods and techniques employed

2.1 Infrared methods

The infrared products produced for the algorithm intercomparison were based upon variations of the Bristol PERMIT method (Barrett and D'Souza 1985, Barrett *et al.* 1986a, 1986b). Originally developed for a relatively long-period, convective regime, use with polar-orbiting satellite data, this technique seeks to identify rainy days rather than individual rain events. In the basic implementation, one or more occurrences of cloud colder than a fixed threshold are deemed sufficient to indicate that a pixel area has experienced some precipitation during a 24-hour period. Precipitation days so identified are assigned a rainfall equal to a mean-rain-per-rain-day statistic ('morphoclimatic weight'), obtained from climatological atlases or other sources. In previous work four images a day had been successfully employed to produce rainfall estimates for periods of 10 days or longer. However, given the availability of hourly GMS data in the Japan data set, the potential existed to produce effective estimates for considerably shorter time intervals.

The procedure described above generates first-order estimates based upon climatological predictors only. If synoptic data are available from local ground-stations, further corrections for meteorology become possible. In previous work, a piece-wise global linear correction function had been derived from a comparison of monthly rainfall estimates for ground-station locations and the rain-gauge data themselves. This function related the first order products generated by the initial stage of the algorithm to improved rainfall values more in accord with the meteorological data (Barrett and Richards 1989).

2.2 Modifications to the PERMIT algorithm for use over Japan

A number of significant differences existed between the intercomparison data set for the Japan study and the data sets used for previous applications of PERMIT. These included: the present availability of hourly infrared images for the study area, the lack of any calibration data for the first stage of the present study, and the availability of numerical model outputs and passive microwave data as possible additional inputs to the rainfall estimation process.

The choice of a temperature threshold for the identification of 'probably precipitating cloud' is a difficult procedure; no clear rules are available to determine the most appropriate values to use for different latitudes, climatic conditions, etc. In previous implementations of the PERMIT method the selection of the threshold temperature had been accomplished using a combination of information from atmospheric soundings and the experience of implementors. Given the complexity of the weather regimes around the Japan test area, involving both tropical and mid-latitude systems, significant advantages were seen in the employment of a more objective approach to the choice of the key cold-cloud threshold. The initial stage of the PERMIT method is primarily a mechanism for identifying rainy days. This property of the algorithm implies that the utility of any particular threshold function must be assessed by the precision to which its application generates rain-day counts. To this end, optimal thresholds were obtained by matching, in a broad statistical sense, rain-day-count outputs from the front end of the PERMIT algorithm with equivalent precipitation-day information derived from collateral data for the study area.

Two sources of collateral rain-day data were employed for the generation of suitable cold-cloud thresholds, namely climatological data from Takahasi and Arakawa (1981) and outputs from the JMA Global Spectral Model. The former were only available for a limited number of randomly distributed ground-station locations while the latter were available for all points on a 2.5° grid covering the study region (and areas beyond). Although it would be possible to define a threshold function which varied with both spatial dimensions, the sparseness of the collateral data suggested that for present purposes it would be more practicable to derive cold-cloud thresholds which varied with latitude alone.

The study region was split into a number of regions, each of which spanned a 2.5° range in latitude. Area-averaged rain-day outputs for each region were produced using a range of fixed cold-cloud thresholds. Equivalent regional statistics derived from the collateral data sources were then matched to these products, yielding an optimal threshold value for each latitude range. Cubic spline interpolation produced cold-cloud thresholds which were a smooth function of latitude (Fig. 2). The use of climatological data for threshold selection proved unsatisfactory over the July–August period — a combination of the available monthly statistics for July plus August did not produce reliable rain-day counts for the intermediate period from 15 July to 15 August and these counts in turn gave rise to totally unconvincing threshold functions. Hence PERMIT runs for this later study period exclusively employed the thresholding functions derived from JMA model data.

The same two sources of collateral data (climatological records and numerical model outputs) used to generate cold-cloud thresholds were employed to derive the required background fields of morphoclimatic weights. For the climatological source, mean-rain-per-

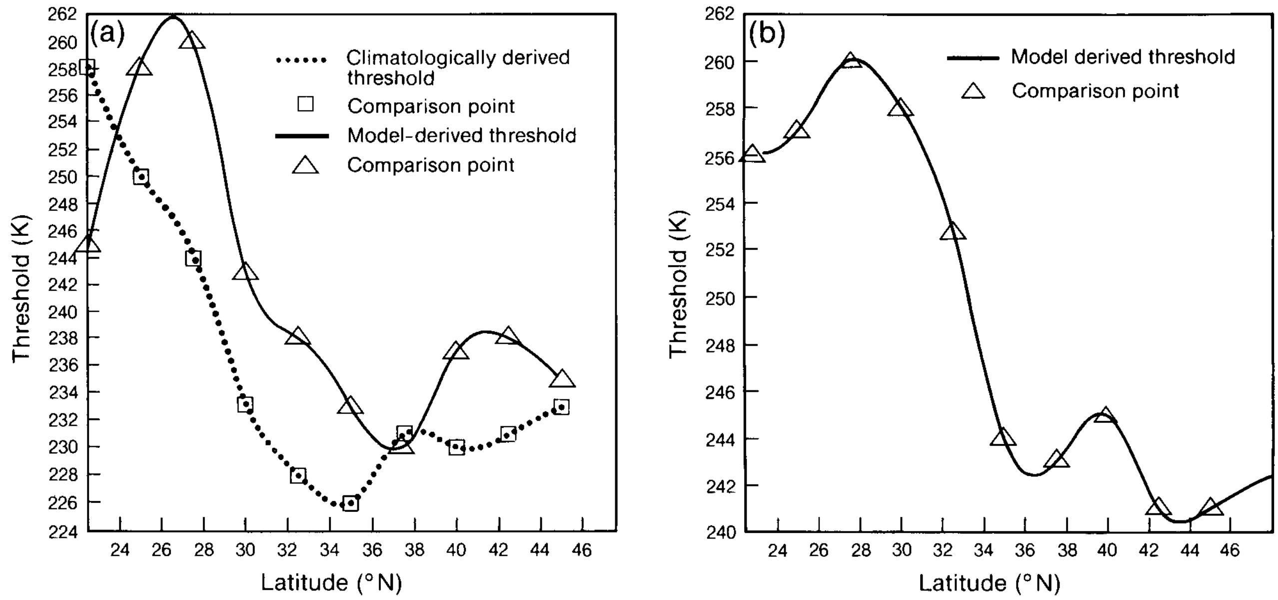

Figure 2. Cold-cloud thresholds for the PERMIT algorithm for (a) June 1989 and (b) 15 July–15 August 1989.

rain-day values for the various climatological stations were plotted on a map onto which, taking account of the local geography, the contours of the overall morphoclimatic weight field were drawn by interpolation. The resulting contour map was digitized and interpolated to the required 441×476 grid using a simple algorithm employing repeated 3×3 selective mean filtering (Fig. 3(c)). The model-derived background field of morphoclimatic weights was interpolated from the 2.5° square grid of the JMA Global Spectral Model precipitation product using the same successive filtering technique (Figs 3(a) and 3(b)).

When combining the various possible permutations of the two sources for each of the two non-satellite inputs to the algorithm, it was discovered that the most reasonable results came from matching the data sources used to derive both the thresholds and the morphoclimatic weights. Errors of a relatively small magnitude in the model precipitation estimates had a significant effect upon the number of rain-days counted by the thresholding of daily rainfall totals above 0.25 mm. When the model-derived rain-day products were used to generate both functions and background weights, the errors introduced by these inaccuracies tended to cancel themselves out; in contrast, mixing input sources lead to a considerable over- or under-estimation of total rainfall.

When the validation data set was received it was found that this contained rainfall totals to a resolution of only 1 mm. It was therefore not possible to use this data set to assess directly the procedures used to derive threshold functions and background fields of morphoclimatic weights. Such an investigation would have required data with at least 0.25 mm resolution if rain-day counts could be derived and compared.

2.3 Extending the PERMIT algorithm to produce daily rainfall totals and time-series to a resolution of one hour

The basic PERMIT technique is a good estimator of long-term rainfall totals but gives little information on the distribution of individual precipitation events. This property of the algorithm is a deliberate result of its structure; precipitation events are assigned rainfall values in such a manner as to ensure correct long-term totals rather than accurate instantaneous rain-rate estimates. In order to generate rainfall products for shorter periods without sacrificing this basic advantage of the algorithm, the PERMIT technique was modified in such a manner as to leave unchanged any longer-term, larger-scale rainfall totals, but to ensure that daily and even hourly estimates might be as accurate as possible.

Fig. 4(a) shows a simple, linear function relating the effective number of rain-days represented by one rainy day (daily rainfall divided by mean-rain-per-rain-day) to the cold-cloud count for that day. This function was derived by noting that the mean number of mean-rain-days rainfall for sufficiently large data set must, by definition, be equal to the mean number of rainy days. Using this constraint, the slope of the linear function could be calculated simply from the occurrence histogram for the 24 possible daily cold-cloud events taken over the entire infrared data set (Fig. 4(b)). From Fig. 4 it may additionally be seen that the true slot-weight function (mean radar/rain-gauge derived rainfall associated with each slot-count category) is non-linear. However, the low frequencies at which the higher slot counts occur (Fig. 4(b)) do permit some deviation from linearity without significant alteration to the magnitudes of any resulting rainfall estimates. It should be noted that this method of assigning daily rainfall leaves the

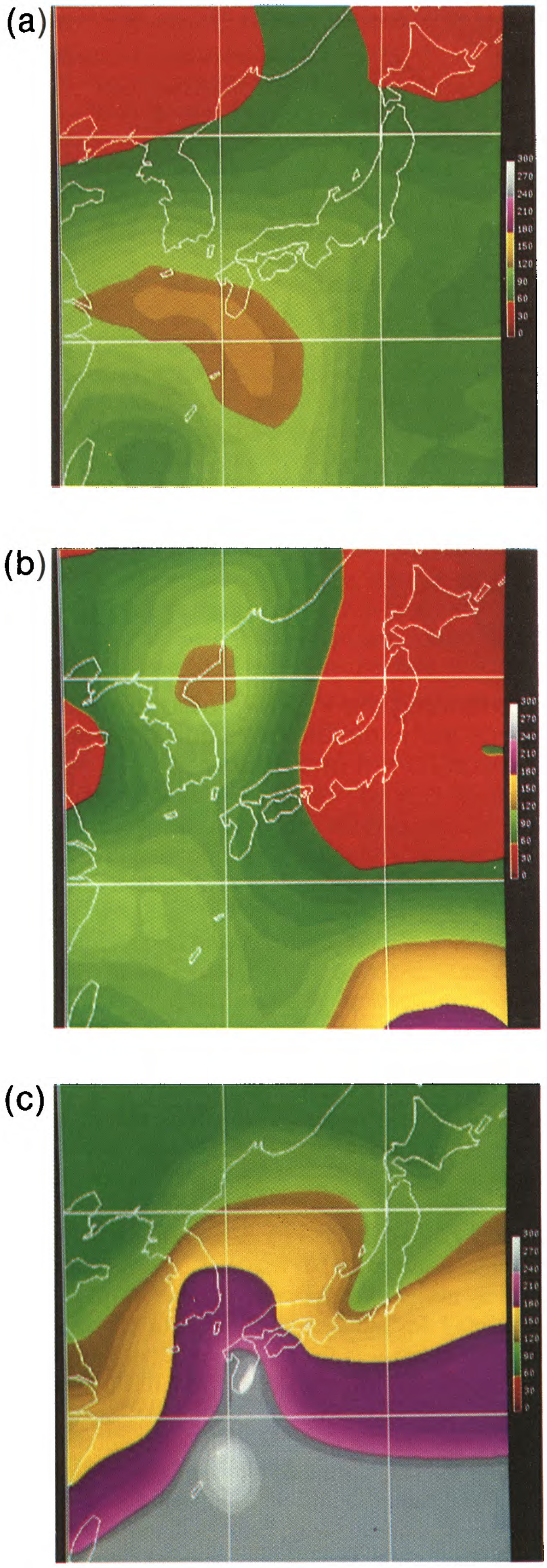

Figure 3. Backgrounds fields of morphoclimatic weights. The values on the scale indicate tenths of millimetres rainfall for (a) June 1989 derived using JMA model data, (b) 15 July–15 August 1989 derived using JMA model data, and (c) June 1989 derived using climatological data.

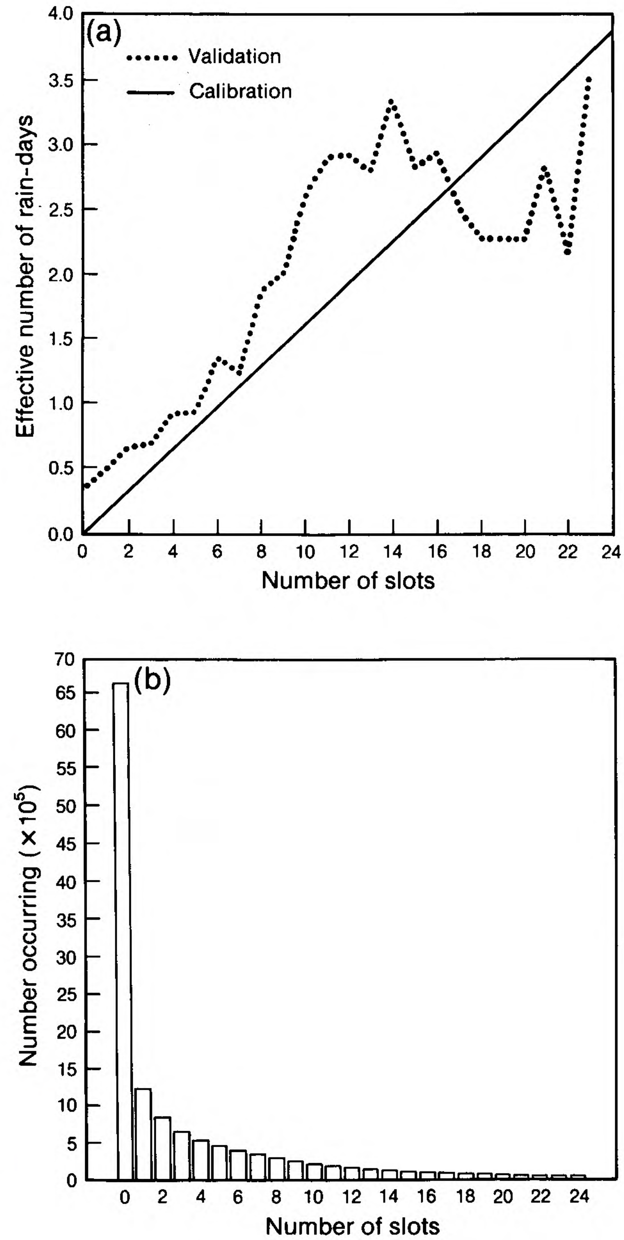

Figure 4. (a) The linear function used in the PERMIT algorithm to relate daily rainfall (in terms of the mean-rain-per-rain-day) to the cold-cloud count for that day. Also shown is the 'true' function relating mean daily rainfall (in terms of the mean-rain-per-rain-day) to the cold-cloud count for that day, derived by comparing the PERMIT products to the composite radar/rain-gauge validation data, and (b) frequency histogram for daily cold-cloud counts derived from the entire AIP infrared data set using model-output derived temperature thresholds.

mean number of mean rain-days rainfall for the entire study area over the entire study period unchanged with respect to the output from the basic PERMIT algorithm; the daily estimates may be said to be derived by a form of 'weighted interpolation' from the longer-term product. Continuing this same 'progressive-refinement' approach, hourly rainfall estimates were obtained by equally dividing each daily rainfall estimate between the identified cold-cloud events for that day.

2.4 Correction of PERMIT outputs using rain-gauge data

While the initial data set for the intercomparison study did not contain any ground data, the validation data set included both rain-gauge data and a combined radar/rain-gauge product. The former of these two data sets was used to derive a correction function for selected infrared products, the corrected versions of which could then be verified against the latter, composite, product. Previous work involving the improvement of PERMIT products using data from ground-stations had concentrated upon the derivation of a global non-linear correction function relating preliminary rainfall estimates to improved values more closely reflecting the ground data. In the case of the Japan study data, however, the primary discrepancy between the rainfall products and the validation data involved a lack of detail in the former with respect to the structure of the rainfall distribution over the islands of Japan. For this reason a simple multiplicative correction factor was calculated for each ground-station based upon the ratio of estimated to observed monthly rainfall and interpolated using a repeated 3×3 selective averaging filter to derive a global, spatially varying, field of correction factors.

2.5 Passive microwave techniques

A considerable amount of research concerning the extraction of rain area and rain-rate information from passive microwave products had been conducted at the RSU prior to the commencement of the Japan Algorithm Intercomparison Project (e.g. Kidd 1988, Kidd and Barrett 1990). However, a number of severe deficiencies in the passive microwave data supplied with the intercomparison data set significantly hindered the generation of both instantaneous and accumulated rainfall products by the methods which had been developed at Bristol for these purposes. The most severe difficulty encountered was the lack of data from the 85 GHz vertical channel, compounded by serious doubts about the quality of the 85 GHz horizontal channel data. This problem precluded the implementation of the RSU Bristol's preferred rainfall-estimation technique for mixed land/sea areas — a polarization-corrected temperature (PCT) algorithm operating at 85 GHz, calibrated against a 85 GHz/37 GHz frequency difference algorithm operating over land areas only. An additional difficulty resulted from the lack of any proper calibration data set for the Japan Project as a whole. This substantially hindered the assessment and calibration of any replacement technique.

The algorithm eventually chosen comprised:

(a) Over sea areas uncontaminated by proximity to land, a polarization difference technique operating at 19 GHz using a global calibration already developed at the RSU Bristol for other purposes (Barrett and Kidd 1991)

(b) Over land and coastal areas, a 37 GHz polarization-corrected temperature technique (Grody 1984), separately calibrated for each monthly period against the polarization difference method by comparing respective values for points within sea areas uncontaminated by land.

Preliminary investigations into the use of the passive microwave data over Japan employed a slightly different algorithm, identical to the above except that a 37 GHz polarization difference technique was used over the sea. This provisional method, which employed an earlier, less effective, global calibration, considerably overestimated all rainfall totals. Parallel research in progress at the RSU yielded improved calibrations for the polarization difference technique at both 19 GHz and 37 GHz and additionally indicated that the lower frequency channel gave a better response for higher rainfall rates. These two factors lead to the adoption of the final algorithm described above.

To summarize:

$$\text{Rainfall} = f(V_{19} - H_{19}) \text{ (over open sea)}$$

$$= g\{(1+\Gamma)V_{37} - \Gamma H_{37}\} \text{ (over land or coastal areas)}$$

Here f and g are piece-wise linear functions, V_{37} is the vertical brightness temperature at 37 GHz and H_{37} is the horizontal brightness temperature at the same frequency. Fig. 5 shows the mask used to classify land, sea and coastal areas.

The Γ parameter to the PCT algorithm was separately calculated for each of the monthly study periods through a comparison between the 37 GHz vertical channel brightness and polarization difference values occurring over uncontaminated land areas and the same variables measured over uncontaminated sea areas. Polarization differences and PCT values could then be compared over the ocean to calibrate the latter method in terms of rain-rates. All calibrations comprised piecewise linear functions. Pixel-resolution 'monthly' rainfall totals were obtained by compiling mean rain-rate statistics in mm h^{-1} for each pixel and multiplying these average values by the total number of hours in the appropriate 30- or 32-day period. The required grid of 1.25°-resolution monthly rainfall values were derived using a weighted averaging technique which took account of the number of individual overpasses contributing to each monthly accumulated pixel value.

Fig. 6 shows the PCT calibration functions for each month together with equivalent curves derived from the validation data (mean PCT) associated with each rain-rate category. The calibration functions are several degrees too severe, indicating that the algorithm should, as a whole, underestimate the amount of rainfall.

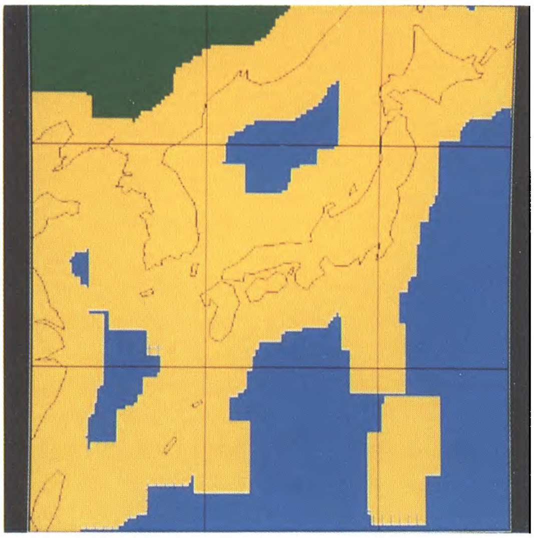

Figure 5. The mask employed to classify land, sea and mixed land/sea (coastal) areas in the passive microwave algorithms.

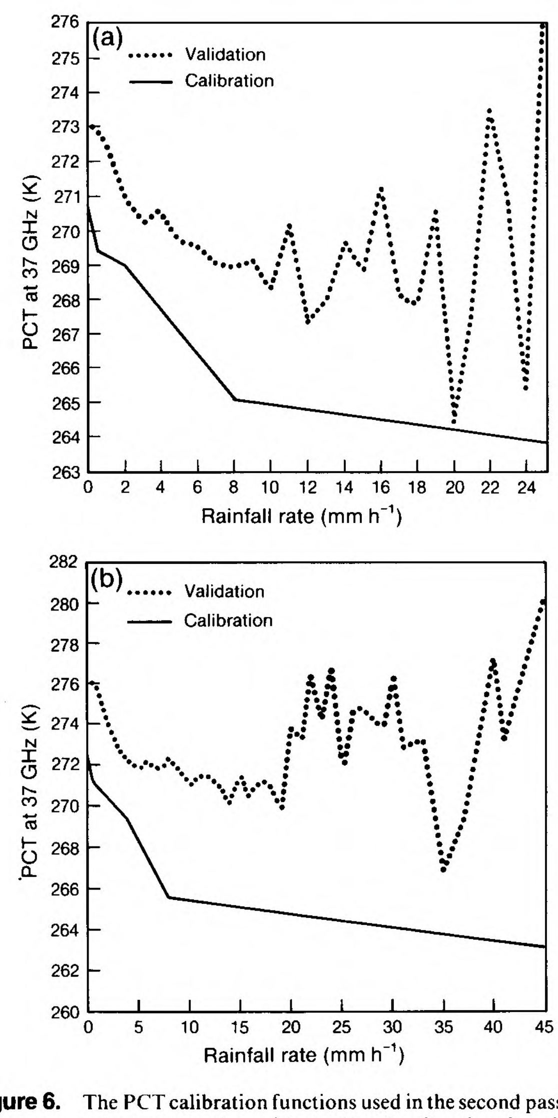

Figure 6. The PCT calibration functions used in the second passive microwave technique together with the 'true' calibration functions (mean PCT associated with each rain-rate category) derived by comparing the passive microwave and composite radar/rain-gauge data set for (a) June 1989, and (b) 15 July–15 August 1989.

3. Results

The primary purpose of the RSU study was to provide intercomparison products for the GPCP project which could then be compared with results produced by other centres using alternative algorithms, ultimately providing valuable information upon the relative strengths and weaknesses of different satellite rainfall monitoring strategies. This central comparison is currently being performed by the Algorithm Intercomparison Centre of NOAA, and the results are scheduled to be available later in 1991. Much of the work performed by the RSU with regards to the First GPCP Algorithm Project was algorithm development; this has been discussed in the section on development of methods and techniques (section 2).

Upon receipt of the validation data set it was possible to perform a preliminary evaluation of the effectiveness of the various algorithms developed throughout the course of the Japan Study. These results are presented here. Fig. 7 shows the monthly rainfall for June 1989 and for July–August 1989 derived from the composite rainfall/rain-gauge product supplied as a part of the validation data set. The most notable feature in these products is the diminution of rainfall with distance from the Japanese mainland; a number of zero monthly rainfall totals (highlighted in white) ring the validation area. This fall-off suggests that radar range effects have a strong influence upon the composite product. While there will certainly be some concentration of rainfall over the mainland, such a relationship will be difficult to differentiate from the radar range effects. As a consequence of this problem we believe that the algorithm validation exercise may take the form more of an intercomparison, between satellite techniques and the radar/rain-gauge composite method, than of a direct comparison/validation of the former.

Figs 8–11 show the estimated total monthly rainfall distributions for the two study periods (June 1989 and July 15–August 15 1989) while Table I gives r.m.s. errors between the various 1.25°-resolution monthly rainfall products and the validation data. The best results were produced by the model-calibrated version of the PERMIT infrared algorithm; the better of the two pure passive microwave algorithms generated estimates with twice the error magnitude of this infrared technique. In general, the infrared based results for the July–August period were much less satisfactory than those for June. There are a number of possible reasons for this: for example the PERMIT method may be less suited to the tropical convective regime predominating during the later period than to the persistent frontal regime ('Baiu') present in June; the July–August period may be untypical, deviating considerably from climatological norms and numerical model predictions; or the validation data for the latter period may be less representative than those for June, creating a false impression that one set of infrared derived results are more satisfactory than the other.

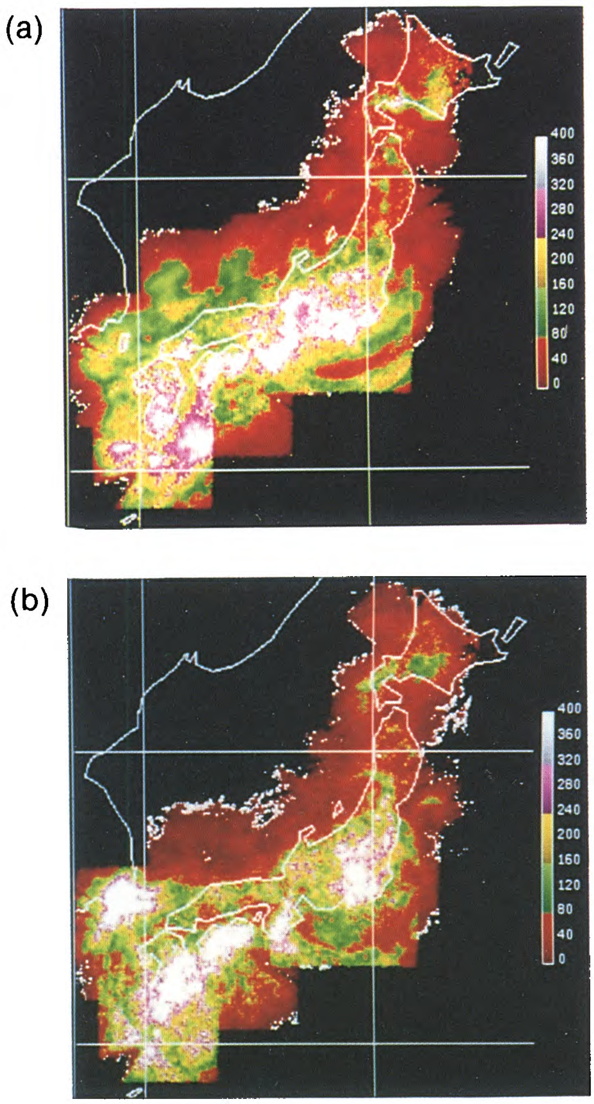

Figure 7. Monthly rainfall derived from the composite radar/rain-gauge product supplied as a part of the AIP validation data set for (a) June 1989 and (b) 15 July–15 August 1989.

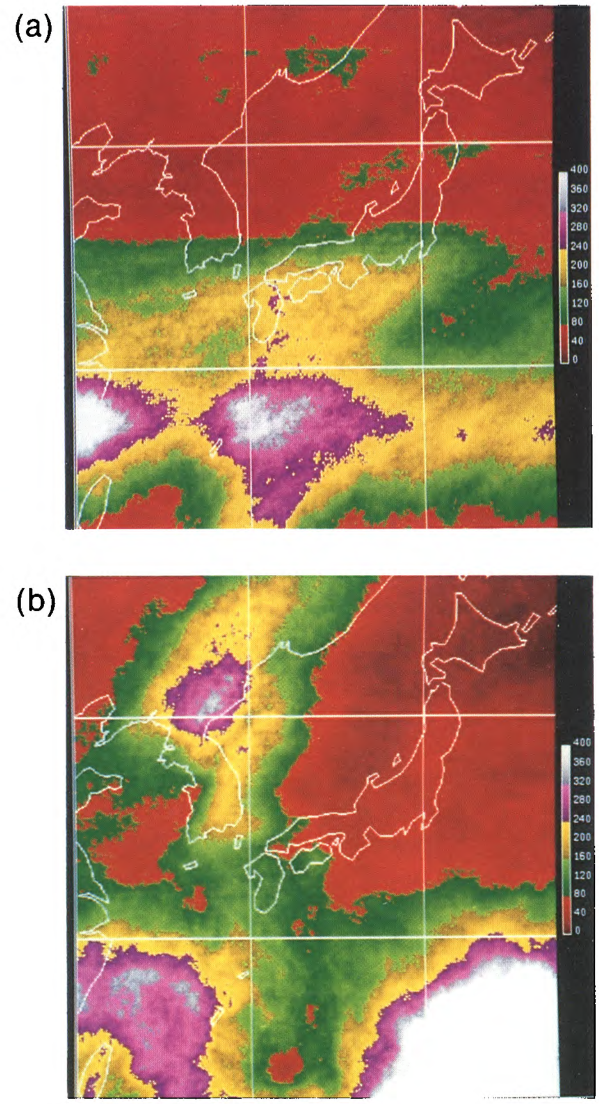

Figure 8. Model-calibrated PERMIT monthly products. The scale indicates monthly rainfall totals (mm) for (a) June 1989, and (b) 15 July–15 August 1989.

Table I. R.m.s. differences between monthly rainfall 1.25°-resolution products and validation data

Product	R.m.s. error (% of mean rainfall) June 1989 (mm)	(%)	15 July–15 August 1989 (mm)	(%)
Model-calibrated infrared	72.5	(47)	122.0	(81)
Climatologically calibrated infrared	100.4	(66)	N/A	
SSM/I	148.7	(97)	187.0	(113)
SSM/I infrared	123.0	(81)	105.7	(71)

(a)
(b)
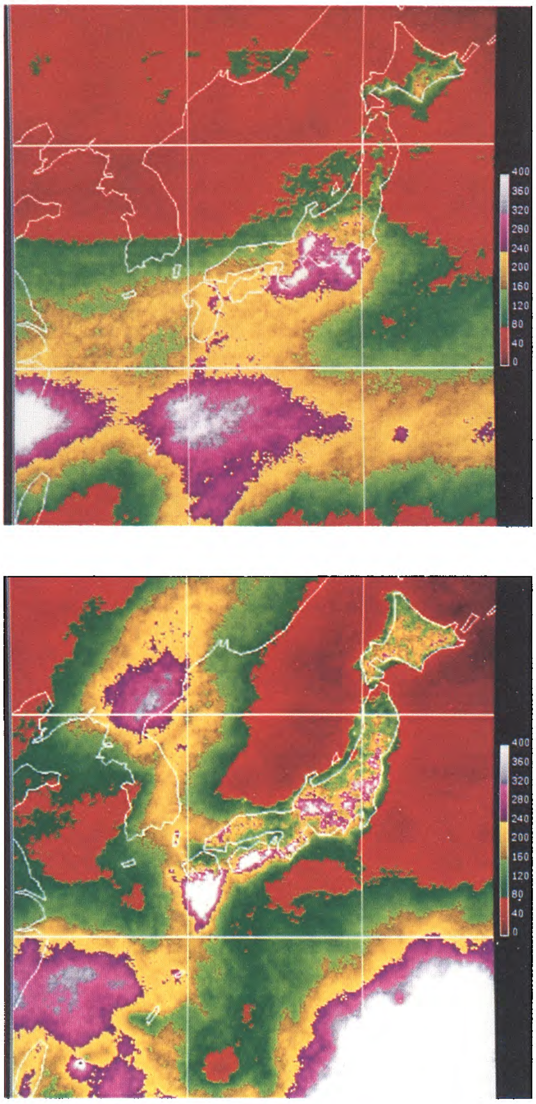

Figure 9. Model-calibrated PERMIT monthly products corrected using ground data. The scale indicates monthly rainfall totals (mm) for (a) June 1989, and (b) 15 July–15 August 1989.

(a)
(b)
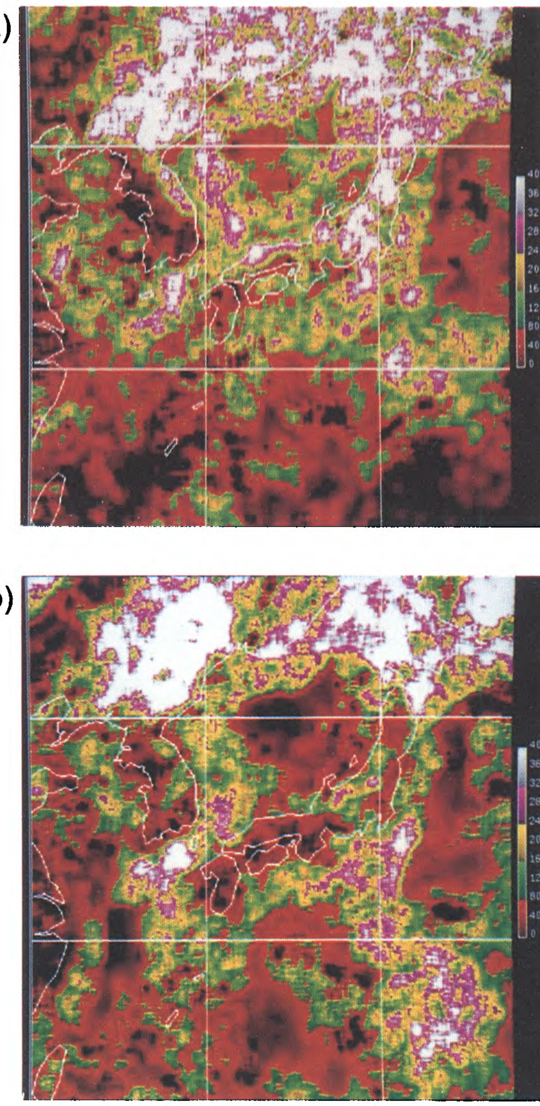

Figure 11. Monthly products produced using the passive microwave algorithm. The scale indicates monthly rainfall totals (mm) for (a) June 1989, and (b) 15 July–15 August 1989.

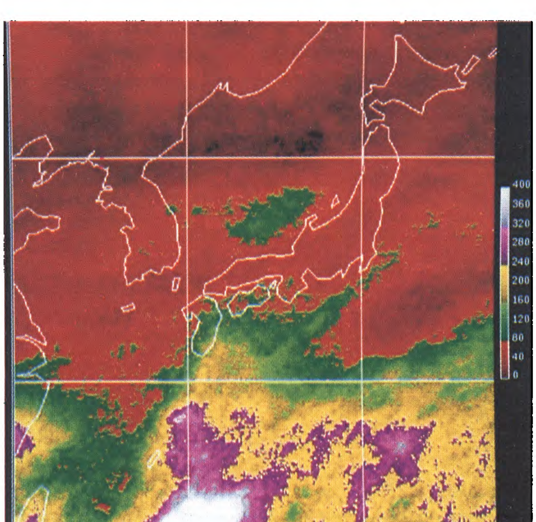

Figure 10. Climatologically calibrated PERMIT monthly products for June 1989. The scale indicates monthly rainfall totals (mm).

The poor quality of the passive microwave results with respect to calibrated infrared outputs may be attributed to a number of causes, chief among which may be as follows:

(a) The bulk of the passive microwave estimates for the validation area were produced using the 37 GHz PCT algorithm. Previous work at the Bristol RSU on PCT algorithms had concentrated upon the 85 GHz channels; the method has not adapted well to the lower frequencies available for this project.
(b) The return rate of SSM/I overpasses was poor. Fig. 12 maps the number of overpasses visiting each part of the survey area over June 1989. While it is reasonable to estimate monthly rainfall from just under two overpasses per day, the lower sampling rates encountered in the Intercomparison Data Set

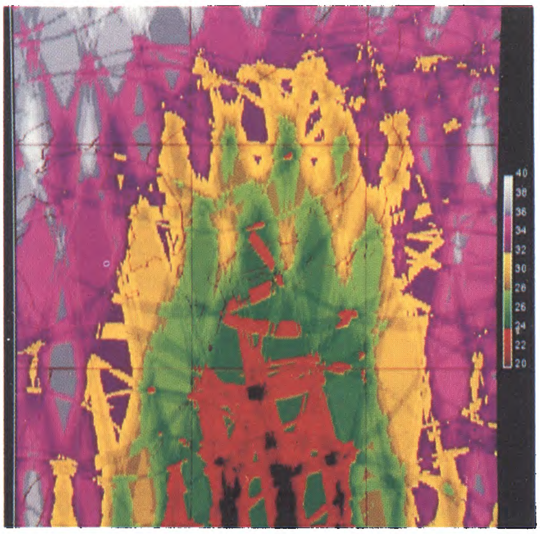

Figure 12. The number of SSM/I overpasses for each pixel for June 1989.

will give rise to significant sampling errors (Laughlin 1981).

(c) The 85 GHz PCT algorithm has been found to perform less well than simple frequency or polarization difference algorithms over open land and open sea areas respectively. The nature of the study region, however, was such that the bulk of the pixel areas had to be classified as 'coastal', i.e. mixed sea or land, or close enough to land or sea to suffer from contamination of the reading and/or errors in swath position.

(d) A variety of meteorological regimes existed within the study area, which itself spanned more than 20° of latitude. Previous work at the RSU had shown that the 'gamma' parameter of the PCT algorithm should be varied with latitude and meteorological regime. The calculation of this parameter for any particular region, however, requires the presence of uncontaminated sea and land areas. The geography of the test area allowed only one, global, value for gamma to calculated.

The combined passive/microwave infrared technique appears to give a better result than the passive microwave data used alone. Given an effectively calibrated passive microwave algorithm operating upon a more complete data set, this technique could show considerable potential, combining as it does the rainfall-resolving properties of the SSM/I instrument with the high spatial and temporal resolutions of the infrared data to provide an effective, purely satellite-based, product.

Table II shows the contributions made by the various components making up the monthly corrected model-calibrated infrared product. The first entry shows the results of employing the calibration data alone. This product was produced by interpolating between rain-day counts derived from the collateral data for each 2.5° latitude range rather than the temperature threshold values derived from these counts. In this manner a field of rain-day counts was produced directly from the collateral data without employing the infrared imagery. Multiplication of this latitudinally varying field of rain-day values by the background field of morphoclimatic weights produced a rainfall product indicative of the contribution of the collateral data to the overall precipitation estimation process. The entries which follow the Table II show the errors for the unweighted and weighted PERMIT products and the weighted PERMIT product corrected using rain-gauge data. Figs 13–15 show this comparison in graphical form.

Table II. Comparison of monthly 1.25°-resolution rainfall products and validation data for various stages of the enhanced PERMIT algorithm

Inputs	R.m.s. error (% of mean rainfall) June 1989 (mm)	(%)	15 July–15 August 1989 (mm)	(%)
Calibration data	70.1	(45)	119.5	(80)
Calibration data + IR imagery	61.8	(40)	115.4	(77)
Calibration data + IR imagery + weighting function	72.5	(47)	122.0	(81)
Calibration data + IR imagery + weighting function + rain-gauge data	45.0	(29)	65.0	(43)

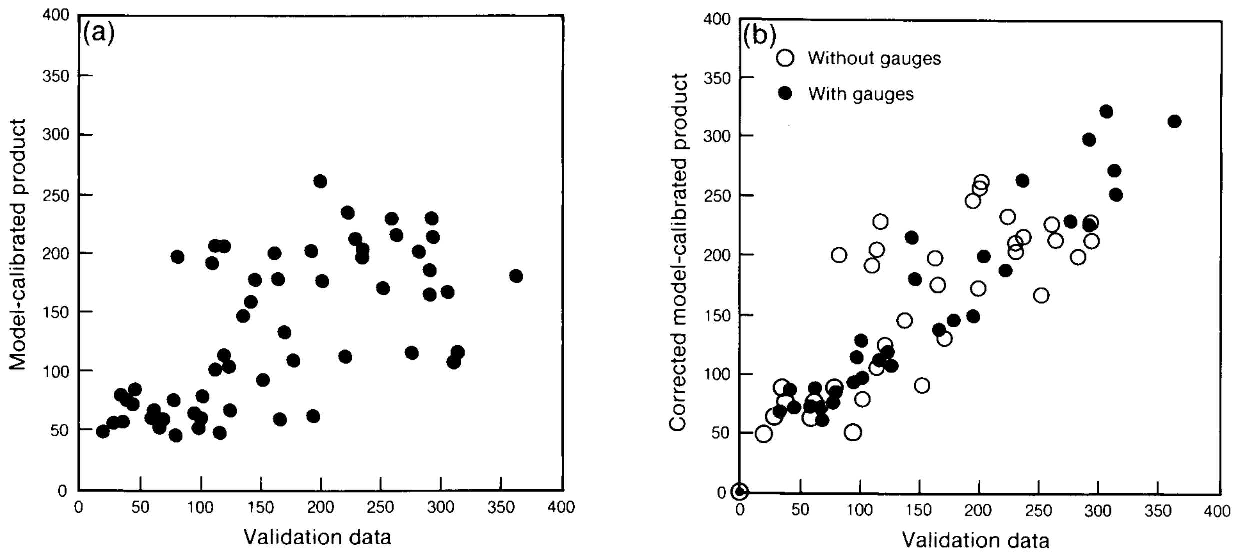

Figure 13. Scatter plots showing a comparison of monthly 1.25°-resolution model-output-calibrated PERMIT products for June 1989 and equivalent values derived from the composite radar/rain-gauge validation data set, (a) not corrected using ground data, and (b) corrected using ground data.

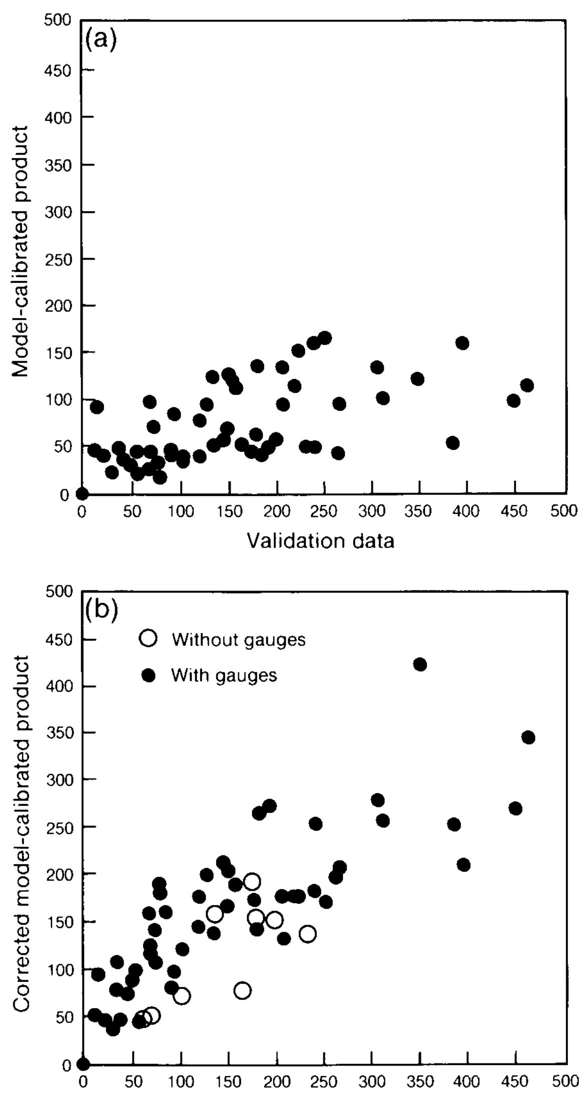

Figure 14. As Fig. 13 but for 15 July–15 August 1989.

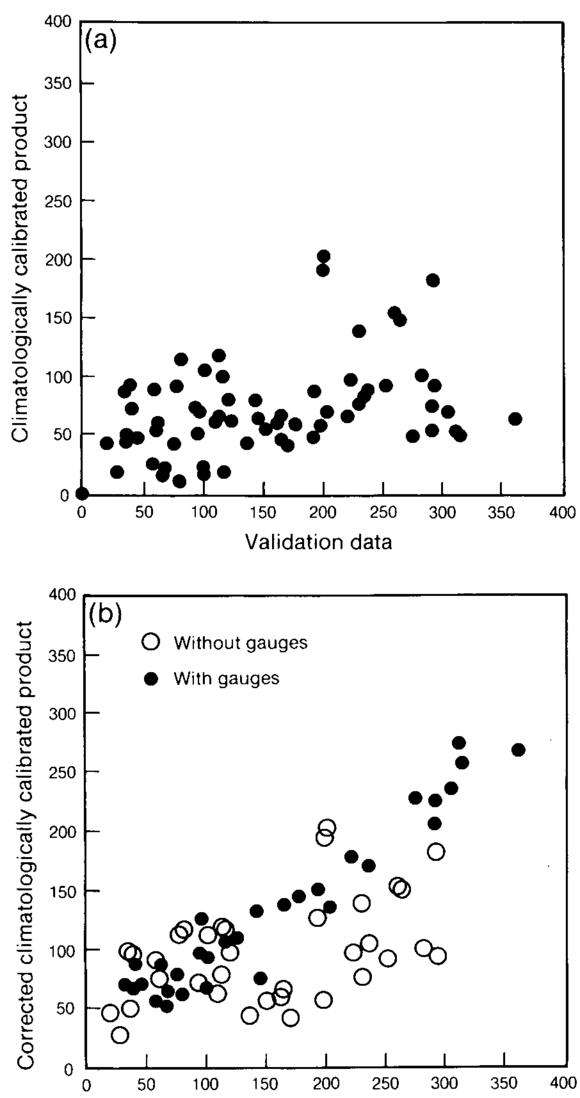

Figure 15. As Fig. 13 but for climatologically-calibrated PERMIT products.

Table III shows the errors in the daily estimates for the same series of products. In this case the collateral-data-only product was derived by evenly dividing the appropriate monthly product between the days of that month.

The inclusion of each data source (collateral, satellite, rain-gauge) creates a successive improvement in the rainfall estimates. The employment of the slot-count weighting function improved the daily estimates but degraded the monthly results to the point where the satellite input has no effect! This last result vindicates the use of the progressive refinement approach employed to improve the temporal resolution of the PERMIT method. Indeed, in light of these comparisons, it may be concluded that no attempt should have been made to improve the monthly estimates using slot-count information at all. A more strict implementation of the progressive refinement philosophy may well produce better daily estimates. For example, monthly estimated rainfall totals produced by the basic PERMIT algorithm could be unevenly distributed among the days of each month with the relative magnitude of each daily rainfall estimate related to the slot count for that 24-hour period.

4. Conclusions

Participating in the Pilot Algorithm Intercomparison Project of the GPCP, the RSU has successfully modified a number of satellite rainfall algorithms to operate over Japan. The PERMIT infrared algorithm was greatly enhanced to meet the product requirements of the intercomparison study. A number of promising new approaches to satellite rainfall monitoring techniques have been investigated. In particular, the progressive refinement approach used to enhance the PERMIT method appears to provide an effective strategy for the optimal extraction of rainfall information from infrared imagery despite the rather poor correlation of cloud-top temperature to rainfall area, intensity and duration. Also a combined passive microwave/infrared technique has been developed which gave an improved result over pure passive microwave techniques for the Japan data set.

These conclusions represent only a part of the scientific yield of the project. The comparison of the RSU products with results from other groups may be expected to generate considerable information upon the strengths and weaknesses of different satellite rainfall estimation strategies.

The GPCP AIP is part of an ongoing programme: a further algorithm intercomparison study, taking into account the lessons learned in the pilot Japanese study, is now being planned. This new study will cover a region of north-west Europe for a period in the late winter and early spring of 1991.

The use of the new progressive refinement approach to the generation of rainfall products from satellite and collateral data merits further investigation. In particular, much more work needs to be undertaken on the realistic assessment of the contribution made by each data source to the final product and upon the optimal integration of these individual components so as to maximize the information content of the final rainfall estimates. The results obtained from the validation stages of the present study indicates that the approach adopted did not employ the progressive refinement strategy to a sufficient extent, although to have done so would have been to be wise before the event. It would now be profitable to investigate a technique in which longer-term products are obtained from satellite images and other sources using one process, and then used in the derivation of shorter-term rainfall products by a completely separate procedure. In this manner the two stages could be independently developed and calibrated

Table III. Comparison of daily 1.25°-resolution rainfall products and validation data for various stages of the enhanced PERMIT algorithm

Inputs	R.m.s. error (% of mean rainfall) June 1989 (mm)	June 1989 (%)	15 July–15 August 1989 (mm)	15 July–15 August 1989 (%)
Calibration data	16.12	(187)	15.91	(215)
Calibration data + IR imagery	14.77	(171)	14.99	(203)
Calibration data + IR imagery + weighting function	13.73	(160)	13.22	(179)
Calibration data + IR imagery + weighting function + rain-gauge data	12.72	(148)	13.31	(180)

so as to make optimal use of all available data. Such an approach seems likely to be the best suited to presently available types of satellite and collateral data.

Further development of the combined passive microwave/infrared algorithm developed as a part this project would certainly benefit from the further application of the above strategy. The availability of a complete SSM/I data set including 85 GHz channel information would facilitate a much more realistic evaluation of this promising technique.

Acknowledgements

This Bristol participation in the GPCP AIP was funded by NERC under research grant GR3/7405.

References

Barrett, E.C. and D'Souza, G., 1985: The development of an objective range of dry day products for drought monitoring by Meteosat over Africa. Final Report for ESA and EARSeL (31 Dec. 1985) ESA Contract No. 6137/84/D/JS(SC).

Barrett, E.C., D'Souza, G. and Power, C.H., 1986a: Bristol techniques for the use of satellite data in raincloud and rainfall monitoring. *J Br Interplanet Soc*, **39**, 517–526.

Barrett, E.C. and Kidd, C., 1991: The mapping and monitoring of rainfall and other key variables by the SSM/I: some global and regional results. Final Report (Stage II) to the Universities Space Research Association, Columbia MD.

Barrett, E.C., Power, C.H., Beaumont, J., and Richards, T.S., 1986b: Cloud cover and rainfall in the Western Sahel. Final report to the NERC, Contract No. F60/C1/19 (30 June 1986).

Barrett, E.C. and Richards, T.S., 1989: Towards an operational system for the use of AVHRR data in Pakistan. Remote Sensing for Operational Applications. Technical Contents of the 15th Annual Conference of the Remote Sensing Society (13–15 September 1989), 41–46.

Grody, N.G., 1984: Precipitation monitoring over land from satellite using microwave radiometry. International Geoscience and Remote Sensing Symposium (IGARSS 1984). Strasbourg, France, 27–30 August, ESA SP-215-417-423.

Kidd, C., 1988: Passive microwave monitoring of rainfall over land. Ph.D. thesis, University of Bristol.

Kidd, C. and Barrett, E.C., 1990: The use of passive microwave imagery in rainfall monitoring. *Remote Sensing Rev*, **4**(2), 415–450.

Laughlin, C.R., 1981: On the effect of temporal sampling on the observation of mean rainfall. Precipitation measurements from space, Workshop Report. Goddard Spaceflight Centre, Greenbelt, MD. p D.59-D.66

Takahasi, K. and Arakawa, H., 1981: World survey of climatology. Vol. 9, Climates of Southern and Western Asia. Editor-in-Chief H.E. Landsberg. Amsterdam, Elsevier Scientific.

551.551:551.553.6(425)

Are gusts and lulls associated with directionality?

A.J. Baran

Meteorological Office, Bracknell

Summary

The question 'do gusts back or veer?' is addressed. It is generally believed that a gust should veer and a lull should back. This belief is tested using sonic anemometer wind measurements carried out by the Meteorological Research Unit at Cardington. The data represent near neutral and unstable conditions and were measured at a height of 6 m and 20 m on the 6 July 1990 and 19 June 1990 respectively. The resulting gusts and lulls have been analysed statistically by fitting a von Mises Probability Density Function to the gust and lull frequency distributions. From the data collected on the 6 July 1990 there is not enough evidence for asymmetry in the gust distribution to be able to state that gusts have a directional tendency. From the data collected on the 19 June 1990 there is evidence for an asymmetric gust frequency distribution but there is no evidence for asymmetry in the lull frequency distribution. A 10-second block average filter was applied to the 19 June 1990 data set in order to examine longer duration gusts. The results from this analysis indicate that there is no evidence, at the 5% level of significance, of asymmetry in the gust and lull frequency distributions. It is concluded that there is at most only very weak evidence for gusts and lulls being associated with a preferred direction.

1. Introduction

The motivation for the study of the veering of wind in gusts has come chiefly from the observed effects of gusts on structures, where the rapid fluctuations give rise to large lateral forces on a structure. This is particularly important from the point of view of wind turbines, as wind loading and wind directionality are important considerations for design. If gusts do have a directional tendency then this would be an important consideration at the design stage of a structure. Kristensen (1989) using different engineering examples, such as a building and an aeroplane, has constructed gust definitions for these situations.

It is generally believed that the wind veers in gusting. This is certainly believed by mariners and pilots: see for example Meteorological Office (1967, 1971). These books state, as literal truth, that the wind veers in gusts, but is the statement correct? The belief comes about because it is generally thought that a gust must be due to winds that originate higher in the atmosphere and, since winds veer across the boundary layer, low-level gusts must also veer. However, there are problems associated with this belief. Gusts are a turbulence phenomenon and turbulence can arise from frictional surface effects, shearing and convection. The frictional surface effect is determined by surface properties and should have no systematic influence on wind direction. If shear turbulence is produced locally then the gusts would not represent faster moving air being brought down from a higher level in the atmosphere to the surface, so there would be no reason for the winds to veer in gusts. In an atmosphere well mixed by convection, directional changes in the boundary layer are small, see Meteorological Office (1975).

The view that wind veers with increasing strength was initially supported by Giblett (1932) who measured changes in wind speed and direction over a period of 10–30 minutes. Giblett's period is not representative of the time-scale associated with gusts. The chosen period of between 10 and 30 minutes is within the spectral gap of the power spectrum representing surface wind speeds reported by van der Hovan (1957) and Ishida (1989), i.e. the region of little fluctuating wind speed. However, these results do not rule out the possibility that fluctuations do occur on some occasions. Lemone (1973) found fluctuating wind speeds of a period of 30 minutes associated with mesoscale convection. Brettle (1990) using 30-second averages of speed and direction came to the conclusion that wind veering in gusts could not be relied upon by mariners. Hisscott and Roberts (1991) using an independent method to Brettle found no evidence to support wind veering in gusts.

2. Data and site

The data were collected at the Meteorological Office Research Unit at Cardington. The horizontal (u, v) and vertical (w) components of the wind were measured with sonic anemometers 6 m and 20 m above the ground. The data were collected digitally with sampling at 20 Hz and 10 Hz respectively during near neutral and unstable conditions. Table I shows the basic statistics of the data set. Each set is 30 or 40 minutes long. There were no significant trends in the time-series of wind speeds over the recording duration. The 6 July 1990 and 19 June 1990 data sets were both filtered using a 1-second block average in order to remove the highest frequencies. A 10-second block average filter was applied to the 19 June 1990 data set to analyse longer-duration gusts. L = Monin–Obhukov length defined as

$$L = -\frac{u_*^3 T_a}{kg\overline{w'T'}}$$

where u_* is the friction velocity, k von Kärmän's constant, g acceleration due to gravity, T_a the absolute temperature, $\overline{w'T'}$ is the surface temperature flux and σ_s is the standard deviation of the horizontal wind. Estimates of L show that the 6 July 1990 data set is near neutral whilst the 19 June 1990 data set is slightly unstable. The area around Cardington is generally very flat: The local roughness length at the anemometer site is about 0.01 m; the area average roughness length is around 0.1 m, typical of land with fields, hedges and occasional trees.

3. Gust definition

The definition of a gust and a lull used was taken to be an increase or decrease in wind speed to an amplitude which was at least 1 σ away from the mean wind speed. The speed s and direction θ of the gust were calculated from the u, v components making up the gust where $s = \surd(u^2 + v^2)$ and $\theta = \arctan(v/u)$, the direction being measured relative to the mean wind direction. The duration of the gust was defined as the time taken for the gust to reach an amplitude and return to a minimum, usually taken to be a return to the mean wind. A similar definition was used by Bergström (1987) in analysing statistical characteristics of gusts.

4. The von Mises distribution function

In meteorology, wind direction measurements are based on angular measures defined on the circle. It is often tempting to use linear estimates of the mean,

Table I. Summary of Cardington data used, see text for explanation of symbols

Date (1990)	Start time (UTC)	Duration (min)	z (m)	$\bar{U}$ (m s^{-1})	σ_s (m s^{-1})	L (m)
6 July	1130	30	6	7.4	1.3	−250
"	1200	30	6	7.6	1.3	−182
"	1230	30	6	6.7	1.5	−286
"	1300	30	6	7.7	1.3	−250
"	1330	30	6	7.9	1.5	−200
"	1400	30	6	6.5	1.8	−158
19 June	1218	40	20	8.1	1.4	−63
"	1436	40	20	7.4	1.4	−79
"	1528	40	20	6.8	1.5	−94
"	1618	40	20	6.6	1.1	−47

though this is clearly erroneous as the following example illustrates. Let there be two measured angles 1° and 359° respectively, then the linear mean would give 180° which is absurd. The example given, though extreme, illustrates that when dealing with directional data it is more appropriate to use statistical measures defined on the circle rather than on the line. The data presented in this paper are directional and are best represented by a probability density function defined on the circle. A widely used model for directional data is the von Mises distribution function, first introduced by von Mises in 1981 when investigating whether atomic weights were integers. The von Mises probability density function is defined by the equation,

$$M(\theta, \mu, \kappa) = \frac{1}{2\pi I_0(\kappa)} \exp^{\kappa \cos(\theta-\mu)} \quad (1)$$

where $I_0(\kappa)$ is the modified Bessel function of the first kind and order zero defined by

$$I_0(\kappa) = \frac{1}{2\pi} \int_0^{2\pi} \exp^{\kappa\cos\theta}\, d\theta = \frac{1}{\pi} \int_0^{\pi} \exp^{\kappa\cos\theta}\, d\theta,$$

μ is the location point, κ the concentration parameter. The distribution function is analogous to Gauss's normal distribution function defined on the line. The location point behaves like a mean, being the point around which the wind direction tends to congregate. The concentration parameter corresponds to a variance about the mean wind direction. If the value of κ is large then the distribution function is highly concentrated about μ. The maximum likelihood estimates, $\hat{\mu}$ and $\hat{\kappa}$, of μ and κ are determined as follows. Let

$$\overline{\sin}\,\theta = \frac{1}{n} \sum_{i=1}^{n} \sin \theta_i,\ \overline{\cos}\,\theta = \frac{1}{n} \sum_{i=1}^{n} \cos \theta_i$$

then

$$\hat{\mu} = \arctan\left(\frac{\overline{\sin}\,\theta}{\overline{\cos}\,\theta}\right),\ R = \sqrt{\{(\overline{\sin}\,\theta)^2 + (\overline{\cos}\,\theta)^2\}}.$$

R is the length of the resultant, $\overline{OP}$, of a point P ($\cos \theta_i$, $\sin \theta_i$), $i = 1, ..., n$, defined on the circle, centre O. The value of $\hat{\kappa}$ corresponding to R is determined from a table such as that given by Mardia (1972). The fitting of the von Mises Probability Density Function (PDF) to the actual data can be tested by using the goodness-of-fit test (chi-square) defined by

$$\chi^2 = \sum \frac{(A-E)^2}{E} \quad (2)$$

where A is the actual frequency of events occurring within a bin width of size 10 or 15° and E is the expected frequency of events occurring within the bin width. E is calculated by integrating the PDF from equation (1) across the size of the bin width and then multiplying the integrated function by the total number of observations. In using equation (2) care must be exercised because the χ^2 distribution is only an approximation to the exact distribution of the quantity represented by the equation. It is known that E in each bin width should be greater or equal to 3 for the approximation to be valid. This is why the above bin widths have the range shown in Tables II–IV in order to ensure that the number of events in each bin width is large. The number of degrees of freedom is defined as the total number of bin widths minus the number of parameters in the PDF estimated from the data. Hypothesis testing is employed in order to ascertain whether there is a significant veering or backing. If μ is constrained to be zero in the PDF then the PDF will be symmetric about zero, which means there is no preferred direction. If μ is not constrained to be zero then the PDF will not be symmetric about zero and a preferred direction will be evident. From these two distribution functions, and from the difference between their χ^2 distributions, it is possible to test whether there is evidence for asymmetry in the distribution functions. For large samples the difference is distributed approximately as χ_1^2 (chi-square distribution of one degree of freedom). This property enables a goodness-of-fit test for the hypothesis that $\mu = 0$.

$$\chi^2_{\hat{\mu}=0} - \chi^2_{\hat{\mu}>0} = \chi^2_1. \quad (3)$$

Equation (3) comes from the mathematical theory of statistics. For a more detailed theoretical treatment the reader is referred to Silvey (1975) and Plackett (1971). Equation (3) describes the goodness-of-fit test where an extra constraint has been imposed on the distribution function by setting $\hat{\mu} = 0$. If $\chi^2_{\hat{\mu}=0} - \chi^2_{\hat{\mu}>0} > \chi^2_1$ then the hypothesis $\mu = 0$ is rejected. If $\chi^2_{\hat{\mu}=0} - \chi^2_{\hat{\mu}>0} < \chi^2_1$ then the hypothesis $\mu = 0$ is accepted. This does not mean that the distribution is symmetric, simply that there is no (or not enough) evidence for asymmetry.

5. Data analysis

The total number of gusts defined in the time-series for the 6 July 1990 using the 1-second filter was 198 out of a total time period of 3.0 hours. 58% of the gusts show backing whilst 42% show veering. The following distributional estimates were found using the procedure outlined in section 4: $\hat{\mu} = 1.9508$ and $R = 0.9815$. For $R = 0.98$, $\hat{\kappa} = 25.2522$ and for $R = 0.99$, $\hat{\kappa} = 50.242$, and by linear interpolation the maximum likelihood estimate of $\hat{\kappa}$ is 29.00. Table II shows the expected frequency calculated from the von Mises PDF against the actual frequency of gusts and lulls. It can be seen that the von Mises PDF fits well to the real data.

The data set obtained on the 19 June 1990 was similarly analysed. The number of gusts in this time-series was 129 with 58% veering and 42% backing which is opposite to what was found in the first data set. For the lulls there were a total number of 109 with 55% backing and 45% veering again opposite to the first data set. The distributional estimates were obtained as above

Table II. Expected and actual frequencies for a 1-second block average on 6 July 1990, using von Mises probability density function

Bin range	Gusts: $\hat{\kappa}=29$, $\hat{\mu}=1.95$		Bin range	Lulls: $\hat{\kappa}=21.0$, $\hat{\mu}=-2.91$	
	Frequencies			Frequencies	
	Actual	Expected		Actual	Expected
0–10	66	66.51	0–10	34	36.56
10–20	40	35.93	10–180	25	21.87
20–180	8	10.36	−(0–10)	40	43.59
−(0–10)	54	57.29	−(10–20)	36	28.40
−(10–20)	22	23.04	−(20–180)	8	12.57
−(20–180)	8	4.84			

Table III. As Table II but for 19 June 1990

Bin range	Gusts: $\hat{\kappa}=18.2$, $\hat{\mu}=-2.591$		Bin range	Lulls: $\hat{\kappa}=20.0$, $\hat{\mu}=2.74$	
	Frequencies			Frequencies	
	Actual	Expected		Actual	Expected
0–10	35	31.94	0–15	40	44.99
10–20	12	16.50	15–180	19	18.67
20–180	5	6.26	−(0–15)	39	36.03
−(0–10)	38	36.62	−(15–180)	11	9.29
−(10–20)	29	24.78			
−(20–180)	10	12.88			

Table IV. As Table III but for 10-second block averages

Bin range	Gusts: $\hat{\kappa}=45.0$, $\hat{\mu}=3.53$		Bin range	Lulls: $\hat{\kappa}=17.5$, $\hat{\mu}=2.56$	
	Frequencies			Frequencies	
	Actual	Expected		Actual	Expected
0–10	14	12.15	0–15	17	17.14
10–180	3	2.48	15–180	8	8.09
−(0–10)	17	17.70	−(0–15)	11	14.25
−(10–180)	9	9.68	−(15–180)	8	4.51

and are contained in Table III for 1-second average data.

A 10-second block average filter was also applied to this particular data set in order to examine the longer duration gusts. Table IV shows the resulting actual frequencies against the expected frequencies for the gusts and lulls. Table V shows the statistical results. The goodness of fit between the actual and expected frequencies can be tested using equation (2), noting that (from look-up tables) $\chi_1^2=3.841$.

The statistics show that there are gusts and lulls which may either back or veer, and in the last three cases there is no preferred sense in unstable conditions. Thus, the evidence for a preferred direction when such an event occurs is inconclusive, and is not supportive of the wind veering in gusty conditions. The behaviour would seem to indicate randomness.

6. Conclusion

The data set recorded on the 6 July 1990 suggested an asymmetry in the gust and lull frequency distribution functions opposite to the sense that one might expect, though the asymmetry present in both cases is weak. The second data set recorded on the 19 June 1990 has an asymmetrical gust distribution function but in the case of lulls there is no evidence to suggest an asymmetry. In the case of longer-duration gusts there is no evidence for an asymmetry in the gust and lull frequency distribu-

Table V. Statistical results, where G = gust, L = lull, B = backing, V = veering, NP = no performance, N = neutral, U = unstable, A = accepted and R = rejected.

G or L	Table	$\chi^2_{\hat{\mu}>0}$	$\chi^2_{\hat{\mu}=0}$	$\chi^2_{\hat{\mu}=0} - \chi^2_{\hat{\mu}>0}$	$\hat{\mu} = 0$	Sense	Stability
G	II	3.302	7.330	4.028	R	B	N
L		4.616	10.450	5.834	R	V	N
G	III	3.165	9.245	6.080	R	V	U
L		1.119	2.970	1.851	A	NP	U
G	IV	0.597	4.080	3.482	A	NP	U
L		3.462	3.841	0.378	A	NP	U

tions. The deviations from symmetry when they occur are only slight and are not significant enough to establish that the wind veers or backs in gusts. These results are very suggestive of random incidence of veering or backing in neutral or convective conditions. Although only one longer time-scale was examined there is no evidence to suggest that different results will be found for longer time-scales. The reproducibility of the fitting of the von Mises PDF to meteorological wind data which is directional in nature is also noted in all cases used in the analysis.

Acknowledgements

I would like to express my thanks to the following colleagues for their useful dialogue. R. Maryon for meteorological discussion and comments which have led to the improvement of the presentation of the paper. A. Grant for meteorological discussion and supplying the 6 July 1990 data set. Dr P. Hignett for supplying the 19 June 1990 data set. Dr M. Farrow for discussion on mathematical properties of the von Mises PDF.

References

Bergström, H., 1987: A statistical analysis of gust characteristics. *Boundary-Layer Meteorol*, **39**, 153–173.

Brettle, M.J., 1990: Wind direction and gusts. *Weather*, **45**, 373–375.

Giblett, M.A., 1932: The structure of wind over level country. *Geophys Mem, Meteorol Off*, No. 54.

Hisscott, C.A. and Roberts, A.P., 1991: Wind direction and gusts at Ronaldsway. *Weather*, **46**, 215–216.

Ishida, H., 1989: Spectra of surface wind speed and air temperature over the ocean in the mesoscale frequency range in JASIN-1978. *Boundary-Layer Meteorol*, **47**, 71–84.

Kristensen, L., 1989: In search of a gust definition. RisøNational Laboratory, Risø-M-2796.

Lemone, M.A., 1973: The structure and dynamics of horizontal roll vortices in the planetary boundary layer. *J Atmos Sci*, **30**, 1077–1091.

Mardia, K., 1972: Statistics of directional data. London, New York, Academic Press.

Meteorological Office, 1967: Meteorology for mariners. London, HMSO.

—, 1971: Handbook of aviation meteorology. London, HMSO.

—, 1975: Handbook of weather forecasting. (Unpublished, copy available in the National Meteorological Library, Brascknell.)

Plackett, R.L., 1971: An introduction to the theory of statistics. Edinburgh, Oliver and Boyd.

Silvey, S.D., 1975: Monographs on statistics and applied probability 7. Chapman and Hall.

van der Hovan, I., 1957: Power spectrum of horizontal wind in the frequency range 0.00007 to 900 cycles per hour. *J Meteorol*, **14**, 160–164.

The winter of 1990/91 in the United Kingdom

G.P. Northcott
Meteorological Office, Bracknell

Summary

The winter of 1990/91 was generally cold and, in most areas, wet; many areas had more sunshine than usual, although it remained dull over part of north-west Scotland.

1. The winter as a whole

Mean temperatures over the winter season were below normal nearly everywhere, apart from Shetland, Orkney and the Isle of Lewis, ranging from 0.4 °C above normal at Lerwick, Shetland to 1.6 °C below normal at Fowey, Cornwall. Rainfall amounts over the winter period were above normal in western and southern Scotland, but below normal in Orkney, Shetland, eastern Scotland and Northern Ireland; much of England and Wales was wet, with the notable exception of the Merseyside and Greater Manchester areas, parts of Lincolnshire and East Anglia, and the southern coastal counties from Cornwall to Kent. Amounts ranged from nearly 179% at Kielder Castle, Northumberland to 68% at Manston, Kent. Sunshine amounts were about normal over Scotland as a whole, although part of north-west Scotland had a very dull winter, and generally above normal over England, Wales and Northern Ireland, and ranged from 187% of average at Buxton, Derbyshire to as little as 55% of average at Kinlochewe, Highland Region.

Information about the temperature, rainfall and sunshine during the period from December 1990 to February 1991 is given in Fig. 1 and Table I.

2. The individual months

December. Mean monthly temperatures were generally about normal for the month, and ranged from 0.8 °C above normal at Fyvie Castle, Borders Region to 1.4 °C below normal at Fowey, Cornwall. Brooms Barn, Suffolk reported the coldest December since 1982. Monthly rainfall totals were generally above normal in the north and west and below normal in the south and east, with nearly twice the average in parts of southern Scotland and northern England but only just over half the average on the south coast. Monthly sunshine amounts were generally above average except for parts of western Wales, eastern England and central areas of Scotland, ranging from more than 180% at Belfast Airport to 61% in the Edinburgh area.

On the 7th and 8th snowfall was very heavy over northern England, Wales, the Midlands and south-west England, with heavy drifting in gale-force winds, causing considerable disruption to traffic of all sorts and cutting power lines. The snow did not freeze, however, but melted very rapidly during the next few days, as the temperature rose a little. On the 11th and 12th storm-force winds swept down the North Sea; Fair Isle, Shetland had a gust to 73 kn. From the 23rd until the

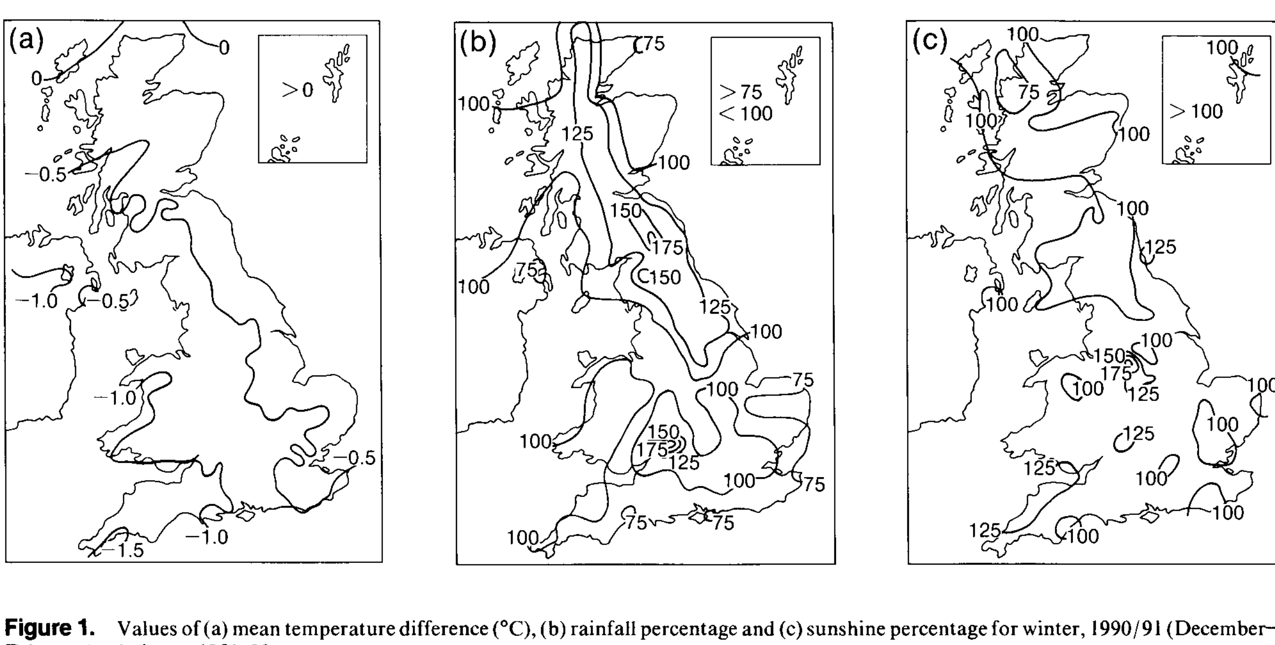

Figure 1. Values of (a) mean temperature difference (°C), (b) rainfall percentage and (c) sunshine percentage for winter, 1990/91 (December–February) relative to 1951–80 averages.

Table I. District values for the period December 1990–February 1991, relative to 1951–80 averages

District	Mean temperature (°C)	Rain-days	Rainfall	Sunshine
	Difference from average		Percentage of average	
Northern Scotland	−0.1	−1	96	98
Eastern Scotland	−0.3	−2	112	104
Eastern and north-east England	−0.3	0	128	104
East Anglia	−0.6	−2	88	107
Midland counties	−0.8	−1	100	112
South-east and central southern England	−0.7	−1	98	108
Western Scotland	−0.6	−1	104	100
North-west England and North Wales	−1.0	−2	110	113
South-west England and South Wales	−1.4	−2	101	121
Northern Ireland	−0.7	−2	90	122
Scotland	−0.3	−2	102	101
England and Wales	−0.7	−1	105	111

Highest maximum: 14.8 °C in Midland counties in February.
Lowest minimum: −14.8 °C in western Scotland, also in February.

end of the month very strong winds and bands of rain, often prolonged and heavy at times, crossed many parts. On the 25th and 26th gales and storm-force winds affected many areas. Gusts of more than 70 kn were reported at Greenock Port, Strathclyde Region, Langdon Bay, Kent, Camborne, Cornwall, Plymouth, Devon and Killough and Orlock Head in Northern Ireland and on the 25th there were reports of tornadoes over Devon, Somerset and Avon. Sleet and snow were reported as far south as South Wales on the 27th and Towy Castle, Dyfed reported hailstones of 15 mm diameter. On the 29th a whirlwind caused extensive damage to houses in Gorseinon, South Wales, and a cottage in North Wales was hit by lightning. Towy Castle reported a whirlwind crossing the station with a maximum height of 35 m at 11 h on the 30th.

January. Mean monthly temperatures were above normal in northern Scotland and central and south-eastern England including East Anglia, and below normal elsewhere, ranging from 1.5 °C above normal at Bexhill, East Sussex to 1.5 °C below normal at the Lizard, Cornwall. Monthly rainfall totals were above normal everywhere, except in eastern Scotland, the Western Isles, East Anglia, and in northern and eastern England; the area around Aberdeen had about 30% of normal and nearby Fyvie Castle had as little as 20% of normal. In contrast Ardtalnaig, Tayside Region and Newton Rigg, Cumbria had more than 160% of normal rainfall. Over Northern Ireland as a whole it was the driest January since 1972. Monthly sunshine amounts were above average nearly everywhere, although it was rather dull over much of western and south-western Scotland, and ranged from 202% of average at Tynemouth, Tyne and Wear to as little as 69% of average at Kinlochewe, Highland Region. It was the sunniest January over Northern Ireland since 1959 and at Wick, Highland Region since records began there in 1946.

The weather was frequently stormy during the first week, with strong winds, rain and snow, and long sunny periods in between. On the 1st, periods of heavy rain aggravated by rapidly melting snow caused flooding in many areas of southern Scotland. On the 5th, gales coupled with high tides caused extensive and costly damage to parts of western and southern coasts from Strathclyde to Sussex, as the sea breached defences. There was considerable flooding in many areas and disruption to power supplies and transport, especially in the west. After the 10th the month was generally dry, although there was rain in many places between the 17th and 20th, and snow in some western areas on the 30th and 31st. Thundery outbreaks were frequent and widespread between the 3rd and 7th. There were isolated reports of thunder on the 9th and 10th and a broad area of thundery activity over south-east England on the 11th.

February. Mean monthly temperatures were below normal nearly everywhere and ranged from 0.1 °C above normal at Lerwick, Shetland to 3.1 °C below normal at Greenwich, Greater London. Monthly rainfall totals were above normal in most parts of eastern Scotland and eastern England and generally below normal elsewhere, ranging from 187% at Durham to as little as 36% at Fort William, Highland Region. Monthly sunshine amounts were generally above average in western areas and below average on eastern coasts, ranging from 142% at Tiree, Strathclyde to 62% at Boulmer, Northumberland.

February was unsettled throughout, with cold weather and frequent falls of snow during the first half. Some sleet or snow showers fell during the first five days of the month. Between the 6th and 14th snowfall was heavy in many places and it became very cold for a few days. On the 6th many parts had snow showers during the day, especially in the east: Anvil Green, Kent reported 6 cm of snow lying. Snow showers over the North Downs overnight gave a cover in most areas by the morning of the 7th; later that day up to 14 cm of level snow lay in some places. During the following night falls of snow over England and Wales, heavy at times, gave up to 20 cm in places as far apart as Essex, mid Wales and Yorkshire. Depths were very variable, however, with 47 cm at Wilsden, West Yorkshire, 35 cm at Pencelli, Powys and 20 cm at St James's Park, central London, probably the greatest depth in London since the end of December 1962. On the 9th some areas had heavy snowfall; some notable depths included 51 cm at Wilsden, 35 cm at Pencelli and 30 cm at Honington, Suffolk; over the next few days snow depths included 45 cm at Fylingdales, North Yorkshire on the 12th, 46 cm at Longframlington, Northumberland on the 13th, and 15 cm at East Hoathly, East Sussex on the 14th. After mid month it became somewhat milder, although remaining generally wet and at times windy. On the 8th there was some thundery activity over eastern parts of England. A thunderstorm was reported to the west of London during the 27th.

551.593.653(4).551.506.1

Noctilucent clouds over western Europe during 1990

D.M. Gavine
29, Coillesdene Crescent, Edinburgh EH15 2JJ

Summary

Noctilucent cloud observations by voluntary and professional observers in the British Isles, Denmark and The Netherlands suggest a lower incidence of the phenomenon than in recent years.

Table I summarizes the noctilucent cloud (NLC) reported to the Aurora Section of the British Astronomical Association (BAA) during 1990. The times (UT) are the reported sightings, not necessarily the duration of a display. 'Negative' nights (Table II) are based on the judgement of two or more experienced observers north of 54° N with clear or nearly clear sky conditions over the period of the night when NLC is likely to occur.

Table I. Displays of noctilucent clouds over western Europe during 1990

Date — night of	Times UT	Notes
22/23 May	2135–2310	Bands, billows and whirls at Chelmsford, Reading and Godalming; NLC at Rotterdam; faint structures visible in Denmark — suspected auroral light with NLC at Vildbjerg 2230–2310, and at Kemnay near Aberdeen.
23/24	2229–2300	Faint bands at elev. 16°, Vildbjerg; no NLC in clear sky in Scotland and I. of Man.
24/25		Suspected faint NLC at Ronaldsway but no NLC in clear sky in Scotland and Morpeth.
25/26	2345–0130	Moderately bright veil and bands to elev. 12° at Vildbjerg, greenish NLC in dawn sky at Rotterdam. No NLC in Scotland and Morpeth.
2/3 June	0000–0200	Suspect faint NLC at Kemnay. No NLC at Edinburgh and Morpeth.
7/8	0240	Suspect billows to elev. 45° at Upton on Severn.
12/13 June	2300	'Silvery' NLC in NW to elev. 40°, Co. Clare, aurora observed at Rønne, Bornholm.
17/18	2240	Moderately bright bands in tropospheric cloud breaks at Rønne.
19/20	2140–0230	Moderately bright and extensive display, all forms, described by 16 observers from Kirkwall to London. Maximum elevs 70° (Alness), 56° (Morpeth), 40° (Upton), 10° (Witham, Essex).
22/23	2110–2150	Suspect bands and patches at Upton. No NLC in I. of Man or in Scotland 2230–2300.
23/24	2130–0115	Faint bands, billows and patches visible in binoculars at Morpeth and Upton. No NLC at Rønne or in Scotland 2305–0030.
24/25	0020–0115	No NLC up to 0000. Faint bands in Ayrshire, very faint NLC at Morpeth.

Date — night of	Times UT	Notes
27/28 June	0005–0130	No NLC before 0000. Very faint bands, slight billows, Ayrshire, Machrihanish and Edinburgh.
28/29	0100–0200	Faint bands at Dundee and Aberfeldy. No NLC at Alness 2315.
29/30	2200–2330	Faint bands and whirls to elev. 9°, Vildbjerg. No NLC visible at Rønne.
30/01	2100–2130	Bands and billows to elev. 15°, Rotterdam.
2/3 July	2300	Moderately bright bands reported at Aberfeldy but NLC reported absent at Machrihanish, Milngavie and I. of Man.
3/4	2315–0000	Faint bands at elev. 6°, Rønne.
7/8		Positive NLC sighting at Kemnay, no details.
8/9	2330–0130	Faint bands in trop. cloud at Morpeth, NLC at Kemnay. No NLC at Rønne but very faint bands visible in binoculars at Vildbjerg.
10/11	2120–0145	Fairly bright display, all forms, visible from Kinloss to Chichester, and Wadebridge, Cornwall. Max. elev. at Morpeth 24°. Photographed by Mr Trafford at Cambridge. 'Chaotic' silvery-blue NLC at De Bilt, bands and billows at Rotterdam and Deventer.
11/12	2156	Very faint bands visible in binoculars, Vildbjerg. No NLC at Morpeth and I. of Man.
14/15	2350	Small faint NLC patch reported at Stirling but negative reports from 3 other Scottish stations, Morpeth and Rønne.
16/17	2240–0240	Moderately bright veil, bands, billows and patches at Wick (elev. 22°), Kinloss, Ayrshire and Pensarn (N. Wales). No NLC in Scotland before 2345.
17/18 July	2200–0320	Fairly faint veil, bands, billows and patches from Wick to N. Wales. NLC in zenith at Carlisle 2200.
19/20	2200–0030	Fairly faint bands, billows and whirls to elev. 11° at Vildbjerg, NLC reported 0030 to dawn by MV *Selectivity* in Kiel Canal. Faint bands suspected near zenith in Carlisle 2200 but no NLC reported in I. of Man.
21/22	2115–2245	No NLC in Scotland 2200–0000. Faint veil at Wick and Morpeth, faint patches at Carlisle. No NLC at I. of Man.
23/24	2025–2215	No NLC in Scotland, I. of Man or Morpeth. Dr Smeaton observed NLC at Helsinki.
24/25	2300	Faint veil at Alness. No NLC at Morpeth or I. of Man. Mr Trafford observed NLC at Helsinki 2100.
25/26	2130–0115	Faint bands, billows and whirls at Vildbjerg elev. 9°, to 2330. MV *Selectivity* at 56° 47′N, 12°E reports bands at elev. 40°, 0045–0115. No NLC at I. of Man and Machrihanish.
26/27	2145–0250	Bright bands and patches at Kinloss and Alness, described as intense electric-blue, photographed by Mr Fraser. No NLC at Rønne but faint bands at Vildbjerg and MV *Selectivity* in the Baltic. Drs Fischer and Hombich photographed very bright horizontal bands with aurora above from Baltic ferry at lat. 59°N.
31/Aug 1	2055–2325	Very faint veil, bands and billows visible in binoculars at elev. 6° at Vildbjerg. No NLC at Rønne.

Table II. Negative nights (British Isles) north of latitude 54° N

May 18/19; 19/20; 20/21; 26/27; 27/28; June 1/2; 3/4; 5/6; 13/14; 14/15; 18/19; 20/21; 21/22; July 5/6; 18/19; 20/21; 22/23; 28/29 (aurora), 30/31; Aug. 1/2.

Despite many clear nights there were 25 positive and 6 suspected sightings, a lower incidence than in recent years. Of these, only 4 displays were noteworthy, many were very faint, some were found only by a binocular search by dedicated amateur observers.

Contributions were received from 27 individual observers and 5 meteorological stations in the United Kingdom, 3 stations of the Royal Netherlands Meteorological Institute, 3 observers in Denmark, 1 in Eire and 1 UK observing vessel. Again, the superb photography by Mr Olesen and Mr Andersen of Denmark has enhanced BAA meetings and exhibitions. Details of Finnish-Estonian NLC sightings are not now mentioned here, but are published annually in the journal *Ursa Minor* of the URSA Astronomical Association (Laivanvarustajankatu 3, SF-00140 Helsinki 14).

As before, the intention of the BAA Aurora Section is to provide a data bank in both aurora and NLC for professional workers. Details of individual NLC nights are available from the author, but all NLC data up to 1988 are held in the Balfour Stewart Archive at the University of Aberdeen.

Our thanks to all observers, amateur and professional (we would like to encourage more professional input into the survey), and to Mr Ron Livesey, Director of the BAA Aurora Section, Mr Tom McEwan, Director of the Junior Astronomical Society Aurora Section, Mr V. Mäkelä (Finland), Dr B. Zwart (The Netherlands), Mr M. Zalcik (USA–Canada NLC Network), and Dr M. Gadsden (University of Aberdeen).

Correction

Meteorological Magazine, September 1991, p. 168, Table III.

The heading above the years should read 'Effective precipitation' and not 'Soil moisture deficit'.

Reviews

Principles of air pollution meteorology, by T.J. Lyons and W.D. Scott. 157 mm × 235 mm, pp. vi+224, *illus.* London, Belhaven, 1990. Price £25.00. ISBN 1 85293 079 9.

This very readable book is a very useful addition to the library of anyone concerned with air pollution. The text covers a wide range of relevant topic-areas: the nature of the atmospheric boundary layer, diffusion theory, the chemical and physical properties of pollutants, the techniques of monitoring and the impact of pollution on crops and the environment. It ends with brief descriptions of many current commercially available computer models developed mainly in the USA.

However, being only some 200 pages long one cannot expect, and one does not get, anything like a complete cover of all these topics. What you do get is a useful 'flavour' of the subject, a background which will be helpful in reading other more up-to-date and specialized papers and books. The authors develop some aspects within each area, giving them fullish treatment, whilst other aspects are glossed over rather more hurriedly. For example, the section on atmospheric diffusion goes into *K*-theory in some detail, but gives too little emphasis (if any) to higher-order closure schemes, to similarity theory or random-walk techniques and allied methods which are much more widely used these days than *K*-theory. There is also little discussion on modern perceptions of dispersion in convective conditions or on gravity flows at night. The effects of complex terrain on dispersion and rain-out from precipitating clouds are not mentioned. These are all important matters.

But I do not wish to damn the book; on the contrary it has many good points, many points are very well explained and overall the book gives a very helpful introduction provided the reader goes on to read other texts. It is very readable, you can dive in almost anywhere and quickly pick up and understand the message, a virtue that is to be highly commended! The book is nicely produced with clear text and good diagrams, with very few typographical errors, and all at a sensible price.

F.B. Smith

Impact models to assess regional acidification, edited by J. Kämäri. 162 mm × 245 mm, pp. xvi+310, *illus.* Dordrecht, Kluwer Academic Publishers, 1990. Price Dfl.195.00, US$115.00. £71.50. ISBN 0 7923 0710 0.

When summoned to meetings at the National Radiological Protection Board at Harwell, I frequently drive across country from Theale to East Ilsley, saving miles and gaining solitude from the quiet leafy lanes of Berkshire. Over the last few years, however, the journey has been tinged by sadness at seeing so many once-splendid beech trees slowly dying, their leaves turning a sickly yellow long before the autumn frosts bring natural colouring to our woodlands.

I feel some guilt too, since my car's exhaust gases are adding their small share to the acidification of the land, which in part may be the cause of the sorry state of the beeches that once ennobled the surrounding landscape.

Questions race through my mind as I drive: just how much pollution can the land take before it really begins to suffer? Are we already overloading the soil and will devastation become increasingly apparent across the land as the years go by? When and where and by how much do we need to reduce emissions? What will be the cost? ...

For 20 years scientists have been trying to come to terms with acidification problems. At first the emphasis was on trying to discover the extent and rate of acidic deposition. Then came attempts to model the complex processes taking place within the atmosphere from emissions, through transport and dispersion, through complex chemical changes, and eventually through removal processes leading to deposition. At the same time others have been studying the effects of acidic depositions on soils, trees, waters, fish and other wildlife. Much has been learnt. The concept of critical loads has been proposed — the idea that any area can cope with long-term depositions up to some critical level above which serious damage to the environment will occur. Due to many spatially varying factors the critical loads can be expected to vary from one area to another. Work has also started on so-called emission abatement strategies whereby over a large area like Europe emission–deposition relationships are studied so that emissions may be 'intelligently' reduced in those areas where the benefit to the environment as a whole will be greatest, taking into special account areas where current loads exceed their critical loads.

This brings me to the book under review. It contains 14 papers either presented during, or written as a result of, a Task Force Meeting on 'environmental impact models designed to assess regional acidification' held in 1987 in Warsaw. The papers have been brought together in this useful and nicely produced volume by Juha Kämäri, one of the organizers of the meeting.

Although not of great direct meteorological interest, the book does provide much useful information concerning the topics outlined above, and in so doing has considerable bearing on the development of environmentally orientated meteorological transport and deposition models. The book should therefore find its place in all meteorological libraries where such models are developed.

F.B. Smith

A field test of thermometer screens, by T. Andersson and I. Mattisson. 209 mm × 296 mm, pp. 40, *illus.* Norrköping, Sweden, SMHI, 1991. ISSN 0347 2116.

This gives results from an 11-month-long experiment comparing the performance of three standard SMHI 'Stevenson' screens with that of five smaller commercial screens (the Vaisala, Young, Lambrecht...on ordinary and long poles...also the Teledyne). One Stevenson screen was small (40 cm × 40 cm × 68 cm); the other two were large (70 cm × 53 cm × 81 cm), one having clean white louvres while the other was older and deliberately left in 'bad' condition with some paint having flaked off, leaving bare wood in places.

The 'Teledyne 327B' is motor-aspirated (and may be regarded as a development of the Assman psychrometer). In the opinion of the authors, it was taken as the reference for this experiment 'to get as good an estimate as possible of the air temperature', but that premise calls into question the validity of the American manufacturer's (1984) claims for accuracy and performance of the ventilated Teledyne, which appear to have been merely presented at face value (as Appendix 1) where engineering drawings would have helped an appreciation of the instrument, not to mention prior testing and results.

One difficulty with taking a ventilated instrument as the standard reference (against which non-aspirated thermometers are compared) concerns probable artificiality of the temperature where naturally stagnating air is forced into motion during calm conditions. Aspirated entrainment of air from non-standard heights above ground level could have produced the large differentials (of 2–3 °C) recorded on 13 December 1989, a day of clear skies, light winds and a snow cover...see p. 10. Other situations of (1) strong temperature inversion or (2) rapid lapse rate changes (e.g. during showers) were found to produce large differentials of between 3 and 3.5 °C (e.g. on 28 June 1989).

This latter situation, of summertime showers producing sudden cooling of surfaces appeared to show a pronounced 3 °C 'lag' of temperatures recorded by the large 'Stevenson' screen in bad condition. Alternatively, it could be argued that some of the instruments in the smaller, novel screens read too low because they did not shield their thermometers well enough! This is because, to some extent, the temperature of the enclosure surfaces (aluminium in the case of the Lambrecht's) is being measured. Nevertheless, solar heating from received radiation was more-efficiently absorbed, stored, and re-radiated by the bare wooden patches on the older 'Stevenson' and the moral to observers is that screens should not be allowed to fall into neglect — temperature discrepancies will result if louvres are not kept clean and white.

Despite the rather-limited test period (from April 1989 to February 1990) which included a relatively mild winter in Sweden, some interesting comparisons were made by continuous monitoring in various weather conditions, and the results are well presented. However, the basic purpose of a thermometer screen is to isolate its instruments from ambient radiative surfaces, and this commendable experiment has shown that some of the smaller commercial screens do not achieve this because they are influenced by the materials of which they are made.

The difficulties in keeping roadside 'Stevenson' screens in good condition are noted and, one hopes, more-modern construction techniques may allow improvements (such as white plastic lamination of the wooden louvre surface) in their manufacture.

W.S. Pike

Books received

The listing of books under this heading does not preclude a review in the Meteorological Magazine at a later date.

Satellite remote sensing in climatology, by A.M. Carleton (London, Belhaven Press, 1991. £39.50) emphasizes the contribution of satellite data to climate theory. Also emphasized is the monitoring of possible human impacts on the climate system. ISBN 1 85293 039 X.

Fractals: endlessly repeated geometrical figures, by H. Lauwerier (London, Penguin Books, 1991) explains the basic mathematics of fractals, and is intended for a wide audience. Constructing fractals with computer programs (answers in the back) is included. ISBN 0 14 014411 0.

Mid-latitude weather systems, by T.N. Carlson (London, Routledge, 1991. £75.00 (hardback), £19.95 (softback)) attempts to present a fusion of synoptic and dynamic meteorology. Conventional weather charts together with equations are used to illustrate the evolutions of weather patterns. ISBN 0 04 551115 2, 0 04 551116 0.

GUIDE TO AUTHORS

Content

Articles on all aspects of meteorology are welcomed, particularly those which describe results of research in applied meteorology or the development of practical forecasting techniques.

Preparation and submission of articles

Articles, which must be in English, should be typed, double-spaced with wide margins, on one side only of A4-size paper. Tables, references and figure captions should be typed separately. Spelling should conform to the preferred spelling in the *Concise Oxford Dictionary* (latest edition). Articles prepared on floppy disk (IBM-compatible) can be labour-saving, but only a print-out should be submitted in the first instance.

References should be made using the Harvard system (author/date) and full details should be given at the end of the text. If a document is unpublished, details must be given of the library where it may be seen. Documents which are not available to enquirers must not be referred to, except by 'personal communication'.

Tables should be numbered consecutively using roman numerals and provided with headings.

Mathematical notation should be written with extreme care. Particular care should be taken to differentiate between Greek letters and Roman letters for which they could be mistaken. Double subscripts and superscripts should be avoided, as they are difficult to typeset and read. Notation should be kept as simple as possible. Guidance is given in BS 1991: Part 1: 1976, and *Quantities, Units and Symbols* published by the Royal Society. SI units, or units approved by the World Meteorological Organization, should be used.

Articles for publication and all other communications for the Editor should be addressed to: The Chief Executive, Meteorological Office, London Road, Bracknell, Berkshire RG12 2SZ and marked 'For Meteorological Magazine'.

Illustrations

Diagrams must be drawn clearly, preferably in ink, and should not contain any unnecessary or irrelevant details. Explanatory text should not appear on the diagram itself but in the caption. Captions should be typed on a separate sheet of paper and should, as far as possible, explain the meanings of the diagrams without the reader having to refer to the text. The sequential numbering should correspond with the sequential referrals in the text.

Sharp monochrome photographs on glossy paper are preferred; colour prints are acceptable but the use of colour is at the Editor's discretion.

Copyright

Authors should identify the holder of the copyright for their work when they first submit contributions.

Free copies

Three free copies of the magazine (one for a book review) are provided for authors of articles published in it. Separate offprints for each article are not provided.

Contributions: It is requested that all communications to the Editor and books for review be addressed to the Chief Executive, Meteorological Office, London Road, Bracknell, Berkshire RG12 2SZ, and marked 'For *Meteorological Magazine*'. Contributors are asked to comply with the guidelines given in the *Guide to authors* (above). The responsibility for facts and opinions expressed in the signed articles and letters published in *Meteorological Magazine* rests with their respective authors.

Subscriptions: Annual subscription £36.00 including postage; individual copies £3.25 including postage. Applications for postal subscriptions should be made to HMSO, PO Box 276, London SW8 5DT; subscription enquiries 071—873 8499.

Back numbers: Full-size reprints of Vols 1—75 (1866—1940) are available from Johnson Reprint Co. Ltd, 24—28 Oval Road, London NW1 7DX. Complete volumes of *Meteorological Magazine* commencing with volume 54 are available on microfilm from University Microfilms International, 18 Bedford Row, London WC1R 4EJ. Information on microfiche issues is available from Kraus Microfiche, Rte 100, Milwood, NY 10546, USA.

February 1992

Vol. 121
No. 1435

Contents

ISSN 0026–1149

ISBN 0-11-728980-9

9 780117 289802

Printed in the United Kingdom for HMSO
Dd 291241 C13 2/92 12521

The Meteorological Magazine

March 1992

Assessment of model fluxes
Traffic accidents in hail showers

HMSO

Met.O.1004 Vol. 121 No. 1436

First published 1992

HMSO

HMSO publications are available from:

HMSO Publications Centre
(Mail and telephone only)
PO Box 276, London, SW8 5DT
Telephone orders 071-873 9090
General enquiries 071-873 0011
(queuing system in operation for both numbers)

HMSO Bookshops
49 High Holborn, London, WC1V 6HB 071-873 0011 (counter service only)
258 Broad Street, Birmingham, B1 2HE 021-643 3740
Southey House, 33 Wine Street, Bristol, BS1 2BQ (0272) 264306
9–21 Princess Street, Manchester, M60 8AS 061-834 7201
80 Chichester Street, Belfast, BT1 4JY (0232) 238451
71 Lothian Road, Edinburgh, EH3 9AZ 031-228 4181

HMSO's Accredited Agents
(see Yellow Pages)

and through good booksellers

The
Meteorological Magazine

March 1992
Vol. 121 No. 1436

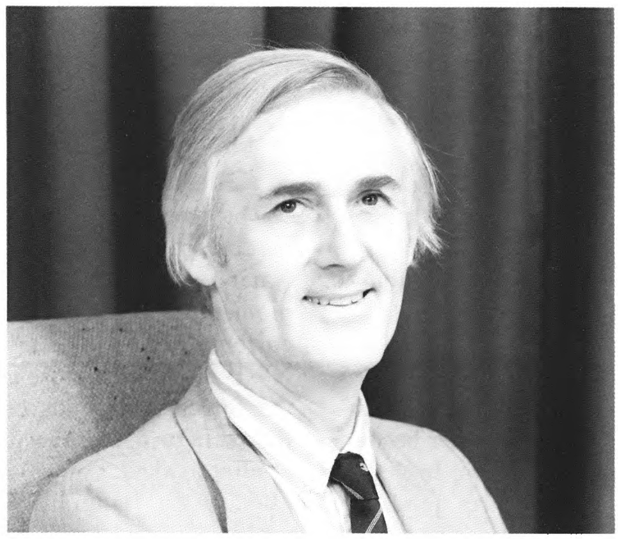

Appointment of Chief Executive of the Meteorological Office

Professor Julian Hunt, MA, PhD, FIMA, FRMetS, FRS was appointed to succeed Sir John Houghton as Chief Executive of the Meteorological Office from 1 January 1992.

Professor Hunt was previously Professor of Fluid Dynamics with the University of Cambridge's Department of Applied Mathematics and Theoretical Physics. Recently he has been involved in a project with his University, the Meteorological Office and National Power to develop an advanced method of calculating dispersion in the atmosphere and also making more use of the advances in meteorological understanding. He held a Readership there from 1978 to 1990, when he was promoted to a Personal Chair. He was elected a Fellow of the Royal Society in 1989.

Professor Hunt, now 50, was a pupil at Westminster School and then gained First Class Honours in Mechanical Sciences at the University of Cambridge. He was awarded his PhD for his work on Aspects of Magnetohydrodynamics.

His appointment reflects the importance the Meteorological Office attaches to retaining the high professional and scientific standards for which it is noted throughout the world.

Professor Hunt's impressive career has fitted him superbly to direct further improvements in forecast accuracy, and research into climate change. His management and commercial experience will also be invaluable: the Meteorological Office as an Executive Agency must satisfy a vast range of technical and financial requirements.

Professor Hunt, accepting the appointment, said:

For a large part of my career I have been intimately involved in scientific research allied to meteorology. I am delighted and honoured to have been chosen as Chief Executive of such a prestigious organization. I have for many years been impressed by the developing range of high-quality services provided by the Meteorological Office to its clients, as well as to the quality of its research. The Office has a well deserved international reputation of the highest order and I am excited at the prospect of becoming identified with it.

Ocean Forecasting

Nina Morgan
Science writer

1. Introduction

Ocean forecasting lags far behind atmospheric weather forecasting. In theory the oceans and the atmosphere obey the same physical laws, but in practice, ocean forecasting has some special requirements.

People who depend on the land for their livelihood can rely on daily, detailed, accurate forecasts of the weather thanks to the development of numerical weather prediction (NWP) methods which use mathematical models, real-time weather observations and large computers which project motions of the atmosphere forward in time-steps using physical equations.

The Royal Navy, concerned with events in the oceans, require detailed daily ocean forecasts, and those which give information about temperature and salinity throughout the ocean depths. Horizontal resolutions of 10 km or less for these ocean models will probably not be available before the end of the century.

2. Related circulation systems

The oceans, which cover more than 70% of the Earth's surface, have a great influence on the weather because they act as a huge heat and moisture reservoir. In climate modelling, which concentrates on long-term trends, the effects of clouds and the oceans are two major unknowns. Because ocean circulation occurs over a very long time-scale, ocean models are commonly coupled to climate models.

3. Important differences

The ocean and the atmosphere interact at the sea surface by exchanging fluxes of momentum, heat and moisture across the sea–air interface. There are, however, some important differences between atmospheric and ocean circulation systems which affect the way their behaviour can be modelled.

Atmospheric circulation is driven by heat from the Sun and the Earth's rotation with pressure systems ranging up to thousands of kilometres wide. Ocean circulation is driven primarily by fluxes of heat (including heat from the sun), fresh water, and momentum, or wind stress, at the interface between the air and the sea surface. The oceanic equivalent of atmospheric pressure systems are on scales of tens to hundreds of kilometres. Therefore, accurate modelling of ocean systems requires a higher resolution than that needed to model the atmosphere. This, in turn, requires greater computing power.

4. Improving ocean forecasts

Models suitable for ocean forecasting are being used for long-term ocean climate studies. Input of the surface fluxes; heat, moisture and momentum, calculated from atmospheric NWP forecasts, is essential. The quality of these flux data from the NWP must be very high, and this can be achieved by iterative changes to the flux equations.

Further improvements will come with more accurate real-time weather data gathered from global weather observations. Weather stations are particularly sparse over the oceans, but the new generation of meteorological satellites, such as the recently launched ERS-1, will help to fill the data gap.

5. Quality of fluxes

The three major fluxes which influence the ocean models are heat (which affects ocean temperature), fresh water (which affects the salinity of the ocean), and momentum (or wind stress) which drives the ocean currents. The forecasts and the fluxes produced by NWP models are closely interlinked. The accuracy of the forecasts depends on the calculation of accurate fluxes. In turn, more accurate forecasts will lead to more accurate calculation of fluxes. The formulae used to calculate the fluxes in NWP models are approximations, which give results that may have significant errors.

In 1991, J.O.S. Alves of the Meteorological Office suggested improvements to the calculation of momentum fluxes in the North Atlantic (*Meteorological Magazine*, November 1991). In this issue, he goes on to analyse the problems involved in accurate calculation of heat and fresh-water fluxes.

Many of Alves' suggestions have already been incorporated in the new Meteorological Office Unified Model. His next task will be to assess the fluxes in the Unified Model. Suggestions made by Alves for improvements in the formulae for calculating fluxes will be relevant to all oceans, even though the study concentrated on analyses of North Atlantic fluxes.

6. Help for oceanographers

The work done by Alves is part of the FOAM (Forecasting Ocean Atmosphere Model) project at the Meteorological Office. The project aims to introduce daily ocean forecasts from an ocean model by the mid 1990s. Further improvements in resolution, for example, to that of the mesoscale weather forecast model grid used by the Meteorological Office, will require more-accurate measurements of the state of the ocean each day and greater computing power than currently available.

To prepare accurate forecasts for the Royal Navy, who are primarily interested in the surface layers, the multilayered model will be run throughout the ocean depth extending to about 6 km below the ocean surface. As a spin-off, this complete 3-dimensional coverage of the oceans will provide valuable information to oceanographers interested in studying ocean circulation.

7. Looking forward to the past

An improved fine-resolution ocean model will lead to a greater understanding of the factors which influence ocean circulation, making it possible to unravel ocean circulation patterns associated with climate change in the geological past. For example, it has been suggested that circulation patterns in the Atlantic were very different during the last ice age from what they are today.

A better understanding of the interaction between ocean circulation and climate in both the present and the past will help to predict the climate in the future.

551.509.313:551.509.5:551.551.8(26)

An assessment of the surface fluxes from the Meteorological Office numerical weather prediction models. Part II: Heat and fresh water

J.O.S. Alves
Meteorological Office, Bracknell

Summary

Interaction between the ocean and the atmosphere is brought about by the exchange of fluxes of momentum, heat and moisture across their interface. Estimates of these come from numerical weather prediction models. Surface heat and moisture fluxes from the Meteorological Office's fine- and coarse-mesh models are assessed and their parametrizations reviewed. The response of the ocean to these fluxes and any biases they may have is investigated using an ocean model of the North Atlantic.

1. Introduction

Fluxes of heat, momentum and fresh water are exchanged between the ocean and atmosphere. An ocean forecasting model is being developed by the FOAM group (Forecasting Ocean Atmosphere Model) of the Meteorological Office (MO). This model will require the specification of the surface fluxes, up to six days ahead of time, as its upper boundary condition. The only source of forecast surface fluxes, i.e. estimates of the surface fluxes ahead of time, is NWP (Numerical Weather Prediction) models. As a first stage in the development of FOAM an assessment of the surface fluxes from the current MO operational NWP models has been carried out. The results for the heat and fresh water fluxes form the contents of this document. A similar paper by Alves (1991) reports on the assessment of the surface momentum fluxes.

Three main types of error can occur in the surface fluxes from a NWP model. The forecast error depends on the ability of the model to represent the real atmospheric situation and to forecast it correctly. Such errors will be ignored as the main interest is in the calculation of the surface fluxes themselves. A second source of errors is the parametrization of the fluxes from the model fields. Thirdly, the model parametrizes the surface fluxes as functions of the basic model fields; wind, temperature and humidity. Calculation of the radiation fluxes is also sensitive to the parametrization of other physical processes, such as the representation of cloud and convection, which themselves depend on the basic model fields. The representation of the basic fields in the NWP models will be discussed briefly.

An ocean model was used to assess the quality of the surface fluxes. The aim was to reveal any biases in the surface fluxes and to quantify the sensitivity of the ocean model to these biases by comparing results from ocean model integrations using the NWP fluxes with similar integrations using climatological fluxes. Fluxes from the two MO operational models were compared and their parametrizations were discussed.

A brief description of the operational NWP models used by the MO and a fuller description of how they parametrize the surface fluxes is given in section 2. Section 3 describes the ocean model and the experiments carried out. Results from the ocean model test, including a discussion of the flux parametrizations, for the heat fluxes (excluding solar), solar heat flux and fresh water flux are given in sections 4, 5 and 6 respectively. In section 7 a summary is presented and conclusions are drawn.

2. The NWP models

2.1 The MO NWP models

The MO used two fully operational numerical weather prediction models, described by Bell and Dickinson (1987). The 'Coarse-Mesh' (CM) model is global and used a latitude/longitude resolution of $1.875° \times 1.5°$. The 'Fine-Mesh' (FM) model had twice the resolution of the CM, this being $0.9375° \times 0.75°$, and covered an area from 30° N to 80° N and from 40° E to 80° W. Output from the global CM model was used to supply boundary conditions for the limited-area FM model. Both models were run twice a day, at 0000 UTC and 1200 UTC. The CM model produced forecasts up to six days ahead and the FM model up to 36 hours ahead. Only the first twelve hours of each forecast were used in this study.

From each model, monthly mean fields consisting of the first twelve hours of each forecast were formed for the month of October 1989. The fields available from the NWP archives are shown in the Table I.

Table I. Fields extracted from NWP archives. X = not available

	FM	CM
σ_1, temperature	✓	X
Surface temperature	✓	✓
σ_1, relative humidity	✓	✓
Precipitation minus evaporation	✓	✓
Latent heat flux	✓	✓
Sensible heat flux	✓	✓
Net surface solar radiation	✓	✓
Net surface IR radiation	✓	✓
σ_1, wind components	✓	X
10-metre wind components	✓	✓

2.2 Parametrization of the surface processes.

The parametrization of the boundary-layer processes is described fully in Bell and Dickinson (1987). A brief summary and modifications are outlined below. The surface latent heat flux (λE), evaporation rate (E) and sensible heat flux (H) were defined in terms of bulk aerodynamic formulae. For the CM model the bulk formulae took the explicit form

$$H = -\rho c_p C_H |v_1| (\theta_1 - \theta_*) \quad (1)$$

$$\lambda E = -\rho \lambda C_E |v_1| (q_1 - q_s(\theta_*)) \quad (2)$$

where C_H is the exchange coefficient for heat, C_E is the exchange coefficient for moisture, $|v| = (u_1^2 + v_1^2)^{1/2}$, u_1 and v_1 are the first model-level horizontal wind components, θ_1 is the first sigma-level model potential temperature, θ_* is the sea-surface potential temperature (the sea surface temperature was kept constant throughout each NWP model integration), λ is the latent heat of vaporization, q_1 is the specific humidity at the model's first sigma level and $q_s(\theta_*)$ is the saturated specific humidity at the potential temperature θ_* (given by Clausius–Clapeyron relation). In the FM model an implicit finite difference scheme (Kitchen 1986) was used for the turbulent fluxes in the boundary layer and the bulk aerodynamic formulae took the form

$$H = -\rho c_p C_H |v_1| \{\alpha(\theta_1^{t+\Delta t} - \theta_*) + (1-\alpha)(\theta_1^{t} - \theta_*)\}$$

$$\lambda E = -\rho \lambda C_E |v_1| (\alpha(q_1^{t+\Delta t} - q_s(\theta_*)) + (1-\alpha)(q_1^{t} - q_s(\theta_*))$$

where $\alpha = 0.5$ and the superscripts t and $t+\Delta t$ refer to successive time levels; Δt represents a time-step.

The exchange coefficients C_H and C_E depend on the surface roughness length z_o and the bulk Richardson number Ri_B. They were calculated using empirical functions which depend on the stability of the boundary layer (see Bell and Dickinson (1987)). Bell and Dickinson indicate that in the CM model z_o over the sea was a constant value of 10^{-4} m. For the FM model the surface roughness length z_o was a variable and was calculated using the Charnock formula (Charnock 1955)

$$z_o = M u_*^2 / g$$

where M is a constant (taken to be 0.019), u_* is the surface friction speed and g is the acceleration due to gravity.

2.3 The parametrization of the radiative fluxes

Net infrared radiation flux at the sea surface was calculated by the difference between the upward long-wave radiation flux from the sea surface (assumed to be a black body) and downward long-wave flux (see Bell and Dickinson (1987) for full details). The downward long-wave flux at the surface was a combination of the clear sky downward flux and the downward flux from the cloud base. In the CM model the cloud distribution was taken to be a zonally averaged climatology. In the FM model an interactive cloud scheme was used where for each model layer the fraction of cloud cover Q is calculated from the relative humidity field (for relative humidity $H > H_{crit}$) from the equation

$$Q = (H - H_{crit})^2 / (1 - H_{crit})$$

where H_{crit} is taken to be 0.85. Clouds are then divided into 'low', 'medium' and 'high' by finding the largest value of Q in each of three bands of model layers. Convective cloud was diagnosed from the convection scheme and was treated as a fourth cloud type by the radiation scheme. Clear sky downward flux was calculated taking into account the absorption by water vapour, carbon dioxide and ozone (see Bell and Dickinson (1987) for full details). Water vapour distribution was obtained from the models humidity field and the carbon dioxide was assumed to be well mixed throughout the atmosphere (mixing ratio of 4.9×10^{-4} kg kg^{-1}). Ozone mixing ratios were specified above 200 mb from monthly climatological zonally averaged values (Bolton 1981).

In the CM model the solar radiation flux reaching the surface was calculated by taking into account absorption by cloud whose distribution was given by a zonally averaged climatology. The FM model had a solar radiation scheme which took account of the diagnosed cloud (Bell and Dickinson 1987). The total downward short-wave radiation flux at some height z is given by

$$S(z) = (1-Q)S^{\infty}(z) + Q\Lambda S^{CL}(z)$$

where Q is the fractional cloud cover, $S^{\infty}(z)$ is the clear-sky radiation flux at height z, $S^{CL}(z)$ is the diffuse flux from the cloud and Λ is the transmissivity of the cloud. The clear-sky radiation flux $S^{\infty}(z)$ was calculated by taking into account absorption by three gases: water vapour, carbon dioxide and ozone. Where there was cloud $S^{CL}(z)$ was used which additionally incorporated the effect of diffusion by the cloud. A further adjustment took account of scattering by the atmosphere which is particularly important for low solar elevation.

A fraction α (the surface albedo) of the solar radiation reaching the sea surface was reflected back into the atmosphere. Over the sea and in clear sky conditions $\alpha = \alpha_o$ where $\alpha_o = 0.06$. When there was cloud present there would be multiple reflection of the solar radiation between the bottom of the cloud and the sea surface. This multiple reflection was taken into account by putting $\alpha = \alpha_{eff}$ (effective albedo) where α_{eff} is given by

$$\alpha_{eff} = \alpha_o(1-Q\beta)/(1-Q\beta\alpha_o)$$

where Q is an ensemble cloud amount and β an ensemble reflectivity incorporating the four types of cloud; low, medium, high and convective (see Bell and Dickinson (1987)).

2.4 Parametrization of precipitation

Precipitation was calculated in two forms; dynamic and convective. Dynamic rain was calculated using the model's humidity field. For each model layer where the specific humidity was greater than the saturated specific humidity for that particular layer, excess water was removed as precipitation taking into account changes in temperature due to latent heat release. Precipitation falling from one layer through another which was not saturated was evaporated (approximately 7 mm day^{-1}/100 mb). Precipitation at the surface was therefore the sum of precipitation less evaporation for all the model layers (note precipitation and evaporation do not occur on the same layer). Bell and Dickinson (1987) give a more detailed account of the calculation of the dynamic precipitation rates.

Convective precipitation rate was calculated using parameters from the model's convection scheme which was based on parcel theory modified by entrainment and detrainment (see Bell and Dickinson (1987) for more details). Condensation of cloud water occurred if the depth of the convective cloud was greater than a critical value D_{crit} (4 km over land, 1.5 km over sea and 1 km if the temperature of the layer above was less than 263 K) and the specific humidity is greater than a critical value q_{crit} (the smaller of 1 g kg^{-1} or saturated specific humidity). The precipitation rate was proportional to the difference between the specific humidity and the critical value q_{crit}, and the vertical mass flux in the convective plume. Rain falling from the cloud base was evaporated at a rate proportional to the difference between the specific humidity and the saturated specific humidity in the layers between the cloud base and the surface. The remaining precipitation determined the surface convective precipitation rate.

3. Use of an ocean model to assess the surface fluxes

The ocean model used is based on that of Cox (1984) and is described by Alves (1991). It uses regular latitude/longitude horizontal co-ordinates with a grid spacing of 1° throughout. In the mixed layer a scheme similar to that of Kraus and Turner (1967) is used. In this scheme convective mixing takes place when there is surface cooling. After this, or where there is net surface heating, the mixing energy of the wind is used to overcome the stability of the upper layers and mix the more buoyant water downwards. A mixed layer depth is diagnosed as the depth to which mixing occurs.

Surface fluxes of momentum, non-penetrating heat, solar radiation and fresh water are used as the upper boundary conditions for ocean model integrations. Momentum flux is used by the ocean model to drive the Ekman drift currents and the long-term average wind stress drives the upper-ocean circulation. Water near the surface is mixed downwards using the wind mixing energy. Heat is either input or removed from the ocean through the specification of the heat flux. The salt budget is modified at the surface by the fresh water flux.

For the month of October 1989 forcing fields were extracted from the NWP archives for each forecast starting at 00 UTC and 12 UTC each day. The T+3, T+6, T+9 and T+12 forecasts from the FM model were used to form three-hourly averaged forcing fields. For the CM model only the T+6 and the T+12 fields were available. The T+6 was copied and relabelled the T+3 and the T+12 was copied and relabelled the T+9, so forming a set of three-hourly forcing fields. The fields extracted consisted of the surface sensible heat flux, latent heat flux, infrared radiation, solar radiation and precipitation minus evaporation (PME). Sensible heat, latent heat and infrared radiative fluxes were combined to form the non-penetrative surface heat flux (note that this excludes the solar radiation as this penetrates into the upper few tens of metres of the ocean).

The ocean model's domain covers the Atlantic from 30°S to 80°N. The region covered by the FM is contained within the domain of the ocean model. It is desirable to use the FM model's forcing fields where possible because of its improved physics and higher resolution. To achieve this the FM and CM fields were merged together so that the FM values were used within the FM domain and those of the CM outside the FM domain, with a smoothing applied at the FM boundary. The resulting fields will be from hereon referred to as the 'merged' fields.

The ocean model was integrated using climatological fluxes for seven months as described by Alves (1991). Similar integrations to those carried out by Alves for the NWP momentum fluxes were repeated for each of the fluxes: non-penetrative heat flux (excluding solar), solar radiation flux and the PME flux, where the climatological flux was exchanged with one of the NWP fluxes, for October 1989, in each experiment. In the following sections these will be referred to as the 'NWP' runs or the 'operational' runs. Monthly mean fields for temperature, salinity, currents, mixed layer depth and the forcing fields were obtained for each run and compared with the climatological control run. These will be discussed in the sections to follow. For the purpose of comparison all fields presented which are not from the ocean model have been interpolated onto the ocean model's grid.

4. Non-penetrative heat fluxes

4.1 Results

The monthly mean latent heat flux for October 1989 from the CM model is shown in Fig. 1(a). Areas of maximum latent heat flux are in general associated with northward transport of warm water within the Atlantic Ocean. Maximum latent heat flux occurs in the Gulf Stream region and reaches 300 W m^{-2}. When compared with a climatology (Esbensen and Kushnir 1981), Fig. 1(b), the CM model latent heat flux shows differences of up to 50 W m^{-2} in areas not influenced by strong oceanic heat transport. In the Gulf Stream region itself the CM model exceeds the climatology by up to 100 W m^{-2} (33%), but away from the main thermal gradients associated with the Gulf Stream the CM has a smaller heat flux than the climatology. This appears to be a consequence of the better resolution of the Gulf Stream thermal gradients in the SST field used by the operational models compared with that used to calculate the Esbensen and Kushnir fluxes (on a 5° × 5° grid). Comparing the FM and CM models' latent heat flux (Fig. 2), the FM exceeds the CM by up to 40 W m^{-2} (13%) in the Gulf Stream region. Away from the western Atlantic the differences between the two models is smaller and generally less than 20 W m^{-2}.

Fig. 3(a) shows the monthly mean sensible heat flux for October 1989 produced by the CM model. Throughout the tropical Atlantic the sensible heat flux is small, generally less than 20 W m^{-2} and from the ocean to the atmosphere. In the middle latitudes (North Atlantic) the heat flux shows a larger variability and reaches up to 60 W m^{-2} in the region influenced by the Gulf Stream. Large heat fluxes near the Gulf Stream arise due to cold air flowing across the Gulf Stream from the cold shelf waters into the warm open ocean. Similarly in the extreme north of the domain, large heat fluxes with great variability occur as cold air from the snow and ice covered sea and land flows over the relatively warmer open sea. When compared with the climatology (see Fig. 3(b)) the sensible heat flux from the CM model agrees to within 10 W m^{-2} or so in the tropical ocean, although this is of the same magnitude as the heat flux itself. In the middle latitudes the variability in the difference is large. In the Gulf Stream region the sensible heat flux is up to 45 W m^{-2} (65%) larger than the climatology but is partly due to a better resolution of the SST used by the operational models. The FM model when compared with the CM model (not shown) indicates differences of up to 10 W m^{-2}; the maximum heat flux in the CM model occurs in the mid-latitude western Atlantic and this is simulated by the FM model to be 15% larger.

Monthly mean infrared radiation (IR) from the CM model for October 1989 is shown in Fig. 4(a). The net upward IR flux ranges from 30 to 80 W m^{-2} throughout the whole domain with the maximum occurring in the western Atlantic in the region influenced by the Gulf Stream. Since the IR radiation scheme uses a zonally averaged climatological cloud distribution, the main zonal variability in the IR flux comes from the variability in the SST (sea surface assumed to be black body). Fig. 4(b) shows the IR radiation from the CM model less a climatological field (Esbensen and Kushnir 1981). The CM model has a larger upward IR flux on the western tropical South Atlantic but less on the eastern tropical South Atlantic. Over the whole of the tropical North Atlantic the CM model has a larger IR radiation flux, up to 30 W m^{-2} (50%) more than the climatology. In the middle latitudes, north of about 45°N the CM model has a smaller IR radiation flux than climatology and vice versa south of 45°N. However, in the western Atlantic the Gulf Stream appears to be a divide, with the western side having a smaller IR than the climatology and the warmer waters of the eastern side having a larger IR flux than the climatology. This again emphasizes the better-resolved SST field used by the operational models. The FM model when compared with the CM (Fig. 5) shows a field with a greater zonal variability as a result of the use of an interactive cloud scheme. In the

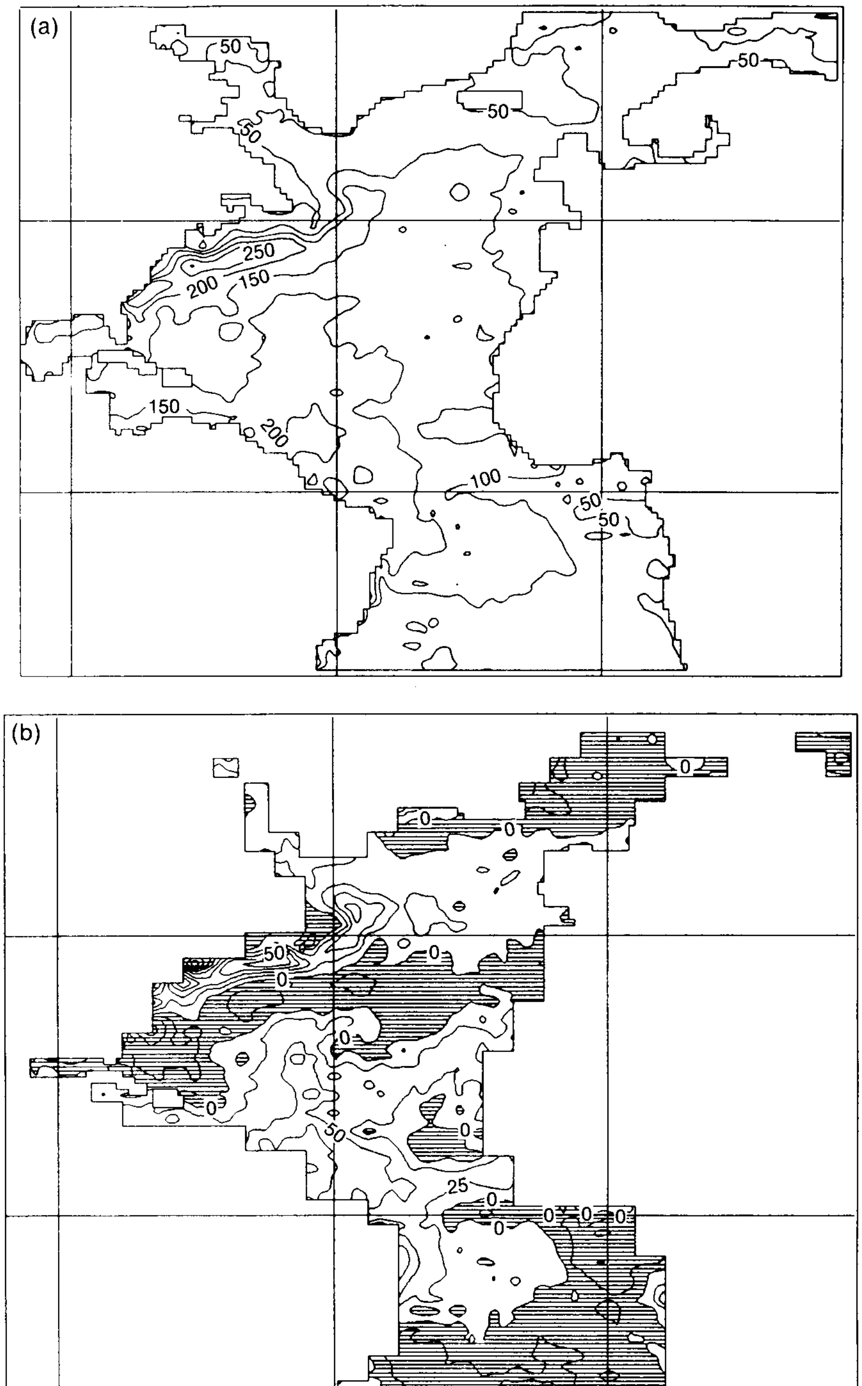

Figure 1. (a) Coarse-mesh monthly mean latent heat flux for October 1989 with contours every 50 W m^{-2}. (b) Difference between the monthly mean latent heat flux from the course-mesh model and climatology. Contours every 25 W m^{-2} with negative areas shaded.

northern and southernmost parts of the FM domain the FM model has a smaller IR flux than the CM (for example 10 W m^{-2}, 25% smaller west of Iceland). Elsewhere the FM has a larger IR flux, for example, 25 W m^{-2} (50%) larger in parts of the mid-latitude west Atlantic.

The three heat fluxes above were combined to form a net non-penetrative heat flux from the operational FM and CM models. An ocean model was integrated with the operational non-penetrative heat flux and all other fluxes being a climatology. Although the influence of each of the separate fluxes above was not tested separately with an ocean model integration, the sensitivity to the net heat flux can be thought of as representing the sensitivity to each of the individual heat fluxes.

Fig. 6(a) shows the climatological heat flux used for the climatological control run. The field is very smooth with the upward heat flux increasing as one moves westwards and towards the tropical North Atlantic. The maximum heat flux occurs in the Gulf Stream region where it reaches 300 W m^{-2}. Fig. 6(b) shows the merged

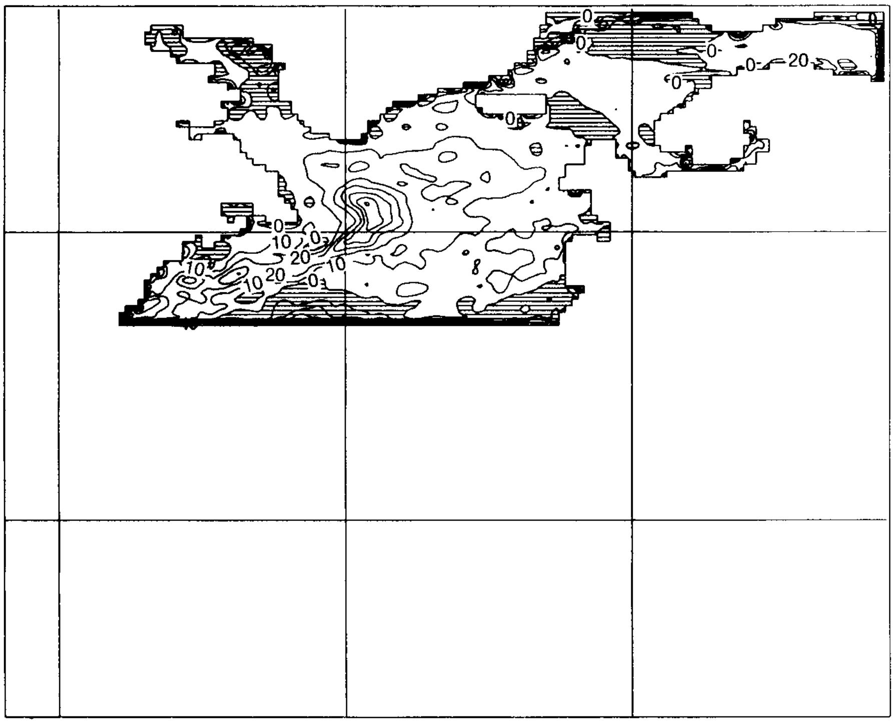

Figure 2. Difference in the monthly mean latent heat flux between the fine-and coarse-mesh models for October 1989. Contours every 10 W m^{-2} with negative areas shaded.

heat flux used for the NWP run less that used for the climatological control run. In the tropical and mid-latitude North Atlantic the NWP model has a generally larger heat flux, up to 100 W m^{-2} away from the Gulf Stream region and up to 200 W m^{-2} in the Gulf Stream area, when compared with the climatology. As already mentioned the higher resolution SST field used by the NWP models produces a larger and more localized heat flux in the Gulf Stream area.

The monthly mean difference in the SST between the NWP heat-flux-driven model and the climatological heat-flux-driven model is shown in Fig. 7. Away from the Gulf Stream region, areas of upwelling and areas of strong near-surface currents, the monthly mean difference in SST (ΔT) between the two runs is related to the monthly mean difference in the heat flux (ΔQ) through the heat equation

$$\Delta Q \simeq 2\rho c_p h \Delta T / \Delta t \qquad (3)$$

where ρ is the sea water density, c_p is the specific heat capacity of water, Δt is the period considered (one month), h is the average of the mean mixed layer depth of the two runs and $2\rho c_p/\Delta t \approx 3.1$. The factor of two in equation (3) arises as a result of using the difference in the monthly mean SST (ΔT) rather than the difference in the SST at the end of the integrations. As an example, applying equation (3) to the area on the Greenwich meridian just south of the equator where the heat flux difference (ΔQ) between the two runs is 50 W m^{-2} yields a monthly mean difference in the SST (ΔT) of approximately 1 °C ($h = 20$ m, see Fig. 8(a)) which agrees well with that shown in Fig. 7.

Equation (3) shows the dependence of the change in the ocean mixed-layer temperature on the mixed-layer depth when there is net heating or cooling of the ocean surface. Generally the mixed layer (Fig. 8(a)) is shallowest in the tropical latitudes (as shallow as 10 m or so in the October climatology of Fig. 8(a)) and increases towards the poles. In the high-latitude North Atlantic the mixed layer depth exceeds 100 m in the climatology for October. The mixed layer depth is usually deeper in mid winter, and in the North Atlantic it can reach depths of several hundred metres during extreme weather conditions.

A positive heat flux into the ocean heats the upper layers and therefore increases the stability. This leads to a reduction in the mixed layer depth which in turn leads to an increase in the sensitivity of the mixed layer temperature to the heat flux. On the other hand, when there is a net cooling, the deepening of the mixed layer through convective mixing decreases the sensitivity of the mixed layer to the heat fluxes. Fig. 8(b) shows the difference in the monthly mean mixed layer depth between the two runs. Generally, where there is more net heating in the NWP-forced run than in the climatology-forced run there is a relative reduction in the mixed layer depth, and vice versa. In the Gulf Stream area the cooling difference of 200 W m^{-2} introduces a relative deepening of the mixed layer by 10 m (15%). In the tropics, where the mixed layer is much shallower, a cooling difference of 50 W m^{-2} between the two runs introduces a relative increase in the mixed layer depth of 10 m (50% deeper). Heating of the sea surface, such as that east of Florida of 50 W m^{-2}, introduces no significant changes in the mixed layer depth, whereas

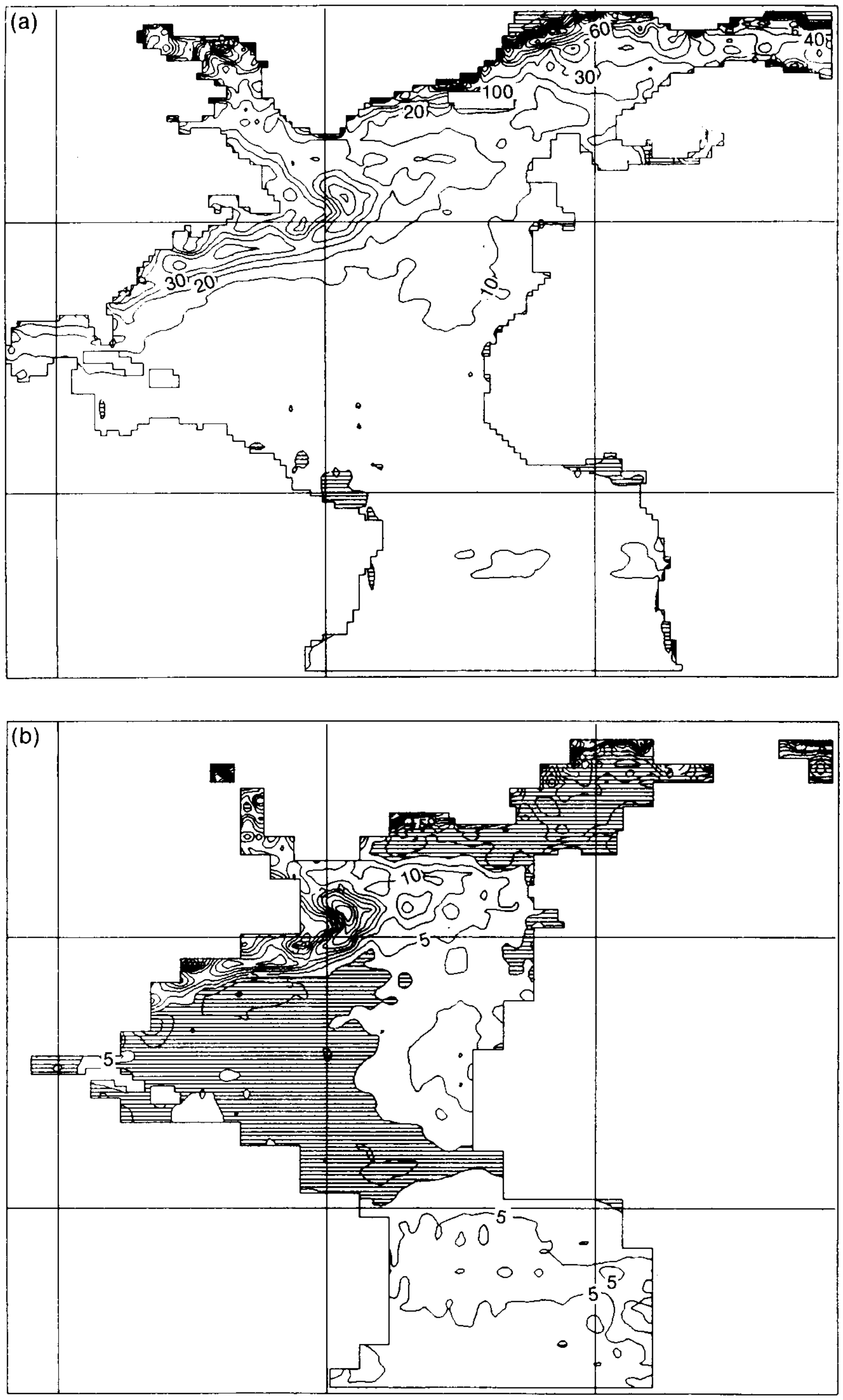

Figure 3. (a) Coarse-mesh monthly mean sensible heat flux for October 1989. Contours every 10 W m^{-2} with negative areas shaded. (b) Difference between the monthly mean sensible heat flux from the coarse-mesh model and climatology. Contours every 5 W m^{-2} with negative areas shaded.

heating differences of less than 50 W m^{-2} in the equatorial ocean, where the mixed layer is shallower, introduces differences in the mixed layer of up to 50% (for example, a shallowing of 15 m where the mixed layer depth in the climatology was 30 m).

Changes in the mixed layer depth will introduce changes in the surface current by changing the depth to which wind stress is applied via the Ekman drift mechanism. The climatology-forced model's current field for October and the vector difference from the NWP-forced models' top-layer current is shown in Fig. 9. The main differences are in the tropics where the largest changes in the mixed layer depth occur. Near the equator, differences of up to 10 cm s^{-1} occur in a region where the surface current is only 20 cm s^{-1}. The complex nature of the ocean–atmosphere system has been demonstrated here, where differences in the heat fluxes between the ocean and atmosphere not only change the ocean mixed layer temperature, but also its vertical stability and current structure.

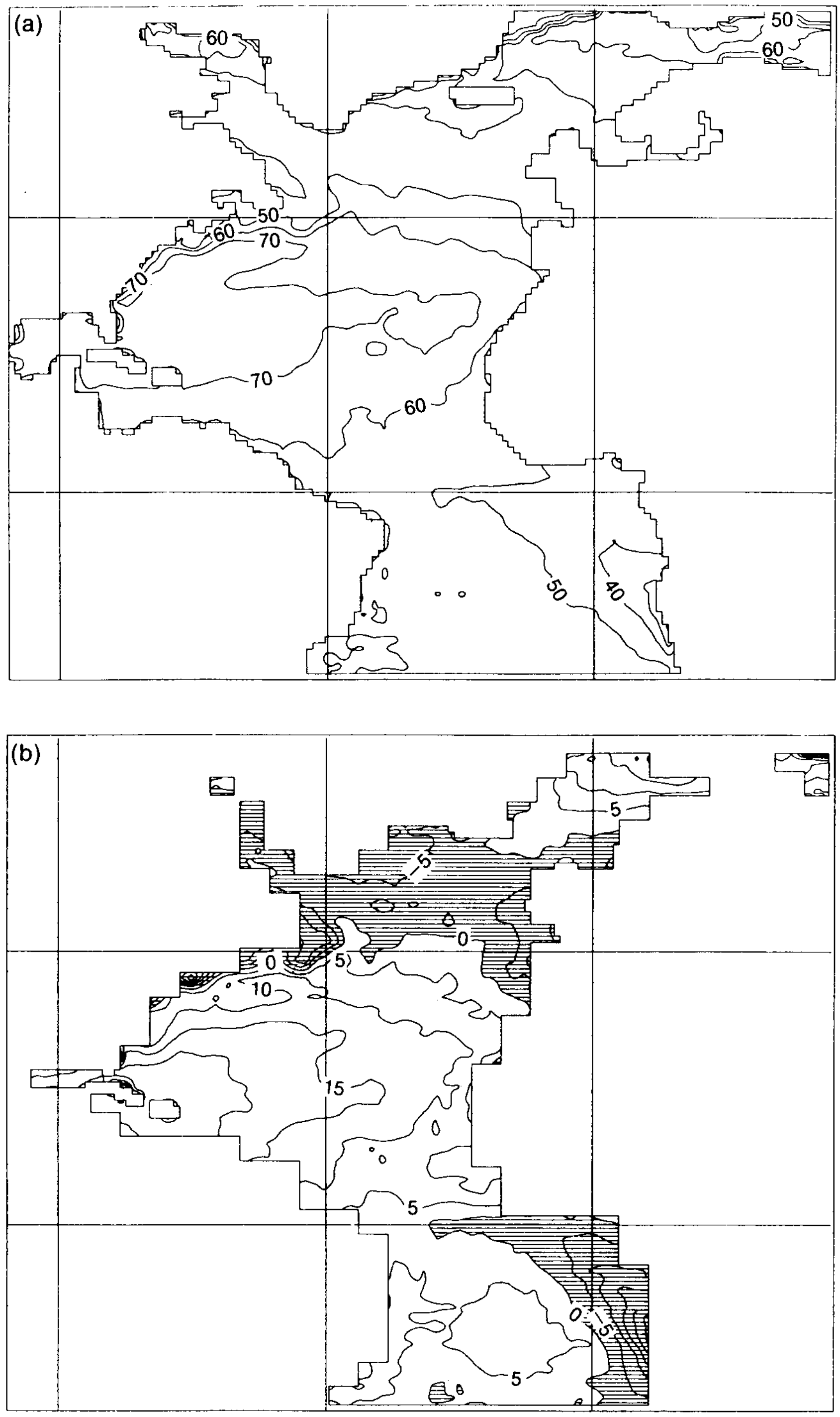

Figure 4. (a) Coarse-mesh monthly mean infrared radiation for October 1989. Contours every 10 W m^{-2}. (b) Difference between the monthly mean infrared radiation from the coarse-mesh model and climatology. Contours every 5 W m^{-2} with negative areas shaded.

4.2 Discussion

The infrared radiation depends on the distribution of cloud. In the CM model, where a zonally averaged climatological cloud distribution is used, the only zonal variability in the IR flux arises due to changes in the SST. In the FM model the cloud distribution is calculated from the humidity field. The proper assimilation of humidity data into NWP models and its representation throughout the forecast is therefore essential for determining the IR flux.

The IR flux (I) from the sea surface (assumed to be a black body) depends on the SST through the Stefan–Boltzman law

$$I = \sigma T^4$$

where σ is Stefan's constant (5.67×10^{-8} W m^{-2} K^{-4}) and T is the absolute temperature. Alves (1990) reported uncertainties of several degrees Celsius in the SST fields used by the NWP models. The uncertainty in the IR field

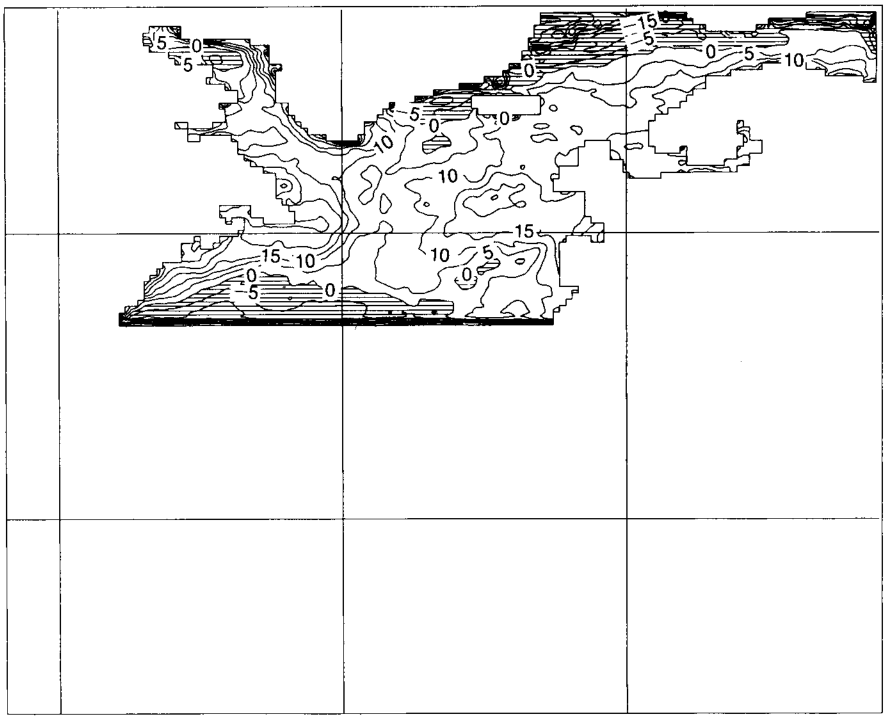

Figure 5. Differences in the monthly mean infrared radiation between the fine- and coarse-mesh models for October 1989. Contours every 5 W m^{-2} with negative areas shaded.

(ΔI) corresponding to an uncertainty in the SST (ΔT) is given by.

$$\Delta T = 4\sigma T^3 \Delta T.$$

An error in the SST of around 2 °C would result in an error in the IR flux of around 10 W m^{-2}, that is 12% to 35% of the values shown in Fig. 4(a), although the value of the IR flux is in general small when compared with the latent heat flux.

Bulk aerodynamic parametrization of the latent and sensible heat fluxes (equations (1) and (2)) makes them directly proportional to the wind speed, ignoring any dependence of the exchange coefficients on wind speed. Alves (1991) compared the FM and CM 10 m winds and an uncertainty of 10% was found. This leads to an uncertainty of 10% in each of the sensible and latent heat fluxes. For the sensible heat flux this could be a few W m^{-2} and as much as 30 W m^{-2} for the latent heat flux in the Gulf Stream region. This uncertainty in the latent heat flux is small when compared with the differences which existed between the NWP heat flux and the climatology discussed earlier.

Sensible heat flux is also directly proportional to the sea–air temperature difference and the latent heat flux is directly proportional to the sea–air humidity difference. The difference in temperature between the SST and the first sigma-level temperature is shown in Fig. 10(a) for the FM model (this was not available for the CM model). The climatological sea–air temperature difference used by Esbensen and Kushnir (1981) in their flux calculations is shown in Fig. 10(b). The climatological sea–air temperature difference is generally positive except in parts of the southern tropics, indicating a general transfer of heat from the ocean to the atmosphere. Largest differences occur along the east coast of North America, Greenland and Iceland where cold air blowing from the continents suddenly passes over a warmer ocean. Differences are also large where air blows across ocean thermal fronts such as the Gulf Stream where the maximum difference resolved in the climatology is 2.5 °C. For the FM model the temperature difference shows the same pattern as the climatology but the values are much larger. In the Gulf Stream area the difference reaches over 5 °C. This would imply a heat flux which would be twice that of the climatology (for the same wind speed and exchange coefficient). The area east of Greenland where cold polar air flows over warmer oceans contains sea–air temperature differences in excess of 7 °C. The reason for this larger value compared to the climatological value of 2.5 °C is because the NWP models use a finer resolution SST, which additionally takes account of ice, compared to the climatology.

Most of the *in situ* observations of the ocean SST are based on the 'bucket' method which involves measuring the temperature of the water collected using a bucket or measuring the temperature of water from engine intake. This water will have originated up to several metres below the ocean surface and in conditions of light winds and strong radiation it may be several degrees cooler than the top few millimetres (skin) of the ocean surface. Liu *et al.* (1979) discuss the difference obtained by using the bulk SST and the 'skin' temperature. They devise a scheme for calculating the skin temperature from the bulk temperature.

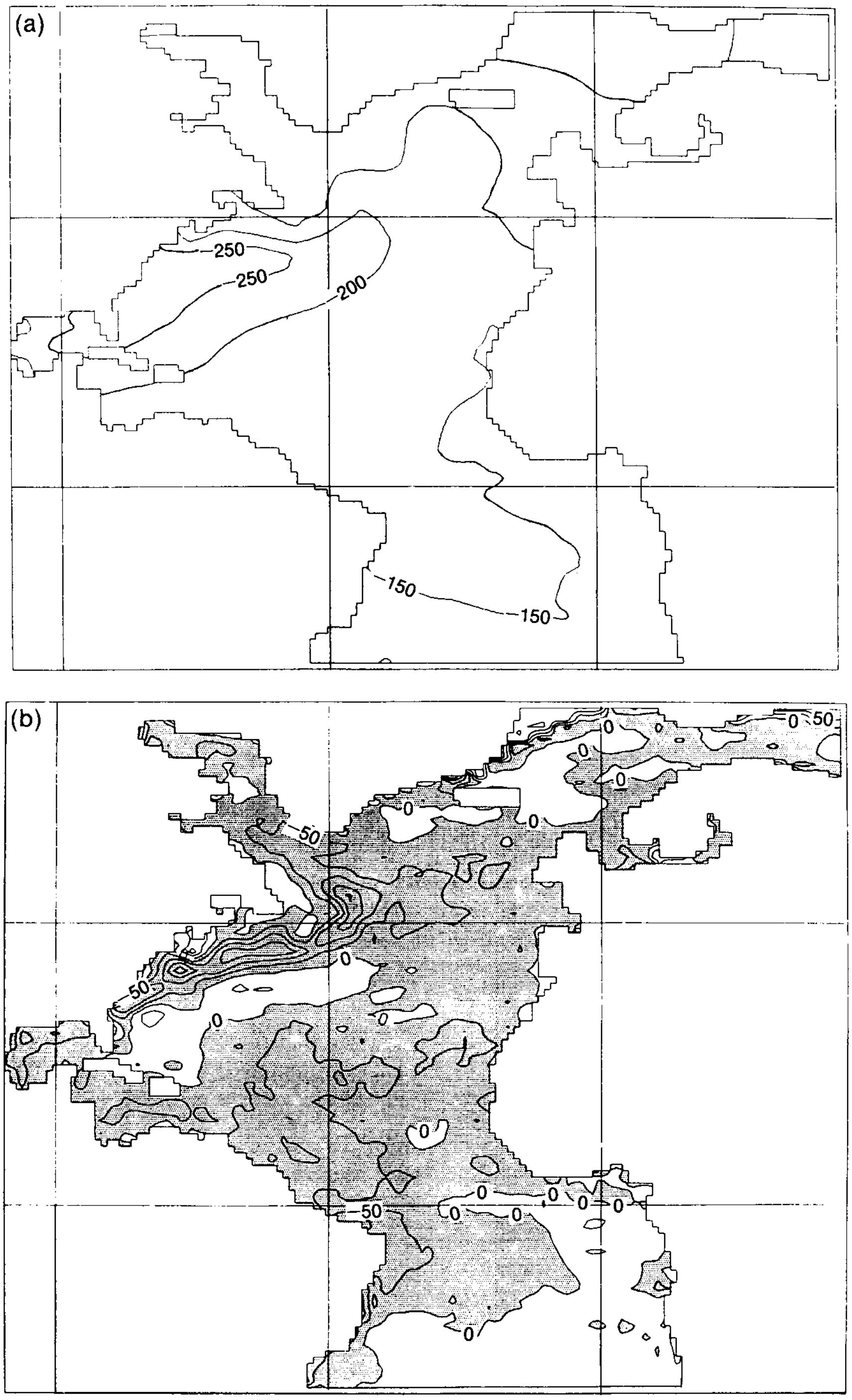

Figure 6. (a) Monthly mean climatological non-penetrative net heat flux for October. Contours every 50 W m^{-2}. (b) Difference between the monthly mean non-penetrative net heat flux between the merged NWP fields and climatology for October 1989. Contours every 50 W m^{-2} with negative areas shaded.

The present data analysis system of the MO does not use near-surface air temperature observations over the sea. This means that the first sigma-level temperature arises as a result of the surface fluxes and it will therefore alter with the SST. Since the first sigma-level temperature responds to the SST it can be argued that a bias in the SST may not seriously effect the temperature difference since the first sigma-level temperature will adjust to that bias through the heat fluxes. What may be important in producing the correct sea–air temperature difference is the correct representation of the SST gradients. This is observed in the Gulf Stream where the sea–air temperature maxima occur across the Gulf stream thermal gradients. This has already been discussed in the results where the SST field used by Esbensen and Kushnir to calculate the climatological fluxes was of a much lower resolution than that used by the NWP models, leading to a larger magnitude and

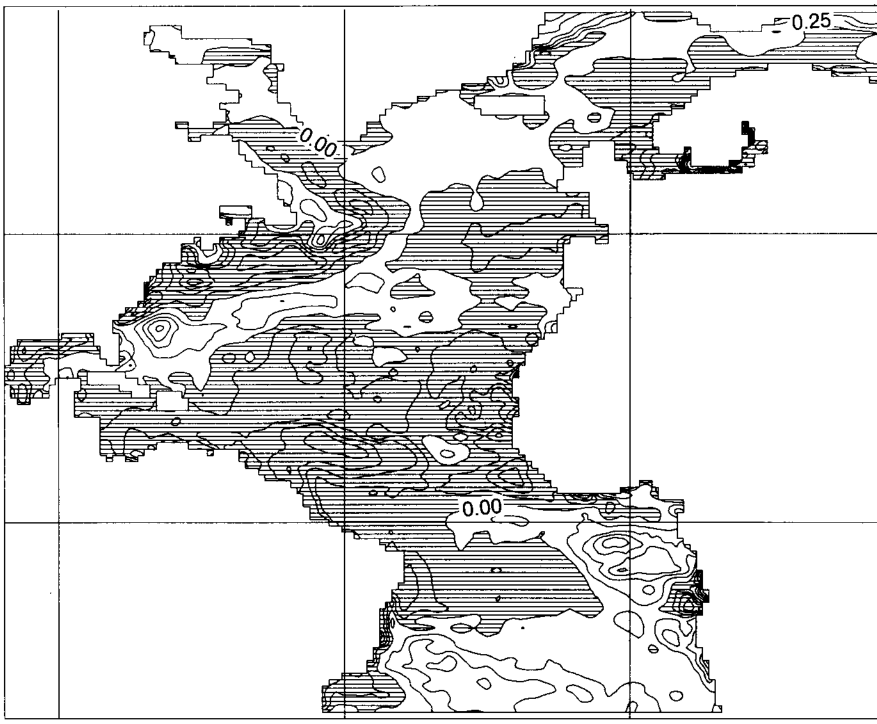

Figure 7. SST monthly mean difference between the NWP net non-penetrative heat-flux-forced run and the climatology-forced run. Contours every 0.25 °C with negative areas shaded.

more localized sensible heat flux in the NWP models. It is therefore essential to represent SST gradients accurately in the SST fields used by the NWP models.

Climatological sea–air specific humidity difference used by Esbensen and Kushnir (1981) is shown in Fig. 11(b). This increases towards the equator and the western North Atlantic. Maxima of just over 6 g kg^{-1} are found in the Gulf Stream area in the West Atlantic. The only humidity field available from the NWP models' archive was the relative humidity (H_1) at the first sigma-level for the FM model. The specific humidity was calculated from this using

$$q_1 = q_{s1}H_1$$

where the saturated specific humidity was calculated using the integrated Clausius–Clapeyron equation

$$q_{s1}(T) = q_{so}(T_o)\exp(\epsilon L/R(1/T_o - 1/T)) \quad (4)$$

where $\epsilon = 0.622$, L is the latent heat of vaporization (2.5×106 J kg^{-1}), R is the gas constant for dry air (287 J kg^{-1} K^{-1}), $T_o = 273$ K and $q_{so} = 3.8$ g kg^{-1}. The surface humidity $q_s(T_*)$ was also calculated using the Clausius–Clapeyron equation (4). Resulting sea–air humidity differences are shown in Fig. 11(a). The pattern is similar to that of the climatology but is less smooth, partly as a result of a higher resolution SST. The maximum in the Gulf Stream area reaches up to 10 g kg^{-1}, which would give a latent heat flux 66% larger than the climatological one (for the same wind speed and exchange coefficient). Dependence of the saturated surface humidity on the SST introduces the same problems which arise in the calculation of the sensible heat flux. These are the requirement to accurately represent thermal gradients in the ocean surface; use of the 'bucket' temperature as the sea surface temperature; and the need to reduce biases in the SST field used by the NWP models. The last of these may be less critical since the first sigma-level humidity field, like the temperature field, does not contain any assimilated data. It will therefore adjust through the latent heat flux to the surface value calculated from the prescribed SST.

In both FM and CM models the exchange coefficients for heat and moisture are made equal. Further, under stable conditions the exchange coefficients are equal to the drag coefficient. Fig. 12 shows the dependence of C_H on wind speed for various stabilities (ΔT) for the CM and FM models. Both models' C_H parametrizations agree well for wind speeds in the range 5–8 m s^{-1}. For wind speeds greater than 7 m s^{-1} there is little stability dependence of the values of C_H used by both models. The CM uses a constant value for the neutral C_H of 1.2×10^{-3} whereas the FM value increases with wind speed as a result of using the Charnock formula to parametrize the surface roughness length. The same problem occurs as for the drag coefficient (since for stable conditions $C_D = C_H = C_E$, see Alves (1991)), for example, for a wind speed of 20 m s^{-1} the FM uses a value for C_H of 2.1×10^{-3}, nearly twice that used by the CM. For low wind speeds and during stable or slightly unstable conditions, differences between the two models' C_H arise due to the Charnock formula used in the FM model decreasing the neutral value of C_H to zero

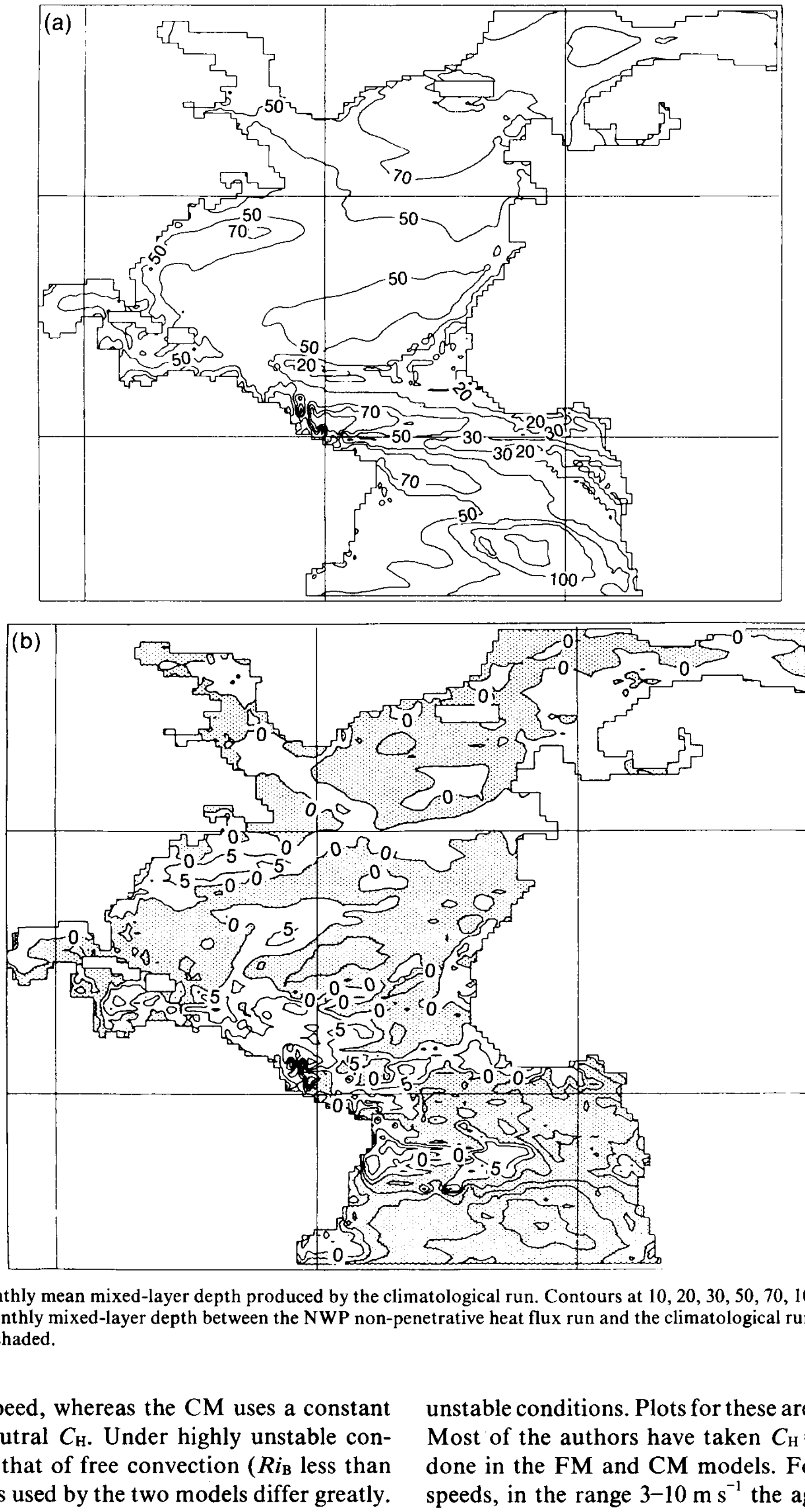

Figure 8. (a) Monthly mean mixed-layer depth produced by the climatological run. Contours at 10, 20, 30, 50, 70, 100, 150 and 200 m. (b) Difference in the monthly mixed-layer depth between the NWP non-penetrative heat flux run and the climatological run. Contours every 5 m with negative areas shaded.

with the wind speed, whereas the CM uses a constant value for the neutral C_H. Under highly unstable conditions, such as that of free convection (Ri_B less than -100), the values used by the two models differ greatly. The values shown on each chart for the lowest wind speed is that when free convection arises. The FM predicts a value of 2×10^{-3}, whereas the CM uses a value of 12.1×10^{-3}, six times greater (Ri_B of -100).

Blanc (1985) compared the empirical formulae for C_H and C_E of several authors under neutral or slightly unstable conditions. Plots for these are shown in Fig. 13. Most of the authors have taken $C_H \approx C_E$ as is indeed done in the FM and CM models. For moderate wind speeds, in the range 3–10 m s^{-1} the agreement between the authors is at its best with the maximum difference being 0.5×10^{-3}, i.e. 50%. The average value in this range for both C_E and C_H is 1.2×10^{-3}, which is in good agreement with the CM and FM models in the range 5–8 m s^{-1}. For stronger winds Masagutov (1981) and Bunker (1976) indicate a wind speed dependence with

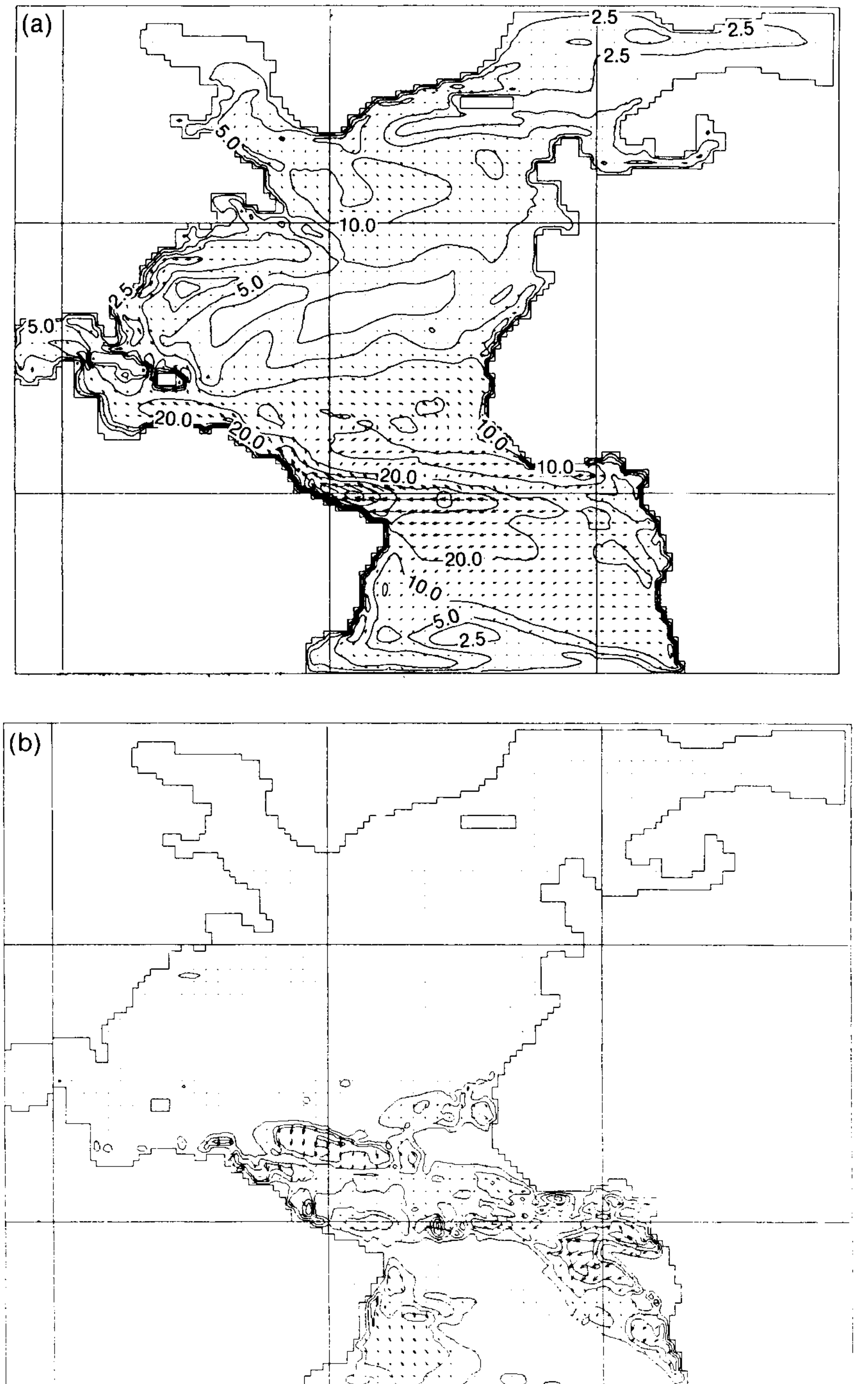

Figure 9. (a) Monthly mean model top-level current vector field produced by the climatological run for October. Contours at 2.5, 5, 10, 20, 40, 60 and 100 cm s^{-1}. (b) Difference in the model top-layer current field between the NWP non-penetrative heat flux run and the climatological run. Contours at 1, 2.5, 5, 10 and 20 cm s^{-1}.

C_H and C_E increasing with wind speed. At 20 m s^{-1} their schemes average to give $C_H = C_E = 1.7 \times 10^{-3}$, 40% larger than the CM value of 1.2×10^{-3} and 20% less than the FM value of 2.1×10^{-3}. Other authors (see Fig. 13) predict neutral C_E and C_H which have little or no wind speed dependence. Their average value is about 1.15×10^{-3} for both C_E and C_H which is in good agreement with the value used by the CM and for a wind speed of 20 m s^{-1} it is 45% less than the FM value. For low wind speeds the neutral C_H is estimated by the various authors to either remain constant or increase slightly, having an average value of about 1.2×10^{-3}. This agrees well with the CM model but disagrees with the FM model where the Charnock formula used to parametrize the surface roughness makes the values of C_H and C_E tend to zero with the wind speed.

Liu *et al.* (1979) devise a model which uses the surface 'skin' temperature, calculated from the 'bulk' sea surface temperature to calculate values for C_H and C_E. Their results indicate that for strong winds both C_E and C_H

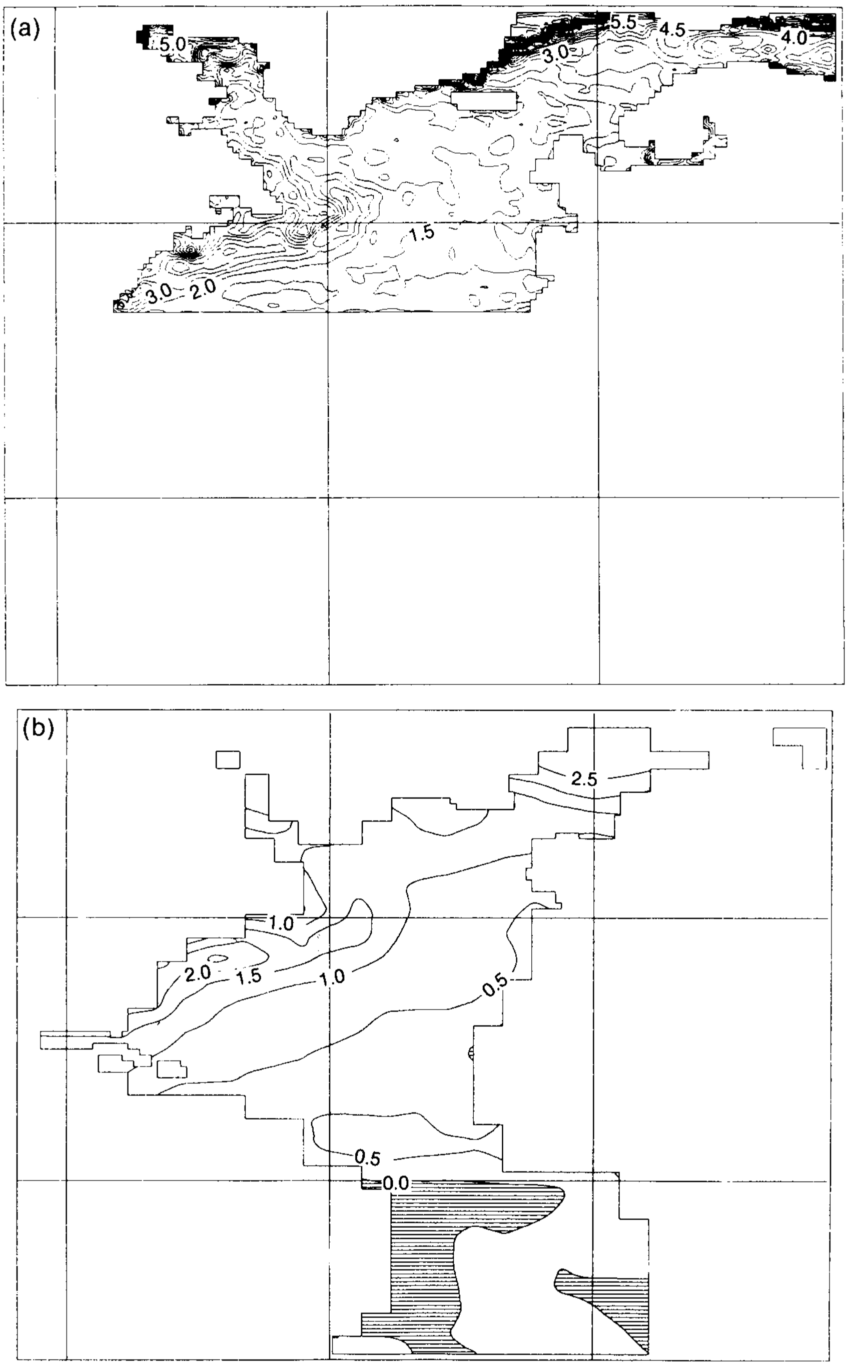

Figure 10. Monthly mean air–sea temperature difference (a) from the fine-mesh model for October 1989, and (b) that used by Esbensen and Kushnir (1981). Contours at 0.5 °C intervals.

decrease slightly with increasing wind speed. Large and Pond (1982) argue that the neutral values for C_H increase with wind speed for unstable conditions but remain constant for stable conditions. Data used by them are shown in Fig. 14 for C_H as a function of stability and wind speed and C_E as a function of wind speed. There is a clear indication of a different behaviour in the value of C_H for stable and unstable conditions. Their results show that for stable conditions the value for the neutral C_H is a constant, 0.7×10^{-3}, much lower than either the FM or CM models. For unstable conditions the neutral value of C_H is 1.1×10^{-3} for wind speeds less than 10 m s^{-1} and increases linearly with wind speed for stronger values, the value for C_H at a wind speed of 20 m s^{-1} being 1.3×10^{-3}. This indicates a wind speed dependence much less than that when the Charnock formula is used for the roughness length. Large and Pond (1982) suggest that the neutral C_E should have a constant value of 1.15×10^{-3} for wind speeds less than 10 m s^{-1}, in good agreement with the CM and the FM in the wind speed range 5–8 m s^{-1}. For stronger winds the linear wind speed dependence is such

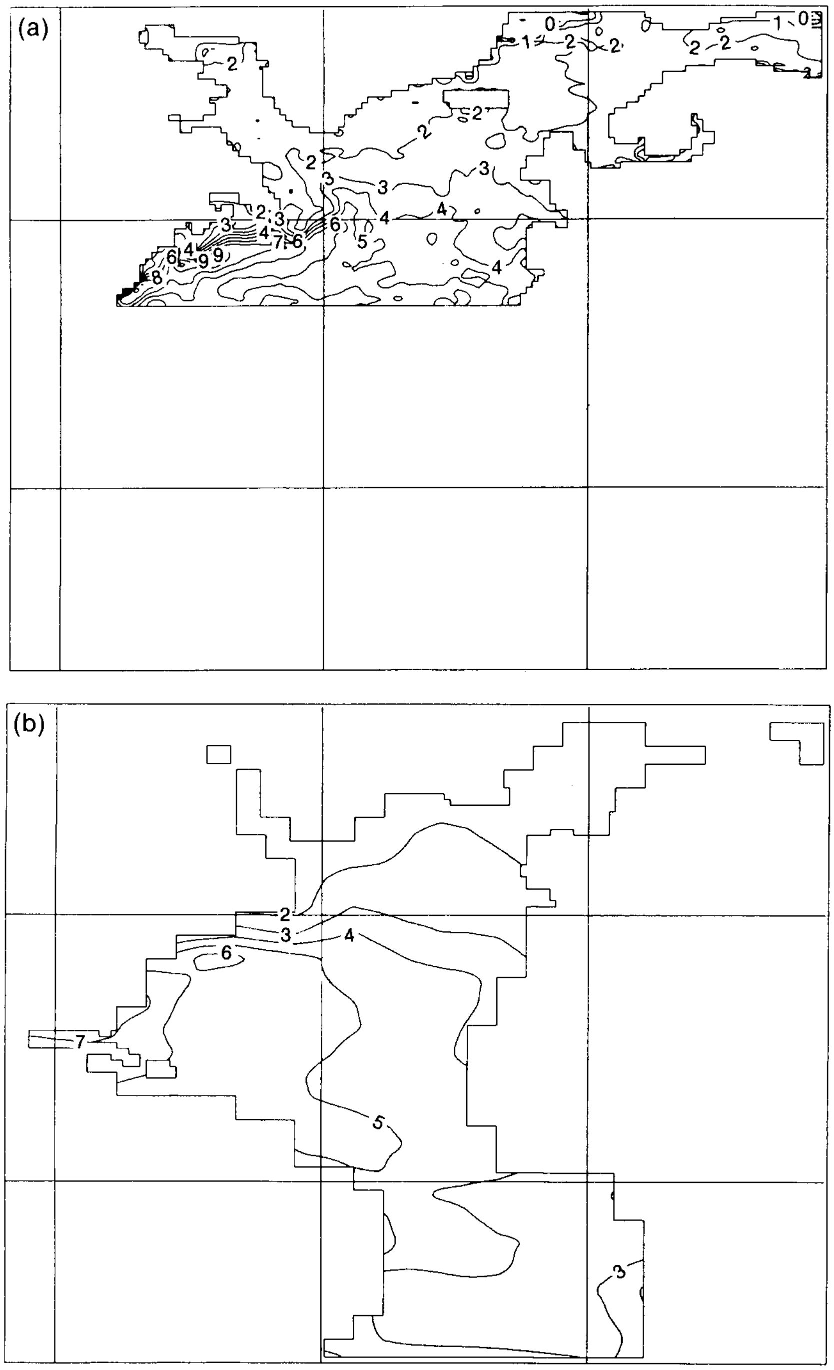

Figure 11. Monthly mean air–sea specific humidity difference (a) from the fine-mesh model for October 1989, and (b) that used by Esbensen and Kushnir (1981). Contours every 1 g kg^{-1}.

that C_E is 1.3×10^{-3} for a wind speed of 14 m s^{-1}. The FM value for a wind speed of 14 m s^{-1} is 1.7×10^{-3}, clearly indicating a much stronger wind dependence.

Under extremely unstable conditions, and conditions of free convection, the values of C_H and C_E become large for the CM model. For the FM model, where the same similarity function is used, the values for C_H and C_E are much less as a result of a smaller surface roughness length. Clearly the Charnock formula is inappropriate at low wind speeds when such conditions occur. Gordon and Hunt (1989) discuss the similarity scheme used for free convection by the CM model, and compare it with other schemes. They conclude that the CM scheme predicts a latent heat flux some 25 W m^{-2} less than the other schemes and suggest some amendments to the present scheme.

The experimental results shown in Fig. 14 show a large scatter and this explains the many differences in the formulations of the various authors considered by Blanc (1985). There is no clear evidence as yet to suggest the dependence on stability or wind speed, if any, of either values of C_H and C_E. The dependence of the drag

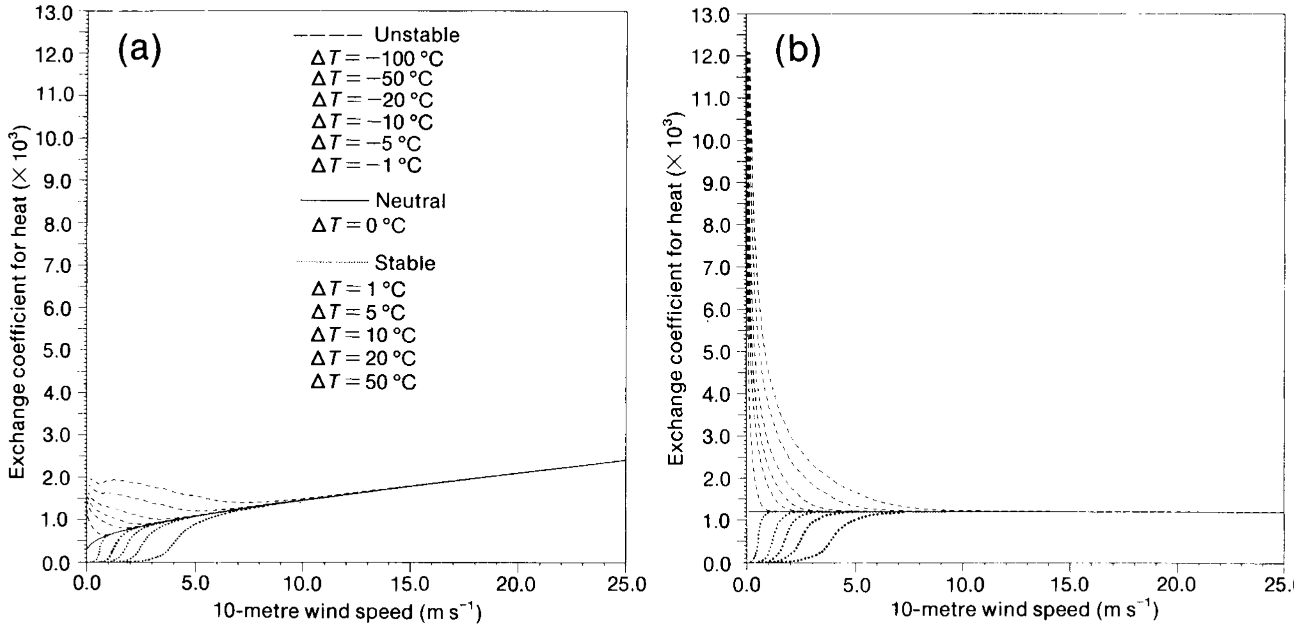

Figure 12. Exchange coefficient for sensible heat as a function of wind speed for various air–sea temperature differences and zero humidity difference for (a) the fine-mesh and (b) the coarse-mesh models.

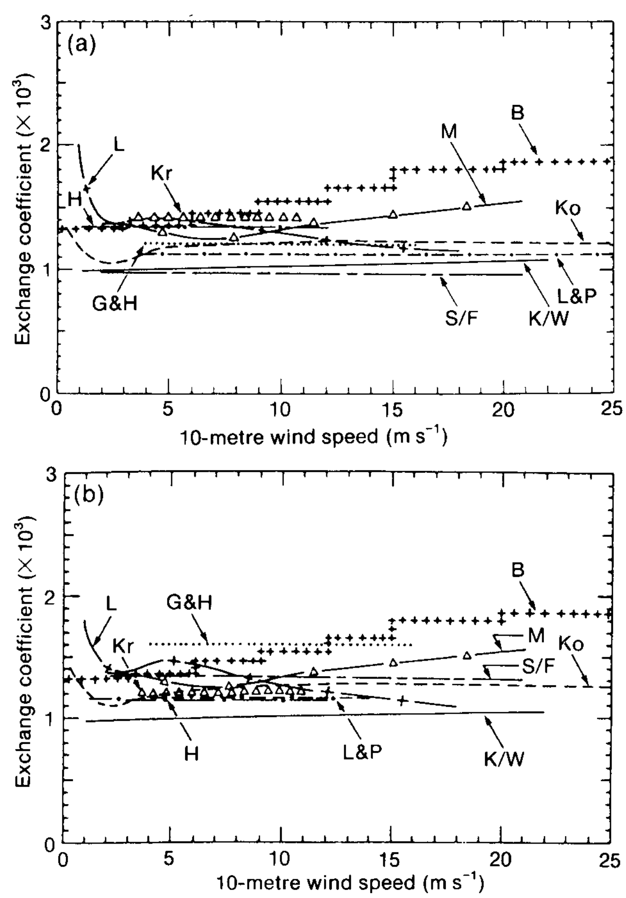

Figure 13. The neutral or slightly unstable exchange coefficients for (a) sensible heat and (b) latent heat as a function of the 10 m wind (from Blanc (1985)). Sources are: K/W = Kitaygorodskiy *et al.* (1973) and Wu (1980); Ko = Kondo (1975); G&H = Garratt (1977) and Garratt and Hyson (1975); B = Bunker (1976); Kr = Krügermeyer (1976); S/F = Smith (1980) and Friehe and Smith (1976); H = Hasse *et al.* (1978); L = Liu *et al.* (1979); M = Masagutov (1981); L&P = Large and Pond (1981, 1982).

coefficient on sea state (discussed by Alves (1991)) would suggest that C_H and C_E may also depend on sea state to some extent. Even so, it is clear that the present formulation used by the FM overestimates the values of C_H and C_E for strong winds and underestimates them for light winds. The CM has a better representation even though it has no wind dependence.

5. Solar heat flux

5.1 Results

The main problem with the solar heat flux is that the CM model uses a cloud distribution which is essentially a zonally averaged climatology. This is apparent in Fig. 15(a) which shows the merged mean solar heat flux for October 1989 used to drive the ocean model. Outside the FM region there is little zonal variation. Fig. 15(b) shows the NWP merged solar heating for October 1989 less a climatological field (Esbensen and Kushnir 1981). The 'bull's-eye' of 130 W m^{-2} (50% more than the climatological value) in the southern tropical ocean clearly indicates that such a zonally averaged radiation could not realistically be used to drive an ocean model. Furthermore, in the NWP model most of the tropical Atlantic has a much larger solar heat flux than climatology, with the departure from climatology increasing as one moves south-eastwards across the equator.

In the FM region the interactive cloud scheme gives a field which varies both meridionally and zonally. When compared with the climatology (Fig. 15(b)) the FM field is generally some 10–50 W m^{-2} (up to 40% of total) higher throughout most of the mid-latitude North Atlantic.

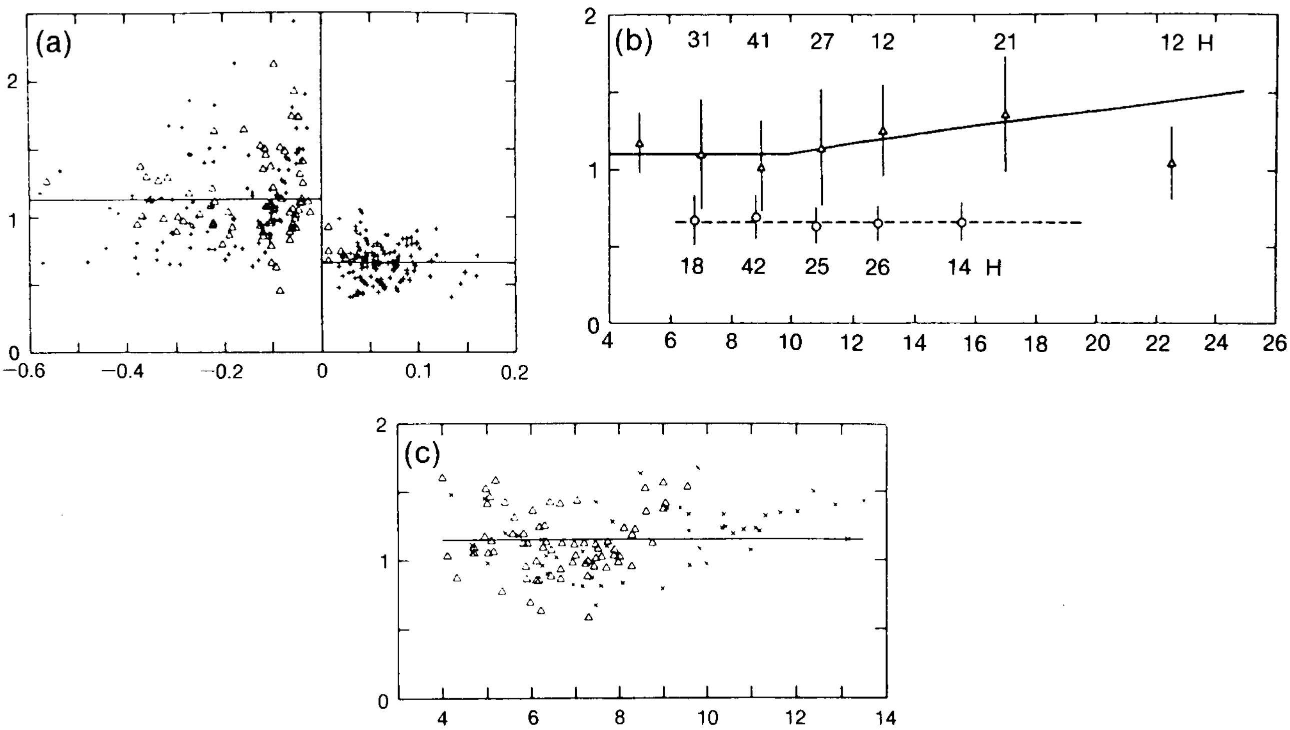

Figure 14. Experimental plots of the exchange coefficient for (a) sensible heat as a function of stability, (b) as a function of the 10 m wind speed (m s^{-1}) and (c) the exchange coefficient for latent heat as a function of the 10 m wind speed (m s^{-1}) (from Large and Pond (1982)).

Fig. 16 shows the difference in the ocean model's top-level temperature between the solar and climatology runs. A monthly mean SST warming of over 1.8 °C occurs in the region where the 'bull's-eye' (Fig. 15) was located and extends down to a depth of around 30 m (not shown). In the FM region there is also a general monthly mean warming of up to 0.6 °C (corresponding to solar flux difference of 50 W m^{-2}). Solar heating leads to an increase of the stratification in the upper layers of the ocean and therefore a decrease in the mixed layer depth (for constant wind mixing energy). A decrease in the mixed layer depth will increase the sensitivity of the SST to solar heating. The hypothesized decrease in the mixed layer depth due to solar heating can be confirmed in Fig. 17. The 'bull's-eye' heating in Fig. 17 resulted in a reduction in the mean mixed layer depth for that month of around 140 m (over 75% of initial value) and in the FM area the maximum heating difference of 50 W m^{-2} reduces the monthly mean mixed layer depth by around 5 m (about 10% of initial value).

Reduction in the mixed layer depth due to solar heating decreases the depth of water to which the momentum flux from the atmosphere is applied directly through the Ekman drift mechanism. This will, of course, change the structure of the currents in the upper layers of the ocean. Fig. 18 shows the monthly mean vector difference between the solar and climatology runs' model top-layer current field. Large solar radiation differences in the tropical Atlantic introduce relatively large anomalous currents throughout the region. The difference in the magnitude of the currents between the two runs is comparable with the magnitudes of the currents themselves. These are also comparable to differences between model integrations using NWP wind stress and climatological wind stress (see Alves (1991)). In the FM region there are no significant differences in the near surface currents mainly due to much deeper mixed layers. Throughout the Atlantic there is no significant difference between the currents of the two runs below the mixed layer.

5.2 Discussion

The calculation of the solar heat flux is mainly sensitive to two factors, the representation of cloud and surface albedo. Derivation of cloud amount (outlined in section 2) depends upon the model humidity field. In the NWP data-analysis scheme used by the MO only humidity measurements from conventional soundings of the atmosphere are used. Sparseness of these soundings over the ocean and the difficulty in measuring humidity render the humidity fields used by the NWP models to be of poor quality. This is an area which requires a great effort in improving the observations of humidity and their assimilation into NWP models. Inability to represent cloud correctly in NWP models will remain the main source of error in the solar heat flux at the surface.

The value α_0 (0.06 in the FM model) is the value for the sea surface albedo used under clear sky conditions (it is modified for multiple reflection when clouds are present). This value is know to vary with the elevation of the sun and the sea state. The amount of reflection from the sea surface is known to increase as the sun's elevation decreases. Representing this effect may be important to

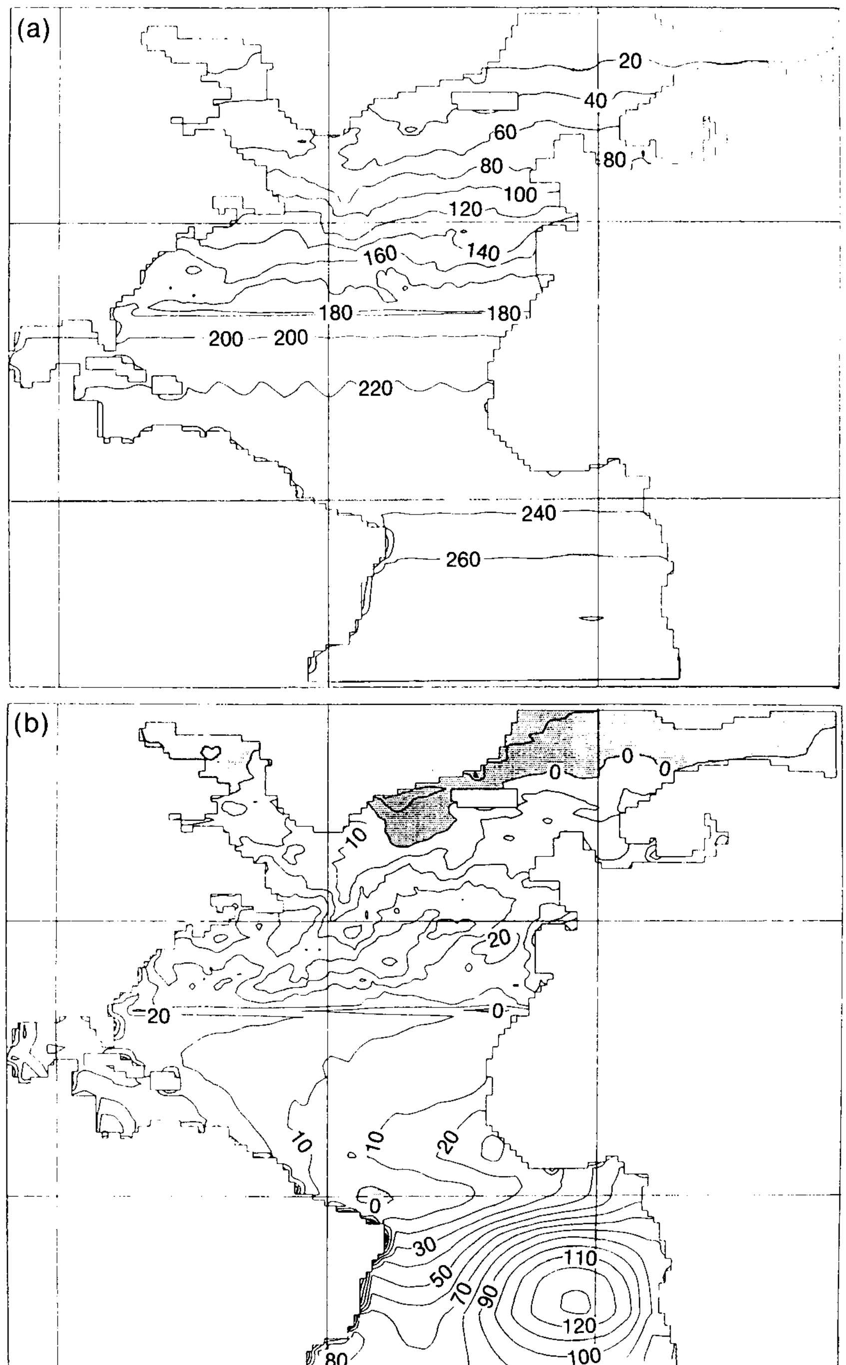

Figure 15. (a) Monthly mean NWP merged solar radiation used by the NWP run for October 1989. Contours every 20 W m^{-2}. (b) Difference in the monthly mean solar radiation between the NWP merged field for October 1989 and climatology. Contours every 20 W m^{-2} with negative areas shaded.

model the daily cycle of the oceanic mixed layer.

Dependence of the surface albedo on the sea state becomes important during periods of strong winds. The formation of whitecaps (foamy mixture of water and air produced by breaking waves) increases the surface albedo since the whitecaps themselves are believed to have an albedo of about 0.5 (Stabeno and Monahan 1986). Spillane *et al.* (1986) show maps of monthly mean whitecap distribution. The maximum whitecap coverage occurs during winter in the North Atlantic and covers about 4% of the ocean. Taking the albedo of the whitecap-free sea surface to be 0.06, the surface albedo under the maximum whitecapping conditions above would be 0.08 (30% greater). It must be emphasized that this is the maximum influence of whitecapping on the surface albedo and it would only be of importance under strong winds and clear skies.

Even where there are no breaking waves, for increasing roughness of the sea, the albedo increases for small zenith angles (near 0°) and decreases for large zenith angles (near 90°) (Nunez *et al.* 1972). The opacity of the water also effects the surface albedo with the albedo increasing with a decrease in transparency (Kondratyev 1972).

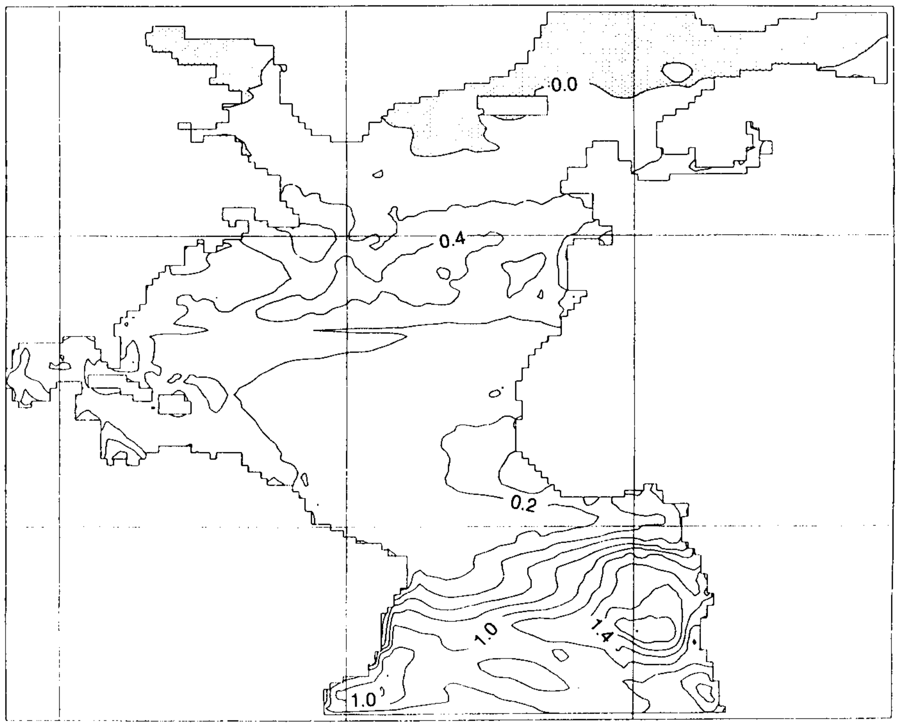

Figure 16. Monthly mean SST difference between the NWP solar run and the climatological run. Contours every 0.2 °C with negative areas shaded.

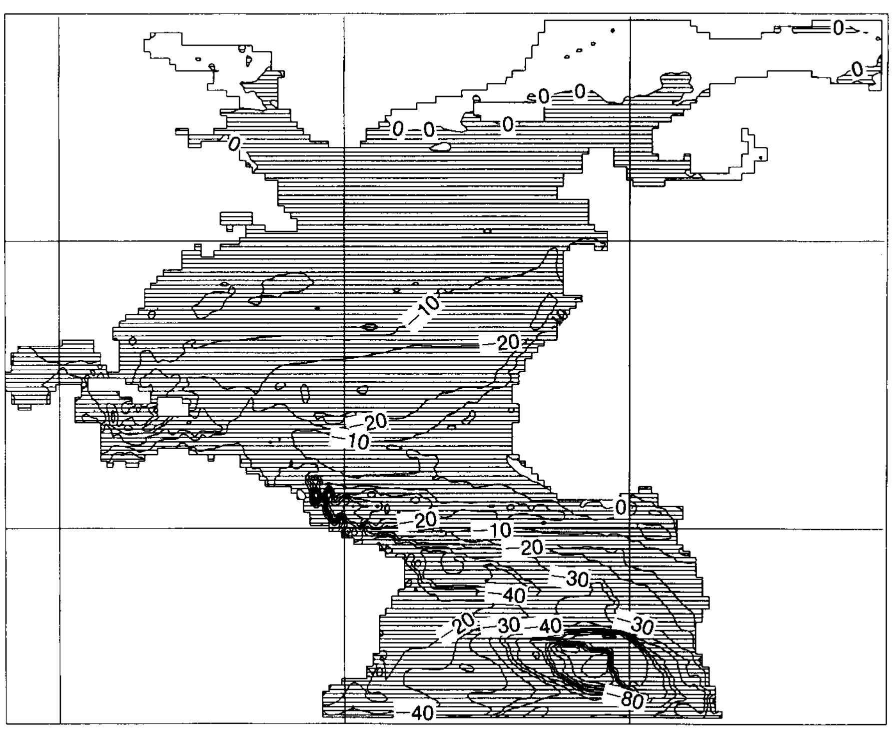

Figure 17. Monthly mean difference in the mixed-layer depth between the solar NWP run and the climatological run. Contours every 10 m with negative areas shaded.

6. Fresh water flux

6.1 Results

The PME (Precipitation Minus Evaporation) field gives a value for the net fresh water flux into the ocean from the atmosphere. Fig. 19(a) shows the climatological PME field for October (precipitation is due to Jaeger (1983) and evaporation is from Esbensen and Kushnir (1981)). Generally evaporation exceeds precipitation except for the region of the ITCZ (Inter Tropical Convergence Zone) in the east tropical North Atlantic, parts of the Caribbean and in the latitude range 50° N–60° N. A region of excess rainfall associated with the ITCZ is concentrated off the west coast of Africa from

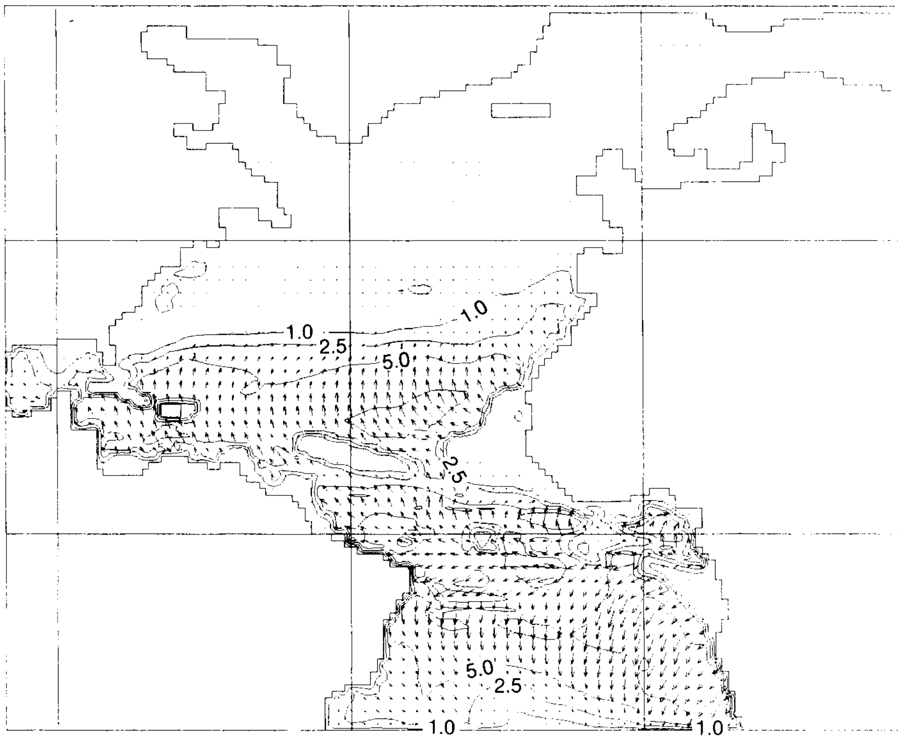

Figure 18. Monthly mean vector difference in the surface current between the solar NWP run and the climatological run. Contours at 1, 2.5, 5, 10 and 20 cm s^{-1}.

around 10°S to 15°N, with the PME reaching 7.5 mm day^{-1}. Fig. 19(b) shows the merged PME field from the NWP models. The ITCZ is represented by a narrower band of larger PME extending from the equator to about 10°N in the east Atlantic. Excess of precipitation over evaporation extends into the west tropical Atlantic, along the Brazilian coast and into the South Caribbean. In the east Atlantic it reaches values of up to 10 mm day^{-1} in the region of the climatological ITCZ and in the west Atlantic it reaches 5 mm day^{-1} in a region where the climatological value is of the opposite sign. Clearly the NWP PME has a stronger ITCZ which spreads out over a longer band across the tropical Atlantic. Confirmation of this actually happening has not been sought.

The difference between the two PME fields is plotted in Fig. 20(a). It emphasizes the large PME in the CM model in the north-western tropical Atlantic which is up to 7.5 mm day^{-1} greater than the climatology. In the west Atlantic, between the latitudes 15°N and 45°N where the climatology shows a negative PME of about 2.5 mm day^{-1}, the NWP model produces much less evaporation and/or much more precipitation, with the PME reaching a positive value of 5 mm day^{-1} in the central part of this region. North of about 45°N the agreement between the two is generally to within 2.5 mm day^{-1} which is of the same magnitude as the PME value.

Temperature and salinity of the ocean affect the ocean circulation by changing the density structure. The PME field, where positive, decreases the salinity of the mixed layer (and vice versa where negative). To establish the importance of a change in salinity on the ocean circulation we need to quantify its relative effect on density. Gill (1982) gives a standard formula relating the density of sea water to the temperature and salinity. Linearizing that formula it can be deduced that the change in density due to a change in temperature ΔT is equivalent to a change in salinity ΔS (in parts per thousand (ppt)) given by

$$\Delta S \simeq \frac{(-0.08-0.02T)}{(0.9-0.004T)}\Delta T$$

where the temperature T is in °C. Taking $\Delta T = 1$ °C, then for the tropics (with $T = 25$ °C) we obtain, that for a similar change in density, it would require $\Delta S = -0.7$ ppt. For the polar regions taking $T = 0$ °C then $\Delta S = -0.09$, nearly an order of magnitude less than in the tropics. This clearly shows that salinity differences due to the PME field will be of greater relative importance in the higher latitudes where the temperature of the mixed layer is cooler.

Differences between the two models top-level monthly mean salinity field are shown in Fig. 20(b). The large difference in the PME field in the region of the ITCZ introduces differences in the salinity field of up to 0.25 ppt, this having a similar effect on the density as a temperature difference of about 0.3 °C which is not significant when compared to the differences produced by the heat fluxes. North of about 45°N differences in the salinity field is generally less than 0.05 ppt, this being equivalent to a temperature change of around 0.5 °C. Therefore a PME difference of 2.5 mm day^{-1} in the polar regions has a similar effect on the upper-ocean density

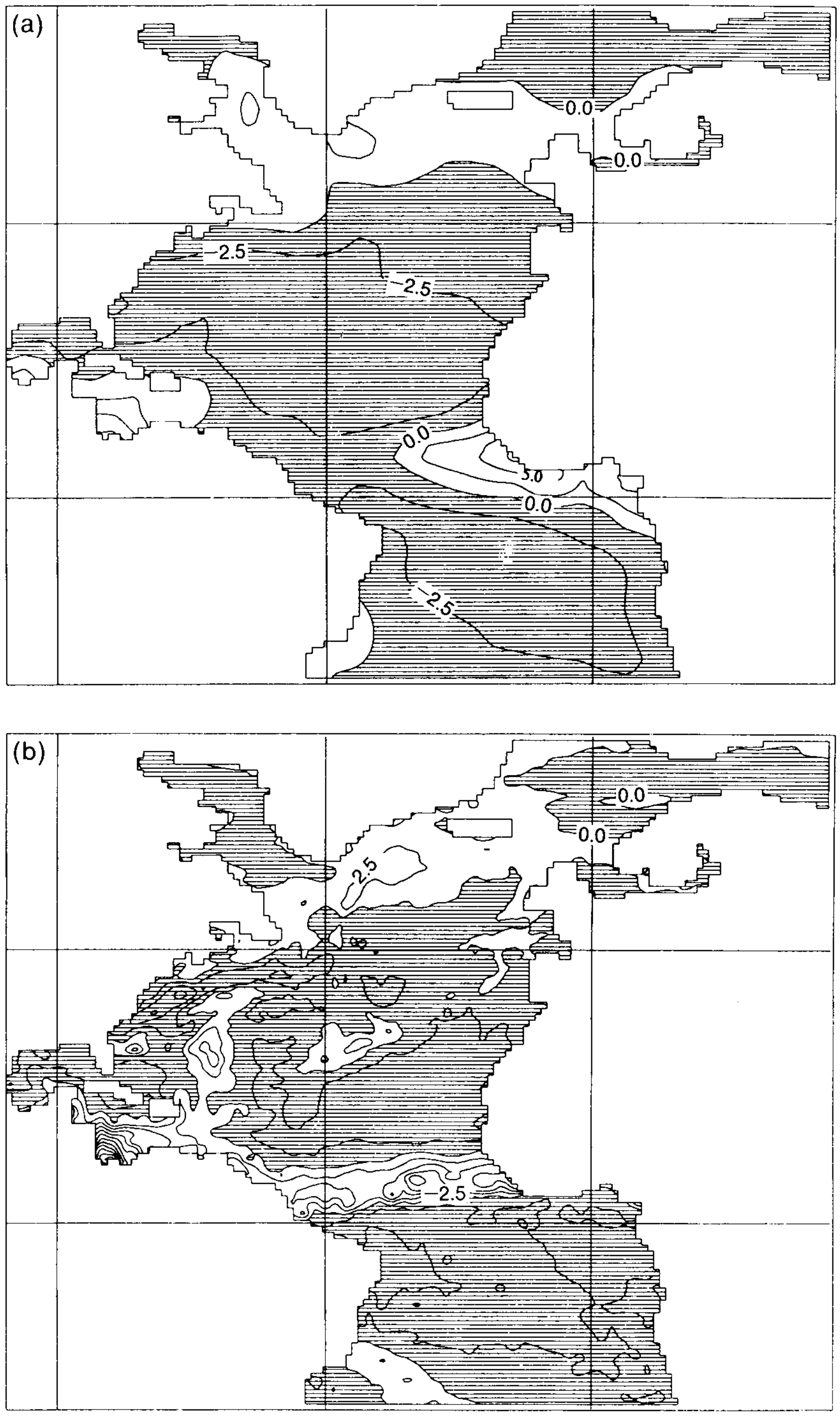

Figure 19. Monthly mean precipitation minus evaporation for (a) climatology and (b) merged NWP field for October 1989. Contours every 2.5 mm day^{-1}.

field as a PME difference of around 10 mm day^{-1} in the tropics.

Fig. 21 shows the difference in the mixed layer depth between the two runs. Where the NWP has excess water flux into the ocean, the increase in buoyancy of the surface water leads to a reduction in the mixed layer depth of up to 30 m in the tropics (on average a 50% reduction). The PME is less than that of the climatology in the Gulf of Guinea and the mixed layer depth there is increased by around 15 m from a monthly mean depth of 25 m. Although these changes in the mixed layer depth do not significantly affect surface temperature (not shown) it does introduce differences in the current field (Fig. 22). Vector differences of over 5 cm s^{-1} occur in a region of the tropics where the surface current is around 20 cm s^{-1}, these differences being restricted to the mixed layer. Away from the region of the ITCZ there are no significant differences in the current field.

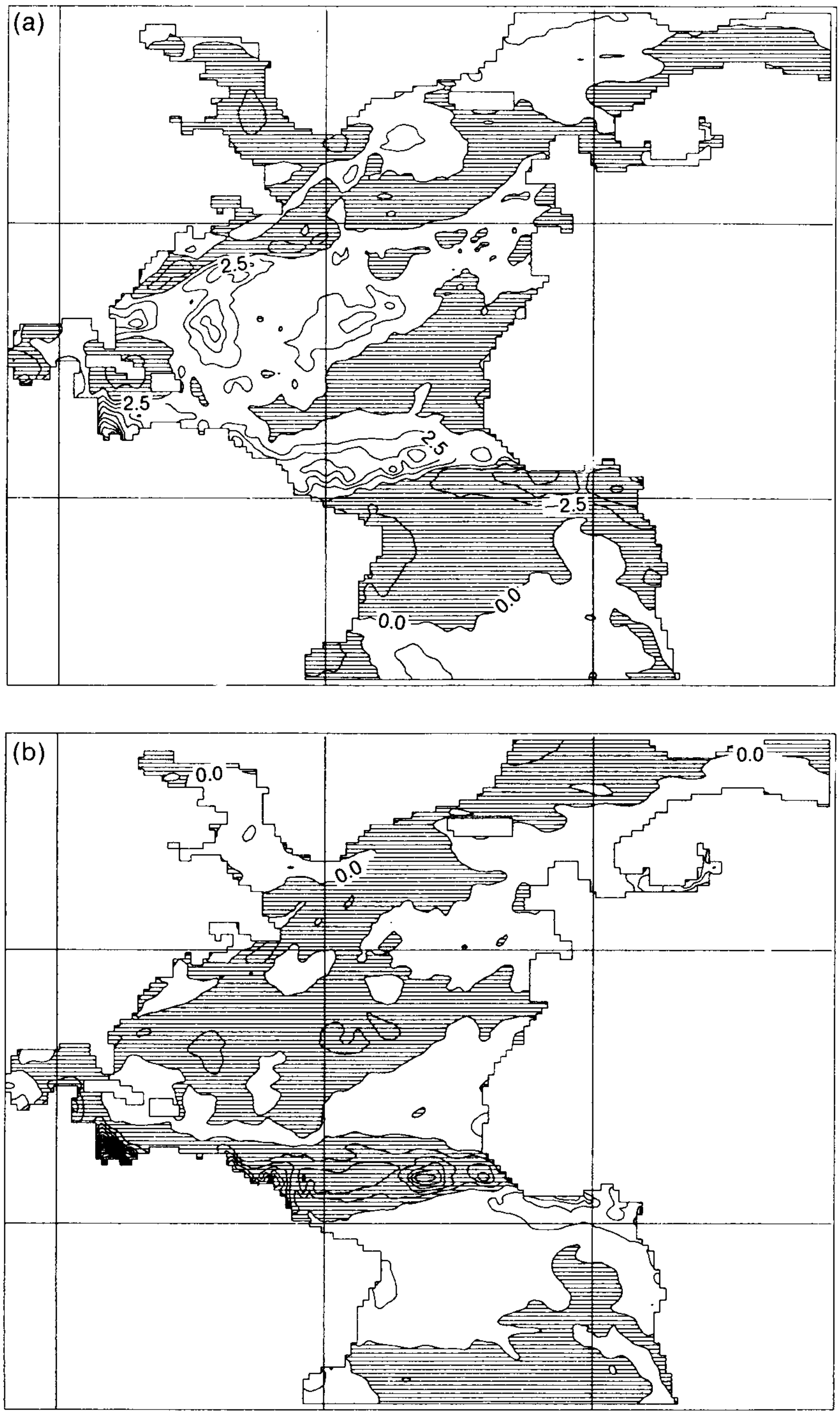

Figure 20. (a) Difference between monthly mean NWP merged and climatology PME fields. Contours every 2.5 mm day^{-1} with negative areas shaded. (b) Monthly mean difference in the top-layer salinity field between the NWP PME integration and the climatological one. Contours every 0.05 ppt with negative areas shaded.

6.2 Discussion

The parametrization of the evaporation flux has already been discussed as the latent heat flux in section 5. The precipitation depends critically upon the humidity field, therefore emphasizing the need to improve the assimilation of humidity data and its representation in NWP models.

Differences in the NWP models' PME field were shown to be more important in areas where the SST was lowest due to the dependence of the density on salinity. However, because of the shallower mixed layers in the warmer SST regions of the tropics, significant differences in the current field were observed. In general, differences were small when compared with the differences due to the heat, solar and momentum fluxes. The specification of the PME field is therefore secondary to that of the other surface fluxes.

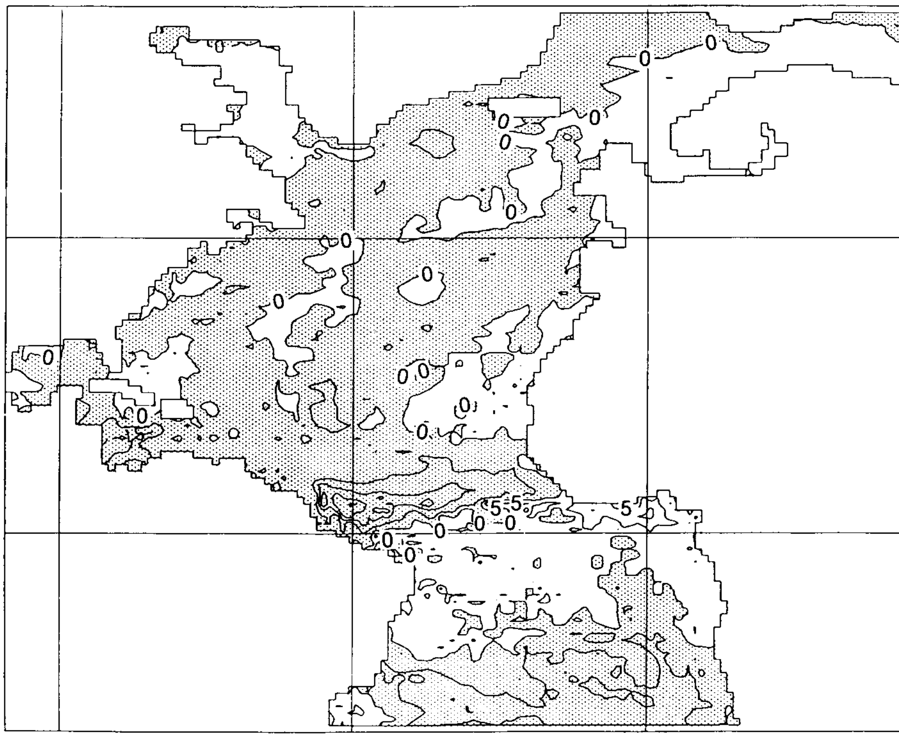

Figure 21. Monthly mean difference in the mixed-layer depth between the NWP PME and climatology runs. Contours every 5 m with negative areas shaded.

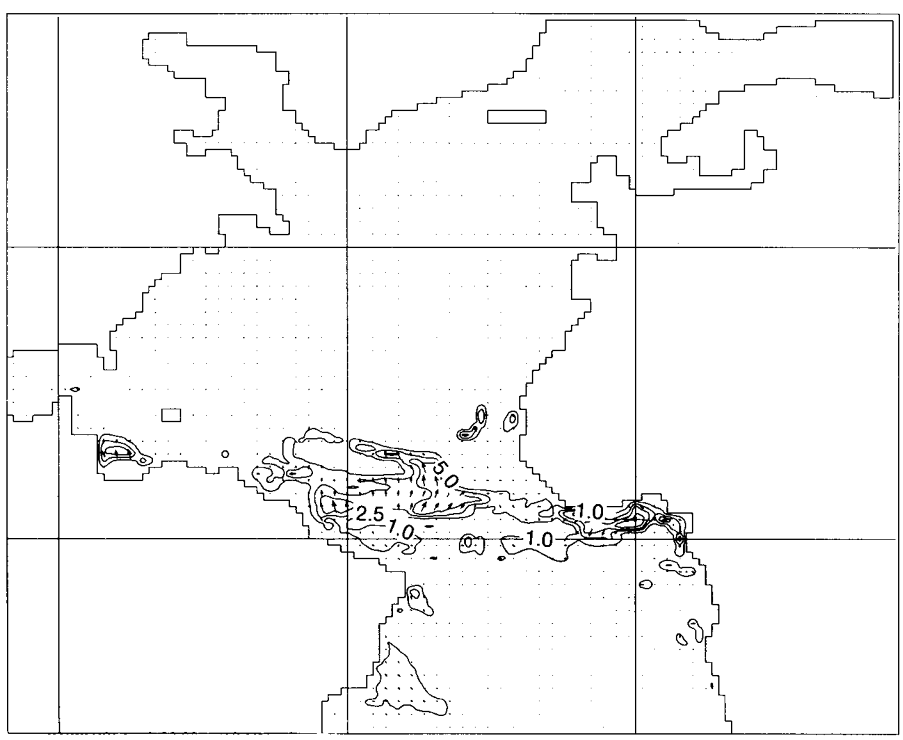

Figure 22. Monthly mean vector differences in the model top-layer current between the NWP PME and climatology runs. Contours at 1, 2.5, 5 and 10 cm s^{-1}.

7. Summary, conclusion and recommendations

7.1 Non-penetrative heat fluxes

The IR flux ranges from 30 to 80 W m^{-2} throughout the North Atlantic. Differences of up to 50% from the monthly mean climatology were noted for the CM model. In the tropical North Atlantic the CM IR flux was some 50% or so greater than the climatology. Comparison of the FM and CM models' IR flux revealed differences of up to 25 W m^{-2}, representing a percentage difference of 50%, this being partly due to the use of a zonally averaged climatological cloud distribution in the CM model. The strong dependence of the IR flux on cloud emphasizes the need to improve the assimilation of humidity into NWP models and its representation throughout the forecast. Possible errors in the SST field used by the NWP models were reported and an uncertainty of 1 °C in the SST field would yield uncertainties in the IR flux of up to 17% in the equatorial Atlantic. This uncertainty represents typically 5 W m^{-2} which is relatively small when compared to uncertainties in the latent heat flux.

In the Gulf Stream area, where the maximum sensible heat flux occurred, the CM predicted values for the sensible heat flux which were 65% or so greater than the climatological values. The FM increased this difference by a further 15%. The 10% uncertainty in the wind speed, due to differences between the FM and CM 10 m winds, leads to uncertainties of 10% in the sensible heat flux. More important, a strong dependence of the sensible heat flux on the SST gradient was shown, with the NWP models producing a more localized and larger magnitude heat flux across the Gulf Stream than the climatology which used a SST field of lower resolution. This emphasizes the need to use high resolution SST fields as the lower boundary condition for the NWP models. The air–sea temperature difference was shown to contribute significantly to the differences between the NWP and the climatological values of the sensible heat flux. Since, over the sea, temperature observations are not assimilated into the lowest level of the NWP model, the air–sea temperature difference is dependent on the model adjustment through the heat fluxes. Whether the assimilation of temperature into the first model level would improve the heat flux is questionable given that the SST fields used at present are known to have relatively large errors (Alves 1990). Values for the exchange coefficient for the sensible heat flux agree well for the two models and published values for wind speeds in the range 5–8 m s^{-1}. For stronger winds the published values show a large spread and there is an uncertainty as to whether there is a stability and/or wind speed dependence. The CM uses a constant value which agrees with some of the published results. The FM value increases with wind speed, due to the use of the Charnock formula to parametrize the surface roughness length, it being nearly twice that used by the CM for a wind speed of 20 m s^{-1}. The FM parametrization clearly overestimates the value of C_H when compared with other authors for strong winds. For light winds the CM keeps its constant value of 1.2×10^{-3}, agreeing with the published values, whereas the FM value decreases to zero with decreasing wind speed. The use of the Charnock formula is clearly not appropriate for light winds. Under conditions of free convection the values for C_H used by the FM model is six times less than that used by the CM model, which itself is reported to be too low (Gordon and Hunt 1989).

The latent heat flux is the dominant of the three heat fluxes (sensible, latent and IR) with its maximum value reaching over 300 W m^{-2} in the Gulf Stream area for the CM model. The monthly mean values from the CM model were up to 100 W m^{-2} (33%) greater than the climatological values. The FM values increased this difference by a further 15% or so. The higher resolution SST field used by the NWP models compared to that used to calculate the climatological heat fluxes resulted in the latent heat flux being more localized and of a larger magnitude where there was strong SST gradients, such us that of the Gulf Stream. The same 10% uncertainty is applicable to the latent heat flux due to uncertainties in the wind speed. The dependence of the latent heat flux on the specific humidity difference was shown to be of importance and this difference was much greater than the climatological value. Similar conclusions can be drawn for the latent heat flux as for the sensible heat flux, these being the need to accurately represent SST gradients and that the humidity difference arises due to the model adjustment to the specified SST through the water flux from the sea surface (constant times the latent heat flux). Again, it is not clear whether the assimilation of humidity observations into the lowest level of the NWP models would improve the latent heat flux due to known biases in the prescribed SST field. The values used for the exchange coefficient for the latent heat flux for both CM and FM models is the same as that used for the sensible heat flux. The same conclusion as for the value of C_H can be made; that there is no clear evidence as yet to suggest the dependence on stability or wind speed, if any, of either values of C_H and C_E. Even so, it is clear that the present formulation used by the FM overestimates the values of C_H and C_E for strong winds and underestimates them for light winds. The CM has a better representation even though it has no wind dependence.

The combination of the three heat fluxes above to form the net heat flux was used to force the ocean model. In general, the monthly mean net heat flux from the NWP models for October 1989 was up to 100 W m^{-2} greater than the climatology away from the Gulf Stream area and up to 200 W m^{-2} greater than the climatology in the Gulf Stream area. The latent heat flux was by far the larger of the three heat fluxes. When there was net heating of the ocean the mixed layer depth was reduced and this decreased the depth of the water column into which heat was input. Thus the sensitivity of the SST to the heat fluxes was shown to depend on the mixed layer depth, this made the tropical ocean much more sensitive to errors in the fluxes than the mid-latitude ocean.

7.2 Solar radiation flux

The solar heat flux, together with the latent heat flux, is the main contributor towards the mixed layer heat balance, with the sensible and IR fluxes, in general, having relatively smaller values. The results presented clearly show that a radiation scheme which uses cloud distribution derived from an interactive cloud scheme is essential. The radiation flux from the CM model which uses a zonally averaged climatological cloud distribution was totally unsuitable for use in ocean model integrations. In the FM region, differences between the NWP solar flux and the climatological solar flux of up to 50 W m^{-2} produces mixed layer temperature differences of up to 0.6 °C in a region of a relatively deep mixed layer, although there was no significant difference in the current field.

The dependence of the solar flux on various physical parameters has been discussed. By far the most important is the dependence on cloud distribution. The cloud distribution is derived from the model's humidity field whose realism over the ocean is based on the assimilation of a relatively small number of conventional atmospheric soundings. Further progress in improving the quality of the surface solar flux must first be in the parametrization of cloud and the representation of humidity in the NWP models. This clearly requires a great effort in improving techniques for measuring humidity and putting them into practice routinely. The solar flux can then be further improved by taking into account the dependence of the surface albedo on the solar zenith angle and the sea state, opacity and its geometry.

7.3 Fresh water flux

The monthly mean PME field from the NWP models represents an ITCZ which extends further into the West Atlantic than the climatology and has a larger intensity. In the western tropical North Atlantic the PME field is up to 7.5 mm day^{-1} more than the climatology (the climatology is of the opposite sign, i.e. excess of evaporation over precipitation). In the middle latitudes the differences are less than 2.5 mm day^{-1}. The effect of the changes in the salinity field on the near-surface density structure, due to differences in the PME field, were shown to depend critically on the SST. The large differences in the PM field between the two runs of 7.5 mm day^{-1} in the tropics had a similar effect on the density structure as a difference of 2.5 mm day^{-1} in the high latitudes. Overall, the changes due to the differences in the PME fields were small when compared to those due to the differences in the heat, momentum and solar fluxes, although significant differences occurred in the equatorial current field as a result of shallower mixed layers.

The specification of the PME field is secondary to that of the other fluxes — momentum, heat and radiation. The evaporation rate is equivalent to the latent heat flux and its deficiencies have already been discussed in the heat fluxes above. The precipitation depends on the model's humidity field. This again emphasizes the need to represent humidity accurately in the NWP models.

References

Alves, J.O.S., 1990: A comparison of sea surface temperatures from three analysis schemes. (Unpublished, copy available from National Meteorological Library, Bracknell.)

—, 1991: An assessment of the surface fluxes from the Meteorological Office numerical weather prediction models. Part I: Momentum. *Meteorol Mag*, **120**, 200–211.

Bell, R.S. and Dickinson, A., 1987: The Meteorological Office operational numerical weather prediction system. *Sci Pap, Meteorol Off*, No. 41.

Blanc, T.V., 1985: Variation of bulk-derived surface flux, stability, and roughness results due to the use of different transfer coefficient schemes. *J Phys Oceanogr*, **15**, 650–669.

Bolton, J.A., 1981: The estimation of zonally averaged climatological cloud data for use in the 5 level model radiation scheme. (Unpublished, copy available from National Meteorological Library, Bracknell.)

Bunker, A.F., 1976: Computations of surface energy flux and annual air-sea interaction cycles of the North Atlantic Ocean. *Mon Weather Rev*, **104**, 1122–1140.

Charnock, H., 1955: Wind stress on a water surface. *Q J R Meteorol Soc*, **81**, 639–640.

Cox, M.D., 1984: A primitive equation, three dimensional model of the ocean. Princeton, Geophysical Fluid Dynamics Laboratory, Ocean Group Technical Report No. 1.

Esbensen, S.K. and Kushnir, Y., 1981: The heat budget of the global ocean: An atlas based on estimates from surface marine observations. Corvallis, Oregon State University, Report No. 29.

Friehe, C.A. and Schmitt, K.F., 1976: Parameterization of air-sea interface fluxes of sensible heat and moisture by the bulk aerodynamic formulas. *J Phys Oceanogr*, **6**, 801–809.

Garratt, J.R., 1977: Review of drag coefficients over oceans and continents. *Mon Weather Rev*, **105**, 915–929.

Garratt, J.R. and Hyson, P., 1975: Vertical fluxes of momentum, sensible heat and water vapour during the air mass transformation experiment (AMTEX) 1974. *J Meteorol Soc Jpn*, **53**, 149–160.

Gill, A.E., 1982: Atmosphere–Ocean dynamics. London, Academic Press.

Gordon, C. and Hunt, D.L., 1989: Surface evaporation during free convection. (Unpublished, copy available from National Meteorological Library, Bracknell.)

Hasse, L., Grünewald, M., Wucknitz, J., Dunckel, M. and Schriever, D., 1978: Profile derived turbulent fluxes in the surface layer under disturbed and undisturbed conditions during GATE. *'Meteor' Forschungsergebnisse*, **13**, 24–40.

Jaeger, L., 1983: Monthly and areal patterns of mean global precipitation. *In* Street-Perrott, A., Beran, M. and Ratcliffe, R. (eds), Variations in the global water budget. Dordrecht, Reidel.

Kitaygorodskiy, S.A., Kuznetsov, O.A. and Panin, G.N., 1973: Coefficients of drag, sensible heat, and evaporation in the atmosphere over the surface of the sea. *Atmos Ocean Phys*, **9**, 644–647.

Kitchen, J.E., 1986: An implicit version of the operational model boundary layer routine. (Unpublished, copy available from National Meteorological Library, Bracknell.)

Kondo, J., 1975: Air-sea bulk transfer coefficients in diabatic conditions. *Boundary Layer Meteorol*, **9**, 91–112.

Kondratyev, K.Ya., 1972: Radiation processes in the atmosphere. Geneva, WMO, No. 309.

Kraus, E.B. and Turner, J.S., 1967: A one-dimensional model of the seasonal thermocline, II. The general theory and its consequences. *Tellus*, **19**, 98–105.

Krügermeyer, L., 1976: Vertical transports of momentum, sensible and latent heat from profiles at the tropical Atlantic during ATEX. *'Meteor' Forschungsergebnisse*, **11**, 51–77.

Large, W.G. and Pond, S., 1981: Open ocean momentum flux measurements in moderate to strong winds. *J Phys Oceanogr*, **11**, 324–336.

—, 1982: Sensible and latent heat flux measurements over the ocean. *J Phys Oceanogr*, **12**, 464–482.

Liu, W.T., Katsaros, K.B. and Businger, J.A., 1979: Bulk parameterization of air-sea exchanges of heat and water vapor including the molecular constraints at the interface. *J Atmos Sci*, **36**, 1722–1735.

Masagutov, T.F., 1981: Calculation of vertical turbulent fluxes in the marine atmospheric surface layer of tropical latitudes. *Sov Meteorol and Hydrol*, No. 12, 47–53.

Nunez, M., Davies, J.A. and Robinson, P.J., 1972: Surface albedo at a tower site in lake Ontario. *Boundary Layer Meteorol*, **3**, 77–86.

Smith, S.D., 1980: Wind stress and heat flux over the ocean in gale force winds. *J Phys Oceanogr*, **10**, 709–726.

Spillane, M.C., Monahan, E.C., Bowyer, P.A., Doyle, D.M. and Stabeno, P.J., 1986: Whitecaps and global fluxes. *In* Monahan, E.C. and MacNiocaill, G. (eds), Oceanic whitecaps. Dordrecht, Reidel.
Stabeno, P.J. and Monahan, E.C., 1986: The influence of whitecaps on the albedo of the sea surface. *In* Monahan, E.C. and MacNiocaill, G. (eds), Oceanic whitecaps. Dordrecht, Reidel.
Wu, J., 1980: Wind-stress coefficients over the sea surface near neutral conditions — a revisit. *J Phys Oceanogr*, **10**, 727–740.

551.578.7:551.501.81:656.1(410.1)

Three motorway traffic accidents in hail showers on 29 March 1986: A radar study

W.S. Pike
19 Inholmes Common, Woodlands St Mary, Newbury, Berkshire RG16 7SX,

Summary

Heavy hail showers caused three major traffic accidents on English motorways when Easter saturday coincided with the last weekend in March 1986. The showers were sometimes accompanied by thunder and often moved quite rapidly at 30–40 m.p.h. The UK weather radar network was able to provide 15 minutes warning of the heaviest showers, and closer liaison with motorway police might eventually result in timely temporary use of speed-limit advisory signs along motorways in future similar situations.

1. Introduction

Holiday road traffic is often particularly dense on motorways, and Easter Saturday, 29 March 1986, was a typical example as drivers were encouraged to venture out in sunny weather during the morning over many central and eastern areas of the United Kingdom.

Three separate major traffic accidents, each involving carriageway-blocking 'pile-ups' of vehicles, occurred as dense and often fast-moving traffic ran into sudden heavy hail showers. These accidents are briefly analysed here together with the UK weather radar network 5 km data (at 15-minute intervals) to see what conclusions may be reached.

2. The synoptic situation

On 29 March 1986 the United Kingdom was affected by a fresh, unstable, westerly polar maritime airstream, in which showery troughs (see Figs 1(a) and 1(b)) were affecting western districts from mid-morning onwards, with clear skies and a deceptively sunny start in most other areas.

Towards midday a pool of very cold air with snow showers even at low levels was making rapid progress over Ireland, associated with a marked upper trough and a north-westerly 'jet streak' in the south. Over the United Kingdom showery surface troughs were generated both ahead of, and in association with, this cold air aloft. The visible image AVHRR satellite picture for 1328 UTC (not shown) gave a good indication of this troughing process which 'banked-up' successive bands of convective cloud over the United Kingdom ahead of more-open 'speckled' cells in the coldest air further west.

Ahead of the first trough the airflow backed west-south-westerly over much of England and the temperatures had risen rapidly to 11 °C at the surface in the south-eastern counties by late morning. Strong convective heating resulted in a scattering of relatively small but heavy showers, often falling as soft hail and occasionally accompanied by thunder, affecting all southern counties by 1145 UTC (see Fig. 2).

3. Radar interpretation

Five-kilometre squares might be considered as really too coarse a grid for accurate interpretation of shower intensities, which are sometimes known to give heavier falls than one is led to believe, in smaller areas. However, the 2 km radar has a lower extreme range (some 77 km) as opposed to the 210 km or so for the 5 km radar and, with quite deep convection involved, the latter network is preferred here.

Fig. 2 gives the radar precipitation rates, as averaged by computer, over 5 km squares at 1145 UTC on 29 March 1986. *Observer's Handbook* definitions of shower intensities do not completely agree with the intensity ranges indicated by the 5 km radar '10-level display scheme'. Therefore, the 'dot screens' used in Figs 3–5 have been interpreted as shown in Fig. 3.

Heavy intensities continued to be analysed throughout the afternoon and evening by the UK weather radar network before dying out later. Particularly violent showers and storms, with precipitation rates in excess of 64 mm h^{-1}, occurred near Evesham (Hereford and Worcester) and just south-west of Faversham (Kent) at

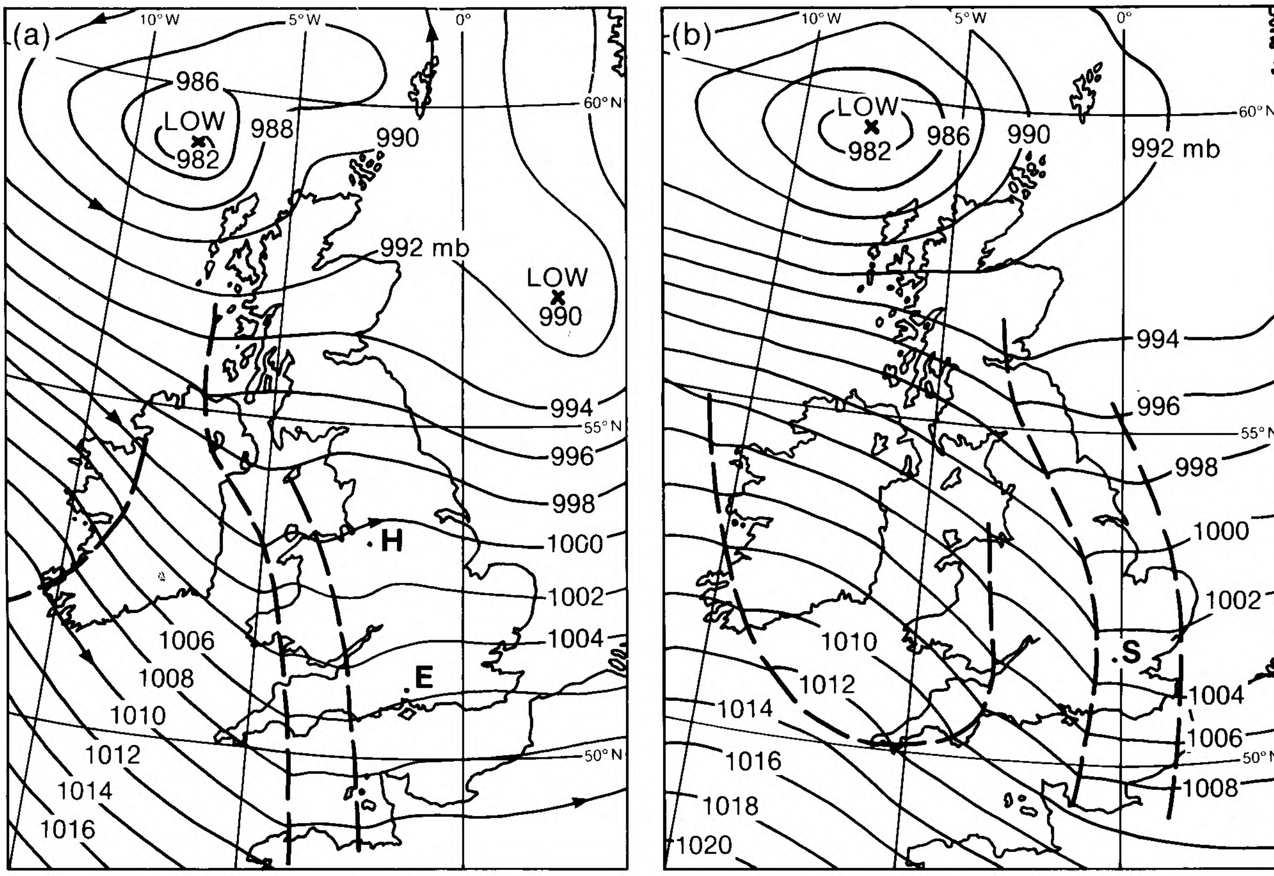

Figure 1. Surface synoptic charts for (a) 1200 UTC and (b) 1800 UTC on 29 March 1986. E, H and S show the locations of Eastleigh, Hassall and Scratchwood, respectively.

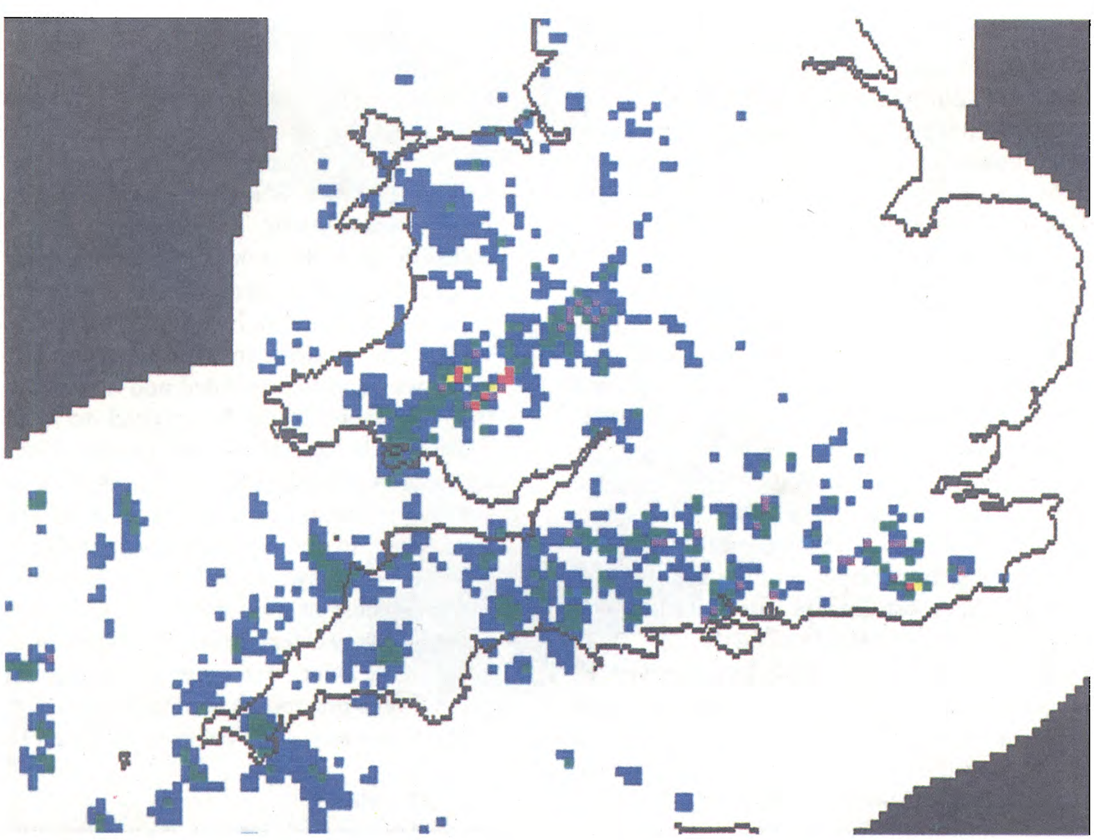

Figure 2. Rainfall distribution from the UK weather radar network at 1145 UTC on 29 March 1986. Rainfall intensities (mm h^{-1}) shown are: dark blue < 1, green 1–4, purple 4–8, light blue 8–16, pink 16–32 and yellow > 32.

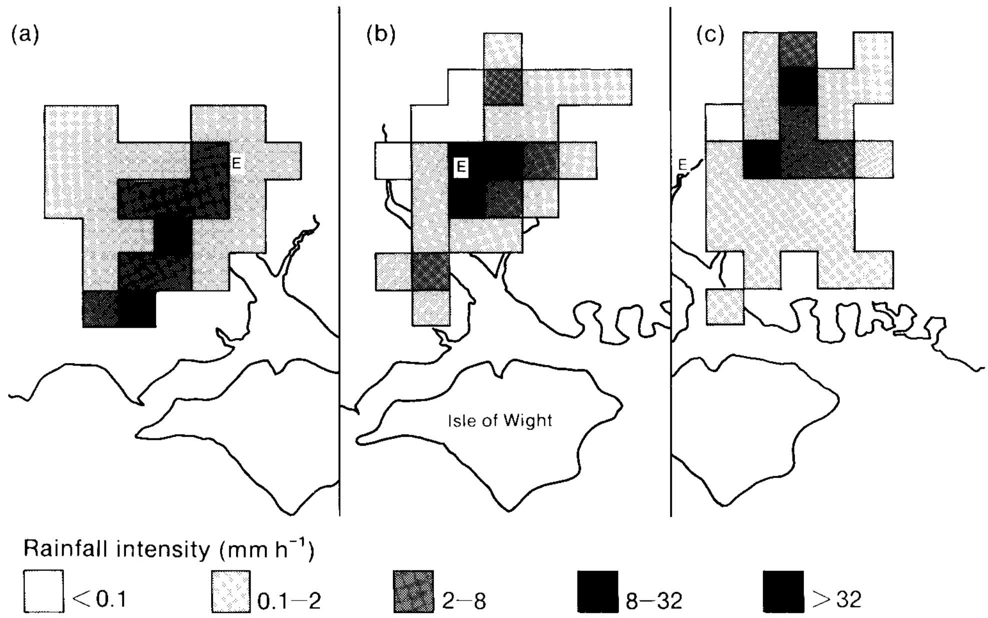

Figure 3. Data from the UK weather radar network at 5 km intervals around Eastleigh (marked E) at (a) 1130, (b) 1145 and (c) 1200 UTC on 29 March 1986. The location of Eastleigh is also shown in Fig. 1(a).

1400 UTC. Further violent storms were indicated near Cheshunt (Hertfordshire) and at Newmarket (Suffolk) by 1545 UTC. The latter East Anglian storms moved north-eastwards to affect the Ely and Thetford areas before decreasing in intensity after 1630 UTC, when approaching Norwich.

4. The traffic accidents

There were three major traffic accidents reported on English motorways during the course of the day, and all apparently occurred when drivers reacted differently as heavy hail showers were suddenly encountered by speeding vehicles:

(a) at Eastleigh, Hampshire (E on Figs 1(a) and 3) at approximately 12 noon near junction 5 of the M27 motorway. It resulted in temporary closure of the entire road. At first six westbound vehicles were involved but, immediately afterwards, four eastbound vehicles collided while attempting to avoid debris from the first accident which had crossed the central reservation. Apart from shock there were no serious injuries sustained. Fig. 3 shows this storm had moved rapidly from the west-south-west at an effective ground speed of 40 m.p.h. (Southampton Weather Centre reported a thunderstorm in the past hour at 1200 UTC). The most intense precipitation was indicated over Eastleigh at 1145 UTC).

(b) At Hassall near Alsager in Cheshire (marked 'H' in Figs 1(a) and 4) at 1237 UTC involving 34 northbound vehicles on the M6 motorway. There was no accident to southbound traffic which continued to flow freely. Fourteen people were injured (12 seriously) and were taken to North Staffordshire Hospital in a fleet of six ambulances. The northbound M6 was closed for nearly 3 hours after the accident. A spokesman from the Operational Support Division of the Cheshire Constabulary said 'The majority of drivers reduced speed in response to the weather conditions, the minority did not slow sufficiently and prosecutions took place for careless driving' (B. Ingham, Cheshire Constabulary, personal communication). Fig. 4 shows a relatively small but intense shower falling just west of Hassall at 1215 UTC, which then proceeded steadily in a north-easterly direction to pass just to the north of the village (and over the motorway) at 1230 UTC.

(c) At Edgware, north London, near Scratchwood Services (marked 'S' in Figs 1(b) and 5) at 1820 UTC. Fifteen southbound vehicles were involved in a collision and thirteen people were injured. The Hertfordshire Fire Service was summoned at 1824 UTC and the London Fire Brigade called out at 1827 UTC. The southbound carriageways of the M1 motorway had to be sanded and hosed down before the motorway could be opened to traffic again (information from D. Norris, London Fire and Civil Defence Authority). Fig. 5 shows a large area of heavy precipitation (associated with the second advancing showery trough) moving quickly eastwards towards Scratchwood just before the accident. The storm appears to have been a typical multicell type with the two western cells merging to form a larger area of heavier precipitation and another cell beginning to precipitate appreciably to the north-east of the motorway — all between 1745 and 1800 UTC.

5. Discussion

The radar network images were generally able to identify heavy precipitation occurring (albeit at this stage mostly in the cloud) from at least 15 minutes

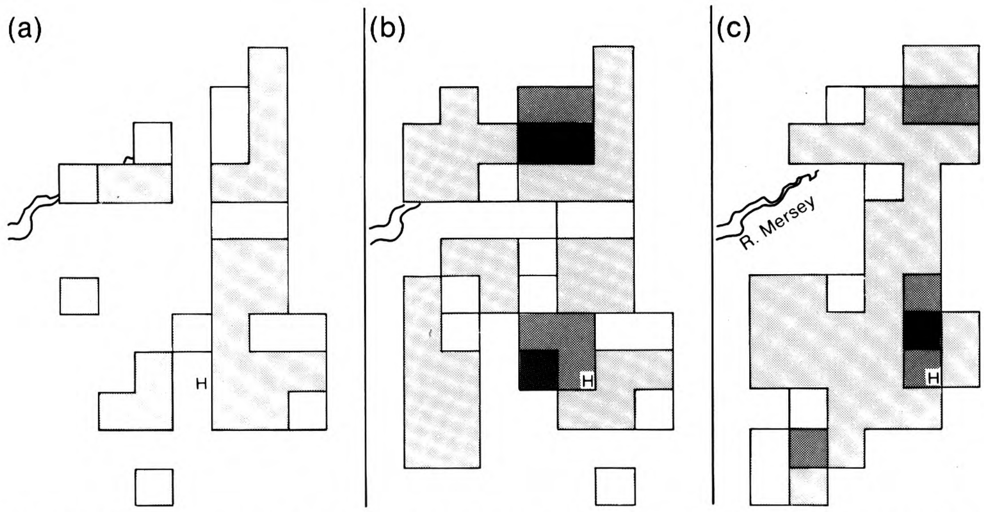

Figure 4. Data from the UK weather radar network at 5 km intervals around Hassall, Cheshire (marked H) at (a) 1200, (b) 1215 and (c) 1230 UTC on 29 March 1986. For intensities see Fig. 3. The location of Hassall is also shown in Fig. 1(a).

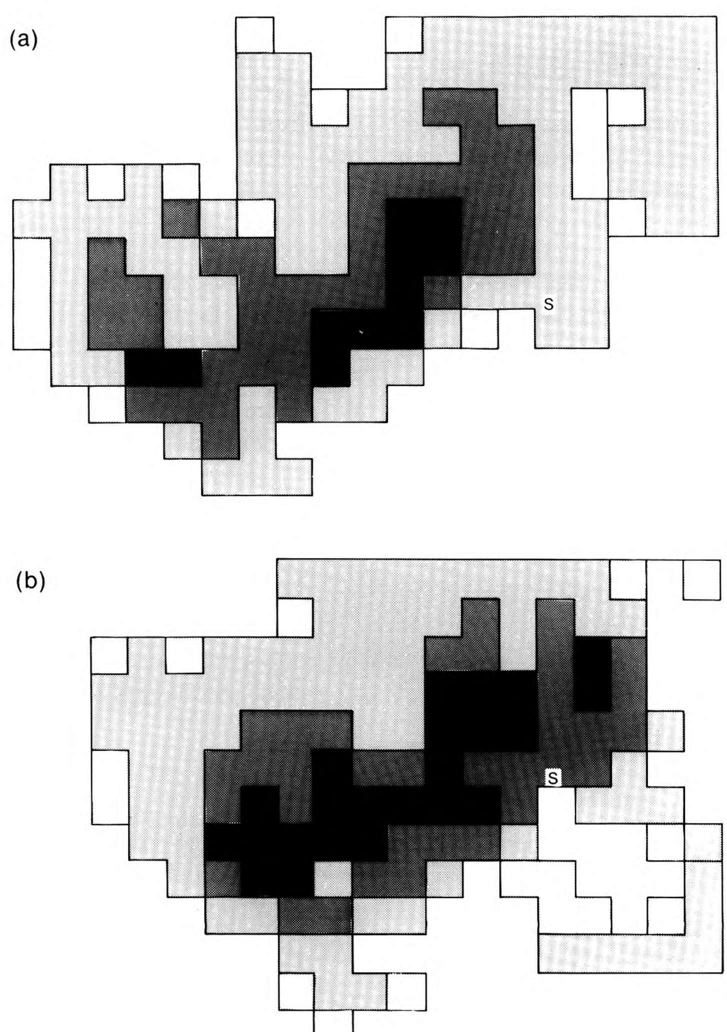

Figure 5. Data from the UK weather radar network at 5 km intervals around Scratchwood (marked S) at (a) 1745 and (b) 1800 UTC on 29 March 1986. For intensities see Fig. 3. The location of Scratchwood is also shown in Fig. 1(b).

before traffic accidents occurred, and such a period of notice could give motorway police and other emergency services a correspondingly useful period of warning as to where the heaviest precipitation is imminent. Speed restriction signs might be switched on temporarily.

At present the advice given by the Department of Transport (DTp) is for drivers to 'use common sense' in adverse weather conditions. However, 'common sense' varies considerably from driver to driver! As occurred in Cheshire, police prosecutions for careless driving may well result from collision with the vehicle in front if speed is not consciously and consistently reduced by each driver. However, the trauma of sudden noise and lack of visibility as one's vehicle runs into a heavy, squally hail shower, perhaps with a clap of thunder, all with a closing (i.e. combined) speed of sometimes in excess of 100 m.p.h., has been observed to result in the exact opposite reaction from some motorists who accelerate in a futile attempt to run through the trouble more rapidly and, hopefully, to come out into the sunshine once again!

It was established (R. Yarwood of the Road Safety Division of the DTp, personal communication) that a reduction of visibility to less than 100 m is officially recognized by the DTp and legal profession generally as being 'poor'.

When driving in poor visibility it is first advisable to check your vehicle's speedometer, as sudden entry into these conditions leads to a special danger of 'spatial disorientation' which can lead to people driving faster than they realize because of the lack of external visual references, which can disastrously affect the driver's judgement of speed and distance. The effect is more usually associated with sudden entry into a fog patch when drivers, similar to airline pilots flying into cloud, must suddenly rely on their instruments.

When encountering a heavy shower, especially of hail, which can instantly reduce visibility to that described as 'poor' above, another important question arises for the vehicle driver as to whether or not it is safer for them to stop for a time on the hard shoulder of the motorway, however briefly, to wait until the shower abates, or else to carry on driving at a much reduced speed and risk being struck from behind!

Because it is illegal (under Motorway Traffic Regulations 1982) to allow one's vehicle to rest on the hard shoulder of a motorway 'except in an emergency', on the basis that it is dangerous to stop near to the free-flowing traffic passing just a few feet away, it is again only officially recommended that drivers 'use common sense within the prevailing conditions'. However, it was conceded that when hail, road spray and greasy windscreens conspire to reduce visibility below 100 m 'it may be prudent for the driver to stop on the hard shoulder' (R. Yarwood, personal communication).

6. Conclusions

The UK weather radar network is usually capable of giving at least a few minutes notice of very heavy showers. Closer liaison with motorway police could lead to timely, temporary use of the recommended speed-limit warning signs, if these were spaced at intervals of 1 mile along carriageways (as emergency telephones are at present). This would help eliminate the 'commonsense' variable which drivers are currently urged to follow in adverse or 'poor' conditions, i.e. below 100 m. If conditions become particularly hazardous it may be prudent to stop on the hard shoulder until conditions improve because violent hail does constitute 'an emergency' due to the reduction in visibility.

Acknowledgements

Thanks to the following information sources: National Meteorological Library and Archives, Bracknell; British Newspaper Library, Colindale; Chief Superintendent B. Ingham, Cheshire Constabulary; Fireman D. Norris, London Fire and Civil Defence Authority; R. Yarwood, Road Safety Division, DTp, and G.A. Monk of the Meteorological Office for supplying the radar imagery.

Books received

The listing of books under this heading does not preclude a review in the Meteorological Magazine at a later date.

The engineering statistician's guide to continuous bivariate distributions, by T.P. Hutchinson and C.D. Lai (Adelaide, Rumsby Scientific Publishing, 1991. $A 44.00, $US 32.00) discusses the subject in various applications, including water in different situations. The ways in which the view of bivariate distributions has changed over recent years are explained. ISBN 0 646 024132.

Air pollution modeling and its application VIII, edited by H. van Dop and D.G. Steyn (New York, London, Plenum Press, 1991. $ 198.00) contains over one hundred papers given at the eighteenth International Technical Meeting 13–17 May 1990 in Vancouver. The authors were drawn from the worldwide scientific community. ISBN 0 306 43828 3.

GUIDE TO AUTHORS

Content

Articles on all aspects of meteorology are welcomed, particularly those which describe results of research in applied meteorology or the development of practical forecasting techniques.

Preparation and submission of articles

Articles, which must be in English, should be typed, double-spaced with wide margins, on one side only of A4-size paper. Tables, references and figure captions should be typed separately. Spelling should conform to the preferred spelling in the *Concise Oxford Dictionary* (latest edition). Articles prepared on floppy disk (IBM-compatible) can be labour-saving, but only a print-out should be submitted in the first instance.

References should be made using the Harvard system (author/date) and full details should be given at the end of the text. If a document is unpublished, details must be given of the library where it may be seen. Documents which are not available to enquirers must not be referred to, except by 'personal communication'.

Tables should be numbered consecutively using roman numerals and provided with headings.

Mathematical notation should be written with extreme care. Particular care should be taken to differentiate between Greek letters and Roman letters for which they could be mistaken. Double subscripts and superscripts should be avoided, as they are difficult to typeset and read. Notation should be kept as simple as possible. Guidance is given in BS 1991: Part 1: 1976, and *Quantities, Units and Symbols* published by the Royal Society. SI units, or units approved by the World Meteorological Organization, should be used.

Articles for publication and all other communications for the Editor should be addressed to: The Chief Executive, Meteorological Office, London Road, Bracknell, Berkshire RG12 2SZ and marked 'For Meteorological Magazine'.

Illustrations

Diagrams must be drawn clearly, preferably in ink, and should not contain any unnecessary or irrelevant details. Explanatory text should not appear on the diagram itself but in the caption. Captions should be typed on a separate sheet of paper and should, as far as possible, explain the meanings of the diagrams without the reader having to refer to the text. The sequential numbering should correspond with the sequential referrals in the text.

Sharp monochrome photographs on glossy paper are preferred; colour prints are acceptable but the use of colour is at the Editor's discretion.

Copyright

Authors should identify the holder of the copyright for their work when they first submit contributions.

Free copies

Three free copies of the magazine (one for a book review) are provided for authors of articles published in it. Separate offprints for each article are not provided.

Contributions: It is requested that all communications to the Editor and books for review be addressed to the Chief Executive, Meteorological Office, London Road, Bracknell, Berkshire RG12 2SZ, and marked 'For *Meteorological Magazine*'. Contributors are asked to comply with the guidelines given in the *Guide to authors* (above). The responsibility for facts and opinions expressed in the signed articles and letters published in *Meteorological Magazine* rests with their respective authors.

Subscriptions: Annual subscription £36.00 including postage; individual copies £3.25 including postage. Applications for postal subscriptions should be made to HMSO, PO Box 276, London SW8 5DT; subscription enquiries 071–873 8499.

Back numbers: Full-size reprints of Vols 1–75 (1866–1940) are available from Johnson Reprint Co. Ltd, 24–28 Oval Road, London NW1 7DX. Complete volumes of *Meteorological Magazine* commencing with volume 54 are available on microfilm from University Microfilms International, 18 Bedford Row, London WC1R 4EJ. Information on microfiche issues is available from Kraus Microfiche, Rte 100, Milwood, NY 10546, USA.

March 1992

Edited by R.M. Blackall
Editorial Board: R.J. Allam, R. Kershaw, W.H. Moores, P.R.S. Salter

Vol. 121
No. 1436

Contents

ISSN 0026–1149

ISBN 0-11-728981-7

9 780117 289819

Printed in the United Kingdom for HMSO
Dd291241 3/92 C13 503 12521

The Meteorological Magazine

April 1992

Notes on radio sounding
Quality of radiosonde observations
Battle of Copenhagen
UK cloud immersion frequencies

HMSO

Met.O.1004 Vol. 121 No. 1437

First published 1992

HMSO

HMSO publications are available from:

HMSO Publications Centre
(Mail and telephone only)
PO Box 276, London, SW8 5DT
Telephone orders 071-873 9090
General enquiries 071-873 0011
(queuing system in operation for both numbers)

HMSO Bookshops
49 High Holborn, London, WC1V 6HB 071-873 0011 (counter service only)
258 Broad Street, Birmingham, B1 2HE 021-643 3740
Southey House, 33 Wine Street, Bristol, BS1 2BQ (0272) 264306
9–21 Princess Street, Manchester, M60 8AS 061-834 7201
80 Chichester Street, Belfast, BT1 4JY (0232) 238451
71 Lothian Road, Edinburgh, EH3 9AZ 031-228 4181

HMSO's Accredited Agents
(see Yellow Pages)

and through good booksellers

The
Meteorological
Magazine

April 1992
Vol. 121 No. 1437

551.508.822:551.5(09)

Some notes on radio sounding in the United Kingdom

R.M. Blackall
Meteorological Office, Bracknell

The earliest upper-air soundings were made by use of 'meteorographs' which were lifted by balloon or kite. Balloon-borne ones were often never recovered or only found some days later! Kite sounding gave readings the same day but with a lightning risk!! The meteorograph was a cunning device which drew a fine stylus across a smoked glass plate or other film. Movement in one direction was controlled by an aneroid capsule and in the other, at right angles, by a temperature sensitive bimetallic strip. Heights reached by captive ballons and kites could be deduced by theodolite readings and knowledge of the length of cable payed-out (30 000 ft could be reached with a train of kites). Otherwise then, as now, height (h) has to be deduced from integration of the hydrostatic equation

$$\delta h = \delta p/(\rho g)$$

where δp is the change in pressure, g is the local acceleration due to gravity and ρ is the density of the air.

Following World War II, and until recently, we used radar to get the exact range and azimuth. Elevation and range should give height by simple trigonometry but in meteorology few things are this simple. First, and most obviously, the curvature of the Earth must be allowed for, the greater the horizontal range the bigger this correction is. The radar's beam of electromagnetic radiation is affected by changes in the refractive index of the air — though not in quite the same way as light. For moderate to large elevations there is no problem, but at low elevations there may be, especially with strong hydrolapses near the surface when the radar equivalent of a mirage can form. If a target is far away and low on the horizon then elevation errors are likely, leading to quite large errors in calculating the height.

Integration of the hydrostatic equation in small steps is capable of giving very accurate height changes provided that ρ and g are known. Now g varies with location and height, so a parcel of air moving at constant geometrical height above sea level may well gain or lose potential energy, it cannot if it moves at a constant geopotential height. The geopotential height, Z, is defined by $Z{=}gz/9.80665$ where z is the geometric height.

The density, ρ, (more accurately the mean density of the layer) depends on the pressure, temperature and absolute humidity. The last is only important with dew-points above about 0 °C. The pressure is accurately measurable if the sensor is immune to the large range of temperature the exterior of the package will experience.

Temperature might be thought easy to measure but in practice it is not. The sensor should not get wet in precipitation or cloud, lest it should become a 'wet-bulb', but should be sufficiently exposed to the air (and of low thermal inertia) to give the air temperature with no lag, or at least with a well-known lag that can be allowed for. The most serious problem though is solar heating from radiation received direct, or by reflection from the clouds below, which may heat the apparatus. (Terrestrial radiation is much less and can usually be ignored). The elevation of the sun can be deduced in advance and its effects allowed for and the distribution of clouds around the sonde taken into account.

Clearly, the sonde's designers' aim is to produce a pressure element that is very well insulated and temperature insensitive, and a temperature sensor that is totally shielded from outside radiation and hydrometeors while freely exposed to the passing air — which is difficult.

When the international radiosonde network became fully available after World War II it was soon noticed that while the air flowed smoothly across international boundaries, the contours of the pressure surfaces often did not. The higher up one went the greater the discontinuities became. It is fundamental to upper-air chart drawing, by hand or by computer, that for a given station, the observed wind velocities (calculated from the difference between two consecutive readings) are more reliable than its calculated heights (where errors accumulate). It was quickly found that the discontinuities were not so much at frontiers as between types of radiosonde and the radiation corrections applied. In the UK Meteorological Office (UKMO) it was assumed that our soundings with the Mk. II sonde were accurate but others might need adjustment. A system of automatic adjustments at 500 mb and above (Hawson corrections) ensured a consistent set of data and smooth contours on our charts. Periodic intercomparisons organized by the WMO now determine differences in a more formal way. Occasional rogue soundings can be treated along the same lines. They are compared with surrounding observations at the highest charted level, often 100 mb, and a correction decided upon. This correction is made up of smaller errors in the layers below and it is possible to make proportional corrections to other charts. However, as Hall shows in his paper, comparison with data for other times may reveal that the errors are not wholly random. In general, where problems are due to solar radiation effects, they will not be apparent in night-time soundings. But we must remember that the Sun's elevation depends on the sonde's height as well as its latitude and longitude.

Until very recently humidity has been measured on UKMO radiosondes using 'gold-beaters skin' these units were ingenious and robust but were rather slow to respond to increases in humidity and ceased to work at temperatures below −40 °C. A truely reliable, accurate, rapid response sensor, light enough to be carried on a radiosonde is a recent development. The 'humicap' element on the RS-80 is small and has a rapid response, but this starts to decline at low air densities (less than about 300 mb).

The UK Mk. III radiosonde is a system of high precision and resolution and is capable of high accuracy. Its main feature is the temperature element. This is a very fine tungsten wire wound in a spiral (rather like a spider's web) on a former above the main casing. Its time constant is only a millisecond or so and its cross-sectional area is so small that that it intercepts hardly any radiation and consequently requires no radiation corrections — in fact WMO comparisons show that it reads a little too low. However, the very fineness of the wire makes it vulnerable to accident, and operational procedures to get the best out of the system are costly in man-hours. The system includes a dedicated computer and software for 'real time' operation. The 40 kbytes of storage on the Ferranti Argus was good by the standards of the early 1970s but was barely sufficient; it is tiny by the standards of the 1990s: winds are obtained by radar tracking. During 1990 the Mk. III was phased out of UK operational use and replaced by the Vaisala RS-80. This device is smaller, lighter, more robust and is used with a modern computer; pre-calibrated by the maker, it can be made ready to fly in less than 15 minutes by one person. It is possible to add a radio receiver to pick up LORAN navigation signals and then the entire system can be run solo.

As mentioned earlier UKMO used to measure winds by radar tracking of a target attached to the sonde train; our main RSW stations are now converting to NAVAID using the LORAN system to provide fixes. Another wind-finding system used internationally is the radio-theodolite. Unlike the active radar, this is a passive instrument which measures the azimuth and elevation of the radio transmitter to which it is tuned. It suffers the same problems with refraction as radar when elevations are low; range cannot be measured directly but the height is computed from the sonde data.

551.509.313:551.509.5:551.508.822:53.088

The use of output from a numerical model to monitor the quality of radiosonde observations

C.D. Hall
Meteorological Office, Bracknell

Summary

To make optimum use of meteorological observations it is essential that regular monitoring is performed to identify those of poor quality. Output from numerical forecast models has proved to be very valuable for this purpose; short-period forecasts or background fields provide accurate global reference values against which observations may be compared. This paper presents some recent results of the monitoring of radiosonde observations, and describes a number of different methods that may be used to identify cases where errors of observation, over a period of a month or more, are significantly larger than normal.

1. Introduction

Hall *et al.* (1991) described some of the ways in which output from a numerical model, in particular the short-term forecast or background values, may be used to provide valuable information on the quality of meteorological observations. Some general principles were outlined, and examples demonstrated how observations of pressure and wind from ships and buoys could be monitored. In this paper it is shown how the quality of observations from radiosondes may be assessed using similar monitoring methods, and some revealing characteristics of the errors are identified.

Radiosondes are the cornerstone of the meteorological observing network, providing in most cases detailed vertical profiles of wind, temperature and humidity of high accuracy. The importance of monitoring radiosonde performance has long been recognized, and this has been achieved at the international level through intercomparisons, sponsored by WMO, where different sondes have been carried on a single balloon. Following the first two phases of the intercomparisons in 1984 and 1985 (Nash and Schmidlin 1987), and a later phase in 1990, systematic differences between many of the sondes in regular use have been identified. The results set a standard which is obtainable under the best operating conditions; in actual practice, performance may not be the same as in a trial, as routine monitoring of the daily observations, received in real time over the GTS, readily reveals. Such monitoring may be performed in various ways. For instance, attention is frequently focused on the reported geopotential height at 100 mb as this value usually reflects the integrated effects of errors in the measured temperature at lower levels. Differences from the observed 100 mb height at neighbouring stations, or between observations made in night-time and daylight conditions are useful indicators of quality. In the absence of nearby stations, comparison is best performed against some reference values, and numerical models, which provide global fields of high quality, have often been used for this purpose (e.g. Kitchin 1989a). Much work in this field has also been performed at ECMWF and results are given in Hollingsworth *et al.* (1986) and Radford (1987). This paper will summarize what can be achieved using output from the UK 15-level model which was operational up to June 1991. Observations of temperature, geopotential and wind will be considered, but not of humidity.

2. Monitoring methods

Central to the monitoring methods described here are differences between the observed value and the value of the model background field interpolated to the observation position (referred to throughout as O−B). The background fields, derived from cycles of data assimilation, reflect the information contained in past observations as well as information relating to the structure of the atmosphere provided by the numerical model. Great advances have been made in numerical modelling in the past two decades, and today global fields are available at high resolution. Their quality is sufficiently high for them to have an important role in observation monitoring. Where the values of O−B relate to observations from one source over a long period of time, the long-term performance of the observing system may be assessed. For instance, a time sequence of values of O−B for radiosonde observations from a given station may reveal changes during the period, of larger magnitude than known errors in the background field, which can only be attributed to changes in the characteristics of the observations. Background, rather than analysis, values are used for the monitoring of observation quality because it is assumed that, being derived prior to the observation time, they are independent of the observation itself. This is probably not always strictly true; persistent systematic observation errors are not always filtered out by the data assimilation system and may influence the background field. A second basic assumption is made, namely that both the systematic and random background errors, averaged over periods of a month or more, vary only smoothly in space. This is probably true in the free atmosphere away from steep orography and the model's upper and lower boundaries. In contrast, errors arising from inaccurate measurements may vary greatly from station to station or between national groupings of stations. Differences from background which are larger than the local average can, in most instances, be attributed to larger-than-average errors at the observing station. Errors in the background fields, which are largest in data-sparse areas, are a limiting factor in their use for observation monitoring, and indeed it is essential that all monitoring results are set in the context of estimates of model errors.

The difference between an observed value (o) and the value of the background interpolated to the observation position (b) may be expressed as

$$o-b = (o-t_o) - (b-t_b) - (t_b-t_o)$$

where t_o is the true value of the observation. If the observation is a spot value, t_o is the true spot value, while if the observation represents some time or space average, t_o is the true value averaged over time or space. Likewise t_b is the true value on the scale that the model can resolve, which in the case of the global model results presented here is approximately a 150 km × 150 km × 80 mb grid-box average. $o-t_o$ will be referred to as the measurement error, $b-t_b$ as the background error, and t_b-t_o as the representativeness error. Squaring and taking an average over many observations the following is obtained

$$\overline{(o-b)^2} = \overline{(o-t_o)^2} + \overline{(b-t_b)^2} + \overline{(t_b-t_o)^2}$$

$$= E_m^2 + E_b^2 + E_r^2.$$

It has been assumed that the various cross-product terms are zero or can be neglected. E_m, E_b and E_r are respectively the r.m.s. measurement, background and representativeness errors.

Several factors contribute to the measurement error (E_m): there are errors due to the malfunctioning of the instrumentation; there are errors arising from the wrong estimate of the pressure level; and finally, there are errors introduced on encoding, either due to truncation (the upper-air code only allows for the direction to be reported to the nearest 5°) or inaccurate ground procedures. The background error (E_b) represents numerical forecast errors on the scale that the model can resolve. There may be additional background errors if account is not taken of the time for the balloon to make its ascent and its horizontal displacement from the release point in strong winds. The representativeness error (E_r) is a measure of the sub-grid-scale detail measured by the sonde but beyond the model resolution. There will be a contribution to E_r from fine structure in the vertical (e.g. temperature changes across an inversion or strong vertical wind shear through a jet stream) as well as from mesoscale features with horizontal scales less than 150 km.

Kitchen (1989b) has estimated values for many of the components of O−B listed above using observations from the UK operational radiosonde network. He finds that E_m is the smallest of the three components of O−B (0.6−1.5 m s^{-1} for wind and 0.06−0.16 °C for temperature) while E_r is typically 2.5−3.0 m s^{-1} and 0.6−0.8 °C for wind and temperature respectively. He shows that a failure to interpolate the background field in space and time to the actual balloon position only leads to large errors in the relatively uncommon cases where the observations are valid 3 hours from the validity time of the background field or the sonde is 100 km downwind of the point of release.

In the monitoring results presented in the next section the background values are taken from the UK operational global model valid at the main synoptic hour (00, 06, 12 or 18 UTC) nearest to the observation time. Interpolation in time has not been performed between model fields, nor has the downwind displacement of the sonde been taken into account. This will lead to errors, as discussed above, but they are not thought to be large on average; in the case of operational radiosondes where most ascents start at, or one hour prior to, one of the main synoptic hours and take perhaps 60–90 minutes before balloon burst, the difference between the actual observation time and the validity time of the model field is seldom more than 1 hour.

For most radiosonde observations the vertical profile obtained from the full TEMP report contains far more detail than is available from the 15 levels of the numerical model. To achieve the best match between observation and background, the reported profile has been averaged across each of the model layers to give a layer-mean value. By smoothing the data in this way its vertical resolution is reduced to exactly that of the model and the contribution to E_r from fine structure in the vertical is eliminated.

3. Monitoring results

Fig. 1 shows vertical profiles of the mean and r.m.s. O−B differences in the 3-month period October–December 1990 at Hemsby (53°N, 2°E). Plots such as these are used routinely to monitor the quality of radiosonde observations, and in all cases it is essential to assess what part of O−B may be attributed to model error and what part to observation error. This question is usually best answered by comparing the values with those obtained at nearby stations, and in the data-rich area round Hemsby, stations over the United Kingdom or other parts of northern Europe may be used. It turns out that these stations show similar values of O−B at all levels. The r.m.s. of O−B for temperature is a little more than 1 °C and for wind it is around 3–4 m s^{-1} rising to 6 m s^{-1} at jet-stream levels. Both values are considerably

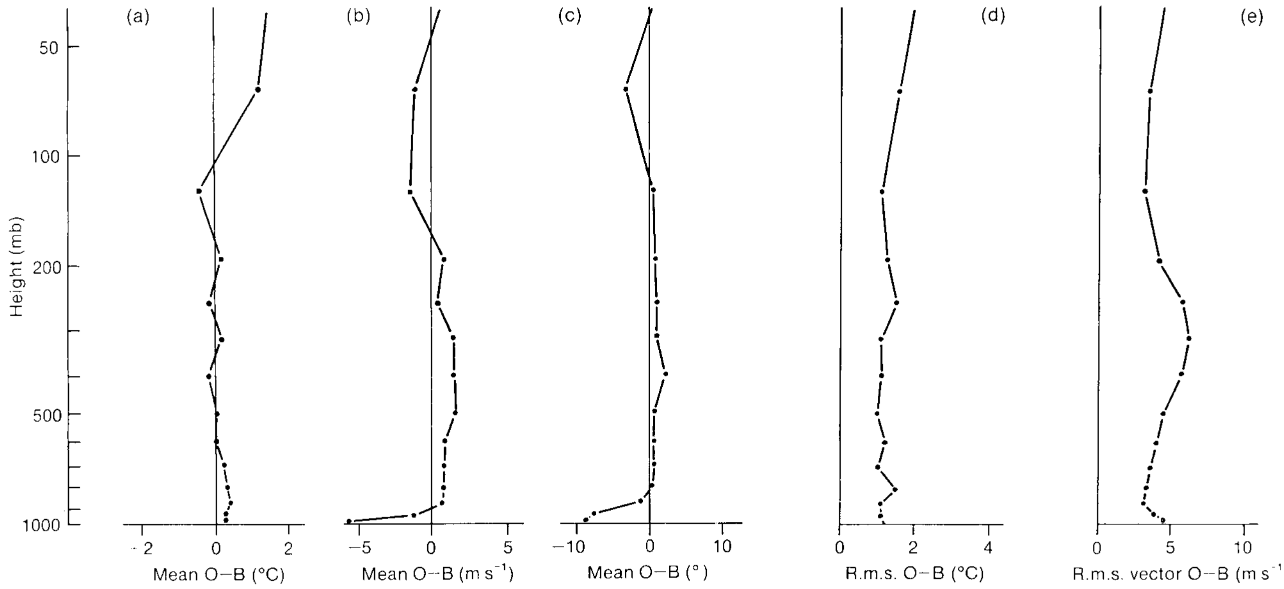

Figure 1. Vertical profiles of O—B for radiosonde observations from Hemsby (53° N, 2° E) in the period October–December 1990 for (a) mean temperature differences, (b) mean wind speed differences, (c) mean wind direction differences, (d) root-mean-square temperature differences, and (e) root-mean-square vector wind differences.

larger than the reproducibility of good quality sonde and wind-finding systems (typically 0.2 °C and 1.0 m s^{-1} respectively) and the major contributions must come from the background error (E_b) and the representativeness error (E_r). From the estimates of E_r noted in the previous section it can be seen that in an area such as northern Europe E_b is a little larger, but not by much; typical values are around 3—5 m s^{-1} for wind and 0.8—1.2 °C for temperature. The bias of O—B is mostly very small, and where there are significant departures from zero, values similar to those at Hemsby are found at all neighbouring stations. Consistent biases such as these point to regional systematic errors in the background values. There are positive O—B temperature biases of around 1 °C above 100 mb showing that the model atmosphere is too cold at these levels. There are negative speed and direction biases close to the surface which is a characteristic found at most land stations and probably reflects inadequacies of the surface processes in the model. The positive speed biases, which are largest in the upper troposphere, are another characteristic found at many middle-latitude stations and shows up most noticeably as a tendency of the model to underestimate the strength of jet streams. Apart from the biases in O—B noted above due to systematic errors of the model, the mean differences from background are small; less than 0.2 °C for temperature, 0.5 m s^{-1} for speed and 2° for direction. The largest values of the r.m.s. vector wind differences are at around 300 mb and are associated with large random model errors within the jet stream and with the strong horizontal wind shears often observed at this level which are beyond the resolution of the model. Consequently the height of this maximum varies with latitude and season in the same way as the level of the jet stream. Where comparisons are required between stations at different latitudes or between statistics in different seasons, it is usually advisable to average the r.m.s. vertically through a deep layer of the upper atmosphere. In this way dependence on the height of the jet-stream maximum is largely avoided.

Time sequences of values of O—B from a single station provide a sensitive test of quality as the paper by Hall *et al.* showed for marine observations. Fig. 2 shows a sequence of monthly mean values of O—B for 100 mb geopotential height at Hemsby over the period September 1989–August 1990. Observations at 00 UTC only have been selected to avoid the complicating effects of solar

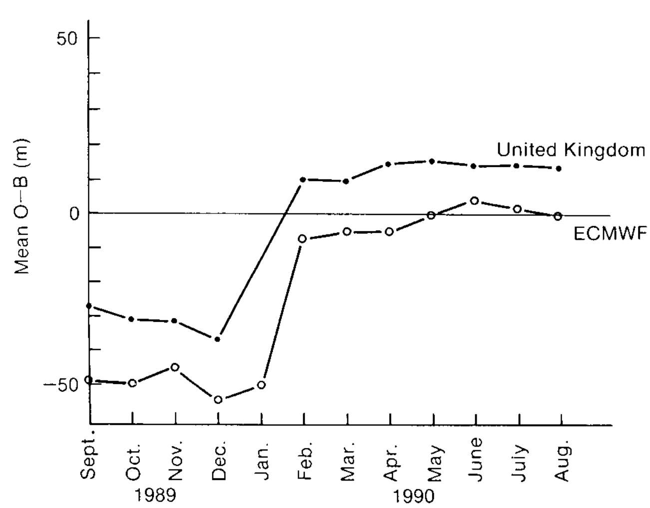

Figure 2. Monthly mean O—B differences for 100 mb geopotential height at Hemsby using the UK and ECMWF operational models. 00 UTC data only.

radiation. For comparison, monitoring values using the ECMWF model are also shown. The backgrounds from both models indicate that a change of bias occurred after January 1990, coinciding closely with the replacement of the Mk. 3 sonde by the Vaisala RS80 at that station on the 23rd of the month. The known tendency for the Mk. 3 to measure too cold is clearly evident as is a 15–20 m systematic difference between the background values from the two models.

The RS80 has now become the most widely used sonde over Western Europe and this allows an intercomparison of O—B statistics for a common instrument to be made over a large region. In Fig. 3 the mean and standard deviation of O—B temperature differences at all stations where it is operational are plotted for the period October–December 1990 using 00 UTC observations only. The values, in tenths °C, represent vertical averages performed over a deep layer of the atmosphere from 850 to 100 mb. To avoid individual observations, differing from background by a very large amount, distorting the sample characteristics, values of O—B have only been included for those observations passing the automatic quality-control checks. In practice very few observations are excluded as quality-control flags are generally raised on less than 1% of the occasions. Mean O—B lies between 0.0 and +0.3 °C at most stations, but there are exceptions principally over Spain and Italy where the mean differences are larger. The larger positive values can almost certainly be attributed to the different radiation correction schemes in operational use. Most stations (indicated by the closed circles at the station position in Fig. 3) use Vaisala '1986' corrections based on an evaluation by Vaisala of results of the WMO International Radiosonde Intercomparisons. A few stations still use earlier '1982' corrections (indicated by open circles) and in almost all cases they are the ones showing the larger mean temperature differences. The sign and magnitude of the difference agrees closely with the difference between the correction schemes at zero solar elevation (Kitchin 1989a). The second set of values in Fig. 3 gives the standard deviation of O—B temperature averaged over the layer and it can be seen that it varies smoothly over the region, confirming the uniform pattern from station to station. As noted earlier, the values, lying between 1.1 and 1.5 °C, principally represent the contributions from E_r and E_b. They are a little larger in the west than in the east, but this is to be expected as background errors are likely to show a similar regional variation rising to a maximum over the data-sparse Atlantic.

Where there is a good coverage of stations providing reasonably accurate observations, as was the case above, values of r.m.s. O—B are found to vary smoothly over the whole region. Stations with a large observation error stand out as having values which are larger than at neighbouring stations. Fig. 4 shows vertically averaged values of r.m.s. O—B differences of the vector wind

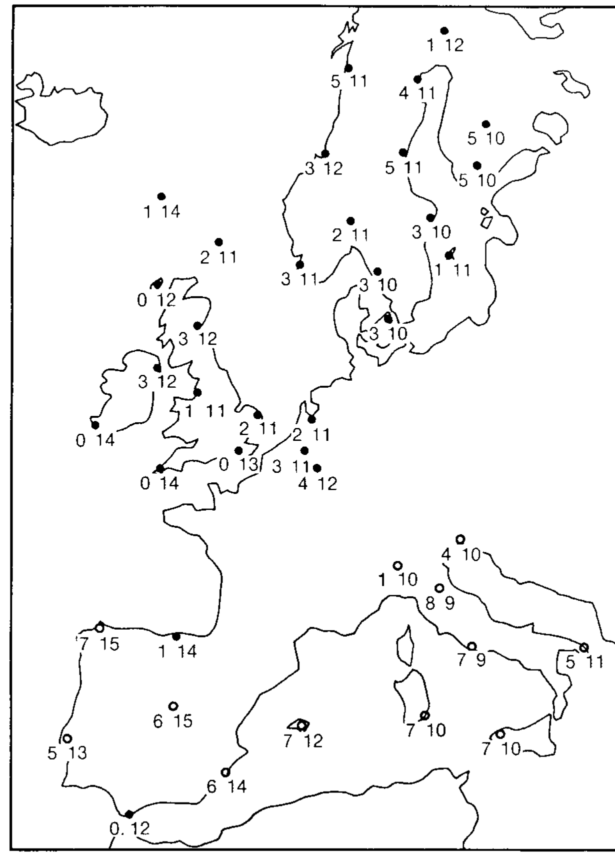

Figure 3. Mean (plotted on the left) and standard deviation (right) of O—B temperature differences at radiosonde stations using the Vaisala RS80 sonde. Values in tenths °C for the period October–December 1990 have been averaged over the layer 850–100 mb. Stations applying the '1982' corrections are marked by an open circle.

in units of tenths m s^{-1} in a data-rich region for the 12-month period January–December 1988. The vertical averaging has been performed over the layer 400–150 mb in order to obtain a representative value through the depth of the jet stream. As in the case above there is an underlying smooth variation over the region and values lie within the range 4–5 m s^{-1}, but this time three stations, identified by the letters A, B and C, stand out with values which are considerably larger than the local average. Large observation errors at these stations are the only reasonable explanation for the large differences from background.

The methods described above are valuable for identifying unreliable stations, but they do not provide much information on the nature of the problems. A more detailed study of O—B differences can reveal much more useful information, especially if it is based on a knowledge of the likely sources of error in the instrumental system in use. Three such examples are presented in sections below.

3.1 Wind direction errors

One type of wind error that is easiest to identify comes from a misalignment of the direction of true north, and

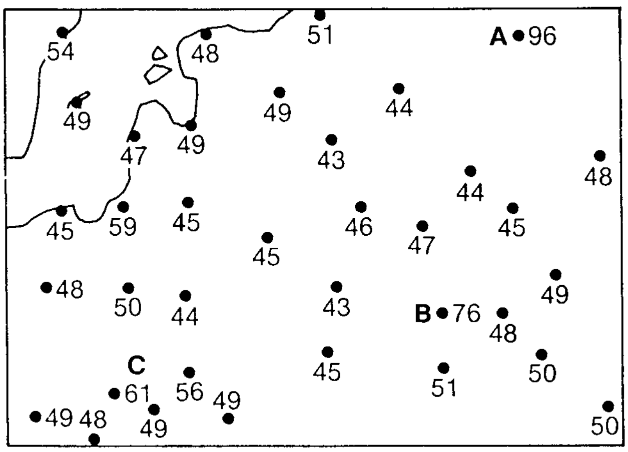

Figure 4. Root-mean-square O—B vector wind differences for radiosonde stations in the period January–December 1988. Values, in tenths m s^{-1}, have been averaged over the layer 400–150 mb. Lettered stations are referred to in later diagrams.

it shows up as a bias in wind direction relative to background and nearby stations which is constant with height. Two of the stations (A and C) identified in Fig. 4 as having abnormally large observation error are found to have a clear direction bias as Fig. 5 demonstrates. In each case the vertical profile of O—B direction differences have been plotted for the station in question and its nearest neighbour. In both cases there is a systematic difference between the pair of profiles: relative to the local average the reported directions are backed by 17° at station A and by 10° at station C. It is interesting to note that at all stations in the region there are negative direction biases in the boundary layer similar to the bias noted at Hemsby (Fig. 1). There are around 20 stations worldwide having O—B direction biases in excess of 10° which can confidently be attributed to observation error, and at least another 20 where the O—B bias is smaller and observation error is considered probable.

3.2 Wind-error dependence on balloon elevation

At some stations abnormally large observation errors occur in strong winds at the level of the jet stream. To understand why, some knowledge of wind-finding systems is required. There are three types in widespread operational use:

(a) Primary radar which measures elevation, azimuth and slant range provides, in general, the most accurate wind finding. Tests made at Beaufort Park, where a balloon was tracked by two independent radars (Edge *et al.* 1986), have demonstrated that the reproducibility of wind measurements from the UK operational radar using 1-minute averaging was better than 1 m s^{-1} r.m.s. vector error at slant ranges less than 60 km, and about 1.5 m s^{-1} r.m.s. vector error at slant ranges of 90 km.

(b) NAVAID (navigation aids) is the general term applied to systems for determining horizontal location at any point on the globe through the use of electromagnetic waves in the radio frequencies. Synchronized signals are transmitted from a number of well-spaced stations, and differences in the time of receipt at a sensor enable its position to be determined. Omega is the NAVAID system in most widespread use and achieves an accuracy of 1–2 m s^{-1} for 2-minute averages on most occasions. Loran systems are in use at some UK stations which achieve a somewhat greater accuracy.

(c) Radiotheodolite is the most common wind-finding system in use today. Radio signals from the sonde are tracked by direction-finding antennas at the ground station enabling azimuth and elevation to be measured. The height is usually determined by integrating the hydrostatic equation using the measurements of temperature, humidity and pressure in the same way as in NAVAID systems. At high balloon elevations and short slant ranges the accuracy obtained from radiotheodolites is comparable to the accuracy of NAVAID winds. However, at low balloon elevations, which are frequently encountered in the strong jet streams in middle latitudes, the reported wind is much more sensitive to errors in the measured elevation. At some stations the operational practice is that winds are not reported where the elevation falls below some critical value. At other stations secondary radar or transponder systems are used to provide direct measurements of the slant range used in the wind finding, eliminating the dependence of the derived wind on measurements of balloon elevation. Both practices lead to a reduction in the largest errors associated with radiotheodolite systems.

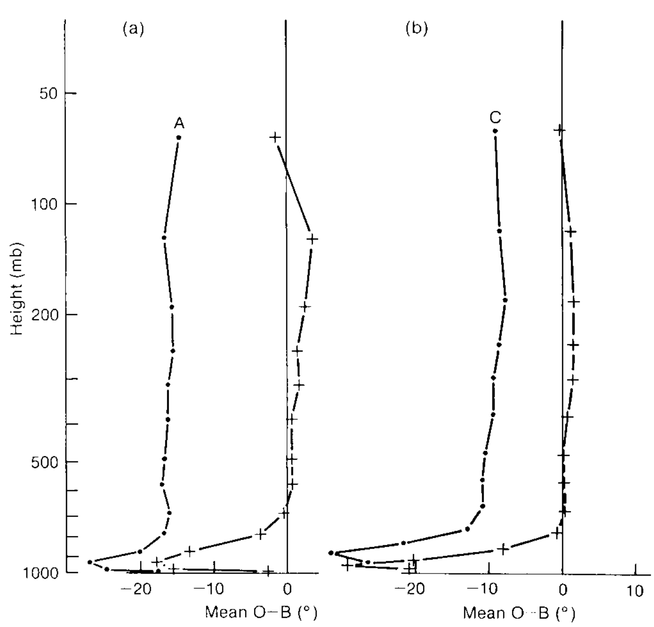

Figure 5. Mean O–B direction differences in the period January–December 1988 at (a) station A and its nearest neighbour in Fig. 4, and (b) station C and its nearest neighbour.

The problems of wind measurement at low balloon elevations at stations using radiotheodolite equipment is a major source of error in the global radiosonde network. Where there is no means of measuring the slant range, winds are calculated from measured values of balloon azimuth, elevation, and a value of the height derived from the pressure–temperature profile from the sonde. If the balloon encounters a strong jet it may be carried 100 km or more downwind and its elevation at the ground station will be less than 10°. Accurate wind measurements require an accurate measurement of the balloon elevation which is critically dependent on the precise alignment of the receiving antenna. Where misalignment occurs, errors are likely to be much larger in the component of wind along the line of sight to the balloon than in the component perpendicular to the line of sight.

The characteristics of radiotheodolite systems at different balloon elevations can be investigated using model background values. It is necessary to work in wind components which lie along the line connecting the balloon and the station (*a*-component) and perpendicular to that line (*p*-component). Differences from background for each of these components can be calculated at various balloon elevations. The balloon downwind range can be estimated from the observed wind profile given in the radiosonde report, and the height can be calculated assuming a constant rate of ascent (taken to be 5 m s^{-1} here). Of course it is not known how model errors in the *a*- and *p*-components of wind differ; for small elevations they are both likely to be larger than average as low balloon elevations result from strong winds at jet-stream level where it is known that model and representativeness errors are large. In addition, the magnitude of model errors at low balloon elevation may depend on location; low elevation implies the existence of a strong (usually westerly) jet, which in turn implies the rapid propogation of errors. In such cases, model errors on the western coasts of continents, just downwind from data-sparse oceans, are likely to be larger than at sites further inland. These model characteristics are impossible to quantify without working from observational results and, as before, background plus representativeness errors will be estimated by reference to wind-finding systems of known high quality.

Fig. 6 shows the dependence on the balloon elevation of the mean and r.m.s. O—B differences for the *a*- and *p*-components of wind. The closed circles represent values from a wide selection of stations in Europe providing observations of good quality from either radar or NAVAID wind-finding systems. All observations have been included with the exception of those making an exceptionally large contribution to the variance of O—B. These outliers have been identified using standard statistical techniques on each sample of observations having values of the elevation within a specified range. In practice far fewer observations are eliminated than have flags raised by the routine quality-control checks. All reports (TEMP and PILOT) received in 1988 have been used and vertical averages have been performed over the band 400–150 mb which includes the jet-stream maxima in most latitudes and seasons. As anticipated there is indeed an increase in O—B differences with smaller values of elevation, and the increase is a little greater in the *a*-component than in the *p*-component. These values provide a standard against which other stations may be compared. The crosses in Fig. 6 are for station B which in Fig. 4 had r.m.s. differences from background considerably larger than at neighbouring stations. It is immediately clear that the suspected observation error is contained in the *a*-component; the r.m.s. O—B of this component becomes very large at low balloon elevations, while that of the *p*-component differs little from the standard. At some stations observations cease where the elevation falls below some critical level, no doubt as a result of the local observing practice. Where observations continue at elevations below 10°, massive r.m.s. O—B differences may be found as the third example in Fig. 6 shows (indicated by the open circles) which is for a station in Asia.

The only reasonable explanation of the characteristics shown in these examples is an error in the radiotheodolite wind-finding systems in use at these two stations. In both cases the mean O—B of the *a*-component is also large and accounts for much of the variance. Quite possibly there is some misalignment of the antennas at these stations resulting in a constant bias in the measured elevation.

3.3 Errors in the assignment of height

The level assigned to a radiosonde observation, reported as a pressure in a TEMP report, may be derived in a number of different ways depending on the instrumentation: the pressure sensor on a sonde gives a direct measurement of the pressure level; alternatively the height in metres, derived from the slant range and balloon elevation, may be converted to a pressure level by applying the hydrostatic equation to the virtual temperature profile measured by the sonde. For systems with range-finding radar and a sonde with a pressure sensor, these two independent estimates of the height may be obtained and cross checked, providing probably the most accurate values of observation level. For systems with a sonde providing pressure and temperature but with no range finding, for example NAVAID and radiotheodolites without secondary radar, the pressure level assigned to the observations is simply the value measured by the sonde.

Some systems have no pressure sensor and rely on the range and elevation provided by the wind finding, and the virtual temperature profile provided by the sonde to give the pressure level. In some cases the elevation is measured by radiotheodolite and, as in the case of wind observations, errors can arise through misalignment of the instrument.

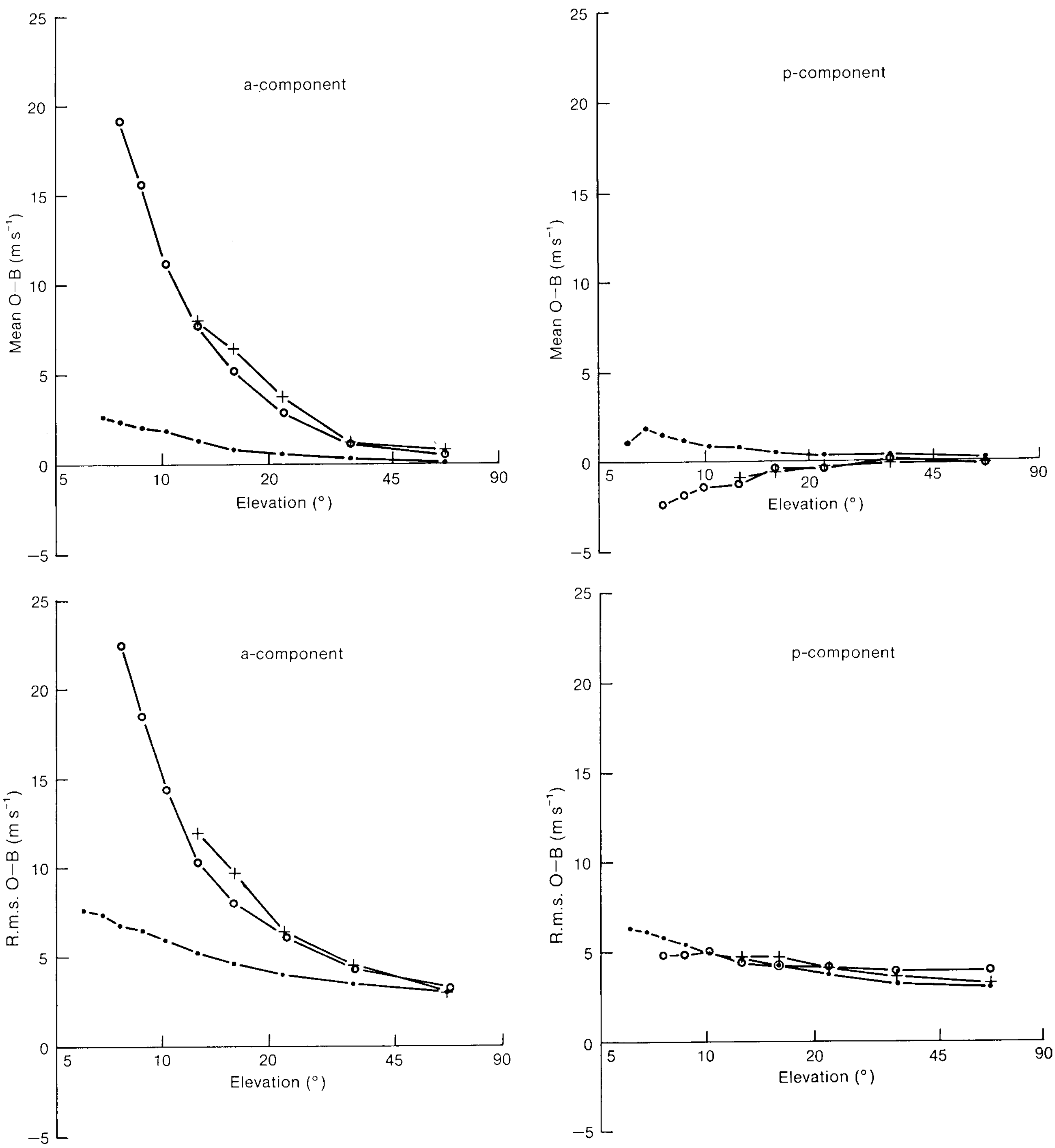

Figure 6. Mean and root-mean-square O–B differences for the wind components across (*a*-component) and perpendicular to (*p*-component) the line of sight to the balloon at various balloon elevations. Values have been averaged over the layer 400–150 mb for the period January–December 1988. The closed circles are for radiosonde stations in Europe using NAVAID or radar wind-finding systems, the crosses for station B in Fig. 4, and open circles for another station appearing to have large wind errors.

A possible way of detecting systematic biases in the height assignment is through an examination of the characteristics of the O—B temperature differences from the sonde and two examples are given in Fig. 7. Both cases are characterized by a sharp discontinuity in the profile of mean O—B at the level of the tropopause. At station D, O—B increases steadily from zero near the surface to a large negative values around 300–400 mb before falling suddenly to values much closer to zero at higher levels. Station E shows a similar profile of O—B temperature differences, but of opposite sign. Neighbouring stations show no such characteristics. It is difficult to imagine how a defect in the temperature element could result in this sudden change with height unless it has a quite exceptionally long response-time. More probable is a bias in the assignment of height which is largest at high levels. In the near-isothermal stratosphere errors in height will not lead to a temperature bias, but just below the tropopause the +3 °C bias implies a systematic error in the height of perhaps as much as +500 m.

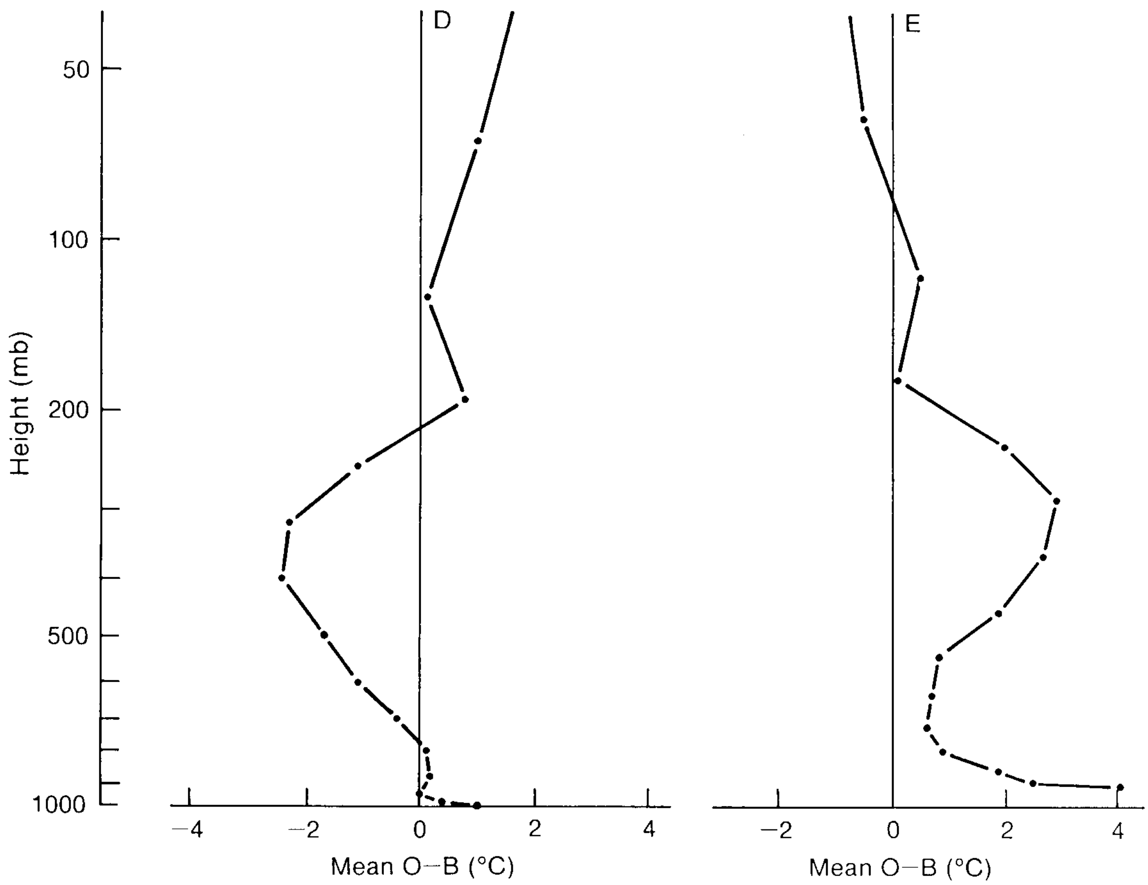

Figure 7. Vertical profiles of the mean O—B temperature differences at two radiosonde stations (D and E) for the period October 1990–March 1991.

Fig. 8 shows the mean and standard deviation of O—B temperature differences at 400 mb for different balloon elevations over the winter period October 1990–March 1991. A very marked relationship is immediately apparent; at both stations the large biases in O—B found at this level occur almost solely at low balloon elevations. In strong winds where the balloon is between 10 and 20° above the horizon the magnitude of the temperature errors is between 4 and 6°. For comparison, values for Hemsby are also plotted. In all cases the standard deviation of O—B is around 1.0–1.5 °C at high evelations rising to 2.0–3.0 °C where the elevation is below 20°. Larger random errors in the background values are to be expected at low balloon elevations, which are indicative of a changeable synoptic type. It is apparent that a systematic bias in the observations accounts for most of the variance of O—B.

According to information provided to WMO, there is no pressure sensor on the sonde at these two stations, and the observation level is obtained from the slant range provided by the secondary radar, the balloon elevation provided by the radiotheodolite, and the temperature profile provided by the sonde. The most likely explanation of the error detected at these two stations is a systematic error in the measured balloon elevation, due no doubt to a misalignment of the antenna of the radiotheodolite system.

4. Concluding remarks

Background values from high-resolution numerical models provide a powerful means of monitoring the quality of observations. Three components contribute to the differences between observations and background: measurement errors, background errors and representativeness errors. For reliable operational radiosonde systems measurement errors are the smallest contribution. Where the observations are of poor quality the measurement error may make up a large part of O—B, and this may be detected through routine monitoring over a period of time. The accuracy of the background is a limiting factor in the success of the monitoring method, and results must be presented in the context of estimates of the background error. The results in this paper seem to provide justification for the assumption that background errors averaged over long periods of time vary only slowly in space. This is critical for identifying stations with larger than average measurement errors. In general, r.m.s. O—B values have uniformly low values highlighting the reliability of the observations, but a few stations stand out with values significantly larger than others in the immediate neighbourhood. Where this is the case, observation error is the prime suspect.

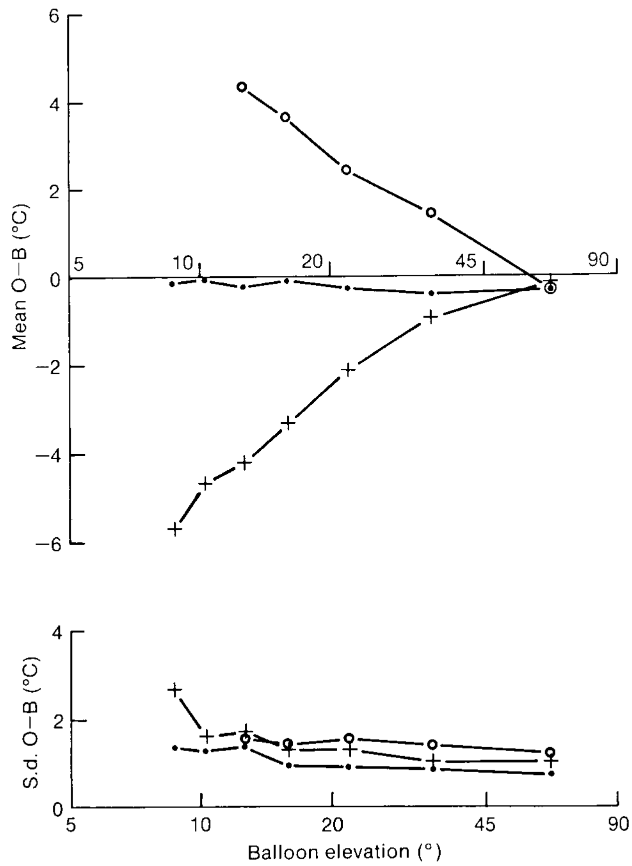

Figure 8. Mean and standard deviation of O–B 400 mb temperature differences at various balloon elevations for the period October 1990–March 1991. The closed circles are for Hemsby, and the crosses and open circles for stations D and E respectively of Fig. 7.

Background values also provide a useful tool for investigating the cause of some of the errors. A number of techniques have been outlined here and no doubt more could be developed. Direction biases in the reported wind, due presumably to the misalignment of true north, are surprisingly common and seem to be a major source of error at some 20 or more stations worldwide. Even more common are problems with radiotheodolite systems where the measurement of wind or pressure level depends critically on the balloon elevation. Large errors have been noted in the examples provided here, and there are many other stations where the errors are equally as large. In many cases the error can be attributed to a systematic bias in the measured elevation, pointing to a levelling problem with the antenna of the instrument.

The methods outlined here provide a basis for the regular monitoring of observations worldwide. Recognizing this, WMO established lead centres for the monitoring of different types of observations. Since 1987 ECMWF has been lead centre for radiosonde data, co-ordinating all results of quality evaluation, and providing those making the observations with monitoring information relating to their station. The information presented here is also of great value for improving the use of observations by the numerical forecast models; estimates of the observation error at each station can be used to give more reliable weights to the observations within data assimilation, and some of the more obvious biases can be corrected. An essential requirement of all these applications of monitoring results is a continual updating of the monitoring information.

Acknowledgements

The author would like to thank John Ashcroft and Jonathan Wright for their help in developing the computer programs needed to provide the results presented here, Alan Radford for providing the ECMWF monitoring results for Hemsby, and John Nash for his helpful comments on the text.

References

Edge, P., Kitchen, M., Harding, J. and Stancombe, J., 1986: The reproducibility of RS3 radiosonde and Cossar WF MK IV radar measurements. (Unpublished, copy available in the National Meteorological Library, Bracknell.)

Hall, C.D., Ashcroft, J. and Wright, J.D., 1991: The use of output from a numerical model to monitor the quality of marine surface observations. *Meteorol Mag*, **120**, 137–149.

Hollingsworth, A., Shaw, D.B., Lönnberg, P., Illari, L., Arpe, K., and Simmons, A.J., 1986: Monitoring of observation and analysis quality by a data assimilation system. *Mon Weather Rev*, **114**, 861–879.

Kitchen, M., 1989a: Compatibility of radiosonde geopotential measurements. WMO Instruments and Methods of Observation, Report No. 36. Geneva, WMO.

—, 1989b: Representativeness errors for radiosonde observations. *Q J R Meteorol Soc*, **115**, 673–700.

Nash, J. and Schmidlin, F.J., 1987: Final report of the WMO international radiosonde intercomparison. WMO Instruments and Methods of Observation, Report No. 30. Geneva, WMO.

Radford, A.M., 1987: ECMWF radiosonde monitoring results. *In* Proceedings of ECMWF/WMO Workshop on radiosonde data quality monitoring.

Meteorological and hydrographical aspects of the Battle of Copenhagen, 2 April 1801

J. Neumann
Emeritus, Department of Atmospheric Sciences, The Hebrew University, Jerusalem, Israel; visiting with the Department of Meteorology, University of Copenhagen, Denmark

Summary

Following diplomatic conflicts between Britain and Russia, on 18 November 1800 the tsar imposed an embargo on British ships in Russian ports. In practice this meant a ban on British ships in all Baltic ports, including the ports from where Britain used to obtain an important fraction of her grain imports (45% in 1800). Toward the end of November, the British Cabinet decided to send a fleet to the Baltic, as soon as ice conditions of that sea permitted, to break the embargo. The plan of naval action against Russia was extended in January 1801 to the navies of the other states of northern Europe when Britain learned that they entered into an Armed Neutrality Pact with Russia. The sequence of the attacks was based on climate.

The winter of 1800/01 was a mild winter in the Baltic region which made it possible for the British fleet to sail on 12 March 1801. The fleet's Second-in-Command was Nelson who formulated the plan of attack on the Danish navy (the first to be attacked) arrayed in defensive positions along Copenhagen's coast. The plan leaned heavily on winds. The battle took place on 2 April and ended in British victory.

The paper makes use of data of Copenhagen's meteorological station of the time (pressure, wind, temperature and weather) as well as on the wind records of two British and one Danish warship.

1. Introduction

In the two successive years 1799 and 1800 the British Isles suffered from crop failure. The winter of 1798/99 was cold, the spring and summer of 1799 cool and rainy, with the consequence that the wheat harvest was down by 50%. The weather characteristics of 1800 were nearly opposite — the spring and summer were warm and rather dry, and in the London area no rain fell in June. The Azores anticyclone extended well into western Europe for weeks. The failure of the 1800 wheat crop was but 25% but, since no reserves were left, the scarcity of bread became even graver and prices rose.

The scarcity led to numerous bread riots, some of them violent and destructive. Among others, such slogans appeared as 'Peace and Large Bread, or a King without a Head'. The memory of the French revolution was still fresh. And, in view of the renewed crop failure, the prospects of still more violent bread riots and danger to the public order during the coming dearth year became even more alarming.

In 1800 the British Isles were able to obtain 45% of their grain imports (wheat, barley, oats, rye, beans and peas) from Baltic ports. But, on 18 November 1800 (NS), the tsar, Paul I, imposed an embargo on British ships in Russian ports and, since the countries around the Baltic were under the tsar's domination, the Russian embargo meant the exclusion of British vessels from all Baltic ports. The loss of these imports portended an even graver scarcity in Britain in 1801. Apparently, on 28 November (1800) the British Cabinet decided on a naval attack on the Russian fleet in the Baltic, as soon as ice conditions permitted sailing, to break the embargo. Soon after mid December the tsar succeeded in bringing together all the countries of northern Europe (Denmark, Prussia and Sweden) to join his empire in an Armed Neutrality Pact which would have entailed armed resistance against the British claim of her right, as a belligerent, of searching neutral vessels for contraband of war (war against France). When the signing of the Pact became known in London in January, this gave additional weight to the earlier decision to go against Russia, but now the plan of attack included all signatories of the Pact. The northern neutrals, especially Denmark, which had a relatively large merchant navy, were called upon to abandon the contract or face the consequences.

The weather conditions of 1799 and 1800 in the British Isles and in some of the grain-growing areas of Europe, the consequences on the harvests, the bread riots in Britain, etc. are described in Neumann and Kington (1992). The diplomatic conflict between Britain, on the one hand, Russia and the other north-European powers, on the other, is described in a book by Pope (1972). Pope also describes the events of the sailing of the (British) 'Baltic fleet' and, especially, the course of the Battle of Copenhagen and its sequels. In an English-language book, the Danish historian Feldbæk (1980) discusses the diplomatic conflict and, in a subsequent book in Danish, he describes (Feldbæk 1985) the events and course of the battle.

2. Climate governs British naval strategy

Referring to the planned naval war in the north, Dudley Pope makes the statement in his book *The Great Gamble* (1972, p. 125) that 'climate governed British naval strategy and planning for the Baltic'. The jacket of the book adds the subtitle 'Nelson in Copenhagen'; the term 'gamble' implies the possibility of failure because the Danish navy represented a strong force.

The plan of attacks on the navies of the northern neutrals is laid out in a memorandum, dated 5 February 1801, submitted to the Admiralty by Vice-Admiral Nicholas Tomlinson (ret.), see *The Tomlinson Papers* (1935, pp. 299–305). Tomlinson saw service previously with the Russian navy on behalf of Britain and, thus, he had personal knowledge and experience of the tsar's Baltic fleet, its bases at Kronstadt (St Petersburg) and Reval (Tallinn) in the Gulf of Finland and the way the fleet is set into operation after its hibernation in winter locked into ice.

Tomlinson's proposal was to attack the Danish navy first, as soon as the ice thawed in the Danish water, and before the ice melted in the Gulf of Finland. In such a case the Russian fleet in the Baltic would not be able to come to the aid of the Danes. He goes on pointing out that the ice at Kronstadt usually thaws 7–10 days later than at Reval and then, assuming the the Danish navy had already been put out of operation, neither the Danish nor the Kronstadt-based warships could help the ships at Reval. Finally, after the presumed defeat of the fleets at Copenhagen and Reval, the British fleet could deal with the fleet at Kronstadt. (We do not know if the Admiralty developed a similar climate-based plan, independently of Tomlinson.)

The figures quoted by Tomlinson for the difference in thawing at the two Russian bases, are in fair agreement with modern data, see Fig. 1.20 in the paper *Physical features of the Baltic Sea* by Mälkki and Tamsalu (1985).

3. The winter 1800–01 in the Baltic

The proviso 'ice conditions in the Baltic permitting', or variants of this phrase, are recurring features of documents of the Cabinet (e.g. in a letter of Henry Dundas, Secretary of State for War, to the Admiralty; reprinted in Clarke and M'Arthur (1859, p. 259) and letters or orders of the Admiralty (see, for example, letter of the Admiralty to Sir Hyde Parker; reprinted in *The Nelson Papers*, 1845, p. 295). Apparently, it was not before the middle of February 1801 that the fact of mildness of the winter in the Baltic became known in London. (The winter was also mild in the British Isles, see Table I below.) The first published indication of the light winter in northern Europe was printed on p. 2 in the issue of *The Times* for 14 February. According to a short report from Memel, a harbour city on the south coast of the Baltic (then part of Prussia, now in Lithuania under the name Klaipeda), dated 10 January, 'the weather is so mild that our harbour has 16 fathoms at the entrance'. The qualification 'the weather is so mild' makes it unlikely that the high water level was due to strong onshore winds. One plausible reason for the high level was a late freezing of the rivers emptying into the sea. Another report of mildness appeared on 20 March in the Copenhagen newspaper *Kjøbenhavnske Tidende.* The news item, dated 3 March, Stockholm, reads as follows in translation: 'The extremely mild weather has favoured the rearmament of the navy. The Åland Sea has been reportedly ice-free'. The Åland Sea is the area of the Baltic sea between Uppsala and the south-west corner of Finland. Lt Col William Stewart, Commanding Officer of the land troops attached to the 'Baltic fleet', writes in his narrative of the Battle of Copenhagen that [in March 1801] 'the openness of those seas had rarely been equalled at this season of the year'. The narrative is reprinted in *The Nelson Papers* (1845, see especially p. 300). His narrative will be mentioned again below.

In Table I are listed the air-temperature data of Copenhagen, Riga and Stockholm, as well as of Central England for late autumn, winter and early spring 1798–99 to 1802–03. The data bring out the fact that the winter of 1800/01 was mild, especially in comparison with winter of 1798/99. The difference between the two winters is even more clearly brought out by the number of days during which the Danish Sound (Sound, for short) was ice-bound in 1798–1803, see Table II. To the

Table I. Mean temperatures (°C) of the months November–March 1798–99 to 1802–03 at stations of the Baltic region, with parallel data of Central England for comparison (World weather records (1927), Wild (1881), Manley (1974)

Years	Copenhagen	Riga	Stockholm	C. England
1798–99	−1.7	−7.6	(−4.0)	2.8
1799–1800	−1.0	−4.0	−4.4	3.2
1800–01	2.6	−1.0	−0.9	5.0
1801–02	−0.4	−1.4	−1.8	3.4
1802–03	1.9	−6.5	−4.0	4.4
1931–60	1.9	−2.6	−0.8	4.9

Table II. Ice data for the Danish Sound, Riga and the Baltic as a whole, 1799–1803. The year date is that of the year into which January falls (Lamb 1977).

	1799	1800	1801	1802	1803
Number of days that the Sound was ice-bound	135	109	0	11	60
Date of final opening of Riga's port for shipping (number of days since 1 January)	107	102	85	79	96
Maximum extent of ice cover of the Baltic, in 1000 km^2	420	400	136	220	400

table have been added the dates of opening of Riga's harbour to shipping in spring, and figures on the greatest extent of ice cover of the Baltic in the same years. All three sets of data are listed in Lamb (1977, pp. 587–589). The figures are particularly relevant to the planned attack.

In 1801 the ice cover of the Neva at St Petersburg broke up on 17 April (NS; see Rykatschew (1887), p. 171), the average date for the recent decades being between 21 April and 1 May (Mälkki and Tamsalu, 1985, Fig. 1.20). As to Reval, the other Russian naval base in the Baltic of the time, a letter dated 30 June 1990 of Dr Andres Tarand (Botanical Gardens, Tallinn) states that the port of Reval became ice-free, according to the State Archives at Tartu (Dorpat) on 1 April OS, which could be either 12 or 13 April NS. The latter dates are very close to the date of the break-up of the ice cover at Tallinn in recent decades. It is reasonable to assume that the date of the 'break-up of ice cover', as used by Mälkki and Tamsalu, occurs a few days before the port becomes 'ice-free', the term adopted in the Estonian record. If this assumption is correct, then the break-up at Reval took place, as we would have expected, earlier than the average date in recent decades.

In view of the reports of a mild winter in the Baltic, the Admiralty issued orders on 11 March for the (British) 'Baltic fleet' assembled at Yarmouth, to set sail. The fleet consisted of just over 50 sail, including 16 (later 17) sail-of-the-line. The Commander-in-Chief of the fleet was Admiral Sir Hyde Parker, with Nelson as Second-in-Command. With the fleet went some 800 land troops, commanded by Lt Col William Stewart of the Rifle Battalion (mentioned earlier).

The voyage in the North Sea was rough. On the 15th (March), a south-west gale dispersed the fleet, but the ships reunited on the 19th off Skagen (The Skaw for the British of the time), the northernmost extremity of Jutland. In a letter of the 16th, Nelson complained that 'our weather is very cold, we have received much snow and sharp frost' (*The Nelson Papers*, 1845, p. 294).

4. Winds in the Danish waters: The Kattegat and the Sound

A wind from the north-west was needed to reach Copenhagen from Skagen. Such a wind blew for a few days from the 19th on, but Parker delayed moving toward Copenhagen. Nelson was irritated by the delay for he wanted to deny the Danes additional time for strengthening their defences. On the 24th, after a journey of some 230 km, the fleet anchored at a point close to Elsinore with its Kronborg Castle or fort, that guarded the entrance to the Sound where this was at its narrowest, that is 4 km. (The fort is the supposed scene of Shakespeare's play *Hamlet, The Prince of Denmark.*) At that point, north-west of Elsinore, a rendezvous was fixed with a British diplomatic delegation to Copenhagen, which tried in vain to persuade the Danish authorities to abandon the Armed Neutrality Pact, or the Danish navy would be attacked. The diplomats also spoke of the intense preparations and heavy defence works at the capital.

It seems that the fleet was favoured by the occurrence of north-west winds between the 19th and the 24th, as mentioned above. This follows from a comparison with wind-direction frequencies of the recent decades. Frequencies, as observed at the rather open site of the sea fort Trekroner (3K in Fig. 1), built on a shoal some 700 m from Copenhagen's coast, are summarized by Lysgaard (1969, pp. 9–10). His tables are based on eight observations a day in the years 1931–60. The data from

Table III. Frequency distribution, in %, of wind direction at the open site of the entrance from the north to the Copenhagen Roads section of the Sound (Lysgaard 1969)

Month	N	NE	E	SE	S	SW	W	NW	Calm
March	8.6	9.0	14.0	15.3	8.1	10.2	16.4	11.8	6.6
April	8.3	6.5	9.8	13.3	11.1	12.6	16.9	12.8	8.7

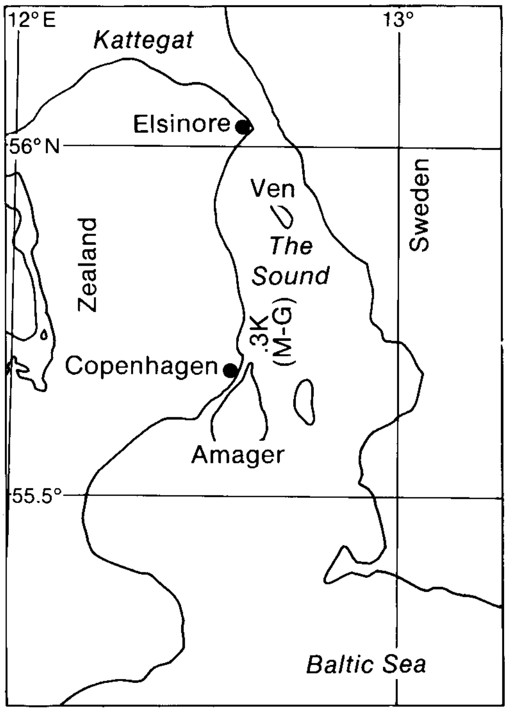

Figure 1. Map of area of the Danish Sound. Kronborg Castle is situated on a tongue of land jutting out from Elsinore (Helsingør in Danish). The symbol 3K stands for Trekroner (= Three Crowns, also called Crown Island by the British). (M-G) indicates the position of the top layer of a major shoal (about 3 km long and 1½ km wide), covered by a shallow layer of water. Copenhagen Roads or Roadstead is on the west side of the shoal. Trekroner was the largest of the sea forts guarding the approaches to Copenhagen. The scale of the map follows from the fact that at Copenhagen's latitude the distance between two longitude lines 1° apart is close to 60 km.

March and April are listed in Table III. The table shows that northerly winds are, on the average, much less frequent than southerlies.

A reference to the pressure and wind observations of the time at the meteorological station on the 'Round Tower' (36 m above street level), in what is now the Old City of the Danish capital, suggests the passage of two high-pressure systems which produced two spells of north-west winds with little time in-between for winds from the south, see Fig. 2. Presumably, the col passed at night between the observations at 21 LST and the observations at 07 LST the next morning, 31 March–1 April.

5. Currents in the Kattegat and the Sound

The currents in these two sea areas are predominantly north-west to northgoing, even when the wind is from the north, excepting the cases of strong winds from the north.

Table IV. Directions of currents in the Sound, 1931–60 (Nielsen 1976)

Sea area	Direction	% of time
In the north	From the SSE	67
(Lappegrunden fire ship)	From the NNW	32
	Other directions	0
	Calm	1
In the south	From SW	59
(Drogden fire ship)	From the NE	36
	Other directions	1
	Calm	4

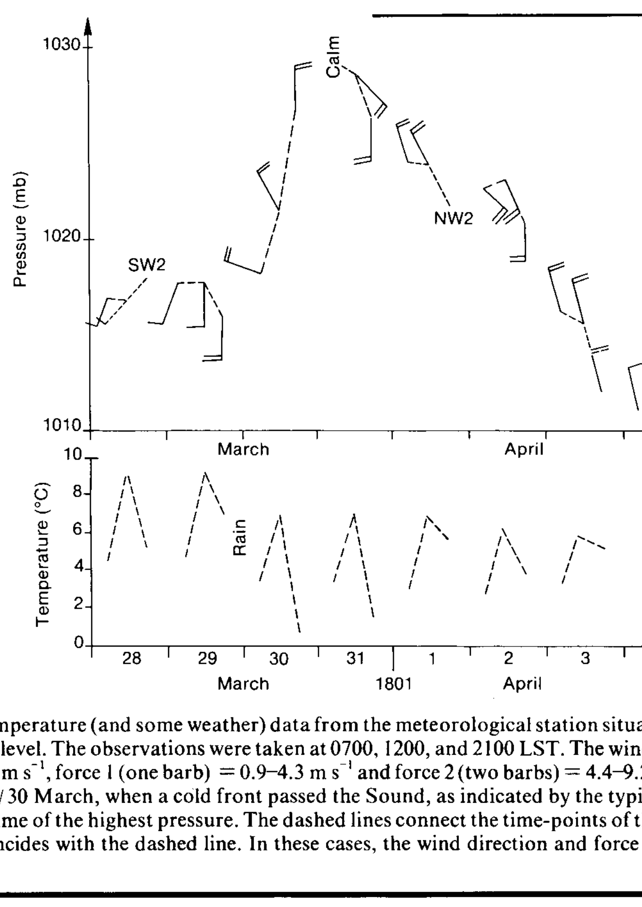

Figure 2. Pressure, wind, temperature (and some weather) data from the meteorological station situated near the top of the Round Tower of Copenhagen, 36 m above street level. The observations were taken at 0700, 1200, and 2100 LST. The wind-force scale used at the time was on the scale of 0 to 4: 'Force' 0 = 0–0.8 m s^{-1}, force 1 (one barb) = 0.9–4.3 m s^{-1} and force 2 (two barbs) = 4.4–9.2 m s^{-1}. The weather was mainly cloudy. Rain fell during the night of 29/30 March, when a cold front passed the Sound, as indicated by the typical wind shift and drop in temperature. Note the wind calm about the time of the highest pressure. The dashed lines connect the time-points of the three observations of the day. In two cases the direction of wind coincides with the dashed line. In these cases, the wind direction and force are indicated by letters and numerals.

Table IV lists the directions of currents in the Sound in 1931–60 (Nielsen 1976, p. 29). The high percentage of northgoing currents is due to the fact that in the Baltic the sum of freshwater inflow and precipitation greatly exceeds evaporation. According to Mikulski and Falkenmark (1986, p. 121), the main items of the annual water balance of the Baltic in 1931–50 were as follows: river inflow 436 km^3, precipitation 250 km^3 — or a total of 686 km^3; evaporation 250 km^3. That is, the sum of the first two is nearly three times as great as the third. Since the only outlet of the Baltic is the North Sea, the flow of surplus waters is to the north-west to north in the Great Belt and the Sound.

Dietrich (1951, pp. 130–131) publishes a table of vectorial velocity of the current in the Sound. For 1901–30 he gives a vectorial velocity of 0.92 knots in March and 0.77 knots in April in the north of the Sound (Lappegrunden fire ship) and, respectively, 0.11 and 0.18 knots in the south (Drogen fire ship). All these vectorial velocities are directed northward. As could be expected, the velocities are higher in the narrow north. In his Table II, Dietrich reports maximum velocities of northgoing currents of 3.6 knots in the north, and 3 knots in the south.

The occasional high current velocities in the north make it likely that the Baltic fleet may have encountered strong northgoing currents on its approach to the Sound. As examples for the disturbing effects of the northward current on the movement of the British fleet in the Sound and the waters on the way to the Sound, two cases are cited. On 27 March, the fleet was virtually immobilized at an approximate distance of 15 km north-west of Elsinore, on account of strong south-south-westerly winds; on the 28th, the wind veered west for some hours and Parker ordered the fleet to weigh anchor but found that 'the ships would not steer owing to a counter-current' (Pope (1972) p. 296, quoting the Admiral's diary). In fact, the fleet was swept northward and Parker had to order the fleet to anchor with Kronborg Castle in sight to the south-east. A second case occurred the day of the battle in the Copenhagen Roads (2 April) when a British frigate (*Jamaica*), with a convoy of gun-boats and other small craft, fell in with the counter-current and had to signal the Admiral that it is unable to proceed (Clarke and M'Arthur, Vol II (1859), pp. 266–267).

6. Sailing to the Sound — Copenhagen's meteorological observations and wind records of British and Danish warships

Since the orders of the Admiralty were to attack the Danish navy if their authorities refused to come to terms with the British demands, and since the Danes refused, the British fleet was to proceed to battle. There were two possible routes to Copenhagen: one was south in the Great Belt, the relatively wide (but shallow) sea area to the west of Zealand, the island on which the Danish capital was situated and then, turn north at the southern extremity of the island as soon as a suitable wind-direction change took place. The other possibility was to sail directly to the Sound by Kronborg Castle at Elsinore where the Sound is, as was mentioned above, at its narrowest. The fort was guarding the entrance to the Sound, and it was equipped with about 100 guns. The first solution was disliked by Nelson because it would have given the Danish authorities more days to advance their preparations and training. Parker, on the other hand, was alarmed by the reports of the serious defence works of the capital, and preferred the first solution.

From now on we shall make use of the data of Copenhagen's meteorological station of the time (pressure, wind, temperature and weather at 0700, 1200 and 2100 LST) as well as the wind data (mainly of direction) recorded in the original logbooks of the British sail-of-the-line *St George* and *Elephant* (the logbooks are preserved at the Public Record Office, Kew, near London), as well as of the Danish sail-of-the-line *Elefanten* (kept at the Danish State Archive, Copenhagen). The 98-gun *St George* was Nelson's flagship until 27 March when, in preparation for the battle in the shallow Sound, he shifted his flag to the lighter, shallower-draught 74-gun *Elephant*. We shall also make some use of Lt Col Stewart's account of the days before the battle and the day of the battle. We shall cite some of his wind reports and consequences of the winds on the movement of the fleet. However, as his account was written from memory, we shall take notice of some corrections put forward by Pope (1972) who studied the events of the journey and the battle on the basis of documents. In addition to Pope's detailed account, there is a detailed account in Danish in a book by Feldbæk (1985).

On the 26th in the forenoon a west wind blew for some hours. The fleet sailed a few leagues (one league equals just under 5 km) in the Great Belt when Parker ordered return to the previous anchorage. Apparently, the fact that some of the small craft hit rocks and the navigational difficulties in the shallow waters prompted him to change his mind. From the 27th to the 29th, the winds were from the south most of the time, both according to Copenhagen's data and logbooks of all the three warships, see Fig. 2 for Copenhagen's data. In the figure, the wind force is on the scale from 0 to 4, used around 1800, before the introduction of the Beaufort scale. According to information received from Dr Knud Frydendahl (Danish Meteorological Institute), 'force' 0 corresponded to a speed of 0–0.8 $m\ s^{-1}$, force 1 to 0.9–4.3 $m\ s^{-1}$ and force 2 to 4.4–9.2 $m\ s^{-1}$.

On the 29th a Council of War was held on Parker's flagship the *London*, where Nelson presented his plan for the battle which heavily leaned on winds. Before describing the plan in brief, we have to refer to Fig. 1 which shows that the west side of the Copenhagen section of the Sound is divided by a major underwater shoal, the Middle Ground, running north–south; the shoal is covered by a shallow layer of water. Nelson proposed to take part of the fleet (Nelson's division) southward, on the east side of the shoal, at a safe distance from the Danish guns. This phase required a north wind. The division would then anchor at a point south of the shoal and, as soon as the wind blew from the south, the division would sail northward on the west side of the shoal, in the channel called King's Deep, to give battle. This roadstead, including the channel was, roughly, 1200 m wide. The Danish navy was arrayed in stationary defensive positions in two lines on the west side of the channel, close to and parallel with the Copenhagen shore line. According to Nelson's proposal, the remaining ships of the fleet, including Parker's flagship, would take up positions north of, and close to, the roadstead, and assist Nelson's division in the battle with their fire. The plan was approved, and, if we follow the printed literature (e.g. Lt Col Stewart's account), Nelson then shifted his flag from this flagship the heavy, 98-gun *St George* to the lighter and of lesser draught 74-gun *Elephant*. (According to the original logbook of the *Elephant*, the shift took place on the 27th, as mentioned above, but this discrepancy is of no meteorological relevance.)

Between the 29th and 30th a cold front passed the area, see Fig. 2. Aside from the wind shift and a drop in temperature, there was some rain during the night. On the 30th, following the passage of the front, the pressure rose sharply, north-westerly winds blew and an anticyclone travelled across. The north-westerly wind enabled the fleet to sail eastward, to a point close to 25 km from Copenhagen (near the island of Ven, made famous by the astronomer Tycho Brahe), see Fig. 1. It seems that the next night the centre of the anticyclone crossed the area. At 0700 LST, the Round Tower Observatory recorded a pressure of 1030 mb and a calm wind, see Fig. 2.

7. Winds and the Battle of Copenhagen

Copenhagen's meteorological data indicate (Fig. 2) that during the night of 31 March/1 April the wind veered to the north-west. The same is indicated by logbooks of the three warships, see Table V. The sequence of direction shifts suggests that another anticyclone, albeit with a lower central pressure, traversed the area, that is, if we assume that the travel of the system was from west to east.

In the forenoon of 1 April the whole fleet sailed with a favourable north-westerly wind to an anchorage about 9 km from Copenhagen, off the north end of the Middle Ground. While Parker's division took up positions north of Roads, the brisk north-westerly wind enabled Nelson's division to sail south on the east side of the

Table V. Winds and some weather information, as reported by Copenhagen's meteorological station and recorded in the logbooks of two British and one Danish warship. The figures on the left-hand side of each column state the hour LST. A complete copy of the entry for 2 April in the logbook of HMS *Elephant* (Nelson's flagship in the battle) is printed in a volume edited by Jackson, Vol. II, 1900, 91–92. Note that in the logbooks the day begins at noon with the date of the next day.

Date	The Round Tower station in Copengahen		HMS *St. George*		HMS *Elephant*		*Elefanten*	
	LST		LST		LST		LST	
1 April 1801	07	NNW 2; scattered skies		Moderate breezes S to NW, cloudy		SSW NW in the morning. Moderate breezes, fair	08	NW
	12	NW 2; nearly overcast					13	NW
	21	NW2; overcast	13	NNW. At 15.30 Nelson's division sails south on the east side of the Middle Ground. At 16.40 the division anchors south of Copenhagen	15	Nelson's division weighs anchor and sails through the east side of the Middle Ground	18	Calm
							24	Calm
					17	Division anchors south of Copenhagen		
			19, 21, 23	Light breezes, cloudy				
			24	Winds S to E				
2 April 1801	07	SE 2; overcast	13	Moderate breezes and cloudy. Engagement continues	A.M.	Fresh breezes, cloudy	01	SE
	12	SSE 2; nearly overcast			10.10	Van division sails to attack	08	ESE
	21	S 2; overcast					13	SSW
					P.M.	Moderate breezes and fair. Truce etc.	18	S to E
							22	S

shoal and anchor about 3 km from the southernmost Danish warship (but within range of a few coastal guns of the island (Amager, see Fig. 1) to the south-south-east and close by the capital.

The next morning, 2 April, another wind-direction shift took place (see Fig. 2 and/or Table V), just as required for Nelson's plan. At about 1000 LST, Nelson's division set sail northward, with an essentially southerly wind, into the roadstead between the capital's coast and the shoal. As stated earlier, in these waters were arrayed the Danish warships in stationary defence. The Danish defenders put up a resolute fire against the British attack, so much so that at 1315 or 1330 LST Parker deemed that the course of the battle did not favour the British fleet. But Nelson saw the situation differently. It was at this time that the famous incident occurred. Parker signalled Nelson to disengage, but Nelson put his telescope to his blind eye and ignored the instruction. By 1400 LST the Danish fire became sparse — it was clear that the Danish navy was defeated. At 1430 Nelson sent a flag of truce to Copenhagen.

Pope (1972), Appendix III, p. 530, summarizes the casualties of the two sides — about 1035 on the Danish side and 944 on the British side. (Pope remarks that the British losses may have been slightly larger, because some who did not report wounded, may have died later.) Nelson reported that all the Danish sail-of-the-line south of the Trekroner fort, 17 in number, were either sunk, burnt or captured. In his Appendix II, Pope (1972) lists the ships in Nelson's division that suffered damages. Of 17 ships in action, one suffered severe damage, slight to somewhat more than slight damage was inflicted on 15, and one was unharmed. An armistice of 14 weeks was agreed upon and signed by the two sides on 9–10 April.

Fig. 3 is a copy of an etching *The Battle in the Roadstead, 2 April 1801* by the Danish engraver Johan Frederik Clemens (1749–1831), made after a painting of the same title by the Danish painter Christian August Lorentzen (1746–1828). It shows the burning Danish warships. Since the ships were aligned in an approximately north–south line (north to the left), the painter shows that the smoke was drifting to the north-west. As stated earlier, the wind was from the south-east or south-south-east, see Table V.

Acknowledgments

The writer is pleased to thank Drs Knud Frydendahl and Povl Anker Skovmand, Danish Meteorological Institute, for their ready assistance with data and

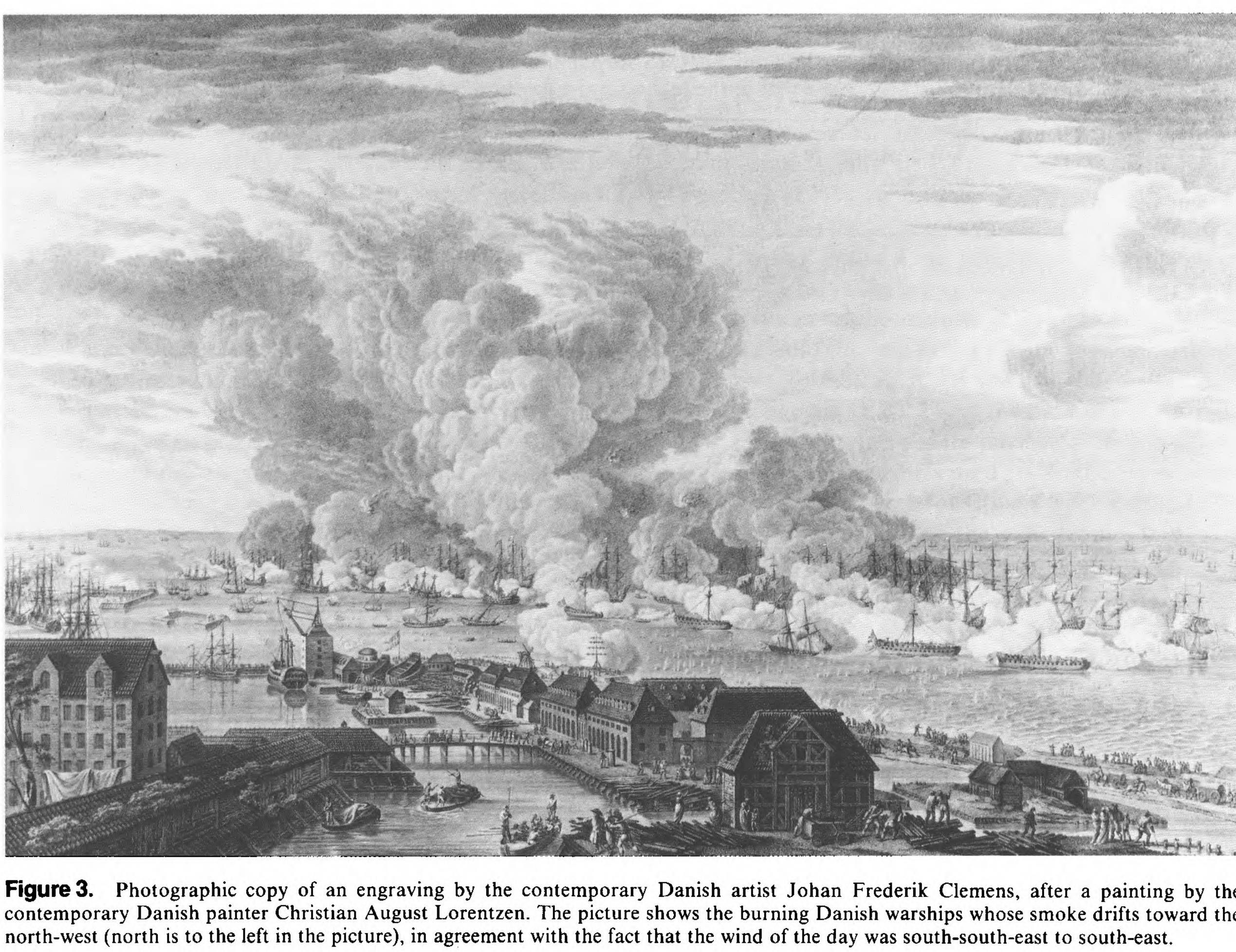

Figure 3. Photographic copy of an engraving by the contemporary Danish artist Johan Frederik Clemens, after a painting by the contemporary Danish painter Christian August Lorentzen. The picture shows the burning Danish warships whose smoke drifts toward the north-west (north is to the left in the picture), in agreement with the fact that the wind of the day was south-south-east to south-east.

comments. Commander A. Holm, Librarian, Danish Marine, and his staff are thanked for naval literature, and Dr Torben Jacobsen, Technical Highschool, Lyngby, is thanked for literature on the physical oceanography of the Baltic Sea. Further thanks are due to Prof C.C. Tsacherning, Institute of Geophysics, University of Copenhagen, for the map in Fig. 1. Finally, credit is due to the Danish State Museum of Art, Copenhagen, for a copy of Johan Frederik Clemens' engraving *The Battle in the Roadstead, 2 April 1801*.

References and bibliography

a. Manuscript sources

Monthly records sheets of observations at the Copenhagen Round Tower Observatory, March–April 1801. Danish Meteorological Institute, Copenhagen.

Logbooks of HMS *St George* and *Elephant*. Public Record Office, Kew, near London.

Logbook of the Danish sail-of-the-line *Elefanten*. Danish State Archive (Rigsarkivet), Copenhagen.

b. Printed sources or printed secondary material

Clarke, J.S. and M'Arthur, J., 1859: The life and services of Horatio Viscount Nelson, Vol II. London, Fisher, Son and Co.

Dietrich, G., 1951: Oberflächenströmungen im Kattegat, im Sund und in der Beltsee. *Deutsche Hydrogr Z.* **4**, 129–150.

Feldbæk, O., 1980: Denmark and the armed neutrality 1800–1801. Small power policy in a world war. Univ of Copenhagen Inst of Econ Hist, Publication No. 16. Copenhagen, Academic Publisher.

Feldbæk, O., 1985: Slaget på reden (Battle in the roadstead). Copenhagen, Politikens Forlag.

Jackson, T.S. (editor), 1900: Logs of great sea fights 1794–1805, Vol II. London, Navy Records Society.

Lamb, H.H., 1977: Climate, present, past and future. Vol 2. Climatic history and the future. London, Methuen and Co.

Lysgaard, L., 1969: Forelobig oversigt over Danmarks Klima 1931–60. Report No. 19. Danish Meteorological Institute, Copenhagen.

Manley, G., 1974: Central England temperatures: Monthly means 1659–1973. *Q J R Meteorol Soc*, **100**, 389–405.

Mälkki, P. and Tamsalu, R., 1985: Physical features of the Baltic Sea. Finnish Marine Res. No. 252, Helsinki.

Mikulski, Z. and Falkenmark, M., 1986: Calculated freshwater budget of the Baltic as a system. *In* Water balance of the Baltic Sea. Baltic Sea Environment Proceedings No. 16. Baltic Marine Environment Protection commission, Helsinki Commission.

The Nelson Paper, 1845: The dispatches and letters of Vice Admiral Lord Viscount Nelson. With notes by Sir Nicholas Harris Nicolas, Vol IV: September 1799 to December 1801. London, Henry Colburn Publisher.

Neumann, J. and Kington, J., 1992: Great historical events that were significantly affected by the weather. Part 10, Crop failure in Britain in 1799 and 1800 and the British decision to send a naval force to the Baltic early in 1801. *Bull Am Meteorol Soc*, **73**. To be published in the February issue.

Nielsen, A., 1976: The Øresund, the Bælt Sea and Kattegat. *In* The Bælt project, Physical investigations. Copenhagen, Environmental Authority.

Pope, D., 1972: The great gamble. London, Weidenfeld and Nicolson.

Rykatschew, M., 1887: Über den Auf- un Zugang der Gewässer des russichen Reiches. Zweiter Supplementband zum Repertorium für Meteorologie. St Petersburg, Imperial Academy of Sciences.

Skovmand, P.A., 1988: The Round Tower and Danish meteorology. Pt I: The observatory periods. *Vejret*, **10**, 30–40. Pt 2: Measurements and instruments. *Vejret*, **10**, 41–47. (Both parts in Danish.)

The Tomlinson Papers, 1935: Selected from the correspondence and pamphlets of Captain Robert Tomlinson, RN and Vice-Admiral Nicholas Tomlinson. London, Navy Records Society.

Wild, H., 1881: Die Temperatur-Verhältnisse des russischen Reiches. Supplementband zum Repertorium für Meteorologie. St Petersburg, Imperial Academy of Sciences.

World Weather Records, 1927. H.H. Clayton, Ed. Smithsonian Misc Collections, Vol. 79. Washington, Smithsonian Institution.

Objectively analysed cloud immersion frequencies for the United Kingdom

K.J. Weston
Department of Meteorology, University of Edinburgh

Summary

Occult deposition, the scavenging of cloud and fog droplets by the land surface and vegetation, forms a significant contribution to the total wet deposition of chemical species to the surface in elevated regions. To assess the magnitude of this contribution it is necessary to have reliable estimates of time spent in cloud on a spatial scale of that of the orography. However, direct observations of cloud immersion are grossly inadequate to define the pattern over a topographically complex area such as the United Kingdom, so use must be made of proxy data. A method is described which makes use of statistics which are routinely available to estimate cloud immersion frequencies for any given land elevation in any part of the United Kingdom. The detailed results of the analysis are obtainable from the author.

As expected, frequencies are strongly dependent on land elevation. Over Scotland at low elevations frequencies are higher in the east than in the west, due mainly to the effects of North Sea stratus, but at elevations above about 500 m frequencies are higher in the west.

1. Introduction

It has been observed by many workers that the concentrations of all major ions in cloudwater collected at elevated sites exceed those in rainwater at the same sites by factors of two or more (Fowler *et al.* 1988, Schmitt 1988, Waldman *et al.* 1985). The deposition of cloudwater to elevated regions leads to a significant contribution to the total wet deposition of chemical species to the surface, particularly if extensive vegetation is present which, together with strong winds, can lead to efficient scavenging of the cloud droplets.

The decline of elevated forests has been observed in several countries (Blank 1985, Saxena *et al.* 1989) and air pollution is suspected to be a contributing factor. Thus it is important to have information of cloud immersion frequencies so that areas which are especially prone to large occult deposition can be identified more readily.

In the United Kingdom very few meteorological observations sites are at elevations above 300 m, so that direct data of cloud immersion are very few. Moreover, the pattern of cloud immersion frequency is likely to be of a scale equal to, or smaller than, that of the orography, so that a prohibitively large number of stations would be required to define the pattern explicitly.

It is clear from the foregoing discussion that direct observations of cloud immersion are grossly inadequate to define the pattern over a topographically complex area such as the United Kingdom, so use must be made of proxy data.

2. Approach to the analysis

Under most meteorological circumstances the spatial variation of cloud-base level is relatively small. When the air below cloud base is well mixed (either because of convection or due to frictionally generated turbulence), the level of cloud base will be almost uniform — even over hills where orographic lifting of low-level air takes place. When the low-level air is thermally stable, such orographic lifting will normally lead to the level of cloud base being lower over the windward side of hills than the general level of cloud base.

A standard statistic derived from cloud observations made at meteorological stations is the percentage of time that the sky has cloud of ⅝ or more at various specific heights. At Royal Air Force stations the statistics are for ⅜ or more cloud cover. If it is assumed that elevated land is 'passive' in that it samples the cloud without either affecting the cloud-base level or the cloud amount, then data from neighbouring stations can be used to estimate cloud immersion frequencies at a site, given its height above sea level.

The fraction of time that ground in a particular location (x, y) at a particular elevation (z) is in cloud is given by

$$F(x,y,z) = \sum_{i=1}^{8} {}^{i}/_{8}\, f_i\,(x,y,z)$$

where i is the cloud cover in oktas and f_i is the fractional time that the sky is covered by i oktas of cloud at or below the particular elevation considered.

The data being used refer to the fractional time that the sky is covered by either ⅜ or ⅝ (as appropriate) of cloud or greater, given by

$$F_3(x,y,z) = \sum_{i=3}^{8} f_i\,(x,y,z) \text{ and } F_5(x,y,z) = \sum_{i=5}^{8} f_i\,(x,y,z).$$

If the frequency distribution f_i is symmetrical with respect to i, it can easily be shown that

$$F(x,y,z) = F_5(x,y,z) + \tfrac{1}{2} f_4(x,y,z).$$

If $f_3 = f_4$, then $f_4 = \tfrac{1}{2}(F_3 - F_5)$ so that

$$F(x,y,z) = \tfrac{3}{4} F_5(x,y,z) + \tfrac{1}{4} F_3(x,y,z). \qquad (1)$$

This is the expression that is used to calculated the frequency of cloud cover in all three space dimensions, by analysing the three-dimensional fields of F_3 and F_5. In practice the approximations used to derive equation (1) are not very sensitve to the assumption of symmetry of the f_i distribution.

3. Available data and analysis

Data for a 20-year period of frequencies of $5/8$ cover at 15 levels (above station) up to 5000 ft were used from 54 stations in the United Kingdom, and from 46 stations for $3/8$ cover. (The highest ground in the United Kingdom is at 4406 ft.) These stations are shown in Fig. 1. All heights were converted to heights above mean sea level and from these data the fields of frequency were analysed objectively using orthogonal polynomials as base functions (Dixon *et al.* 1972); but to increase the accuracy of the representation in the vertical, the data were split into three overlapping sets covering the height ranges 0–800 ft, 500–2000 ft and 1200–5500 ft. Polynomials were evaluated to third order in all three dimensions, so that the analysed fields were represented by 20 coefficients.

From these analyses the frequencies of cloud cover of $3/8$ or more and of $5/8$ or more were calculated for a particular area of the United Kingdom, using the appropriate average height of ground. At heights falling in the overlap ranges (500–800 ft and 1200–2000 ft), a linear interpolation between the values for the two height ranges was used. Application of equation (1) then gives the estimate of cloud immersion frequency.

4. Results

Before looking at cloud immersion data, first look at maps of the frequency of cloud at or below specific heights. The frequency of cloud cover at or below a height of 500 ft is shown in Fig. 2. Everywhere over the United Kingdom frequencies are very low, nowhere exceeding 6% of the time. Highest frequencies are over the south-west of England and down the east coast, especially over East Anglia. Cloud at such a low height is usually stratus. Mansfield (1988), in an investigation of stratus distrubution over the United Kingdom, identified two summer regimes and one winter regime largely responsible for stratus. One of the summer regimes gives advection stratus/fog on south-western coasts and the other is associated with north-easterly flow and gives highest frequencies of stratus down the east coast, and especially over East Anglia. These regimes of advection

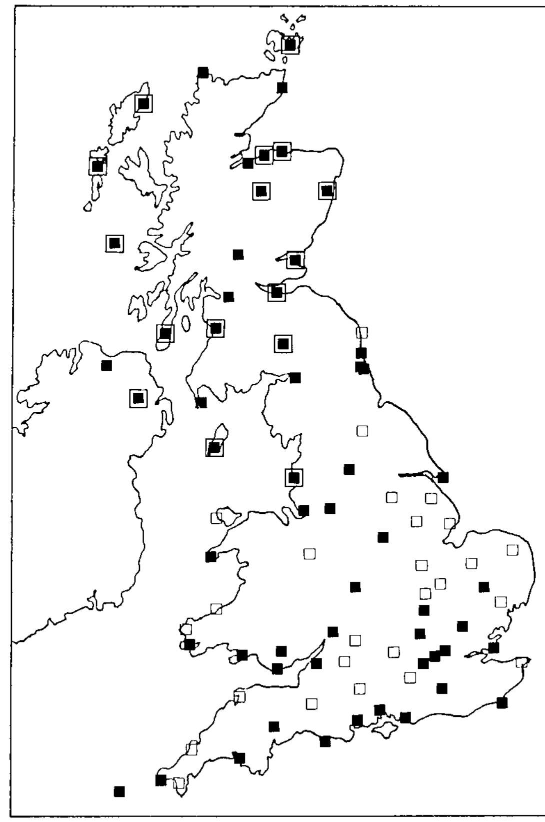

Figure 1. Stations included in the analysis. Solid squares indicate stations for which data were based on $5/8$ cloud cover and open squares on $3/8$ cover. (For 16 stations both were available.)

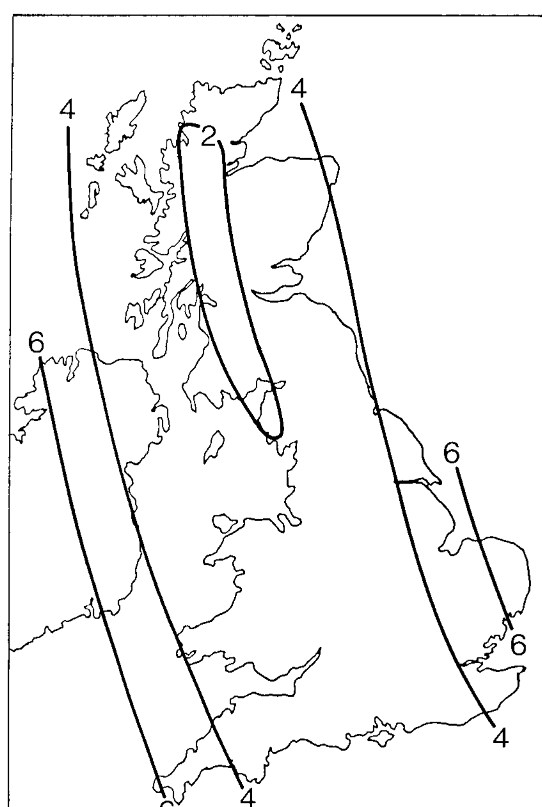

Figure 2. Frequency of cloud cover (%) at 500 ft above sea level.

stratus are the main reason for the form of the cloud frequencies at 500 ft shown in Fig. 2. The third, the winter regime, identified by Mansfield is associated with anticyclonic southerly flow and gives inland stratus due to local cooling.

The pattern of cloud frequency at or below 2000 ft (Fig. 3) shows lowest frequencies over north-east Scotland, with less than 15% frequency. This rather low frequency is probably due to the sheltering effect of the Scottish Highlands, causing a drying of the air in flow from western quadrants. Highest frequencies are in south-west England, East Anglia, and the Western Isles of Scotland, where frequencies reach 25%. Most of the cloud at or below 2000 ft is again likely to be stratiform, but some contribution from cumulus is probable, especially in coastal regions where humidities are higher and hence cloud base is lower.

The results of this analysis (obtainable on request from the author) may be used to derive cloud immersion frequencies on any spatial scale for which land height data are available; but, for illustration, average cloud immersion frequencies are given in Fig. 4 for 15 km squares over Northern Scotland. Highest immersion frequencies of 24% occur over the Cairngorm Mountains, where there are several peaks of over 4000 ft. The immersion frequency, given by the analysis, for the highest summit in the Cairngorms (Ben MacDhui, 4296 ft) is 42%.

Acknowledgements

The author is grateful to the Meteorological Office for the provision of the data, and to D.A. Mansfield for help and advice.

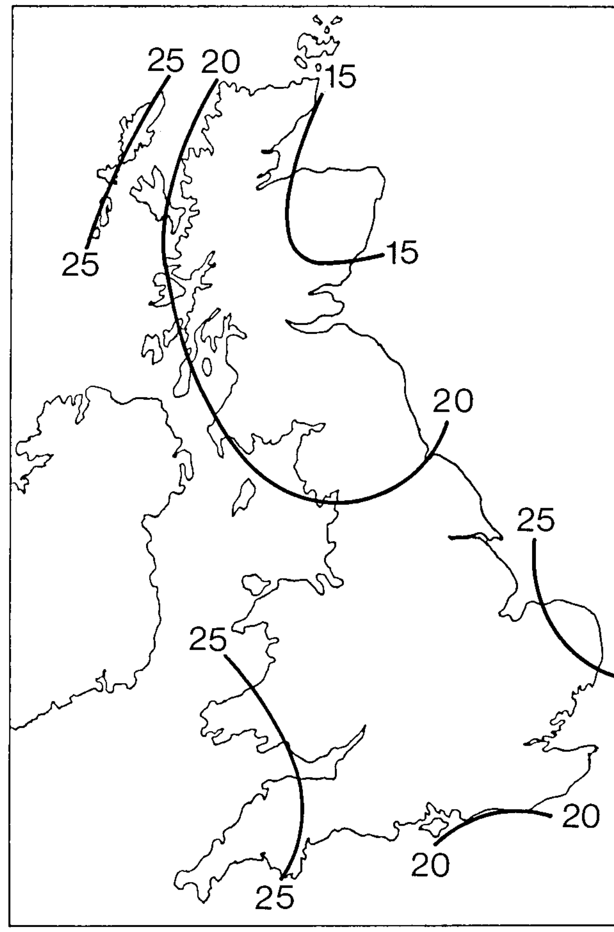

Figure 3. Frequency of cloud cover (%) at 2000 ft above sea level.

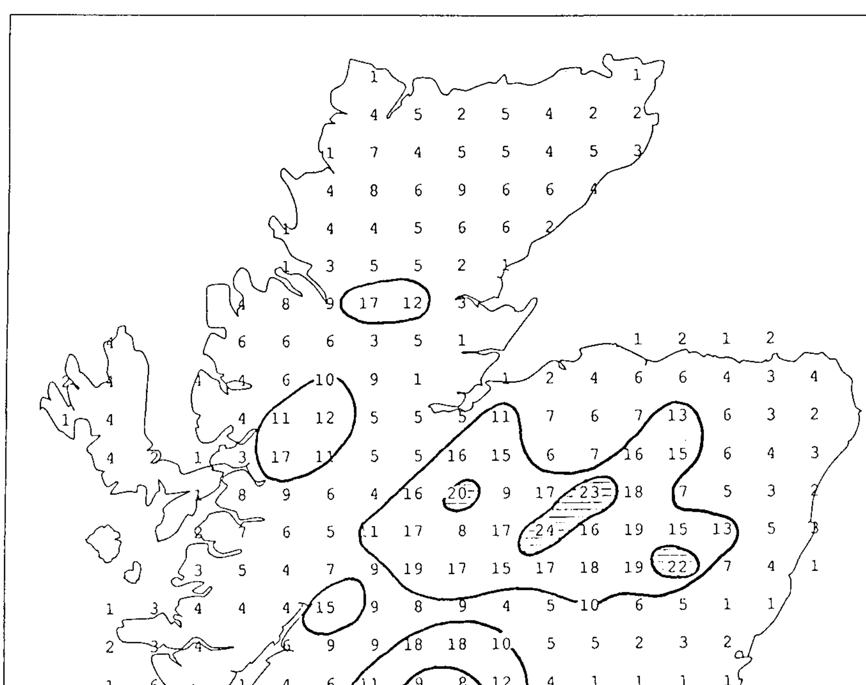

Figure 4. Cloud immersion frequencies (%) for Northern Scotland, averaged over 15 km squares. Contours of 10% and 20% are shown.

References

Blank, L.W., 1985: A new type of forest decline in Germany. *Nature*, **314**, 311–314.

Dixon, R., Spackman, E.A., James, I. and Francis, A., 1972: The global analysis of meteorological data using orthogonal polynomial base functions. *J Atmos Sci*, **29**, 609–622.

Fowler, D., Cape, J.N., Leith, I.D., Choularton, T.W., Gay, M.J. and Jones, A., 1988: The influence of altitude on rainfall composition at Great Dun Fell. *Atmos Environ*, **22**, 1355–1362.

Mansfield, D.A., 1988: An investigation into stratus distribution over the United Kingdom. *Meteorol Mag*, **117**, 236–245.

Saxena, V.K., Stogner, R.E., Hendler, A.H., DeFelice, T.P., Yeh, R. J-Y. and Lin, N-H., 1989: Monitoring the chemical climate of the Mt Mitchell State park for evaluation of its impact on forest decline. *Tellus*, **41B**, 92–109.

Schmitt, G., 1988: Measurements of the chemical composition in cloud and fogwater. *In*: Acid deposition at high elevation sites, NATO ASI Series, Series C, Vol. 252. Dordrecht, Kluwer Academic Publishers.

Waldman, J.M., Munger, J.W., Jacob, D.J. and Hoffman, M.R., 1985: Chemical characterization of stratus cloudwater and its role as a vector for pollutant deposition in a Los Angeles pine forest. *Tellus*, **37B**, 91–108.

Review

Prediction and regulation of air pollution, by M.E. Berlyand. 164 mm × 244 mm, pp. xiii+312, *illus*. Dordrecht, Boston, London, Kluwer Academic Publishers, 1991. Price Dfl.175.00, $108.00, £61.00. ISBN 0 7923 1000 4.

Question: 'Which is the oldest surviving area of research in the Meteorological Office (discounting the everlasting struggle to improve weather forecasting)?'

Answer: 'Surprisingly, it is the study of airborne pollution dispersion which started in the Office in about 1916 when poisonous gas was used as a weapon of war in the trenches.'

You might think we'd learnt a thing or two in those 75 years — and I think we have. On good days, one is tempted to think a very great deal has been learnt, not just in the Office but worldwide — just look at the fat books on the subject. Then comes the bad day! The telephone rings; a caller has a dispersion problem — it's a bit complex, with odd-shaped buildings and a steep valley next-door and downwash from the stack and .... A bit too difficult even for our latest up-market dispersion model with all the most recent science in it. Shattered you tell the caller the best thing he can do is to get it physically modelled in a wind-tunnel, theory cannot fully solve his problem, it can only guide him.

I think this anecdote reflects a tendency in the West to let theory and more practical procedures advance together as complementary partners. Overall, I believe this makes good sense and, aware of the uncertainties involved, we have been rather reticent to push the theory forward beyond what seems sensible in some difficult areas. On the other hand, scientists in Eastern Europe, and in Russia in particular, have apparently tended to develop theories and obtain complex solutions to problems that we have tended to model more tentatively or at best more empirically.

Professor Berlyand's book opens the window to what has been going on in the Soviet Union in the way of practical dispersion modelling. It reveals that many very important issues have been considered — many more than have been really worked on in the West. To give but one small example: the dispersion of gases emanating from a long slit running the length of the roof of an aluminium smelter. Often the approach has been theoretical, as implied earlier, but sometimes the suggested method has had to be empirical. In addition the book contains many of the advances made in the West; lots of references to western studies underline that.

It all makes fascinating reading — a new insight into a world of research all too little revealed in this depth before. Whilst I doubt it will revolutionize what is currently done in the West, I think it will make many of us think about our methods and thereby have a more subtle influence.

A little disappointingly there are many mis-spellings, particuarly of names, and other small but important typographical errors. Particularly disturbing is the occasional use of misleading terminology: to give one example, by 'light' pollutants the authors means 'passive' pollutants, not pollutants whose density is significantly less than that of air!

However these little irritations aside, this is a very important book with a rightful place on the shelf of any pollution meteorologist, and is otherwise very well produced and pleasing to use.

F.B. Smith

Fractals: endlessly repeated geometrical figures, by H. Lauwerier. 139 mm × 216 mm, pp. xiv+209, *illus.* London, Penguin Books, 1991. Price £9.90. ISBN 0 14 014411 0.

This book, an English translation of a work first published in the Netherlands in 1987, deals mainly with the basic mathematics of fractals rather than their applications or occurrence in nature. An appendix of computer programs illustrating the text enables readers with personal computers to generate fractals for themselves. The book is aimed at a wide audience and therefore assumes only a limited mathematical knowledge. Concepts such as number systems other than base ten, Cartesian co-ordinates, irrational numbers and infinite sets are explained in the early chapters. No familiarity with complex numbers is assumed or required but an appendix briefly indicates their use in simplifying some of the mathematics.

After a brief description of work on the length of the British coastline by L.F. Richardson (who is described as a 'somewhat eccentric English meteorologist'), the author describes various types of meandering curves. This is in line with his definition of a fractal as 'a geometrical figure in which an identical motif repeats itself on an ever diminishing scale', a definition which disguises the links between fractals and chaos. The well-known fractals of Sierpinski, Koch and Minkowski, all older than the term 'fractal' itself, are described as well as dragon curves (formed by repeated folding of a strip of paper), spirals, tree fractals and star fractals. Programs to draw all of these are included. A chapter for the mathematically minded reader describes methods for computing fractals of this type using similarity transformations. The backtracking method which is both fast and requires little storage is outlined and illustrated with programs.

It is not until half way through the book that the concept of chance makes its first appearance. This precipitates a succession of fascinating, and often deep, mathematical topics: Brownian motion, chaotic behaviour, Feigenbaum's number, attractors and Julia and Mandelbrot sets. Pure mathematicians will be disappointed to find only two of the book's eight chapters devoted to these subjects. A few illustrative programs are given but some of these topics stretch the present capacity of small computers. (A program to outline the Mandelbrot set is easily the longest running of all those listed.)

The book is well printed and contains a number of attractive illustrations of Julia fractals and detail of the Mandelbrot set as well as two spectacular fractal landscapes from Mandelbrot's book *The fractal geometry of nature*, all in colour but with little or no comment. A few typographical and other errors were detected including the incorrect description of the Mercator projection as 'the projection of a sphere from its centre onto a vertical cylinder surrounding it'. A short bibliography gives suggestions for more advanced reading.

The computer programs presented, written in BASIC for a PC with a high-resolution monochrome screen, form an essential feature of the book. They range from simple ones for drawing spirals to those capable of drawing various repeated-motif fractals at any specified level of detail. A few generate dust fractals illustrating chaotic behaviour. There is a certain fascination in watching a fractal design appearing on the screen like a time-lapse film of a fanatical portrait painter — readers familiar with basic will not be able to resist altering the data input to some programs to see what happens (some suggestions are given in a chapter entitled *Making your own fractals*), or modifying them to produce more detail. Most programs are less than 25 lines long and, although they contain few comments, all are referred to in the body of the text where further description can usually be found. (The graphics statements used are briefly described for users needing to convert to other programming languages.) Of course, accuracy is particularly important where computer programs are presented so it is satisfying to report that this reviewer has tried all of the 41 programs and found them to work as described.

The book cannot be described as a meteorological book — readers interested in the applications of fractals and chaos to clouds, turbulence and predictability will have to look elsewhere. But understanding of any new or unfamiliar scientific topic implies an initial familiarity with basic concepts. Within the limitations of its view of fractals as mathematical curiosities with aesthetic visual appeal rather than a subject related to modern mathematical techniques for describing the real world, this book succeeds in giving the reader a feel for fractals, not least through its computer programs. With these you will be able to demonstrate your skill in computer art to your friends. It certainly makes a refreshing change from holiday slides or home movies.

B.R. Barwell

Books received

The listing of books under this heading does not preclude a review in the Meteorological Magazine at a later date.

Natural weather wisdom, by Uncle Offa (Hanley Swan, Worcester, Images Design and Print Ltd, 1991. £9.50) contains many saws and sayings used by our forefathers as a guide to future weather. This, of course, entails observation of nature and types of weather on Saints' Days etc. ISBN 1 85421 146 3.

Fundamentals of weather and climate, by J.F.R. McIlveen (London, New York, Tokyo, Melbourne, Madra, Chapman and Hall, 1991. £19.95) is an expanded, new edition of *Basic meteorology: A physical outline*. It attempts to collocate the theory and actuality of atmospheric behaviour. ISBN 0 412 41160 1.

GUIDE TO AUTHORS

Content

Articles on all aspects of meteorology are welcomed, particularly those which describe results of research in applied meteorology or the development of practical forecasting techniques.

Preparation and submission of articles

Articles, which must be in English, should be typed, double-spaced with wide margins, on one side only of A4-size paper. Tables, references and figure captions should be typed separately. Spelling should conform to the preferred spelling in the *Concise Oxford Dictionary* (latest edition). Articles prepared on floppy disk (IBM-compatible) can be labour-saving, but only a print-out should be submitted in the first instance.

References should be made using the Harvard system (author/date) and full details should be given at the end of the text. If a document is unpublished, details must be given of the library where it may be seen. Documents which are not available to enquirers must not be referred to, except by 'personal communication'.

Tables should be numbered consecutively using roman numerals and provided with headings.

Mathematical notation should be written with extreme care. Particular care should be taken to differentiate between Greek letters and Roman letters for which they could be mistaken. Double subscripts and superscripts should be avoided, as they are difficult to typeset and read. Notation should be kept as simple as possible. Guidance is given in BS 1991: Part 1: 1976, and *Quantities, Units and Symbols* published by the Royal Society. SI units, or units approved by the World Meteorological Organization, should be used.

Articles for publication and all other communications for the Editor should be addressed to: The Chief Executive, Meteorological Office, London Road, Bracknell, Berkshire RG12 2SZ and marked 'For Meteorological Magazine'.

Illustrations

Diagrams must be drawn clearly, preferably in ink, and should not contain any unnecessary or irrelevant details. Explanatory text should not appear on the diagram itself but in the caption. Captions should be typed on a separate sheet of paper and should, as far as possible, explain the meanings of the diagrams without the reader having to refer to the text. The sequential numbering should correspond with the sequential referrals in the text.

Sharp monochrome photographs on glossy paper are preferred; colour prints are acceptable but the use of colour is at the Editor's discretion.

Copyright

Authors should identify the holder of the copyright for their work when they first submit contributions.

Free copies

Three free copies of the magazine (one for a book review) are provided for authors of articles published in it. Separate offprints for each article are not provided.

Contributions: It is requested that all communications to the Editor and books for review be addressed to the Chief Executive, Meteorological Office, London Road, Bracknell, Berkshire RG12 2SZ, and marked 'For *Meteorological Magazine*'. Contributors are asked to comply with the guidelines given in the *Guide to authors* (above). The responsibility for facts and opinions expressed in the signed articles and letters published in *Meteorological Magazine* rests with their respective authors.

Subscriptions: Annual subscription £36.00 including postage; individual copies £3.25 including postage. Applications for postal subscriptions should be made to HMSO, PO Box 276, London SW8 5DT; subscription enquiries 071–873 8499.

Back numbers: Full-size reprints of Vols 1–75 (1866–1940) are available from Johnson Reprint Co. Ltd, 24–28 Oval Road, London NW1 7DX. Complete volumes of *Meteorological Magazine* commencing with volume 54 are available on microfilm from University Microfilms International, 18 Bedford Row, London WC1R 4EJ. Information on microfiche issues is available from Kraus Microfiche, Rte 100, Milwood, NY 10546, USA.

April 1992

Edited by R.M. Blackall Vol. 121
Editorial Board: R.J. Allam, R. Kershaw, W.H. Moores, P.R.S. Salter, J. Gloster No. 1437

Contents

ISSN 0026–1149

ISBN 0-11-728982-5

9 780117 289826

Printed in the United Kingdom for HMSO
Dd291241 4/92 C22 503 12521

The Meteorological Magazine

May 1992

Ocean models in FOAM
Forecasting seasonal long rains in Kenya
The spring of 1991

HMSO
Met.O.1004 Vol. 121 No. 1438

First published 1992

HMSO

HMSO publications are availabl(

HMSO Publications Centre
(Mail, fax and telephone orders c
PO Box 276, London, SW8 5DT
Telephone orders 071-873 9090
General enquiries 071-873 0011
(queuing system in operation for
Fax orders 071-873 8200

HMSO Bookshops
49 High Holborn, London, WC1
258 Broad Street, Birmingham, I
Southey House, 33 Wine Street,
9-21 Princess Street, Manchester
16 Arthur Street, Belfast, BT1 4J
71 Lothian Road, Edinburgh, EH

HMSO's Accredited Agents
(see Yellow Pages)

and through good booksellers

The Meteorological Magazine

May 1992
Vol. 121 No. 1438

551.509.313:551.465

The role of ocean models in FOAM

S.J. Foreman
Meteorological Office, Bracknell

Summary

FOAM (the Forecasting Ocean Atmosphere Model) is planned to form the basis of an ocean forecast system for the Atlantic and Arctic Oceans. Synoptic features in the ocean have smaller space scales than in the atmosphere, and so require more observations to define them and greater computer power to simulate them. Satellites, such as ERS-1, will supplement the in situ *data during the 1990s, and the power of supercomputers continues to increase. It is now possible to develop model-based systems for forecasting the ocean. FOAM will mimic the numerical weather prediction system at the Meteorological Office. An essential component of FOAM will be the use of manual input to the model to enhance the quality control of observations and to make use of data which cannot be used directly by the computer system.*

1. Introduction

Computers have been used to forecast the weather for many years with increasing accuracy (Meteorological Office 1988). Numerical models, based on the 'laws' of physics, form the basis of the Numerical Weather Prediction (NWP) systems. The ocean obeys the same laws as the atmosphere, and there is no theoretical reason why ocean forecasts should not be produced in the same way.

FOAM, the Forecasting Ocean Atmosphere Model, sets out to provide a physically based system for forecasting the temperature, salinity, and current structure of the Atlantic and Arctic Oceans.

This paper aims to explain why it has not been practical to produce ocean forecast models until the 1990s, and then describes the essential components of a computerized forecasting system. This involves a discussion of the models themselves and of the methods for inserting observations into the models. This is followed by a description of how the quality of forecasts can be improved by involving humans in the forecast cycle. Finally the reasons for using models in the FOAM system are summarized.

2. Evolution of the ocean circulation

Just as the atmospheric circulation is driven by the sun's energy, that of the ocean is driven primarily by the fluxes of heat, fresh water, and momentum across the air–sea interface (Foreman 1990). In response to these, the physics governing ocean circulation produce the large-scale flow patterns, within which smaller features may develop, such as fronts and eddies.

Atmospheric disturbances (depressions and anti-cyclones) have a major and rapid impact on the upper ocean, determining changes in the depth and temperature of the mixed layer on time-scales of hours to days. The spatial scale of these features is of the order of thousands of kilometres and they have a typical lifetime of a week.

The ocean also generates its own fronts and eddies. Development of eddies in the ocean is slower than in the atmosphere (Gill (1982) p. 569). Typically, Gulf Stream rings grow on time-scales of a week and have lifetimes of a month. Space-scales of ocean eddies are much smaller than those of the atmosphere, typically 200 km (Fig. 1).

On a seasonal time-scale the atmospheric climate influences the large-scale circulation patterns of the ocean. As an example, Fig. 2 shows the impact of

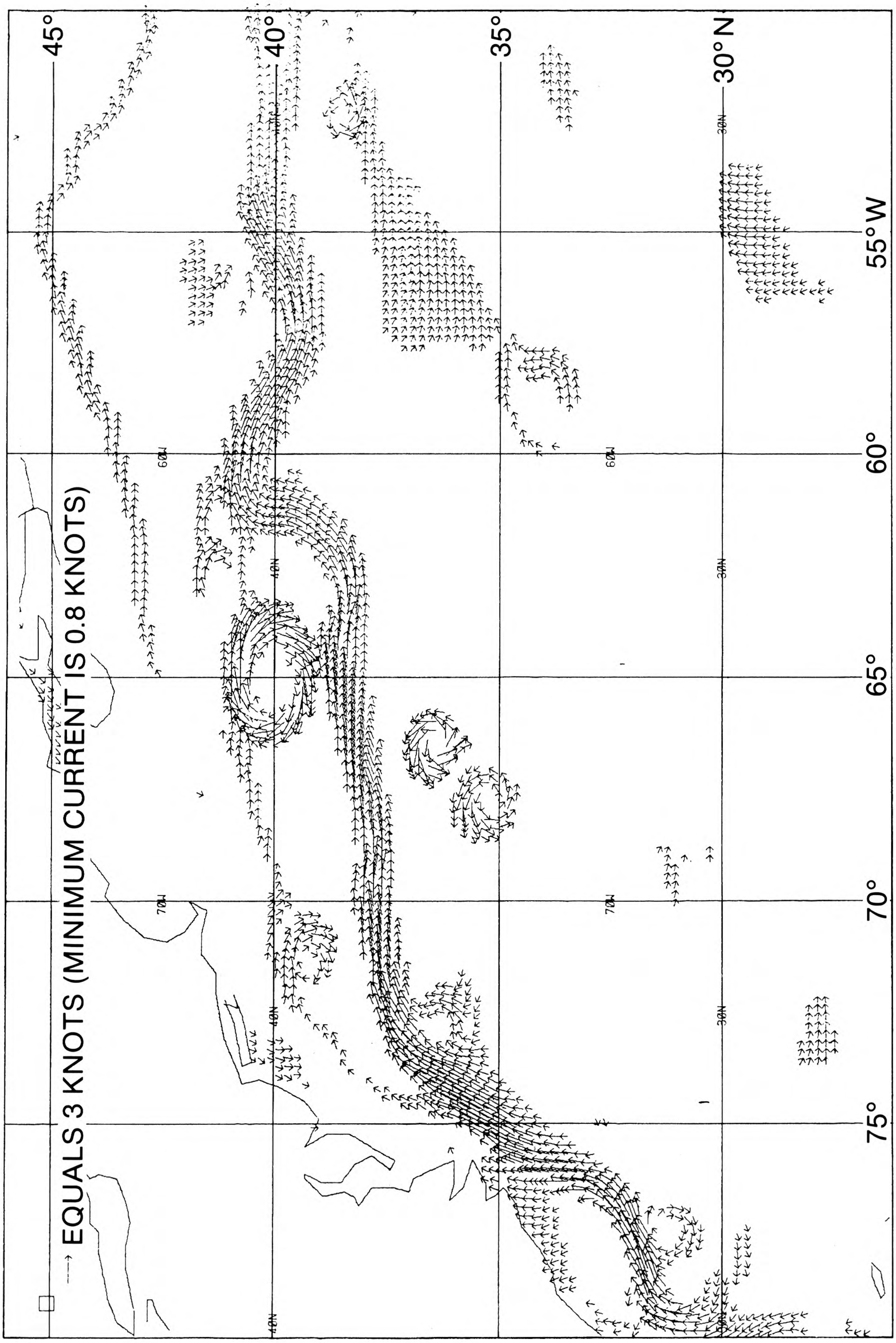

Figure 1. Ocean currents in the north-west Atlantic on 9 June 1991. Only currents greater than 0.8 kn are shown. (Reproduced with permission of M. Clancy, Fleet Numerical Oceanography Center.)

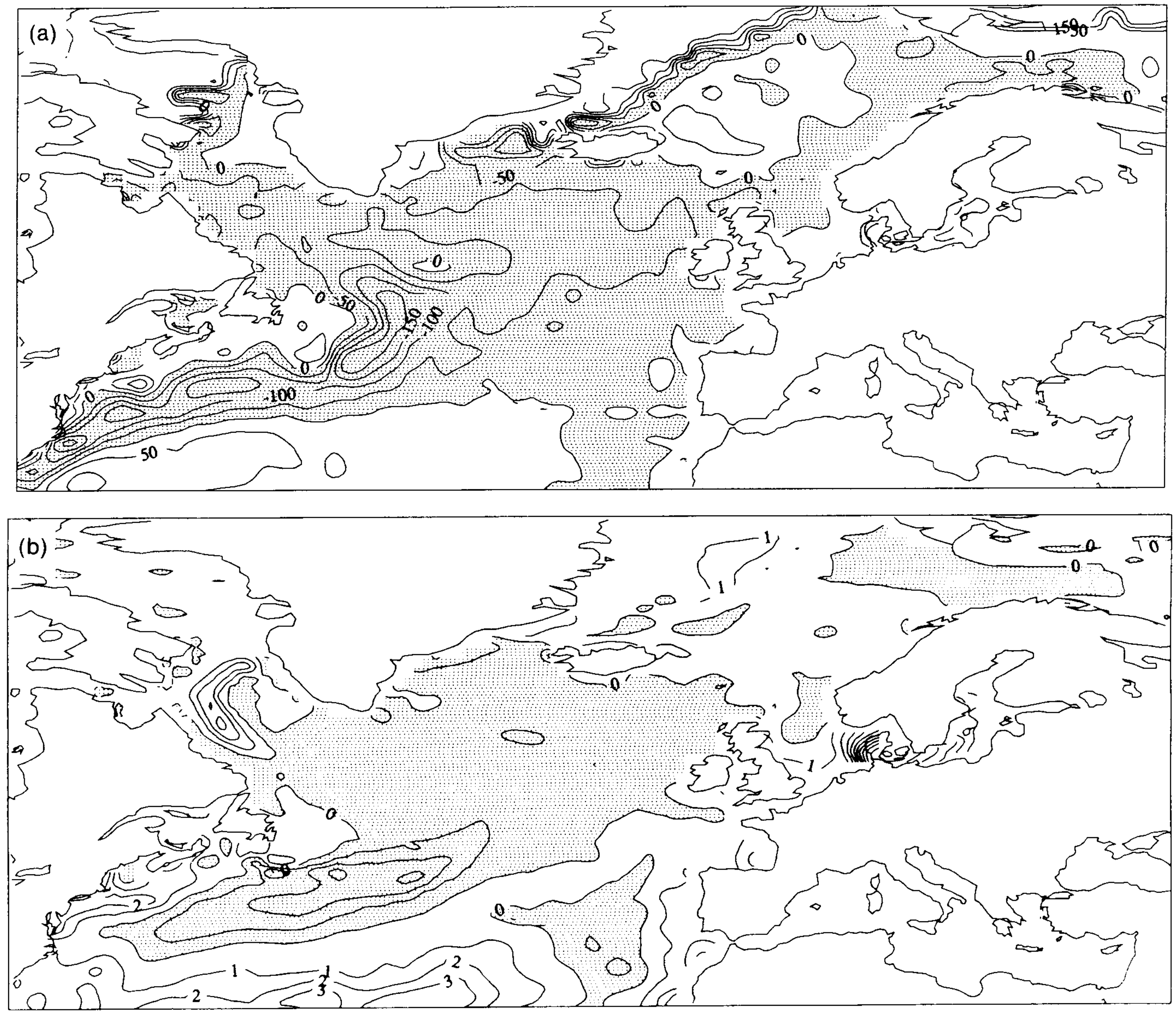

Figure 2. Impact of different surface flux estimates on an integration of a 1 degree resolution Atlantic model in the north-west Atlantic. Differences are for 6-month integrations for the winter of 1989/90 run using climatological fluxes minus a run with NWP derived fluxes. (a) Difference between six-month average of fluxes (50 W m^{-2} contour interval), and (b) difference between sea surface temperatures after 6 months of simulation (1 °C contour interval). Negative areas are stippled.

driving an ocean model with two different sets of surface fluxes. In the control, the fluxes used were derived from observed climatologies. The perturbation integration used surface fluxes from the Meteorological Office NWP suite. In both cases the fluxes were applied to an ocean model of the Atlantic for the 6 winter months. Fig. 2(a) shows the differences between the heat fluxes into the ocean averaged over the six months. Most of the structure in the Gulf Stream region is due to the greater horizontal resolution of the NWP data. There are large differences in other areas which are typical of interannual variability. Fig. 2(b) shows the difference in sea surface temperature (SST) between the two simulations at the end of the 6 months. Differences of one degree are common (and are typical of the observed interannual variability). The ocean therefore responds to the seasonal climate of the atmosphere. The space-scale of this response is large compared to that of the ocean eddies.

3. Observing the ocean

Different aspects of the ocean circulation have different time- and space-scales associated with them. Eddies in the ocean are typically an order of magnitude smaller than in the atmosphere, so that to obtain as accurate synoptic analyses as those from NWP correspondingly more observations would be needed.

Fig. 3 shows the locations of all observations of the ocean vertical structure for the Atlantic received in real time by the Meteorological Office during May 1991. Although there are regions (such as the eastern seaboard of the United States) where there is dense coverage of BATHY data (temperatures only), most of the ocean is unsampled. To resolve eddies would require observations about 25 km apart over the whole region in which eddies are expected (including the Iceland–Faeroes Gap). A full description of the ocean density requires salinity as well as temperature to be reported. The number of TESAC reports (which may contain both temperature

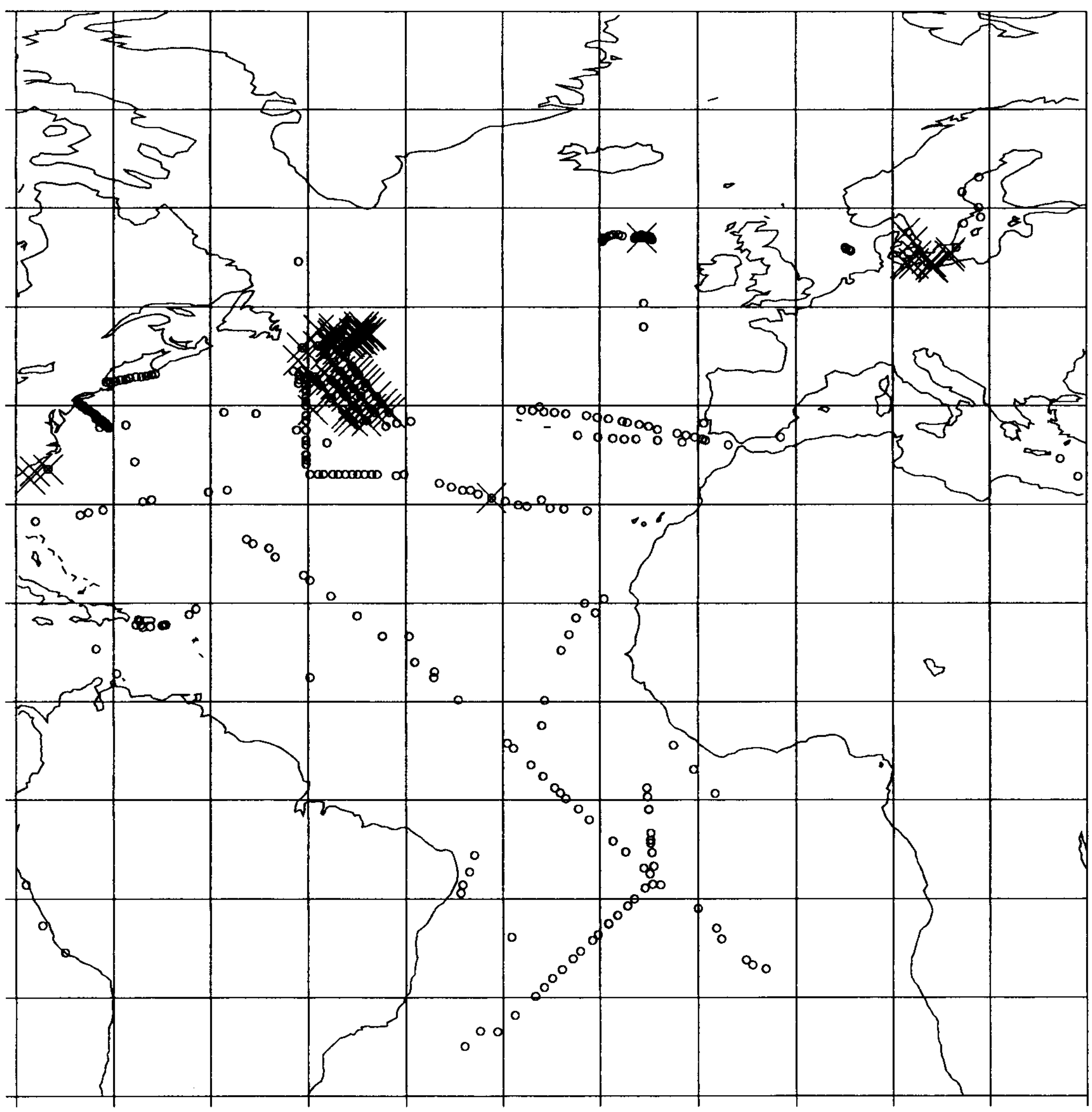

Figure 3. Distribution of BATHY and TESAC reports received at Bracknell in the Atlantic during May 1991. BATHY reports are indicated by circles, TESACs by crosses.

and salinity observations) during May 1991 can be seen to be small.

The horizontal distribution of BATHY and TESAC reports is inadequate for the task of determining the synoptic evolution of ocean eddies without further information. Considering the vertical distribution of reports is even less encouraging. Fig. 4 shows the depths to which observations extended in 1988. Although some of the more useful TESAC reports reached 2000 m, most of these were made by Ocean Weather Ship 'C', which no longer reports. Observations of the ocean below 600 m are rare.

Design of a system to analyse the ocean must also take into account the delays in receiving observations. As may be seen in Fig. 5, many BATHY and TESAC observations were still being received 3 days after the time for which they are valid.

By far the most plentiful observations of the ocean are of its surface temperature. There are two main sources of these data: ship reports and satellite measurements. Satellite infrared measurements have high spatial resolution, but cannot be made through cloud. Some satellites have used microwave sensors to measure sea surface temperature. Although observations may be made through cloud, they are of lower accuracy and resolution than those made using infrared instruments.

SEASAT in the 1970s, and GEOSAT during the 1980s, carried altimeters capable of measuring the height of the satellite above the ocean surface. Several successor satellites to these are planned for the 1990s, starting with ERS-1. After careful correction these observations may be used to derive information about the vertical mean circulation in the ocean. Data are derived along sub-satellite tracks, instead of the more familiar swathes of the sea-surface-temperature measurements. This means that deducing variations along the track is straightforward, but that variations perpendicular to the track can only be determined with the resolution of the spacing between tracks in both space and time. ERS-1 and other oceanographic missions carrying altimeters are designed to be flown in 'repeat orbits' in which the same point on the Earth is overflown on many orbits. A characteristic of the repeating orbits is that high spatial resolution is accompanied by low temporal resolution. The choice of orbit is thus a compromise between the needs of different users, and ERS-1 is expected change its orbit several times during its life.

It is only the introduction of satellites such as ERS-1 and development of new observation systems, such as the Natural Environment Research Council's 'AUTOSUB' project (Baker 1991) which will make it possible to observe the ocean in enough detail to make ocean forecasting a practical proposition.

4. Modelling the ocean

At its heart FOAM will contain numerical models of the atmosphere and ocean. That for the atmosphere will be the same as that used for NWP by the Meteorological Office (Wilson *et al.* 1990). This will communicate with a model of the ocean built using the same physical principles derived from Bryan and Cox (1972).

Underlying the ocean model are Newton's 'laws' of motion as they apply to a continuous fluid. Equations for conservation of heat, salt, momentum, and mass form the basis of the model. These are represented using a 'finite difference' approach, in which the ocean is divided into a large number of cuboids (in the early stages of FOAM these will have dimensions approximately 100 km (later 30 km) in the horizontal and 5 m in the vertical in the upper ocean). Numerical techniques based on finite difference approximations are used to approximate continuous equations governing ocean flow. These are solved using a computer for each model box and for each time-step. The forecast is thus built up of a sequence of 'mini forecasts' of a few minutes duration. The region expected to be covered by the model is shown in Fig. 6 and the physics represented within it in Fig. 7.

In the absence of observations (such as when producing a forecast) the ocean model responds only to its internal physics and to the fluxes of heat, fresh water, and momentum through the ocean surface, which are calculated by the NWP model. In many data-sparse areas forecasts would be the sole source of information about the ocean.

Techniques for modelling the ocean are similar to those used in numerical weather prediction. Computing demands of the ocean models are greater because of the smaller scales of ocean features. Weather forecast models use state-of-the-art supercomputers. It is only during the 1990s that supercomputers will become powerful enough to run ocean models for routine forecasts, and even then the models will continue to be limited by the computer power available.

5. Data assimilation

Data assimilation is the process of including ocean observations into the numerical model. This task is complicated by several factors, including: not enough observations to define the state of the ocean at any one time, observations have errors, observations may not be representative of the larger-scale ocean around them (e.g. through internal wave activity), the ocean model cannot resolve all scales of motion, and the physics included in the numerical model are not complete. Errors introduced by these factors grow during the forecast, and so frequent correction of the model is required to obtain realistic forecasts.

Ocean data could be used to analyse the state of the ocean without use of an ocean model. Fig. 3 demonstrates that analyses produced in this way would be lacking in detail.

Fig. 8 illustrates how observations are used in conjunction with a forecast model to produce estimates of the ocean state at a given time. Information available

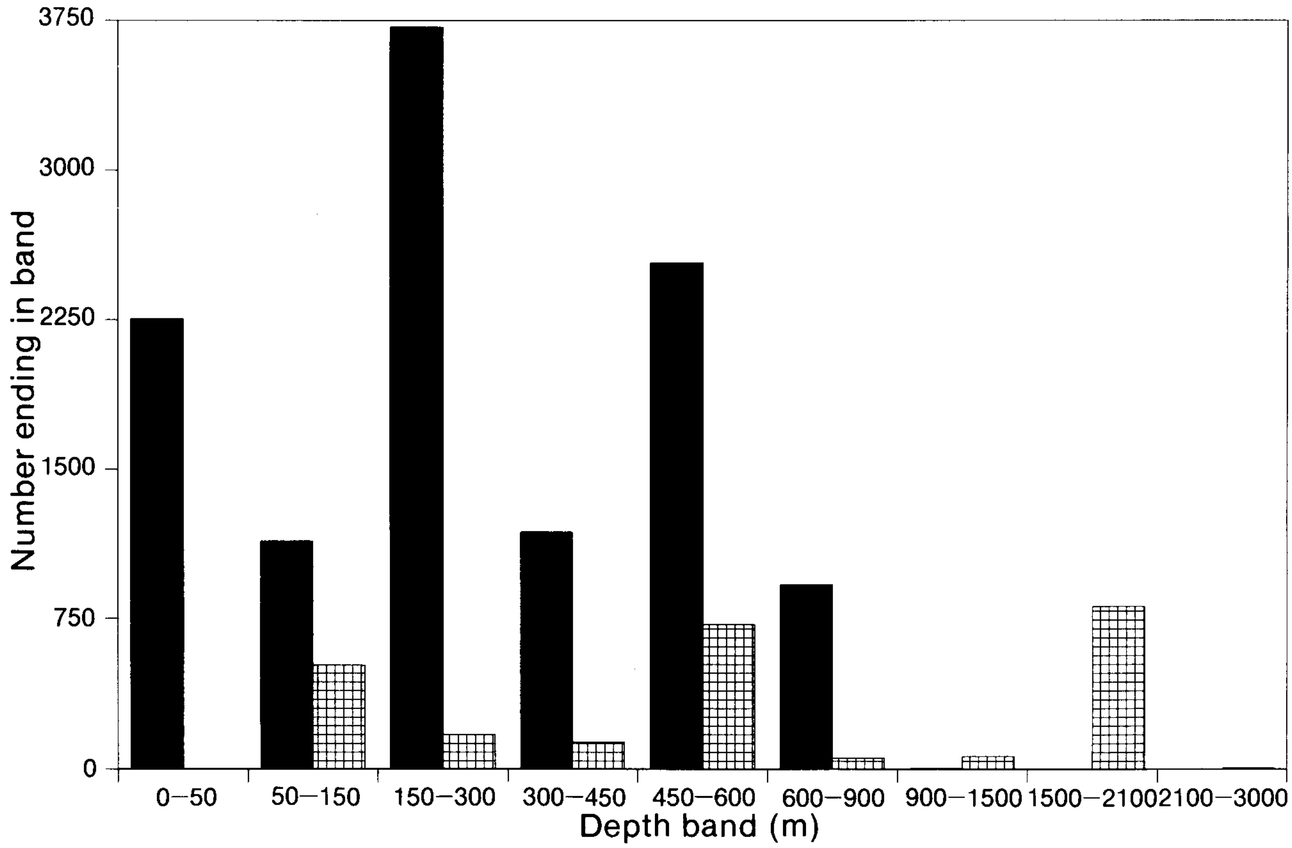

Figure 4. Distribution of maximum depths (in metres) reported in ocean observations for the Atlantic during 1988. BATHY reports indicated by the solid areas and TESAC reports by the shaded areas.

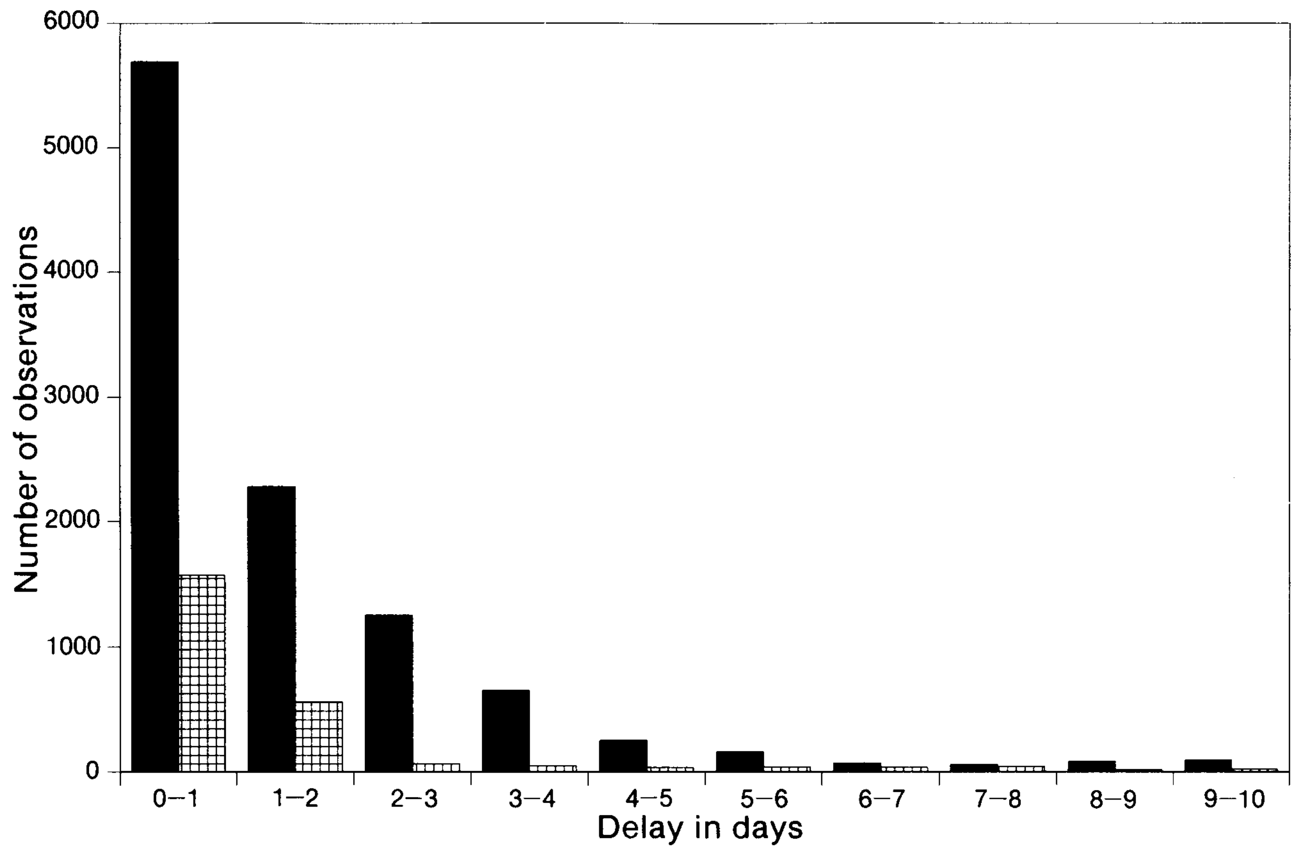

Figure 5. Distribution of the time delay between observations being made and receipt of the reports at Bracknell during 1988. BATHY reports indicated by the solid areas and TESAC reports by the shaded areas.

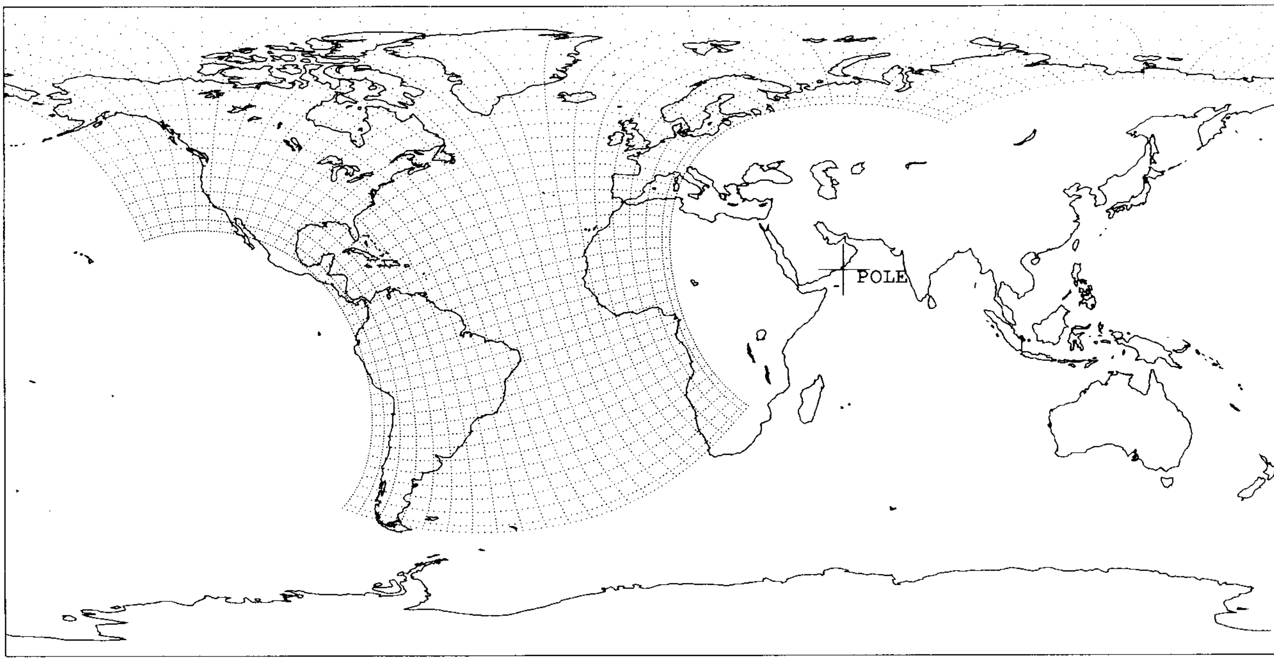

Figure 6. Area which FOAM is expected to cover. Dotted lines represent the mesh to be used by the model, every fourth line of a 1° mesh is shown.

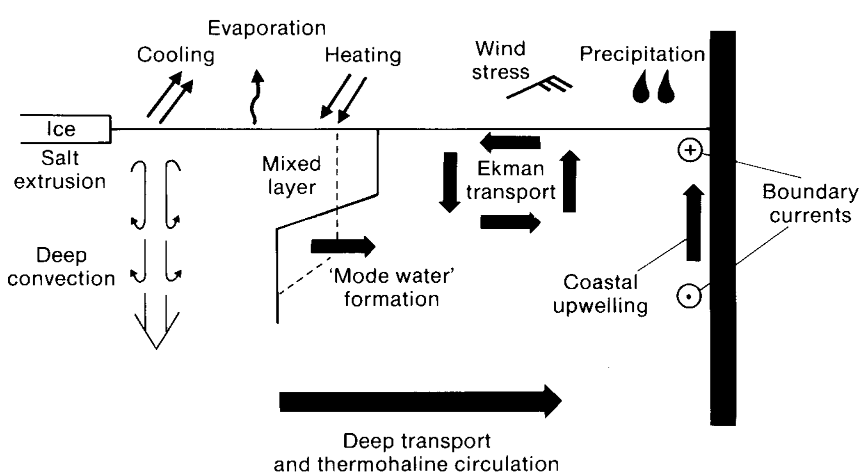

Figure 7. Schematic representation of the processes represented in ocean models.

to the assimilation system includes: observations, typical observation errors, forecasts of the ocean state, and expected errors of the forecasts. Therefore, if the actual state of the ocean is represented by the curve in Fig. 8(a), observations are made as shown in Fig. 8(b), and the model forecast is as shown in Fig. 8(c), the best estimate of the state of the ocean (Fig. 8(d)) does not fit the observations exactly, nor is the forecast field represented precisely. In this case the analysed field is close to the actual state. As time passes the ocean evolves and, because an ocean model forms part of the assimilation system, so does the model estimate of the ocean state. This is illustrated in Figs 8(e) and 8(g). Qualitatively the model and actual fields resemble each other, although errors in the model and the earlier analysis prevent an exact match. Fig. 8(f) shows the observations available at the later time. As will sometimes happen in reality, these add little to the model fields and, taken alone, would misrepresent the actual state of the ocean. The resulting analysis, Fig. 8(h), retains information from the forecast and represents the major development which has occurred. In data-sparse regions the model has the ability to interpolate dynamically in space and time between observations, capturing developments which are not observed directly.

In the FOAM system the assimilation sequence will be performed once each day using a technique similar to that described by Lorenc *et al.* (1991) for an atmosphere model. The assimilation process will consist of an integration of the forecast model with additional calculations performed between the usual forecast steps.

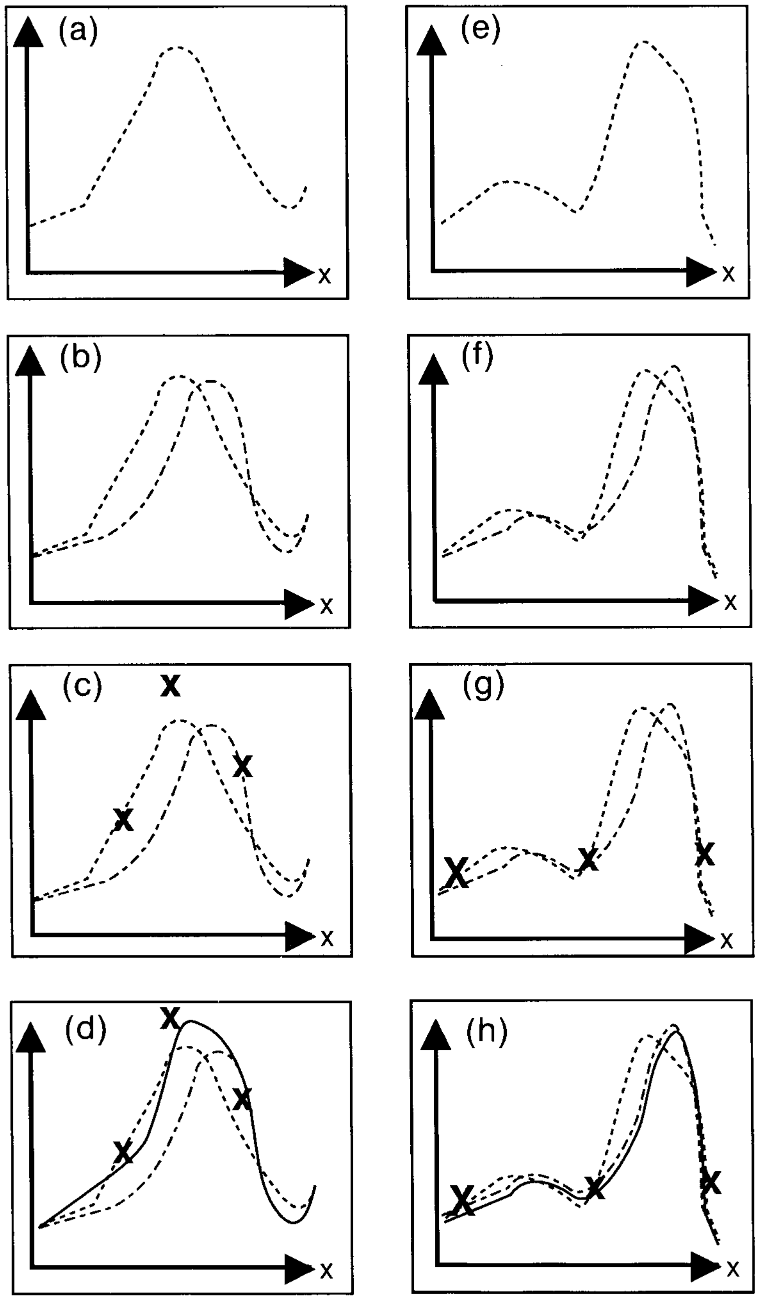

Figure 8. Schematic representation of data assimilation. At the initial time the real state of the ocean is at (a) and is shown dotted in the lower panels. The corresponding forecast is dash-dot (b). Observations are available (marked X) in panel (c). The resulting analysis is a compromise between the observations and forecast (d). At a later time the ocean evolves to the state in panel (e). The forecast (f) carries information not present in the observations (g), and results in a detailed analysis which qualitatively reflects the actual state (h).

These extra calculations will consist of determining the difference between observations and the model values corresponding to each point with observations, and corrections to the surrounding model grid-points to reduce the differences. This 'continuous insertion' of observations results in a smooth adjustment of the model fields towards the observed values. At each time-step the adjustment towards the observations is small, and the model physics have an opportunity to adjust the structure of the model fields to represent the observed values in a manner which the forecast model will be able to use. Without the repeated insertion of observations, an additional stage in the forecast cycle would be required (called 'initialization') in which the fields produced by the analysis would have to be modified to ensure that they were consistent with the needs of the ocean model. Continuous insertion removes the need for an initialization step, and attempts to ensure that the observed values are retained on the scales of motion which the model can represent.

FOAM will use many sources of observations. The order of development of the assimilation scheme reflects their usefulness and the complexity of their use. First to be included will be the BATHY and TESAC reports which are the only direct source of information on the vertical structure of the ocean. Next will be the ship measurements of sea surface temperature (SST). Satellite measurements of SST will be so numerous that additional techniques will need to be developed to handle them efficiently. After satellite SST data have been included, the more challenging altimeter data will be included. These data must be interpreted and the vertical structure of the ocean deduced from the surface information if the potential of these data is to be exploited. Once these major sources of data have been included other types will be used, such as current data.

Even with global satellite coverage of the ocean surface there will be regions of the ocean which are poorly observed. Most obvious of these is the deep ocean. To prevent systematic errors of the model causing unrealistic fields to develop in data-sparse regions, the FOAM will include a mechanism for adjusting the model fields towards climatology.

6. The role of the oceanographer

Numerical models of the atmosphere and ocean will form the basis of FOAM. Observations will be used to ensure that the model products are an adequate representation of the real world. Results will therefore only be as good as the observations available to the models.

Observations are subject to a number of errors. Some are a result of manual coding of the data, such as transposed digits in a temperature or position. Although such simple errors are easy for a human to identify and correct, it is difficult to automate this process. Thus an oceanographer examining observations which are regarded as suspect by the automated quality control might be able to confirm or correct the observation so that it may be used by the models.

Some observations will not be directly available to the automated system, such as the patterns which can be used to identify eddies in satellite imagery. As a result a second area in which human intervention will be necessary is in creating 'bogus' observations. These will arise from the experience of the oceanographer in interpreting observations and the model data, and will be used to influence the evolution of the model in the same way as real observations. Bogus data may consist of single point observations (analogous to TESAC reports), or may describe a larger-scale entity, such as an eddy. It is planned to introduce a database of typical eddies, fronts, and other 'features' into the FOAM system to allow forecasters to allow rapid and accurate interaction with the models. Feature models have been used successfully by Robinson *et al.* (1988). Some of the features in the database will be tools to allow the correction of broad-scale errors in the model fields (for example to allow an eddy to be removed from the model if one had been introduced in error in an earlier assimilation).

Manual intervention was essential in the southern hemisphere for NWP models before the widespread availability of global satellite observations of the three-dimensional state of the atmosphere in the early 1980s. It is still required for specific features such as tropical storms which are not represented fully by the NWP models. Ocean data are sparser than those for the atmosphere, and there is no prospect of three-dimensional information from satellites. Acoustic tomography, the only remote sensing technique which has the potential to yield three-dimensional fields on basin scales, is in its infancy (Cornvelle *et al.* 1989). Manual intervention will, therefore, be a central part of the ocean data assimilation process for many years.

7. Planned operational system

An overview of the proposed operational system is shown in Fig. 9. The ocean system mimics that used at present for the weather forecast models.

Data are received and placed in the main database. These are examined by an experienced oceanographer

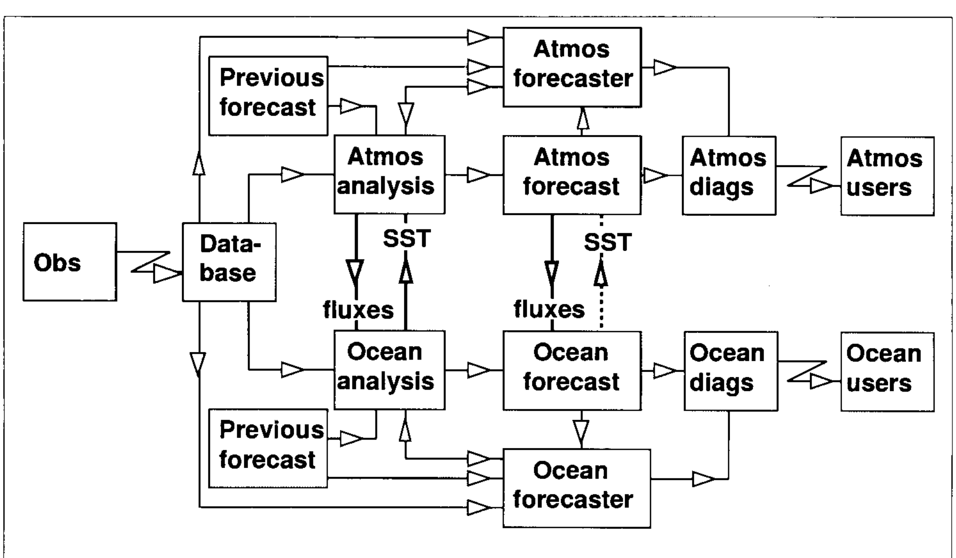

Figure 9. Schematic representation of the FOAM operational system.

who can perform quality control on the observations. Although some quality control will also be performed by the FOAM programs, human experience will be essential if the most value is to be extracted from the few observations available. Examples of errors which a human can rectify more easily than an automatic system include positional errors and transcription errors.

As for the atmosphere forecast models, the ocean forecaster will also be able to influence the model analyses by introducing fictitious 'bogus' observations. As an example of their use, consider a satellite image representing sea surface temperature. A forecaster may be able to identify the positions of several ocean eddies in this. Having identified the eddies, the forecaster can deduce much more information about the ocean structure than the automated system. By introducing additional observations to represent the sub-surface structure, the forecaster will be able to encourage the model to develop realistic representations of the eddies. Instead of introducing a large number of simulated profiles, it is intended that the forecaster will be able to select form a number of conceptual models ('feature models') which would both reduce the workload of the forecaster and improve the consistency of the bogus data. Similar techniques have recently been introduced into the weather forecast models to assist with the analysis of tropical disturbances.

Interactions between the atmosphere and ocean models will initially be loose. Surface fluxes will be calculated during the weather forecast and passed to the ocean model to provide its upper boundary condition. Until the FOAM system had demonstrated its accuracy there would be no feedback from the ocean model to the atmosphere. Once the ocean model had proved its reliability, it would be possible to use the ocean model analyses of sea surface temperature and sea ice as the surface conditions for the next integration of the atmosphere model. FOAM will be based on the Unified Model, and thus will have the mechanisms for coupling the ocean and atmosphere models built in allowing the benefits of coupling the forecasts to be assessed.

8. Summary

Ocean data are sparse and largely describe the surface layer. Information on the three-dimensional structure of the ocean is required on smaller length scales than the observations for any one time can describe. Numerical which the data can interpolate between the observations in both space and time. In performing the interpolation, models can develop features using the physical principles which govern ocean flow. Observations keep the model simulations close to reality, and the models interpolate between the observations.

Computer requirements of high resolution ocean models are so large that until the 1990s it was not feasible to introduce operational forecast models of the ocean. Computer speed will continue to be a limiting factor for model development. Simultaneously with increases in computer power, data from satellites and other sources are expected to increase. The two main restrictions on developing a viable operational ocean forecast system will thus ease simultaneously, making the development of FOAM feasible.

Increased use may be made of observations by using human experience to monitor quality-control decisions made by the automated system. This concentrates the effort where it is most needed, and allows transcription and other common errors to be corrected, enabling the models to use more data.

Some aspects of the observations will not be amenable to automated interpretation. An example is the identification of eddies in the SST fields derived from satellites. Having identified an eddy it may be possible to infer the sub-surface structure from its surface manifestation. Identification of such features is difficult to automate. A man–machine mix is required to produce the best products from FOAM.

References

Baker, D.J., 1991: Toward a global ocean observation system. *Oceanus*, **34**, 76–83.

Bryan, K. and Cox, M.D., 1972: The circulation of the world ocean: a numerical study. Part I, a homogeneous model. *J Phys Oceanogr*, **2**, 319–335.

Cornvelle, C., Munk, W. and Worcester, P., 1989: Acoustic tomography from ships. *J Geophys Res*, **84**, 6232–6250.

Foreman, S.J., 1990: The ocean as a component of the climate system. *In* M.E. Schlesinger (Ed): Climate–ocean interaction. Dordrecht, Kluwer.

Gill, A.E., 1982: Atmosphere–ocean dynamics. New York, Academic Press.

Lorenc, A.C., Bell, R.S. and Macpherson, B., 1991: The Meteorological Office analysis correction data assimilation scheme. *Q J R Meteorol Soc*, **117**, 59–89.

Meteorological Office, 1988: Meteorological Office Annual Report 1987. London, HMSO.

Robinson, A.R., Spall, M.A. and Pinardi, N., 1988: Gulf Stream simulations and the dynamics of ring and meander processes. *J Phys Oceanogr*, **18**, 1811–1853.

Wilson, C.A. *et al.*, 1990: First results from a unified forecast/climate model. *In* G.J. Boer (Ed), Research activities in atmospheric and oceanic modelling. Geneva, Working Group on Numerical Experiments, Report No. 14.

551.509 333:551.509.542:551.513.5(676.2)

Numerical forecast of the onset of the 1990 seasonal long rains in Kenya

V.O. Ahago
Kenya Meteorological Department, P.O. Box 30259, Nairobi, Kenya

Summary

Some model fields from the Global Model of the United Kingdom Meteorological Office (UKMO), and 24-hour rainfall data from various stations in Kenya were examined. This was in an attempt to verify whether the model products could have provided useful medium-range guidance in forecasting the onset of the 1990 seasonal long rains in Kenya. The results showed that the model did have some skill, and was capable of predicting the onset of the rains at least two to three days in advance.

1. Introduction

Kenya experiences a bimodal rainfall regime (Johnson 1962, Tomsett 1969, Potts 1971), with the first wet season occurring in the months March to May and the second in the period late October to early December (Kiangi and Anyamba 1987). These rains are commonly referred to as the 'long' and 'short' rains respectively (Mhita and Nassib 1987). The ability to provide accurate short- or medium-range forecasts of the onset of these seasonal rains would not only be important to the agricultural sector, but even more so to the tourism industry, commercial film industries and the general public at large. Studies in the past have shown that it is very difficult to predict the date of the onset of these rains (Thompson 1957, Alusa and Mushi 1974); equally difficult is the definition of an event to mark their beginning (Stern *et al.* 1982).

The case-study given here attempts to verify whether numerical weather prediction (NWP) products originating from the United Kingdom Meteorological Office (UKMO) could have provided useful medium-range guidance in forecasting the onset of the 1990 long rains in Kenya. The region under study, i.e. Kenya, is roughly enclosed by latitudes 4° N and 4° S and longitudes 34° E and 42° E.

It has been assumed that the onset of the 1990 long rains in Kenya occurred on the first day the country experienced widespread rains at the end of the dry season. These rains then continued interspersed with short, dry spells. It has also been assumed that the 'grass' rains that occasionally precede the long rains as noted by Alusa and Mushi (1974) were part of the proper Long Rains. An inspection of the 24-hour rainfall data from various rainfall stations in Kenya (Table I), identified 20 February 1990 as the date of the onset. No attempt has been made in this paper to explain this early onset, and, although generally occurring in early March, there have been other years in the past which had early onsets.

2. Data

The 24-hour rainfall data for various rainfall stations in Kenya were supplied by the Kenya Meteorological Department (KMD). The model products were retrieved from the archive of fields from the operational global forecast model of the UKMO in Bracknell. The version of the model then in use had a grid-point formulation based on the hydrostatic primitive equations with a horizontal grid of 1.875° longitude by 1.5° latitude and 15 levels in the vertical (Bell and Dickinson 1987).

The fields examined were mean-sea-level pressure (MSLP), accumulation of rainfall during the 6 hours preceding the forecast time, and winds at the standard levels 850 mb and 250 mb. Model analyses and forecast periods of 24, 48 and 72 hours were looked at. Observational data of 24-hour rainfall totals provided by the KMD are given in Table I. Due to the difference in the accumulation period for the forecast and observed rainfall and also the fact that data for the former were evenly distributed whilst those for the latter were not, comparisons were made only on the basis of their relative values.

3. Analysis of charts and discussion

3.1 Forecast from data time 12 UTC on 15 February 1990

An increase in the west to east gradient of surface pressure over central Africa is observed during the forecast and is illustrated in Fig. 1; Fig. 1(a) contains the analysis of MSLP and Fig. 1(b) the 72-hour forecast. Consideration of the 1012 mb isobar over the Gulf of Guinea and the 1008 mb isobar in the east shows a general increase in the gradient just to the west of Kenya. A development of this nature tends to induce a more westerly flow of winds in the lower troposphere of the region (Riehl 1954). Thompson (1957) and Kiangi and Anyamba (1987) observed that, at times, rainfall in

Table 1. 24-hour rainfall totals (mm) from Kenyan meteorological stations for the 15-day period 12–26 February 1990

Station		Date 12	13	14	15	16	17	18	19	20	21	22	23	24	25	26
Northern areas																
Lodwar	(03° 07′N, 35° 37′E)	—	—	—	—	0.1	—	—	0.4	Tr	Tr	11.3	Tr	3.5	0.3	5.4
Marsabit	(02° 18′N, 37° 54′E)	Tr	Tr	—	Tr	Tr	—	Tr	—	5.8	16.0	64.2	—	—	2.0	4.9
Moyale	(03° 32′N, 39° 03′E)	—	—	—	7.1	Tr	—	Tr	16.1	23.0	Tr	4.0	Tr	4.3	3.2	3.0
Garissa	(00° 28′S, 39° 38′E)	—	—	—	—	—	—	—	—	1.1	—	—	—	—	Tr	0.3
Wajir	(01° 45′N, 40° 04′E)	—	—	—	—	—	—	—	—	2.8	—	—	—	16.0	—	2.1
Mandera	(03° 56′N, 41° 52′E)	—	—	Tr	—	—	—	—	—	—	—	—	—	—	—	—
Western areas																
Kitale	(01° 01′N, 35° 00′E)	—	—	—	Tr	—	—	22.6	1.2	2.3	34.4	5.2	2.2	3.4	0.6	—
Kakamega	(00° 17′N, 34° 47′E)	0.4	—	Tr	—	—	24.4	6.8	1.4	18.8	55.3	4.7	1.5	26.6	3.7	0.1
Eldoret	(00° 32′N, 35° 17′E)	—	—	—	—	—	—	—	2.2	10.9	23.4	4.0	49.2	35.5	8.5	1.1
Kericho	(00° 22′S, 35° 21′E)	3.3	—	—	5.8	—	19.0	—	13.6	25.0	33.5	1.5	25.4	41.9	8.3	3.2
Kisii	(00° 40′S, 34° 47′E)	9.1	0.8	0.3	0.6	8.8	58.0	2.9	5.6	2.0	29.0	0.6	1.1	16.1	16.1	7.5
Lake Basin																
Kisumu	(00° 06′S, 34° 45′E)	—	—	—	—	—	21.0	—	1.2	0.5	87.3	0.4	9.9	9.2	1.8	Tr
Rift Valley																
Nakuru	(00° 16′S, 36° 06′E)	—	—	—	—	—	—	0.1	1.1	0.5	20.6	18.7	2.1	8.1	15.3	1.8
Narok	(01° 08′S, 35° 50′E)	—	—	—	2.8	Tr	3.5	—	32.1	Tr	23.0	Tr	0.6	2.8	7.7	30.0
Highlands east of Rift Valley																
Nyeri	(00° 30′S, 36° 58′E)	1.0	—	0.8	Tr	1.4	2.8	Tr	1.6	0.4	30.0	3.3	6.0	0.6	0.1	0.2
Dagoretti	(01° 18′S, 36° 45′E)	—	Tr	—	—	—	—	—	11.8	0.8	8.4	—	0.7	—	—	5.9
Wilson	(01° 19′S, 36° 49′E)	—	—	—	—	—	—	—	8.3	0.3	0.5	—	9.4	—	—	10.3
J.K. Airport	(01° 19′S, 36° 55′E)	—	Tr	—	—	—	—	—	29.4	Tr	0.1	—	6.6	—	—	4.6
Embu	(00° 30′S, 37° 27′E)	—	—	—	—	—	—	—	0.3	0.5	—	5.6	Tr	—	—	—
Meru	(00° 05′N, 37° 39′E)	—	—	0.4	22.2	11.4	—	—	—	0.8	14.1	13.9	Tr	Tr	37.1	4.6
South-eastern districts																
Makindu	(02° 17′S, 37° 50′E)	—	—	—	—	—	—	—	5.6	Tr	0.7	11.8	13.7	—	—	1.4
Voi	(03° 24′S, 38° 34′E)	0.6	—	—	—	—	—	—	1.3	—	—	—	—	—	3.2	0.8
Coast																
Lamu	(02° 16′S, 40° 50′E)	Tr	—	—	—	—	—	—	—	—	—	—	—	—	—	—
Malindi	(03° 14′S, 40° 06′E)	—	—	—	—	—	—	—	—	Tr	—	—	—	—	—	—
Msabaha	(03° 16′S, 40° 03′E)	—	—	—	—	—	—	—	—	Tr	Tr	—	—	—	—	—

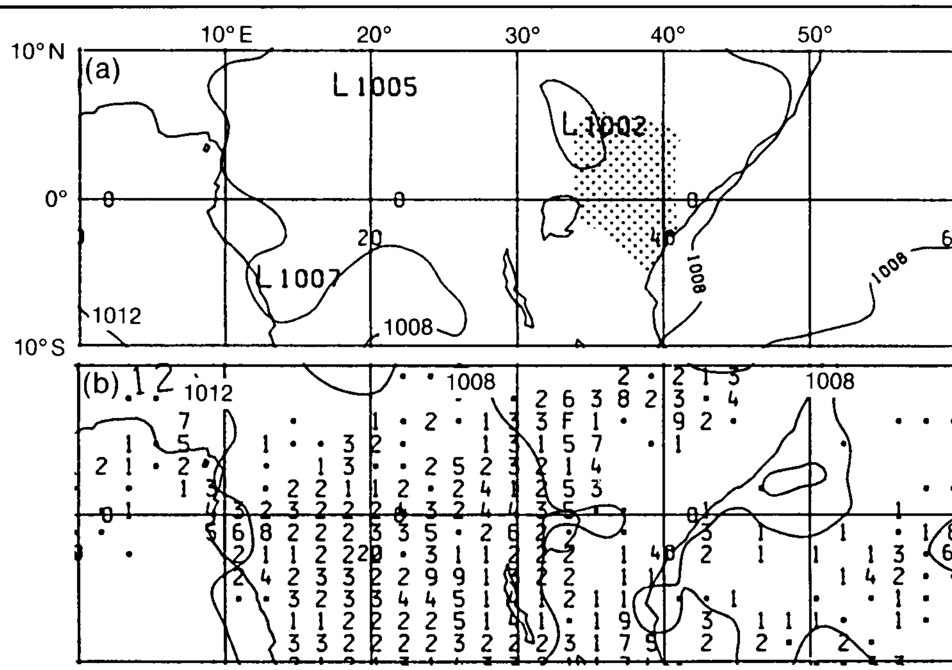

Figure 1. (a) Mean-sea-level pressure (mb) at 12 UTC on 15 February 1990, and (b) 72-hour forecast of 6-hour rainfall accumulation and mean-sea-level pressure valid for 12 UTC on 18 February 1990 (values are in whole millimetres (1–9) or shown as dots (0.1–0.5 mm), A (10 mm), B (11 mm), C (12 mm), etc. Kenya is shown by the shaded area.

Kenya is associated with incursions of unstable westerlies or Congo air, a near stagnant air of high humidity.

Despite this increase in west to east pressure gradient, little or no precipitation is forecast over most of Kenya during the forecast as illustrated by the 6-hourly totals in Fig. 1(b). At 850 mb a largely diffluent flow pattern is dominant over Kenya in both the analysis and forecast, the 72-hour forecast being shown as an example in Fig. 2. A flow pattern of this nature tends to inhibit convective developments (Riehl 1954, Kiangi and Anyamba 1987). At 250 mb there is a generally east or south-easterly flow with little or no diffluence over Kenya. This is apparent throughout the forecast with the 72-hour forecast chart shown in Fig. 3.

3.2 Forecast from data time 12 UTC 17 February 1990

This forecast covers the period of the onset of the rains and a sequence of forecast charts at 24-hour intervals for MSLP and rainfall is given in Fig. 4. An increase in the west to east gradient of pressure is again apparent over central Africa during the forecast, but the 72-hour forecast chart in Fig. 4(d) now shows widespread rain to be predicted over Kenya by this time. This follows 24- and 48-hour forecasts of relatively dry conditions (see Figs 4(b) and 4(c)), and contrasts with the previous forecast described in section 3.1 from a data time two days earlier. The predicted onset of the rains is in good agreement with the date inferred from the observational data in Table I. At 850 mb a line of convergence in the wind field can be identified immediately to the east of Lake Victoria in the analysis (Fig. 5(a)), and moves steadily eastward during the forecast with its position after 72 hours shown in Fig. 5(b). Such a line of convergence would tend to increase the low-level moisture content of the atmosphere, and its forecast movement would imply a surge of westerly or Congo air into Kenya.

During intense surges of westerly air in the lower levels, the effects, which include an increase in precipitation, may be felt as far east as Nairobi (1° 18′S, 36° 45′E). The forecast rainfall charts in Fig. 4 seem to agree with this observation. No marked confluence or diffluence can be observed over Kenya at 250 mb either in the analysis or during the forecast, the 72-hour forecast being given as an example in Fig. 6. Kiangi and Anyamba (1987) have pointed out that upper-level outflow of air from the East African region towards mid-latitude troughs tends to be associated with confluent flow in the low levels.

3.3 Forecast from data time 12 UTC on 21 February 1990

This forecast covers a period after the long rains had started and the sequence of forecast charts for rainfall and MSLP in Fig. 7 shows widespread rain across the country. This sequence also shows the same trend of the two earlier forecasts in increasing the west to east gradient of MSLP.

At 850 mb a convergence line is again in evidence immediately to the east of Lake Victoria in the analysis (Fig. 8(a)), and is predicted to move steadily east during the forecast reaching the extreme east of Kenya after

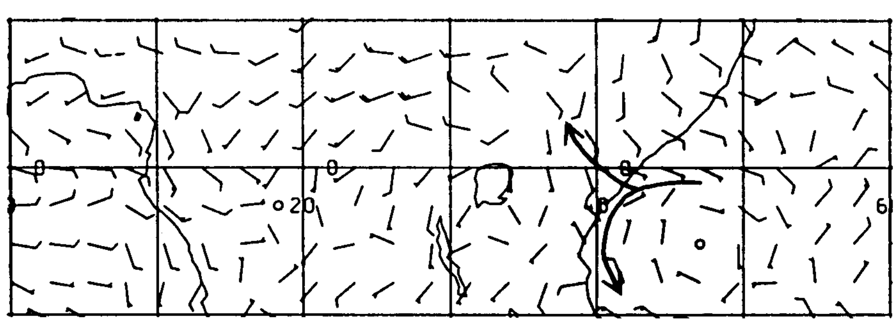

Figure 2. 72-hour forecast of the 850 mb winds valid for 12 UTC on 18 February 1990 with streamlines added over Kenya.

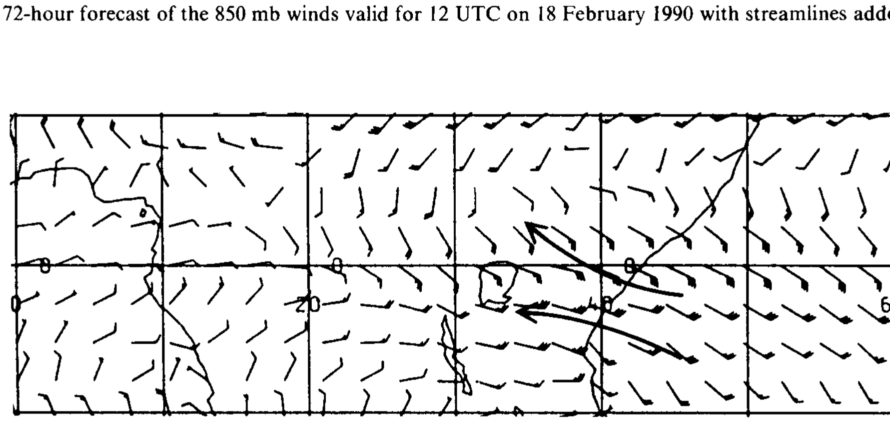

Figure 3. 72-hour forecast of the 250 mb winds valid for 12 UTC on 18 February 1990 with streamlines added over Kenya.

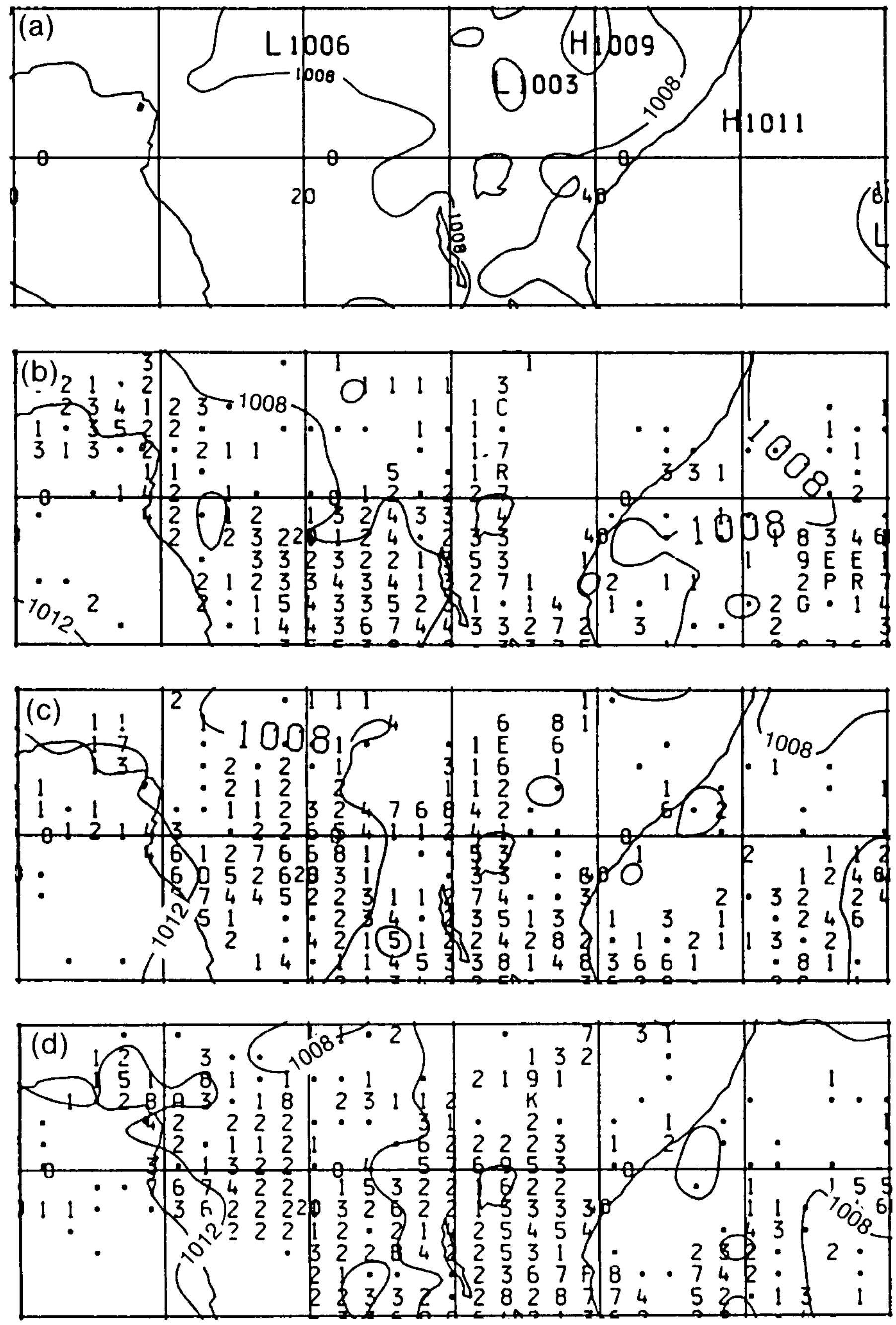

Figure 4. (a) Mean-sea-level pressure (mb) at 12 UTC on 17 February 1990. Six-hour rainfall accumulation and mean-sea-level pressure, (b) 24-hour forecast valid for 12 UTC on 18 February 1990, (c) 48-hour forecast valid for 12 UTC on 19 February 1990, and (d) 72-hour forecast valid for 12 UTC on 20 February 1990. For key to rainfall amounts see Fig. 1.

72 hours (Fig. 8(b)). By this time the forecast low-level winds over most of the country have a strong westerly component. A south-easterly flow is again the dominant feature at 250 mb over Kenya in both the analysis (Fig. 9(a)) and the forecast. The predicted field after 72 hours is shown in Fig. 9(b). A structure of this nature with no marked diffluence in the upper troposphere would not normally be expected to contribute much by way of enhancement or suppression of convective developments over the affected area. Of some interest is the trend for an increase in wind strength over Kenya during the forecast; this was also evident in the two previous examples but to a lesser degree.

4. Summary and conclusions

The principal results from the forecast runs described in section 3 may be summarized as follows:

(a) The onset and spread of rain over Kenya, as indicated by the forecast rainfall charts, are in broad

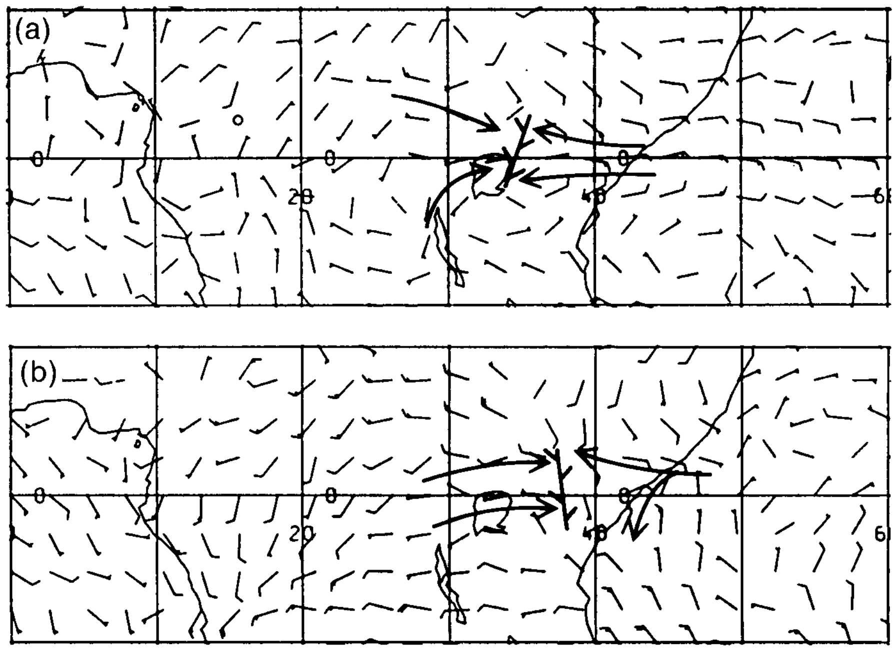

Figure 5. Winds at 850 mb, (a) analysis valid for 12 UTC on 17 February 1990, and (b) 72-hour forecast valid for 12 UTC on 20 February 1990, with streamlines added over Kenya.

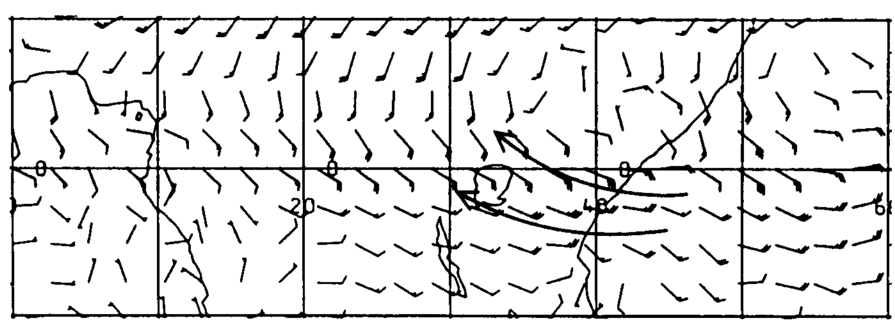

Figure 6. 72-hour forecast of 250 mb winds valid for 12 UTC on 20 February 1990, with streamlines added over Kenya.

agreement with observations.

(b) The forecast charts of MSLP would not have been very helpful in giving the necessary guidance. The otherwise conducive trend to build a west to east pressure gradient during the forecast, occurs in all three examples. It should also be noted that the sequence provided by the analyses in Figs l(a), 4(a) and 7(a) do not show this trend to any marked degree, though this would have been expected.

(c) The 850 mb structure of winds suggests the formation of a line of convergence which shifts eastwards in agreement with the eastward spread of the observed rainfall. This movement of the convergence line, which is first noticed at the start of the widespread rains, is however repeated in the forecast run after the onset. A comparison of Fig. 8(b) with the verifying analysis for this time in Fig. 10 reveals that this pronounced eastward progression is in fact, erroneous.

(d) The 250 mb charts generally show a weakly diffluent pattern, as would be expected at the beginning of the rainy season.

The errors observed on the forecast charts for MSLP and 850 mb winds could possibly be due to lack of adequate additional data in the area under study. In this case, the analyses would closely resemble the background field and the forecasts would often resemble those from the previous run of the model (WMO 1991).

The rains observed over the western and central parts of Kenya before the onset, and not depicted on the forecast charts, could perhaps illustrate deficiencies in both the convective parametrization scheme of the model and the representation of orography. Convective parametrization schemes can have difficulty in handling situations where showers develop in a scattered fashion, and precipitation amounts are generally underforecast in such cases (WMO 1991). Also, poor representation of

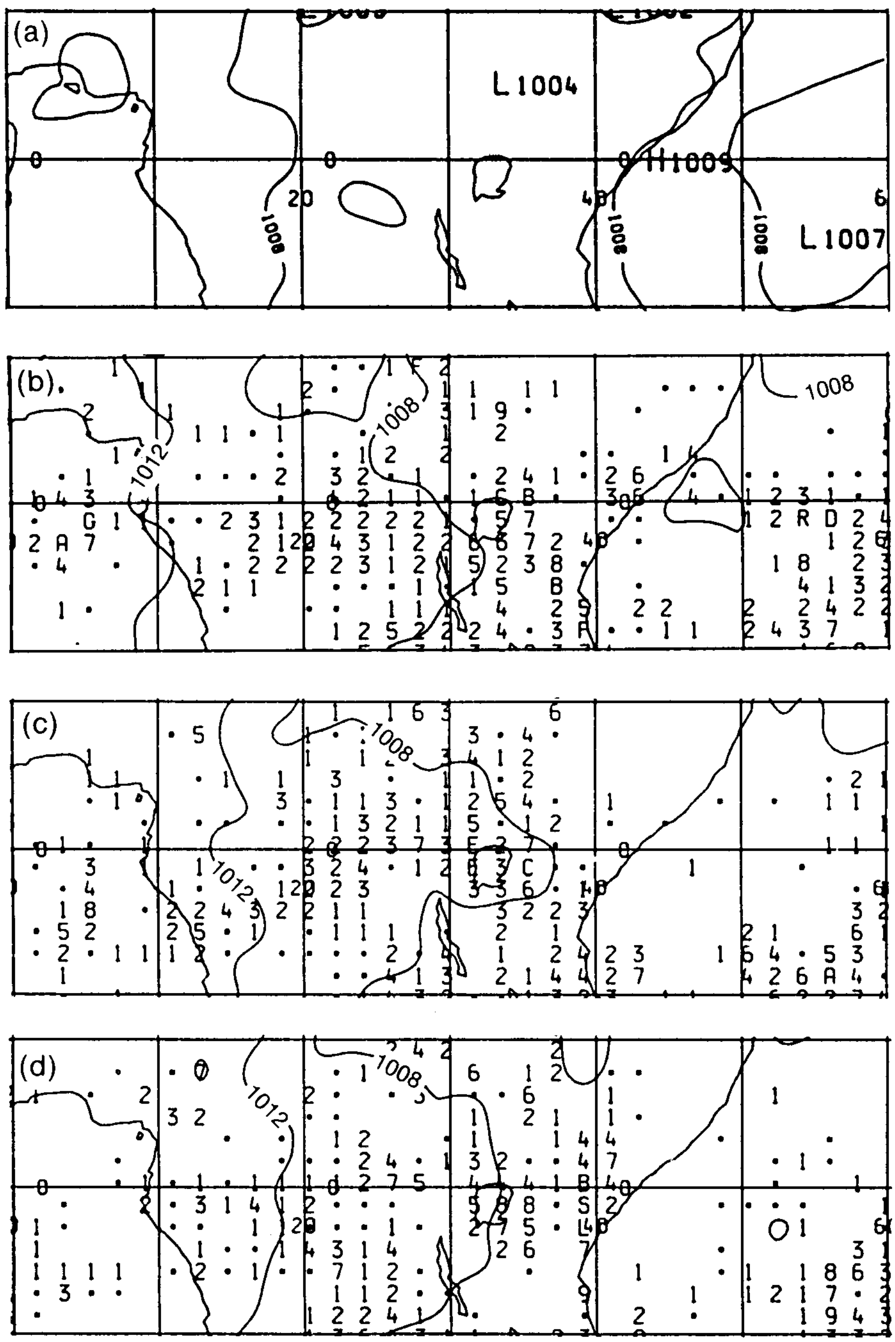

Figure 7. (a) Mean-sea-level pressure (mb) at 12 UTC on 21 February 1990. Six-hour rainfall accumulation and mean-sea-level pressure, (b) 24-hour forecast valid for 12 UTC on 22 February 1990, (c) 48-hour forecast valid for 12 UTC on 23 February 1990, and (d) 72-hour forecast valid for 12 UTC on 24 February 1990. For key to rainfall amounts see Fig. 1.

orography often results in underforecasting precipitation which would otherwise have been enhanced by it (WMO 1991). This study has shown that the model did have some skill and was capable of predicting the onset of the 1990 seasonal long rains in Kenya, at least two to three days earlier. Care has to be taken however, in view of the systematic errors identified in the forecast of MSLP and the movement of the convergence line in the 850 mb wind forecast.

Acknowledgements

This study was made as part of the author's on-the-job training in the interpretation of numerical weather prediction products at the Meteorological Office in Bracknell. Acknowledgements are made to Dr. W.H. Lyne and all the staff in the Central Forecasting Office for their assistance, and thanks are due to the British Government for awarding the VCP fellowship enabling the training programme to be undertaken.

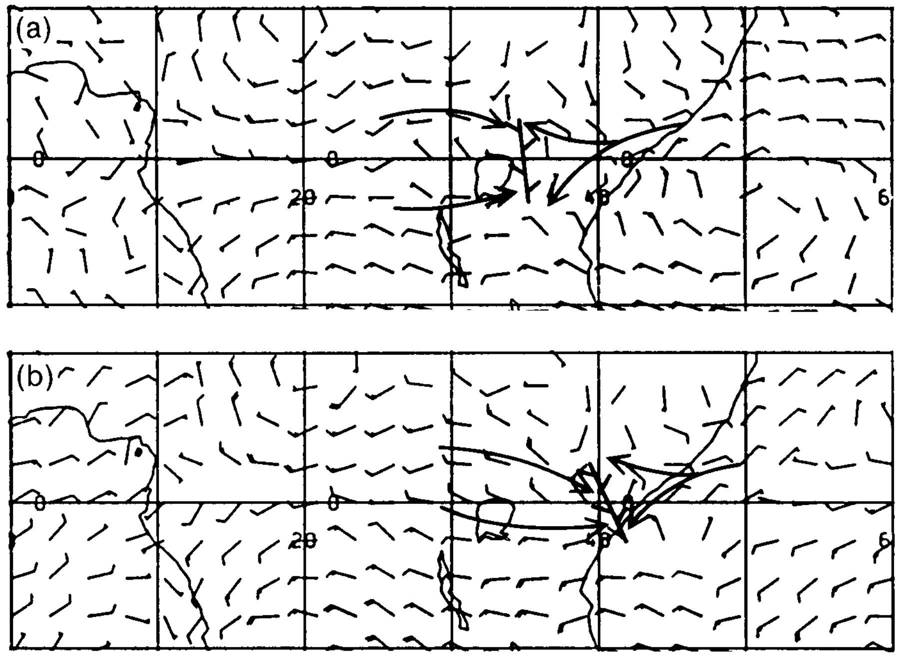

Figure 8. Winds at 850 mb, (a) analysis for 12 UTC on 21 February 1990, and (b) 72-hour forecast valid for 12 UTC on 24 February 1990, with streamlines added over Kenya.

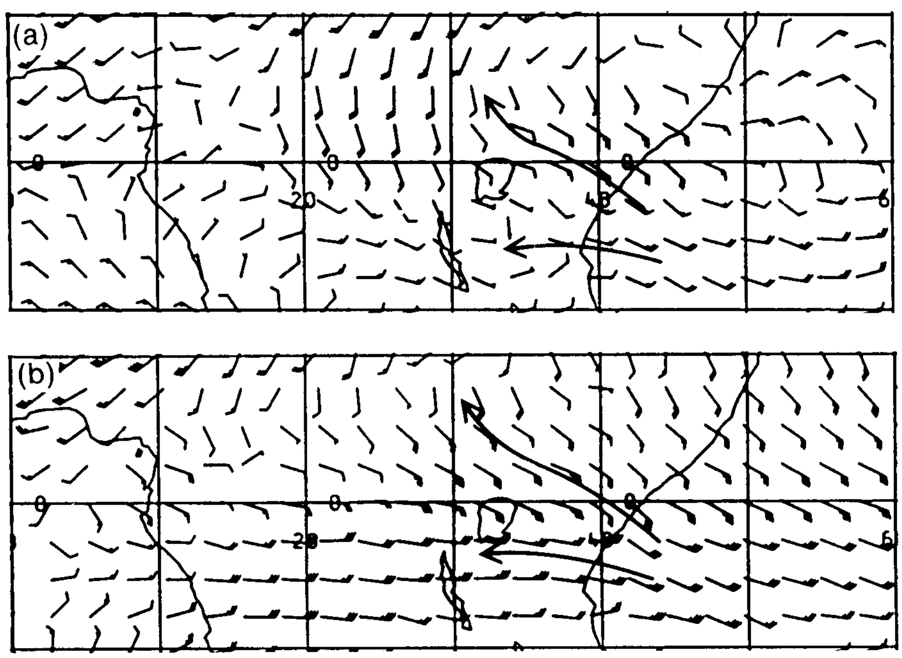

Figure 9. Winds at 250 mb, (a) analysis for 12 UTC on 21 February 1990, and (b) 72-hour forecast valid for 12 UTC on 24 February 1990, with streamlines added over Kenya.

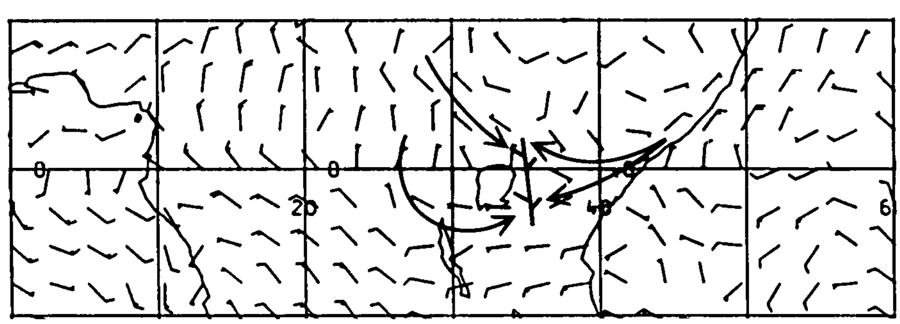

Figure 10. Analysis of 850 mb winds for 12 UTC on 24 February 1990, with streamlines added over Kenya.

References

Alusa, A.L. and Mushi, M.; 1974: A study of the onset, duration and cessation of the rains in East Africa. International Tropical Meteorology Meeting, Nairobi, 31 January to 7 February 1974. Boston, American Meteorological Society.

Bell, R.S. and Dickinson, A., 1987: The Meteorological Office operational numerical weather prediction system. *Sci Pap, Meteorol Off,* No. 41.

Johnson, D.H., 1962: Rain in East Africa. *Q J R Meteorol Soc*, **88**, 1–19.

Kiangi, P.M.R. and Anyamba, E.K., 1987: Some monsoons of East Africa — why the low rainfall productivity? *In* First Technical Conference on meteorological research in eastern and southern Africa, Nairobi, 6–9 January 1987. Nairobi, Kenya Meteorological Department.

Mhita, M.S. and Nassib, I.R., 1987: The onset and end of rains in Tanzania. *In* First Technical Conference on meteorological research in eastern and southern Africa, Nairobi 6–9 January 1987. Nairobi, Kenya Meteorological Department.

Potts, A.S., 1971: Application of harmonic analysis to the study of East African rainfall data. *J Trop Geogr*, **33**, 31–42.

Riehl, H., 1954: Tropical meteorology. New York, McGraw-Hill.

Stern, R.D., Dennett, M.D. and Dale, I.C., 1982: Analysing daily rainfall measurements to give agronomically useful results. I. Direct methods. *Exp Agric*, **18**, 223–236.

Thompson, B.W., 1957: Some reflections on equatorial and tropical forecasting. Nairobi, East African Meteorological Department, Technical Note No. 7.

Tomsett, J.E., 1969: Average monthly and annual rainfall maps of East Africa. Nairobi, Kenya Meteorological Department.

WMO, 1991: Methods of interpreting weather prediction output for aeronautical meteorology. Geneva, WMO.

551.506(41-4)

The spring of 1991 in the United Kingdom

G.P. Northcott
Meteorological Office, Bracknell

Summary

The spring of 1991 was generally rather warm, wet in the north and west but dry in eastern areas, especially in north-east England, and rather dull in practically all parts of the United Kingdom.

1. The spring as a whole

Mean temperatures over the spring months were above average in most areas, ranging from 1.3 °C above average in North Wales and Dorset to 0.2 °C below average at Girvan, Strathclyde Region. Seasonal rainfall amounts were above average in western parts, but below average in central and eastern areas, ranging from 143% of average at Bargrennan, Dumfries & Galloway to 53% at Cromer, Norfolk. Sunshine amounts over the season were below average nearly everywhere; several places in Scotland having just above average, including a figure of 102% in the Glasgow area. In contrast Harrogate, North Yorkshire had a very dull 58% of average and nearby Bradford, West Yorkshire had 63% of average.

Information about the temperature, rainfall and sunshine during the period from March to May 1991 is given in Fig. 1 and Table I.

2. The individual months

March. March was a warm month especially over central and eastern England, although not generally as warm as March 1990. Mean monthly temperatures were above normal over the whole United Kingdom and ranged from 0.9 °C above normal at St Mary's, Isles of Scilly to 3.1 °C above normal at Cromer, Norfolk. Monthly rainfall totals were above normal nearly everywhere, the exceptions being parts of central and eastern England and the northernmost part of the Western Isles where rainfall was below normal, and ranged from 178% at Tynemouth, Tyne & Wear to as little as 40% at Manston, Kent. Monthly sunshine amounts were below average nearly everywhere apart from a few places in East Anglia and along the south coast, where values were average or just above, ranging from 104% of average at Falmouth, Cornwall to as little as 39% of average at Bradford, West Yorkshire.

The first three weeks were wet, although rainfall amounts were greater in the west than in the east; some parts of the east and south-east were unusually dry for March. North-eastern coastal areas had cold and foggy weather between the 6th and 9th. A tornado hit part of south-west Wales early on the 3rd, causing considerable structural damage and uprooting trees. On the 7th deposits of dust or sand in rainfall were reported at a number of places in the west Midlands, including Malvern, Bromsgrove and Solihull. On the 11th deposits of red dust were reported in rain at Northwood, Greater London and Cavendish, Suffolk. An area of thundery activity extended from Lincolnshire to East Sussex on the 16th. Thunder was reported in Surrey and Berkshire on 21st, the Thames Valley, the Cotswolds and Cornwall on the 22nd and on 23rd there was an isolated thunderstorm in the Thames Valley. During the early hours of the 26th brown rain was reported at Towy Castle, Dyfed and Slimbridge, Gloucestershire.

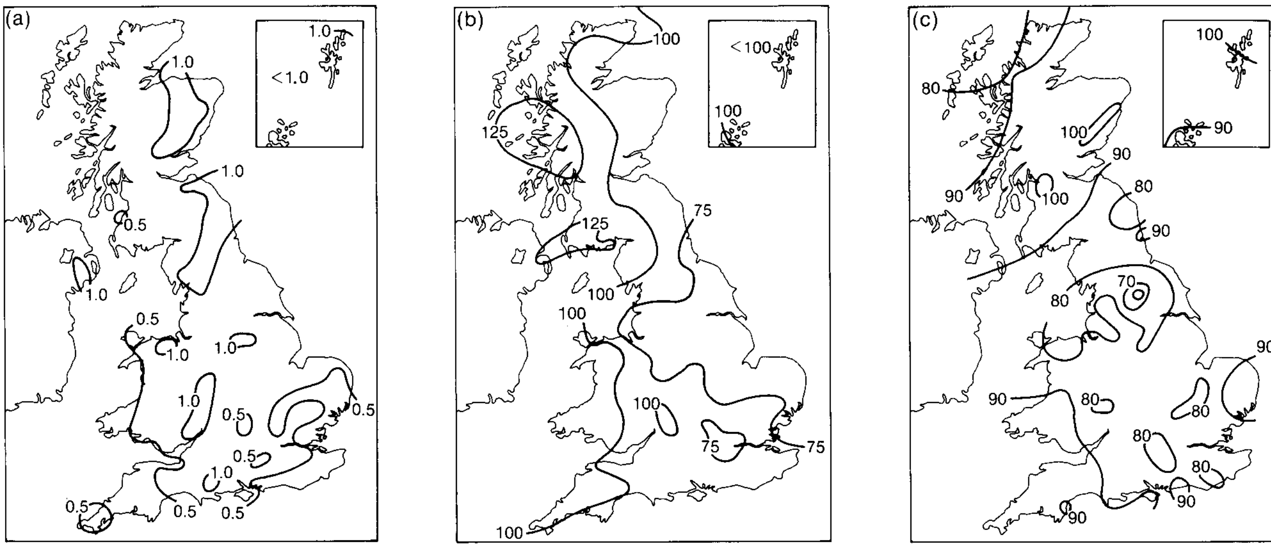

Figure 1. Values of (a) mean temperature difference (°C), (b) rainfall percentage and (c) sunshine percentage for summer, 1991 (March–May) relative to 1951–80 averages.

Table I. District values for the period March–May 1991, relative to 1951–80 averages

District	Mean temperature (°C)	Rain-days	Rainfall	Sunshine
	Difference from average		Percentage of average	
Northern Scotland	+0.8	+1	101	89
Eastern Scotland	+0.9	−2	95	91
Eastern and north-east England	+0.8	−2	75	81
East Anglia	+0.5	−2	72	90
Midland counties	+0.8	−3	80	81
South-east and central southern England	+0.4	−2	86	88
Western Scotland	+0.7	−1	120	92
North-west England and North Wales	+0.7	−2	96	80
South-west England and South Wales	+0.6	−1	101	93
Northern Ireland	+0.8	−1	114	91
Scotland	+0.8	−1	109	91
England and Wales	+0.7	−2	88	85

Highest maximum: 25.0 °C in Midland counties in May.
Lowest minimum: −8.0 °C in western Scotland in March.

April. Mean monthly temperatures were generally near to the monthly normal and ranged from 0.6 °C below normal at Sandown, Isle of Wight to 1.2 °C above normal at Kinloss, Grampian Region. Monthly rainfall totals were above normal everywhere except over eastern Scotland and much of northern England, and ranged from more than twice the normal in parts of western Cornwall and western Scotland to less than half the normal in north-east England and around the Moray Firth. Heavy rain gave falls of 72 mm at Inverinan, Highland Region on the 1st and 81 mm at Isle of Rhum, Highland Region on the 10th, the latter having its wettest April day since records began there in 1958. Heavy rain during the 29th and 30th doubled the month's totals in parts of south-east England, with some places having their wettest April day this century on the 29th, the wettest day over England and Wales as a whole since the very wet Bank Holiday, 25 August 1986. Monthly sunshine amounts were generally above average in eastern areas but below average in western areas, ranging from 129% of average at Edinburgh, East Craigs, Lothian Region to a rather dull 73% of average at Stornoway, Western Isles. Stornoway recorded its dullest April since 1975, whereas Lerwick with 122% of its normal April amount had its sunniest April since 1970.

The weather was unsettled at the beginning of the month with rain or showers during the first week, and some sunny intervals. Rain was often prolonged and heavy over western areas. The second half of the month brought a wintry mixture of hail, sleet and snow showers, with longer periods of rain and a few sunny intervals. On the 12th thundery outbreaks occurred over parts of central and south-eastern England. On the 18th and 19th England and Wales had heavy and prolonged wintry showers, sometimes with thunder, although Wales and south-west England had some good sunny spells. Thunder occurred over Essex on the 21st. There were scattered hail showers on the 22nd and 23rd. Rain in the west on the 25th gave way to thundery showers, while in the north and east it remained dry. Further thundery outbreaks occurred over Wales, the Midlands and Cornwall on the 26th.

May. Mean monthly temperatures were generally about average, ranging from 1.5 °C above normal in parts of Tayside Region to 1.6 °C below normal at Greenwich, Greater London and Wye, Kent. Monthly rainfall totals were well below normal everywhere except for the northernmost part of the Scottish mainland where totals were just above normal. The percentage of normal at Cape Wrath, Highland Region, 124%, contrasts with that in parts of western Scotland and much of south-west England and South Wales where amounts were generally less than 10% of normal. It was the driest May over England and Wales since 1896, and Glasgow had its driest May since 1868. Monthly sunshine amounts were below average nearly everywhere, the exceptions being parts of western Scotland, Devon and Cornwall where sunshine amounts were just above average; amounts ranged from 111% of average at Machrihanish, Strathclyde Region to 60% of average at Manchester. Many eastern and northern areas had one of the dullest Mays this century.

During the first week troughs gave some rain in the north. A brief spell of fine weather during the second week gave some sharp overnight frosts. On the 7th there were some locally heavy thundery showers over parts of southern England and South Wales. After the 10th the predominance of milder westerly winds prevented night frosts in all but a few locations and it was warm during the period, with some rain, mainly in the north-west. During the second half of the month the weather was mainly anticyclonic, although often cloudy, but became sunny and very warm for a time around the 21st, before becoming cold again towards the end of the month.

Books received

The listing of books under this heading does not preclude a review in the Meteorological Magazine at a later date.

Atmospheric transmission, emission and scattering, by T.G. Kyle (Oxford, New York, Seoul, Tokyo, Pergamon Press, 1991. £40.00, $40.00) introduces the physical processes needed to understand the behaviour of radiation in the atmosphere. Various wavelength regions are considered and, while software for solving problems is discussed, an effort has been made to avoid extensive mathematics. ISBN 0 08 040287 9.

Future climatic change and radioactive waste disposal, edited by C.M. Goodess and J.P. Palutikof (Norwich, Climatic Research Unit, University of East Anglia, 1991. Postage and packing only) contains the papers presented at an International Workshop on 1–3 November 1989. The urgency of the radioactive waste problem with its associated long time-scales prompted the organization of the meeting.

Perspectives of nonlinear dynamics, Vols 1 and 2, by E.A. Jackson (Cambridge University Press, 1992. £19.95, $32.95 each) develop the perspectives generated by analytical, topological and computational methods in a variety of contexts. They are aimed at a broad readership across a range of disciplines, with a style intended to stimulate the reader's imagination. ISBNs 0 521 42632 4 and 0 521 42633 2.

A *New Scientist* guide to chaos, edited by N. Hall (London, Penguin Books Ltd, 1992. £9.99) contains a collection of essays explaining the roots of this multidisciplinary phenomenon. Computers' abilities to display and explore the area are demonstrated. ISBN 0 14 014571 0.

Meteorological fluid dynamics: Asymptotic modelling, stability and chaotic atmospheric modelling, by R.K. Zeytounian (Berlin, Heidelberg, Springer-Verlag, 1991. DM 66.00) attempts to develop a rational and coherent theoretical modelling of realistic atmospheric flows. It is aimed at both scientists and students of physics and theoretical meteorology. ISBN 3 540 54446 1.

Solar radiation atlas of Africa, by E. Raschke, R. Stuhlmann, W. Palz and T.C. Steemers (Rotterdam, Brookfield, A.A. Balkema, 1991. £93.75) contains many coloured images for the period 1985-86 derived from the SUNSAT project. The logistics employed are decribed, and a variety of other methods of displaying the results are used. ISBN 90 5410 109 1.

Mountain weather and climate, second edition, by R.G. Barry (London, New York, Routledge, 1992. £60.00 (hardback), £18.99 (paperback)) contains sections dealing with all areas of the subject, with case-studies of selected areas. This edition also includes the results of research during the last decade. ISBN 0 415 07112 7 (hardback), 0 415 07113 5 (paperback).

GUIDE TO AUTHORS

Content

Articles on all aspects of meteorology are welcomed, particularly those which describe results of research in applied meteorology or the development of practical forecasting techniques.

Preparation and submission of articles

Articles, which must be in English, should be typed, double-spaced with wide margins, on one side only of A4-size paper. Tables, references and figure captions should be typed separately. Spelling should conform to the preferred spelling in the *Concise Oxford Dictionary* (latest edition). Articles prepared on floppy disk (IBM-compatible) can be labour-saving, but only a print-out should be submitted in the first instance.

References should be made using the Harvard system (author/date) and full details should be given at the end of the text. If a document is unpublished, details must be given of the library where it may be seen. Documents which are not available to enquirers must not be referred to, except by 'personal communication'.

Tables should be numbered consecutively using roman numerals and provided with headings.

Mathematical notation should be written with extreme care. Particular care should be taken to differentiate between Greek letters and Roman letters for which they could be mistaken. Double subscripts and superscripts should be avoided, as they are difficult to typeset and read. Notation should be kept as simple as possible. Guidance is given in BS 1991: Part 1: 1976, and *Quantities, Units and Symbols* published by the Royal Society. SI units, or units approved by the World Meteorological Organization, should be used.

Articles for publication and all other communications for the Editor should be addressed to: The Chief Executive, Meteorological Office, London Road, Bracknell, Berkshire RG12 2SZ and marked 'For Meteorological Magazine'.

Illustrations

Diagrams must be drawn clearly, preferably in ink, and should not contain any unnecessary or irrelevant details. Explanatory text should not appear on the diagram itself but in the caption. Captions should be typed on a separate sheet of paper and should, as far as possible, explain the meanings of the diagrams without the reader having to refer to the text. The sequential numbering should correspond with the sequential referrals in the text.

Sharp monochrome photographs on glossy paper are preferred; colour prints are acceptable but the use of colour is at the Editor's discretion.

Copyright

Authors should identify the holder of the copyright for their work when they first submit contributions.

Free copies

Three free copies of the magazine (one for a book review) are provided for authors of articles published in it. Separate offprints for each article are not provided.

Contributions: It is requested that all communications to the Editor and books for review be addressed to the Chief Executive, Meteorological Office, London Road, Bracknell, Berkshire RG12 2SZ, and marked 'For *Meteorological Magazine*'. Contributors are asked to comply with the guidelines given in the *Guide to authors* (above). The responsibility for facts and opinions expressed in the signed articles and letters published in *Meteorological Magazine* rests with their respective authors.

Subscriptions: Annual subscription £36.00 including postage; individual copies £3.25 including postage. Applications for postal subscriptions should be made to HMSO, PO Box 276, London SW8 5DT; subscription enquiries 071–873 8499.

Back numbers: Full-size reprints of Vols 1–75 (1866–1940) are available from Johnson Reprint Co. Ltd, 24–28 Oval Road, London NW1 7DX. Complete volumes of *Meteorological Magazine* commencing with volume 54 are available on microfilm from University Microfilms International, 18 Bedford Row, London WC1R 4EJ. Information on microfiche issues is available from Kraus Microfiche, Rte 100, Milwood, NY 10546, USA.

May 1992

Vol. 121
No. 1438

Contents

ISSN 0026–1149

ISBN 0-11-728983-3

Printed in the United Kingdom for HMSO
Dd 291241 5/92 C13 503 12521

The Meteorological Magazine

June 1992

Dr F.B. Smith retires
Fifty years of dispersion
Low wind-speed meteorology
Aircraft incident

HMSO

Met.O.1004 Vol. 121 No. 1439

First published 1992

HMSO

HMSO publications are available from:

HMSO Publications Centre
(Mail, fax and telephone orders only)
PO Box 276, London SW8 5DT
Telephone orders 071-873 9090
General enquiries 071-873 0011
(queuing system in operation for both numbers)
Fax orders 071-873 8200

HMSO Bookshops
49 High Holborn, London WC1V 6HB
071-873 0011 Fax 071-873 8200 (counter service only)
258 Broad Street, Birmingham B1 2HE
021-643 3740 Fax 021-643 6510
Southey House, 33 Wine Street, Bristol BS1 2BQ
0272 264306 Fax 0272 294515
9-21 Princess Street, Manchester M60 8AS
061-834 7201 Fax 061-833 0634
16 Arthur Street, Belfast BT1 4GD
0232 238451 Fax 0232 235401
71 Lothian Road, Edinburgh EH3 9AZ
031-228 4181 Fax 031-229 2734

HMSO's Accredited Agents
(see Yellow Pages)
and through good booksellers

3 8078 0010 2470 4

The
Meteorological Magazine

June 1992
Vol. 121 No. 1439

Dr F.B. Smith retires

In February 1992, Barry Smith retired from the Meteorological Office after an industrious 35-year career throughout which he made many valuable and distinctive scientific contributions, particularly in the fields of atmospheric dispersion and diffusion. Barry's interest in meteorology goes back to his school days when he set out his own meteorological station in his back garden and, when a 6th-former, he bought Sir Napier Shaw's *Manual of Meteorology*. Mathematical inclinations took him from Cheadle Hulme Grammar School to Manchester University where be obtained a first class honours degree in Mathematics in 1953. He remained at Manchester to undertake a PhD under Sir James Lighthill. This was a time of great interest and excitement in aerodynamics but, influenced by a desire to have some independence of Sir James, Barry chose a more meteorological area of work. Such an early manifestation of Barry's renowned independence will come as no surprise to those who know him!

On completing his PhD, Barry joined the Meteorological Office as a Junior Research Fellow at the Chemical Defence Establishment, Porton. In 1958 he became a permanent member of the Office as an SSO and made an energetic start publishing numerous papers including several in the *Quarterly Journal* of the Royal Meteorological Society. The topics varied from the 'analysis of observations of wind fluctuations' to 'the turbulent spread of clusters of particles'. In 1960 the Office sought to broaden his interests and he was sent to Stockholm for 7 months to learn from Dr Phillip Thompson about numerical weather prediction. On his return he worked on objective analysis and the development of Lagrangian forecast models using the Mercury and then the newly installed KDF9 computers. Publications continued to flow, including one on the uncomfortable subject of 'The effect of advection in a region of no data'. Oceanographers take note! Later he joined Bob Murgatroyd to study stratospheric circulations. Barry's real interests however still lay in atmospheric diffusion and dispersion and it was no secret that he continued to spend time on such studies. In 1966 he persuaded the Office to allow him to spend a sabbatical year with Frank Gifford's group at Oak Ridge, Tennessee working on conditional dispersion theories and random-walk ideas. Thus began a close association between Barry and colleagues there, which still continues today. On his return, the Office made a final brief and unsuccessful attempt to divert his attention by posting him to work in the Geophysical Fluid Dynamics Branch. However, Barry's persistence and the Office's recognition of his talents prevailed and from 1967 until his retirement he has been a mainstay of the boundary layer branch. At first he was deputy to Frank Pasquill and in 1974 he became Head of the Branch. Barry's distinctive approach to the in-tray was always to deal efficiently with items he felt important, but to leave other actions either forever or until the third demand. He was also not one to waste time on staff who were obviously getting on with useful work but was always generous with his time in giving help and direction where needed. Close colleagues generally approved of this regime. In spite of the frustration it may have caused senior management at times, one distinct benefit of Barry's individualistic administrative style was his continuing high scientific productivity. This was duly recognized in 1979 on his transfer to an Individual Merit Research post, with a highly deserved promotion in the same capacity to grade 5 in 1986.

Barry's initial contributions to the understanding of atmospheric dispersion were often idealized and involving 'heavy' mathematics. Although he never abandoned such sophistication, the hallmarks of Barry's activities in the last 20 years have been his ability and willingness to tackle real problems and his solutions in the form of practical tools for, as he would say, 'the man in the field'. In many instances, he has converted pages of equations into simple curves and formulae. In particular, the nomograms and overlays which form the basis of the Office's chemical emergency response are due to him. The use of these practical schemes has also been assisted by Barry's skill as a teacher and lecturer. He is known for well-prepared public talks and lecture courses with good diagrams which are easy to follow and capture the essential points.

In 1983, his long-standing collaboration with Frank Pasquill was suitably crowned with their joint authorship of the third edition of the recognized seminal test *Atmospheric Diffusion*. Barry's interests were not confined to short-range dispersion and during the 1970s he became involved in the study of long-range transport in connection with acid rain. This involved studies of synoptic-scale air trajectories and the verification of his models for the transport and deposition of atmospheric pollutants with field studies of marked power-station plumes sampled by the MRF C-130 aircraft. In typical fashion he became involved in the whole problem, from the emissions and the atmospheric dispersion to the atmospheric chemistry and the deposition processes. As a leading European expert on acid rain his impartial advice and scientific integrity were widely sought after on national committees and in international fora. His contributions were recognized in 1981 by the award of the FitzRoy Prize of the Royal Meteorological Society. During the Chernobyl accident in 1986 he was again at the heart of the Office's advice to Government. Subsequently, he undertook a careful and thorough analysis of the meteorological factors which governed the spread of the plume from Chernobyl and the eventual deposition of its radioactive material. Then together with Roy Maryon he helped respond to the Cabinet Office request for an operational system to provide detailed predictions of the transport and deposition of radioactive material that might arise from any future similar accident. The resulting nuclear accident model, NAME, is one of the best of its kind available. The model and Barry's expertise were put to good use in investigating the impact of the oil fires started in the recent Gulf War.

Barry's interests and contributions have by no means been confined to his professional efforts in the Office. Almost simultaneous with the start of his Office career has been his devotion to the Scout Association, in particular the Cub Section. In this context, Barry's exploits are legendary and, not surprisingly, his unique and unstinting efforts have been fully recognized by the Association which has honoured him with medals for his outstanding contributions. Over the years, many colleagues have been charmed or press-ganged by Barry to aid and abet him at Scout functions. In the process, all will have witnessed the unique brand of fun, excitement, encouragement, guidance and education that Barry has provided and continues to provide, for those Cubs privileged to have him as their 'Akela'. His remarkable success with Cubs is undoubtedly linked to his open approachability, friendliness and good humour, which his colleagues in the Office have long appreciated. Although the Met. Office has lost a true expert of high international repute, Barry will continue at large to contribute to the subject. He has accepted positions as an Honorary Professor at the University of East Anglia and as a Visiting Professor at the Centre for Environmental Technology at Imperial College, London, as well as retaining a number of other commitments. Noting the volume of material transferred from his office to his home, both must be at risk of settlement damage. All his colleagues will surely wish him a long and rewarding retirement.

P.J. Mason and D.J. Carson

551.5(09):551.551.8:551.510.42

The first 50 years in the study of atmospheric dispersion

F.B. Smith
Meteorological Office, Bracknell

Before 1914, the Meteorological Office was small and dedicated to the task of making meteorological measurements, drawing charts and issuing forecasts. At the beginning of the World War I, the Office contained only about six professional meteorologists, who had learned their trade in the hard school of experience, and another half a dozen young men from the universities who were at the beginning of their careers.

The geostrophic wind, regarded for over 70 years as a mere theoretical curiosity of an impressionable Frenchman, G. Coriolis in 1835, was still hardly recognized as a practical tool of the working forecaster. However in 1919 Sir Napier Shaw, in the preface to Part IV of his *Manual of Meteorology*, wrote 'Within the past four years...... we have found a guiding principle of great practical utility in the relation of the wind to the distribution of pressure...in the free atmosphere which follows very closely the laws of motion under balanced forces depending on the spin of the earth'.

Nevertheless, the basic ideas of wind structure and turbulence were already under investigation. The idea of a momentum exchange coefficient had been proposed by Boussinesq. The idea was then developed by Schmidt in Germany who called it an austausch coefficient (although his work was not properly written up until 1925), and in 1902 Ekman had published his famous paper on the establishment of ocean currents due to wind stress, which when applied to meteorology led to the Ekman spiral of wind in the boundary layer.

The German school had thus developed some major ideas about turbulence, although it was in Britain where scientists like Reynolds had already established several fundamental concepts. In two papers in 1883 and 1884, Osborne Reynolds explained the conditions in which streamline motion would break down into turbulent motion; it depended on whether or not the velocity V of the fluid was sufficiently high that Vl/v exceeded some critical value of the order of 2000 (where l is the linear dimension of the system and v is the kinematic viscosity). He noted that whereas streamline motion could be described by the use of hydrodynamical equations, turbulent motion has to be treated statistically like the motion of gas molecules. Rayleigh in a Report to the Advisory Committee for Aeronautics (1909–1910) had already set out the principles of dynamical similarity.

Before World War I, G.I. Taylor had been appointed the Schuster Reader at the University of Cambridge. Following the tragic loss of the *Titanic* in the western Atlantic after striking an iceberg in 1912, the government fitted out an old wooden sailing ship, the *Scotia* to look for icebergs in the North Atlantic and to report their positions by the new radio method. Taylor was on of three scientists appointed to accompany the expedition. He decided to study the vertical transfer of heat and momentum and water vapour in the friction layer of the air. He arranged for instrument-carrying kites and balloons to be flown from the ship. He measured wind, temperatures and humidity profiles up to about 2500 m on several occasions. He also needed information of the previous history of the air mass and this he was able to infer from records of water and air temperature and wind data collected by ships upwind of *Scotia*. In a 1915 paper, Taylor gave a rational description of the profiles in terms of the upwind history of the air and a supposed 'eddy conductivity' and a 'mixing length' (defined as the vertical distance over which an element of fluid and its vorticity would move before attaining the same value as its surroundings and losing its identity). Unknowingly his concept of mixing length was similar to that of Prandtl ten years earlier, although Prandtl had thought in terms of momentum rather than vorticity.

Taylor also analysed the approach of the wind to the geostrophic at the top of the boundary layer, showing good agreement between theory and observations. Again he was unaware of the earlier work of Ekman. Taylor however used the better lower boundary condition of assuming stress and wind to be parallel at the surface.

In 1914, Taylor investigated stability. He inferred that an airflow is stable to small disturbances provided:

$$\left(\frac{\mathrm{d}U}{\mathrm{d}z}\right)^2 < \frac{4g\Delta\rho}{\rho L}$$

where $\Delta\rho$ is the drop in density over a layer of vertical thickness L. This work was part of an essay 'Turbulent motion in fluids' which won him the Adams Prize of the University in 1915.

In the same year, G.I. Taylor joined a group of civilians at Farnborough working for the Royal Flying Corps helping to put the design and operation of aeroplanes on a scientific basis. He felt the need to be able to fly aircraft to do his work properly, so unable to do this as a civilian he enlisted and later attained the rank of Major. On 14 February 1916 he became the Professor of Meteorology to the Royal Flying Corps (RFC), attached to the Meteorological Office, but much of his work continued to be concerned with the proper design of aircraft and the study of the flow of air over wings and the resulting pressure distribution. Eventually he left Farnborough in 1917 to concentrate on more meteorological issues for the RFC although little in the way of research into dispersion resulted during the next few years. Before doing so, however, Major Taylor had constructed a sophisticated anemometer which could measure wind speed and its fluctuations in three dimensions. This was set up on a chimney at Pyestock to test the diurnal variation of gustiness.

However it wasn't until 1915 that attention in the Meteorological Office was first directed towards diffusion. This resulted from the use of poisonous gas in the front line. It was first used by the Germans against the Algerian Division of the French Army at Ypres on 22 April 1915 by the simultaneous discharge of chlorine from 6000 emplaced cylinders over a front of about 4 miles. The effects were dramatic; those who could, fled the front line and the front collapsed. On 24 April the 2nd Canadian Brigade was also attacked in this way. British troops were first attacked with gas on 1 May. Army Chiefs requested urgent action and help. The first proper gas-mask was designed in the following August and an Establishment was set up at Porton in 1916 with a Meteorological Station in support. The head of the station was Corporal T.A. Beardsmore, B.Sc., RE, whose responsibility was to make extra meteorological measurements during smoke releases as well as routine meteorological observations. They soon found that experiments were most successful in winds less than 7 m.p.h. and when ground temperatures were lower than the air temperatures (i.e. in stable conditions). The small station came under the direction of Colonel H.G. Lyons who was stationed at a Home Unit on Salisbury Plain (possibly Larkhill).

Their routine work of attending experiments and making standard meteorological observations took up most of their time. One of these experiments concerned the production of smoke screens under widely varying atmospheric conditions and at different ranges. However they did find time to investigate:

(a) The variation of wind with height, and

(b) The eddies and currents of wind in the immediate vicinity of woods.

From May 1916 onwards, field trials were carried out with many liquified gases to determine, amongst other things, how the gas cloud travelled and the effects of ground and air temperatures, ground contours, winds, etc. on the resulting concentrations.

Going back in time just a little, Britain first used gas against the enemy at Loos on 25 September 1915. The meteorologist commissioned to forecast when conditions would be suitable was Capt. Gold. On the 24th the winds were very light, but with observations from the Western Front and from Britain he predicted the wind would turn to the west-south-west and would therefore be suitable for a release. The winds however remained very light and Gold was greatly relieved when reports began to come in of gas rolling towards the enemy lines.

In 1917 an Advisory Committee on Atmospheric Pollution was established at the request of the Department of Scientific and Industrial Research (DSIR) under Sir Napier Shaw. This came under the control of the Meteorological Office in 1919 and remained so until, in 1928, it came under the chairmanship of Warren Spring Laboratory. The objective of the Committee was largely to study levels of pollution in urban areas in collaboration with local Councils. A network of gauges was established to record the levels of smoke.

It is about this time that L.F. Richardson had completed his pioneering work on numerical weather prediction (NWP) whilst serving as an ambulance man at the front. I believe at one stage he temporarily lost his manuscript and calculations in a muddy trench! In 1918 he was out of the war and was stationed in the Meteorological Office Observatory at Eskdalemuir. However he did not stay there long and was soon moved to Benson where W.H. Dines was working on upper winds. Richardson then found time to submit his work on NWP; a paper described by others as 'elaborate'! The paper was sent to the Royal Society where it was published.

He devised a method of measuring the wind at different levels by its differential effect on steel spheres shot nearly vertically upwards so that when they returned to earth the displacement could be noted. The spheres varied in size from a pea to a cherry, and the system was particularly useful in fog or cloud when visual observations of a balloon could not be made. However the system had its dangers, and it was ultimately abandoned mainly because with spheres of a non-lethal size and muzzle velocities below the speed of sound the height reached was not great enough to satisfy the synoptic meteorologist. (But how about it, Cardington 1992?!)

Richardson in 1919 took up G.I. Taylor's idea of eddy conductivity and coined the term 'eddy diffusivity' for *K*. He showed that *K* derived from observations of smoke and thistledown and dandeliondown across different types of land surface, of steamer smoke at sea and of the growth of cumulus clouds, varied from 5 to 10^6 cm^2 sec^{-1}), much more widely than had previously been supposed. In 1920 he published his famous work on the Richardson Number the criterion for deciding whether or not turbulence levels will increase or decrease, given gradients of wind and temperature.

Meanwhile Alcock and Brown had flown the Atlantic for the first time on 14/15 July 1919, and David Brunt had been appointed the Superintendent of the Met. Establishments for the Army (including Porton). Brunt was stationed at Shoeburyness. Up to 31 March 1920, no action had been taken to provide civilian meteorological staff at Porton, since its future programme of research, if any, was uncertain, but after Sir Napier

Shaw resigned as Director of the Office and Dr G.C. Simpson took his place, civilians were sanctioned by the Treasury with N.K. Johnson as the Station's Head. In 1921 the Chemical Defence Establishment at Porton was officially opened with Nelson Johnson as Superintendent of the 'Meteorological Department'. The Department's duties were to carry out research into meteorological problems arising in chemical warfare, and to provide meteorological information to the Establishment as a whole.

G.I. Taylor, now back at Cambridge, carried out a short but crucial study of the relationship between dispersion and turbulent fluctuations which led to the classical formula:

$$\sigma_y^2 = 2\sigma_v^2 \int_0^T \int_0^t R(s)\,ds\,dt.$$

The work was published in the London Mathematical Society in 1921 but it was not until the 1930s that O.G. Sutton took up the method again and applied it to dispersion in the boundary layer, and that the method was applied to laboratory flows by Taylor himself.

At Porton the next few years seem rather quiet, but in reality the staff there were grappling with the problems of measuring velocity and temperature gradients in the lower atmosphere and in carrying out some formative dispersion experiments. In any case, the number of staff in the Met. Department was rather too low to carry out any very extensive work during this period.

In 1923 smoke experiments indicated that at 100 m downwind from the source the width of the cloud, defined by one-tenth peak concentration, averaged about 35 m in neutral conditions for a release duration of 4 minutes but values ranging from 23 m to 47 m were found. R.F. Budden analysed the form of the cross-wind concentration distribution and showed that

$$C(y) = C(0) \exp(-ay^{1.5}),$$

at variance with the Gaussian form, which had been expected. This lower exponent (1.5 rather than 2) was broadly confirmed later in 1931 by E.L. Davies at Cardington.

The staff also endeavoured to measure vertical dispersion. They did this by spacing a number of smoke candles some 4 m apart across-wind and sampling the smoke at various heights on a downwind tower using a hand-pump. The candles were of a pitch composition and the downwind concentrations were inferred by the 'stain-meter' technique devised by Scrase in which the smoke was drawn through a filter and the resulting stain compared with a set of standard stains corresponding to different concentrations. The results implied an average plume-top height of 10 m at a range of 100 m in neutral conditions. These results were later used by Sutton in the 1930s to validate his new diffusion formulation.

In 1922 a name that later became associated with airship meteorology came on to the scene. This was M.A. Giblett, who worked on and published a paper on evaporation from large expanses of water.

In 1925 the Met. Department was strengthened to include not only N.K. Johnson, but E.L. Davies, F.J. Scrase and O.F.T. Roberts. By the following year they had produced an interesting paper entitled *The measurement of the lapse rate of temperature by an optical method.* The team also carried out further dispersion experiments extending the range of travel to 300 m and 1000 m. They showed amongst other things that in neutral conditions the cloud-width varied roughly like $x^{0.8}$.

In the years up to and including 1925, there was considerable interest in the potential of airship travel. In 1925 an Airships Division was set up at the Pulham Airship Station under L.G. Garbett to provide meteorological information. The first major flight was made which was from England to India via Egypt in the R33. A year later a separate Airships Met. Division was established at Cardington under M.A. Giblett as Superintendent. One of their first tasks was to investigate short-period fluctuations of wind speed and direction. They also worked on the horizontal scale of eddies, especially in very strong winds. To this end they set up a network of anemometers. In 1928 this network was modified to three anemometers at the corners of an equilateral triangle of side 700 ft (roughly the dimension of an airship) with a fourth anemometer at the centre.

In 1929 Cardington staff were charged with predicting conditions when it was safe to move the airship from its hangar to the launch-mast, the conditions at the mast itself and to issue warnings of any sudden changes in wind, and to make forecasts of weather along the route.

On 4 October 1930, the R101 set off for India with Mr Giblett on board as Met. Officer. The terrible disaster that followed led to his death and to the end of airship development using hydrogen.

Going back to 1926 we can pick up again developments in the study of dispersion. L.F. Richardson, as noted earlier, had inferred the very wide range of eddy diffusivities appropriate to the diffusion equation on different scales. Richardson recognized the different nature of relative diffusion. He defined a distance-neighbour function q(r) defined as

$$q(r) = \frac{1}{Q} \int_{-\infty}^{\infty} C(x)C(x+r)\,dx$$

where C(x) is the concentration of x, Q is the total number of particles. He proved that if the diffusion was Fickian then q satisfied

$$\frac{\partial q}{\partial t} = 2K \frac{\partial^2 q}{\partial r^2}.$$

In non-Fickian diffusion he suggested replacing $2K$ by $F(r)$ so that

$$\frac{\partial q}{\partial t} = \frac{\partial}{\partial r}\left(F(r)\frac{\partial q}{\partial r}\right).$$

Using the data from different scales including the balloon data described below he inferred $F(r) = 0.6r^{4/3}$ for values of r between 1 m and 10 km. For objects floating on the surface of the sea however, the coefficient 0.6 should be replaced by 0.035, sixteen times less or in the same ratio as the viscosity of air to that of water.

Richardson decided to collect as much longer-range dispersion data as he could. However much of these were rather crude and heterogeneous. His balloon data were obtained largely from balloon competitions organized at Brighton and in Regent's Park, London. He and Proctor found agreement with the 4/3 law given above but that if the data were subdivided into wind-speed classes then $K \propto \sigma^{5/3}$ where σ was the standard deviation of balloons from their mean track. It is important to remember in interpreting this result in terms of relative diffusion that some of the release durations extended over about 10 hours.

In 1929 O.G. Sutton joined the Porton Group and launched a new development of the work there on dispersion which lasted throughout the 1930s. During this time a number of (later famous) scientists joined him: F.J. Scrase, A.C. Best, P.A. Sheppard, K.L. Calder, F. Pasquill and C.H.B. Priestley.

The idea of a constant eddy diffusivity K led to the dimensions of a plume expanding as $x^{1/2}$, but field data showed that this was not generally the case. In the vertical it was generally accepted that K could be made a function of height, reflecting the change in the nature of turbulence as z increases. But it was harder to resolve the problem for horizontal dispersion. As we have already seen, Richardson had thrown some light on this problem but it really remained unresolved. Sutton saw the urgent need for a different approach. He decided to combine Taylor's 1921 statistical theory with the old concept of mixing length. He searched for an appropriate form for $R(s)$. On intuitive and dimensional grounds he suggested in 1934:

$$R(s) = \left(\frac{v}{v + \sigma^2 s}\right)^n$$

where v is the kinematic viscosity and n is a constant to be identified.

The essential equations are

$$K = \overline{w'^2} \int_0^{t_o} R(s)\,ds$$

where t_o is the time for the correlation to fall to effectively zero. Thus

$$K = \frac{v^n}{1-n}(\overline{w'^2}\,t_o)^{1-n}.$$

Then with

$$t_o = l/|\overline{w'}| = |du/dz|^{-1}$$

and

$$l = k|du/dz|/|d^2u/dz^2|$$

and the assumption of a Gaussian distribution in w'

(hence $\overline{w'^2} = \frac{1}{2}\pi|\overline{w'}|^2$)

$$K = \frac{(\pi k^2/2)^{1-n}}{1-n} v^n(|du/dz|^3|d^2u/dz^2|^{-2})^{1-n}.$$

If we then assume that the shearing stress τ is changing only very slowly with height so that $K\,du/dz$ is effectively constant, and that we have a power-law wind profile then

$$u \propto z^{n/(2-n)}$$

and we can then determine n from the shape of the wind profile. It follows, using Taylor's equation for the σ's that

$$\sigma_x^2 = \frac{1}{2}C^2(uT)^{2-n}$$

where T is the time of travel and C is given by

$$C^2 = \frac{4v^n}{(1-n)(2-n)u^n}\left(\frac{\overline{u'^2}}{u^2}\right)^{1-n}.$$

Similar expressions apply for σ_y and σ_z. These values of σ can then be inserted into a Gaussian plume formulation to obtain the concentration distribution.

Despite the success with small-scale boundary-layer studies of vertical transfer, Sutton's form of K-theory ran into difficulties when tested against observations of the vertical diffusion of smoke in the field. It gradually became clear that the significance of surface roughness had not been fully appreciated. Calder and Sheppard were tasked with trying to sort out the problem. Over aerodynamically rough surfaces it proved necessary to replace v by $u_* z_o$ where u_* is the friction velocity and z_o the roughness length. Thus v was replaced by a macro-viscosity. Experimentally the value of n was found to be about ¼ in near neutral conditions.

During much of the 1930s, Sutton's formulation was further developed and much effort was expended in exploring the profiles of wind (and temperature) in more detail to obtain optimum values of n in different conditions. I have rather laboured Sutton's approach because it dominated thinking about dispersion for over 20 years in this country.

In 1931 and 1934 Porton staff carried out further dispersion experiments out in the field at Cardington. To their surprise they found that plume widths over similar sampling durations were greater at Cardington than at Porton even though the general lie of the land was flatter at Cardington.

In 1934 the experiments were accompanied by measurements of turbulence (using a bi-directional vane) which showed that the width of the trace of directional fluctuations compared well with the plume width. They also displayed a close relation between cloud-width and atmospheric stability as indicated by the Richardson Number.

1935 saw the return of G.I. Taylor to our story. In that year he extended his initial 1921 analysis in which he regarded the changes in velocity of a particle as a continuous process by applying the same concept of continuous change to the Eulerian description of the spatial structure of turbulence. In this he defined a length-scale of turbulence as the integral of the space-correlation of turbulent velocities, recognizing that the scale could well be different in the three component directions.

In 1938 Taylor adopted the 'frozen-eddy' concept which related the spatial correlation alongwind to the temporal correlation at a fixed point,

$$\mathrm{R}(t) = \mathrm{R}(x)$$

when $x = ut$. He also introduced into turbulence theory the relation between the correlation coefficient and the spectrum of turbulence through the Fourier integral. The practical importance of this was that it brings out the idea of a continuous range of eddy sizes and helps to identify those eddy sizes which are of most significance as regards kinetic energy and those which are of most importance in creating dispersion. It was these ideas that were later developed first by A.N. Kolmogoroff in the USSR in 1941, and later by G.K. Batchelor in and after 1946 and subsequently by many others.

Frank Pasquill joined the team at Porton in 1937, two years before the outbreak of war. He was given the job of investigating dispersion over the sea. By the beginning of 1939 he had everything organized to measure the profiles of wind, temperature and humidity using equipment sited on a landing-stage at Bognor. After just a few trials, the approaching threat of war changed the priorities and he was told to concentrate on problems of the evaporation and persistence of mustard gas on the ground back at Porton. Sutton had developed a theory for evaporation along the lines outlined earlier. This theory was extended by Calder to give the absolute rate of evaporation. Pasquill was asked to test this using a large wind-tunnel specially built at Porton for this purpose. He showed that the evaporation rate could be well predicted using Sutton and Calder's treatment by knowing the power-law variation of wind with height in the shallow boundary layer over the wind-tunnel floor. The war had, of course, a profound effect on the programme of work at Porton. In 1943 following the disastrous advance of Japanese troops across south-east Asia, the Government feared that chemical warfare might be used by the Japanese in the hot, humid conditions of the tropics, for example in Burma. Uncertain of their possible behaviour, they sent a team out to north Queensland to carry out tests. Pasquill was included in the team as the meteorologist. The role was mainly support, with little chance to do research.

At the end of the war, in 1946, Pasquill returned to the United Kingdom and found himself posted to the School of Agriculture at Cambridge where he again worked on the determination of profiles and evaporation. He was able to show that the eddy diffusivity for water vapour was very close to that of momentum, and that the von Kármán constant was likewise the same as that for momentum, namely 0.4. In 1949, he agreed to be seconded to the Atomic Energy Authority at the Harwell Laboratories. He became involved in studying the distribution of radioactivity in the countryside around Harwell originating from one of the reactors on site. He also took up the work started by C.S. Durst in the Office on the long-range travel of radioactive material both from atomic bomb tests and from nuclear plants on a global scale. In shorter-range studies Pasquill and Crabtree were able to fit small smoke-generators on to the cable of a captive balloon. Individual puffs could be followed for quite some distance downwind. The striking thing which they noted was that the track of an individual puff was surprisingly straight even though there were quite big changes in the wind at the source, implying that the Lagrangian time-scale was much longer than the Eulerian scale.

Meanwhile Calder and Sheppard continued after the war to work on problems of evaporation from aerodynamically rough surfaces as well as from water surfaces. Batchelor was extending the spectral work initiated by Taylor and by Kolmogoroff. In 1950 he had published a paper on the application of Similarity Theory of turbulence to atmospheric diffusion. A big landmark came on the publication of his monograph *The theory of homogeneous turbulence* in 1953 which set out in a coherent way all the new advances in homogeneous turbulence as viewed through these spectral and correlation statistical methods. This laid the way for further advances in dispersion theory which came later in the decade and beyond.

After 1950 the number of scientists working in the study of dispersion began to increase, slowly at first but with ever increasing speed. Highly productive groups became established in the USA at Penn State University under Panofsky, at Oak Ridge under Frank Gifford, and at the Environmental Protection Agency under Ken Calder (who had emigrated in 1949) and other; other groups started in Japan, in Germany, at Roskilde in Denmark, in Sweden and, of course, in the Soviet Union. To tell the story from this point would require many books, suffice it to concentrate on progress in the United Kingdom and at Porton in particular.

In 1954 Pasquill returned to Porton, replacing C.J.M.

Aanensen who in turn had replaced Calder. Aanensen had worked on the diffusion of gases in cities, using the large wind-tunnel to carry out his experiments. He had also been contemplating the use of a new tracer for longer-range dispersion experiments. Pasquill took up this project. One of the key factors in the work at Porton in the next few years was the application of these new methods for evaluating dispersion. New tracers were employed that were easier and more accurate than some of the older methods. The first new tracer was zinc cadmium sulphide which, when released as a fine powder, could be collected on sticky plates and the particles counted subsequently in the laboratory since they fluoresced under ultra-violet light. Another tracer was lycopodium spores that were collected on sticky cylinders and could be counted under a microscope. These enabled dispersion experiments to be carried out to 100 km or more, although many were at much shorter range. J.S. Hay did much to make these tracer techniques practical and effective. One interest was in the longer-range travel of cloud seeding agents (like silver iodide) which could diffuse up into cloud, from generators on the ground, and hopefully enhance rainfall rates. The tests that were carried out had to be done in situations of otherwise rather uniform rainfall so that the effects, if any, could be observed. Unfortunately, since such uniform conditions could only be expected with warm fronts, the silver iodide found it very difficult to penetrate the rather stable inversion at the frontal surface so that little got into the precipitating cloud. The experiments turned out to be rather a failure for this reason.

Another great aid to better field-studies came with the development of much more sensitive and useful instrumentation in which J.I.P. Jones played such an important role. The dispersion work that Pasquill and Crabtree had done at Harwell, and the subsequent studies made at Porton led to the useful concept that the Lagrangian spectrum of turbulence, required to predict dispersion, could be well estimated from the Eulerian spectrum (measurable using fixed anemometers) by assuming the two had the same shape but the Lagrangian spectrum was displaced towards lower frequencies.

F.B. Smith joined the group in 1956. He extended the range of analytical solutions of the diffusion equation then available with u and K profiles more in line with measured profiles through the boundary layer. He was also able to include the effects of dry deposition into some of the these solutions. He was attracted by the possible application of Monte Carlo techniques to atmospheric dispersion but was largely thwarted in this by the lack of computer facilities which did not become available until the early 1960s.

He also obtained the first solutions for dispersion in convective conditions in which thermals and compensating downward subsidence in the air produced concentration distributions in the vertical radically different from those obtained by simple K-theory but much more in line with those observed in the real atmosphere.

Towards the end of the 1950s, Smith presented the results of a theoretical study into the turbulent growth of puffs of heavy particles falling from their release point towards the ground. This was based very much on the extension of Taylor's statistical approach to dispersion and his work on the spectrum of turbulence. Smith and Hay later extended this work to puffs of passive particles, showing that the growth rate accelerates initially as the puff grows but asymptotically approaches the growth rate of a plume from a continuous source. He showed the growth rate could be expressed in terms of an integral of the energy spectrum weighted by a simple factor dependent on the puff size.

Pasquill had been approached in 1958 by the UK Atomic Energy Authority following the Windscale accident for current methods of estimating dispersion using easily obtained meteorological data. Pasquill realized there were no such simple methods. However, an important field experiment had been carried out in Nebraska in the USA called 'Prairie Grass'. The results complemented the results of the Porton experiments, extending these both in terms of range and in the effects of thermal stratification. Grouping all the results together it was possible to associate different rates of vertical dispersion with broad classes of wind speed and incoming solar radiation, or insolation, subjectively assessed, using cloud cover as a guide. He defined six categories of stability called A, B, ..., F. A was the most unstable category to be found only in light winds and strong insolation. Category D was for 'neutral' conditions, most commonly found in overcast conditions with winds above $5\,m\,s^{-1}$. At night, cloud amount replaced insolation as one of the key factors. The most stable category was F which occurred when there was little or no cloud and the winds were light. However, Pasquill's original scheme did not include any guidance at night when the wind speed fell below $2\,m\,s^{-1}$, although later versions associated this state with an even more stable category G. Pasquill provided curves of plume depth with range from the source for each of his six categories. In conjunction with the assumption of an approximately Gaussian profile shape, calculations of downwind concentration became extremely simple. Pasquill emphasized that his scheme was only to be used if wind fluctuation data were unavailable and only for near-ground-level sources.

The scheme was published in 1961 in the *Meteorological Magazine* and with some extensions suggested by Gifford it soon became the accepted method to use, and is still a valuable tool, extensively used, even in 1992.

With the onset of computers, new experimental and theoretical advances would soon become possible, but that is another story. The year 1960 really marks the end of an interesting 50-year initial development of a subject that has not ceased to be of considerable importance.

Sources of information:

Biographical Memoirs of Fellows of the Royal Society:
L.F. Richardson, 1954.
G.I. Taylor, 1976.
O.G. Sutton, Vol. 24, 1978.
Manual of Meteorology, Volume IV, by Sir Napier Shaw., 1931. Cambridge University Press.
Micrometeorology, 1953. by O.G. Sutton. published by McGraw-Hill, London.
Atmospheric Diffusion (first edition), 1962. by F. Pasquill. published by van Nostrand Co. Ltd, London.
The Chemical and Biological Defence Establishment, Porton Down 1916–1991. by G.B. Carter. *RUSI Journal*, autumn 1991, pp. 66–74.
Meteorology at Porton in World War I. Unpublished note by K.P. Norris.
'Dr. F. Pasquill', a transcription of an interview in the R. Met. Soc. Series of Distinguished Fellows of the Society. 1986.
Annual Reports of the Meteorological Office, (1910–1960). HMSO.

551.551.8:551.510.42

Low wind-speed meteorology

F.B. Smith
Meteorological Office, Bracknell

Summary

Low wind-speed conditions are particularly important for the science of air pollution because it is under these conditions that the highest ground-level concentrations are often experienced, and because the state of the lower atmosphere is often least well defined and predictable. Furthermore, most of the conventional models for dispersion are to some extent suspect because of their assumptions when the wind speed falls below about 2 m s⁻¹. This paper explores the meteorological nature of low-wind conditions, and thereby emphasizes many of the difficulties associated with this state.

1. Definition of low wind-speed conditions

1.1 Wind speed less than turbulent velocities

One useful definition of low wind speeds is that the mean wind speed (defined over some specified time interval) is comparable or less than the root-mean-square turbulent horizontal velocity, σ_u. In unstable conditions, the magnitude of σ_u can be defined in terms of the friction velocity u_* and the sensible heat flux H

$$\sigma_u^2 = 0.3w_*^2 + 6.25u_*^2$$

where w_* is the convective velocity

$$w_* = \left(\frac{gHh}{\rho C_p T}\right)^{1/3}$$

and h is the height of the boundary layer, which in many conditions can be approximated for in this calculation by 1000 m. C_p is the specific heat at constant pressure and ρ is the air density.

The friction velocity can be calculated using Monin–Obukhov similarity theory in terms of the measured wind at 10 m, the heat flux H, and the surface roughness z_0. Such a calculation is implicit in Table I where values of σ_u are given for different values of u (10 m) and heat flux H.

Table I. σ_u (m s^{-1}) for $z_0 = 0.01$ m in unstable conditions, with different values of the heat flux H and horizontal wind speed, u. The following algorithm is assumed: $\sigma_u^2 = 0.3w_*^2 + 6.25u_*^2$ for small heights z. See text for explanation of other variables.

u (m s^{-1})	H (W m^{-2})								
—	0	5	10	20	50	100	150	200	250
0.0	0	0.319	0.402	0.507	0.688	0.867	0.992	1.09	1.176
0.5	0.073	0.336	0.419	0.522	0.701	0.879	1.005	1.104	1.187
1.0	0.145	0.366	0.444	0.545	0.722	0.899	1.02	1.12	1.205
1.5	0.218	0.404	0.478	0.575	0.748	0.921	1.04	1.14	1.225
2.0	0.290	0.448	0.518	0.610	0.778	0.948	1.07	1.166	1.248

In these light wind conditions, it can be seen that σ_u is most sensitive to the heat flux. In fact $\sigma_u \approx 0.187 H^{1/3}$ when u is small.

In stable conditions, as long as there is some wind, it seems that σ_u is governed by low frequency meanderings and shallow gravity flows, to the extent that a quasi-minimum value is reached independent of the mean wind speed. This has been noted by Hanna and by others. Hanna (1983) has reported measurements of plume widths from low-level upwind sources, sampled over an hour, one at Oak Ridge, Tennessee, and the other at Idaho Falls. The measurements, reproduced in Fig. 1, are stated to be broadly consistent with a crosswind σ_u of about 0.5 m s^{-1}. However, when looked at rather more closely, the fit is less convincing at each site taken in isolation; at Oak Ridge, as Fig. 2 shows, a better fit is obtained by assuming the angular width of the plume 100 m downwind from the source is given by $\sigma_\theta = 0.3/u$. At Idaho Falls, the fit to any simple relationship is far from convincing, as shown in Fig. 3.

The data on the fluctuations in wind directions over 3-minute sampling periods, reported by Smith and Abbott (1961), are given in Fig. 4. These data are subdivided according to a measure of stability s. On the stable side, an inverse relationship with wind speed is evident, in an averaged sense. The equivalent crosswind value of σ_u is about 0.26 m s^{-1}. This implies a value of about 0.35 m s^{-1} if the sampling period were to be extended to one hour.

1.2 Instruments are inadequate

From a purely practical point of view, it may be argued that a good definition of low wind-speed criterion is provided by the speed when the wind-measuring instruments begin to perform inadequately.

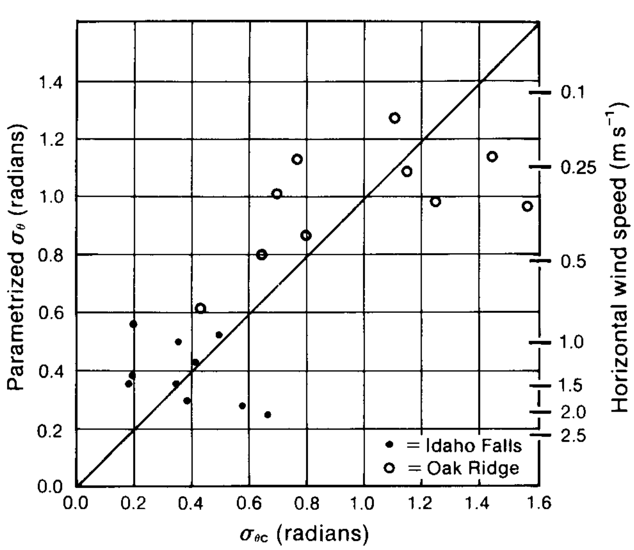

Figure 1. Observations of standard deviation of crosswind distribution of material in plume divided by distance from source ($\sigma_{\theta c}$) determined from the concentration distribution, compared with parametrized $\sigma_\theta = \tan^{-1}(0.5\ \mathrm{m\,s^{-1}}/u)$ based on wind observations.

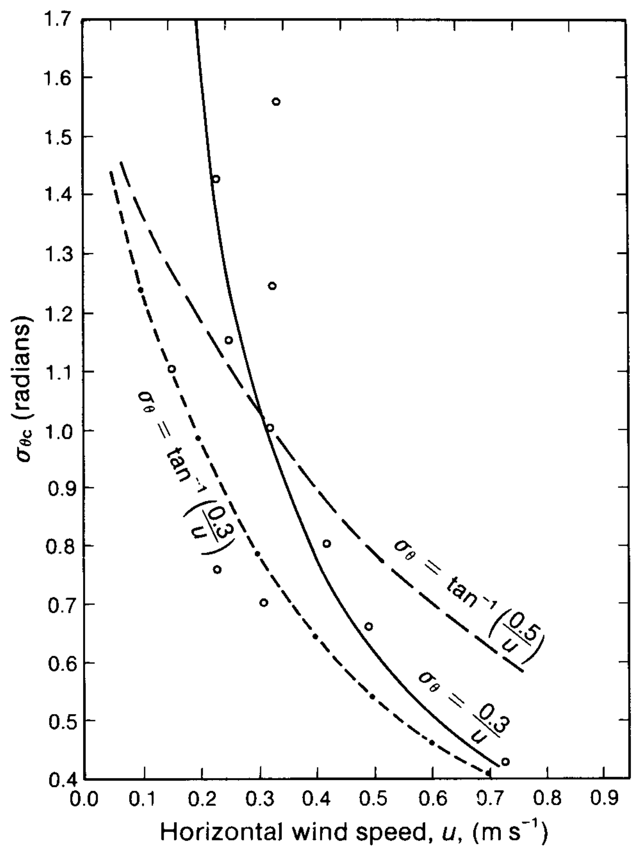

Figure 2. A replot of the Oak Ridge data from Fig. 1 (1-hour averages for stable light-wind cases) showing that the assumption that $\sigma_u = 0.5$ m s^{-1} is not a particularly good fit.

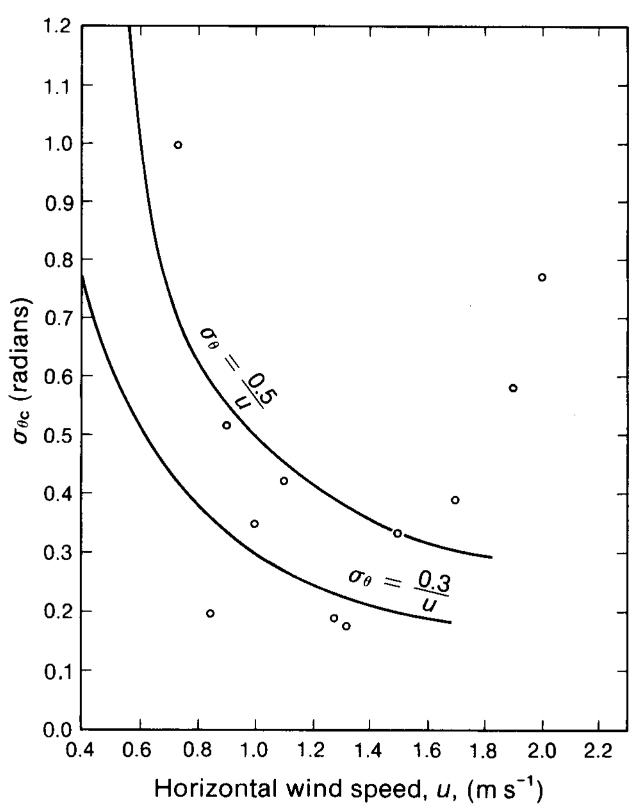

Figure 3. As Fig. 2 but for Idaho Falls data.

This however makes the speed a function of the instruments. Table II shows the recording errors of standard vanes and anemometers; it is clear their performances are not very good for pollution purposes when the winds are light. In particular the cup anemometers can only be trusted when the wind speed is greater than about 6 knots, or 3 m s^{-1}. Such instruments are designed to be very robust in all sorts of extreme weather conditions, and to record accurately conditions that are important to weather forecasting, and to the

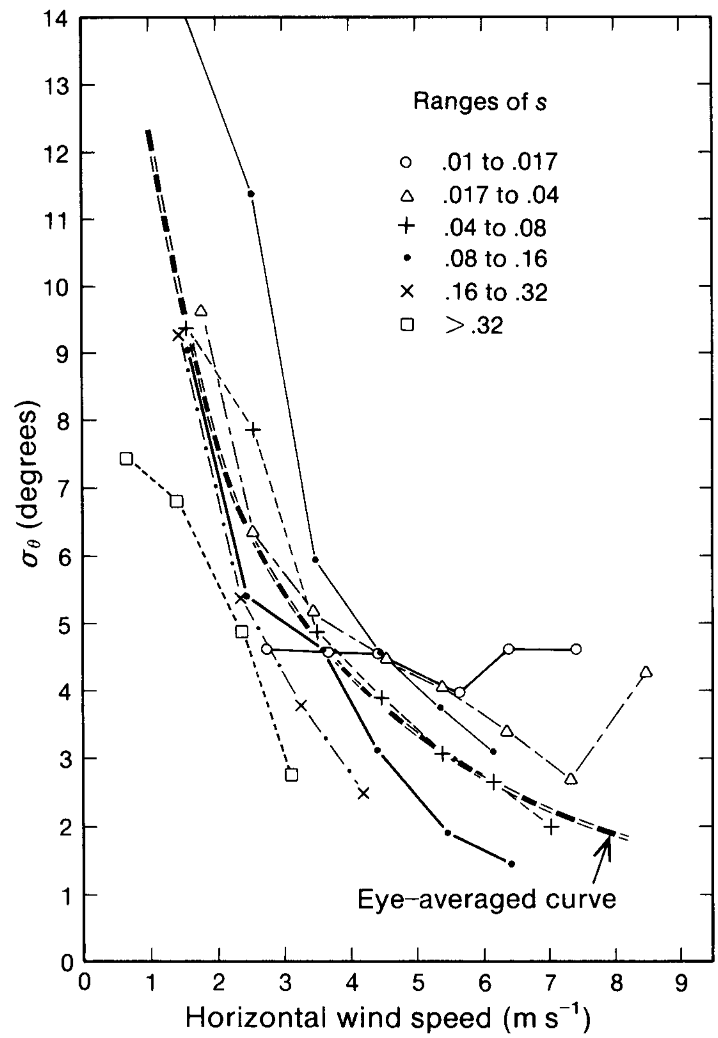

Figure 4. Fluctuations in wind direction (σ_θ) for various ranges of measures of stability (s) over 3-minute sampling periods, from Smith and Abbott (1961). The stability parameter s was defined as $(T_{7.1\ m} - T_{1.2\ m})/u^2_{15.5\ m}$. The eye-fit curve is close to $\sigma_\theta = 15/u$, implying $\sigma_v = 1.26$ m s^{-1} for 3-minute samples.

Table II. The standard procedure for assessing wind speeds by Meteorological Office observers. Instrument movements are assessed over the 10 minutes prior to the observation.

Anemometer	No movement	No movement	Occasional movement	Movement
Wind wave	No movement	Some movement	Some movement	Movement
Classed as:	Calm	2 kn	3 kn	4 kn or above as indicated

Standard instrument and recording errors:
Wind direction (vanes): starting speed 1–2 kn, direction recorded to nearest 10°.
Wind speed (anemometers): cups on standard instruments start to rotate when speed >4–6 kn.

safety of the public. This they do well. However there is obviously a need for more sensitive instruments for pollution purposes. Anemometers of the 'Porton' type are good examples and many automatic weather stations now on the market are equipped with one of these. Wind speeds can be measured accurately down to 1 knot. Unfortunately, although there are believed to be over 200 of these in operation around the United Kingdom, the great majority are privately owned and are not connected up to any network where the results are available to other potential users. Ideally, what is required is for a network of such improved instruments to be installed and maintained by some authority with pollution responsibilities at sites across the country where pollution episodes are most probable.

Unfortunately with the standard instruments commonly used the wind speed has to be subjectively assessed at low values using the procedure set out in Table II. Inevitably this must introduce some error.

1.3 Topographical control greater than geostrophic control

A third possible criterion could arise from consideration of the relative importance of geostrophic and topographical controls over the motion of the air. In light winds the geostrophic control becomes weak, and the influence of slopes, hills and valleys and coastlines becomes relatively more important. Theoretical and experimental studies would be required in any locality to establish some sensible criterion for that locality.

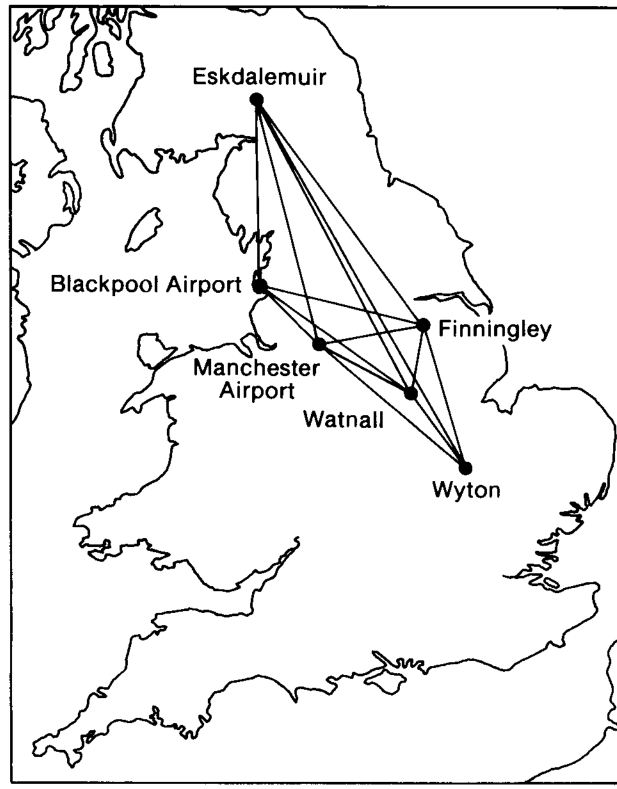

Figure 5. The locations of the six stations used in the study of wind differences as a function of station separation.

2. Measurement problems

2.1 Representativeness

Most releases, whether they be continuous or accidental, usually occur some distance away from where meteorological data are available. In applying algorithms or models to predict the likely consequences, the best meteorological data are required. Wind direction is probably the most important of all these data since this determines whether or not any potential receptor is likely to be affected by the plume. In interpolating the winds from neighbouring meteorological stations to the site, or from instruments on the site of the emission to points in the plume at various distances downwind, the danger of introducing significant errors is all too clear.

Fig. 5 shows the location of six meteorological observing stations in the United Kingdom. Four of these are lowland inland stations, Blackpool Airport is an exposed coastal site and Eskdalemuir is in the Scottish Southern Uplands at an altitude of 242 m above sea level.

Hourly values of wind direction (which are recorded to the nearest 10°) have been compared between all the stations whenever the wind speed at Wyton was less than 5 knots or, separately, greater than 20 knots. The station separations range from 55 km (between Watnall and Finningley) and 370 km (between Wyton and Eskdalemuir). For Wyton wind speed less than 5 knots the r.m.s. wind direction difference increases sharply with range from under 35° at 55 km to 63° at 370 km in January and February, 1990. The results are plotted in Fig. 6. Although there is scatter, the points above the dashed lines contain all the points involving Blackpool, the site most influenced by a major topographical feature — a coastline.

The implied values of σ_θ for the low wind speeds are significantly larger than those for the high wind speed class plotted on the same figure. This implies, of course, that at low wind speeds the geostrophic control becomes less and topographical influences are more important. It may also imply that the geostrophic wind itself is more spatially variable in situations of light winds. Fig. 7 compares the r.m.s. differences for light winds for June with those for Jan.–Feb. 1990. It shows that the June values tend to be significantly larger by some 20°. This is probably due to the generally weaker and more variable synoptic winds in June compared to the winter adding an extra factor to the effect of nocturnal surface inversions creating light low-level winds.

A similar study has been made by Lockhart and Irwin (1981) on the St Louis RAPS data. Here the station separations were on a rather smaller scale ranging from 0.1 to 80 km. The values are given in Table III and are

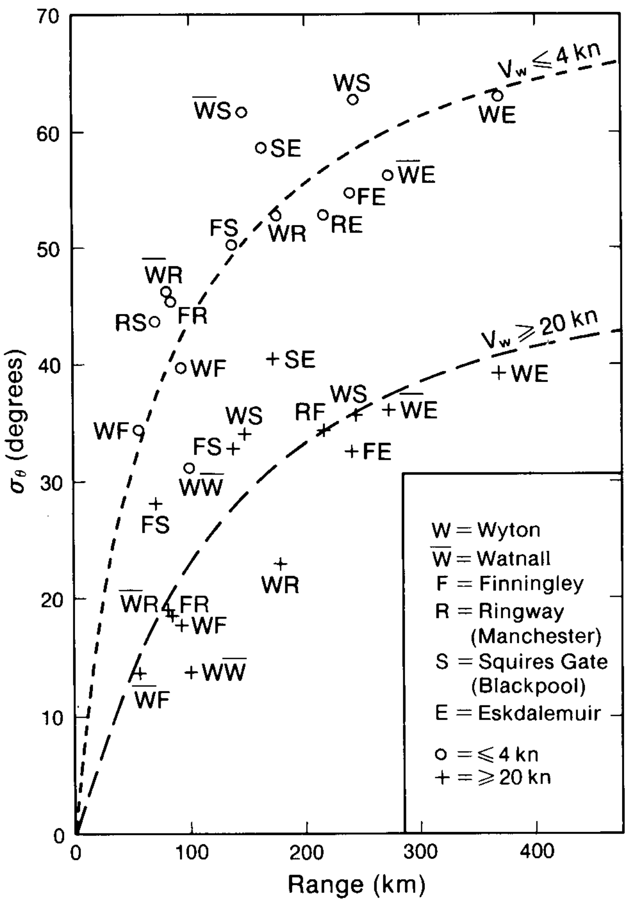

Figure 6. A comparison of r.m.s. wind-direction differences with range between six sites in the United Kingdom for Jan.–Feb. 1990. See Fig. 5 for station locations and text for an explanation of layout.

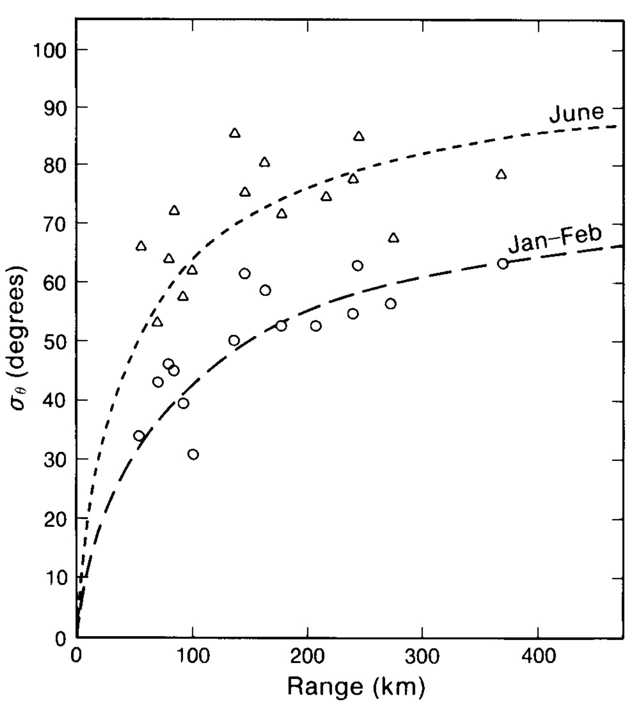

Figure 7. A comparison of r.m.s. wind direction differences in June and Jan.–Feb. 1990 for light winds at Wyton (occurring mainly at night) with distance separation between sites. See Fig. 6 and text for explanation of symbols.

Table III. Root-mean-square differences in hourly wind speed (u) and direction (θ) from 25 stations (with separations between 3 and 80 km) within the St Louis network as a function of distance, using high-quality instruments. The following empirical formulae appear to represent these values: $\sigma(u_a-u_b) = 0.47 + 0.24\ln(x)$ and $\sigma(\theta_a-\theta_b) = 15 + 5.7\ln(x)$. The constant first terms on the right-hand side of the two formulae could be larger if less accurate instruments were to be employed.

Separation (x (km))	$\sigma(u_a-u_b)$ (m s^{-1})	$\sigma(\theta_a-\theta_b)$ (°)
0.1	—	2
0.5	0.3	11
1.0	0.5	15
2.0	0.64	19
5.0	0.86	24
10	1.02	28
20	1.2	32
40	1.4	36

broadly consistent with the values and curves shown in Figs 6 and 7. Fig. 8 show the RAPS values plotted against wind speed for stable, neutral and unstable conditions. The values from all combinations from the 25 stations are grouped together, and the curves show that the r.m.s. differences in both direction and speed increase significantly as the wind speed becomes small.

2.2 Accuracy in low winds

The problems in accuracy of measurement have already been touched on earlier, and won't be repeated. As we saw, the accuracy depends very much on the instruments being used, and the recent improvements point to a gradual improvement in general accuracy in the future.

2.3 Surrounding topography and roughness length (z_0) changes

Almost all stations are influenced to a greater or lesser degree by the inhomogeneous nature of the terrain surrounding the site and its instruments. At most stations, the wind profile suggests an increase in effective roughness length with height, so that in neutral conditions for example the profile is not logarithmic as predicted by theory. In light winds, especially at night in stable conditions, the wind profile may be strongly influenced by a wide variety of features stretching up to many kilometres upwind. An example of this will be seen later when we compare the statistics of light winds at Eskdalemuir with those at other stations.

3. Frequency of occurrence and persistence

3.1 Time-of-day occurrence

Inspection of records of wind speed at observing

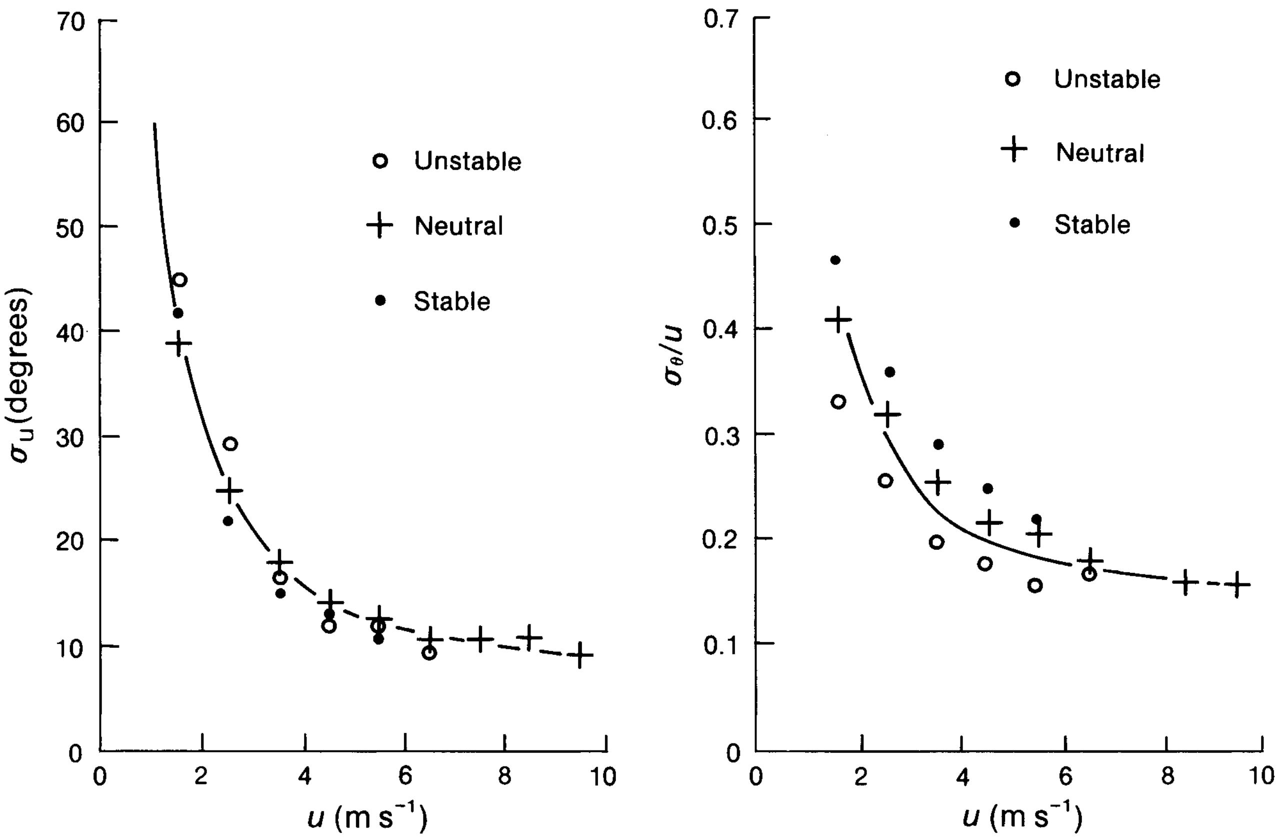

Figure 8. Variation of spatial σ_θ and σ_u/u with wind speed and stability for hourly St Louis data. The spatial standard deviations are calculated from concurrent observations at 25 monitoring stations. Empirical equations are also drawn on the figures: $\sigma_\theta^2 = (5°)^2 + (60°/u)^2$ and $(\sigma_u/u)^2 = (0.15)^2 + (0.6/u)^2$.

stations reveals, as expected, that the majority of light-wind cases occur at night with clear skies or broken cloud, when the lower boundary layer becomes stably stratified. This is particularly true whenever the surrounding terrain has sufficient trees, or other large obstacles, to extract momentum from these lower layers to leave almost windless conditions below the height of the obstacles. Immediately above, a rather turbulent jet tends to exist, which may be only a few metres deep, with a more quiescent airflow above. Cases of daytime calm or light winds tend to occur in the centre of large regions of high pressure in winter or summer (although in the latter, convectively driven motions may give a semblance of a mean light wind).

Data from Finningley are fairly representative of the diurnal cycle. The four months of January, February, June and July, 1990, have been analysed in terms of time of day. The results are shown in Fig. 9. The size of the sample is small and may have introduced unrepresentative aspects of detail, but the general trends are probably correct. It can be seen that calms are a feature of night-time and the early morning, with no cases occurring in the sample from 11 to 19 UTC. Light winds, recorded as 2 knots, show a marked maximum between midnight and 09 UTC with a smaller maximum around 18 UTC and two minima around 14 and 20 UTC. The curves for slightly higher wind speeds (3 knots and 4 knots) show a much more uniform diurnal distibution with, however, a minimum around 18 UTC and a maximum around 22 UTC.

3.2 Monthly occurrence

Fig. 10 gives an example from Ringway (Manchester Airport) of the month-to-month variation in the percentage frequencies of light winds with speeds less than or equal to 3 knots. The figure shows not only the mean monthly frequencies, but also the year-to-year r.m.s. variations in the mean and the extreme values over a 10-year period from 1981 to 1990. The figure also shows that the period from January to March tends to have the fewest light-wind hours, with the greatest number occurring in November, and the season with the greatest number being summer.

Fig. 11 shows the percentage probability of the hourly averaged wind being less than any specified value calculated from data collected during the four months January, February, June and July, 1990. It implies an almost constant probability of the speed lying in any fixed speed band out to about 4 knots.

Fig. 12 shows the percentage number of hours with the wind speed less than or equal to 3 knots, by month, averaged over the same six stations used earlier. As at Ringway, the winter period shows the least number with the greatest number during the summer months and in November.

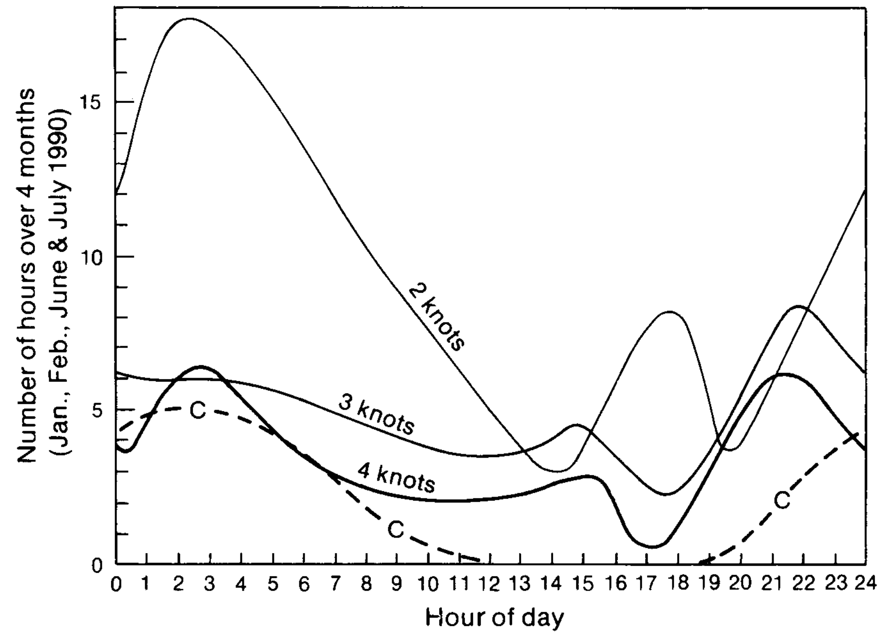

Figure 9. The diurnal cycles of light-wind frequencies (C = calms) at Finningley during the four months shown.

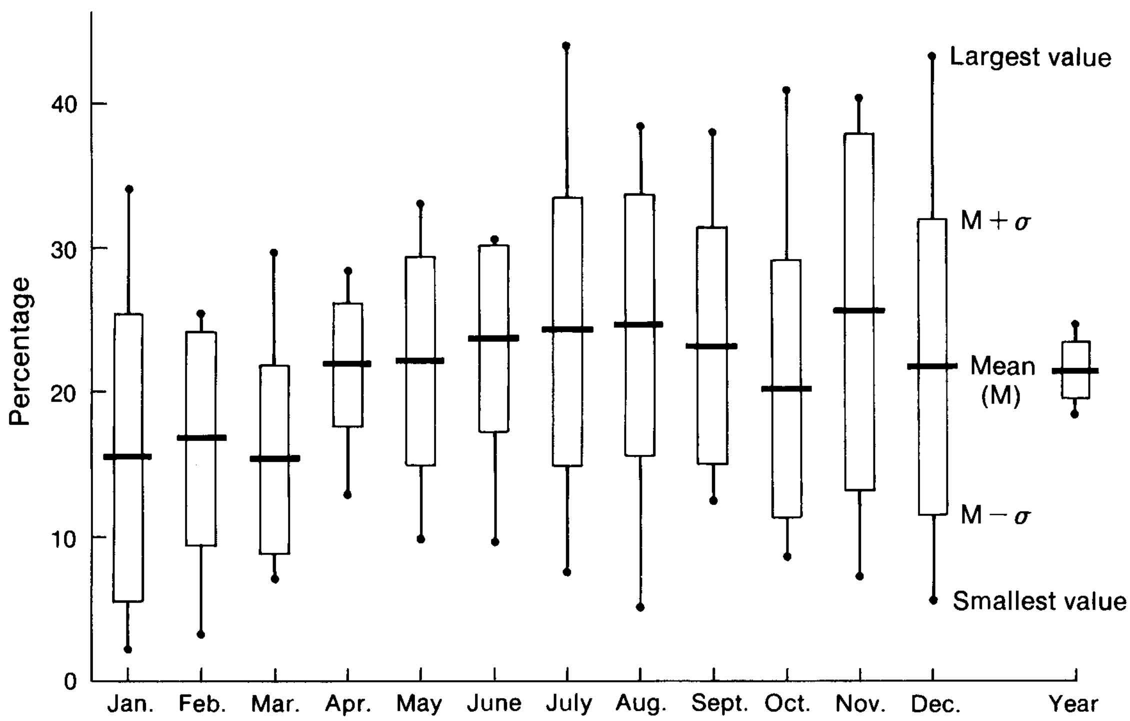

Figure 10. The percentage mean-monthly frequencies of winds ≤ 3 knots at Manchester Airport over the 10 years from 1981 to 1990. A measure of the variation is also included.

3.3 Location occurrence

Table IV gives value of percentage frequencies of hours when the wind speed at 10 metres was less than 4 knots at the same six stations, divided accorded to month. Table V gives the annual figures averaged over the 10 years from 1981 to 1990. It comments on the large frequencies found at Eskdalemuir where it seems that the influence of higher hills within several kilometres of the site causes significant sheltering whenever the gradient wind is fairly light. At first it was thought that the sheltering may have been due rather more to the surrounding forests, but this seems to be unlikely since a comparison of comparable statistics for the decade 1961–70 shows relatively small differences even though the conifers were much smaller at that time. Such differences as are evident can easily be explained by: natural decade-to-decade variations, and a change during the mid 1960s to a better anemometer at Eskdalemuir. Overall the table shows that the frequency

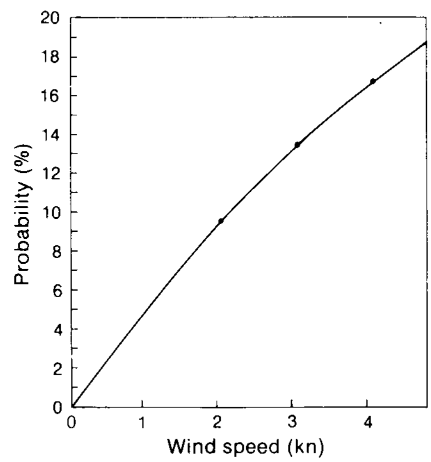

Figure 11. Percentage probability of the hourly 10 m wind lying below a specified value at Manchester Airport during the same months as in Fig. 9.

of light winds varies quite markedly between sites, and this must provide a warning that simple interpolation to any potential emission site has to be carried out with considerable care taking into account all the factors involved.

3.4 Persistence

The persistence of light-wind situations is revealed from an analysis of hourly data from the inland lowland site at Ringway. Fig. 13 shows the cumulative percentage probabilities that the wind speed is less than or equal to 2, 3 or 4 knots for any specified number of consecutive hours. Between 40 and 60% of cases last for one hour only, but beyond that the probability distribution is consistent with a Guassian or Normal distribution, giving straight lines on the graph. Thus there is a 10% probability that given one hour of wind speed 2 knots or

Figure 12. Percentage number of hours with wind speed ≤ 3 knots averaged over the six stations of Fig. 5 for the 10-year period from 1981 to 1990.

Table IV. Percentage frequencies of hours when the wind speed at 10 m was less than 4 knots at six stations in the United Kingdom, divided according to month

Month	Watnall	Ringway	Squires Gate	Finningley	Eskdalemuir	Wyton
Jan.	11.2	15.5	7.6	13.1	25.9	8.9
Feb.	11.6	16.8	6.7	17.1	27.1	10.1
Mar.	12.1	15.3	7.5	13.0	22.8	7.8
Apr.	15.0	21.8	11.2	18.7	30.5	12.0
May	15.2	22.0	9.8	18.7	29.2	14.3
June	18.4	23.5	9.6	20.8	30.8	15.3
July	19.1	24.0	8.8	21.8	32.2	15.0
Aug.	19.2	24.4	9.6	21.9	28.3	15.2
Sept.	19.0	23.0	10.1	20.8	32.5	15.8
Oct.	18.2	20.0	9.4	21.5	30.4	14.7
Nov.	17.4	25.3	11.0	19.8	33.6	15.2
Dec.	14.1	21.5	9.7	16.8	32.5	11.1
Year	15.8	21.1	9.2	18.7	29.7	13.0

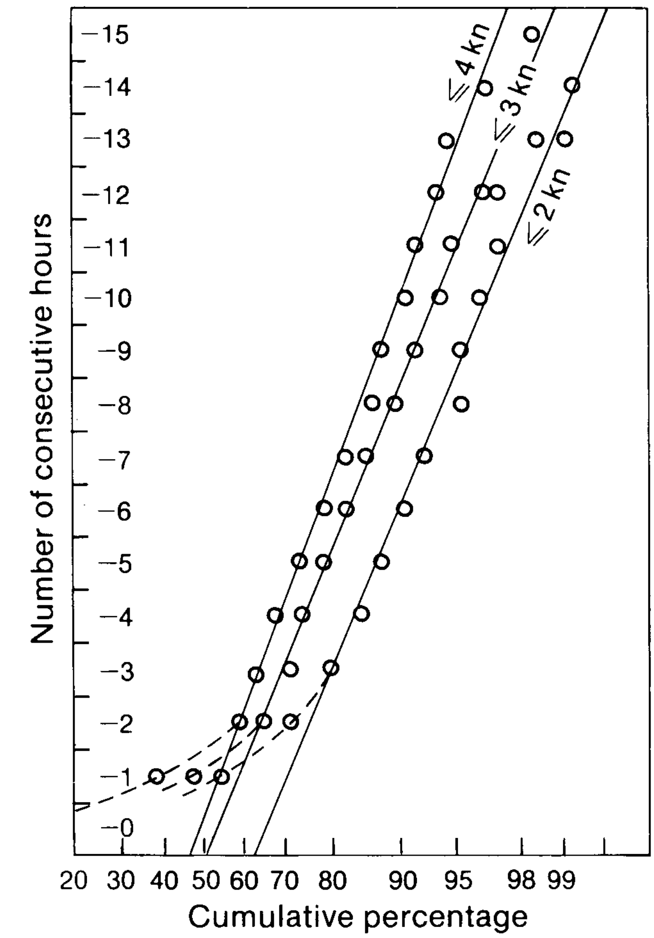

Figure 13. Persistence of light winds at Ringway, e.g. 90% of runs with wind ≤ 2 knots last 6 hours or less, and 7% of all runs with wind ≤ 2 knots last between 6 and 10 hours.

less, the speed will persist in this band for six consecutive hours or more.

4. Relation between surface and upper winds

Rossby Similarity Theory predicts that, over a very uniform and extensive terrain in rather stationary conditions, the surface wind and the geostrophic wind should be related as functions of Kazanski–Monin Stability parameter μ (which includes the heat flux), the surface roughness z_0, and the Coriolis parameter f. Arya (1975) provided empirical forms for this relationship, but as his data showed, considerable scatter is apparent, in part due to the lack of ideal conditions almost always prevailing (see Fig. 14).

The same sort of scatter is apparent in Fig. 15, which shows a comparison of the ratio V_{10}/V_{1000} plotted against the 1000 m wind V_{1000}. The 10 m wind was taken from a surface-based anemometer, and the 1000 m wind from radiosonde data, both originating from Crawley (Gatwick) in Surrey. The results are subdivided according to time of day: 00, 06, 12 and 18 UTC. All show considerable scatter and no obvious systematic varation with V_{1000}. At night the average value of the ratio is about 0.23 with most points lying within ±0.10 of that value. At 06 UTC the scatter is even more extreme with no obvious division according to estimated sensible heat flux at the ground. Conditions are clearly too transitional to provide any guide to the magnitude of the ratio.

At 12 UTC, the amount of scatter is still very large with no certain division according to estimated heat flux, although there is a suggestion that the average value of the ratio is somewhat higher (0.63) in clearly

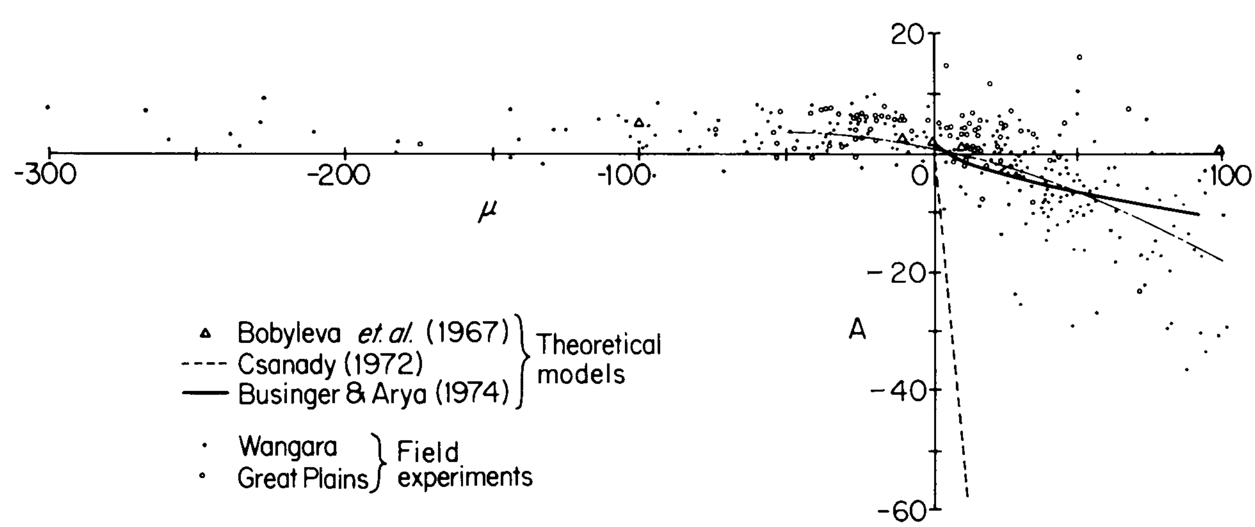

Figure 14. The form of one of the parameters in Rossby Similarity Theory, showing the amount of data scatter.

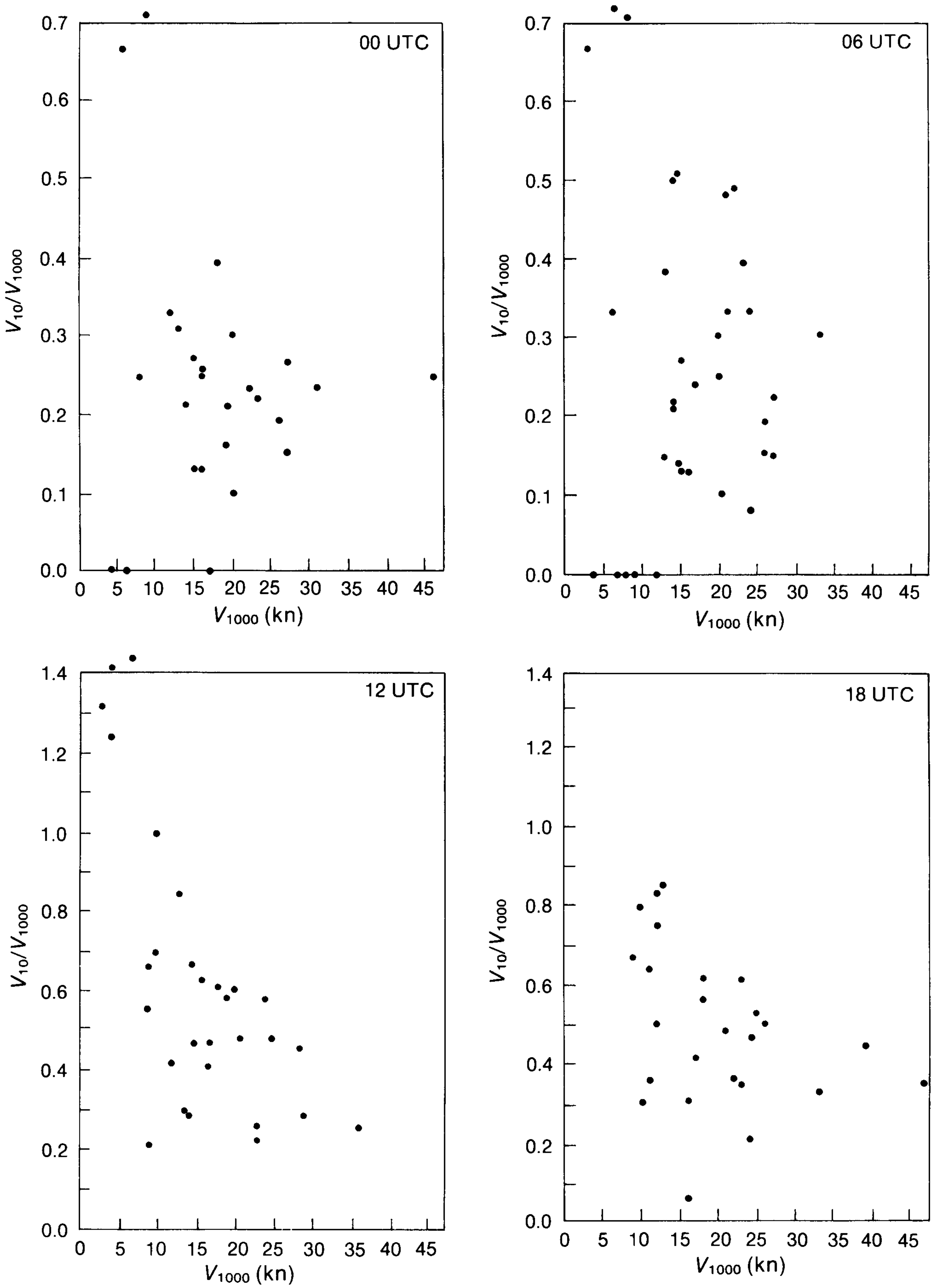

Figure 15. A comparison of the ratio V_{10}/V_{1000} plotted against the 1000 m wind, V_{1000}, at the times shown for Gatwick during June 1990.

Table V. Percentage frequencies of hours of calms and light winds over the 10-year period 1981–90, for the six stations in Table IV

Station	Calms	<4 kn
	Percentages	
Watnall	1.4	15.8
Ringway	2.3	21.1
Squires Gate	0.6	9.2
Finningley	2.7	18.7
Eskdalemuir	6.6	29.7
Wyton	2.0	13.0

Note. The frequencies for Eskdalemuir are somewhat surprisingly large for a station 242 m above mean-sea-level in the Scottish Uplands. The area around the site is largely forested except to the north. It is in a slight hollow on the shoulder of a valley running north–south. At a range of a few miles it is surrounded by higher hills. It seems that the hills provide sufficient sheltering to produce very low 10 m winds when the gradient winds are fairly light. From a directional analysis of these light-wind cases (often at night) it seems that the anemometer is often being affected by northerly gravitational flows.

unstable conditions, than in near neutral conditions (0.46). There is perhaps also an increase in the scatter at lower wind speeds which implies that Rossby Similarity Theory is on even more shaky ground at low speeds.

At 18 UTC, the scatter is slightly less with a mean value of the ratio again lying somewhat near 0.46 (with most points lying within 0.26 of the mean) apparently appropriate to near neutral conditions.

Similar studies, concentrating on higher wind speeds and on coastal sites, are reported in the *Handbook of Weather Forecasting* produced by the Meteorological Office, and come to similar conclusions.

References

Arya, S.P.S., 1975: Geostrophic drag and heat transfer relations for the atmospheric boundary layer. *Q J R Meteorol Soc*, **101**, 147–161.

Hanna, S.R., 1983: Lateral turbulence intensity and plume meandering during stable conditions. *J Clim and Appl Meteorol*, **22**, 1424–1430.

Lockhart, T.J. and Irwin, J.S., 1981: Methods of calculating the 'representativeness' of data. Oak Ridge, Tennessee, National Laboratory.

Smith, F.B. and Abbott, P.F., 1961: Statistics of lateral gustiness at 16 m above ground. *Q J R Meteorol Soc*, **87**, 549–561.

551.551.5:551.558(235.13):629.7

Incident above Zanjan

R.W. Lunnon*
Meteorological Office

At 2347 UTC on 29 November 1989, a British Airways Boeing 747 was near the town of Zanjan (Fig. 1) in the Zagros mountains while *en route* from Bahrain to London. Suddenly the aircraft pitched up, lost air speed, and fell from flight level (FL350 (238 mb, approximately 35 000 ft)) to FL260 (360 mb, approximately 26 000 ft). The pilot was so disconcerted by this occurrence (understandably!) that he issued a 'mayday' call. However, at FL260 he managed to level off and the flight continued to London.

The nearest radiosounding was from Lenkoran (WMO number 37985) on the south-west coast of the Caspian Sea. Fig. 2 shows it has almost neutral static stability from 210 mb (FL390) down to 425 mb (FL220) at potential temperature of 47 °C; in conjunction with the fairly light winds at low levels this would seem to rule out classical mountain waves.

The infrared image from Meteosat at the time of the incident is shown at Fig. 3, with coastlines and the approximate track of the aircraft shown, ending at the location of the incident. The topography of this region is dominated by ridges running from south-east to north-west with valley bottoms at about 1500 m and ridge tops at 2500 m — this is shown in Fig. 1. The spacing between the ridges is about the same as that of the lines convection apparent in Fig. 4, an enlargement of the area of interest. It is believed that the incident was caused by convection whose scale and orientation were determined by orographic effects. It is considered that the aircraft encountered a downdraught associated with the convection and that this caused the 9000 ft height loss. The wind at the time and location was south-westerly at 60 knots, which is roughly perpendicular to the ridges and convective lines.

It is not known how common this type of occurrence is. What are believed to be classical mountain waves are seen quite frequently in satellite imagery, but it is rare for a check to be made on the stability to establish the true cause. It is worth noting that downdraughts are inherently more dangerous than updraughts, partly because they cause aircraft to accelerate downwards, and partly because they are not usually marked by cloud or precipitation and are therefore invisible. Downdraughts at high level should be apparent on water-vapour imagery as dry zones, as was the case here. It would probably be worth inspecting water-vapour imagery in the vicinity of mountains for evidence of mountain wave activity in cloud-free conditions for this particular threat to aircraft safety.

* The preliminary investigation of this incident was carried out by Dr D.A. Forrester and K. Grant.

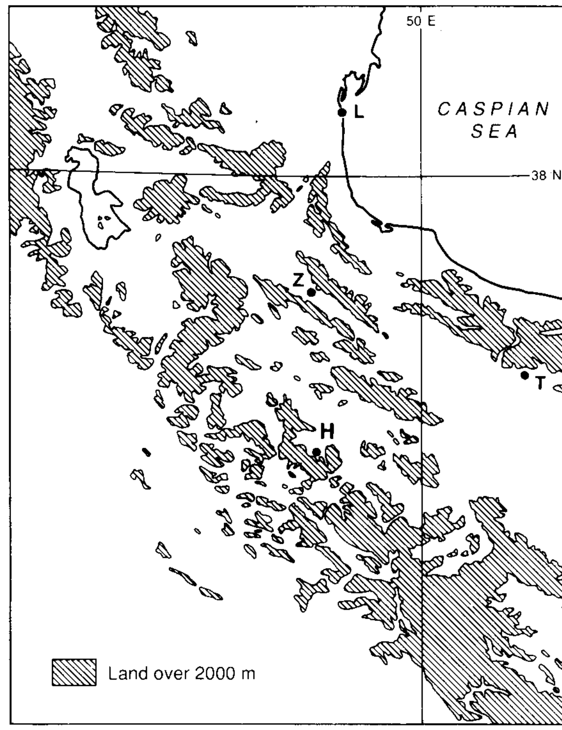

Figure 1. Map of the area of the incident showing the south-east to north-west orientation of the ridges. Z is Zanjan; L is Lenkoran; T is Tehran; H is Hamadan.

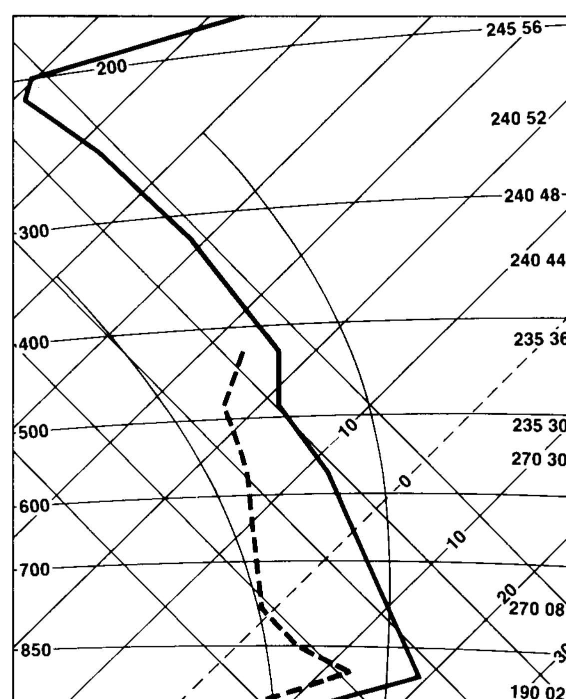

Figure 2. Tephigram for Lenkoran 0000 UTC on 30 November 1989 showing near-static stability between 210 mb and 425 mb. Pressures in mb, wind speeds in knots and temperatures (°C).

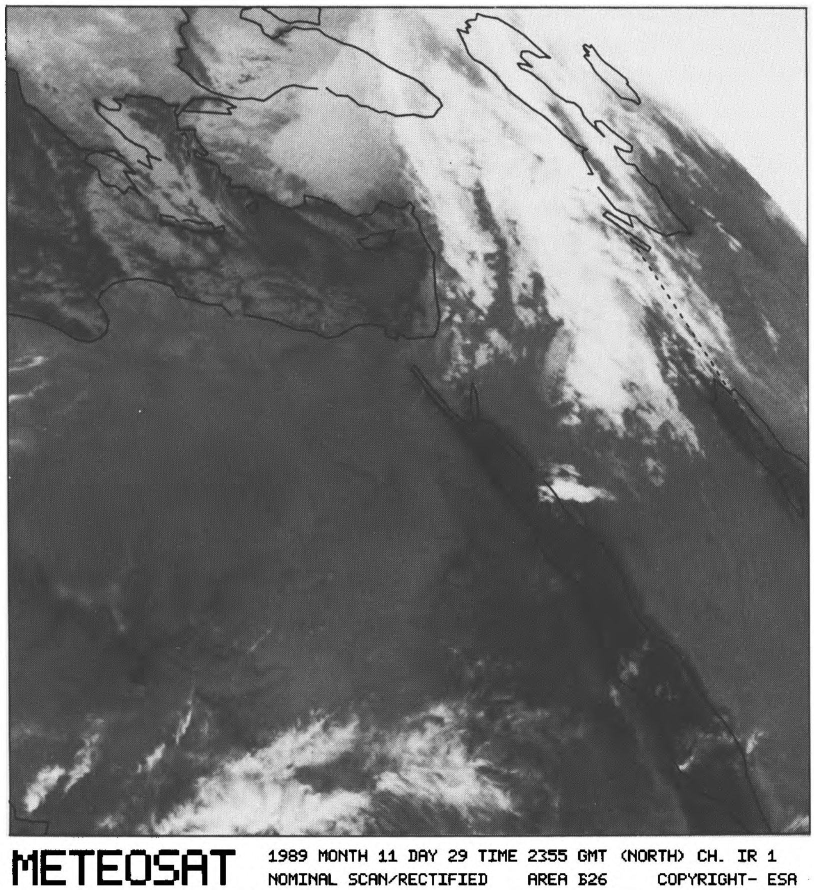

Figure 3. Meteosat infrared image around the time of the incident showing the flight path from Bahrain to Zanjan.

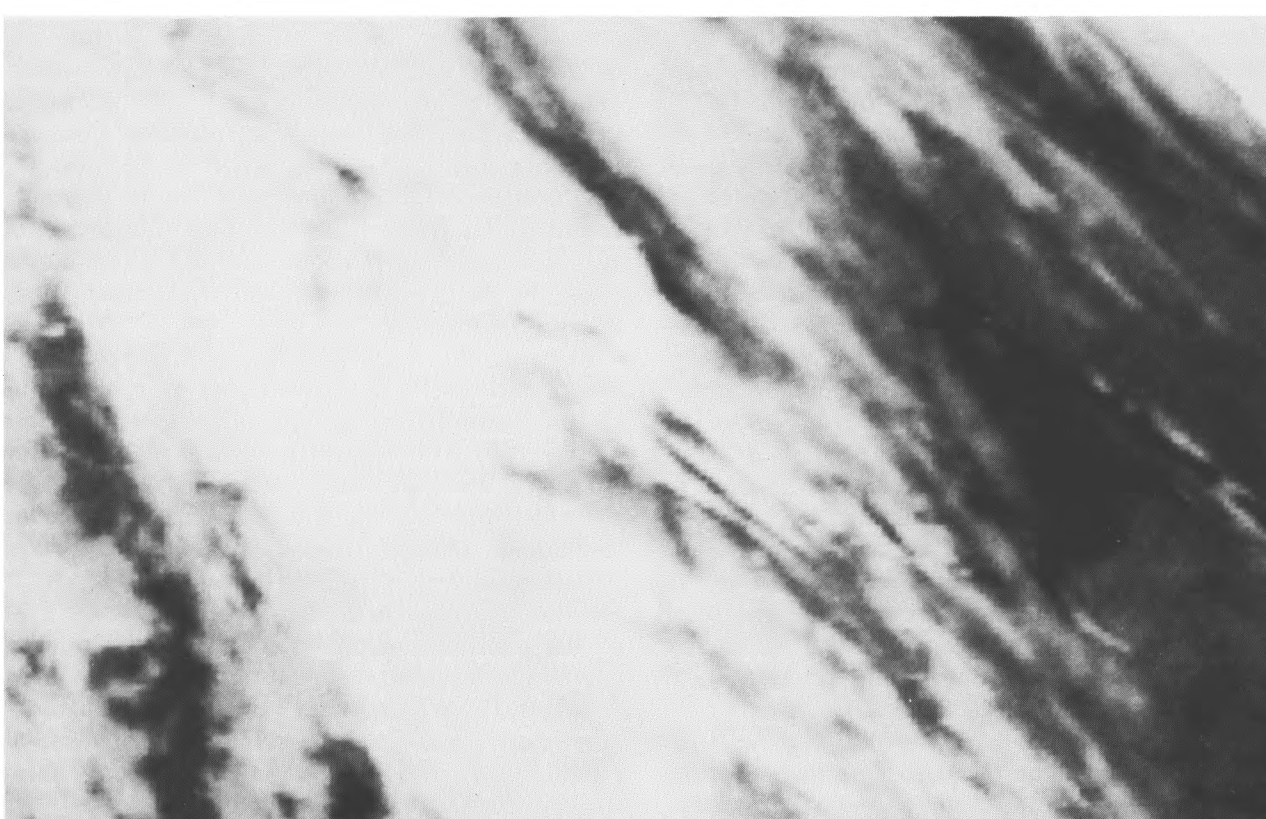

Figure 4. This is an enlargement of part of Fig. 3 showing clear-cut straight edges to the clouds in the area of the incident.

Reviews

Theoretical geophysical fluid dynamics, by A.S. Monin. 165 mm × 246 mm, pp. xii+399, *illus.* Dordrecht, Boston, London, Kluwer Academic Publishers, 1990. Price £99.00, $149.00. ISBN 0 7923 0426 8.

In this ambitious monograph based on a lecture course delivered at the Moscow Institute of Physics and Technology, Professor Monin presents a valiant attempt to cover an astonishing range of topics in the study of the dynamics of some geophysical fluids, namely the Earth's liquid core where the geomagnetic field originates, the mantle of the Earth, the oceans, and the lower atmosphere. With the exception of the mantle, which behaves like a highly viscous fluid when subjected to long-term forcing (but like an elastic solid at seismic frequencies), Coriolis forces due to the Earth's general rotation relative to an inertial frame exert a dominant dynamical influence on large-scale flows. Buoyancy forces associated with stable (i.e. bottom-heavy) density stratification are also dynamically important in the cases of the atmosphere and oceans; Lorentz forces associated with electric currents and concomitant magnetic fields are dynamically important in the liquid core. Professor Monin is one of a very small number of scientists who have studied the dynamics of all these regions of the Earth, and his book amounts to a personal (not always up-to-date) view of his areas of interest.

General concepts and basic dynamical processes are treated in the first two sections of the book, which deal with the basic equations of geophysical fluid dynamics, the theory of small amplitude oscillations in rotating stratified fluids, including oscillations of an isothermal atmosphere and Rossby waves, baroclinic and other types of instability, and turbulent flows. A fluid is often thought of as differing from a solid through its inability to support shear (vorticity) waves. Rotation, stable density stratification or, in the case of electrically conducting fluids, magnetic fields, bestow a quasi-rigidity to the fluid which enables disturbances to propagate over large distances through the agency of shear waves, which in general are both dispersive and anisotropic. Finite amplitude effects can give rise to soliton-type behaviour. In many cases the waves are generated by internal instabilities (e.g. baroclinic instability associated with horizontal density gradients) or interactions with irregular boundaries.

Applications are treated in the final section of the book, with chapters on the general circulation of the atmosphere and ocean, theory of climate, and the dynamics of the Earth's core and mantle. As in previous sections, for reasons that are by no means clear, the references cited in the text are not always up-to-date and many do not appear in the reference list at the end of the book. These and other shortcomings in the editing of the monograph make it hard for this reviewer to give more than a qualified recommendation to this interesting and wide-ranging discussion of geophysical fluid dynamics by one of its most distinguished practitioners.

R. Hide

History of the Commission for Agricultural Meteorology of the World Meteorological Organization, prepared by W. Baier, I.G. Gringof, N.D. Strommen. 205 mm × 292 mm, pp. x+197, *illus.* Geneva, WMO, 1991. WMO/TD No. 440.

At the 1987 Commission for Agricultural Meteorology (CAgM) Meeting in Madrid delegates approved the appointment of a Task Force to write a history of CAgM. The result is a very readable book packed with vital information about the work done by CAgM and those who have contributed to its success.

The book comprises four chapters and a series of annexes. To quote from Dr Baier's preface 'Chapter 1 presents an introduction to the historical development of the Commission within the International Meteorological Organization and the World Meteorological Organization. Chapter 2 looks at the early history and development of IMO and the Commission for Agricultural Meteorology. Chapter 3 deals with the transition of IMO to WMO, the formation of CAgM and its relationship to other technical bodies of WMO and to the Regional and international organizations. Chapter 4 forms the main body of the report. It describes the development of CAgM from the first to the ninth session, primarily from the viewpoint of policy, plans and goals including terms of reference, collaboration with other WMO bodies and with other national and international agencies.'

There are nine Annexes to the report. They include a Who's Who of all those who have ever served the Commission including rapporteurs, delegates, observers and members of the Secretariat — it is a long list running from page 79 to page 155. Details of all the CAgM Sessions are given in Annex 2, together with a list of the resolutions, recommendations and appointments made by each session. There are also lists of WMO and WCP publications related to the activities of CAgM and a list of the published proceedings of seminars, training courses and technical conferences sponsored by CAgM or attended by WMO. Annex 8 gives a brief chronology of relevant events from the First International Meteorological Conference, Brussels in 1853 up to the Fourth Norbert Gerbier Mumm Award in 1990.

As already indicated the heart of the book is chapter 4 — it gives readers abbreviated biographies of the six presidents and describes the progress made by CAgM under the individual presidencies.

In the early period under Burgos (Argentine) and Bourke (Ireland), the role and limits of agrometeorology were examined; attempts to merge the Commission with the Commission for Climatology were successfully resisted and the terms of reference of the Commission more rigorously defined; technical regulations were devised and co-operation with international organizations was established and set on a firm footing. Among the topics of special interest studied during the latter part of this period were forestry, tropical agrometeorology, and locust control.

The presidencies of Smith (United Kingdom) and Baier (Canada), spanning the years from 1967 to 1974, were a time during which there were increasingly prolonged periods of drought in many areas of the world and major food shortages. The problems were exacerbated by the massive rises in oil prices which affected the economies of both developing and developed countries all over the world. As a result of these pressures there was a major change in direction of the Commission's work, from data gathering to solving urgent operational problems such as the role of meteorology in the protection of the environment and natural resources, how agrometeorology could aid world food production and how relevant technologies could be transferred to developing countries. It was during this period that the World Weather Watch programme was devised and the CAgM was able to advise on, among other matters, the information required for the monitoring of global food production from weather data.

During this period two innovations were made that are still operational today, namely the setting up of an Advisory Working Group (AWG) and the system of appointing Rapporteurs.

The AWG is a small select group of experts appointed by the Commission to assist the President with various statutory duties and to assist with urgent unforeseen business arising between sessions. This was necessary because of the greatly increased workloads faced by the presidency during L.P. Smith's time.

Prior to this period the technical work of the Commission had been handled by working groups but financial restrictions on the Commission now meant that only ten could be sustained at any one time. During an era when giant strides were being made in new technologies this was seen to be a serious problem. The solution hit upon was to appoint Rapporteurs, i.e. acknowledged experts in particular fields who were willing, voluntarily and freely, to undertake specific investigations, for the benefit of CAgM, and to provide written reports for CAgM, to be issued later as WMO publications.

The most recent period considered by the Task Force covers the years from 1974 to 1986 under the presidencies of Baier, Gerbier (France) and Kassar (Tunisia). The critical food shortages of the early years were eventually turned into food mountains in some countries, largely due to improved agricultural practices and new technologies but also improved global weather conditions. The 5th President, Norbert Gerbier (who died in October 1985), pointed out that in 1982, while overall world food production looked good it had in fact fallen in 33 of the 69 developing countries, with significant losses being caused by pests and diseases and thus there was considerable scope for agrometeorology to play a decisive role in minimizing losses and increasing production.

These recent years have very busy ones for the Commission, both technically and administratively, and it was particularly pleasing for the Commission to see their roving seminars, fellowship schemes and their training missions to 55 countries, bear fruit in the form of an increased involvement of developing countries in the Commission's affairs.

There is a note on page ii that this book has been produced without editorial revision by the WMO Secretariat and it comes as no surprise to find a number of small, irritating typographical errors — for instance, did the first meeting of Directors of European Meteorological Services really take place in 1735 as indicated on page 2? The new Chairman of CAgM, Professor C. Stigter, has no doubt noticed that his name has been misspelt on page 180 (but not on pages 143 or 189). The readability of the book would have been improved significantly if the three periods described above had been treated as separate chapters, or if the various subsection headings had been emphasized differently.

The Task Force have produced a most interesting book which deserves a wide readership. It will be of particular value to CAgM delegates both old and new; the latter will find it very useful for reference purposes — the Who's Who Annex especially. It will also be welcomed by those interested in the history and development of agrometeorology, though they will not be able to identify contributions made by individual countries. Bearing in mind that these Commissions do have political influence, they will perhaps find clues as to why particular policies were followed at particular times. They will also find this book a very good complement to the descriptive history of CAgM given in Sir Arthur Davies' book *40 Years of Progress and Achievement: a Historical review of WMO.*

Finally it is worth noting that the recent CAgM meeting urged Members to produce histories of their own agrometeorological services as a way of increasing awareness of the value of agrometeorology. We can already look forward with anticipation to the histories, soon to be published, of the Canadian and Chinese agrometeorological services.

P. Harker

Air traffic and the environment — Background, tendencies and potential global atmospheric effects, edited by U. Schumann. 165 mm × 241 mm, pp. vi+170, *illus.* Berlin, Heidelberg, New York, London, Paris, Tokyo, Hong Kong, Springer-Verlag, 1990. ISBN 3 540 53352 4.

This slim review of the potential environmental impacts of air traffic can be broken down into three main sections: the nature and extent of aircraft emissions, potential chemical impacts leading to changes in radiatively active trace species and perturbations to the distribution of water vapour and cirrus clouds.

These notes start off by considering the geographic extent and likely magnitude of aircraft emissions, noting that the number of passenger miles is set to increase significantly over the next decade and that some of that increase will be above the more remote areas of the planet than is presently the case. Chapters 3 and 4 stay on the emissions theme and consider new hydrogen technology and the likely improvements in efficiency and reductions in emissions which may accrue from improvements to conventional engines.

The bulk of the fuel burnt in an aircraft engine is converted into carbon dioxide and water vapour, with much smaller quantities of nitrogen oxides, carbon monoxide and unburnt hydrocarbons. Chapter 5 reviews the background composition of the upper troposphere and lower stratosphere and tries to put the magnitude of aircraft emission into a relevant atmospheric context by assessing the likely perturbation to the background concentrations for a given, highly idealized, emission and dispersion scenario. From this analysis it is concluded that the aircraft emissions most likely to influence background distributions significantly are water vapour and nitrogen oxides. Chapters 6 and 7 describe the results from 2-D and 1-D model runs respectively, both employing emission scenarios which include a major growth in the number of high-speed civil transports (HSCT) flying in the mid-stratosphere. These studies conclude that if there is a major increase in HSCT and at the same time we manage to reduce the chlorine loadings from CFCs, then NO_x from HSCT may become the dominant anthropogenic sink of stratospheric ozone.

In addition to the chemical impacts which ozone may have in the stratosphere, the emission of large quantities of water vapour into a part of the atmosphere which is close to saturation may promote a change in the frequency of cirrus clouds. Chapters 8 and 10 considers the climate impacts from increased incidences of contrails and from extra water vapour generally, while chapter 9 considers methods for determining contrail coverage globally from space.

In the preface Schumann points out that the papers on which this document is based were gathered together prior to a 2-day seminar and there was little time to revise or edit those papers before publication. He asks that the deficiencies which arise from this approach be excused because of the more 'precise information' (perhaps he means more up to date?) and the early publication of the results. While it is clear that some of the material could have been improved had more time been taken, I am inclined to side with Schumann. While this will never be a classic text, it should provide a useful source document for scientists who are interested in the potential impact that aircraft emissions may have in the atmosphere.

Where this document is likely to be deficient is that it is directed in large part at the potential impacts of a fleet of high flying HSCT which may never be built, while not considering as fully the impact of the assured growth in conventional air traffic which could have dramatic impacts on the ozone and water budgets adjacent to the tropopause.

D.S. McKenna

Books received

The listing of books under this heading does not preclude a review in the Meteorological Magazine at a later date.

Climate, data and resources: A reference and guide, by E. Linacre (London, Routledge, 1992. £50.00 (hardback, £16.99 (paperback)) focuses especially on the sorts of observation which are made at a single climate station. Also included are modern-day methods of parametrization of surface conditions for computer modelling and interpretation of satellite observations. ISBN 0 415 05702 7 (hardback), 0 415 05703 5 (paperback).

Seasonal snowpacks: Processes of compositional change, edited by T.D. Davies, M. Tranter and H.G. Jones (Berlin, Heidelberg, New York), 1991. DM 288.00 (hardback)) contains the papers presented at the NATO Advanced Research Workshop held at Maratea, Italy, 23–27 July 1990. Biological, chemical and physical aspects of the subject are considered. ISBN 3 540 51760 X.

GUIDE TO AUTHORS

Content

Articles on all aspects of meteorology are welcomed, particularly those which describe results of research in applied meteorology or the development of practical forecasting techniques.

Preparation and submission of articles

Articles, which must be in English, should be typed, double-spaced with wide margins, on one side only of A4-size paper. Tables, references and figure captions should be typed separately. Spelling should conform to the preferred spelling in the *Concise Oxford Dictionary* (latest edition). Articles prepared on floppy disk (IBM-compatible) can be labour-saving, but only a print-out should be submitted in the first instance.

References should be made using the Harvard system (author/date) and full details should be given at the end of the text. If a document is unpublished, details must be given of the library where it may be seen. Documents which are not available to enquirers must not be referred to, except by 'personal communication'.

Tables should be numbered consecutively using roman numerals and provided with headings.

Mathematical notation should be written with extreme care. Particular care should be taken to differentiate between Greek letters and Roman letters for which they could be mistaken. Double subscripts and superscripts should be avoided, as they are difficult to typeset and read. Notation should be kept as simple as possible. Guidance is given in BS 1991: Part 1: 1976, and *Quantities, Units and Symbols* published by the Royal Society. SI units, or units approved by the World Meteorological Organization, should be used.

Articles for publication and all other communications for the Editor should be addressed to: The Chief Executive, Meteorological Office, London Road, Bracknell, Berkshire RG12 2SZ and marked 'For Meteorological Magazine'.

Illustrations

Diagrams must be drawn clearly, preferably in ink, and should not contain any unnecessary or irrelevant details. Explanatory text should not appear on the diagram itself but in the caption. Captions should be typed on a separate sheet of paper and should, as far as possible, explain the meanings of the diagrams without the reader having to refer to the text. The sequential numbering should correspond with the sequential referrals in the text.

Sharp monochrome photographs on glossy paper are preferred; colour prints are acceptable but the use of colour is at the Editor's discretion.

Copyright

Authors should identify the holder of the copyright for their work when they first submit contributions.

Free copies

Three free copies of the magazine (one for a book review) are provided for authors of articles published in it. Separate offprints for each article are not provided.

Contributions: It is requested that all communications to the Editor and books for review be addressed to the Chief Executive, Meteorological Office, London Road, Bracknell, Berkshire RG12 2SZ, and marked 'For *Meteorological Magazine*'. Contributors are asked to comply with the guidelines given in the *Guide to authors* (above). The responsibility for facts and opinions expressed in the signed articles and letters published in *Meteorological Magazine* rests with their respective authors.

Subscriptions: Annual subscription £36.00 including postage; individual copies £3.25 including postage. Applications for postal subscriptions should be made to HMSO, PO Box 276, London SW8 5DT; subscription enquiries 071–873 8499.

Back numbers: Full-size reprints of Vols 1–75 (1866–1940) are available from Johnson Reprint Co. Ltd, 24–28 Oval Road, London NW1 7DX. Complete volumes of *Meteorological Magazine* commencing with volume 54 are available on microfilm from University Microfilms International, 18 Bedford Row, London WC1R 4EJ. Information on microfiche issues is available from Kraus Microfiche, Rte 100, Milwood, NY 10546, USA.

June 1992

Edited by R.M. Blackall
Vol. 121
No. 1439

Contents

ISSN 0026–1149

ISBN 0-11-728984-1

Printed in the United Kingdom for HMSO
Dd 291241, 6/92, C13, 543, 24503

The Meteorological Magazine

July 1992

Road temperature variations
Hoar frost
Extreme rainfall 1956

HMSO

Met.O.1004 Vol. 121 No. 1440

First published 1992

HMSO

HMSO publications are available from:

HMSO Publications Centre
(Mail, fax and telephone orders only)
PO Box 276, London, SW8 5DT
Telephone orders 071-873 9090
General enquiries 071-873 0011
(queuing system in operation for both numbers)
Fax orders 071-873 8200

HMSO Bookshops
49 High Holborn, London, WC1V 6HB
(counter service only)
071-873 0011 Fax 071-873 8200
258 Broad Street, Birmingham, B1 2HE
021-643 3740 Fax 021-643 6510
Southey House, 33 Wine Street, Bristol, BS1 2BQ
0272 264306 Fax 0272 294515
9-21 Princess Street, Manchester, M60 8AS
061-834 7201 Fax 061-833 0634
16 Arthur Street, Belfast, BT1 4GD
0232 238451 Fax 0232 235401
71 Lothian Road, Edinburgh EH3 9AZ
031-228 4181 Fax 031-229 2734

HMSO's Accredited Agents
(see Yellow Pages)

and through good booksellers

The
Meteorological
Magazine

July 1992
Vol. 121 No. 1440

551.525.2:625.7:551.509.329

A description of a local climatological model used to predict temperature variations along stretches of road

J. Bogren, T. Gustavsson and S. Lindqvist
Department of Physical Geography, University of Gothenburg

Summary

This paper includes a discussion of the factors causing large variations in temperature along stretches of road. These factors can be integrated into a local climatological model, and it is also shown how a model of this kind can be used to predict temperature variations along roads.

1. Introduction

Surveys of winter road conditions are traditionally based on information from field stations located in areas where large variations in temperature are found, as well as where road slipperiness frequently occurs. The most common methods for detecting such areas involve the use of instruments attached to cars, as reported by, for example, Lindqvist (1976), Thornes (1985), Smith (1988). Other methods involve the use of infrared equipment mounted on, for example, helicopters, as discussed by Stove *et al.* (1987) and Gustavsson and Bogren (1991). Several studies have demonstrated that a temperature survey of stretches of road using road weather sensors is very useful for the local road authorities (Lindqvist and Mattsson 1979, Lindqvist 1982, Thornes 1989). However, as discussed in several studies, e.g. Bogren (1990) and Gustavsson (1990a), recordings from field stations give only very localized information about road temperatures. There is therefore a need to extrapolate temperatures from the field stations to make them valid for larger areas. Such an extrapolation is not possible without taking the local topography into account. Variations in temperature can be dealt with, however, by constructing a model of the local environment along specific stretches of road.

The central focus of other studies dealing with the modelling of local climate has been to develop models in order to predict the variation in, for example, frost sensitivity, as discussed by Laughlin and Kalma (1988, 1990). The present paper describes how a local climatological model can be used to calculate air and road surface temperatures in an area with road weather sensors.

The paper consists of two parts. The first section deals with analyses of temperature recordings from field stations and from thermal mappings along stretches of road in order to determine the relationship between topography, weather and temperature variations. The second part starting with section 5 includes a discussion of the principles behind the modelling of local climate, as well as the procedure for adapting a model to a specific area.

2. Data

In order to study temperature variations along stretches of road, different types of recordings have been used. The data are obtained from:

(a) thermal mapping of road sections by use of instruments attached to a specially designed car, and
(b) field stations in the Swedish Road Weather Information System (RWIS) sited in different climatological environments along road sections.

2.1 Thermal mapping

The location of the sensor sites in the Swedish RWIS is determined after analysing thermal-mapping records obtained from cars. Thermal mapping produces continuous recordings along road sections. Air temperature is measured at 2 m and 0.3 m above the surface, humidity at 2 m and surface temperature by use of a thermal radiometer, all of which are recorded every 5 metres. The temperature recordings are stored in a computer, into which the driver feeds other parameters of interest to the analysis, such as information on road cuts, bridges, fog and changes in road surface construction.

In this study the thermal recordings have been used for analyses of the relationship between topography, weather and temperature variations. Using topographical maps (scale 1:50 000) in combination with field observations makes it possible to distinguish several types of topographical areas and their temperature differences compared with a reference temperature obtained from nearby neutral areas.

2.2 Field stations

The field stations are located at road sites which frequently suffer from slipperiness. Typical locations are, for example, valleys, bridges and road cuts. At all stations the air temperature and humidity are measured at the height of 2 m and the road surface temperature by use of a probe in the top layer of the road coating. Some of the stations have extra equipment, such as sensors for wind speed, wind direction, precipitation and for detecting dry or wet road surfaces.

As the field stations are located in different types of area, these recordings allow a good overall evaluation of temperature variations between different types of location. The method used for the analyses comprises a comparison between neutral and exposed location. From the integration of weather parameters obtained from nearby synoptic weather stations and wind recordings from field stations, the variation caused by these parameters can be determined.

3. Repetition of temperature patterns

The fundamental idea behind modelling local climates for prediction of temperature variations is that the temperature pattern is repeated during situations with similar weather. Huovila (1964) and Mattsson and Börjesson (1978) have shown that there is a high correlation between different measuring trips carried out along the same route during clear, calm nights.

Air temperature recordings from three measuring trips along road 60 between Falun and Borlänge in the county of Kopparberg, Sweden, are shown in Fig. 1. The recordings were carried out on 19, 22 and 23 January 1986, all three at approximately 2200 LST. During the three nights the sky was cloudless. A light wind of approximately 1 m s^{-1} was blowing on 19 January, but the other two nights were calm. The correlation between the lowest air temperatures is very high, as can be seen in the figures, and the temperature patterns along the road during the three nights are very similar. The lowest air temperature was to be found in three distinct valleys along the road, as well as in an open arable area at a distance of 13 km from the start. However, during 19 January when light winds were blowing, this area did not have such a low temperature as on the two other measuring trips. This can be explained by the fact that the open area is very exposed to the wind, a factor obstructing stabilization of cold air during windy nights.

The three measuring trips presented in Fig. 1 show the same result as the measurements presented by Huovila (1964) and Mattsson and Börjesson (1978) discussed above. This theorem forms the basis for modelling local climate. It is possible to make a highly accurate prediction of the temperature variation in an area, especially when discussing forecasting of temperature variations along a road section which is thermally mapped. This reasoning is also valid for weather situations which are not clear and calm, as the temperature pattern is to a high degree controlled by local topography and other factors which it is possible to determine. This is discussed further in the following sections, in which each factor is treated separately.

4. Analyses of geographical factors controlling temperature variations

4.1 Valleys

Accumulation of cold air in valleys during clear, calm nights results in a varying air temperature pattern along road stretches. In a study by Bogren and Gustavsson (1991) it was demonstrated that the variation in temperature between valley bottoms and summits can be related to such factors as the valley geometry, i.e. the width and depth of the valley. Another important factor was found to be the wind exposure of the valleys. The return period of the occurrence of the cold air pool, as well as the magnitude of the temperature difference, increased if the valley location was in any way sheltered from the wind by, for example, trees.

Gathering of cold air in valleys causes a reduction of the road surface temperature (RST) compared to the RST of nearby neutral areas. As shown in Gustavsson (1990b) and Bogren and Gustavsson (1991), the lowering of the road surface temperature is linearly related to the lowering of the air temperature, i.e. the

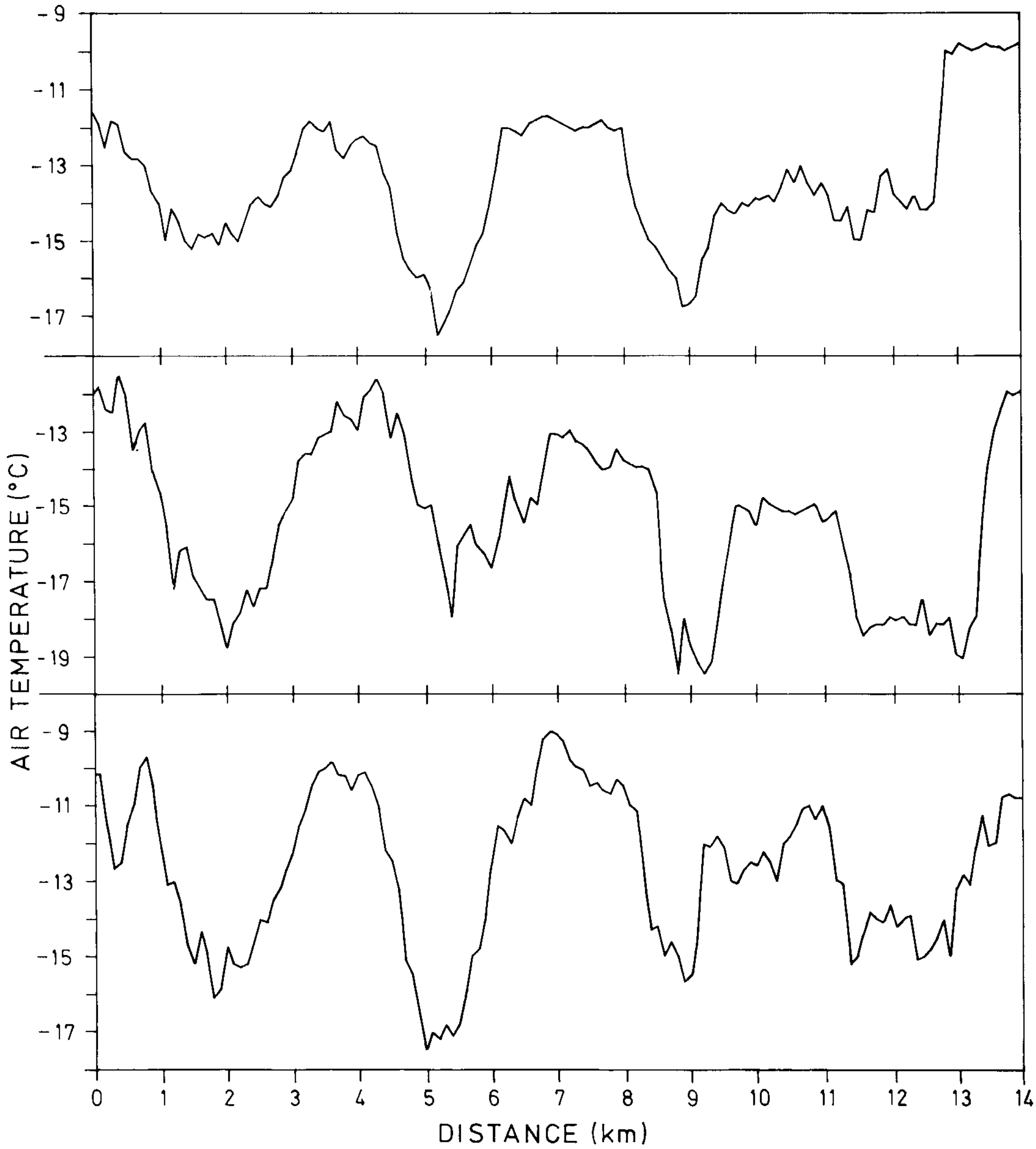

Figure 1. Thermal mapping along a road during three clear nights: 19, 22 and 23 January 1986.

intensity of the cold air pool (see Fig. 2). An air temperature difference of, for example, 6 °C results in a lowering of the RST by approximately 2.5 °C. By use of the relationship between the geometric factors and the variation in air temperature, it is possible to calculate the variation in road surface temperature.

4.2 Variation in altitude

Under cloudy, windy conditions variations in temperature are largely due to changes in altitude, and the influence of local topography is most reduced. By the action of wind and counter radiation from clouds the temperature differences are generally small.

In order to calculate the temperature variations during this type of weather, the heights above sea level at

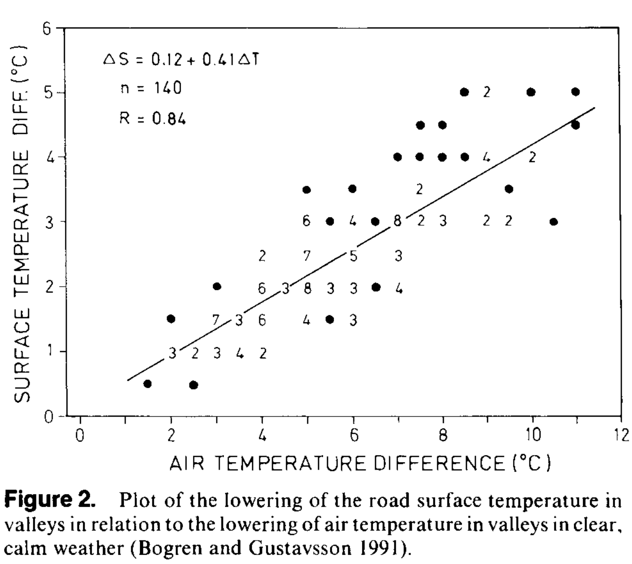

Figure 2. Plot of the lowering of the road surface temperature in valleys in relation to the lowering of air temperature in valleys in clear, calm weather (Bogren and Gustavsson 1991).

which the stations are sited are used together with air and road surface temperatures as inputs to a regression model. From the regression equations, the distribution of air and road surface temperature as a function of altitude is determined. Under fully mixed conditions, the temperature falls by approximately 1 °C per 100 m. This tendency is a general one and can be used for both night and day.

The effect of cloudy, windy conditions on the temperature lapse rate is illustrated in Figs 3(a) and 3(b). The two RWIS stations which are used in this example cover an altitudinal range of 150 m. Station 20 is situated at 170 m, while station 26 is sited at 320 m. The relation between the minimum road surface temperatures (RST) of the two stations is expressed by the equation $RST_{20} = 0.7 + 0.96\, RST_{26}$, with a correlation coefficient of $r = 0.97$. The number of observations was 29. This implies a decrease in road surface temperature of 0.64 °C per 100 m change in altitude. The minimum air temperature (AT) behaves in the similar way as the road surface temperature. The regression for the air temperature is $AT_{20} = 0.98 + AT_{26}$ with $r = 0.96$, i.e. a change in temperature of 0.67 °C per 100 m.

4.3 Screening

On clear days the screening effect must be considered when analysing temperature variations along road sections. Especially during the spring and autumn, screened areas can be prone to localized risk of slipperiness. A study by Bogren (1991) demonstrates that the factors of greatest importance when considering screening effects are the position of the sun in relation to the site (time of day and season) and the type of object, together with its orientation in relation to the orientation of the road. The intensity of the temperature difference which develops between the screened and exposed sites is also affected by the amount of cloud. That the orientation and geometrical configuration of the screening object are the most important factors controlling the variation in surface temperature during sunny days has also been documented in a study by Gustavsson and Bogren (1991).

The effect of screening objects on the road surface temperature is illustrated by a thermal recording from a measuring trip by car on a clear day, Fig. 4. The measuring trip was conducted on highway No. 40 between Gothenburg and Landvetter, in the western part of Sweden. This is a good example of a road section where screened and open areas alternate. The screening objects are mainly in the form of road rock cuts. Since the orientation of the road is primarily east–west, parts of it are screened during the middle of the day and afford a good opportunity for study.

The measuring trip was carried out in the early afternoon on 6 March 1990. The weather preceding the measuring trip was clear and calm; these conditions also prevailed during the thermal recording. The areas which were not screened from the sun had a relatively high surface temperature, approximately 11 °C. The difference in temperature between the screened and exposed parts of the road section varied between 5.7 and 2.3 °C. The variation among the 13 screened areas can be explained by two of the major factors, the exact orientation of the road rock cut and its height.

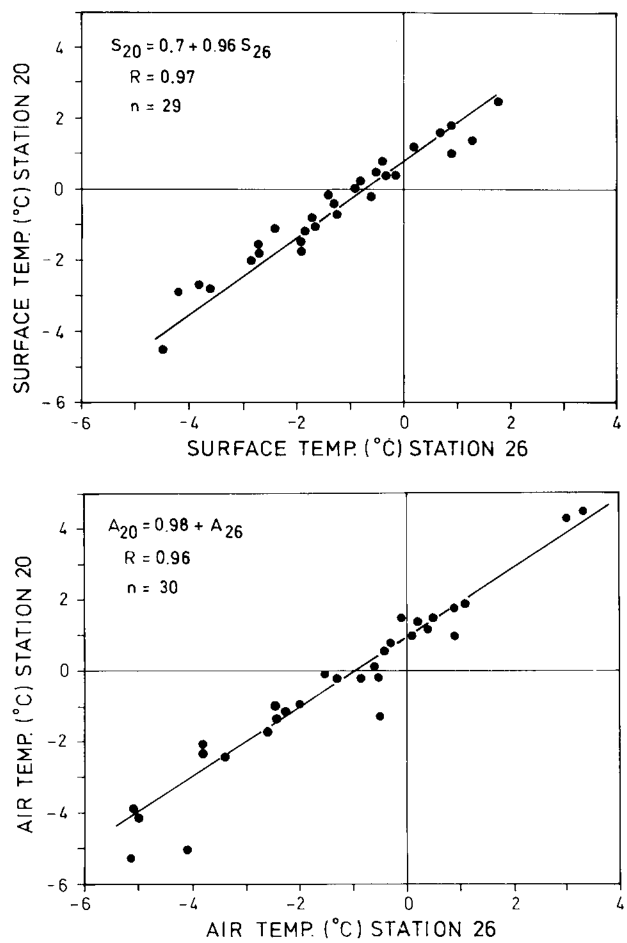

Figure 3. Plots of (a) minimum road surface temperature, and (b) minimum air temperature for cloudy, windy nights from two field stations whose altitudes differ by 150 m.

By use of information about the position of the sun together with data on the screening objects, it is possible to calculate the temperature difference between screened and sun-exposed areas. An additional input is gained from the road surface temperature values recorded at the RWIS stations along the road sections in question.

5. Modelling of local climatological areas

The following section describes the principles of the local climatological model used to predict temperature variations along stretches of road. The different units described in the previous section form the basis for calculations of temperature variations. Since different weather conditions require that different factors are taken into account, the model is subdivided into five sections each dealing with a specific weather condition. This subdivision is further described below together with the background information needed for an

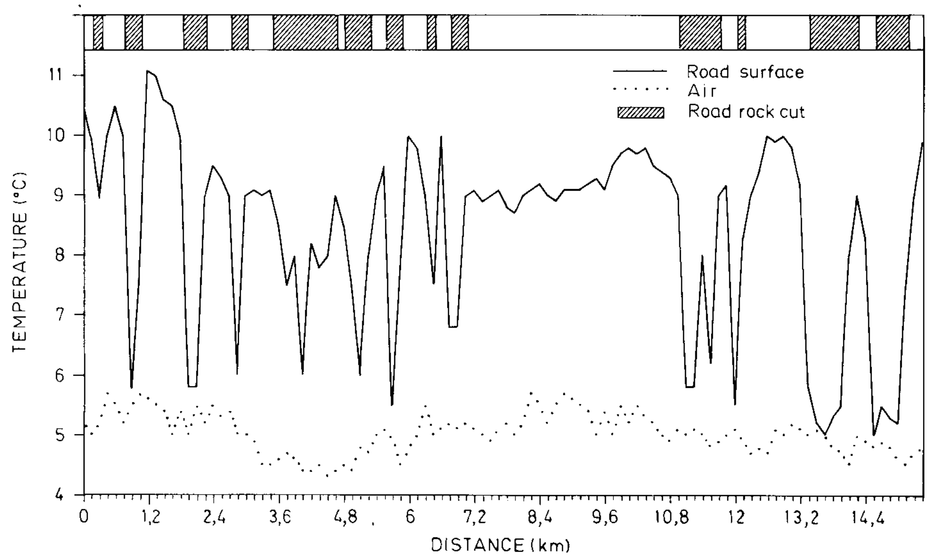

Figure 4. Thermal mapping along a road during a clear sunny day, 6 March 1990.

adaptation of the model to a specific area. An example of the procedure behind the adaptation of the model to the county of Halland, south-west Sweden, is presented in Gustavsson and Bogren (1990).

The data required for adapting the model to a specific area include thermal mappings along the road sections, and historical data from the field stations in the area. Both types of recordings are necessary, as they serve as a basis for the model adjustment in two different ways. The thermal recordings give information about the location and extent of variations in air and road surface temperatures, as well as the relative differences in the temperature between specific areas, while historical recordings are used to confirm the temperature variations determined from the thermal mappings. These recordings are also used to study the temperature differences which occur and to link them up with the prevailing weather conditions.

The road sections included in the model are classified and subdivided into segments with the help of topographical maps on a scale of 1:50 000 and field measurements and checks of the topographical properties (see Fig. 5, for example). The field checks are very important, especially for determining the exact orientation of road stretches and the type and density of objects causing shadow patterns. The extent and position of each type of variation which must be dealt with in the model are derived from analyses of the temperature recordings and maps.

The local climatological model uses four different types of temperature patterns depending on the prevailing weather situation. These types are:

day/clear
night/clear
cloudy, windy
regional pattern.

A subdivision of these types of pattern is made according to the amount of wind and cloud which is indirectly measured by the temperature variations at the field stations in the area discussed.

The algorithm which is used for the calculation of the temperature pattern along the stretches of road has different criteria for the decision as to which temperature pattern is currently valid. The criteria are successively considered until the temperature information can be applied on the different segments along stretches of road.

The first level in the algorithm includes a determination of actual time, and in the daytime the system starts to compare the theoretical calculations for screening effect with the values that are recorded from the RWIS system. If the required criteria are not fulfilled the algorithm continues to investigate if there is a temperature decrease with increasing height — if not, the model chooses the regional temperature distribution.

At night the criteria for pooling of cold air and its effect on the road surface temperature are tested. If the required criteria regarding wind speed and temperature differences match the actually recorded values the model uses the night/clear temperature pattern. If the wind speed is high and the temperature pattern smooth, the algorithm tests the correlation between absolute height and temperature fall. In situations with a high correlation between increasing height and falling temperature, the model output results in the temperature pattern decreasing temperature with increasing height. The regional temperature pattern is used if the criteria for decreasing temperature with increasing height are rejected.

If an external temperature forecast is added as an input to the model it is possible to use the algorithm for prediction of temperature values.

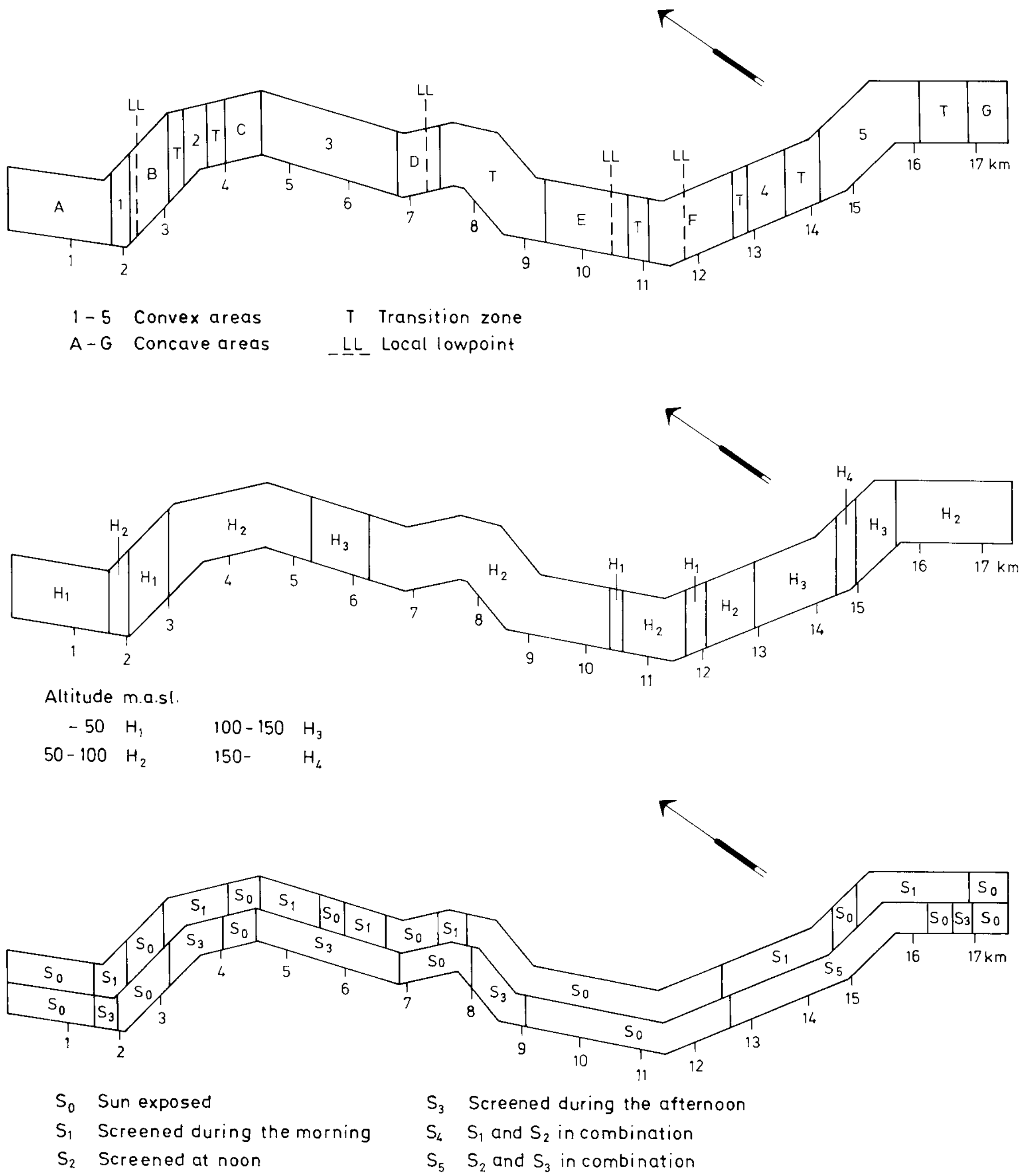

Figure 5. Subdivision of a road into segments used in the local climatological model for (a) calm nights, (b) cloudy, windy situations, and (c) clear days.

To be able to model the temperature patterns along a stretch of road under varying weather conditions, the stretch must be divided into significant topographical segments. Fig. 5 shows three different segments for road No. 156, western Sweden. The topographical units used to determine the temperature pattern in situations with potential for development of cold air pools are convex areas, concave areas, transition zones and local low-points.

On a clear calm night, the pooling of cold air is concentrated in the concave areas where the local low-points form the lowest temperatures. The concave areas are often open and relatively well exposed, which makes them favourable to accumulation of cold air but also sensitive to disturbance by the wind. Convex areas are neutral areas which are relatively elevated and thus do not permit pooling of cold air. The transition zones are located in the stretch between the convex and concave areas and they can be affected by cold air in extreme situations. Calculated air temperature differences between the concave and convex areas in relation to the geometric properties of the valley are shown in Table 1 for a clear, calm night. The table also includes measured temperature differences for the same situation.

The variation between measured and calculated temperatures is generally small. The maximum error is 1.0 °C for area F (see Fig. 5(a)).

When the weather situation is characterized by cloudy, windy conditions the model takes advantage of the relation between the temperature lapse rate and altitude. In such situations, the temperature pattern is calculated using the topographical units which are based on the absolute height above sea level of a certain road section. For road section No. 156, Fig. 5(b), four different levels, H_1–H_4 are used. The segments cover an interval of 50 metres starting with H_1 for the 0–50 m interval. The temperature pattern may be calculated with the help of a regressions calculation where the values recorded at the RWIS stations in the area are used as input data. The result from a calculation referring to a cloudy, windy situation is given in Table II. On this occasion the temperature decreased by 0.8 °C per 100 m. The input temperature which is given from a reference station (H_0) along the road is −1.2 °C in this situation, this temperature thus yielding for the H_0 segment.

The temperature pattern under clear-day conditions is determined by topographical object which can give a shadow pattern. The segmentation for these occasions is done according to the time period during which there is a shadow pattern. Five differently screened classes are used, where S_0 represents a sun-exposed area, S_1 — screening during the morning, S_2 — screening at noon, S_3 — screening during the afternoon, S_4 — S_1 and S_2 in combination and S_5 — S_2 and S_3 in combination (Fig. 5(c)). The calculated RST variations along road No. 156 under clear-day conditions are shown in Table III. The road surface temperature is calculated as the difference between sun-exposed and screened sections for 15 January, 15 February and 15 March at 1000 and 1300, respectively. As a result of the variation in the maximum solar elevation during the period, the maximum temperature difference varies accordingly.

The examples given in Fig. 5 cover three of the weather situations included in the model. Variations of these weather conditions are also taken into account, i.e. the temperature pattern is calculated using subdivisions where various wind and cloud conditions are considered. Weather situations other than those discussed above are dealt with using, for example, the regional temperature distribution determined by the regional climate. A more detailed description of how this is performed is given in Gustavsson and Bogren 1990. Here, the influence on the road surface temperature of variations in traffic density and road construction material is dealt with in a more general way, and not in relation to specific weather situations.

6. Discussion

Ideas similar to those presented in this study concerning prediction of temperature variations along stretches of road have been used in the United Kingdom. However, a much more simplified technique was used as a base for the extrapolation of temperatures. From temperature recordings along a specific stretch of road, thermal maps are constructed for three types of atmospheric conditions: extremes (i.e. clear, calm nights), intermediate (some influence from clouds and

Table I. Air temperature difference between concave and convex segments in a clear-night situation, see also Fig. 5(a)

Segment	Valley width (km)	Valley depth (m)	Cold air pool intensity		
			Calculated (°C)	Measured (°C)	Calculated−measured (°C)
A	1.8	5	5.0	5.4	−0.4
B	1.0	20	4.0	3.5	0.5
C	0.5	5	2.0	2.0	0
D	0.6	35	4.0	4.0	0
E	1.6	0	3.0	3.5	−0.5
F	1.6	0	3.0	4.0	−1.0
G	0.6	20	3.0	3.0	0

Table II. Calculated road surface temperatures under cloudy, windy conditions, see also Fig. 5(b)

Segment	H_{abs} (m)	H_{rel} (m)	RST_{cal} (°C)	RST_{actual} (°C)
H_1	0–50	0	T_r	−1.2
H_2	50–100	50	T_r−0.4	−1.6
H_3	100–150	100	T_r−0.8	−2.0
H_4	150–200	150	T_r−1.2	−2.4

H_{abs} — Absolute height, interval 50 m.
H_{rel} — Height relative to H1.
RST_{cal} — Calculated road surface temperature relative to T_r, T_r is the road surface temperature at the reference station.
RST_{actual} Actual road surface temperature.

Table III. Calculated road surface temperature differences under clear-day conditions on 15 January, 15 February and 15 March at latitude 57°N at 1000 and 1300, see also Fig. 5(c). These are the differences between sun-exposed and screened areas.

Segment	15 January RST_{diff} (°C)		15 February RST_{diff} (°C)		15 March RST_{diff} (°C)	
	10h	13h	10h	13h	10h	13h
S_0	0	0	0	0	0	0
S_1	−0.8	0	−2.5	0	−7.4	0
S_2	0	−2.2	0	−3.2	0	−4.3
S_3	0	0	0	0	0	0
S_4	−0.8	−4.1	−2.5	−7.6	−7.4	−15.8
S_5	0	−2.2	0	−3.2	0	−4.3

S_0 — Sun-exposed area
S_1 — Screening during the morning
S_2 — Screening at noon
S_3 — Screening during the afternoon
S_4 — S_1 and S_2 in combination
S_5 — S_2 and S_3 in combination

wind) and damped (fully mixed conditions). A weather forecast is used for the decision which type should be used.

The model presented in this paper uses, as previously described, several types of background data in order to develop the empirical relationships used for extrapolation of temperatures. Different segmentation is further used for different weather conditions as well as time of the day and the Julian date in the year. With the aid of all this information together with the real-time observations from the field stations a much more diversified temperature pattern can be obtained and the accuracy of the temperature forecast improved.

The benefits of using a local climatological model such as the one described in this paper are several compared with a road weather information system based only on field stations, the most important naturally being that the area covered by the information system is much larger, resulting in a more diversified snow and ice control. Computerized maps of the temperature variations along stretches of road can be used by the road authorities and by others to determine the local risk of slipperiness. The information from the model may be combined with a temperature forecast to obtain a prognosis of the temperature pattern for the coming 4–6 hours, as well as a prognosis of the risk of road slipperiness, not only at specific locations but for the whole area covered by the model. Another advantage is that the information received by the superintendent includes greater details, which results in a more restricted use of means of combating snow and ice, such as salt.

Acknowledgements

The project described in this paper was sponsored by the National Swedish Road Administration. The figures were drawn by Solveig Svensson.

References

Bogren, J., 1990: Application of a local climatological model for prediction of air and road surface temperatures. GUNI Report 31. Gothenburg, Department of Physical Geography.

—, 1991: Screening effects on road surface temperature and road slipperiness. *Theor Appl Climatol*, **43**, 91–99.

Bogren, J. and Gustavsson, T., 1991: Nocturnal air and road surface temperature variations in complex terrain. *Int J Climatol*, **11**, 443–455.

Gustavsson, T., 1990a: Modelling of local climate — with applications to winter road conditions. GUNI Report 30. Gothenburg, Department of Physical Geography.

—, 1990b: Variation in road surface temperature due to topography and wind. *Theor Appl Climatol*, **41**, 227–236.

Gustavsson, T. and Bogren, J., 1990: Use of a local climatological model for the prediction of air and road surface temperatures along road stretches. GUNI Report 29. Gothenburg, Department of Physical Geography.

—, 1991: Infrared thermography in applied road climatological studies. *Int J Remote Sensing*, **12**, 1811–1828.

Huovila, S., 1964: On precautions against crop damage due to radiation frost within hilly regions. Societas Scientarum Fennica, Commentationes Physico — Mathematicae XXIX, **4**.

Laughlin, G.P. and Kalma, J.D., 1988: Frost risk mapping and frost control. *In* Proceedings of the IGN precongress symposium August 1988, Christchurch.

—, 1990: Frost risk mapping for landscape planning: a methodology. *Theor Appl Climatol*, **42**, 41–51.

Lindqvist, S., 1976: Methods for detecting road sections with high frequency of ice formation. GUNI Report 10. Gothenburg, Department of Physical Geography. (In Swedish with English summary.)

—, 1982: New methods for ice-surveillance in Sweden. GUNI Report 16. Gothenburg, Department of Physical Geography. (In German with English summary.)

Lindqvist, S. and Mattsson, J.O., 1979: Climatic background factors for testing an ice-surveillance system. GUNI Report 13. Gothenburg, Department of Physical Geography.

Mattsson, J.O. and Börjesson, L., 1978: Lokalklimatologiska temperaturstdier inom ett skånskt fruktodlingsdistrikt — med särskilt bektande av frostläntheten. Swedish University of Agricultural Sciences, Trädgård, 131. (In Swedish with English summary.)

Smith, K., 1988: Highway meteorology comes to Scotland. *Scott Geogr Mag*, **104**, 123–125.

Stove, G.C., Kennie, T.J.M., and Harrison, A., 1987: Airborne thermal mapping for winter highway maintenance using the Barr and Stroud IR18 thermal video frame scanner. *Int J Remote Sensing*, **8**, 1077–1084.

Thornes, J.E., 1985: The prediction of ice formation on roads. *J Inst Highw Transp*, **32**, 3–12.

—, 1989: A preliminary performance and benefit analysis of the UK national road ice prediction system. *Meteorol Mag*, **118**, 93–99.

Persistent hoar frost

W.S. Pike
19 Inholmes Common, Woodlands St Mary, Newbury, Berkshire RG16 7SX

The frosty period of weather in southern England from 6 to 15 December 1991 provided opportunities for the photographic observations of persistent hoar frost and its growth in the author's garden (183 m above mean sea level).

Passage of a weak cold front from the east on Thursday, 5 December 1991 effectively cleared a persistent blanket of stratocumulus which had been causing 'anticyclonic gloom'. After six frosty nights, with negligible thawing by day in the shade, Fig. 1 shows the sharp, crystalline, vertical hoar frost growths some 1–2 cm high on short grass (at the edge of the path) and beech leaves over bare soil — the photograph being taken at 1430 UTC on the 11th. There is very little growth of crystal on the clay earth itself, suggesting that the capture of moisture from a saturated atmosphere by projections near the ground had occurred. Small movements of air in the light, variable winds within the sheltered garden probably account for the more randomly orientated profusion of crystals which had formed on the blade edges of longer grass.

Following three more frosty nights, some freezing fog causing rime deposition, and a little thawing by day, the hoar frost growths had become 2.5 cm high (Fig. 2, taken at 1430 UTC on the 14th). A maximum of 3 cm was measured early on the 15th before a very rapid thaw ensued during the morning.

Hewson and Gait (1992) do not appear to have mentioned if surface friction bears any relation to hoar frost 'deposition'. From the above photographic evidence (albeit taken in a sheltered situation) one suspects that a rough road surface (e.g. loose chippings) is more likely to capture low-level moisture from the atmosphere than a smooth one (e.g. tarmacadam).

Reference

Hewson, T.D. and Gait, N.J., 1992: Hoar-frost deposition on roads. *Meteorol Mag*, **121**, 1–21.

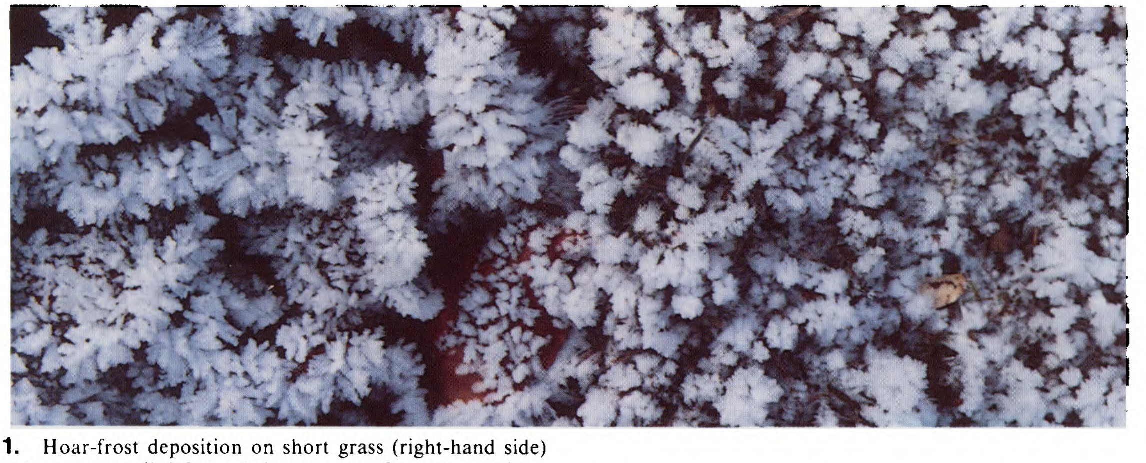

Figure 1. Hoar-frost deposition on short grass (right-hand side) and beech leaves and soil (left-hand side), see text for date and time.

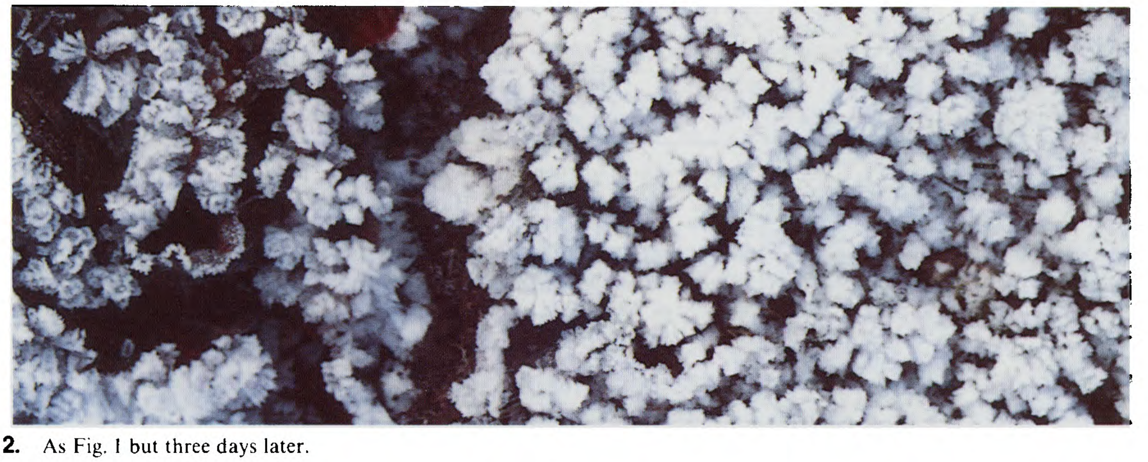

Figure 2. As Fig. 1 but three days later.

551.557.37:551.515.42:551.579.4:556.16(234.631)

Extreme rainfall at Hewenden Reservoir, 11 June 1956

V.K. Collinge, J. Thielen and J.F.R. McIlveen
University of Lancaster

Summary

One of the most intense rainfalls within a 2-hour period in Great Britain was recorded during a severe thunderstorm on 11 June 1956 at Hewenden Reservoir. Later, doubts were raised about the validity of this observation, because the storm efficiency appeared to be too high. However, a re-examination of the meteorological situation on that date and investigation of the scale of the resulting flood seem to suggest that the original measurement may have been correct.

1. Introduction

The 11th of June 1956 was a day noted for the development of severe and widespread thunderstorms in Britain, with damage reported from places as far apart as the Isle of Wight, Wales and Inverness-shire. The outstanding storm, however, was in West Yorkshire between Bradford and Keighley where a rainfall of 155 mm in 105 minutes beginning at 1745 UTC was reported at Hewenden Reservoir. This was of particular interest because, at that time, it substantially exceeded the highest recorded rainfall in a comparable period (122 mm in 2 hours (1895)); and even today remains one of the highest rainfalls observed in a period of about 2 hours (Table I). But the observation was rejected as 'not acceptable' in the Flood Studies Report (FSR) (Natural Environmental Research Council 1975), based on studies of the storm efficiencies of six other major 2-hour storms and an estimated dew point of 12 °C on 11 June 1956. In fact the fall was down-rated to 102 mm on the implicit assumption that the original observation exceeded the local Probable Maximum Precipitation (PMP).

It is important to establish, as far as possible, the facts about this observation, particularly because, of the four highest falls in about 2 hours, only the Hampstead one is fully authenticated (Table I). In the case of Walshaw Dean Lodge the reading was not accepted by the Meteorological Office on the grounds that the gauge overflowed and the reading exceeded the PMP for the area. Also the radar observations were much lower; but recent analyses (Acreman and Collinge 1991) provide a possible explanation for this, and evidence provided by Acreman (1989) also supports the original rainfall observation. In the case of Camelford substantial amounts of hail fell during this storm. The officially accepted value is 139 mm (Meteorological Office 1957) but Bleasdale (1957) states that a minimum of 25 mm water equivalent of hail was not collected by the gauge.

Unfortunately no investigation of the Hewenden Reservoir storm was published at the time, though the Meteorological Office made some enquiries. However, the authors have made an extensive search for information, the results of which are described in this paper.

It seems that the representative dew-point for the Hewenden storm was underestimated, which has led to a considerable overestimation of the storm efficiency associated with the observed rainfall. It is believed that the validity of the original observation has been restored.

Table I. Maximum observed rainfall values for durations of 1½–2½ hours

Rainfall (mm)	Duration (min.)	Date	Place
193	120	19 May 1989	Walshaw Dean Lodge
171	150	14 Aug. 1975	Hampstead
161	150	8 June 1957	Camelford
155	105	11 June 1956	Hewenden Reservoir
137	135	10 Aug. 1957	Llansadwrn
136	150	4 Aug. 1938	Torquay
132*	120	6 June 1963	Southery
130	120	5 Sept. 1958	Knockholt
126	120	11 July 1932	Cranwell

* An unofficial gauge; reading reported by Jackson (1979)

2. Meteorological situation on 11/12 June 1956

On the 11th, Great Britain was under the influence of a weakening ridge joining two high pressure systems, one east of Scandinavia and one west of Spain (Fig. 1). Blocked by this ridge, a low had moved north to Iceland and its cold front moved slowly east as the ridge weakened. At the same time a depression over northern Germany moved slowly west towards the Netherlands. Associated weak north-easterly surface winds over Britain were bringing warm air from Scandinavia to Central England. The accompanying warm front was almost stationary on 11 June, but was replaced on the 12th by the cold front associated with the approaching Atlantic depression.

At 1200 UTC on the 11th, over the whole of Great Britain, light north-easterly surface winds of 5–15 knots brought in moist, warm air from Scandinavia. The air was particularly moist on the east coast of England with dry-bulb temperatures of 13–15 °C and dew-points of 9–14 °C (relative humidity ≈ 85%); whereas the air mass over the western British Isles was drier, with higher temperatures (15–21 °C) and dew-points (12–16 °C) (relative humidity ≈ 70%). The skies were only partly cloudy in the west, allowing the surface to be heated by direct sunlight and producing convectively unstable conditions. Most stations in the east recorded complete cloud cover.

During the afternoon convection developed and cumulonimbus clouds were widespread over Great Britain. Showers and thunderstorms were reported from the south of England up to Scotland.

3. Development of storms on 11 June

The general weather situation on 11 June 1956 in Great Britain provided all the necessary features for the development of severe convective storms.

3.1 Availability of moist air in the lowest levels.

The dew-point maps for 1200 UTC show rather high dew-points of 14–16 °C over central England. The warm, moist air mass expanded north during the day and at 1800 UTC a warm air tongue stretched from central England to southern Scotland, producing rather steep dew-point gradients in northern England (Fig. 2).

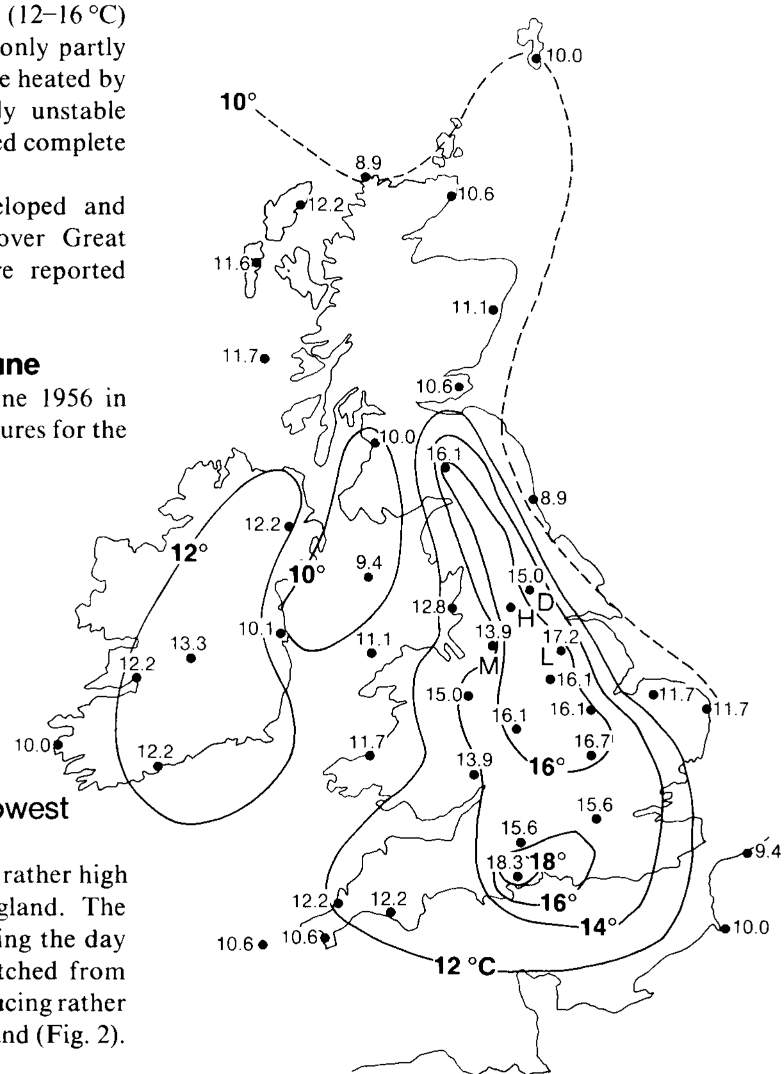

Figure 2. Readings and isotherms of dew-point for 1800 UTC on 11 June 1956. M, L, D and H label the positions of Manchester, Lindholme, Dishforth and Hewenden respectively.

Hewenden Reservoir is located between Manchester, Lindholme and Dishforth, with the last two being upwind of the storm. The dew-point in Manchester fell during the afternoon, while at Lindholme and Dishforth the dew-points rose (see Table II). This suggests that the dew-point at Hewenden Reservoir probably lay between 15° and 16 °C at the time of the outbreak of the Hewenden storm on the evening of 11 June (Fig. 2).

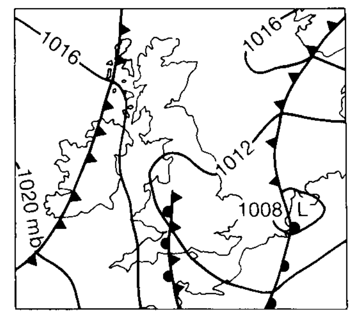

Figure 1. Surface chart for 1800 UTC on 11 June 1956.

3.2 Wind shear between lower and upper levels

The surface flow was light north-easterly, associated with the depression over the Netherlands. The flow in the middle troposphere was veering during the day from easterly to south-westerly, implying an increasing wind shear in the lower troposphere. This wind shear is important for the development and duration of severe storms, because it feeds the system with fresh, moist air from the lower levels and it also facilitates the venting of air descending from middle levels (Sumner 1990). It separates updraughts and downdraughts, so that they can co-exist and co-operate, rather than interfere destructively (Ludlam 1980).

3.3 Convective instability

The combination of wind field, warm, moist air masses over central and northern England, and the approaching cold front produced a high degree of convective instability over most parts of Great Britain, especially in the south and the central part of England. In the afternoon convection developed, giving rise to the formation of cumulonimbus clouds and thunderstorms, which were reported mainly in regions of high dew-points (Figs. 2 and 3).

The map showing the location of thunderstorms on 11 June 1956 (Fig. 3) proves that convective instability was widespread over Great Britain, though concentrated over central England. Thunderstorms were reported in Scotland (Inverness-shire) around 1300 UTC, in northern Cumbria around 1400 UTC, but most of the storms broke out between 1700 UTC and 1900 UTC in central and southern England.

4. The Hewenden storm

Details of the storm and the resulting damage have been obtained from several sources: articles in two local newspapers (the *Keighley News* and *The Yorkshire Observer*), photographs in the archives of those newspapers, a report by Mr J.S. Lattin (at that time Surveyor to Bingley Urban District Council), the Meteorological Office and Yorkshire Water plc.

The storm occurred between Bradford and Keighley, in an area where the land is rising from the river Aire in a generally west-south-westerly direction to the moors which form part of the Pennines (Fig. 4).

The newspapers reported a violent thunderstorm which struck the area bounded by the villages of Cullingworth, Oxenhope and Oakworth. A member of the British Thunderstorm Census, living in Oakworth, recorded 115 flashes of lightning. Information about the time of the storm comes mainly from the rainfall observations —at Hewenden Reservoir the rain lasted from 1745 to 1930 UTC, and at Stubden Reservoir from 1745 to 1900 UTC. According to the *Keighley News* the storm was 'at its height' between 1745 and 1830 UTC.

Table II. Dew-points for Manchester, Lindholme and Dishforth for the times shown 11/12 June 1956

Stations	11th 1200	11th 1800	12th 0000
	Dew-points (°C)		
Manchester	15.6	13.9	10.6
Lindholme	14.4	17.2	12.2
Dishforth	12.8	15.0	11.7

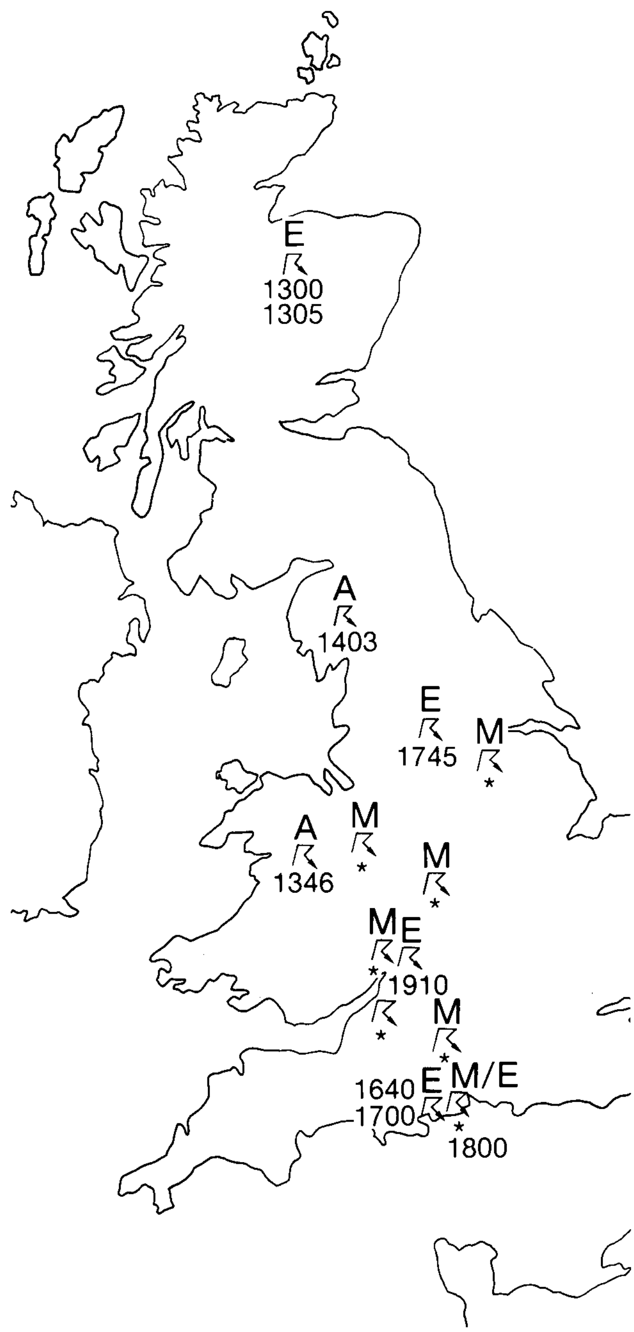

Figure 3. Thunderstorms with times of commencement over Britain on 11 June 1956. The storms were reported by Meteorological Office (M), Autographic records (A) (Meteorological Office 1956), Eye observations (E) (Meteorological Office 1956). Onset time between 1500 and 1800 UTC is indicated by *.

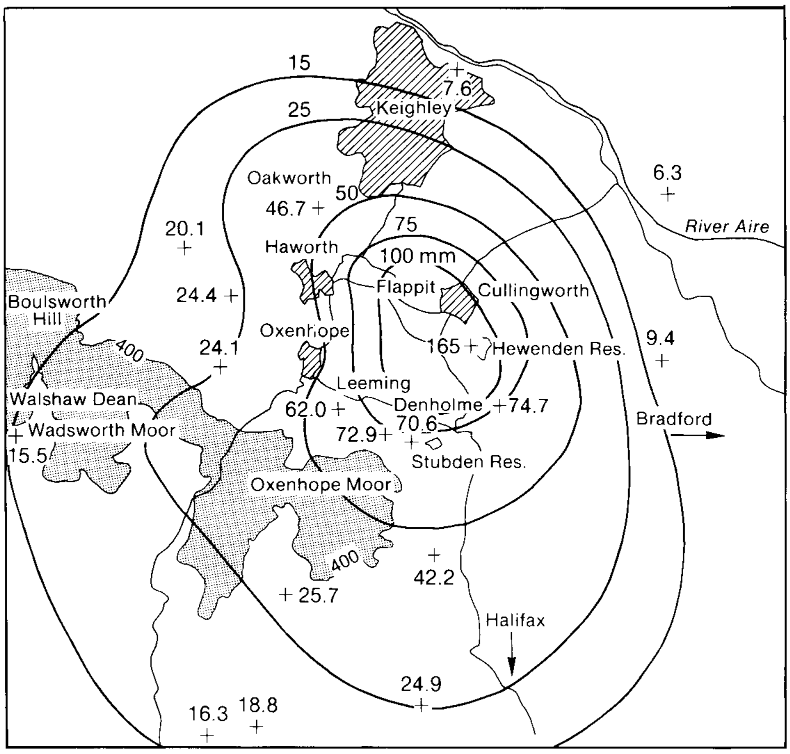

Figure 4. Twenty-four hour rainfall totals and isohyets on 11 June 1956 for the Hewenden Reservoir area.

Accounts of the damage are copious and graphic and leave no doubt about the severity of the rainfall and the accompanying flooding (Fig. 5). Fortunately there is good evidence to establish the location of the storm centre. According to Mr Lattin, the storm appeared to be worst on the hills above the Halifax–Keighley road, between Flappit and Denholme, which is some 2 km west of Hewenden Reservoir, where the maximum rainfall was observed (Fig. 4). This was presumably based on the fact that the worst flooding was in Cullingworth, through which Manywell's Beck flows, draining 2.05 km^2 of moorland in the area he identified. Just upstream of Cullingworth Gate the stream is conveyed under a mill yard in a culvert. This was so overloaded that the culvert burst, and the arch of a road bridge just downstream was also unable to accommodate the flow.

An estimation of the minimum rainfall that must have fallen in order to exceed the capacity of the bridge is found to be 115 mm (see Appendix). The actual value is likely to have been considerably larger than this, since the bridge capacity was conspicuously exceeded and since flood water was rushing down the three roads (from the west, south-west and east) that converge on Cullingworth Gate, resulting in extensive flooding and damage to properties and roads (Fig. 5). There are accounts of minor flooding in surrounding villages — Oakworth, Haworth, Oxenhope and Leeming, but only in the last was there evidence of something exceptional. Here residents 'saw the hillside break into streams' and tried to build barriers to prevent their homes from being flooded.

5. Rainfall

Evidence about the maximum observed rainfall is contained in British Rainfall 1956, and is supported by a letter from the Waterworks Engineer, City of Bradford to the Director, Meteorological Office dated 16 July 1956. (Times referred to are BST.) He wrote — 'The reservoir keeper at Hewenden informs me that the rain started at 6.45 p.m. The gauge was then empty after a fine day. The rain ceased by 8.30 p.m. and the gauge was read at 9.00 p.m. when 6.09 inches of rain was measured. A further 0.41 inches fell during the early hours of the 12th. At Stubden reservoir the keeper observed that the rain started at 6.45 p.m. and finished at 8 p.m. He then read the gauge, which was empty at 6.45 p.m. and found the rainfall to be 2.45 inches. A further 0.42 inches fell before 9 a.m. on the 12th'.

Daily (0900–0900 UTC) rainfall totals have been obtained from 19 gauges, including Hewenden and Stubden. There is also a storm total reading from an unofficial gauge in Oakworth of 1.6 inches (41 mm) from which the 24-hour fall at that site has been estimated to be 46.7 mm. All these data and the corresponding isohyets have been plotted in Fig. 4. There are places where clearly considerable doubt must exist, notably around the centre of the storm and also in the north-east quadrant. However, the overall pattern and the location of the 25 mm and 50 mm isohyets have been established with reasonable confidence. The isohyets have been drawn on the assumption that the centre of the storm was correctly located by Mr Lattin, and this therefore suggests a maximum rainfall in excess of that observed at Hewenden Reservoir.

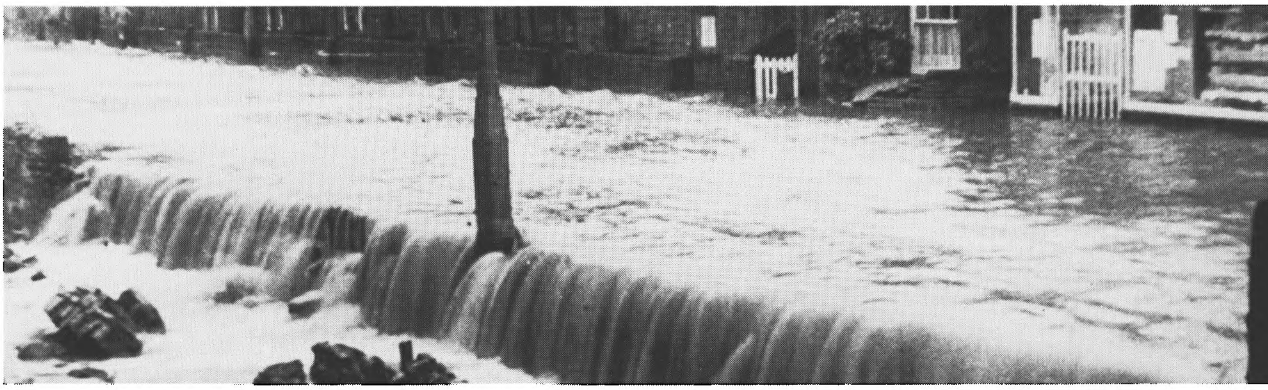

Figure 5. Flood-water flowing down the Halifax Road, Cullingworth, on the evening of 11 June 1956, causing severe damage in houses and breaking down 36 metres of the wall along the road *The Yorkshire Observer*.

6. Storm efficiency

One method of classifying storms for the purpose of Probable Maximum Precipitation (PMP) studies (Wiesner 1970, WMO 1969) is to calculate the corresponding storm effiency (S_{eff}) which is defined as the ratio of maximum observed rainfall to the amount of precipitable water in the representative air column during the storm (NERC 1975).

The amount of precipitable water, W (mm) in a column of air of height z is defined as

$$W = \int_0^z \rho_w \mathrm{d}z = -\int_{p_0}^{p_z} \frac{\rho_w}{\rho} \frac{\mathrm{d}p}{g} = -\int_{p_0}^{p_z} \frac{s}{10^3 g} \mathrm{d}p$$

where ρ and ρ_w are the densities of air and water vapour respectively in kg m^{-3}, s is the specific humidity or mixing ratio in g kg^{-1}, p the atmospheric pressure (mb $\times$ 10^{-2}) and g is the gravitation constant 9.81 m s^{-2}.

If no vertical soundings are available, it is assumed that the air mass in the storm is saturated and that the vertical humidity profile is represented by the screen level dew-point, following the saturated pseudo-adiabatic lapse rate. The precipitable water W can then either be calculated by using tephigrams to determine the mixing ratio s or by using tables which directly give the precipitable water as a function of height and dew-point (Wiesner 1970).

For the present study W was determined with help of the tephigram for an air column between 1000 and 200 mb, in 100 mb steps. Three storm efficiencies were then calculated for surface dew points of 12, 14 and 16 °C and an observed rainfall of 155 mm. The results are shown in Table III, which demonstrates clearly that the storm efficiency is very sensitive towards changes in the dew-point.

Attempts to reproduce the FSR calculations of S_{eff} have failed. Assuming a dew-point of 12 °C, a value of 5.93 is obtained as above, and 6.10 is found using Wiesner's (1970) tables, both substantially larger than the 5.3 quoted by FSR. To obtain an S_{eff} of 5.30 as above, the precipitable water content would have to be 29.2 mm, which corresponds to a dew-point of 13.5 °C.

Even with allowance for station and cloud-base altitudes as well as for a storm duration of 105 minutes rather than 120 minutes, a value of 5.3 could not be obtained. However, none of these possible allowances are mentioned in the FSR. Practical and theoretical problems inherent in defining effective precipitable water for this purpose deserve careful future examination.

In any case, examination of surface meteorological data for 11 June has revealed no evidence for a dew-point as low as 12 °C at Hewenden Reservoir during the storm (as assumed in the FSR); examination of Fig. 2 and Table II suggests instead a value of 16 °C. Although not explicitly mentioned in the FSR, it seems that the quoted low value was taken to be representative of the Hewenden storm on the grounds that it was the highest dew-point persisting for a 6-hour period. Though consistent with WMO advice for long-lasting storms (WMO 1969), this approach is suspect on two counts:

(a) Convective storms break out rapidly once critical conditions have been reached. Averaging over 6 hours may remove significant peaks, especially those related to the important diurnal cycle of surface heating.

(b) On this occasion it would seem that the 6-hour period chosen ran from the beginning of the storm (1800 UTC) to well after its end (0000 UTC, 12 June). Dew-points at the latter time are representative of the cool air deposited from the middle troposphere, rather than the warm air rising from surface layers which provides the high precipitable water content powering the storm, and should not be used to estimate storm efficiency.

Table III. Calculated storm efficiencies (S_{eff}) for dew-points of 12, 14 and 16 °C

Dew-point (°C)	Precipitable (mm)	S_{eff}
12	26.11	5.93
14	31.30	4.95
16	37.55	4.17

In the FSR, similar storm efficiency calculations were carried out for six other major 2-hour storms in England and Wales, giving values ranging from 3.04 to 3.86. On this basis it was concluded in that report that a probable maximum storm efficiency in the United Kingdom for a 2-hour storm is 3.86, whilst the value the present authors obtained for the Hewenden Reservoir (Table III) is 4.17. The difference is not great, and indeed is remarkably small given the uncertainties in the calculation, and doubts about the concept of storm efficiency.

Note that the probable maximum storm efficiency multiplied by the maximum observed precipitable water content gives the PMP which was originally derived to provide useful assessments of very intense precipitation for hydrological purposes, but seem now to be widely regarded as the Maximum Possible Precipitation (MPP). It is implicit in the FSR case against the Hewenden reservoir rainfall observation that it must be incorrect because it exceeds the local and national 2-hour PMP. Problems inherent in the concept of PMP are the subject of considerable controversy. The dangers of assuming identity between the practically useful PMP, and the probably indefinable MPP, will be addressed by the authors in another paper.

7. Conclusions

In the Flood Studies Report doubts were raised about a gauge rainfall observation of 155 mm in 105 minutes on 11 June 1956 on the basis that the corresponding storm efficiency was too high when compared with other storms (NERC 1975). In this study evidence is brought together that supports the original observation.

The authors estimated the dew-point, which is an essential variable for the calculation of the storm efficiency, to be considerably higher than that quoted in the Flood Studies Report, which then leads to an acceptable lower value for the storm efficiency. This suggests, that the original measurement of 155 mm was correct and that this event was indeed an outstanding storm in Great Britain with one of the highest observed rainfalls in 2 hours.

In any case, as the storm efficiency is very sensitive to changes in the dew-point, which generally has to be estimated for a particular site, it should not be used as the basis for the rejection of an actual rainfall measurement.

The controversy over the rainfall observation for this storm shows how important it is to investigate extreme events immediately and to summarize the facts in a report that is published and made available to the scientific community.

8. Acknowledgements

Two of the authors (J.F.R.M. and J.T.) wish to acknowledge the primary role and enthusiastic interest of our colleague V.K. Collinge to within a few weeks of his death. J.T. acknowledges support from an NERC studentship during the course of this work.

The authors wish to acknowledge the help of the following in providing data and other information about the Hewenden storm: Mick Wood (Archivist, National Meteorological Archives), the Meteorological Office, Yorkshire Water plc, National Rivers Authority (Yorkshire Region), the *Keighley News* and *The Yorkshire Observer*. We also acknowledge the help of Ewan Archibald and the advice of Dr N.A. Chappell, both of the University of Lancaster, and the valuable comments of Dr R.W. Riddaway and D. Hollis on a first draft.

References

Acreman, M.C., 1989: Extreme rainfall in Calderdale, 19 May 1989. *Weather*, **44**, 438–446.

Acreman, M.C. and Collinge, V.K., 1991: The Calderdale storm revised: an assessment of the evidence; Proceedings of BHS 3rd National Hydrology Symposium, Southampton, pp. 4.11–4.16.

Bleasdale, A., 1957: Rainfall at Camelford, Cornwall on June 8, 1957. *Meteorol Mag*, **86**, 339–343.

Jackson, M.C., 1979: The largest fall of rain possible in a few hours in Great Britain. *Weather*, **34**, 168–175.

Ludlam, F.H., 1980: Clouds and Storms. The behaviour and effects of water in the atmosphere. Pennsylvania State University Press.

Meteorological Office, 1956: British Rainfall. London, HMSO.

—, 1957: British Rainfall. London, HMSO.

Natural Environmental Research Council, 1975: Flood Studies Report, Vol. II, Meteorological Studies. London, Whitefriars Press.

Shaw, E.M., 1984: Hydrology in Practice; Wokingham. Van Nostrand Reinhold Co.

Sumner, G., 1988: Precipitation, process and analysis; Chichester, John Wiley and Son.

Wiesner, C.J., 1970: Hydrometeorology. London, Chapman and Hall Ltd.

WMO, 1969: Estimation of Floods; Technical Note 98, Geneva, World Meteorological Organization.

Appendix

The discharge at Cullingworth Gate Bridge at the point of overtopping can be estimated with Manning's formula (Shaw 1984)

$$Q_P = \frac{AR^{2/3}\,S^{0.5}}{n}$$

With the area (A) of the bridge that had to be overtopped of 8.1 m^2, a hydraulic depth (R) of 1.62, a slope S of 0.015 and a roughness coefficient for unlined earth of 0.015 the discharge would be $Q_P = 91\ m^3\,s^{-1}$.

The precipitation generating the discharge between the rise and peak storm-flow is given by

$$P = 0.5(Q_P T_P)SA^{-1}R$$

where P is precipitation (mm), Q_P the peak discharge in $m^3\,s^{-1}$, T_P is time (seconds) to peak discharge, S is the shape function for the rate of hydrograph rise (0.8), A is the catchment area (2 050 000 m^2) and R is the index of the discharge coefficient (90% run off $\equiv$ 0.9).

Assuming: (i) a time to peak discharge (from start of hydrograph rise) of two hours (7200 s), and (ii) a discharge coefficient (R) of 0.9, the catchment mean precipitation would be 115 mm. This minimum value is already higher than the point value at the storm centre as calculated in the Flood Studies Report.

Review

Atmospheric data analysis, by R. Daley. 182 mm × 260 mm, pp. xiv+457, *illus.* Cambridge University Press, 1991. Price £55.00, $79.50. ISBN 0 521 38215 7.

In the past, when asked to recommend reading material on analysis methods, I have had to scratch around and suggest several articles in order to give a balanced approach. This book brings the material all together and fills a gap in the atmospheric science literature. The scope is wider than the title might suggest, including initialization and related dynamical theory as well as the spatial analysis aspects. It has an emphasis on the theoretical foundation, but includes practical applications. It is the second title in the Cambridge Atmospheric and Space Science Series.

Chapter 1 forms an introduction, including brief descriptions of the types of observations available and a short historical review of data assimilation from subjective analysis to the present via the start of computer predictions and analysis *circa* 1950. Most of the rest of the book requires a substantial mathematical background (advanced undergraduate level).

Chapters 2–5 cover early analysis methods including function fitting and successive corrections and then move on to statistical interpolation (sometimes called optimum interpolation or OI). The statistical interpolation equations are derived from the minimum variance (least-squares) principle, the alternative probabalistic viewpoint is not given. A continuous analogue of the equations is provided to illustrate properties of the algorithm, and some atmospheric physics, in the form of multivariate constraints, is introduced. A renewed interest in successive correction methods came from the realization that they could be formulated so as to converge to the statistical interpolation solution (appendix F).

Initialization is the process of adjusting the initial conditions so that they do not excite inertia–gravity waves in the early part of the forecast. Starting with geostrophic adjustment of the shallow-water equations the theory is developed, via quasi-geostrophic constraints and variational procedures, into normal mode initialization of the primitive equations (chapters 6–10). Dynamic initialization using damping time integration schemes and continuous data assimilation (motivated by the asynoptic nature of satellite observations) are dealt with in chapters 11 and 12.

Most operational forecast centres use an intermittent data assimilation cycle with a statistical interpolation analysis and non-linear normal mode initialization. To be different, the Meteorological Office uses a continuous (dynamic relaxation) data assimilation cycle with a modified successive correction method and no explicit initialization.

Statistical assimilation methods have the disadvantage of relying on average covariance functions to represent atmospheric structures/dynamics. Four-dimensional variational assimilation allows a two-way interaction between model dynamics and observations in the search for the optimum analysis. It is currently the subject of active research at several centres. The Kalman–Bucy filter evolves the forecast error covariance matrix (with dimension = number of grid-points squared!) using linearized dynamics. With recent forms of initialization (Laplace transform and bounded derivative) and notes on assimilation of hydrological, mesoscale and ocean data, these are introduced as 'Future directions' in chapter 13.

The chapters each have a set of questions at the end, some quite testing. A series of appendices give background material on several topics including normal modes and Bessel functions. There is an extensive bibliography.

Roger Daley covers the subjects comprehensibly and well, as one might expect from his contributions over the years. The book is well produced and up to date, however it is not light reading. I would have liked to have seen an abstract or summary for each chapter. The book is obviously useful as a textbook for advanced courses in meteorology and also as reference material for meteorologists and oceanographers involved in data analysis.

N.B. Ingleby

GUIDE TO AUTHORS

Content

Articles on all aspects of meteorology are welcomed, particularly those which describe results of research in applied meteorology or the development of practical forecasting techniques.

Preparation and submission of articles

Articles, which must be in English, should be typed, double-spaced with wide margins, on one side only of A4-size paper. Tables, references and figure captions should be typed separately. Spelling should conform to the preferred spelling in the *Concise Oxford Dictionary* (latest edition). Articles prepared on floppy disk (IBM-compatible) can be labour-saving, but only a print-out should be submitted in the first instance.

References should be made using the Harvard system (author/date) and full details should be given at the end of the text. If a document is unpublished, details must be given of the library where it may be seen. Documents which are not available to enquirers must not be referred to, except by 'personal communication'.

Tables should be numbered consecutively using roman numerals and provided with headings.

Mathematical notation should be written with extreme care. Particular care should be taken to differentiate between Greek letters and Roman letters for which they could be mistaken. Double subscripts and superscripts should be avoided, as they are difficult to typeset and read. Notation should be kept as simple as possible. Guidance is given in BS 1991: Part 1: 1976, and *Quantities, Units and Symbols* published by the Royal Society. SI units, or units approved by the World Meteorological Organization, should be used.

Articles for publication and all other communications for the Editor should be addressed to: The Chief Executive, Meteorological Office, London Road, Bracknell, Berkshire RG12 2SZ and marked 'For Meteorological Magazine'.

Illustrations

Diagrams must be drawn clearly, preferably in ink, and should not contain any unnecessary or irrelevant details. Explanatory text should not appear on the diagram itself but in the caption. Captions should be typed on a separate sheet of paper and should, as far as possible, explain the meanings of the diagrams without the reader having to refer to the text. The sequential numbering should correspond with the sequential referrals in the text.

Sharp monochrome photographs on glossy paper are preferred; colour prints are acceptable but the use of colour is at the Editor's discretion.

Copyright

Authors should identify the holder of the copyright for their work when they first submit contributions.

Free copies

Three free copies of the magazine (one for a book review) are provided for authors of articles published in it. Separate offprints for each article are not provided.

Contributions: It is requested that all communications to the Editor and books for review be addressed to the Chief Executive, Meteorological Office, London Road, Bracknell, Berkshire RG12 2SZ, and marked 'For *Meteorological Magazine*'. Contributors are asked to comply with the guidelines given in the *Guide to authors* (above). The responsibility for facts and opinions expressed in the signed articles and letters published in *Meteorological Magazine* rests with their respective authors.

Subscriptions: Annual subscription £36.00 including postage; individual copies £3.25 including postage. Applications for postal subscriptions should be made to HMSO, PO Box 276, London SW8 5DT; subscription enquiries 071-873 8499.

Back numbers: Full-size reprints of Vols 1-75 (1866-1940) are available from Johnson Reprint Co. Ltd, 24-28 Oval Road, London NW1 7DX. Complete volumes of *Meteorological Magazine* commencing with volume 54 are available on microfilm from University Microfilms International, 18 Bedford Row, London WC1R 4EJ. Information on microfiche issues is available from Kraus Microfiche, Rte 100, Milwood, NY 10546, USA.

July 1992

Vol. 121
No. 1440

Contents

ISSN 0026–1149

ISBN 0-11-728985-X

Printed in the United Kingdom for HMSO
Dd 291241 7/92 C13 543 24503

The
Meteorological Magazine

August 1992

Indian monsoon indices
Cyclone tracks in the south-west Indian Ocean
Summer of 1991

HMSO

Met.O.1004 Vol. 121 No. 1441

First published 1992

HMSO

HMSO publications are available from:

HMSO Publications Centre
(Mail, fax and telephone orders only)
PO Box 276, London, SW8 5DT
Telephone orders 071-873 9090
General enquiries 071-873 0011
(queuing system in operation for both numbers)
Fax orders 071-873 8200

HMSO Bookshops
49 High Holborn, London, WC1V 6HB
(counter service only)
071-873 0011 Fax 071-873 8200
258 Broad Street, Birmingham, B1 2HE
021-643 3740 Fax 021-643 6510
Southey House, 33 Wine Street, Bristol, BS1 2BQ
0272 264306 Fax 0272 294515
9-21 Princess Street, Manchester, M60 8AS
061-834 7201 Fax 061-833 0634
16 Arthur Street, Belfast, BT1 4GD
0232 238451 Fax 0232 235401
71 Lothian Road, Edinburgh EH3 9AZ
031-228 4181 Fax 031-229 2734

HMSO's Accredited Agents
(see Yellow Pages)

and through good booksellers

The Meteorological Magazine

August 1992
Vol. 121 No. 1441

Editorial

Dear readers,

I do not intend to make it part of my duties to bore you with editorial comment very often, but I will avail myself of the opportunity from time to time.

I write this time about the contents and our circulation. We would like to increase our circulation by about 15% over the next year — this would help to keep the price down and increase the number of pages. To do this we need to know more about our readers and what they want; a questionnaire will be included soon. Meanwhile, we are trying to make the magazine both useful, and more readable, by having occasional review articles to accompany major papers or to introduce topics that are to be covered in future issues.

Most of the papers submitted to us are major works that occupy nearly half an issue. These are very welcome and we hope they will continue to come in from all over the world at the rate they have been recently. However, difficulty arises because there is often room for only two topics in one issue — and neither may be of interest to you. I would like you all to consider whether you might be able to write, or encourage colleagues to write, some shorter items of perhaps 2000 words, but please glance at the inside back cover. An issue with one main article and six short ones is more likely to be interesting than one with two main articles. Why not write a letter to me? We do not publish 'letters to the editor' because we do not have any to print!

I will close on the rather vexed question of style and language. A recent article in *New Scientist*, 9 May 1992 tells of the growing incomprehensibility of specialist scientific journals. On a scale where 'comics' score −26, newspapers 0 and more difficult works above zero, two prestige journals scored 0 in the 1930s (i.e. were easily read and understood) but by 1990 their scores were about +30 (too hard for many specialists). Those of you who have English as your mother tongue, please consider your foreign readers and use simple English and, if it is at all possible, the present tense and first person (write 'I saw' NOT 'it was observed that'). If English is not your first language, you should still write in simple English because it is easier for you and your first readers — the editor and his helpers. It is most unlikely that we will reject work because the language is too simple. We do reject what WE cannot understand!

Rodney Blackall

Write to:
The Editor of Met. Mag.
Room 707a
Meteorological Office
London Road
Bracknell
Berkshire RG12 2SZ
England

551.577.2(540):551.557.32:551.553.21

Indian summer monsoon rainfall indices: 1871–1990

B. Parthasarathy, K. Rupa Kumar and D.R. Kothawale
Indian Institute of Tropical Meteorology, Dr Homi Bhabha Road, PUNE-411008, India

Summary

The Indian summer monsoon rainfall, because of its importance to the country's economy and in the global atmospheric circulation, has motivated many studies pertaining to its behaviour, characteristics, teleconnections with global/regional features and long-range prediction. These studies have used various types of rainfall series, most of them based on a variable network of rain-gauges, with the consequent inhomogeneities in the data series. The present paper describes some homogenous representations of the Indian summer monsoon rainfall for the period 1871–1990, prepared on the basis of a fixed and well-distributed network of 306 rain-gauges. An Indian Summer Monsoon Rainfall (ISMR) Index, indicating the net excess or deficient rainfall conditions over the country, is proposed. This index, and some others are listed in the papers, for ready use in the studies of monsoon, its teleconnections and other related aspects.

Statistical analysis of the above series identifies 18 large-scale dry years and 15 large-scale wet years during the last 120 years. The decadal means of ISMR index were continuously negative for three decades 1901–30, positive 1931–60 and again became negative during the current period 1961–90.

1. Introduction

The importance of the Indian monsoon rainfall to the country's economy and also as a major global circulation parameter has motivated many studies during the last century, pertaining to its characteristics, variability, teleconnections with regional/global circulation features and long-range prediction. A systematic study of the variability in annual rainfall and droughts over British India (including present-day Pakistan, Sri Lanka, Bangladesh and Burma (now Myanmar)) was first made by Blanford (1886), using areal mean rainfall (annual) during 1867–85, based on a varying network of about 500 rain-gauges. Later, Walker (1910) estimated the monsoon (June–September) rainfall of India (subsequently updated (Annual Reports of IMD) for the period 1841–1935), using a variable rain-gauge network as follows: 20–71 stations prior to 1865; 500–1500 stations for the period 1866–90 and 1500–2000 stations from 1891 to 1935. The monsoon rainfall series for the Post-independence India (as one unit) has been prepared by Parthasarathy and Dhar (1976), Parthasarathy and Mooley (1978), Thapliyal (1990) and Thapliyal and Kulshrestha (1991) with the number of rain-gauges varying from 300 to 3000 spread all over India for the different lengths of period starting from 1865 onwards. Subdivisional monsoon rainfall of India has also been estimated and studied by Rao and Jagannathan (1963), Parthasarathy and Dhar (1974), Banarjee and Raman (1976), Shukla (1987), Chowdhury *et al.* (1989) and Chowdhury and Mhasawade (1991) for the period starting from 1875 onwards using a variable rain-gauge network. However, due to the obvious inhomogeneities introduced by the variable rain-gauge network, these data sets are not suitable for advanced statistical analysis.

Monsoons also play an important role as major energy sources in the global-scale circulation. There are many recent studies notably Drosdowsky (1990), Joseph *et al.* (1991), Yasunari (1990, 1991) and Kiladis and Sinha (1991) have brought out that the Indian summer monsoon rainfall is used as an input parameter in forecasting or estimating the other regional parameters. In view of this, there is a great demand by scientists all over the world for a homogeneous data series representing the monsoon rainfall of India for their further investigations.

In this context, a long, homogeneous rainfall time-series having adequate spatial and temporal representativeness would be a very useful tool, as the amount of latent heat energy released to the atmosphere through condensation of water vapour can be obtained completely from relevant precipitation amounts (Fleer 1981). Mooley and Parthasarathy (1984) and Parthasarathy *et al.* (1987) put in considerable efforts to prepare a homogeneous rainfall series for whole India as well as different meteorological subdivisions, on the basis of a fixed network of 306 rain-gauges for the period 1871 onwards. These series have been well recognized and extensively used by many scientists (Gregory 1986, 1988, 1989; Mooley and Shukla 1987; Hastenrath 1991, etc.).

For a country as vast as India, with spatial variability of monsoon rainfall, there would almost always be some areas of deficient rain even in the best of monsoons (or some areas of floods even in the worst of monsoons). It is very difficult to incorporate all such complex spatial and temporal variabilities in a single series. Therefore, it becomes necessary to express the Indian monsoon rainfall in a variety of ways depending on the application. The present paper addresses itself to this problem.

2. Details of rainfall data

The total number of rain-gauges in India varied from 50 in 1850 to 5000 in 1990. After an initial screening of all the available data series, a fixed number of 306 well-distributed rain-gauge stations, one from each of the districts (a small administrative area) in the plain regions of India, have been selected for the present study. Care has been taken to exclude non-homogeneous records and only reliable or corrected station data have been used in the calculation of area averages. The Symon's pattern rain-gauge with a 127 mm (5 inches) diameter funnel, one foot above the surface, was used in the data period, and there had been no changes in instruments. The earliest year for which reliable data is available for these stations is 1871. The relevant rainfall data at these 306 stations have been obtained for the period 1871 to present from the records of the India Meteorological Department, Pune (for further details of data see the publications of Mooley *et al.* 1981; Mooley and Parthasarathy 1984 and Parthasarathy *et al.* 1987). The hilly regions consisting of four subdivisions in the Himalayas (hatched areas in Fig. 1) have not been

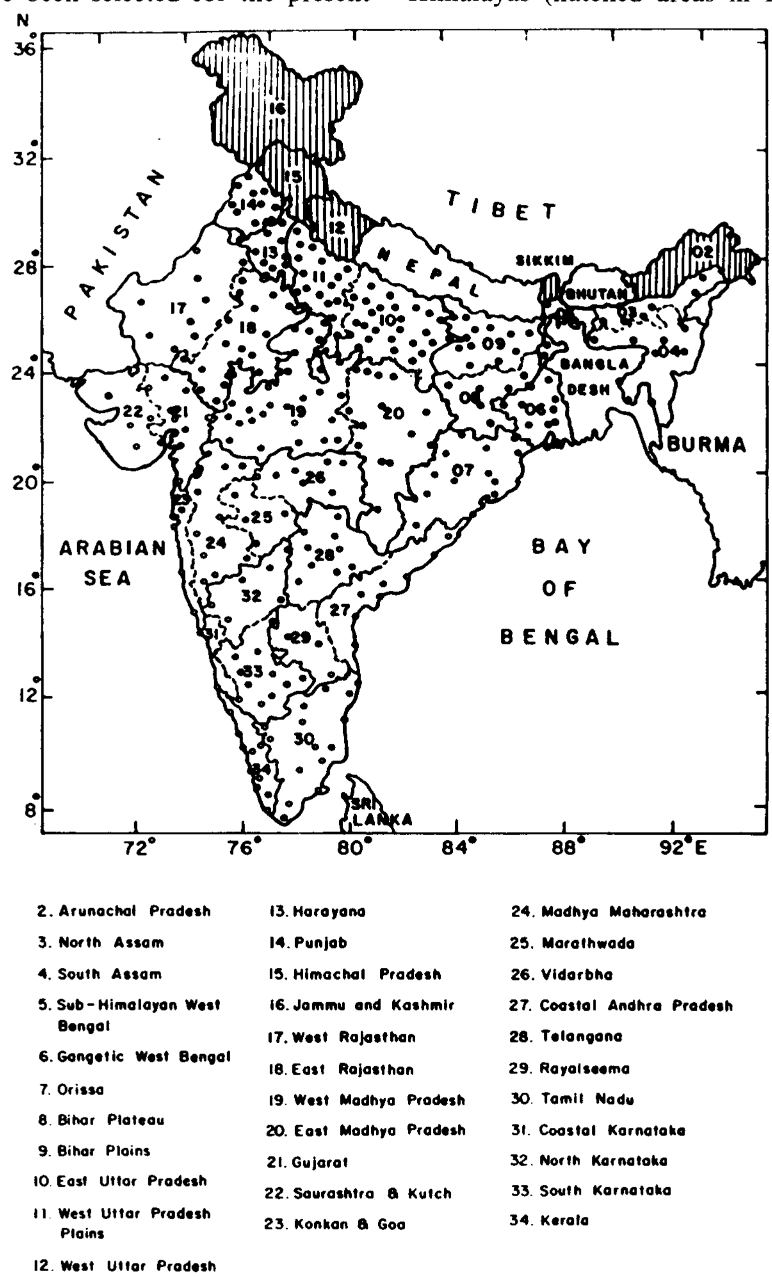

Figure 1. Latest Meteorological subdivisions of India with network and locations of rain-gauges considered. Hatched hilly subdivisions are not considered.

considered in view of the inadequate rain-gauge network, their limited representativeness and non-monsoonal nature of rainfall there. The islands in the Bay of Bengal (subdivision number 1) and the Arabian Sea (subdivision number 35), not shown in Fig. 1, have also not been considered for the present study to maintain contiguity. The contiguous area considered measures 2.88×10^6 km^2, which consitutes about 90% of the country's total area. The spatial pattern of mean summer monsoon rainfall based on data for 306 stations over the period 1871–1978 (Parthasarathy 1984a) is in good agreement with the climatological (normal) map prepared by the India Meteorological Department (IMD) on the basis of about 3000 rain-gauge stations for the period 1901–50; (IMD 1981, Rao 1976). This shows that the rainfall stations selected here are adequately representative. Also, the rainfall data of all the individual stations used in this analysis have been found to be homogeneous, Gaussian-distributed and free from persistence for the period 1871–1978 (Parthasarathy 1984a).

Fig. 1 shows the latest meteorological subdivisions into which the country has been divided and the area considered along with the location of rain-gauges used in this study. Area-weighted mean summer monsoon rainfall (June through September) for each of the 29 meteorological subdivisions have been prepared by assigning the district area as the weight for each representative rain-gauge station for the period 1871–1984 (Parthasarathy *et al.* 1987). Similarly, the All-India (India taken as one unit) mean monsoon rainfall is computed by taking the weighted average of the subdivisional monsoon rainfall, with the subdivisional areas as the weights. For the recent period after 1985, the rainfall data for some of the 306 stations are not readily available in published form; however, to make the study up-to-date, the following procedure has been followed. The Hydrology Unit of IMD, Pune compiles the monthly and seasonal rainfall data based on all reported observatory stations (about 350) soon after every season for different meteorological subdivisions of India, and these are published in the subsequent issues of official IMD Journal *Mausam*. From these and from other IMD publications, we obtained the seasonal rainfall data (R_{ij} for the *i*th subdivision and *j*th year) for the period 1985–1991 for each of the 29 subdivisions used in this study; however, the number of reporting stations varied from year-to-year. The IMD seasonal normal rainfall ($\bar{R}_{ij}$ period 1901–1970) of each of the subdivisions prepared on the basis of reporting stations are also available for each year. From these data, the estimates of subdivisional monsoon rainfall R^*_{ij} for the period 1985–1991 are obtained from the expression

$$R^*_{ij} = R_{ij} \, (R^*_i / \bar{R}_{ij})$$

where R^*_i is the subdivisional normal based on the stations used by Parthasarathy *et al.* (1987) for the period 1871–1978. As such, these data may be considered to be approximate and realistic for immediate use.

The 29 subdivisional and All-India monsoon rainfall series are found to be homogeneous, random and normally distributed (Mooley and Parthasarathy 1984; Parthasarathy *et al.* 1987) for the period 1871–1978. The values for the period 1981–91 are presented in Table I, i.e. updating the values of the Table II of the paper by Parthasarathy *et al.* (1987).

3. All-India monsoon rainfall series

The yearly All-India monsoon rainfall data, along with the percentage departure from the long term (1871–1984) average, are listed in Table II for the period 1871–1990. The mean (R), standard deviation (S) and coefficient of variation (CV) of the All-India monsoon rainfall respectively are 852 mm, 83 mm and 9.8% for the period 1871–1984. The highest rainfall was 1017 mm in the year 1961 and lowest 604 mm in 1877. The range of All-India rainfall during a period of 120 years is 413 mm which is 48% of the average. The monsoon rainfall of an individual year is classified as large-scale deficient (dry year) when it is less than $\bar{R}-S$ and excess (wet year) when it is more than $\bar{R}+S$. With this criterion, there are 21 dry and 18 wet years during the period 1871–1990 (Fig. 2). It is also observed that there are many negative departures during the periods 1899–1920 and 1962–87 and positive departures during 1874–94 and 1942–61. A general increase in the rainfall from 1899 to 1961 can also be seen. To delineate the slow variations, the rainfall series has been subjected to a binomial low-pass filter (Mitchell *et al.* 1966, Tyson *et al.* 1975) and the filtered rainfall curve along with the percentage departure of All-India rianfall series are shown in Fig. 2. It is observed that the low-pass filter curve is generally below the normal rainfall during the periods 1899–1920 and 1962–87 and positive departure during 1874–94 and 1942–61.

This All-India data set gives a generalized picture but does not satisfactorily quantify the spatial extents of anomalous situations. Therefore, an attempt has been made to prepare data sets indicating the spatial extent of excessive and deficient rainfall conditions, by adopting suitable criteria.

4. Methodology

Various definitions have been used to define drought/flood over a region, depending on the context. In a tropical country like India, rainfall invariably becomes the dominant parameter in almost all the definitions of droughts and floods. The India Meteorological Department (1971) (see also Raman (1975) Government of India (1976)) consider drought to have occurred in a year over a subdivision when the seasonal rainfall is less than 75% of the normal. However, this criterion does not take into account the variability of the rainfall over the different

Table I. Summer monsoon (June–Sept.) rainfall values (mm) for 29 subdivisions of India for the period 1981–91 with long-term means for comparison

Subdivision number and name	Area of India (%)	1871–1984 mean	1981	1982	1983	1984	1985	1986	1987	1988	1989	1990	1991
03 North Assam	1.96	1451	1314	1363	1503	1502	1598	1339	1698	1676	1595	1552	1235
04 South Assam	4.28	1451	1113	1258	1308	1312	1304	1082	1350	1449	1497	1353	1294
05 Sub-Himalayan West Bengal	0.75	1991	1838	1636	2051	2316	2080	1775	2718	2439	2146	1832	2462
06 Gangetic West Bengal	2.30	1143	1158	905	981	1519	1305	1317	1460	1561	1421	1429	1602
07 Orissa	5.41	1168	1094	1074	1009	1288	1373	1258	781	1132	1263	1237	1283
08 Bihar Plateau	2.27	1100	936	889	987	1220	952	1005	1186	1125	1180	1427	1230
09 Bihar Plains	3.27	1032	1113	721	895	1502	1096	1002	1682	1075	1013	860	920
10 East Uttar Pradesh	5.09	912	1085	989	958	1032	1037	796	541	893	921	1051	807
11 West Uttar Pradesh	3.36	771	639	681	1059	814	883	595	425	994	686	726	663
13 Haryana	1.59	458	435	315	622	497	537	331	167	843	326	548	352
14 Punjab	1.75	492	283	338	413	549	570	544	160	1086	456	829	481
17 West Rajasthan	6.77	256	215	197	383	208	180	176	102	280	237	445	133
18 East Rajasthan	5.11	641	602	467	691	580	488	551	322	695	506	679	458
19 West Madhya Pradesh	8.07	923	817	912	1061	865	807	893	712	855	707	1066	742
20 East Madhya Pradesh	7.79	1205	964	987	1167	1098	1185	1041	954	1081	1061	1384	1114
21 Gujarat	2.99	873	974	580	1110	1032	395	426	354	1148	786	1001	601
22 Saurashtra and Kutch	3.82	437	490	232	607	388	195	261	84	721	454	329	220
23 Konkan and Goa	1.18	2382	2598	2383	3556	2389	2510	1632	2420	2695	2370	2660	2427
24 Madhya Maharashtra	4.00	581	725	415	732	500	393	460	410	933	627	654	703
25 Marathwada	2.24	690	757	616	1054	367	479	556	571	1324	1055	940	613
26 Vidarbha	3.39	900	1136	726	1038	613	654	870	569	1076	793	1140	715
27 Coastal Andhra Pradesh	3.23	505	599	425	758	381	458	468	313	722	749	420	639
28 Telangana	3.98	718	916	728	1083	576	513	697	580	1103	988	740	667
29 Rayalseema	2.40	421	471	396	690	291	295	344	373	636	546	397	485
30 Tamilnadu	4.52	308	398	185	402	322	451	259	275	441	343	294	333
31 Coastal Karnataka	0.64	2852	3271	3376	3654	2491	2474	2476	2274	3358	3010	2744	3277
32 North Karnataka	2.77	603	764	590	819	551	467	490	491	765	692	500	685
33 South Karnataka	3.24	503	568	376	599	499	339	564	529	751	611	356	689
34 Kerala	1.35	1940	2526	1749	2054	1622	1656	1531	1469	2114	1826	1435	2405

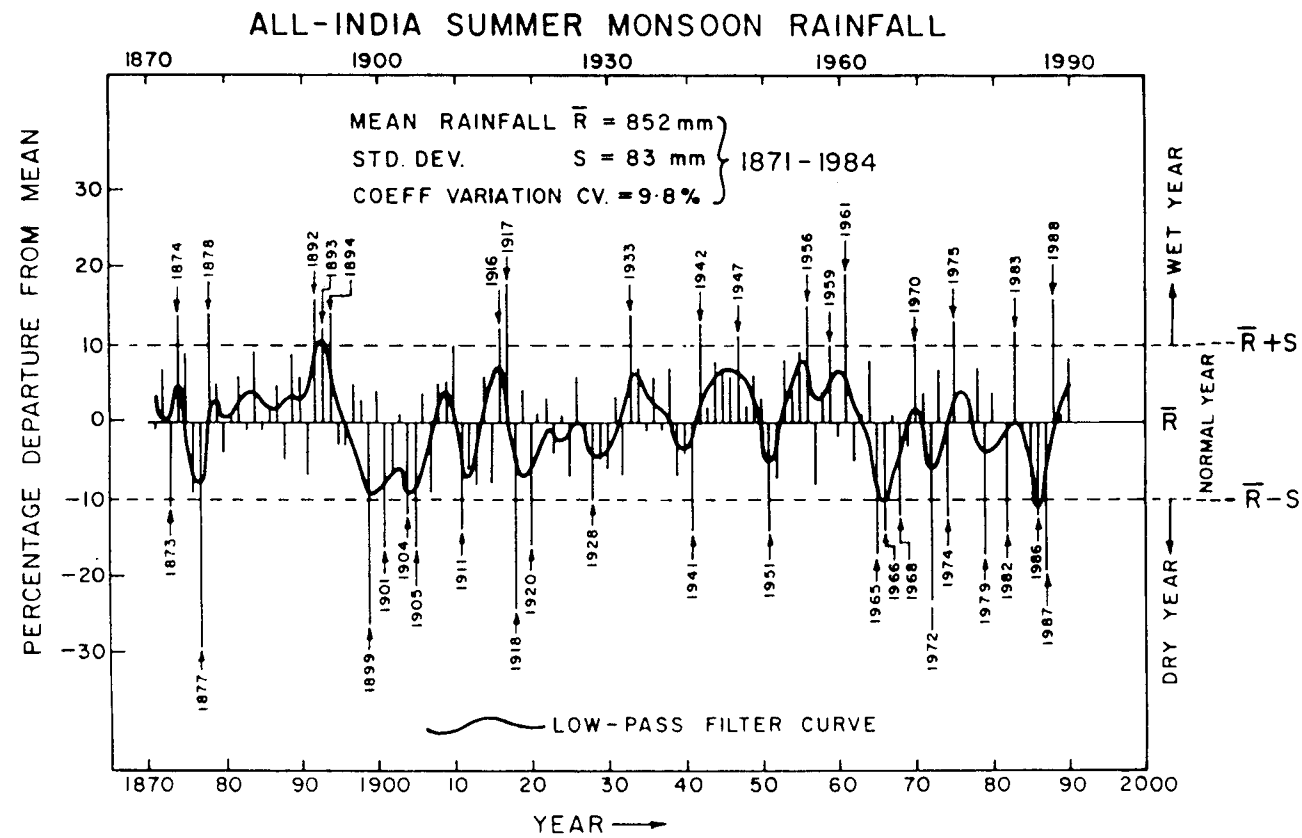

Figure 2. Year-to-year percentage departure (from mean) of All-India summer monsoon rainfall from 1871 onwards. Excess/deficient years are marked against the bars.

subdivisions of the country which varies from 12% in Assam to 44% in Gujarat. In any region, human activities are adapted to the prevailing climatic pattern of the region and also to the average rainfall variability. Therefore, it may be presumed that only rainfall deficits/excesses exceeding the average variability of the season are felt by the people of the respective region as being significantly detrimental. In general terms it can be regarded as the condition where there is lack of sufficient water to meet the requirements of plants, animals and human population of the region. It appears reasonable to define normal rainfall over a region in terms of the standard deviate, $(R_i-\bar{R})/S$, since CV over different parts of India varies between 15% and 45%. Parthasarathy *et al.* (1988, 1992) classified the All-India monsoon rainfall of an individual year as deficient when it is less than $\bar{R}-S$ and excessive when it is more than $\bar{R}+S$, and showed the impact of these extreme rainfall years on the total as well as rainy-season food-grain production of the country. Similar reasoning can be extended to the subdivisional scale also. Thus, the seasonal rainfall (R_i) for a meteorological subdivision in the ith year is classified as being deficient when it is less than $\bar{R}-S$ and excess rainfall when R_i is more than $\bar{R}+S$. If R_i is within $\bar{R}\pm S$, the rainfall is treated as normal.

5. Area under deficient/excess rainfall conditions

On the basis of the criterion described in the earlier section, the seasonal rainfall values over each of the 29 meteorological subdivisions are classified into deficient, excess and normal categories in each year of the period from 1871 to 1990. In each year, the total area of the country falling under the deficient/excess rainfall conditions has been computed and expressed as percentage of the total area of the country and is presented in Table II. The year-to-year variation in the area under deficient monsoon rainfall can be seen in Fig. 3. The number of subdivisions reporting deficient/excess monsoon rainfall conditions are also shown in Fig. 3. The mean, standard deviation and CV are 15.1 (D), 16.3 (S_D) and 108% respectively for Deficient area (DA) series and 15.3 (E), 12.0 (S_E) and 78% for Excess area (EA) series, respectively, for the period 1871–1984. It can be noted that the mean for DA and EA series is almost same, but the variability is relatively more for DA series.

A large-scale deficient (Dry) and Excess (Wet) rainfall year can be defined as that when the area under deficient and excess rainfall exceeds the corresponding long-term (1871–1984) mean area by one standard deviation (i.e. Dry year, $d \geqslant D+S_D$ and Wet year, $w \geqslant E+S_E$). Based on this criterion, there are 21 large-scale excess (Wet)

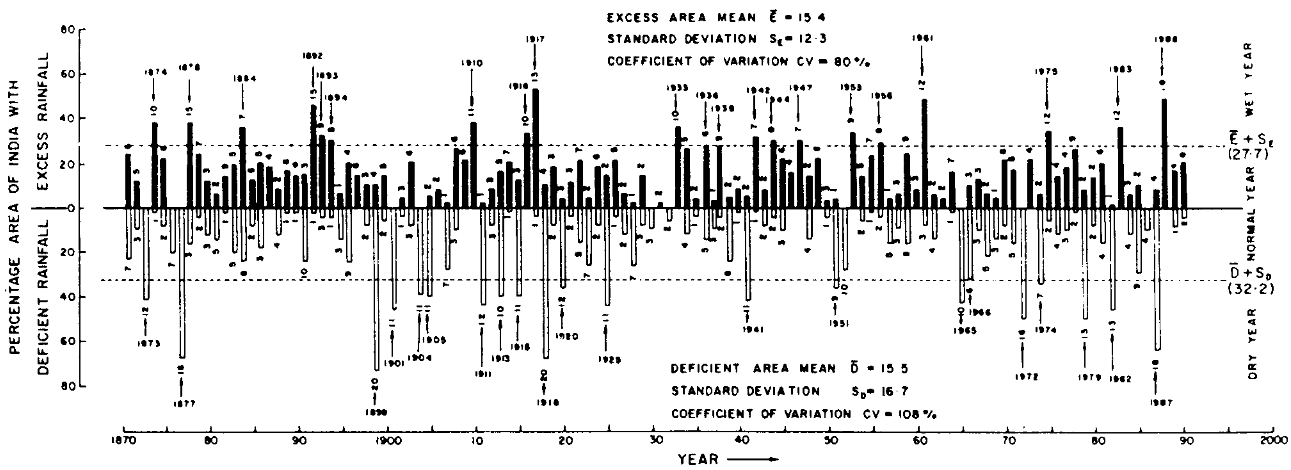

Figure 3. Year-to-year variations in the percentage area of India with excess and deficient monsoon rainfall conditions for the years from 1871 onwards.

years and 20 large-scale deficient (Dry) years (see Tables III and IV) during the period 1871–1990 (Fig. 3). It may be mentioned here that the DA and EA series are skewed and the use of standard deviation to define the thresholds may be of doubtful effectiveness. To examine this aspect, Gamma distribution has been fitted to the series and the extreme years have been identified by following the extreme 15% criterion on either side. It has been observed that these years are closely tallying with those identified by means of standard deviation (Tables III and IV). Therefore, the authors have proceeded with the use of standard deviation. It can be seen that the wet and dry years are clustering alternatively in two groups:

(a) during 1874–1894, six wet years,
(b) during 1899–1925, ten dry years,
(c) 1933–61, nine wet years, and
(d) 1965–87, seven dry years.

The country suffered the six worst dry years 1877, 1899, 1918, 1972, 1979 and 1987 when the deficient area (DA) was more than D+2S_D and the five wettest years 1878, 1892, 1917, 1961 and 1988 when the excess area (EA) was more than E+2S_E. The highest value of DA is 66.8 for the year 1877 and that of EA is 52.8 for the year 1917.

To examine the long-term variability in the DA and EA series, their decadal means are presented in Fig. 4. It can be seen that most of the decadal means of EA are close to the overall mean, while those of DA show several decades of large departures from mean. There is a gradual increase from the decades 1881–90 to the highest value in 1911–20, and then a decrease to the lowest in 1931–40. Subsequently, the DA shows a monotonic increase up to the recent decade, 1981–90. Seven decadal means of DA are more than the long-period mean D, of which three are in the recent period. In two decades, 1931–40 and 1951–60, the decadal means of both EA and DA are lower than their overall means.

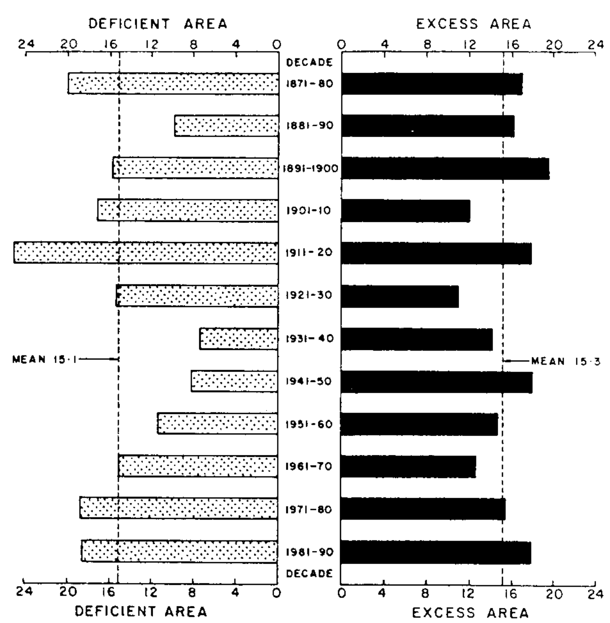

Figure 4. Decadal percentage area of India with deficient/excess monsoon rainfall conditions.

6. Indian summer monsoon rainfall (ISMR) index

It may also be of interest to know the net performance of the monsoon over the country as a whole. Subtracting DA from EA yields our Indian Summer Monsoon Rainfall (ISMR) Index (=EA−DA). The ISMR index values for the period 1871–1990 are shown in Fig. 5 and listed in Table II. The ISMR index gives the net total

Table II. Different Indian summer monsoon (June–Sept.) rainfall indices for the period 1871–1991 of contiguous India

Year	All-India rainfall (mm)	Departure from mean (%)	Deficient rainfall Area of DA (%)	Deficient rainfall Number of subdivisions	Excess rainfall Area of EA (%)	Excess rainfall Number of subdivisions	ISMR index (EA−DA) (%)
1871	846.1	−0.7	23.0	7	23.4	6	0.4
1872	910.1	6.8	9.0	3	11.8	5	2.8
1873	754.5	−11.4	40.9	12	0.0	0	−40.9
1874	971.2	14.0	2.3	1	38.5	10	36.2
1875	928.5	9.0	7.2	2	21.9	6	14.7
1876	776.4	−8.9	19.8	7	0.0	0	−19.8
1877	604.0	−29.1	66.8	18	0.0	0	−66.8
1878	973.8	14.3	16.0	3	39.0	15	23.0
1879	893.6	4.9	3.6	2	23.8	7	20.2
1880	817.1	−4.1	11.7	3	12.0	3	0.3
1881	860.2	1.0	13.2	5	5.7	2	−7.5
1882	900.7	5.7	2.0	1	13.6	5	11.6
1883	848.9	−0.4	19.8	5	19.0	5	−0.8
1884	929.4	9.1	23.2	8	36.2	7	13.0
1885	842.4	−1.1	7.2	2	11.4	5	4.2
1886	870.2	2.1	17.2	3	19.3	5	2.1
1887	896.8	5.3	0.0	0	18.1	4	18.1
1888	810.0	−4.9	12.2	4	8.4	2	−3.8
1889	926.9	8.8	2.3	1	16.0	6	13.7
1890	903.6	6.1	1.3	1	14.5	4	13.2
1891	789.2	−7.4	24.5	10	14.8	3	−9.7
1892	989.8	16.2	2.3	1	46.7	15	44.4
1893	953.5	11.9	3.9	3	32.2	9	28.3
1894	969.3	13.8	3.2	1	29.8	8	26.6
1895	825.2	−3.1	13.1	3	5.4	1	−7.7
1896	824.3	−3.3	24.4	9	19.2	4	−5.2
1897	890.2	4.5	0.0	0	13.3	6	13.3
1898	880.3	3.3	7.0	2	10.7	3	3.7
1899	628.5	−26.2	73.0	20	10.3	4	−62.7
1900	885.4	3.9	6.2	2	13.9	5	7.7
1901	718.9	−15.6	45.4	11	0.0	0	−45.4
1902	791.4	−7.1	3.4	1	3.3	3	−0.1
1903	858.1	0.7	8.3	3	20.1	6	11.8
1904	749.5	−12.0	38.9	11	0.0	0	−38.9
1905	715.2	−16.1	40.1	11	5.0	2	−35.1
1906	882.8	3.6	0.0	0	7.5	2	7.5
1907	776.4	−8.9	27.8	7	1.3	1	−26.5
1908	894.7	5.0	9.1	3	25.3	6	16.2
1909	888.8	4.3	0.0	0	20.8	6	20.8
1910	934.8	9.7	0.0	0	37.3	11	37.3
1911	733.1	−14.0	43.5	12	2.8	1	−40.7
1912	804.4	−5.6	7.3	3	8.4	3	1.1
1913	782.0	−8.2	40.3	10	15.1	5	−25.2
1914	899.0	5.5	2.8	1	20.2	7	17.4
1915	780.1	−8.4	39.7	11	11.6	3	−28.1
1916	949.7	11.5	0.0	0	33.0	10	33.0
1917	1003.2	17.7	4.3	1	52.8	13	48.5
1918	648.3	−23.9	68.2	20	10.3	4	−57.9
1919	884.8	3.8	8.3	2	18.6	3	10.3
1920	717.6	−15.8	36.5	12	4.9	3	−31.6
1921	863.4	1.3	4.5	2	10.8	3	6.3
1922	867.4	1.8	15.6	5	20.9	7	5.3
1923	818.7	−3.9	25.6	7	4.1	2	−21.5
1924	861.8	1.1	8.8	2	18.2	6	9.4
1925	802.9	−5.8	43.1	11	13.2	2	−29.9
1926	901.4	5.8	4.0	1	21.0	5	17.0
1927	849.4	−0.3	11.3	2	6.2	2	−5.1
1928	766.4	−10.0	25.4	7	2.3	1	−23.1
1929	819.5	−3.8	7.2	3	13.2	2	6.0

Table II. (Continued)

1930	800.4	−6.1	8.5	3	0.0	0	−8.5
1931	876.8	2.9	0.0	0	2.5	2	2.5
1932	800.6	−6.0	5.6	2	0.0	0	−5.6
1933	972.8	14.2	0.0	0	35.5	10	35.5
1934	913.4	7.2	12.4	4	26.4	5	14.0
1935	843.5	−1.0	3.2	1	4.4	2	1.2
1936	904.1	6.1	14.4	5	27.7	6	13.3
1937	843.3	−1.0	9.2	3	3.0	1	−6.2
1938	908.1	6.6	4.4	2	28.4	9	24.0
1939	788.8	−7.4	23.0	6	5.1	2	−17.9
1940	850.4	−0.2	1.6	1	8.8	2	7.2
1941	729.3	−14.4	41.8	11	5.1	2	−36.7
1942	958.4	12.5	0.8	1	32.1	7	31.3
1943	866.3	1.7	7.9	2	8.2	2	0.3
1944	921.5	8.2	4.7	2	29.5	6	24.8
1945	907.6	6.5	10.1	3	21.9	6	11.8
1946	901.4	5.8	0.0	0	15.2	4	15.2
1947	942.5	10.6	0.0	0	29.8	7	29.8
1948	872.6	2.4	13.7	4	13.2	2	−0.5
1949	901.8	5.8	0.0	0	22.2	8	22.2
1950	875.1	2.7	3.4	1	3.1	3	−0.3
1951	737.1	−13.5	36.3	9	4.3	1	−32.0
1952	792.0	−7.0	27.9	10	0.0	0	−27.9
1953	919.9	8.0	0.0	0	33.9	9	33.9
1954	885.4	3.9	5.1	2	13.6	5	8.5
1955	930.0	9.2	2.8	1	22.8	7	20.0
1956	979.6	15.0	3.3	2	28.8	8	25.5
1957	784.5	−7.9	15.5	5	3.2	1	−12.3
1958	886.5	4.0	8.5	3	6.1	3	−2.4
1959	938.4	10.1	15.3	5	24.4	9	9.1
1960	839.6	−1.5	0.0	0	8.3	3	8.3
1961	1017.2	19.4	7.0	3	48.9	12	41.9
1962	807.2	−5.3	14.8	4	5.0	2	−9.8
1963	855.5	0.4	0.0	0	3.4	2	3.4
1964	920.2	8.0	2.3	1	15.7	7	13.4
1965	706.9	−17.0	43.0	10	0.0	0	−43.0
1966	735.4	−13.7	31.3	8	10.8	3	−20.5
1967	858.9	0.8	9.5	3	11.2	3	1.7
1968	753.7	−11.5	22.0	5	5.6	2	−16.4
1969	829.3	−2.7	14.5	3	4.0	1	−10.5
1970	939.6	10.3	8.6	2	20.6	8	12.0
1971	886.1	4.0	16.3	5	17.0	5	0.7
1972	653.4	−23.3	49.5	16	0.0	0	−49.5
1973	911.7	7.0	0.0	0	21.7	4	21.7
1974	747.1	−12.3	34.1	7	6.2	2	−27.9
1975	960.2	12.7	6.2	2	33.4	12	27.2
1976	854.9	0.3	12.3	4	13.1	4	0.8
1977	880.6	3.4	9.8	3	17.2	4	7.4
1978	908.1	6.6	2.7	2	25.4	9	22.7
1979	707.7	−16.9	49.2	13	7.1	2	−42.1
1980	882.7	3.6	8.8	2	12.9	2	4.1
1981	852.7	0.1	16.6	4	20.0	6	3.4
1982	735.3	−13.7	46.4	13	0.6	1	−45.8
1983	955.6	12.2	0.0	0	36.7	12	36.7
1984	835.7	−1.9	11.3	4	6.3	3	−5.0
1985	786.8	−7.7	28.8	9	9.9	2	−18.9
1986	746.5	−12.4	9.8	4	0.0	0	−9.8
1987	687.9	−19.3	64.3	16	8.3	4	−56.0
1988	990.6	16.3	0.0	0	48.9	18	48.9
1989	862.3	1.2	8.1	1	17.4	6	9.3
1990	917.1	7.6	4.6	2	19.2	6	14.6
1991	814.5	−4.3	29.1	6	14.9	6	−14.2

Table III. Large-scale deficient (dry) years of India, identified on the basis of different analysis of All-India/29 meteorological subdivisional monsoon rainfall data for the period 1871–1990

Serial number	Year	All-India monsoon rainfall Amount (mm)	All-India monsoon rainfall Departure from normal (%)	Area of India with deficient rainfall conditions (%)	ISMR Index (%)	Rank based on ISMR Index
1	1873	755	−11.4	40.9	−40.9	10
2	1877	604	−29.1	66.8	−66.8	1
3	1899	629	−26.2	73.0	−62.7	2
4	1901	719	−15.6	45.4	−45.4	7
5	1904	750	−12.0	38.9	−38.9	12
6	1905	715	−16.1	40.1	−35.1	14
7	1907+	776	−8.9	27.8	−26.5	21
8	1911	733	−14.0	43.5	−40.7	11
9	1913*	782	−8.2	40.3	−25.2	22
10	1915*	780	−8.4	39.7	−28.1	18
11	1918	648	−23.9	68.2	−57.9	3
12	1920	718	−15.8	36.5	−31.6	16
13	1925*	803	−5.8	43.1	−29.9	17
14	1928+	766	−10.0	25.4	−23.1	23
15	1941	729	−14.4	41.8	−36.7	13
16	1951	737	−13.5	36.3	−32.0	15
17	1952+	792	−7.0	27.9	−27.9	19
18	1965	707	−17.0	43.0	−43.0	8
19	1966	735	−13.7	31.3	−20.5	24
20	1968*	754	−11.5	22.0	−16.4	25
21	1972	653	−23.3	49.5	−49.5	5
22	1974	747	−12.3	34.1	−27.9	20
23	1979	708	−16.9	49.2	−42.1	9
24	1982	735	−13.7	46.4	−45.8	6
25	1986+	747	−12.4	9.8	−9.8	26
26	1987	688	−19.3	64.3	−56.0	4

+ Identified by one index
* Identified by two indices

area over the country under rainfall deficiency (negative area) or excess (positive area). It is shown by Parthasarathy *et al.* (1991a) that the *Kharif* food-grain production (rice, wheat, sorghum, pearl millet, maize, chick-pea, pulses, etc.) of the country and ISMR index for the period 1966–88 had a high correlation of 0.865 (however, with All-India rainfall series the CC is 0.878) indicating that this index also adequately represents the net monsoon performance over the country. This index could be very useful to the governmental agencies for resource assessment and planning purposes. The mean (A) and standard deviation (S) of ISMR index are 0.2 and 24.1 respectively for the period 1871–1984. The lowest index value was −66.8 in the year 1877 and the highest 48.9 in the year 1988.

For identifying the extreme rainfall years based on ISMR index, the similar procedure as adopted in the earlier section is used, i.e. the index in any year if it is less than $A-S$ denoting a dry year and more than $A+S$ denoting wet year. It is observed that there were 17 wet years and 21 dry years during the data period (Fig. 5). There is a conspicuous clustering of dry and wet years in two periods:

(a) 1899–1925 containing eleven dry monsoon years, and

(b) 1933–1961 containing seven wet monsoon years.

The frequent occurrence of dry years during the period 1899–1925 caused severe hardship as the crop production was critically dependent on the rainfall in this period, with agricultural technology not as developed as at present. The Census reports of Mitra (1978) indicate that the population growth rate decreased from +5.8 per thousand during 1901–11 to −0.3 per thousand during 1911–21. This population decrease is mainly noticed over West Bengal, Bihar, Madhya Pradesh Orissa, Rajasthan, Maharashtra and Karnataka states, where many deficient rainfall years are also noticed during the decade 1911–20, clearly showing the disastrous impact of the monsoon failure.

Fig. 6 shows the decadal means of ISMR index during the period 1871–1990. It is interesting to note

Table IV. Large-scale excess (wet) years of India, identified on the basis of different analysis of All-India/29 meteorological subdivisional monsoon rainfall data for the period 1871–1990

Serial number	Year	All-India monsoon rainfall Amount (mm)	All-India monsoon rainfall Departure from normal (%)	Area of India with excess rainfall conditions (%)	ISMR Index (%)	Rank based on ISMR Index
1	1874	971	+14.0	38.5	36.2	7
2	1878*	974	+14.3	39.0	23.0	19
3	1884+	929	+9.1	36.2	13.0	21
4	1892	990	+16.2	46.7	44.4	3
5	1893	954	+11.9	32.2	28.3	12
6	1894	969	+13.8	29.8	26.6	15
7	1910	935	+9.7	37.3	37.3	5
8	1916	950	+11.5	33.0	33.0	10
9	1917	1003	+17.7	52.8	48.5	2
10	1933	973	+14.2	35.5	35.5	8
11	1936+	904	+6.1	27.7	13.3	20
12	1938+	908	+6.6	28.4	24.0	18
13	1942	958	+12.5	32.1	31.3	11
14	1944*	922	+8.2	29.5	24.8	17
15	1947	943	+10.6	29.8	29.8	12
16	1953*	920	+8.0	33.9	33.9	9
17	1956	980	+15.0	28.8	25.5	16
18	1959+	938	+10.1	24.4	9.1	23
19	1961	1017	+19.4	48.9	41.9	4
20	1970+	940	+10.3	20.6	12.0	22
21	1975	960	+12.7	33.4	27.2	14
22	1983	956	+12.2	36.7	36.7	6
23	1988	991	+16.3	48.9	48.9	1

+ identified by one index
* Identified by two indices

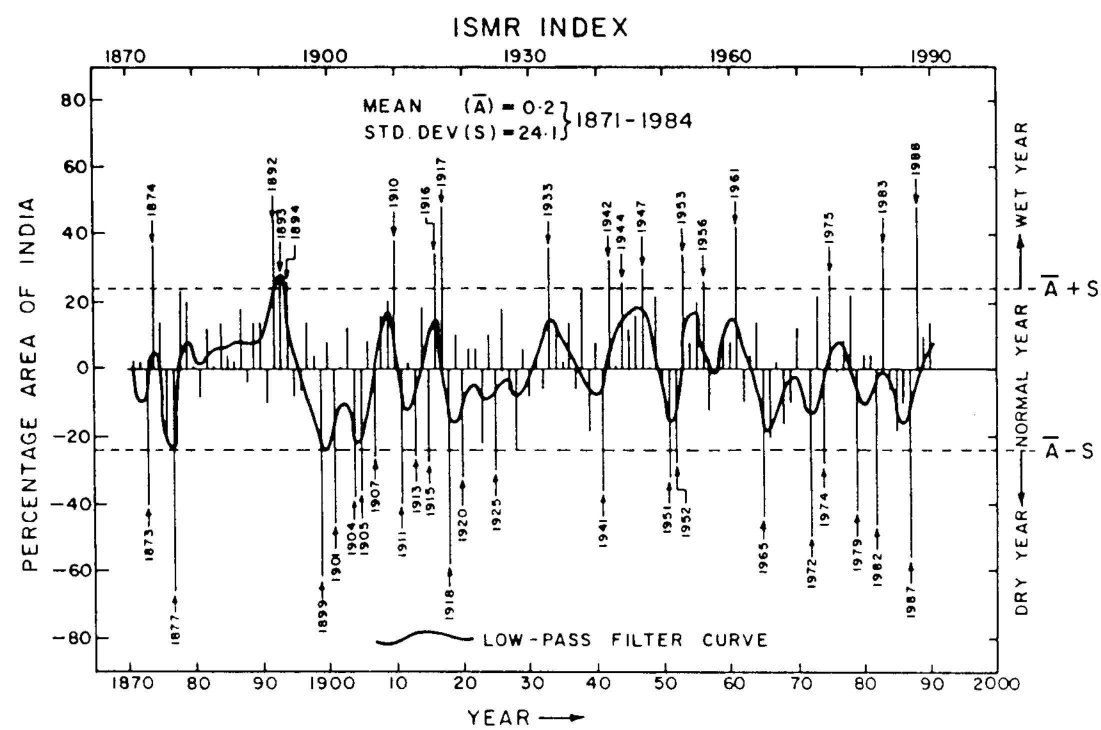

Figure 5. Year-to-year variation of Indian summer monsoon rainfall (ISMR) index for the years from 1871 onwards, wet/dry years are indicated against bars.

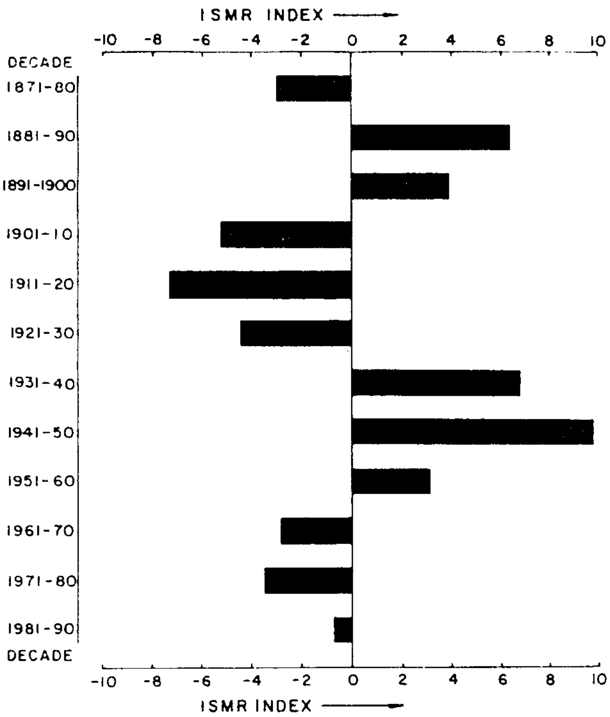

Figure 6. Decadal mean of ISMR index, for the period 1871–1990.

from Fig. 6 that three continuous decades (1901–30) reported negative index followed by three decades (1931–60) of positive index and, later again, three decades (1961–90) of negative index. It is well known that the release of latent heat energy over the Indian subcontinent is responsible for some of the low/middle latitudinal circulations over the globe (Fleer 1981). It can clearly be seen how this energy source has varied from long-term normal during the decades 1871–1990 (Fig. 6), further suggesting that some major circulation changes over India or other parts of the tropical regions might have taken place during these decades in response to the latent heat changes over India. Parthasarathy *et al.* (1991b), Fu and Fletcher (1988) and Elliott and Angell (1987, 1988) have shown that some evidence of large signals of decadal-scale climatic variations over the tropical regions of the globe. The present study provides some supporting evidence to their work.

To identify the significantly prolonged occurrence of extremes in the series, the 10-year moving *t*-test (called Cramer's test) as suggested by Lawson *et al.* (1981) has been applied on all the four series for the period 1871–1990. The calculated Cramer's *t*-values exceeding the table value of ± 1.96 (significant at 5% level) have been found for:

(a) five decades in All-India rainfall series (1896–1905; 1897–1906; 1898–1907; 1899–1908 and 1965–74),
(b) three decades in DA series (1898–1907; 1899–1908 and 1911–20),
(c) four decades in EA series (1897–1906; 1898–1907; 1908–17 and 1923–32), and
(d) three decades in ISMR indices (1896–1905; 1898–1907 and 1899–1908).

The decade 1898–1907 (deficient rainfall period) was common in all the series. Thus, it can be seen that there were definite clusters of positive and negative extremes in the rainfall roughly in the periods separated by the turning point mentioned above. These are not gradual changes but are in the form of epochs.

The above four series have also been subjected to power spectrum analysis following the Blackman–Tukey algorithm (Mitchell *et al.*, 1966) to find significant periodicities if any. The only significant cycle at 5% level corresponding to Quasi-Biennial Oscillation (2–3 years) in the series. However, this cycle accounts for only about 10% or less of the total variance and therefore is of limited practical application.

The intercorrelations among the four indices are presented in Table V. All the Correlation Coefficients (CCs) are high and statistically significant at 0.1% level. The CC between DA and EA, though negative as expected, is relatively low, indicating that they do not necessarily exclude each other. The ISMR index is highly sensitive to both DA and EA as well as the All-India monsoon rainfall.

7. Discussion

In this study, the monsoon rainfall performance over India has been quantified in four different ways, which may be useful for different purposes. Identification of large-scale deficient (dry) or excess (wet) years of the country are of primary concern to the planners, as the economy is dependent upon these vagaries.

Out of the 26 dry years based on different indices (Table III), 18 years are common to all types of the indices. Three years (1913, 1915 and 1925) are identified as dry years by only two indices while five years (1907, 1928, 1952, 1968 and 1986) are identified as dry years by only one index. Therefore, it can be inferred that the country has suffered from large-scale deficient conditions in 18 years during 1871–1990 and the other years might have had marginal rainfall deficiency. Out of the 23 wet years based on different indices (Table IV), 15 years are common to all types of the indices. Three wet years 1878, 1944 and 1953 indicated by only two indices while five wet years 1884, 1936, 1938, 1959 and 1970 are indicated by only one index.

8. Conclusions

Suitable indices are presented to represent the Indian summer monsoon rainfall during the data period 1871–1990 based on area-weighted mean rainfall series of 29 subdivisions, in turn computed from the rainfall data at 306 well-distributed rain-gauges over the country. The following are the main conclusions of the study:

(a) The mean All-India monsoon rainfall for the period 1871–1984 is 852 mm, with a standard deviation (S) of 83 mm and CV of 9.8%.
(b) The rainfall was below average in many years during 1899–1920 and 1962–87, and above average during 1874–94 and 1942–61.

Table V. Interrelationships (CCs) between the indices for the period 1871–1984

Indices	SMRF	DA	EA	ISMR
All-India summer monsoon rainfall (SMRF)	1.0			
Deficient area (DA)	−0.84	1.0		
Excess area (EA)	+0.78	−0.45	1.0	
ISMR index	+0.95	−0.90	+0.80	1.0

(c) The mean percentage area of the country with deficient area (DA) rainfall condition is 15.1 with an S of 16.3 and CV 108%, respectively and those for the Excess Area (EA) are 15.3, 12.0 and 78%, respectively.
(d) On the basis of different classifications there are mainly 18 large-scale dry years and 15 large-scale wet years. Many dry years are bunched during 1899–1925 while many wet years during 1933–1961.
(e) The ISMR index was continuously negative for three decades 1901–30, positive 1931–60 and again became negative during the current period 1961–90.

Acknowledgements

The authors are thankful to D.R. Sikka, Director, Indian Institute of Tropical Meteorology (IITM), Pune-411008 for the interest and facilities and to the Additional Director General (Research), IMD, Pune-411005 for supply of necessary meteorological data. They are also grateful to Dr G.B. Pant, Head, C&H Division, IITM for critically going through the manuscript and offering valuable suggestions. Thanks are also to Mrs N.A. Sontakke and Mr A.A. Munot for help in computations and to Mrs J.V. Revadekar for keying in the manuscript.

References

Banerjee, A.K. and Raman, C.R.V., 1976: One hundred years of southwest monsoon rainfall over India. *Scientific Report* No. 76/6 Pune, India Meteorological Department.

Blanford, H.F., 1886: Rainfall of India. *Mem India Meteorol Dept*, Pune, Vol. 3.

Chowdhury, A., Dandekar, M.M. and Raut, P.S., 1989: Variability in drought incidence in India — A statistical approach. *Mausam*, **40**, 207–214.

Chowdhury, A. and Mhasawade, S.V., 1991: Variations in meteorological floods during summer monsoon over India. *Mausam*, **42**, 167–170.

Drosdowsky, W., 1990: A simple index of the second POP component of Southern Oscillation. *Trop Ocean-Atmos Newsl (TOAN)*, **54**, 13–15.

Elliott, W.P. and Angell, J.K., 1987: The relation between Indian monsoon rainfall, the Southern Oscillation and hemispheric air and sea temperature: 1884–1984. *J Clim Appl Meteorol*, **26**, 943–948.

—, 1988: Evidence for changes in Southern Oscillation relationships during the last 100 years. *J Clim*, **1**, 729–737.

Fleer, H. 1981: Large-scale tropical rainfall anomalies. *Bon Met Abh* No. 26.

Fu, C. and Fletcher, J., 1988: Large signal of climatic variation over the ocean in the Asian monsoon region. *Adv Atmos Sci*, **5**, 389–404.

Government of India, 1976: Climate and Agriculture. Part IV of the report of the National commission on Agriculture. New Delhi, Ministry of Agriculture and Irrigation.

Gregory, S., 1986: Data base aspects of temporal patterns of climatic fluctuations: An Indian case study. *Trans Inst Indian Geogr*, **8**, 35–44.

—, 1988: El Niño years and the spatial pattern of drought over India, 1901–1970. *In* Recent climatic change — A regional approach. London, Belhaven Press.

—, 1989: Macro-Regional definition and characteristics of Indian summer monsoon rainfall, 1871–1985. *Int J Climatol*, **9**, 465–483.

Hastenrath, S., 1991: Climate Dynamics of the Tropics. Dordrecht, Netherlands, Kluwer Academic publications.

India Meteorological Department., 1971: Rainfall and droughts in India. Report of the drought unit, Pune, Indian Meteorological Department.

—, 1981: Climatological Atlas of India: Part A (Rainfall). Pune, Indian Meteorological Department.

Joseph, P.V., Liebmann, B. and Hendon, H.H., 1991: Interannual variability of the Australian summer monsoon onset: Possible influence of Indian summer monsoon and El Niño. *J Clim*, **4**, 529–538.

Kiladis, G.N. and Sinha, S.K., 1991: ENSO, Monsoon and drought in India. *In* (Eds M.H. Glantz, R.W. Kalz and N. Nicholls) Teleconnections linking worldwide climate anomalies — scientific basis and social impact. New York, Cambridge University Press.

Lawson, M.P., Balling, R.C., Jr., Peters, A.J. and Rundquist, D.C., 1981: Spatial analysis of secular temperature fluctuations. *J Clim*, **1**, 325–332.

Mitchell, J.M., Dzerdyeevskii, B., Flohn, H., Hofmeyr, W.L., Lamb, H.H., Rao, K.N. and Wallen, C.C., 1966: Climatic Change. Technical Note 79, (WMO No. 195-TP-100), Geneva, World Meteorological Organization.

Mitra, A., 1978: India's population: Aspects of quality and control. Vol. II, (Appendix-I). New Delhi, India, Abhinov Publications.

Mooley, D.A. and Parthasarathy, B., 1984: Fluctuations in All-India summer monsoon rainfall during 1871–1978. *Clim Change*, **6**, 287–301.

Mooley, D.A., and Shukla. J., 1987: Variability and forecasting of the summer monsoon rainfall over India. *In* C.P. Chang and T.N. Krishnamusti (eds), Monsoon Meteorology. Oxford University Press.

Mooley, D.A., Parthasarathy, B., Sontakke, N.A. and Munot, A.A., 1981: Annual rain-water over India, its variability and impact on the economy. *J Climatol*, **1**, 167–186.

Parthasarathy, B., 1984a: Some aspects of large-scale fluctuations in the summer monsoon rainfall over India during 1871–1978. Ph.D. Thesis, University of Poona, Pune, India.

—, 1984b: Interannual and long-term variability of Indian summer monsoon rainfall. *Proc Ind Acad Sci (Earth & Planetary Sci)*, **93**, 371–385.

Parthasarathy, B. and Dhar, O.N., 1974: Secular variations of regional rainfall over India. *Q J R Meteorol Soc*, **100**, 245–257.

—, 1976: A study of trends and periodicities in the seasonal and annual rainfall of India. *Indian J Meteorol Hydrol and Geophys*, **27**, 23–28.

Parthasarathy, B. and Mooley, D.A., 1978: Some features of a long homogenous series of Indian summer monsoon rainfall. *Mon Weather Rev*, **106**, 771–781.

Parthasarathy, B., Munot, A.A. and Kothawale, D.R., 1988: Regression model for estimation of Indian foodgrain production from summer monsoon rainfall. *Agric For Meteorol*, **42**, 167–182.

Parthasarathy, B., Rupa Kumar, K. and Munot, A.A., 1991a: Evidence of secular variations of Indian monsoon rainfall — Circulation relationships. *J Clim*, **4**, 927–938.

—, 1991b: Forecast of Kharif foodgrain production based on monsoon rainfall. *In* Statistical Methodology for dry-land Agriculture, January 1991 at Hyderabad. Hyderabad, CRIDA and IASRI.

—, 1992: Forecasting of rainy-season foodgrain production based on monsoon rainfall. *Indian J Agric Sci*, **62**, 1–8.

Parthasarathy, B., Sontakke, N.A., Munot, A.A. and Kothawale, D.R., 1987: Droughts/floods in summer monsoon season over different meteorological sub-divisions of India for the period 1871–1984. *J Climatol*, **7**, 57–70.

—, 1990: Vagaries of Indian monsoon rainfall and its relationships with regional/global circulations. *Mausam*, **41**, 301–308.

Raman, C.R.V., 1975: A new approach to rainfall climatology for agricultural planning. *Sci Today*, **19**, 13.

Rao, K.N. and Jagannathan, P. 1963: Climatic changes in India. *In* proceedings on Changes in Climate. Rome, UNESCO and WMO.

Rao, Y.P., 1976: Southwest Monsoon. Meteorological Monograph, No. 1. Pune, Indian Meteorological Department.

Shukla, J. 1987: Interannual variability of Monsoons. *In* Monsoons (Eds J.S. Fein and P.L. Stephens). New York, Wiley and Sons.

Thapliyal, V., 1990: Long-range prediction of summer monsoon rainfall over India: Evolution and development of new models. *Mausam*, **41**, 339–346.

Thapliyal, V. and Kulshrestha, S.M., 1991: Climate changes and trends over India. *Mausam*, **42**, 333–338.

Tyson, P.D., Dyer, T.G.J. and Mametse, M.N., 1975: Secular changes in South African Rainfall: 1880 to 1972. *Q J R Meteorol Soc*, **101**, 817–833.

Walker, G.T., 1910: On the meteorological evidence for supposed changes of Climate in India. *Mem India Meteorol Dept*, **21**, 1–21.

Yasunari, T. 1990: Impact of Indian monsoon on the coupled atmosphere/ocean system in the Tropical Pacific. *Meteorol Atmos Phys*, **44**, 29–41.

—, 1991: The monsoon year — a new concept of the climatic year in the tropics. *Bull Am Meteorol Soc*, **72**, 1331–1338.

551.509.57:551.515.23(267.2)

Tropical cyclones in the south-west Indian Ocean — track prediction and verification 1989–91

J.H. Vermeulen
Weather Bureau RSA, Pretoria
M.R. Jury
Oceanography Dept, University of Cape Town

Summary

The skill of the United Kingdom Meteorological Office weather prediction model in forecasting cyclone tracks in the south-west Indian Ocean is evaluated for the period 1989–91. The track predictions of the model are shown to be useful up to day 3. Mean track errors grow from an initialization value of 172 km to over 500 km by day 3. Cyclones which cross the highlands of Madagascar are not well handled by the model, recurving poleward while predictions maintain westward movement due to model resolution, the steep topography, and consequent entrainment of flow around Madagascar. The forecasting skill of the model is affected by the background flow patterns. Tropical westerlies increased in the 15° S zone in the first season and model errors were smaller.

1. Introduction

On average, ten tropical cyclones (TCs) form and move across the south-west Indian Ocean (5–30° S, 30–90° E) each summer from November to April (Crutcher and Quayle 1973). Approximately two reach the intense cyclone stage causing destruction to the islands of Mauritius, Rèunion and Madagascar and posing a threat to busy shipping lanes (Padya 1989). TCs form most frequently along the Inter-Tropical Convergence Zone (ITCZ) near 13° S, 63° E where low-level horizontal shear between equatorial monsoon westerlies and subtropical trade winds is overlain by an anticyclonic circulation above 200 mb. Sea surface temperatures (SSTs) average 28 °C in the December–March period (Halpert and Ropelewski 1989) and zonal upper-level flow is often absent (Arkin *et al.* 1986). Pre-existent forcing of cyclogenesis by easterly waves and by surges of the north-west monsoon has been noted (Jury *et al.* 1991, Jury 1992). TCs usually move in a south-westerly direction north of 20° S and east of 50° E (Neumann and Randrianarison 1976). To the south-west, the encroachment of subtropical westerlies, the highlands of Madagascar and a semi-permanent subtropical trough all contribute to poleward recurvature (Jury and Pathack 1991).

In recent years numerical weather prediction systems such as the United Kingdom Meteorological Office (UKMO) model have shown increasing usefulness in forecasting the evolution of large-scale weather systems, primarily in the extratopical baroclinic zone. The accurate prediction of TC intensity and track remains elusive, as evidenced by comparisons of numerical forecast errors in the tropical zone and persistence errors (Flood 1985). Towards improving forecasts for these small-scale tropical systems, the model data assimilation and analysis scheme, and spatial resolution are continually being upgraded (Bell and Dickinson 1987). Such improvements may not become immediately evident owing to the interannual variability of tropical circulation. Brankovic *et al.* (1988) point out that model skill response to climatic fluctuations may be more variable than the improvement in skill brought about by model reformulation or resolution change. Over the 1989–91 period considered here, it can be noted that the UKMO model data assimilation and meteorological analysis scheme remained unchanged.

Morris (1989) reviews the capabilities and attributes of the UKMO numerical weather prediction model. The model has a horizontal resolution of about 200 km in the tropics and is thus only able to resolve the large-scale structure of tropical cyclones. In the physics parametrization, radiation is non-interactive and convective processes are crudely represented. The specification of upper winds by geostationary satellite presents a significant problem in the Indian Ocean region. Meteosat provides SATOB data to 60° E while GMS data begins at 90° E. INSAT data have thus far proved unreliable. Hence the quality of model analyses in the central Indian Ocean is compromised, not only by lack of geostationary satellite coverage, but also by the reduced volume of shipping and aircraft reports.

A bogusing procedure is implemented for TCs which makes use of local TC Warning Centre data and satellite imagery to correct the position of or locate a warm-core vortex through the input of winds in the 850–500 mb layer. In the UKMO numerical model, TC motion appears to be controlled by the interaction of the mean flow and the vorticity advection above 500 mb. The model assumes an in-phase and predominantly symmetrical relationship between wind and temperature fields below 500 mb (Morris and Hall 1987). The TC steering level is typically around 500 mb, but can be higher for intense systems with convection overshooting the tropopause (Padya 1989).

2. Background

The aim of this paper is to evaluate the skill of TC track predictions of the UKMO model for the 1989–90 and 1990–91 seasons in the south-west Indian Ocean. The TCs include:

Name	Date	Min. pressure (mb)	Max. sustained wind ($m\ s^{-1}$)
Alibera	16 Dec. 89–6 Jan. 90	975	30
Baomavo	3 Jan. 90–8 Jan. 90	945	33
Cezera	3 Feb. 90–9 Feb. 90	990	20
Dety	3 Feb. 90–9 Feb. 90	990	20
Edisaona	2 Mar. 90–8 Mar. 90	955	35
Felana	10 Mar. 90–15 Mar. 90	986	22
Gregoara	15 Mar. 90–24 Mar. 90	930	40
Hanta	13 Apr. 90–14 Apr. 90	1000	10
Ikonjo	14 May 90–21 May 90	984	22
Alison	4 Jan. 91–9 Jan. 91	975	27
Bella	23 Jan. 91–4 Feb. 91	942	35
Cynthia	15 Feb. 91–20 Feb. 91	990	20
Debra	23 Feb. 91–3 Mar. 91	965	27
Elma	28 Feb. 91–2 Mar. 91	970	25
Fatima	23 Mar. 91–2 Apr. 91	975	25
Gritelle	10 June 91–15 June 91	984	20

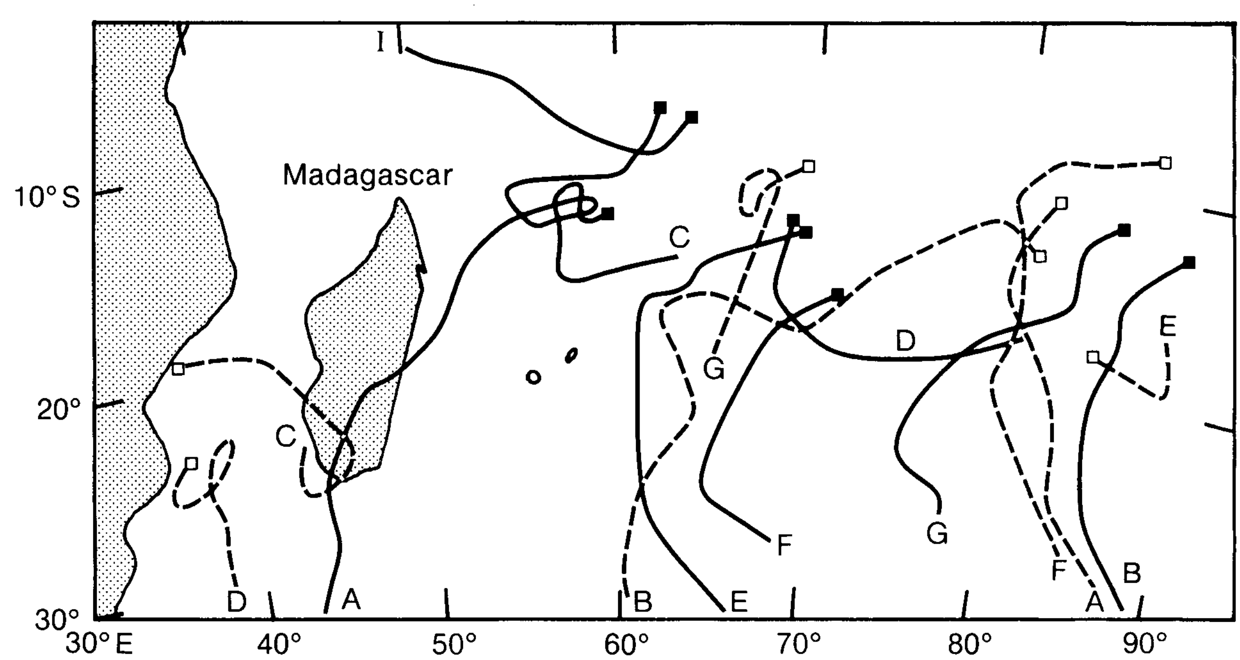

Figure 1. Tropical cyclone (TC) genesis points and tracks for 1989–90 (solid squares and solid lines) and 1990–91 (open squares and dashed lines). Letters refer to alphabetical names of TCs, see text for full names.

The 1989–90 summer is more active with nine TCs; close to the average for the region. The last cyclones of both seasons were quite late (May, June). TC genesis and tracks are shown in Fig. 1 and a general south-westward displacement is evident. The track of the late cyclone, Ikonjo was slightly equatorward. TCs which moved or formed near South Africa include Alibera, the first cyclone of the 1989–90 season, which tracked south-westward over Madagascar in early January 1990 and Debra which developed at 24°S, 37°E, on 23 February 1991. Cezera, Dety, Hanta and Elma have been excluded from further analysis owing to lack of data or limited lifespan.

3. Data

All available weather data on TC track and intensity were analysed by the shipping forecaster at the headquarters of the Weather Bureau of the Republic of South Africa (RSA) in Pretoria at 00 and 12 UTC. The south-west Indian Ocean observations, both direct and indirect, include warnings from TC Warning Centres at Réunion, Mauritius and Madagascar; ship, coastal and island synoptic reports and radiosonde and pibal profiles; Meteosat, NOAA and INSAT satellite images, UKMO advisories and gridded numerical output from the ECMWF and UKMO models. According to forecasters at the south-west Indian Ocean TC Warning Centres at Mauritius and Réunion, the discrepancy between the analysed and observed TC eye is about 55 km. The UKMO model analysed TC positions for 00 and 12 UTC were taken from GTS advisories. The distance or displacement error between the observed and predicted TC position was calculated. Seasonal mean errors were computed by weighting the contribution by each TC according to the number of forecasts. Emphasis is placed on the evaluation of the day 1 forecasts. As shown in Table I, the day 0 initialization error is 163–182 km, and this impacts on subsequent forecast errors. The initialization error is due to the lack of eye in many of the weaker systems, leaving room for subjective errors in the observed position, and to the model resolution as previously mentioned.

4. Results

4.1 Observed climatology, anomalies and seasonal differences

The genesis and tracks for all TCs in the 1989–91 seasons is shown in Fig. 1. The genesis positions can be distinguished by area: two in the Mozambique Channel in February 1992, three near 10°S, 60°E in 1989–90, four in the 70°E longitude, and six to the east of 80°E. A break in cyclone tracks appears in the vicinity of Réunion (21°S, 55°E). The genesis points to the east of Madagascar were more zonally aligned than usual possibly due to the orientation of SST isotherms (Climate Analysis Centre bulletins 1989–1991). During the 1989–90 December–March TC season, the south-west Indian Ocean anticyclone and associated trade winds in the 30°S band were above normal. In addition, tropical monsoon westerlies were persistently above normal to the north-east of Madagascar (contributing to formation of the TC pair Cezera and Dety). Together these circulation features enhanced 850 mb cyclonic

Table I. Mean distance error (km) between the UKMO forecast and the true positions of the cyclones for different forecast periods (days) for all the cyclones. The values in brackets are the number of forecasts used to calculate the mean distance error.

Cyclone names	Forecast period (days) 0	1	2	3	4	5
1989/90 season						
Alibera	172 (15)	395 (13)	614 (12)	792 (11)	969 (9)	924 (8)
Baomavo	180 (10)	274 (9)	356 (7)	493 (5)	777 (4)	965 (2)
Edisaona	267 (8)	255 (7)	296 (8)	311 (8)	454 (8)	464 (5)
Felana	221 (5)	394 (5)	478 (5)	614 (3)	393 (1)	399 (1)
Gegoara	208 (11)	303 (10)	401 (9)	309 (6)	541 (7)	1074 (5)
Ikonjo	117 (15)	161 (14)	265 (13)	250 (7)	344 (3)	248 (1)
Seasonal means	182 (64)	287 (58)	401 (54)	478 (40)	646 (32)	803 (22)
1990/91 season						
Alison	299 (8)	317 (10)	481 (10)	677 (8)	586 (6)	510 (3)
Bella	158 (20)	256 (20)	413 (18)	642 (15)	702 (12)	861 (6)
Cynthia	223 (8)	144 (4)	240 (4)	238 (3)	157 (1)	111 (1)
Debra	138 (17)	231 (12)	344 (7)	503 (4)	917 (3)	—
Fatima	112 (18)	223 (18)	435 (16)	594 (14)	669 (12)	835 (8)
Gritelle	139 (6)	211 (7)	339 (6)	686 (4)	891 (4)	679 (2)
Seasonal means	163 (77)	241 (71)	404 (61)	601 (48)	696 (38)	742 (20)

vorticity during the 1989–90 season. In 1990–91, 850 mb wind anomalies were less intense and the flow pattern was dominated by subtropical Rossby waves of short wavelength. One such trough was located over the Mozambique Channel in February 1991 (Climate Analyses Centre bulletins 1991), spawning two cyclones there. The 200 mb 10 m s^{-1} isotach retreated south of 20°S in January and March 1990 and in February 1991 Outgoing Long-wave Radiation (OLR) anomalies to the north-east of Madagascar were below normal (convective) in December 1989 and February 1990. In the 1990–91 season a low/west–high/east convective dipole moved slowly across the region from southern Africa to the south-west Indian Ocean. In February 1991 the convective part of the dipole, as seen in the OLR pattern, crossed into the Mozambique Channel in association with the eastward movement of the low-level subtropical trough.

4.2 Track errors for individual TCs

Table I and Fig. 2 show the accumulated track errors associated with forecasts from 0 to 5 days for individual TCs. The displacement errors of the UKMO model in forecasting TC position increases after day 2. For individual TCs such as Edisaona, Felana and Ikonjo in 1990 the day 4 and 5 skill is reasonable (i.e. below 400 km error). It is notable that the early season TCs of 1989 were poorly forecast, particularly Alibera the first of the season.

TCs of the 1990–91 season also show the trend of decreasing errors in mid season, with Cynthia forecast best and Alison faring worst in day 2 and 3 forecasts. Debra in the Mozambique Channel, was well forecast up to day 2, but looped back instead of heading poleward, causing day 4 and 5 forecasts to 'explode'. In many cases TCs were dissipated too soon by the UKMO model. Debra lasted 9 days, but was forecast to dissipate after day 4. It would appear that the model drifts to the climatological mean too quickly, possibly due to insufficient observations which impair thermodynamic forcing in the model. The seasonality of forecasting skill is seen after day 3 for TC Gritelle which dissipated quickly after merging with a mid-latitude front in June 1991.

A closer look at Alibera December 1989 and Debra February 1991 is taken in Fig. 3. These two contrasting examples were chosen by virtue of their influence on the weather of south-east Africa. Alibera formed on 16 December 1989 to the north-east of Madagascar and tracked reasonably close to the climatological mean. However, on reaching the highlands of Madagascar, Alibera recurved poleward (996 mb, 20 m s^{-1} winds), while the forecast track was south-westward. Track errors grew to 969 km as a result of the poor handling of orographic friction and interaction with a weak mid-

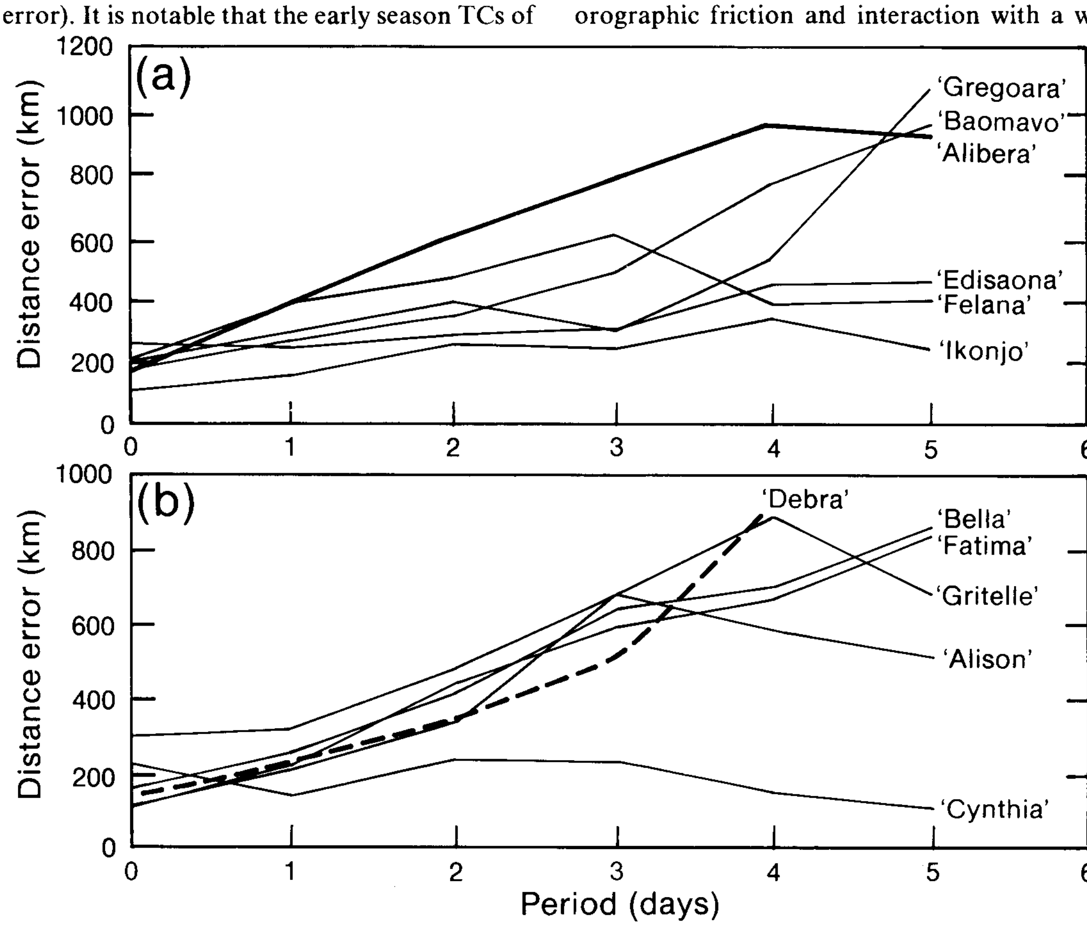

Figure 2. Distance error of predicted versus observed tropical cyclone positions for 0–5 day forecast periods for (a) season 1989–90, and (b) season 1990–91.

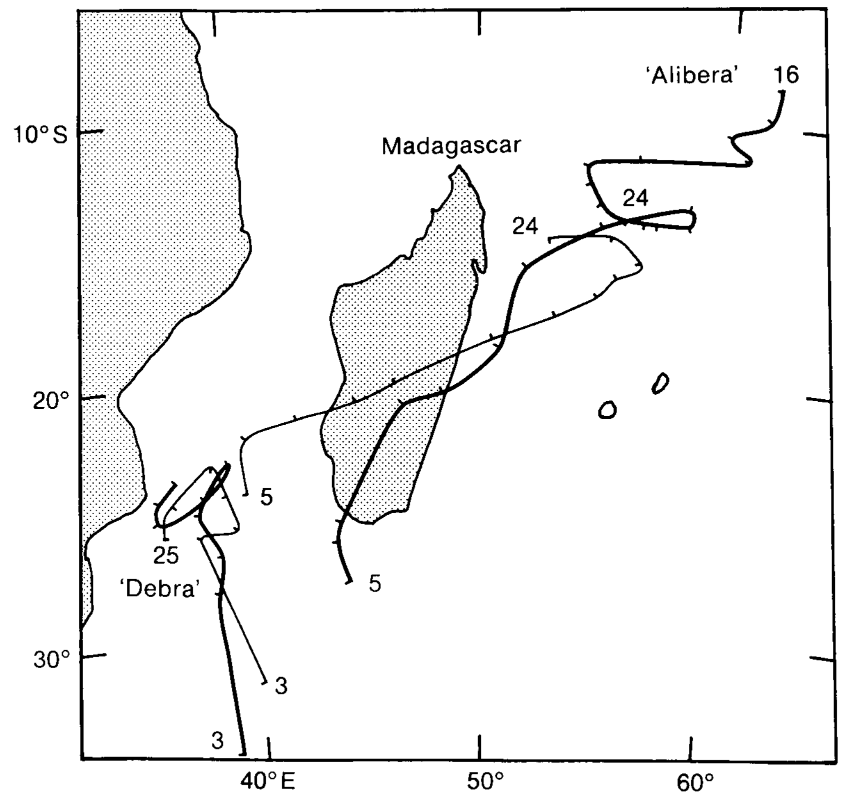

Figure 3. Tropical cyclone observed track (bold line) and 1-day forecast track (thin line) for Alibera and Debra. Numbers refer to dates, tick marks show daily positions.

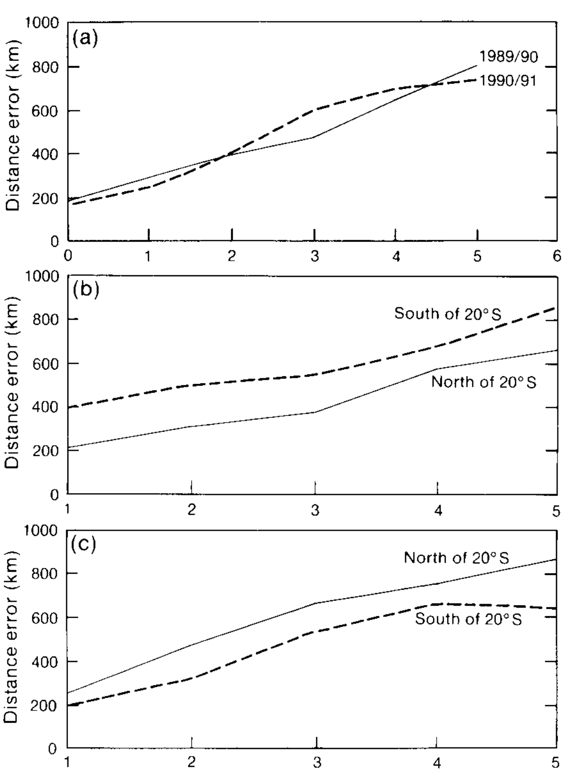

Figure 4. Mean distance error of predicted versus observed tropical cyclone positions for (a) 0–5 day forecast periods for 1989–90 and 1990–91 (dashed) seasons, (b) distance error for 1–5 day forecast periods for zone north and south (dashed) of 20° S for 1989–90 and (c) as in (b) except for 1990–91.

latitude trough. Morris (1989) indicates that the UKMO model often transfers a TC which approaches Madagascar from the north-east in a westerly track across the mountainous island. Debra, in contrast, formed and looped in the subtropical Mozambique Channel (992 mb, 20 m s^{-1} winds) then became extratropical after 4 March 1991. Debra was forecast with reasonable skill up to day 3. The day 1 forecast track handled the looping and poleward acceleration reasonably well (Fig. 3).

4.3 TC track errors by season and latitude zone

The seasonal mean initialization error declined slightly from 1990 to 1991. Errors for day 1 and 2 forecasts in 1989–90/1990–91 grew from 287 km/241 km to 401 km/404 km, respectively. The greatest difference between the seasonal means is at day 3 (Fig. 4(a)) where errors in the second season were 123 km larger than the first. The average difference for all forecast times is only 8 km and the UKMO model performance appears unchanged over the two seasons. The error budget compares well with similar results reported by Morris and Hall (1987) for TCs in the North Atlantic and north Pacific Ocean basins.

The mean recurvature latitude of 20° S for TCs in the south-west Indian Ocean (Neumann and Randrianarison 1976) was utilized to make comparisons of track errors to the north and south (Table II and Figs 4(b) and 4(c)). In the first season, mean errors north of 20° S were much

Table II. As Table 1 but for demarcation at 20° S

Cyclone names	Forecast period (days) 1	2	3	4	5
1989/90 season		North of 20° S			
Alibera	269 (6)	444 (5)	570 (5)	819 (4)	920 (3)
Baomavo	107 (3)	163 (2)	—	—	—
Edisaona	255 (7)	331 (6)	377 (5)	488 (3)	493 (2)
Felana	351 (1)	—	—	—	—
Gegoara	317 (3)	369 (2)	—	—	—
Ikonjo	161 (14)	265 (13)	250 (7)	344 (3)	248 (1)
Seasonal means	214 (34)	311 (28)	381 (17)	577 (10)	666 (6)
		South of 20° S			
Alibera	504 (7)	737 (7)	977 (6)	1089 (5)	926 (5)
Baomavo	358 (6)	433 (5)	493 (5)	777 (4)	965 (2)
Edisaona	—	194 (2)	201 (3)	434 (5)	444 (3)
Felana	405 (4)	478 (5)	614 (3)	393 (1)	399 (1)
Gegoara	298 (7)	411 (7)	309 (6)	541 (7)	1074 (5)
Ikonjo	—	—	—	—	—
Seasonal means	391 (24)	499 (26)	549 (23)	677 (22)	854 (16)
1990/91 season		North of 20° S			
Alison	453 (5)	548 (6)	571 (4)	440 (2)	—
Bella	273 (12)	580 (10)	859 (7)	954 (3)	1068 (4)
Cynthia	—	—	—	—	—
Debra	—	—	—	—	—
Fatima	183 (13)	406 (11)	552 (9)	632 (7)	618 (4)
Gritelle	211 (7)	339 (6)	686 (4)	1031 (3)	1023 (1)
Seasonal means	254 (37)	472 (33)	667 (24)	751 (15)	863 (9)
		South of 20° S			
Alison	181 (5)	381 (4)	784 (4)	660 (4)	510 (3)
Bella	232 (8)	204 (8)	453 (8)	618 (9)	449 (2)
Cynthia	144 (4)	240 (4)	238 (3)	157 (1)	111 (1)
Debra	231 (12)	344 (7)	503 (4)	917 (3)	—
Fatima	326 (5)	499 (5)	670 (5)	720 (5)	1051 (4)
Gritelle	—	—	—	471 (1)	334 (1)
Seasonal means	198 (39)	322 (28)	535 (24)	660 (23)	643 (11)

lower than to the south (Fig. 4(b)). A Wilcoxon sum of ranks test indicates that the difference between track errors in the two areas is significant at 95% for day 1. In the 1989–90 season nine TCs formed in random positions in the tropical monsoon westerlies, but were subsequently better predicted.

While TC track errors were lower in the tropical zone in the first season, Fig. 4(c) reveals the opposing trend in the second season. The 1990–91 season had seven TCs, most forming east of 80° E. Given the lower intensity of monsoon westerlies (Climatic Analysis Centre bulletins, 1991) it is likely that many TCs formed as an outgrowth of easterly waves. Poor short-term forecasts of TC tracks in the tropical zone could be attributable to the interaction of an eastward-moving low-frequency mode in the subtropics and higher frequency westward-moving barotropic waves in 1990–91. Although the extratropical band was better predicted in the latter season, no statistically significant differences in the two latitude zones could be found.

5. Discussion

A study of TC track prediction based on the UKMO model advisories has been made for the south-west Indian Ocean. The day 1 to 3 forecasts were shown to be useful, keeping in mind the large day 0 displacement error. Little forecasting skill was found beyond day 3. Problems were encountered when TCs moved across the large mountainous island of Madagascar. From statistical analyses, track errors in different latitude zones reveal that differing climatological background patterns can have a varying effect on the forecast skill of the model. The tendency in the model to dissipate cyclones too early may be a drift in the model to background climatology. Other deficiencies in the model (Morris 1989) include the inability to discriminate between depressions and cyclones, and the absorption of a TC pair by the poleward system. A positive attribute is the ability of the model to predict TC genesis in response to upper dynamical forcing.

In general, TC interaction with baroclinic waves and subsequent poleward acceleration appears less easily predicted, in the seasons considered here, than steering by steady tropical flow. In the south-west Indian Ocean predictability is complicated by: low-frequency surges of the north-west monsoon (Wang and Rui 1990), the absence of a background zonal easterly flow in the 500–300 mb layer, the intermittent nature of high-frequency barotropic easterly waves, and a lack of upper-level observations near the ITCZ over the central ocean basin. Further studies are planned using detailed ECMWF and UKMO model analyses to elucidate meteorological processes influencing TC formation and steering, and kinematic–thermodynamic interactions in the south-west Indian Ocean. It is hoped that the upgraded capabilities of the next generation of weather satellites and high-resolution numerical models will assist in this endeavour.

Acknowledgements

Thanks are due to K. Estie, G. Schulze and C. Archer of the Weather Bureau RSA, and B. Pathack of the Oceanography Dept, University of Cape Town for advice and guidance.

References

Arkin, P.A., Konsky, V.E., Janowiak, J.E., and O'Lenic, E.A., 1986: Atlas of the tropical and subtropical circulation derived from NMC operational analyses. *NOAA Atlas*, 7, Washington, CAC/NMC/NOAA.

Bell, R.S., Dickinson, A., 1987: The Meteorological Office operational numerical weather prediction system. *Sci Pap, Meteorol Off*, No. 41.

Brankovic, C., *et al.*, 1988: Predictability in the medium and extended range, *In* Proceedings ECMWF workshop.

Climate Analysis Centre, 1989–1991: *Climate Diagnostic Bulletin*, for December to March.

Crutcher, H.L. and Quayle, R.G., 1973: Mariners worldwide climatic guide to tropical storms at sea. Washington, Naval Weather Service.

Flood, C.R., 1985: Forecast evaluation, *Meteorol Mag*, **114**, 254–260.

Halpert, M.S. and Ropelewski, C.F., 1989: Atlas of tropical sea surface temperature and surface winds, *NOAA Atlas*, **8**, Washington, CAC/NMC/NOAA.

Jury, M.R., 1992: Tropical cyclones in the SW Indian Ocean. Submitted to *Weather Forecasting*.

Jury, M.R. and Pathack, B., 1991: A study of climate and weather variability over the tropical southwest Indian Ocean. *Meteorol Atmos Phys*, **47**, 37–48.

Jury, M.R., Pathack, B., Wang, B. and Landman, W., 1991: Transient convective waves in the tropical southwest Indian Ocean, *Meteorol Atmos Phys*, **47**, 27–36.

Morris, R.M., 1989: Provisional report on forecasting the evolution of tropical storms over the South Indian and South Pacific during 1988-1989 season using the UKMO operational global model. Unpublished, copy available in the National Meteorological Library, Bracknell.

Morris, R.M. and Hall, C.D., 1987: Forecasting the tracks of tropical cyclones with the UKMO operational global model, *In* Proceedings WMO Typhoon Comm An Rev, Manilla.

Neumann, C.J. and Randrianarison, E.A., 1976: Statistical prediction of tropical cyclone motion over the southwest Indian Ocean. *Mon Weather Rev*, **104**, 76–85.

Padya, B.M., 1989: Climate and weather of Mauritius. Mauritius, M. Gandhi Inst.

Wang, B. and Rui, H., 1990: Synoptic climatology of transient tropical intraseasonal convection anomalies: 1975–1985, *Meteorol Atmos Phys*, **44**, 43–61.

551.506.1(41-04)

The summer of 1991 in the United Kingdom

G.P. Northcott

Meteorological Office, Bracknell

Summary

Despite the very cold and rather miserable June, the summer as a whole was rather warm, rather dry, though with average sunshine.

1. The summer as a whole

Although June was unusually cold, over the summer as a whole temperatures were above average nearly everywhere, except in parts of Wales and south-west England, and ranged from 1 °C above average in western Scotland and on the Norfolk/Suffolk coastal stretch to 0.5 °C below average in parts of south-west England. Rainfall amounts over the summer season were generally below average, although in southern England amounts of rain were generally above average and reached more than 150% of average along the coast of East Sussex, as against only 41% of average in Lincolnshire. Sunshine amounts were about average generally, although it was rather sunny over northern and western Scotland and eastern and central parts of England, but dull over North Wales, north-west England, and much of south-western and central Scotland, ranging from more than 120% in South Yorkshire to less than 80% in North Wales.

Information about the temperature, rainfall and sunshine during the period from June 1991 to August 1991 is given in Fig. 1 and Table I.

2. The individual months

June. Mean monthly temperatures were below normal in all areas of the United Kingdom, ranging from 2.7 °C below normal at Macclesfield, Cheshire to

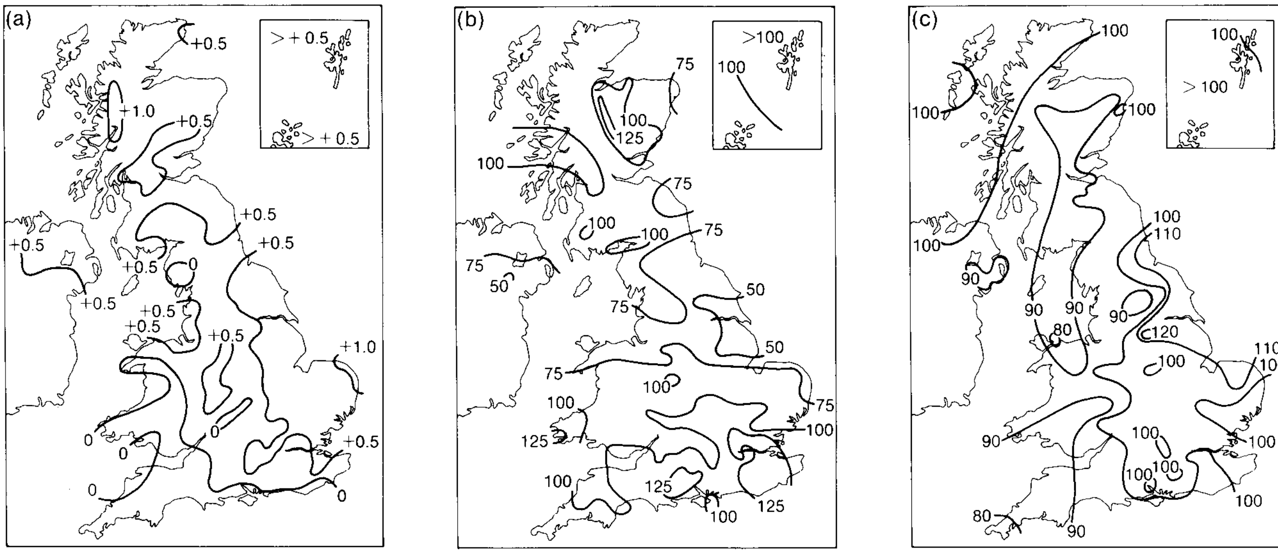

Figure 1. Values of (a) mean temperature difference (°C), (b) rainfall percentage and (c) sunshine percentage for summer, 1991 (June–August) relative to 1951–80 averages.

Table I. District values for the period June–August 1991, relative to 1951–80 averages

District	Mean temperature (°C)	Rain-days	Rainfall	Sunshine
	Difference from average		Percentage of average	
Northern Scotland	+0.7	0	88	103
Eastern Scotland	+0.6	0	96	93
Eastern and north-east England	+0.6	0	70	105
East Anglia	+0.6	+1	94	104
Midland counties	+0.3	0	94	105
South-east and central southern England	+0.2	+2	125	104
Western Scotland	+0.5	+1	97	95
North-west England and North Wales	+0.3	+2	86	90
South-west England and South Wales	+0.3	+3	108	92
Northern Ireland	+0.6	+1	82	98
Scotland	+0.6	0	94	97
England and Wales	+0.3	+2	95	100

Highest maximum: 30.6 °C in East Anglia in July.
Lowest minimum: −3.8 °C in western Scotland in June.

0.7 °C below normal at Lowestoft, Suffolk. Frost occurred quite widely during the first week. Bastreet, Cornwall had a minimum of −1 °C on the 2nd. The temperature over grass at Birmingham Airport fell to −6 °C on the 5th and this was the coldest June night since records began at a number of places; this included the lowest of the month (−3.8 °C) at Carnwath, Strathclyde Region, the lowest for June at that station since the record began in 1952. Monthly rainfall amounts were above normal nearly everywhere apart from a few locations, mainly in western areas where it remained dry; nearly three times the normal in East Sussex contrasted with as little as half the normal in western Scotland. Monthly sunshine amounts were below average everywhere except for a few places, mainly in northern Scotland, where they were above or near normal, and ranged from 109% of average at Tiree, Strathclyde Region to 50% of average at Bexhill, East Sussex. The month was one of the dullest Junes this century over a wide area. Sunny days were mainly limited to the 3rd and 13th in the south-west of England and the 20th more widely across England and Wales, apart from the south-east.

The weather was generally unsettled, with outbreaks of rain or drizzle, and more prolonged rain from time to time, heavy in places, or showers, often thundery and sometimes of hail. Sleet and snow fell on the Grampian Mountains on the 2nd and 3rd, and on the Southern Uplands on the 3rd; snow lay at Cairngorm Carpark for three days. Snow fell on the northern Pennines on the 3rd, hail was reported at Inverness, over North Yorkshire and north Norfolk, and thunder over Salisbury Plain. On the 23rd torrential rain over the south and west caused extensive flooding, particularly in Plymouth and Torquay, Devon and Bridport, Dorset, while in Cornwall some rivers burst their banks.

Thunderstorm frequency was very high during the month, particularly in eastern areas, with thundery activity reported somewhere in the United Kingdom on nearly every day.

July. Mean monthly temperatures were above normal nearly everywhere, ranging from more than 3 °C above normal in the western Highlands to nearly 1 °C below normal in the Isles of Scilly. Scotland had one of the warmest Julys on record. Monthly rainfall totals were above normal in northern Scotland, Shetland and Orkney, the Forth–Clyde Valley, and England and Wales south of a line from Anglesey to Essex, and below normal elsewhere, and ranged from 280% in the Isles of Scilly to as little as 26% in Lincolnshire. Monthly sunshine amounts were above average over westernmost areas of Scotland and the whole of England apart from the south-west peninsula, and below average elsewhere, ranging from 138% at Cromer, Norfolk to just over 50% in west Cornwall.

The weather was changeable, with showers, sometimes accompanied by thunder, and longer periods of rain. Heavy rain fell in parts of Scotland, Northern Ireland and northern England on the 1st. During the afternoon of the 2nd rain spread across Kent and Sussex, where thunder was reported, later spreading across south-eastern England, East Anglia and the Midlands; thunderstorms occurred over North Wales and north-west England, with heavy showers, some of hail. Thunderstorms, some severe with hail, moved northwards over southern England late on the 5th, and crossed parts of Wales and the Midlands during the night; further thunderstorms occurred over Wales and north-west England early on the 6th and again widely on the 7th. Lightning caused structural damage in North Wales and Scotland on the 8th. On the 13th a short-lived tornado caused damage to roofs and power lines at Castle Bytham, south-west Lincolnshire. Thundery outbreaks over south-west England on the 23rd became widespread by the evening, with the south-east being the worst affected. The main thundery activity moved to East Anglia and eastern England on the 24th. Further heavy rain fell over parts of south-east England and the Midlands on the 30th.

August. Mean monthly temperatures were above normal nearly everywhere, ranging from near normal in the Isles of Scilly to 2.0 °C above normal in parts of East Anglia. Monthly rainfall amounts were below normal nearly everywhere, ranging from 112% at Stornoway, Western Isles to as little as 6% at Finningley, South Yorkshire. This was generally the driest August since that of 1976. Apart from parts of Scotland and northern England, most places had no rain after the 23rd. August was the driest at Valley, Gwynedd since 1976, at Coventry, Warwickshire since 1947, and over Northern Ireland since 1983. Monthly sunshine amounts were above average nearly everywhere and ranged from 143% in East Kent to 82% at Benbecula, Western Isles. Sunshine amounts were generally higher than those of August 1990 in north-western areas. Northern Ireland had its sunniest August since 1977.

Very moist air brought cloud and mist and kept sunshine amounts as well as temperatures low in some places in the west, while fronts, although they crossed all areas, soon weakened as they moved south-eastwards, giving negligible amounts of rain in the east. However, thundery showers produced localized heavy rainfall. On 1 August thunderstorms over East Anglia and south-east England caused flooding and disrupted traffic: lightning killed one person in Kent, injured two people in Essex, and caused structural damage in south-east London. Further thundery outbreaks occurred over northern England and Scotland on the 6th, 16th, 17th and 22nd, and over Wales and south-west England on the 23rd. Late on the 30th lightning was observed over Cornwall and the Channel Islands as thunderstorms drifted northwards over the English Channel and on the 31st thunderstorms occurred over Cornwall and South Wales.

Latest Climate Assessment

28 May saw the publication of the authoritative update on climate change which has been produced by the Scientific Assessment Working Group of the United Nations Intergovernmental Panel on Climate Change (IPCC).

For world leaders and officials who attended the UNCED 'Earth Summit' in Rio de Janeiro, Brazil — where a key item on the agenda was the the signing of a convention on Global Climate — the Report provided a timely reminder of the continuing scientific concerns about global warming due to the emission of greenhouse gases.

Climate Change 1992: The Supplementary Report to the IPCC's Scientific Assessment, published by Cambridge University Press, is the result of 12 months of intensive work by IPCC Working Group I.

The Report is an update to the definitive and widely accepted first *Scientific Assessment* published in 1990. Read in conjunction with the 1990 Report, it provides policymakers worldwide with the best available consensus of contemporary scientific opinion on climate change, and essential reading for the Rio delegates and all those who have an interest in the future of global climate.

The 1992 Supplementary Report upholds the major conclusions of the 1990 Assessment but introduces new research which sheds light on such subjects as the climate effects of pollution, ozone depletion by CFCs and volcanoes. Recent UN projections of future world population and economic growth are all incorporated in a range of predictions of global warming.

Under the chairmanship of Sir John Houghton, the Supplementary Report was compiled on the basis of contributions from 118 scientists from 22 countries, and was reviewed by a further 380 specialists from 63 countries and 18 UN and non-governmental organizations.

Review

Mid-latitude weather systems, by T.N. Carlson. 152 mm × 234 mm, pp. xx+507, *illus.* London, Routledge, 1991. Price £19.95 (paperback, ISBN 0 04 551116 0), £75.00 (hardback, ISBN 0 04 551115 0).

In this book the author attempts to fuse together two differing disciplines within meteorology, that of the synoptician and that of the dynamicist. The stated aims are to enable students of dynamical meteorology to relate their knowledge to processes depicted on weather charts and, at the same time, allow those more familiar with chart material to interpret synoptic patterns in terms of dynamics. The author is particularly well qualified to tackle this difficult task, having studied synoptic meteorology under one of the best-ever exponents of the art, the late Professor Ludlam, and having since published many papers involving both aspects of meteorology.

The first three chapters give a rather brief overview of the basic equations of dynamical meteorology, more an *aide-mémoire* for those already familiar with the subject than a formal introduction. Thereafter most aspects of synoptic-scale meteorology are explained in terms of simplified dynamical models based on quasi-geostrophic theory and appropriate to the scale of mid-latitude cyclones. Wherever possible concepts are illustrated by well-documented case-studies. Not surprisingly, a large amount of space is devoted to the role of vorticity advection and thermal advection in cyclogenesis. There are two fairly lengthy chapters devoted to fronts and one on upper fronts and jet streaks. On the synoptic side the concept of warm and cold conveyor belts and the air flow through cyclones and fronts is explained with the use of isentropic analysis. I was disappointed to find that use of isentropic potential vorticity in the diagnosis of cyclone development is not covered, though the other fashionable diagnostic aid, Q-vectors, is explained in some detail.

A comprehensive bibliography is ordered by broad subject headings, perhaps unnecessarily since each chapter has its own list of references often very similar to a subject list in the complete bibliography. There are mathematical and synoptic exercises at the end of each chapter to test the understanding of the student, but I would have liked to have seen some brief solutions as well to help those who may use the book in the absence of guidance from lecturers or tutors.

The book is well presented with the many line diagrams especially clear, though a few of the reproductions of satellite images are less so. The case-studies are taken almost exclusively from the USA and students should be aware that a few aspects may not be completely transportable to other regions. Some readers may find the strange mix of units still used by the US Weather Service irritating if not confusing. For example, vertical velocities in micro-bars per second are combined with rainfall in inches per day! However, there is a clearly defined list of symbols and subscripts, etc. for use in equations, which is adhered to throughout, making interpretation of the quantitative examples relatively easy. On the negative side there are a large number of typographical errors especially within the mathematics, a few of which are not immediately obvious as such and may be a serious drawback for those not very familiar with dynamics.

It is very difficult in writing a book of this sort to avoid falling between two stools and the author is not entirely successful in avoiding this. Those already familiar with dynamics will find the first four chapters largely unnecessary whereas there is probably insufficient explanation included for those tackling the subject for the first time. A knowledge of maths approximately at the level of a first-year science undergraduate is needed to make good use of the dynamical meteorology presented. Because of this, the book is best considered as a text on dynamical mid-latitude meteorology, but a rather novel one in that the theory is at every opportunity related to real synoptic situations. In this way the first aim of the author is achieved but the reciprocal aim will only be realized where the reader already has a reasonably sound if undetailed knowledge of dynamics. Assuming such a prior knowledge most of the chapters are reasonably self-contained and this combined with the independent bibliographies makes the book particularly useful for reference.

In conclusion I would strongly recommend the book to all undertaking a course in dynamical meteorology (though not as a first text because of its deliberate omission of certain aspects such as tropical meteorology and numerical modelling). Those engaged in practical meteorology who wish to pursue the dynamics on which their work is based, and have a sufficient mathematical background, would also find this book useful.

D.A. Mansfield

Book comment

The *New Scientist* Inside Science, published by Penguin at £10 is a useful handbook giving brief résumés (about 12 pages) on 26 topics of current interest. The articles are by research scientists, science teachers and *New Scientist*'s team of science writers and editors. They have tried to steer clear of topics which are well handled in readily available textbooks. As their target audience is probably scientific, but knowing only a little of the topic, they cover a large amount of ground and assume good general knowledge.

Of particular interest are essays on acid rain, the ozone layer, the greenhouse effect and risk assessment, which should go a long way towards answering the questions put to us by non-meteorologists. One difficulty is the use of large two-column footnotes which intrude on the main text to the point of obfuscation. However, the index is as likely to contain the topic of a search as many larger, more costly, encyclopaedias.

R.M. Blackall

Books received

The listing of books under this heading does not preclude a review in the Meteorological Magazine at a later date.

Perfect symmetry, by H.R. Pagels (London, Penguin Books, 1992. £7.99) contains a non-technical account of the origin and evolution of the universe. The text proceeds to the farthest frontiers of scientific thought. ISBN 0 14 015826 X.

Glaciers–Ocean–Atmosphere INTERACTION, edited by V.M. Kotlyakov, A. Ushakov and A. Glazovsky (Wallingford, IAHS Press, 1991. $60.00) contains the proceedings of the International Symposium held at St Petersburg on 24–29 September 1990. A number of glacial phenomena related to large-scale variations are identified, and areas requiring knowledge intensification are described. ISBN 0 947571 33 7.

The year without a summer? World climate in 1816, edited by C.R. Harington (Ottawa, Canadian Museum of Nature, 1992. $42.80) includes 40 papers from experts in many disciplines, and countries, concerned with the unusual weather worldwide around 1816. The data gathering and their interpretation are explained and demonstrated from various viewpoints. ISBN 0 660 13063 7.

GUIDE TO AUTHORS

Content

Articles on all aspects of meteorology are welcomed, particularly those which describe results of research in applied meteorology or the development of practical forecasting techniques.

Preparation and submission of articles

Articles, which must be in English, should be typed, double-spaced with wide margins, on one side only of A4-size paper. Tables, references and figure captions should be typed separately. Spelling should conform to the preferred spelling in the *Concise Oxford Dictionary* (latest edition). Articles prepared on floppy disk (IBM-compatible) can be labour-saving, but only a print-out should be submitted in the first instance.

References should be made using the Harvard system (author/date) and full details should be given at the end of the text. If a document is unpublished, details must be given of the library where it may be seen. Documents which are not available to enquirers must not be referred to, except by 'personal communication'.

Tables should be numbered consecutively using roman numerals and provided with headings.

Mathematical notation should be written with extreme care. Particular care should be taken to differentiate between Greek letters and Roman letters for which they could be mistaken. Double subscripts and superscripts should be avoided, as they are difficult to typeset and read. Notation should be kept as simple as possible. Guidance is given in BS 1991: Part 1: 1976, and *Quantities, Units and Symbols* published by the Royal Society. SI units, or units approved by the World Meteorological Organization, should be used.

Articles for publication and all other communications for the Editor should be addressed to: The Chief Executive, Meteorological Office, London Road, Bracknell, Berkshire RG12 2SZ and marked 'For Meteorological Magazine'.

Illustrations

Diagrams must be drawn clearly, preferably in ink, and should not contain any unnecessary or irrelevant details. Explanatory text should not appear on the diagram itself but in the caption. Captions should be typed on a separate sheet of paper and should, as far as possible, explain the meanings of the diagrams without the reader having to refer to the text. The sequential numbering should correspond with the sequential referrals in the text.

Sharp monochrome photographs on glossy paper are preferred; colour prints are acceptable but the use of colour is at the Editor's discretion.

Copyright

Authors should identify the holder of the copyright for their work when they first submit contributions.

Free copies

Three free copies of the magazine (one for a book review) are provided for authors of articles published in it. Separate offprints for each article are not provided.

Contributions: It is requested that all communications to the Editor and books for review be addressed to the Chief Executive, Meteorological Office, London Road, Bracknell, Berkshire RG12 2SZ, and marked 'For *Meteorological Magazine*'. Contributors are asked to comply with the guidelines given in the *Guide to authors* (above). The responsibility for facts and opinions expressed in the signed articles and letters published in *Meteorological Magazine* rests with their respective authors.

Subscriptions: Annual subscription £36.00 including postage; individual copies £3.25 including postage. Applications for postal subscriptions should be made to HMSO, PO Box 276, London SW8 5DT; subscription enquiries 071–873 8499.

Back numbers: Full-size reprints of Vols 1–75 (1866–1940) are available from Johnson Reprint Co. Ltd, 24–28 Oval Road, London NW1 7DX. Complete volumes of *Meteorological Magazine* commencing with volume 54 are available on microfilm from University Microfilms International, 18 Bedford Row, London WC1R 4EJ. Information on microfiche issues is available from Kraus Microfiche, Rte 100, Milwood, NY 10546, USA.

August 1992

Vol. 121
No. 1441

Contents

ISSN 0026–1149

ISBN 0-11-728986-8

Printed in the United Kingdom for HMSO
Dd 291241, 8/92, C13, 543, 24503

The Meteorological Magazine

September 1992

Improving road ice prediction models
United Kingdom observing
Quality assurance in observations
Rime deposition

HMSO

Met.O.1004 Vol. 121 No. 1442

First published 1992

HMSO

HMSO publications are available from:

HMSO Publications Centre
(Mail, fax and telephone orders only)
PO Box 276, London SW8 5DT
Telephone orders 071-873 9090
General enquiries 071-873 0011
(queuing system in operation for both numbers)
Fax orders 071-873 8200

HMSO Bookshops
49 High Holborn, London WC1V 6HB
071-873 0011 Fax 071-873 8200 (counter service only)
258 Broad Street, Birmingham B1 2HE
021-643 3740 Fax 021-643 6510
Southey House, 33 Wine Street, Bristol BS1 2BQ
0272 264306 Fax 0272 294515
9-21 Princess Street, Manchester M60 8AS
061-834 7201 Fax 061-833 0634
16 Arthur Street, Belfast BT1 4GD
0232 238451 Fax 0232 235401
71 Lothian Road, Edinburgh EH3 9AZ
031-228 4181 Fax 031-229 2734

HMSO's Accredited Agents
(see Yellow Pages)
and through good booksellers

The
Meteorological
Magazine

September 1992
Vol. 121 No. 1442

551.509.324.3:625.7

Objective method for improving the operational performance of a road ice prediction model using interpolated mesoscale output and a templet for correcting systematic error

J.E. Thornes and J. Shao
School of Geography, University of Birmingham

Summary

Two techniques for improving the operational performance of numerical road ice prediction models are presented. The first uses the output from a mesoscale model to estimate the inputs for site-specific forecasts. The second uses a templet to reduce systematic bias in model output.

1. Introduction

The Meteorological Office numerical road ice prediction model (MORIPM) is now widely used in the United Kingdom to produce OpenRoad forecasts (Rayer 1987, Thompson 1989, Thornes and Shao 1991a). This paper presents the results of two possible methods designed to improve its operational performance. Both methods could be used with other similar models.

In an attempt to reduce the considerable time taken to input data into MORIPM each winter day, for over 100 forecast sites around the United Kingdom, the output of the Meteorological Office mesoscale model has already been tailored to provide input into the model on an experimental basis (Buchanan 1990, Farmer and Tonkinson 1989). As the mesoscale model grid-points are not exactly coincidental with specific forecast sites, this paper examines the most appropriate interpolation of grid-point values to the forecast sites.

Another important task in improving the operational efficiency of road ice prediction models is to reduce the systematic errors of the ice prediction model. MORIPM has a negative bias of about 1 °C (Thornes and Shao 1991a). However, a small negative bias (of say 0.25°C) is preferred to no bias at all in order to reduce the risk of skidding accidents (Thornes 1989). The negative bias is caused by both model failure in simulating physical processes and the necessary use of 'blank' parameters that the model has to adopt, such as the thermal properties and construction of the road, topography, shadow angles and traffic. The use of an averaging templet is suggested which takes the mean hourly error over the previous 7 days and applies it as a correction factor to the hourly forecast curve for the next 24 hours.

2. A combination scheme for the mesoscale output

A convenient formulation that expresses the value of a variable at a specific field site in terms of a linear combination of grid values is an equation such as

$$V^f = \sum_{i=1}^{n} W_i V_i^g \qquad (1)$$

where V^f is the interpolated or analysed value of the variable V at the field site f, W_i represents the weight applicable at the grid-point i, V^g is the mesoscale output of variable V at the grid-point i, and n is the number of neighbouring grid-points which are assumed to be of influence to the site.

The weights in equation (1) are obtainable from distance–neighbour functions called 'weight parameters'. It is the derivation of these parameters and how they enter the weight calculation procedure that is of concern. Here, the weight parameter for the grid-point i in the field site f is given by the formula

$$W_i = w_i / \sum_{i=1}^{n} w_i \qquad (2)$$

where

$$w_i = (R^2 - D_{fi}^2)/(R^2 + D_{fi}^2) \qquad (3)$$

$$D_{fi}^2 = (x_f - x_i)^2 + (y_f - y_i)^2. \qquad (4)$$

Here, D_{fi} is the distance between site f and grid-point i, and R is the 'radius of influence' beyond which grid-points cease to be considered. For the first stage of the investigation, R is assumed to be the length of a diagonal line in the four-g-id-point network which is shown in Fig. 1.

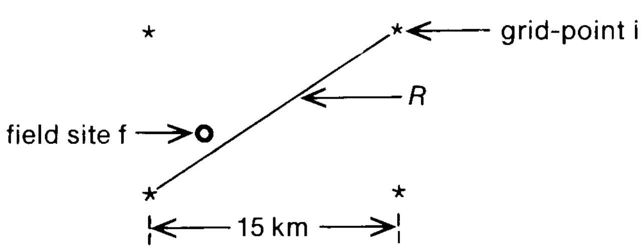

Figure 1. The four mesoscale grid-points and field site.

In order to take altitude into account, the grid-point values of each variable such as air temperature and wind speed need to be extrapolated to an equivalent value at the same altitude as that of the field site, before using equations (1) to (4). Here air temperature is extrapolated according to an average lapse rate, i.e. −0.65 °C/100 m. Wind speed is extrapolated by an equivalent power law exponent

$$U_2 = U_1(z_2/z_1)^a \qquad (5)$$

where 'a' is given analytically by (for simplicity, under neutral stability, e.g. high winds)

$$a = \frac{1}{\ln(z_g/z_0)} \qquad (6)$$

and

$$z_g = (z_1 z_2)^{1/2}. \qquad (7)$$

Here z_0 is the surface roughness length (m), which is always assumed to be 0.03 m, as for low grass, steppe.

In order to find the best combination of the considered mesoscale outputs, they were combined in the following three schemes:

(a) Meso-4a method: neither air temperature or wind speed is extrapolated,

(b) Meso-4b method: only air temperature is extrapolated, and

(c) Meso-4c method: both air temperature and wind speed are extrapolated.

The whole procedure of the objective analysis is shown in Fig. 2.

3. Application of the combination scheme

The scheme was applied to MORIPM for 11 sites in England and Scotland. The sites chosen for the

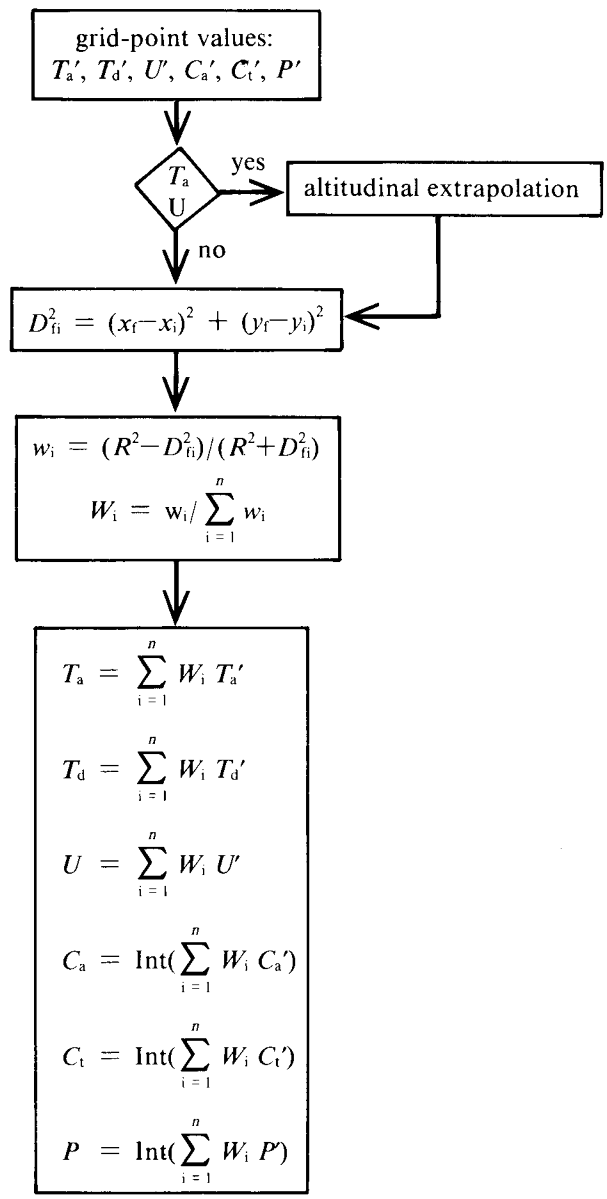

Figure 2. Flow chart of the procedure of the objective analysis. T_a=air temperature, T_d=Dew-point, U=wind speed, C_a=cloud amount, C_t=cloud type and P=rainfall.

application and their relevant four mesoscale grid-points are listed in Table I with coordinates and height. The required input data for MORIPM includes air temperature, dew-point, wind speed, total and low-cloud amount, dominant cloud type, and rainfall. They are all required at 3-hourly intervals. The input data used in this study covers the period from 2 to 24 January 1991. For comparison actual roadside measurements at the sites were used, and cloud data was derived from the nearest airport or Weather Centre for each site.

In order to verify the method introduced below, MORIPM was run first against the actual roadside input (called perfect prognosis) and then against the mesoscale inputs. The results are given in Table II. As root-mean-square (r.m.s.) error can be regarded as a measure of total prediction error, the mean r.m.s. errors averaged over 11 sites are listed at the bottom of the table. It is seen from the table that for perfect prognosis (with actual roadside input) a cold bias exists at most of these sites.

Comparing the model forecasts with a single mesoscale grid-point (column '2') with those with four-grid-points (columns '3', '4' and '5'), it is clear that the combination method gives better results in overall and minimum-temperature prediction for most of the sites. The method combining four grid-point values without any extrapolation (column '3') is generally superior to the single grid method (column '2', comparing SD of overall errors 8 out of 11 sites are better) and other combination methods with wind speed and/or air temperature extrapolations. This is probably due to the fact that the assumption of a general or neutral extrapolation profile of air temperature and wind speed is not suitable.

4. Templet for site specific correction

Results (Thornes and Shao 1991a, Farmer and Tonkinson 1989) have shown that the Meteorological Office road ice prediction model has an obvious cold bias, which may be caused by both its simulation of

Table I. Coordinates (NGR) and height (m) of specific sites and the nearby mesoscale grid-points

Site code/name			Site	Grid a	Grid b	Grid c	Grid d
BO001	West Linton	X	3149	3100	3250	3100*	3250
		Y	6520	6550	6400	6400	6550
		height	200	361	361	270	317
BR006	Windsor Park	X	4945	4900	5050	4900*	5050
		Y	1724	1750	1600	1600	1750
		height	88	53	42	73	38
CH007	Siddington	X	3844	3700	3850*	3700	3850
		Y	3709	3850	3700	3700	3850
		height	30	46	94	34	37
GR003	Tyrebagger	X	3840	3700*	3850	3700	3850
		Y	8120	8200	8050	8050	8200
		height	36	151	102	150	108
HW010	Chapman's Hill	X	3964	3850	4000	3850	4000*
		Y	2775	2800	2650	2650	2800
		height	200	79	106	39	184
IN002	Slochd Summit	X	2626	2500	2650	2500*	2650
		Y	8262	8350	8200	8200	8350
		height	380	—	—	—	—
KB003	Grange Moor	X	4224	4150	4300	4150*	4300
		Y	4155	4300	4150	4150	4300
		height	220	235	168	404	80
RO013	Stubbin Road	X	4420	4300	4450	4300	4450*
		Y	3977	4000	3850	3850	4000
		height	60	168	48	211	51
SF001	Barton Mills	X	5726	5650*	5800	5650	5800
		Y	2738	2800	2650	2650	2800
		height	10	34	17	61	39
WN002	Ray Hall	X	4022	4000	4150	4000	4150*
		Y	2938	2950	2800	2800	2950
		height	123	162	128	184	98
XM005	Thurcroft	X	4478	4450	4600*	4450	4600
		Y	3885	4000	3850	3850	4000
		height	100	51	63	48	47

* The grid was chosen by the Meteorological Office as a representative site for the road site and is used in a single grid-point data set.

Table II. Bias and standard deviation of model forecasts with roadside and mesoscale inputs (January 1991)*

Site code		Overall errors 1	2	3	4	5	Errors in minimum temperature 1	2	3	4	5
BO001	bias:	−0.91	0.33	−0.44	−0.08	−0.25	−1.24	0.59	−0.265	0.12	−0.10
	SD:	1.28	1.33	1.30	1.35	1.35	1.46	1.42	1.35	1.41	1.41
BR006	bias:	−0.70	−0.25	−0.40	−0.52	−0.50	−0.64	0.11	−0.15	−0.26	−0.24
	SD:	0.97	2.05	2.05	2.07	2.07	1.08	2.26	2.26	2.26	2.28
CH007	bias:	−0.59	0.22	0.07	0.17	0.02	−0.57	0.57	0.41	0.50	0.30
	SD:	0.85	1.83	1.76	1.79	1.75	0.86	2.14	1.98	1.97	1.91
GR003	bias:	−1.12	−0.85	−0.67	−0.40	−0.69	−1.14	−0.90	−0.81	−0.53	−0.86
	SD:	1.18	1.64	1.61	1.54	1.65	1.25	1.35	1.59	1.61	1.62
HW010	bias:	−1.33	−1.06	−1.06	−1.32	−1.29	−1.47	−0.85	−0.97	−1.25	−1.21
	SD:	1.39	2.65	2.63	2.61	2.63	0.89	3.11	3.03	3.00	3.02
IN002	bias:	0.30	1.80	0.88	—	—	0.82	2.34	1.49	—	—
	SD:	1.20	1.59	1.39	—	—	0.63	1.70	1.54	—	—
KB003	bias:	0.50	0.71	0.57	0.75	0.64	0.80	1.33	1.07	1.27	1.14
	SD:	0.84	1.59	1.60	1.61	1.62	0.87	1.76	1.85	1.83	1.85
RO013	bias:	−0.93	−0.72	−0.76	−0.79	−0.81	−1.22	−1.06	−0.87	−1.10	−1.04
	SD:	1.07	1.95	1.88	1.95	1.95	1.11	2.24	2.19	2.27	2.30
SF001	bias:	−0.34	−0.94	−0.99	−0.89	−1.00	0.27	−0.36	−0.40	−0.28	−0.44
	SD:	0.83	1.71	1.73	1.73	1.71	0.81	2.06	2.04	2.03	1.97
WN002	bias:	−1.36	−1.28	−1.44	−1.36	−1.45	−1.56	−1.46	−1.51	−1.43	−1.55
	SD:	1.68	2.35	2.32	2.31	2.33	0.92	2.74	2.86	2.85	2.87
XM005	bias:	−0.40	−0.84	−0.80	−0.96	−0.94	−0.56	−1.00	−0.88	−1.07	−1.06
	SD:	0.78	2.23	2.00	2.00	2.00	0.77	2.63	2.32	2.33	2.33
Mean	r.m.s.	1.31	2.09	1.99	2.04	2.05	1.37	2.40	2.28	2.32	2.33

* 1 — forecasts with roadside input;
2 — single mesoscale grid-point;
3 — four mesoscale grid-points without any extrapolation;
4 — four mesoscale grid-points with air temperature extrapolated;
5 — four mesoscale grid-points with both air temperature and wind speed extrapolated;
SD — standard deviation (°C);
r.m.s. — root-mean-square error (°C).

physical processes, and by the unpredictable influences of topography, altitude, traffic and many other unknown factors, such as the thermal properties of road construction. To eliminate the cold bias or any other systematic error, the use of a templet is introduced here. The mean error (E) and variance (σ^2) of the model prediction are estimated by:

$$E = \frac{1}{n}\sum_i(\hat{X}_i - X_i) = \frac{1}{n}\sum_i(\mathrm{d}x_i) \qquad (8)$$

$$\sigma^2 = \frac{1}{n}\sum_i[(\hat{X}_i - X_i) - E]^2 = \frac{1}{n}\sum_i(\mathrm{d}x_i - E)^2 \qquad (9)$$

where $\hat{X}_i$ is initial hourly prediction, X_i observation (reality), and $\mathrm{d}x_i$ an unknown error of prediction. In order to reduce prediction error, an hourly averaging templet is applied to each hourly predicted value, i.e.

$$\hat{X}_i' = \hat{X} - \mathrm{d}x_i' \qquad i=1, 2, ..., 24. \qquad (10)$$

Here, $\hat{X}_i'$ is the corrected prediction, $\mathrm{d}x_i'$ the mean hourly error of prediction of previous days. The mean error (E') and variance ($\sigma^{2\prime}$) of the prediction with a templet are

$$E' = \frac{1}{n}\sum_i(\hat{X}_i' - X_i) = \frac{1}{n}\sum_i(\mathrm{d}x_i - \mathrm{d}x_i') \qquad (11)$$

and

$$\sigma^{2\prime} = \frac{1}{n}\sum_i[(\hat{X}_i' - X_i) - \frac{1}{n}\sum_i(\hat{X}_i' - X_i)]^2$$

$$= \sigma^2 - \frac{2}{n}\sum_i(\mathrm{d}x_i - \overline{\mathrm{d}x})(\mathrm{d}x_i' - \overline{\mathrm{d}x'})$$

$$+ \frac{1}{n}\sum(\mathrm{d}x_i' - \overline{\mathrm{d}x'})^2 \qquad (12)$$

where an overbar stands for averaging.

The estimation of hourly prediction error ($\mathrm{d}x_i'$) is expected to approximate to the real error ($\mathrm{d}x_i'$) with a small deviation (e_i), i.e.

$$\mathrm{d}x_i = \mathrm{d}x_i' + e_i \quad (13)$$

and

$$\overline{\mathrm{d}x} = \overline{\mathrm{d}x}' + \overline{e}. \quad (14)$$

Substituting equations (13) and (14) into equations (11) and (12), E' and $\sigma^{2\prime}$ are rewritten as

$$E' = \frac{1}{n}\sum_i e_i \quad (15)$$

and

$$\sigma^{2\prime} = \sigma^2 - \frac{2}{n}\sum_i(\mathrm{d}x_i' + e_i - \overline{\mathrm{d}x}' - \overline{e})(\mathrm{d}x_i' - \overline{\mathrm{d}x}') + \frac{1}{n}\sum_i(\mathrm{d}x_i' - \overline{\mathrm{d}x}')^2$$

$$= \sigma^2 - \frac{1}{n}\sum_i(\mathrm{d}x_i' - \overline{\mathrm{d}x}')^2 - \frac{2}{n}\sum_i(e_i - \overline{e})(\mathrm{d}x_i' - \overline{\mathrm{d}x}'). \quad (16)$$

It is seen from equation (15) that the mean error of the corrected prediction is approximately zero as e_i is expected to be the difference between $\mathrm{d}x_i$ and $\mathrm{d}x_i'$. In equation (16), if the third term is neglected (i.e. estimated hourly error approximates to real error), the variance or standard deviation ($\mathrm{SD} = +\sqrt{\sigma^2}$) of corrected prediction will be smaller than that of initial prediction. Therefore, it is reasonably expected that with a proper estimation of hourly initial prediction error, the accuracy of model prediction can be improved by subtracting the estimates from the initial predictions. After the correction, the bias is expected to be around zero and the standard deviation to be reduced. The simplest way to get an estimation of hourly prediction error is to average the error of previous days by comparing observations and predictions. This method is called an 'averaging templet'.

In getting the above results, an assumption has been implicitly introduced, i.e. initial prediction error is systematic and easily estimated. Thus the question arises: how can the estimation of initial prediction error be optimized before using the templet method?

A meteorological variable, as well as the road surface temperature (RST) or the model prediction error in RST, is expected to consist of periodic components. To draw as much information as possible from the difference between model predictions and actual observations for estimating the initial model prediction error, the hidden periodicity in the series of the RST difference should be revealed so that the averaging time for a templet is able to cover an integral period of the variation of the series. This has been done by using spectral analysis on road surface temperature data for the winter of 1988/89 at the Chapman's Hill road weather site on the M5 (Thornes and Shao 1991b). The results showed that the series of model prediction has dominant periodicity around 3, 5 and 7 days. An estimation of initial prediction error over one of these periods is representative of the optima.

5. Validation of the templet

The templet method was first used for winter 1990/91 for the 11 sites given in Table I, with actual roadside input to validate the effectiveness of the method. The results are given in Table III. As a demonstration, the hourly biases and standard deviations of sites GR003 and WN002 without and with a templet are shown in Figs 3 and 4. From the figures, it is seen that the cold bias has been removed by the templet. The frequency distribution of the difference between actual and predicted minimum temperatures for the model is shown in Figs 5 and 6. About 40% of the minimum road temperature forecasts with the templet are of an accuracy ±0.5 °C, and 57.3% (Tyrebagger) and 74.2% (Ray Hall) of the forecasts are within ±1 °C. The improvement in minimum forecast using a templet is 10–20%.

In order to see its generality and usefulness in real-time model runs, the method was then applied for ten sites using realistic or forecast inputs. Table III summarizes the results.

From Table III and Figs 3–6, an improvement in the model prediction by using an averaging templet is obvious. The most notable improvement is in the bias which is reduced very significantly. No matter how big the bias is, the templet reduces it close to zero. On the other hand, there is very little change in the standard deviation. Comparing the results in both bias and standard deviation, the corrected predictions are much better than those without a templet in both overall hourly predictions and minimum temperature prediction for almost all of the sites. For the real-time application of the method, Table IV shows that:

(a) the method improved the model real-time forecasts for most sites by significantly removing bias, especially for the overall forecasts;

(b) there is no large difference between using a 5-day or 7-day templet;

(c) for some sites (Barton Mills (SF001) and Grange Moor (KB003)), the method deteriorates the forecasts where the initial model forecasts were of small bias.

The above results demonstrate that an averaging templet is a useful tool to delete systematic errors in model predictions. It is clear that the method is potentially useful to increase the accuracy of real-time forecasts, although the results may not be so good as with perfect prognosis. It must also be remembered that for real-time use a negative bias of about 0.25 °C is desirable, as discussed in Thornes (1989). The templet can easily be adjusted to achieve this.

Table III. Bias and standard deviation of model forecasts with an averaging templet* (roadside input, November–February 1990/91)

Site code		Overall errors A	B	C	D	T_{min} errors A	B	C	D
BO001	bias:	−0.83	−0.01	0.01	0.01	−1.15	−0.20	−0.13	−0.11
	SD:	1.22	1.21	1.21	1.18	1.19	1.19	1.24	1.23
BR006	bias:	−0.56	0.00	0.01	0.03	−0.34	0.05	0.21	0.27
	SD:	0.98	1.04	1.00	0.98	0.87	1.06	1.00	0.94
CH007	bias:	−0.31	−0.01	−0.02	−0.01	−0.17	0.11	0.16	0.19
	SD:	0.98	1.02	1.00	0.97	0.93	0.94	0.95	0.95
GR003	bias:	−0.98	−0.02	−0.02	0.04	−0.97	−0.12	0.16	0.05
	SD:	1.07	1.14	1.00	1.12	1.14	1.20	0.95	1.20
HW010	bias:	−0.77	−0.03	0.00	0.01	−0.78	−0.59	−0.14	−0.03
	SD:	1.20	1.33	1.19	1.16	0.96	1.76	1.08	0.98
IN002	bias:	0.05	−0.01	0.01	0.03	0.32	0.02	0.17	0.22
	SD:	1.14	1.32	1.22	1.19	0.97	1.14	1.04	0.97
KB003	bias:	0.26	−0.02	−0.02	−0.01	0.65	0.13	0.23	0.29
	SD:	0.95	1.05	1.00	1.00	0.98	1.08	1.06	1.08
RO013	bias:	−0.76	−0.01	0.00	0.01	−0.93	−0.07	−0.01	0.04
	SD:	0.88	0.85	0.82	0.81	0.78	0.85	0.82	0.83
SF001	bias:	−0.37	−0.01	0.00	0.01	0.01	0.11	0.18	0.22
	SD:	0.88	0.92	0.88	0.88	0.83	0.89	0.88	0.87
WN002	bias:	−0.87	−0.04	−0.02	0.00	−0.90	−0.20	−0.06	0.01
	SD:	1.11	1.17	1.11	1.09	1.01	1.19	1.07	1.04
XM005	bias:	−0.29	0.00	−0.01	0.00	−0.21	−0.01	0.04	0.06
	SD:	0.83	0.86	0.82	0.81	0.72	0.6	0.73	0.73
Mean	r.m.s.	1.19	1.08	1.02	1.02	1.15	1.10	0.98	0.98

* A — without templet
B — with a 3-day templet
C — with a 5-day templet
D — with a 7-day templet.

6. Conclusion

From the above results the following conclusions can be drawn:

(1) The output of the Meteorological Office mesoscale model can be linearly combined using four-grid-point values to give a better input data set for a specific site for the Meteorological Office road ice prediction model. For the 11 sites chosen for the investigation, eight of them showed improvements in the predictions of overall temperatures.

(2) The averaging templet method is a useful tool to delete systematic prediction error and increase prediction accuracy for the Meteorological Office road ice prediction model in overall and minimum temperature predictions.

As for an optimal averaging period for the templet method, 3, 5 and 7 days are suitable candidates. Too short a period may be unable to cover a necessary range of road-surface temperature variations in order to smooth the fluctuation of prediction error. A longer period (more than 7 days) contains too much 'old' information that has lost its usefulness, especially for minimum prediction. To take into account the weekly cycle of traffic, a 7-days averaging period is preferable.

For real-time use the forecaster should be able to deselect the templet option if the weather conditions are set to change significantly from the previous few days weather.

Acknowledgements

This research was funded by the UK Meteorological Office and our thanks go to Peter Buchanan, Anthony Astbury and Sarah Rawlins for their support and encouragement.

References

Buchanan, P., 1990: The application of the Meteorological Office mesoscale model to critical weather situations in the UK. *In* Proceedings of the 5th International Road Weather Conference, Tromso, March 1990. Public Roads Administration, Norway.

Farmer, S.F.G. and Tonkinson, P.J., 1989: Road surface temperature model verification using input data from airfields, roadside sites and the mesoscale model. Bracknell, Meteorological Office, Special Investigations Technical Note No. 58. (Unpublished, copy available from National Meteorological Library, Bracknell.)

Rayer, P.J., 1987: The Meteorological Office forecast road surface temperature model. *Meteorol Mag*, **116**, 180–191.

Thompson, N., 1989: The Meteorological Office road surface temperature prediction model. *In* Proceedings of the 4th International Conference on Weather and Road safety, Florence, November 8–10 1988. Accademia dei Georgofili - Logge degli Uffizi Corti, Italy.

Thornes, J.E., 1989: A preliminary performance and benefit analysis of the UK national road ice prediction system. *Meteorol Mag*, **118**, 93–99.

Thornes, J.E. and Shao, J., 1991a: A comparison of UK road ice prediction models. *Meteorol Mag*, **120**, 51–57.

Thornes, J.E. and Shao, J., 1991b: Spectral analysis and sensitivity tests for a numerical road surface temperature prediction model. *Meteorol Mag*, **120**, 117–124.

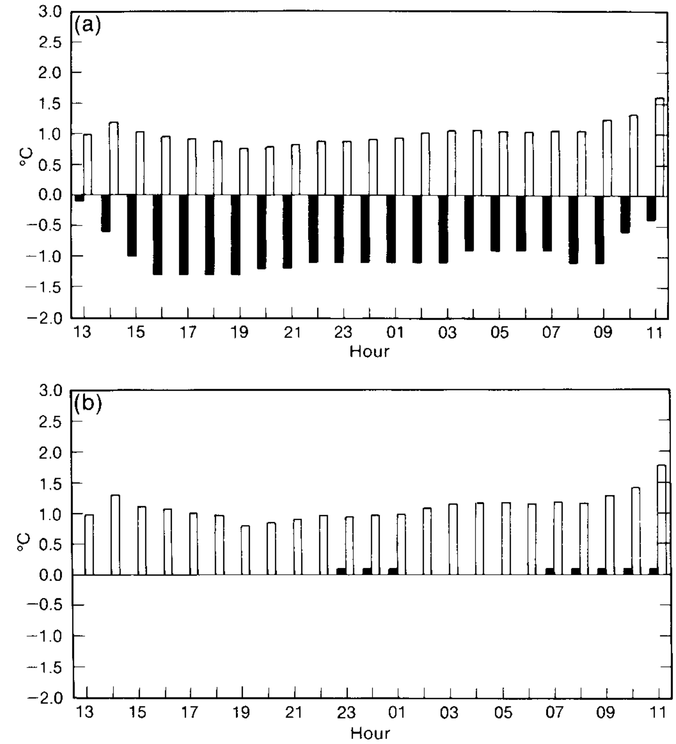

Figure 3. Mean hourly bias (shaded) and standard deviation (unshaded) of model forecasts (a) without a templet and (b) with a 7-day templet (roadside input for Tyrebagger, winter 1990/91)

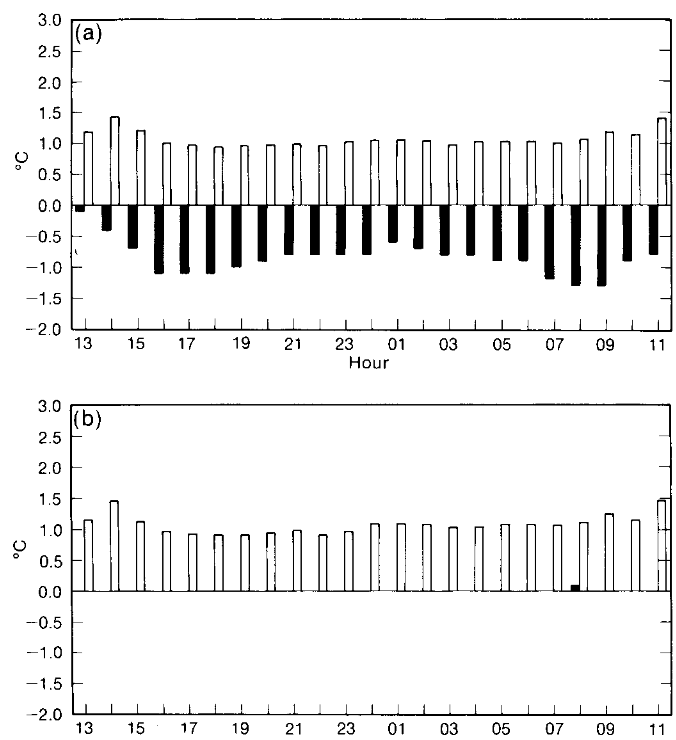

Figure 4. Mean hourly bias (shaded) and standard deviation (unshaded) of model forecasts (a) without a templet and (b) with a 7-day templet (roadside input for Ray Hall, winter 1990/91).

Table IV. Comparison of Meteorological Office model forecasts with and without a templet (realistic inputs, November 1989)

Site code		No templet bias	No templet SD	5-day templet bias	5-day templet SD	7-day templet bias	7-day templet SD
XM005	overall	−0.55	1.119	0.02	1.150	0.05	1.178
	min. temp.	−0.36	1.197	0.23	1.372	0.20	1.378
GR003	overall	−1.47	1.730	−0.10	1.866	−0.21	1.955
	min. temp.	−1.79	1.652	−0.37	2.223	−0.24	2.456
IN002	overall	−0.83	1.457	−0.08	1.276	−0.29	1.266
	min. temp.	−0.50	1.441	0.20	1.341	−0.09	1.306
SF001	overall	−0.69	1.737	0.18	1.772	0.23	1.878
	min. temp.	−0.36	1.260	0.41	1.330	0.52	1.439
BR006	overall	−1.24	1.521	−0.18	1.616	−0.22	1.519
	min. temp.	−1.15	1.409	−0.24	1.854	−0.22	1.461
CH007	overall	0.67	2.075	0.13	2.471	0.33	2.444
	min. temp.	1.39	1.927	0.92	2.477	1.20	2.343
KB003	overall	0.02	1.362	0.03	1.641	0.13	1.456
	min. temp.	0.15	1.445	−0.07	2.013	0.06	1.733
RO013	overall	−0.76	1.973	−0.20	1.787	−0.31	1.615
	min. temp.	−1.37	1.990	−0.15	2.146	−0.30	2.059
WN002	overall	−0.77	2.085	−0.06	2.364	−0.16	2.259
	min. temp.	−0.61	1.729	−0.03	2.107	0.05	2.060
BO001	overall	−0.88	2.171	−0.21	2.274	−0.21	2.265
	min. temp.	−1.54	2.385	−0.49	2.554	−0.32	2.425
Mean r.m.s.	overall	1.93		1.83		1.80	
	minimum	1.93		1.98		1.91	

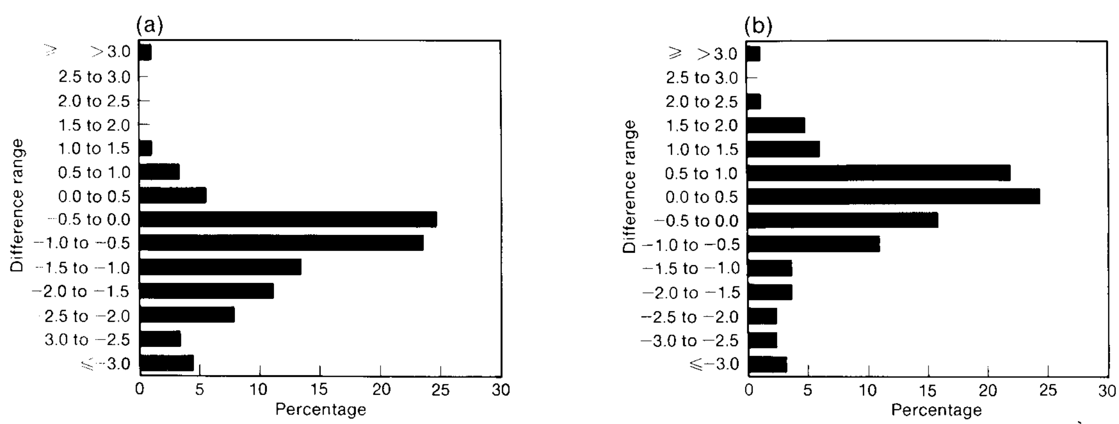

Figure 5. Frequency distribution of the difference of minimum temperature (a) without a templet and (b) with a 7-day templet (roadside input for Tyrebagger, winter 1990/91).

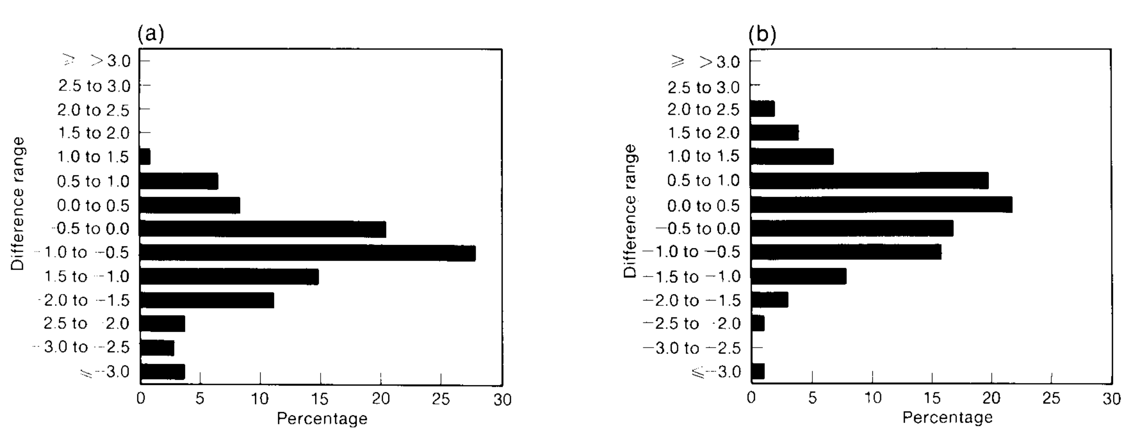

Figure 6. Frequency distribution of the difference of minimum temperature (a) without a templet and (b) with a 7-day templet (roadside input for Ray Hall, winter 1990/91).

551.501.9(410):551.5(09)

United Kingdom synoptic meteorological observing — past, present and future

F. Singleton
Meteorological Office, Bracknell

Summary

The history and current state of the UK synoptic network is reviewed in the light of current developments in the automation of observing.

1. Introduction

This paper describes the UK synoptic observing network and its current configuration. Developments in the network are discussed and also the ways in which the needs of the user will be met. These needs relate to the WMO requirements for data for exchange over the Global Telecommunication System (GTS), to numerical weather prediction models of increasing resolution, to or national forecasters and to the local forecasting or nowcasting requirement, especially for aviation. A look is taken at the UK observing scene in some 20 years' time.

2. Observing network

The need for a network of observations all made at the same time and in the same way had been recognized by Robert Hooke in 1663. In 1838 John Ruskin rationalized upon the need for an observing network, noting that '... the individuals should think, observe and act simultaneously, though separated from each other by each other by distance on the greatness of which depended the utility of the observations'.

The potential value of such a network was demonstrated when Napoleon III asked his astronomer royal, Le Verrier, to study a storm in the Black Sea (14 November 1854) during the Crimean War, when some 40 allied ships were lost. Le Verrier was able to show that the storm was a coherent circulation of winds, around a centre of low pressure, which had moved as an entity in a gently curving track. From this study it was apparent that, on the basis of extrapolation alone, weather prediction over a few hours at least was possible in principle. Observing networks for operational purposes began to be developed from the mid to late 1850s when the first meteorological services were created and when, importantly, the electric telegraph was developing as a means for transmitting data quickly. The Great Exhibition of 1851 saw the first 'near real-time' maps of actual weather derived from these messages. The maps sold for one penny a piece (then the price of a postage stamp).

3. The UK surface synoptic network

Admiral FitzRoy started the early operational observing networks run by the Meteorological Office, but these were limited in that the observers had to have access to the telegraph. In 1880 there were some 36 synoptic stations, many of which were at lighthouses or coastguard stations. In 1920 the Office came under the aegis of the newly formed Air Ministry and a major component of its work was directed to serving aviation in general and to the Royal Air Force in particular. Observations became available from airfields.

In the early 1920s there were around 45 to 50 synoptic observing stations, 20 or so of these were official stations — observatories or distributive stations. The latter name was coined because their data were collected on a distributed scheme through collecting centres. The remaining 25 or so stations continued to be known as telegraphic stations for obvious reasons, and they corresponded to the current auxiliary synoptic stations in that they were manned by coastguards, lighthouse keepers, etc.

Just prior to the Second World War the annual report of 1939 quoted the total number of stations at 51. During the war the number of airfields rapidly increased and the reporting network reached its densest ever at 550, mostly in the eastern half of Britain with the many RAF and US Air Force bases. Within 18 months of the war's end the number of observing sites had halved and subsequently the number of officially manned stations decreased to around 80; the number of auxiliary stations increased to around 180 in the 1970s, but has now decreased to about 100.

The manned official observing sites are still mostly at airfields, while the auxiliary sites are chosen to fill gaps in the network and to meet specific operational requirements. Clearly, throughout its history the Office has had little real control over the shape and size of its observational base. In the ideal situation the network observing sites would be planned in such a way as to represent those weather features sufficiently long-lived to be worth predicting, and at the same time represent adequately the different climatological areas of the United Kingdom.

Because the ideal is far removed from the practical, the Meteorological Office Working Group on United Kingdom Observing Networks (WGUKON) was created to consider the needs for observations. It advises upon network design and has developed policies for all networks, synoptic, offshore, climatological, rainfall stations and radar (but radiation and sunshine have yet to be completed). These enable the actuality to be compared to an ideal and point to actions necessary to bring each network up to an acceptable standard. A policy for synoptic networks is contained in a paper known as UKON 1. The basics of this are as follows:

(a) There will be a key synoptic station network, comprising some 30 stations reporting hourly throughout the 24 hours. These stations will be fully equipped and manned by professional meteorologists for the observing function, so that every observation complies with the full WMO requirements for a SYNOP from a principal land station. These stations are about 90 km apart on average, although the network is not very even and in some areas the spacing approaches 200 km. The WMO recommendation is that the space between stations on a regional basic synoptic network should not exceed 250 km.

(b) There will be a number of secondary stations associated with each key station depending upon the area in which the latter is considered to lie. These stations will represent coastal areas facing representative directions, inland areas, both high and low ground and areas of particular interest, e.g. the Thames Valley, the Upper Clyde Valley, major conurbations and recreational areas. Secondary stations may be fully manned to WMO PLS (Principal Land Stations) standard and they may be fully manned, automatic or part-manned/part-automatic. The minimum requirement for secondary stations is that they should report pressure, winds, temperatures and precipitation, not less frequently than every 3 hours. The UKON 1 policy currently calls for 85 secondary stations, with at least one being fully manned in each key station area.

(c) There will be an unspecified number of Supplementary Observing Stations, these stations will report as necessary to meet the needs of local forecasting and other operational requirements for weather observations. Some conform to the full WMO PLS specifications, others fall far short.

4. Implementation of UKON 1 policy

4.1 Key stations

The UKON key stations, secondary stations and associated areas are shown in Fig. 1: six of the key stations are located at radiosonde stations, a further three are at locations where the main function is surface weather observing, and the remainder are at aviation stations where there is a current need for full-time professional observers. Such a need does of course depend upon the operational requirement, and where a local user need ceases then the Meteorological Office may keep staff on site, upgrade another station to key status or, sometimes, open an office purely for synoptic observing function. For example, Dunkeswell opened when there was no longer a need for Office staff at Exeter Airport. However, such offices are regarded as undesirable in terms of the use of staff time, and whenever possible the policy is to try to collocate surface synoptic observing with other functions, such as upper-air observing, observatory work or aviation services. As well as being chosen for their meteorological attributes, key stations should also have a reasonable likelihood of a long operational life — major airports and important RAF bases are good examples.

4.2 Secondary stations

Airfield closures, availability of suitable sites, and the pressure to reduce costs have made it impossible to sustain a Meteorological Office-manned secondary station network to the levels defined in the UKON policy paper. Application of the policy has led to the selective recruitment of auxiliary observers and to the deployment of some fully automatic stations, typically the Synoptic Automatic Weather Stations (SAWS) in order to fill gaps in the network.

4.3 Supplementary stations

At other meteorological stations where there is a flying commitment, observers have to be present during flying hours. Such stations may be closed at weekends and nights so the density of stations reporting depends upon the time of day and the day of week. Requirements for data to meet specific user requirements, other than on operational airfields, may be met by the recruitment of auxiliary observers, by automatic stations, or by Meteorological Office staff on an opportunity basis. Fig. 2 shows the maximum hourly coverage of observations when all are reporting, while Fig. 3 shows the minimum observational coverage. Both of these figures are valid for spring of 1992.

5. Implementation of automated observing systems

The initial concept for automated observing in the United Kingdom was for a system that would operate at remote sites, generating limited SYNOPs consisting only of temperature, dew-point, pressure, wind and 6-hourly rainfall totals. Subsequently these SAWS systems were enhanced to measure hourly rainfall totals, extreme temperatures and hourly mean winds and gusts. They were also able to accept observations of radiation, visibility and cloud base, and to have extra temperature sensors fitted to give grass minimum and ground temperatures. The enhanced SAWS therefore not only provides better observational data than the original, but

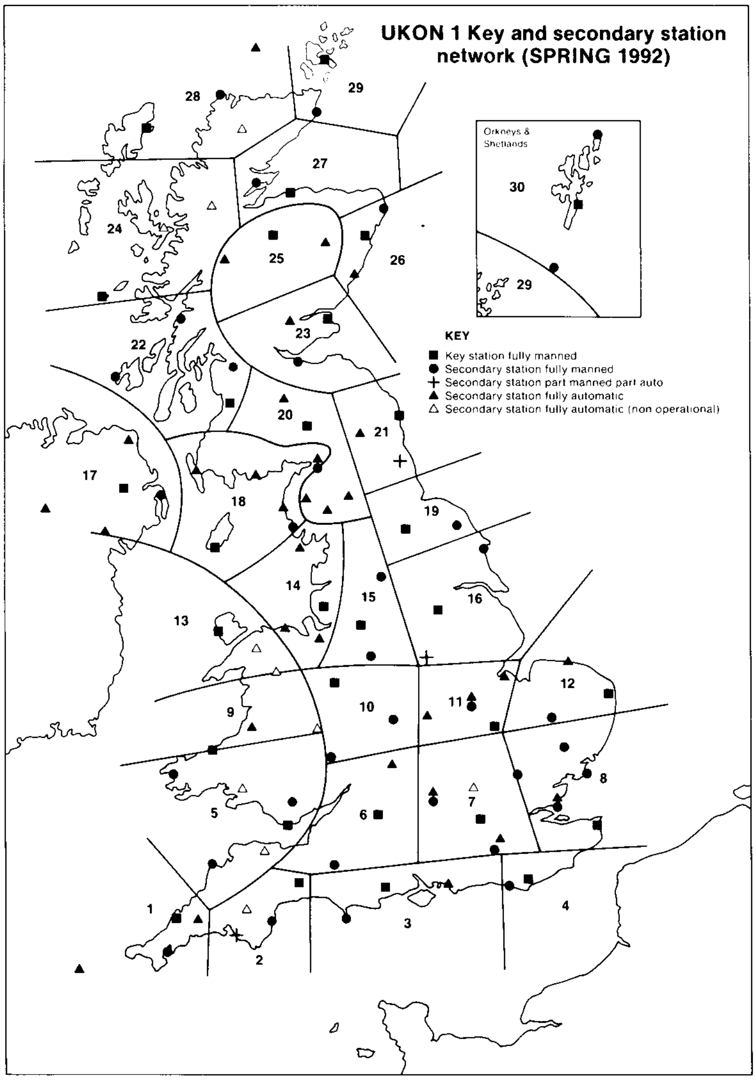

Figure 1. The UKON 1 key and secondary station network as at the spring of 1992. Note that several areas, e.g. 9, 13, 21 and 25 do not meet UKON 1 policy in that there are no manned secondary stations.

is also able to act as a principal automatic climatological station within the WMO definitions. Although initially limited in scope and application, the SAWS has become a successful operational system. Since their introduction the concept of applying automation to the observing functions has developed. There is still a need for systems to operate unattended like SAWS, but there is now also a requirement for systems to be able to accept additional or modified data generated by a human observer. The applications for such Semi-Automatic Meteorological Observing Systems (SAMOS) or the commercial derivative, Computer-Aided Meteorological Observing Systems (CAMOS) are seen as being fivefold:

(a) Manpower is released from the mechanical aspects of observing, such as reading, transcribing and keying of instrumental data, coding them into SYNOP or METAR format, completing the *Daily Register*, checking the data and generating the national climate message. This may allow some merging of functions, e.g. those of observer and forecaster, at quiet times.

(b) A reduced SYNOP is provided when observers are totally or partially withdrawn for reasons of economy and so maintain observing networks up to the standard for UKON 1 secondary station purposes.

(c) Night-time and weekend gaps in the observing network are filled to bring it up to the UKON 1 requirements when necessary. A station that was previously capable only of meeting supplementary station needs, because of its operating hours, can fairly cheaply be brought up to the frequency of observing that is required of a secondary station.

(d) With minimum interference to their ATC functions, Air Traffic Control staff are enabled to produce METARs and, as a by-product, to generate the SYNOP.

(e) Uniform standards of observing and coding are maintained at all stations, thus saving some time and costs of training observers.

Even when envisaging the most advanced automation of observing there are still some parameters which

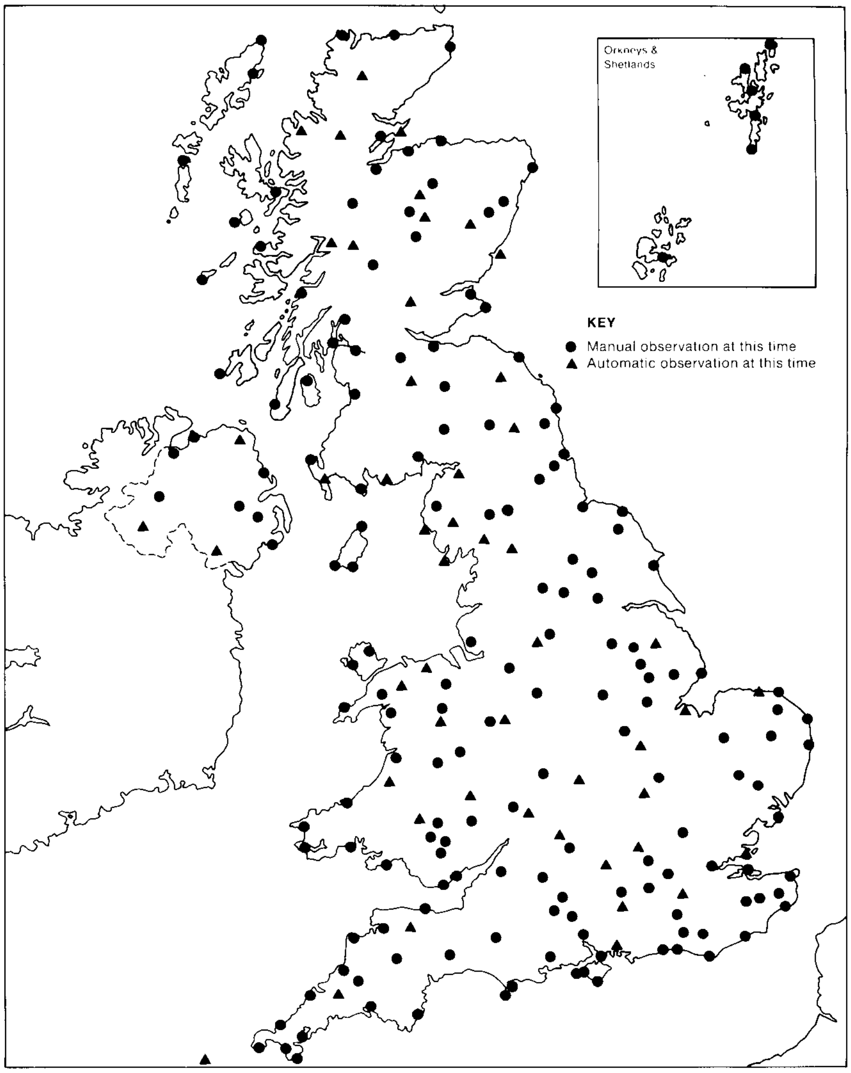

Figure 2. The maximum hourly cover of observations (at 0900 UTC on weekdays) as at the spring of 1992.

require human input for correct observing. These are visibility, the amount, height and type of cloud, present weather and state of ground. Visiometers now available have been shown to be at least as good as a human being (at night they are somewhat better) except that they cannot cope with directional variation in visibility. Cloud-base recorders still require some degree of interpretation. While they might be programmed to give estimates of low cloud amount they are unlikely to cope with higher-level cloud amounts, they are adversely affected by some precipitation and cannot, of course, describe cloud type. Present weather devices cannot, and are unlikely ever to, cope with the '99' description of the WMO code.

From the above it is clear that an automatic system requires human assistance to produce a SYNOP to WMO standards or a METAR to ICAO requirements. It follows therefore that Meteorological Office observing policy is as follows:

(a) SYNOPs at key stations and for regional basic synoptic network purposes, i.e. for exchange over GTS, will be made with human input for the visual element and to check input from SAMOS where used.

(b) SYNOPs and METARS at Meteorological Office-manned stations where flying is taking place will be made with human input for the visual elements and to check input from SAMOS where used.

(c) At all other stations or times, SYNOPs may be made by automated systems, and if there is no human input available, will be transmitted in limited form. From remote sites such as buoys, oil rigs and platforms, such limited data may also be transmitted over GTS.

6. SAMOS programme

The programme for SAMOS includes implementation at all observing offices where there are Meteorological Office staff. The result will be that the number of stations providing hourly data throughout the 24 hours will increase, and in some areas exceed UKON 1 secondary station needs, to give a degree of redundancy in the network. SAMOS may be provided to auxiliary stations, if that is the only way that UKON 1 secondary stations can be found in some parts of the United Kingdom. Whether CAMOS is used to provide assist-

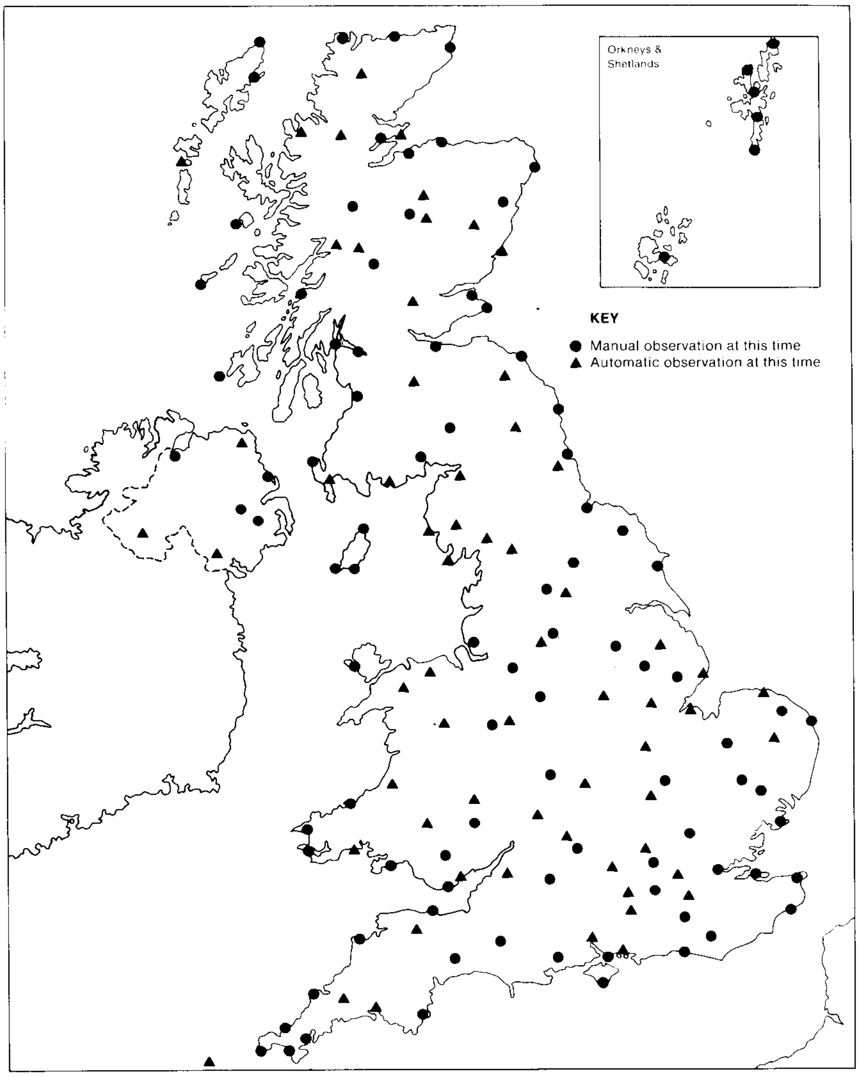

Figure 3. Minimum observational coverage (at 0300 UTC at weekends) in 1992.

ance to ATC staff at civil airports with no Meteorological Office staff is, of course, a matter for the CAA or the local airfield management. It is hoped that CAMOS will be seen as sufficiently user friendly for this, since it will improve further the UK observational network to the benefit, amongst others, of civil aviation itself.

There are still a few SAWS installations to complete. The SAMOS programme is scheduled for completion by the end of 1995/6. By then the 'maximum' network of Fig. 2 should have been augmented, with many of the SAWS and SAMOS sites being equipped with visiometers and cloud-base/low-cloud amount recorders. More importantly the 'minimum' network at Fig. 3 will also have increased in numbers to that shown in Fig. 4. Should CAMOS be implemented at civil airports where there are currently no SYNOPs provided, then the network densities will be greater than shown.

7. Message transmission and exchange

The above is a description of the current observing policies for the United Kingdom. However, it must be remembered that the SYNOP code forms and data needs, as identified by WMO, had their origins in the days before numerical weather products, and long before radar networks and satellite sensing. The use of groups of five figures, with the location of each number indicating the elements reported, dates back to 1863 when Admiral FitzRoy produced instructions for the construction of weather messages with simple present- and past-weather codes, dew-point depression, gust speeds and directions, pressure, mean winds, etc.

The form of the current WMO SYNOP report was designed to give as complete a description as possible to enable subjective and detailed analyses of small-scale weather features. Nowadays much forecasting is undertaken by computers using objective analysis techniques, enhanced by human input based on satellite cloud and radar rainfall imagery. Therefore it is pertinent to question the need for continuation of, or adherence to, the SYNOP format.

Given improvements in communication systems and data compression techniques, it is possible to consider large numbers of automatic stations producing continuous data streams of some, but not necessarily all, of the

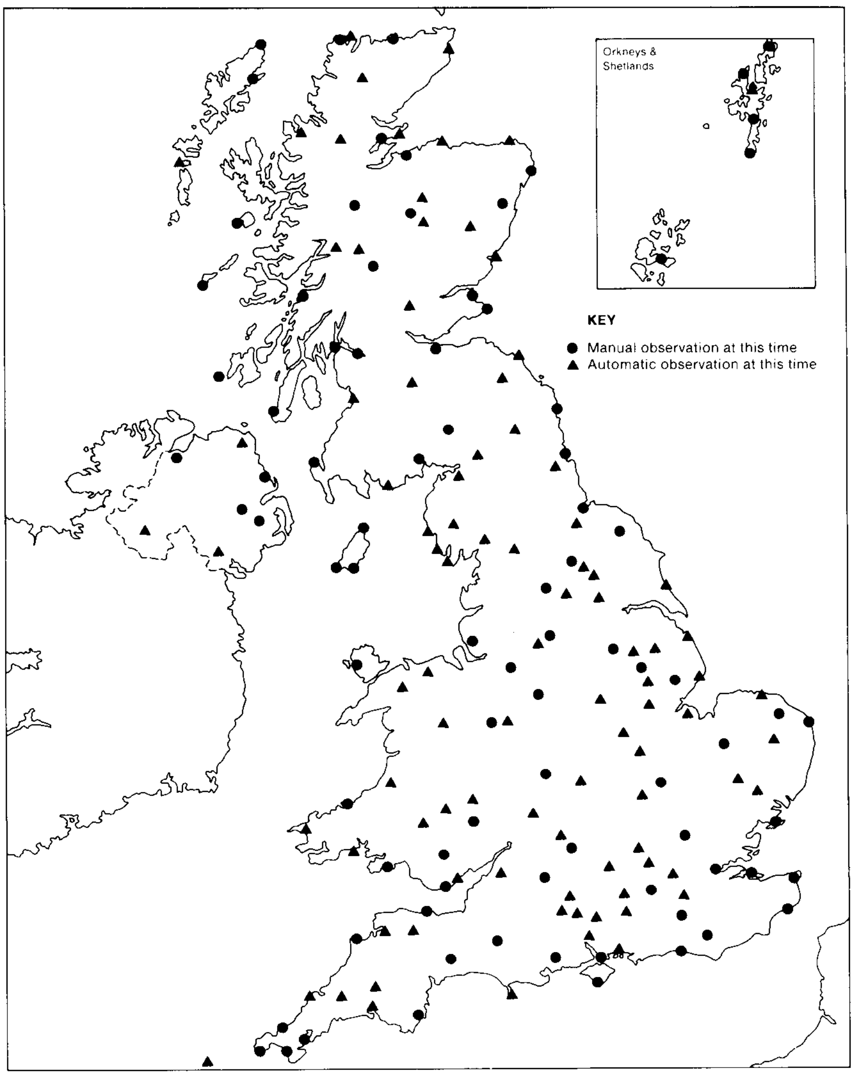

Figure 4. Minimum observational coverage at 0300 UTC by late 1996. Note the number of automated observations (cf. Fig. 3). Use of CAMOS at smaller civil airports will give even better SYNOP cover than shown.

basic data of winds, pressures, temperatures, rainfall, visibility, low-cloud amounts and heights. The climatological network is a potential source for these extra sites. At present it is largely manual, but there is an increasing need to introduce automatic stations. Fig. 5 shows the 1992 voluntary climate network. The increasing power of computers coupled with developments in objective analysis techniques is leading to the possibility of being able to use such data with near-continuous assimilation. The use of imagery in such analysis methods is also being actively explored.

For such internal, national processing of data, a coded SYNOP becomes inappropriate for either data collection or dissemination. Local area forecasters are increasingly likely to become supplied with data analyses in pictorial or digital forms, coupled with short-period predictions of the same fields. There will be no need for individual forecasters to analyse fields of pressure, wind, temperature, cloud, precipitation, etc.

8. The UK upper-air network

The radiosonde, developed during the 1930s, became an operational tool during the latter part of that decade and during the Second World War, after which there was rapid development and expansion of networks worldwide.

Early wind finding from radiosonde ascents in the United Kingdom used radio direction-finding systems with a triangle of stations around each radiosonde station, but has been replaced by radar since the mid 1940s. As part of current cost-saving measures, NAVAID wind finding has been introduced at some UK radiosonde stations using the LORAN system. From ships the NAVAID–OMEGA system is already used and is adequate, but it is unable to produce wind data of the accuracy and resolution required over the UK mainland. The main shortcoming of the radiosonde is that, for cost and logistic reasons, operational systems, typically, are only launched at 6-hour intervals. The UK

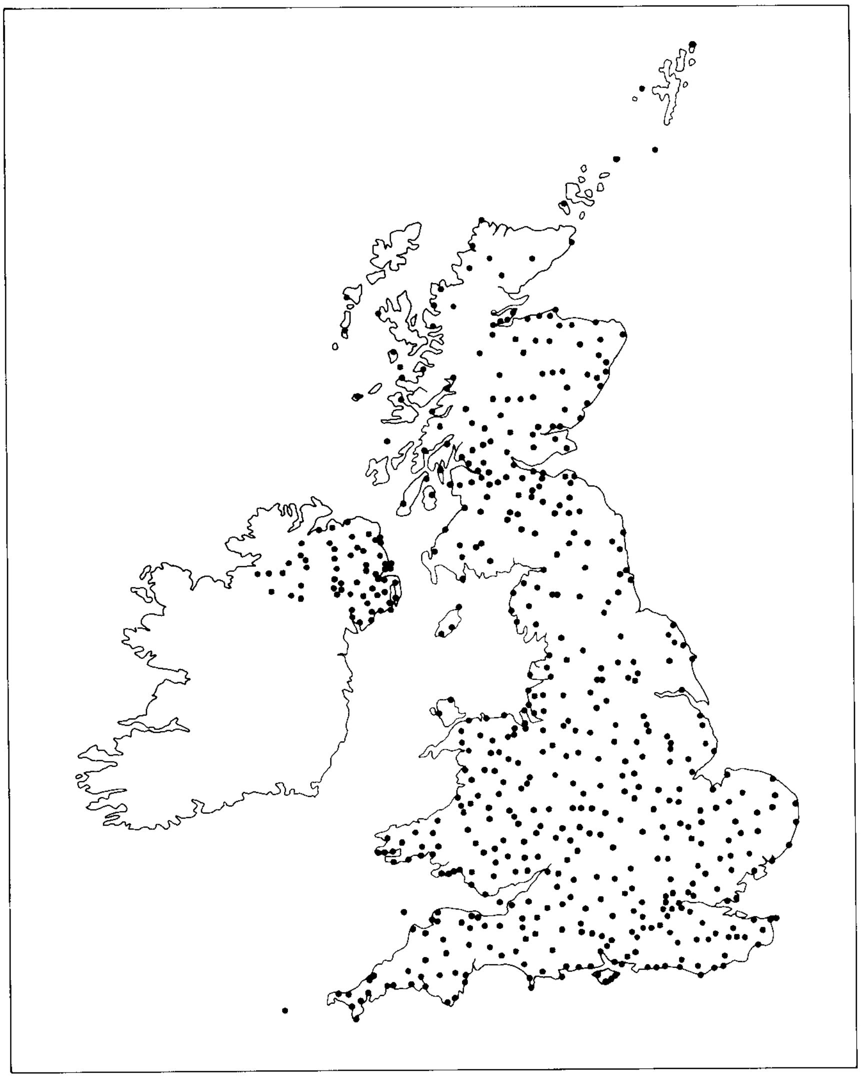

Figure 5. The voluntary climatological observing network as at early 1992. Some of these sites have the potential for a simple automatic weather station and the provision of instrumental data to enhance the synoptic networks.

radiosonde network is roughly at the WMO recommended spacing. All the stations produce wind data at 6-hour intervals, but where winds are measured by radar, the temperature and humidity ascents are made only twice a day. Because a radiosonde is needed for LORAN wind-finding these stations make temperature and humidity ascents 6-hourly. For local forecasting purposes the so-called boundary layer radiosonde is used. This is a conventional sonde system typically used up to 500 mb but not measuring winds.

In the future, satellite sounding techniques are expected to produce data of sufficient quality for large-scale temperature, humidity, pressure contour and wind analyses but are unlikely to provide detailed soundings of the kind used by forecasters. Future ground-based remote sounders may be able to produce useful detailed temperature profiles up to about 2 km, but without humidity data. At present it seems unlikely that either ground- or space-based remote sensing will completely replace the radiosonde for observing temperature and humidity profiles with great accuracy and resolution from the surface up into the stratosphere. However, early results with aircraft-to-satellite data relay (ASDAR) have shown that aircraft can produce good temperature profiles up to normal cruising altitude, but without humidity data.

Wind profilers (high-power vertical-looking Doppler radars detecting inhomogeneities in clear air) are capable of producing measurements of wind from 200 m to 14 km (working at 400 mHz) or 2 km to 20 km (at 50 mHz) with resolutions of 150 to 300 m. These systems are being studied in a number of countries, notably the USA where a network of thirty or so 40 mHz profilers is being created. Profilers operating at 400 mHz have typically a 10 × 10 m aerial array and may be adversely affected by precipitation. At 50 mHz a 100 × 100 m aerial array is needed, there is little effect from precipitation, but no wind data below 2 km. So there are a number of problems with this technique, including some associated with frequency clearance. In principle, however, profilers offer the possibility of frequent measurements of wind over a network at least as dense as the radiosonde network. Should the data prove adequate, then profilers at around 400 mHz could prove a cost-effective method of generating wind data in lieu of either radar or NAVAID systems. Further work is necessary to evaluate wind profilers. Data from the 50 mHz profiler run by the University College of Wales, Aberystwyth, are being evaluated by the Meteorological Office, and several European countries are also undertaking trials. Much will be learnt from the experience in the United States.

9. The UK observing scenario in 2010 — long-term forecasts

Firstly, there will probably be more observing sites, some possibly only producing one or two parameters with a greater flow of instrumental objective data than at present. This could be achieved using some of the 500 climate stations if they were equipped with low-cost automatic systems. Such data could include visibility, some limited present-weather indicators with cloud height and amount of low cloud. Human observers, if used at all, will be limited to a relatively few stations where full weather and cloud descriptions are still needed, or where required for safe aircraft operation.

Secondly, SYNOPs will not be used for dissemination of observational data within the United Kingdom. Data will come to the centre in basic numerical form in much larger volumes than at present and be redistributed as analyses and short-range predictions. Of course this concept is already being developed for radar data.

Thirdly, SYNOPs if used at all, will be generated only for a limited number of stations and at times needed for broadcast on the Global Telecommunication System. Their generation will be at a central location and not necessarily on site.

Fourthly, upper-air wind-finding by radar with balloon-borne reflectors will have been phased out in favour of NAVAID techniques, using LORAN or GPS or wind profilers. There will be increasing use of aircraft-produced wind data.

Finally, ground-based remote soundings, and aircraft data on the ascent and descent phases, will provide a near-continuous description of temperature distribution with height. Radiosonde flights to provide humidity data and detailed temperature profiles in depth may be made only 12-hourly.

551.50

Quality Assurance in the observations area of the Meteorological Office

R.J. Shearman
Meteorological Office, Bracknell

Summary

The Meteorological Office is heavily dependent upon data for service provision. Considerable effort and resources are devoted to maintaining the quality of the data, far exceeding the correction of identifiable errors. This paper describes the overall quality assurance system which has evolved in the observations area of the Meteorological Office.

1. Introduction

The Meteorological Office has much in common with industry in that raw material in the form of observations is taken into the system and subjected to a number of processes leading to the production of a forecast or consultancy service. In the case of forecasts, there is some monitoring against ensuing events which acts as an indicator of quality in absolute terms. There is also considerable feedback from the customer based on a comparison with his perception of what the quality should be. Customer perception of quality is more important in some ways to a service provider than absolute quality. Customer perception is strongly linked with price paid and sales stance. When product improvement operates on a diminishing return, with costs escalating rapidly for small technical gain, it is easy for the actual quality of service to fall far short of the customer's preconceived perception. The inherently variable nature of the weather is such that customers' expectations of weather forecasts cannot always be met.

The problem is rather less critical in the climatological consultancy field as verification is more difficult in the short term and the customer's assessment is more likely to be made on presentation and fitness of the product for the intended purpose. However, climatological advice can be very sensitive to the quality of data from an individual site, sometimes more so than forecasting products which are based upon numerical models and broader areal analyses.

The Meteorological Office differs from many retailers in that it creates its own raw materials, the data archive, and produces the tools to do this, i.e. the observing instrumentation, the networks, communications and the archiving software. Thus the Meteorological Office must also monitor the quality performance of all the processes affecting the input data.

2. The traditional approach to Quality Assurance

Meteorological observations have been relatively labour intensive until fairly recently, and the quality assurance procedures tend to reflect this situation. Typically, the instruments are designed to measure the atmosphere to specified accuracies and are located in a manner conforming to the best achievable meteorological exposure. The synoptic observer is given a manual of complicated codes designed more for telecommunication convenience than ease of use and is constrained to carry out the whole observing/coding process to tight deadlines. Climatological observing is rather simpler, but those sites reporting on a daily basis via communication lines, rather than in delayed mode in manuscript, still have to deal with codes. It is not surprising that errors do occur, and the Meteorological Office has become very good at detecting and correcting errors in data, having twenty or so staff engaged upon this work.

The advent of automation seems at first sight to have stimulated a different approach, in that most of the problems associated with manual observing, e.g. instrument reading and coding, have been removed. However, automatic observing systems develop faults and monitoring is necessary to initiate repair or replacement action. In severe cases, the data may be deleted until monitoring indicates that the fault has been cleared.

Training and experience are essential parts of quality assurance, and the Meteorological Office has a good record in this respect. Professional observers are trained at the Meteorological Office College early in their careers and attend refresher courses from time to time. The Meteorological Office is fortunate in enjoying the cooperation of a large number of auxiliary and climatological observers who are not professional meteorologists, but who make a major contribution to the observing network. Auxiliary or cooperating observers are encouraged to attend courses. Their observations are monitored by the Meteorological Office station which collects their data, and their observations can be discussed both during collection and the two- to three-yearly inspection visit. Many auxiliaries are being equipped with personal computers which will encode their observations and pass them direct to Bracknell via telephone lines. This will remove the possibility of discussion during collection, but contact between cooperating observers and their professional colleagues is so important that specific meteorological offices are to be made responsible for groups of auxiliaries and will contact them for an informal chat on a regular basis.

The training given to cooperating observers is aimed at encouraging good practice and adherence to standard procedures. The instructors pay special attention to aspects of the work which give rise to difficulty. However, the main objective is to develop observing skills and capitalize upon the interest and dedication of both Meteorological Office and cooperating observers.

3. The concept of Total Quality Assurance

Over the years, the Meteorological Office has developed most of the elements of a Total Quality Assurance programme, but these have yet to be integrated to create a comprehensive system.

The elements are as follows:

(a) Specification of the user requirement for an observing system.
(b) Creation of a technical response.
(c) User field trial, usually preceded by an engineering trial.
(d) Installation for operational use.
(e) Quality evaluation.
(f) Quality control.
(g) Corrective action.
(h) Initiate feedback from user of data.

In what follows, the interrelationships of an integrated and comprehensive system of quality assurance are described. The system is described schematically in Fig. 1.

3.1 The user requirement for an observing system and technical response

The users' requirement should be established by thorough discussion and will be expressed initially as a need for a particular type of data with stated accuracy and resolution. Many users will not state their expectation of reliability or mean time between failures although it is now customary to quote the amount of data which may be lost before a system becomes unacceptable. Often this is expressed in term of the minimum amount of data to be provided, expressed as a percentage of the total possible. Thus a system which is expected to lose no more than 5% of data is said to have a minimum percentage data capture of 95%. However, every user has a preconceived idea of what system performance should be and this must be quantified at this stage. Realism is established and an acceptable target included in the user requirement. The user is likely to base his judgement of satisfaction in terms of quality on whether that target is met.

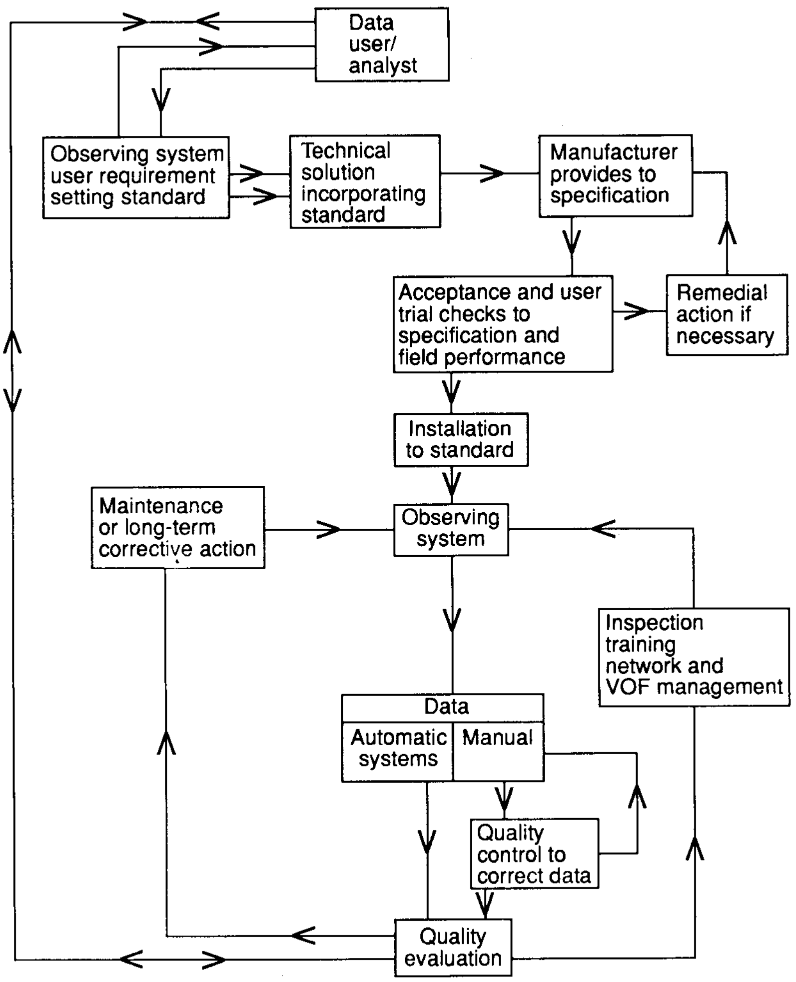

Figure 1. The Total Quality Assurance system.

The technical solution is a response to the user need and should balance what is possible in terms of cost, delivery time, accuracy and performance against the requirement. This is an interactive process leading to an agreed solution. It is vital that the technical specification contains a clear performance target as well as the desired percentage data capture. The time-scale to achieve operational installation should also be agreed at this stage, because the extent to which it is achieved will also affect the users' perception of the quality of the system.

Procurement action is also part of quality assurance because it either helps or prevents the meeting of delivery targets.

3.2 The trial phase

Equipment being tested should meet the technical specification regarding safety, construction and durability. These factors are tested during engineering trials while gaining some evidence of equipment performance and how this matches the users' perception of (agreed) quality.

After the engineering trials, a user trial is set up to determine the performance and reliability of the system under field conditions. For example, a laser cloud-base recorder has been operated at Hemsby, a key operational observing site where there are good data for comparison. Thus the equipment has been evaluated under realistic conditions. Apart from assessing the reliability and performance of the equipment against the original specification, the views of the staff actually using it are canvassed to give an indication of eventual user satisfaction.

3.3 Operational installation

The eventual quality of the data and performance of a system are inevitably related to its operational environment. The quality, effectiveness and durability of the installation are vital if a high rate of failure is to be avoided in operation. Clear and established standards and procedures have evolved as a result of long and hard-won experience. The resulting quality of installation is high and has to meet health, safety and associated legislation.

3.4 Quality evaluation

The function of quality evaluation is to assess the performance of any system by examining the data produced on a routine basis. Any unacceptable features of performance are investigated to identify the underlying cause and to seek means of eliminating it at source, if this is cost-effective. Errors in individual items of data may be corrected, but this is not an essential part of the work. It is much more important that the errors detected in the data are viewed in the light of insight into the workings of the system. Thus the services of a technician may be requested to carry out essential maintenance work on an automatic system (e.g. Synoptic Automatic Weather Station) and subsequent monitoring will check that the problem is solved. However, if the problem persists, the Quality Evaluation Team must identify this. The cost of continually fixing the system is compared with that of a longer term and permanent technical solution, if one is available. All the Meteorological Office automated observing systems, both on land and at sea, are routinely monitored and evaluated.

With auxiliary observers, the parenting action by professionally manned Meteorological Office stations provides a mix of quality evaluation and quality control, in that errors are also corrected. The professional Meteorological Office staff discuss problems with the observer while collecting the observation. Often these are related to coding but there can be more deeply seated misconceptions regarding observing practice. Parenting stations routinely pass to Bracknell summaries of such problems, so that the staff responsible for inspection and training can target their activities. The introduction of automated data collection resulting from the use of personal computers by auxiliary observers should remove most of the coding errors, leaving only observing errors. This is a major step in quality assurance but, unfortunately, it will also remove the routine contact between parenting station and auxiliary. If quality is to be maintained, a regular contact must be set up to replace the current arrangement. Meteorological Office staff will have to ensure that the auxiliary observer remains fully aware of the value of, and need for, his observations. The contact must not be allowed to relax to 'contact only when errors occur' because this will adversely affect auxiliary observer morale and therefore quality.

Fostering a sense of involvement in the meteorological process is an important step towards Total Quality Assurance. This applies equally to those professionally manned stations established solely to provide observations. Such stations have to be provided with forecast data and other material to maintain interest in the weather and, consequently, in observing standards.

For various data, e.g. from ships, buoys and other platforms, monitoring software within the operational analysis suite of programs produces statistics of errors (Hall 1991). These statistics are analysed and Port Meteorological Officers (PMOs) visit ships to discuss sources of error with observers. Monitoring and quality evaluation is also carried out for upper-air data.

Quality of observations from professionally manned stations is maintained largely by means of a long-established checking system whereby each observer reviews his predecessor's work. More formal objective checking may be introduced later.

It is essential that the quality evaluation manager continues to review the entire observing/data gathering operation to ensure that all possible actions are taken to eliminate sources of error. This involves liaison with staff from the instrument branch, the network managers and inspectorate, and the monitoring team in the Central Forecasting Office.

3.5 Quality control

From its earliest days, the Meteorological Office has always been active in quality control of data, particularly in the areas of climatology and rainfall; some quality control is performed for real-time data entering the Synoptic Data Bank. In general, errors are identified and removed or corrected, sometimes after consultation with the observer. Considerable resources are devoted to this activity, which continues to be developed. For example, a new system is on trial to quality control rainfall data using a personal computer. The gauge totals are compared with radar data and corrections made as required.

The level of quality achieved in the data before presenting them to a user is a matter of agreement and compromise. There should always be some element of user validation, particularly in the case of extreme events. Ideally all the data from any noteworthy event would be subjected to a full and exhaustive spatial and temporal analysis by quality-control staff. This is obviously not practical because of the large volume of data received and the need to approach quality control in a routine and orderly manner. The Meteorological Office does not have sufficient resources to mount detailed investigations. This means that those analysing data from a climatological archive must be satisfied that an agreed standard has been reached in terms of rejection of outliers while attempting to retain climatological extremes. The user should be wary when dealing with extreme cases and discuss doubts and inconsistencies in the data with those responsible for the quality control.

The first priority for quality-control staff is to check and correct the data, and although some effort is made to detect underlying trends or causes, this is a secondary and somewhat *ad hoc* process. Summaries of errors found are passed to the network and inspectorate staff on a monthly basis. This process will be formalized and automated so that it follows quality evaluation principles in trying to eliminate the cause of the problem.

3.6 Corrective action — the role of the Inspectorate

The Meteorological Office has a team of inspectors who visit each auxiliary observing site, climate station and rainfall site approximately every three years. This level of activity conforms to WMO guidelines, and seeks to ensure that observing practices and instrument exposure meet the accepted standard. Details of errors detected by quality control are available to inspectors visiting climatological and rainfall stations. Auxiliary sites will also be included shortly.

The inspector should discuss the whole process with the observer in detail to establish the individual's *modus operandi* and related ergonomics. The object should be to detect error-prone practices as well as to discuss errors which have actually occurred. All inspectors are well aware of their public relations role, and take great care to commend, encourage and motivate observers.

A number of auxiliary and voluntary climatological observers' training courses are run each year. However, the observers are volunteers and either they or their parent organizations have to fund the time spent on a course. The Meteorological Office pays travel costs and provides accommodation.

The Inspectorate encourages the observers to perform well and this includes attendance on courses. There is no question of compulsion but if a station consistently falls below an acceptable standard it should be discontinued and if a replacement station is required for the network, action taken to identify a suitable candidate. PMOs carry out duties which are broadly similar to those of the station Inspectorate. However, they encounter difficulties in that crew changes are frequent and some UK ships do not enter UK ports at any time. PMOs do offer to visit ships of other nationalities, and bear in mind monitoring results. However, there is little to be done when errors are caused by poor or damaged equipment on board ships of other nationalities. The Meteorological Office can, and does, recruit foreign ships to its voluntary observing fleet, but cannot replace poor equipment on ships from the voluntary observing fleets of other countries.

3.7 Feedback from the users of the data

The user requirement for any observing system reflects the accuracy and performance dictated by the use intended for the data. Quality assurance seeks to maintain the whole data management system to that level of performance. However, it is important that feedback is sought regularly from users of the data to ensure that their perception of the quality achieved matches their expectations and that the expectation matches the level aimed at by the quality-assurance staff. Responsibility for this activity rests with the Quality Assurance Manager.

4. The Management role in Quality Assurance

Management must make it quite clear that there are quality targets and that they will be adhered to at all times. Policies should be determined for data standards as they are for the composition of the various observing networks maintained by the Meteorological Office. Such standards must be defensible when it comes to overall resource allocation. In times of financial stringency it can be all too easy to cut back an apparently non-productive function such as quality assurance. However, the results of doing so with data can have repercussions for future generations. Most companies who have adopted Total Quality Assurance recognize that regulatory systems have a role to play, but largely it is one of reinforcement. Quality will be determined mainly by the attitude of mind of the work force and their pride in producing a worthwhile end result. This means that each member of staff must be encouraged to value their professional contribution.

5. Conclusion

The Meteorological Office is data dependent, and as such the reputation of its products depends upon quality assurance. Standards set must be consistent with the requirement of those producing the highest grade of commercial service, because the same data feed all the services. Maintenance of quality is largely a question of attitudes and management must make it quite clear what is required and stand by that statement. Good communication must be maintained between the various component parts of the data management system with effective feedback on quality, and well coordinated action. The Quality Assurance Manager has a key role to play in this respect. However, none of the regulatory mechanisms will result in a high level of quality unless the members of staff concerned take professional pride in their output, and the value of their contribution is continually emphasized.

Reference

Hall, C.D., Ashcroft, J. and Wright, J.D., 1991: The use of output from a numerical model to monitor the quality of marine surface observation. *Meteorol Mag*, **120**, 137–149.

Rime deposition

W.S. Pike
19 Inholmes Common, Woodlands St Mary, Newbury, Berkshire RG16 7SX

Following two days and nights of freezing fog in a light easterly airflow, the following photographs were taken on 31 January 1992. Fig. 1 shows 2–3 cm of rime deposition as the fog was beginning to clear on the Lambourn Downs. The beech trees showed characteristic translucent or transparent rime on all east-facing twigs, increasing with height above ground level.

Fig. 2 shows the effect of a miniature funnelling of 'upslope' airflow between 'Armco' steel fencing and the ground, leaving transparent rime on the stems of dried grass. Again, depositions of up to 3 cm have occurred where the airflow is strongest.

Fig. 3 shows thin transparent rime on twigs, becoming translucent where thicker accumulations occur at buds. Small trees are on a causeway leading to a narrow bridge over the M4 motorway, standing in an 'upslope' effect as the easterly airflow crosses the embankment.

Fig. 4 is the 'upslope' effect seen in rime depositions on a vertical twig — a close-up of Fig. 3 but viewed (with back light) to the north-east. Rime was transparent and 2–3 cm in length.

Transparent growth occurs when larger fog (or freezing drizzle) droplets strike the obstruction at temperatures just below 0 °C, allowing some 'spreading' of liquid before freezing occurs. Compare these photographs to those of hoar frost (*Meteorol Mag*, **121**, p. 165) which is translucent or opaque white because water vapour (or smaller droplets invisible to the naked eye) were frozen more rapidly on contacting low-level obstructions. The freezing of droplets, or the appearance of crystals, on the edges of blades of grass may challenge the exclusive theory of condensation (as in dew formation) when explaining the appearance of hoar frost crystals.

Perhaps initially hoar frost is 'deposited' by condensation and later the crystals grow by 'accretion' of droplets, similar in essence to rime formation?

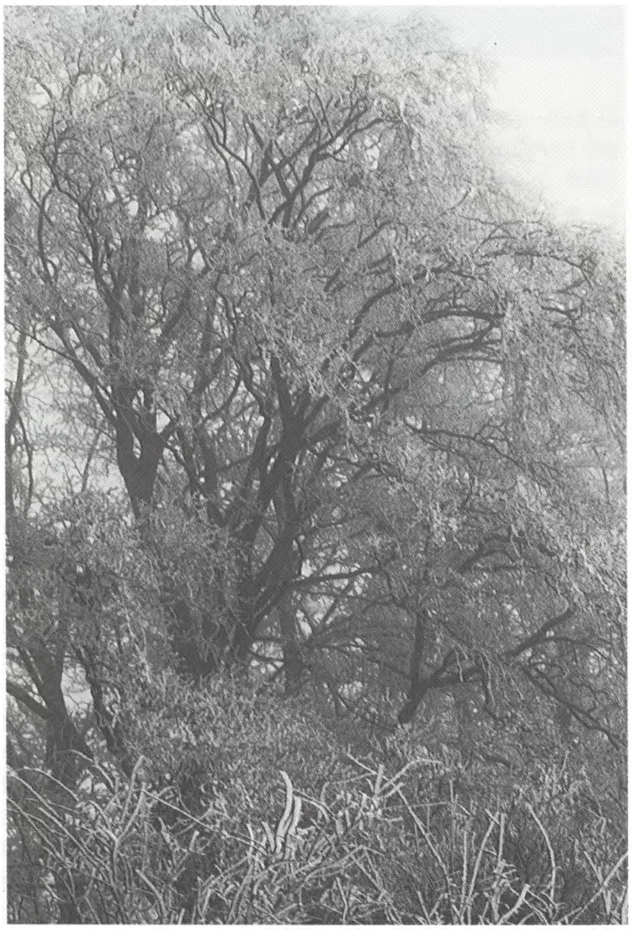

Figure 1. Translucent rime on beech trees on the Lambourn Downs at 1145 UTC.

Figure 2. Rime on grass at 1200 UTC.

Figure 3. Rime deposition on east-facing twigs at 1200 UTC.

Figure 4. Close-up view of Fig. 3.

Reviews

Mountain weather and climate (Second edition), by R.G. Barry. 57 mm × 240 mm, pp. xx+402, *illus.* London, Routledge, 1992. Price £60.00 (hardback), £18.99 (paperback), ISBN 0 415 07112 7, 0 415 07113 5.

It is over ten years since the first edition of this book was published and during that time there have been several important field programmes carried out in mountainous areas, for example, the ALPEX programme. A second edition of this admirable book was therefore long overdue.

The author is a Professor of Geography at the University of Colorado and has had an interest in the mountain world since childhood and his keenness comes through in the text.

Mountain weather and climate is a comprehensive account of our knowledge of the mountain environment. Much of the contents can only be found in scientific reports and magazines which may not be easily available to the general reader. The book is divided into seven sections, each describing a specific topic and accompanied by a detailed list of references, several pages long. The first section provides an introduction to the history of mountain meteorology from the early experiments on the effects of altitude on pressure at the Puy-de-Dôme in 1648 to the design of an Alpine experiment (ALPEX) as part of the Global Atmospheric Research Programme in the 1980s. This is followed by four sections giving more detail on the weather and climate of the mountains, a section on human bioclimatology, weather hazards and pollution and a final section on climatic change. The first five sections are very comprehensive but the final two are quite short. Personally I would have liked to have seen more in the penultimate section on the effects of the mountain environment on the human frame and the expansion of the subsection on weather hazards — avalanches in particular. At the end of the book, beside the general index, the author has provided an additional author index in response to reviews of the first edition.

A book of this kind is obviously expensive. However it is a pity that certain economies appear to have been made. All photographs are in black and white and sometimes are of poor contrast. For example, the first photograph in the book is of the Sonnblick observatory but it is difficult to identify the building against the black sky. Surely it would have been possible to print the photographs in colour. Surprisingly too there are only fifteen photographs throughout the book. This omission is compensated for by the large number of diagrams. In certain cases these could also have been improved by colour, for example, the figures on pages 113 and 114.

The book is really intended to be the definitive reference book on the subject and it performs this task admirably. The reviewer also found it interesting to read but I doubt if many will be of similar mind. The book's cost will mean that few will be willing to buy it in hardback. However, it is a book that any serious library should add to its collection and they should find it more often out on loan than mouldering on their shelves.

T.R. Spalding

Natural weather wisdom, by Uncle Offa (F. Hingston). 142 mm × 221 mm, pp. 160, *illus.* Hanley Swan, Worcester, Image Design and Print Ltd, 1991. Price £9.50. ISBN 185421 146 3.

Once a month since September 1990 Uncle Offa (a *nom de plume* of Frederick Hingston) has offered his natural weather wisdom to Saturday addicts of BBC Radio 4's farming programme, during the course of which he has built up not only a fully paid-up fan club but also, according to the fly of this book, 'an astonishingly high success rate foretelling the weather "according to the ancients" '. So how does he, and others professing similar expertise, do it? What signs do the experts use and which do they ignore? I approached this book in anticipation hoping to discover the secrets of using swallows, frog spawn and St. Swithin's Day for weather prediction in both the long and the short term, to be able to anticipate cold winters, sunny summers and late frosts and to become a sage in forecasting next year's crop yields. Was I satisfied; do I feel I have gained the knowledge basic to the countryman's lore? Well, no, not really. Uncle Offa retains a few of his secrets.

In fewer than 150 pages of widely spaced text, liberally interspersed with pleasant line drawings, Uncle Offa presents a large number of basic prediction rules, for short-, medium- and long-term forecasts. In the first chapter he deals with the 'Days of Prediction', days known to the Druids on which weather patterns for the forthcoming few weeks are set (*As the wind is on St. Michael's Day so 't' will be for three months*). St. Swithin's Day is the best known Day of Prediction. The moon's links to the weather are dealt with in chapter 2 (*it will be a wet month that has two full moons in it*). The next three chapters cover various 'Monthly signs', mainly sayings which relate to predictions of winter (*if in October the leaves still hold, the coming winter will be cold*) and, bearing in mind the country origins of this wisdom, summer (*a green Christmas brings a good harvest next year*). 'Signs of rain', or chapter 6, not only has "*Red sky at night....*" but also "*when eager bites the thirsty flea clouds and rain you'll surely see*". Birds (*in Richmondshire, some persons say that the breastbone of ducks after being cooked are observed to be dark-coloured before a severe winter and much lighter-coloured before a mild winter*) and miscellaneous matters (*when lobsters end the crawling season early, there will be an early winter*) form the subject matter of the next two chapters. Throughout all of this Uncle Offa identifies lores he considers either particularly reliable or probably questionable (I leave it to the reader to decide into which categories the above samples fall); in most cases, however, no comment is passed.

Finally, chapter 9 promises to put it all together. I started this chapter in expectation, I ended it in disappointment. I must learn to recognize those signs of local significance, although giving precedence to the Days of Prediction, then the phases of the moon and then the monthly signs. How do I put it all together? Concentration, observation and persistence. No cook book here, I'm afraid. But I was forewarned: 'forecasting by weather signs is a very local business and the signs are unlikely to give a true reading beyond the confines of the parish'.

And how accurate is it? Uncle Offa claims 85% (whatever that means). Tim Finney, editor of the BBC farming programme, admits in his introduction to the book to having created a deafening silence on air by asking this question. There is a book, *Red sky at night, shepherd's delight? Weather lore of the English countryside* (Sheba Books) by P.J. Marriott, in which some attempt is made to validate similar saws. I spot-checked a large number of Uncle Offa's sayings against verifications in Marriott's book. Results were mixed, with few of those sayings I checked having validity according to Marriott. I should also note that Duncan (*Weather*, **46**, 377–383) expresses caution about the value of long-term prediction saws from north of the border.

So, would any reader wish to make a careful analysis of Uncle Offa's radio predictions? I doubt it. The ways of the countryside have been handed down generation to generation and are part of our natural heritage. We would be the poorer were scientific incredulity to interpose upon this culture. This is not the only book on this subject, but it is one of the easier ones to read. Uncle Offa's fan club members will no doubt purchase it with glee. But how many of them will admit to making hard decisions on the basis of Uncle Offa's predictions?

M.S.J. Harrison

The engineering statistician's guide to continuous bivariate distributions, by T.P. Hutchinson and C.D.Lai. 143 mm × 206 mm, pp. xxii+246, *illus.* Adelaide, Rumsby Scientific Publishing. Price $A44.00, $US32.00. ISBN 0 646 024132.

As the title implies, Hutchinson and Lai's book is concerned with continuous bivariate distributions and the emphasis is very much on the distributions themselves and not on related matters such as statistical tests or statistical modelling. Bivariate distributions have a much greater range of possible forms than univariate distributions, and a large part of this book is devoted to presenting examples of this rich variety. The examples in the book arise in various ways such as mixing and compounding of simpler distributions, transformation of other multi-dimensional random variables, series expansions for the distribution functions, and the combination of a marginal distribution and a given set of conditional distributions. One of the recurring themes of the book is the idea of separating the study of the relationship between the two variables in question from the study of the univariate marginal distributions. This is achieved by separately transforming the two variables so that their marginal distributions have a standard form (usually uniform, normal or exponential). The book also contains discussions of reliability (e.g. how does the failure rate of a component depend on its age?) in the bivariate context, ways of measuring the degree of dependence and correlation between two variables, and techniques for generating pairs of random numbers with various distributions. Many applications are mentioned (including several meteorological examples) but in most cases these are dealt with rather briefly.

The book is to be welcomed as it brings together information which is not readily accessible outside of journal articles and conference proceedings. It has an extensive list of references which provide a good starting point for someone who wants to 'get into' the subject and it also has a good, if somewhat unusual, index (some of the sub items listed under one heading are so numerous that one loses track of which 'level' of the index one is looking through). However, the contents of the book give the impression of a loose collection of facts rather than a well-developed theory. Although this is partly a consequence of the nature of the subject, it is in places taken to the extreme. Many ideas are only given as references 'X did such and such while Y did so and so' and in a few places details of the figures and chapters from other books are listed. I also found the lack of theory in the book rather disappointing. In reading the book I found questions kept occurring to me to which the book provided no answers. For example, in discussing bivariate extreme-value distributions, the marginal distributions are transformed to a particular extreme-value form without discussing whether this preserves the bivariate extreme-value property. Also a number of concepts and distributions are presented with little probabilistic motivation.

The book is well produced with good quality text and mathematical typesetting. There are a number of errors and the meaning is not always as clear as one would like (for instance in discussing extreme-value distributions the authors say careful attention is needed as to whether one is dealing with maxima or minima — however they fail in most of their discussions to say which they are considering). However, these errors and lack of clarity are not a serious problem — it is usually possible with a little thought to see what's going on. There are also one or two oddities in the ordering of the book, with concepts being introduced after they have been used, but again these are not a significant hindrance to understanding.

Despite the above criticisms, the book fills a useful role. It would be an appropriate starting point for someone with a reasonable background in statistics who wishes to learn about different types of bivariate distribution.

D.J. Thomson

GUIDE TO AUTHORS

Content

Articles on all aspects of meteorology are welcomed, particularly those which describe results of research in applied meteorology or the development of practical forecasting techniques.

Preparation and submission of articles

Articles, which must be in English, should be typed, double-spaced with wide margins, on one side only of A4-size paper. Tables, references and figure captions should be typed separately. Spelling should conform to the preferred spelling in the *Concise Oxford Dictionary* (latest edition). Articles prepared on floppy disk (IBM-compatible) can be labour-saving, but only a print-out should be submitted in the first instance.

References should be made using the Harvard system (author/date) and full details should be given at the end of the text. If a document is unpublished, details must be given of the library where it may be seen. Documents which are not available to enquirers must not be referred to, except by 'personal communication'.

Tables should be numbered consecutively using roman numerals and provided with headings.

Mathematical notation should be written with extreme care. Particular care should be taken to differentiate between Greek letters and Roman letters for which they could be mistaken. Double subscripts and superscripts should be avoided, as they are difficult to typeset and read. Notation should be kept as simple as possible. Guidance is given in BS 1991: Part 1: 1976, and *Quantities, Units and Symbols* published by the Royal Society. SI units, or units approved by the World Meteorological Organization, should be used.

Articles for publication and all other communications for the Editor should be addressed to: The Chief Executive, Meteorological Office, London Road, Bracknell, Berkshire RG12 2SZ and marked 'For Meteorological Magazine'.

Illustrations

Diagrams must be drawn clearly, preferably in ink, and should not contain any unnecessary or irrelevant details. Explanatory text should not appear on the diagram itself but in the caption. Captions should be typed on a separate sheet of paper and should, as far as possible, explain the meanings of the diagrams without the reader having to refer to the text. The sequential numbering should correspond with the sequential referrals in the text.

Sharp monochrome photographs on glossy paper are preferred; colour prints are acceptable but the use of colour is at the Editor's discretion.

Copyright

Authors should identify the holder of the copyright for their work when they first submit contributions.

Free copies

Three free copies of the magazine (one for a book review) are provided for authors of articles published in it. Separate offprints for each article are not provided.

Contributions: It is requested that all communications to the Editor and books for review be addressed to the Chief Executive, Meteorological Office, London Road, Bracknell, Berkshire RG12 2SZ, and marked 'For *Meteorological Magazine*'. Contributors are asked to comply with the guidelines given in the *Guide to authors* (above). The responsibility for facts and opinions expressed in the signed articles and letters published in *Meteorological Magazine* rests with their respective authors.

Subscriptions: Annual subscription £36.00 including postage; individual copies £3.25 including postage. Applications for postal subscriptions should be made to HMSO, PO Box 276, London SW8 5DT; subscription enquiries 071–873 8499.

Back numbers: Full-size reprints of Vols 1–75 (1866–1940) are available from Johnson Reprint Co. Ltd, 24–28 Oval Road, London NW1 7DX. Complete volumes of *Meteorological Magazine* commencing with volume 54 are available on microfilm from University Microfilms International, 18 Bedford Row, London WC1R 4EJ. Information on microfiche issues is available from Kraus Microfiche, Rte 100, Milwood, NY 10546, USA.

September 1992

Vol. 121
No. 1442

Contents

ISBN 0-11-728987-6

Printed in the United Kingdom for HMSO Dd 291241, 9/92, C13, 543, 24503

The Meteorological Magazine

October 1992

International radar networking
Sea-breeze front on radar
Cloud-head image

HMSO

Met.O.1004 Vol. 121 No. 1443

First published 1992

HMSO

HMSO publications are available from:

HMSO Publications Centre
(Mail, fax and telephone orders only)
PO Box 276, London SW8 5DT
Telephone orders 071-873 9090
General enquiries 071-873 0011
(queuing system in operation for both numbers)
Fax orders 071-873 8200

HMSO Bookshops
49 High Holborn, London WC1V 6HB
071-873 0011 Fax 071-873 8200 (counter service only)
258 Broad Street, Birmingham B1 2HE
021-643 3740 Fax 021-643 6510
Southey House, 33 Wine Street, Bristol BS1 2BQ
0272 264306 Fax 0272 294515
9-21 Princess Street, Manchester M60 8AS
061-834 7201 Fax 061-833 0634
16 Arthur Street, Belfast BT1 4GD
0232 238451 Fax 0232 235401
71 Lothian Road, Edinburgh EH3 9AZ
031-228 4181 Fax 031-229 2734

HMSO's Accredited Agents
(see Yellow Pages)
and through good booksellers

The
Meteorological
Magazine

October 1992
Vol. 121 No. 1443

551.501.81:551.501.9

International radar networking

C.G. Collier
Meteorological Office, Bracknell

I am going to talk about International Radar Networking, the COST-73 project, which ran from 1986 to 1991. I was Chairman of the Management Committee responsible for organizing parcels of work. I notice Colin Fair at the back and he takes a lot of responsibility for much of the work that was actually done by the United Kingdom. What I want to do is to outline the programme for this research project, and then give illustrations of some the work that has actually been undertaken. Before I do that I will begin by explaining what the COST programme is, because some of you may not be familiar with it.

COST is a European Commission programme Co-Operation in Science and Technology, and it was a programme established in 1970. In fact we also celebrated, in November 1991, the joining to that programme of some Eastern European countries. Many subjects other than meteorology, for example materials and social sciences, are all part of the COST programme. Meteorology was included from the beginning. Indeed, perhaps the greatest achievement of COST (you possibly might not be aware) was that it led directly to the formation of the European Centre for Medium-range Weather Forecasts from COST-70. It has had some further successes. You can judge whether it has led to improvements in the surface observational database in part from what I am going to say. However, the programme has also been concerned with buoys, with radiosondes, and now wind profilers. The United Kingdom have the Vice Chairmanship of COST-74, the wind profiler project. The Met. Office, rightly or wrongly, has taken part in several COST projects over a very large number of years. What is the strength of COST? Well the informality and the fact that there is no money (laughter), some might say it is a talking shop, but in reality it is an enabling mechanism for getting like-minded scientists and engineers together with industry. This is what COST is about; encouraging European industry to transfer technology to commercial applications. Although the strength of COST is its informality, it does depend upon national programmes. Without the goodwill of the participants nothing would actually be done in COST.

Let us begin then by trying to put radar network developments within Europe into context. Roughly in 1970 Europe, USA, east and western Europe and Japan were more or less at the same position in terms of radar networking, not in terms of radar meteorological science, but certainly in terms of networking. Many countries had networks of analogue radars, but from that point on developments started to diversify. The Japanese started to digitize all their radars, and being Japanese they did this almost instantaneously, such that they now have the densest radar network in the world, and have actually gone further and Dopplerized some of the radars. I'll say a little more about Doppler radar later, but basically a Doppler radar, as well as measuring precipitation, measures wind speed and direction (direction with a little bit of ingenuity). Eastern Europe is more or less in the same position now as it was in 1970. The eastern European countries still have a very dense network of analogue radars, and many of these are actually dual frequency radars which is something we don't have many of in the west. These radars operate at two frequencies (usually X and S band), and that has provided some interesting science although most of the science has been carried out using analogue data. The situation may change very rapidly because of their involvement in COST, certainly Hungary, Czechoslovakia and Poland, in particular, are actually seeking now to modernize their National Meteorological Services and, providing money can be found, action will be taken. The money will obviously limit what can actually be done.

In America things began to take off rather slowly from 1970. There was a project known as D-RADEX concerned with digitizing an analogue radar and trying to measure precipitation quantitatively. It actually paralleled fairly closely the work which some of you may have heard of, the Dee Weather Radar Project at the beginning of the 1970s which was carried out in North Wales, and in which the Met. Office played a leading role. A further project known as RADAP extended the digitization programme in the USA. These were really projects concerned with one or two radars, and looked at how to digitize them, and how to develop them for operational use. However, there was no very strong radar networking programme until work began on to the specification of the NEXRAD (NEXt generation RADar) system and its associated communications and display system AWIPS-90. This project aims to establish perhaps the most sophisticated radar that has yet been deployed, to be used by operational meteorologists. It is a Doppler radar, a high-powered system, and I will return to this subject later in my talk to give an indication, as to the type of performance these systems can have. However, what you should remember is that they are of an order 2 or 3 times as expensive as the kind of Doppler radars that we are familiar with in Europe.

Coming back to Europe, several European countries by 1970 had established radar programmes. I have already mentioned the Dee Weather Radar Project in the United Kingdom which was concerned with looking at whether you could measure precipitation with a digital radar. There was similar work going on in Switzerland and similar work starting in Sweden. In a sense, these projects were brought together by COST-72, which was the forerunner of the present project, concerned with investigating whether you could actually make quantitatively useful measurements with a digital radar. As we will see shortly, COST-72, certainly in the rest of Europe, although perhaps not in the United Kingdom, stimulated the rapid deployment of digital radars, and this trend has continued during COST-73. COST-73 has led to specifications for new technology projects, and proposals for operational implementation of international exchanges of radar data, so it could be argued that the COST programme has been the catalyst for rapid developments in operational radar networking in Europe. Just to follow that up, this is the actual deployment of radars that took place from 1970 to 1995 (Fig. 1). In 1970 there was a single digital weather radar in Europe, and that was actually located in northern Sweden. It was a military radar, and it can be seen from the figure that in the next 20 years there was an almost exponential increase in the deployment of digital radars

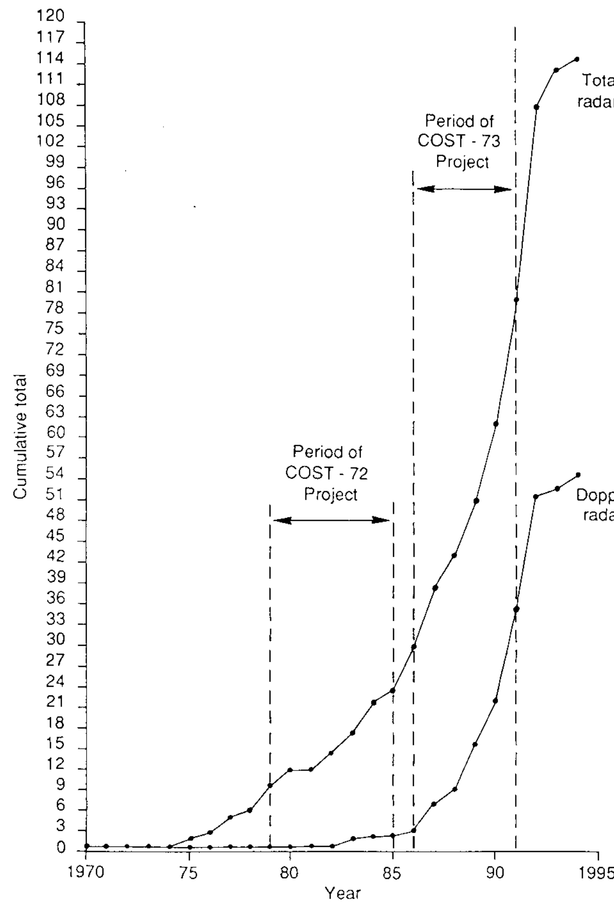

Figure 1. Radar deployment in European COST countries.

in Europe, spanned by the COST-72 and then COST-73 projects. In fact almost parallel to that deployment, starting in round about the early 1980s, a similar deployment of Doppler radars began, although that seems to have peaked for the time being. Doppler radars measure winds as well as precipitation. You can see that now there are approaching 100 digital radars in western Europe of which about a third are Doppler radars.

So what has COST-73, done and how was it structured? Well first of all COST-73 involves pretty well every country in western Europe and included as a full participant the European Commission itself. It involved all these countries and they pooled their expertise through the management committee of the project. The work, which I'll talk about in detail in a second, was tackled in two ways: offline studies involving asking all these countries how they were processing data and what were their plans, how we might use their data in radar networks, and real-time sub-projects. The aim was to demonstrate if data could be actually transferred between countries, and whether it was possible to use European-wide data in ways which were useful. The work was roughly partitioned in that way.

The work covered all aspects of radar networking, starting with the radar systems themselves, the characteristics of the radar hardware, what they could and couldn't do, and, most importantly, what radar systems were just round the corner that might actually produce some new information. Various work was carried out trying to detail (really for those countries that were just starting off in networking) how to write a specification for radar network software. Clearly European industry was involved in this programme as members of the Management Committee; representatives from the Ericsson radar company in Sweden, Siemens Plessey in the United Kingdom, Gematronik in Germany, SMA in Italy and various software houses have been involved, and one had to write this type of specification to a rather high level. Also, specifications for display systems for radar network data were reviewed. Underpinning most of the work was analysis of data transmission methods and standardization of codes. Data transmission underpins so much of radar networking, so it is a very important topic that had to be addressed. We looked at bilateral data exchanges. These are already beginning to move ahead. The United Kingdom has exchanged data with the Republic of Ireland for some years now, between the Shannon radar and Bracknell. Likewise France exchanges data with Switzerland. During the project some (if you like) 'rules of play' for these exchanges were partially developed, but I will come back to this later. It is necessary to look at actually who wants all the data from other countries. COST-73 examined the requirements, data archiving, how to sensibly exchange data in real time, and how to operate Doppler radars within a conventional radar network because some countries have Doppler radar and some countries don't. Finally, and this caused untold problems, it was actually stated in our terms of reference that we must look at a *modus operandi* for a co-ordinated European Weather Radar Network. This led to some political difficulties.

What were the kinds of real-time project that we looked at? A composite image using data from several countries was produced in COST-72, and this work was carried on in COST-73 with some improvements and extensions to include other radar data. We looked at whether you could use radar data generally, and specifically COST data, for detecting severe weather and I'll touch on these severe weather algorithms a little later. An experiment was carried out both in the United Kingdom, at London Weather Centre later Aberdeen, and in the Netherlands to try to assess the utility of COST images to forecasters responsible for forecasting in maritime areas in the North Sea. I will touch on the results later. COST-73 began in the post-Chernobyl era, and of course here in the United Kingdom in particular we led the way in using wide area radar data to say something about where radioactivity was going to be deposited.

I have already shown the rapid growth in radars in Europe (Fig. 1) but how does this transfer into actual radar distributions in all countries. Have all countries got the same densities of radars? Well of course the answer is 'no'. Fig. 2 shows the present coverage from weather radars in Europe where the shading represents the lowest radar beam that is used, really the coverage where the radar beam is below 1½ kilometres above the surface. You can see that there is a very dense network of radars being installed now in Spain, for example, and really throughout the whole of northern Europe there is a very dense radar network. There were, before the current troubles in Yugoslavia, a lot of radars in Croatia and we think some of them have been destroyed. So this is a little bit out of date. The square frame here is the area over which the United Kingdom on behalf of COST produced European radar composites beginning with the COST-72 project and carrying on right through COST-73. These images were distributed to a number of countries including Finland. The open areas in Fig. 2 show radars which are planned, but not yet installed, although firm plans have been made with funds being committed. No radars are shown over Poland, Czechoslovakia, Romania and other Eastern European countries. In fact there are a lot of radars in these countries but they are analogue systems, as I have already mentioned. It is likely that radar coverage over the next few years will increase quite significantly. Fig. 3 shows the radar installation at Hohenpeissenberg in Bavaria, complete with Christmas tree, to prove that the United Kingdom doesn't have any prerogative on radar design.

Besides the conventional type of radar, Doppler radars can detect motion towards the radar and away from the radar within a range of plus and minus 48 metres per second. This information can be interpreted by making certain assumptions to give some information about the actual motion as opposed to the radial motion towards and away from the radar. Fig. 4 shows an example of the radial motion display. This is the actual type of data that one gets out of these radars. The colours represent the motion towards the radar and away from the radar so the blue colours are, I think, towards the radar and the red ones are away from it, a convention which they happen to use in Sweden as this is a Swedish radar. We in the United Kingdom are getting such a radar. It'll probably be installed in south-west England at Cobbacombe. Fig. 5 shows the kind of information that we can derive from the types of image shown in Fig. 4. Height against time is plotted, and the contours are actual wind speed. In a single Doppler radar you really don't get the three-dimensional motion vector, so it may be appropriate to interpret these data in the context of a numerical model. In Sweden they have actually started to do this, and they can produce measurements of wind velocity, but only where there is precipitation, because these radars in Europe are of low power and in general do not make measurements in the clear air. In the USA with their NEXRAD systems, which are very high powered systems, and they can actually make measurements in the clear air. So NEXRAD will be able to observe clear air turbulence for example, and a whole variety of phenomena which

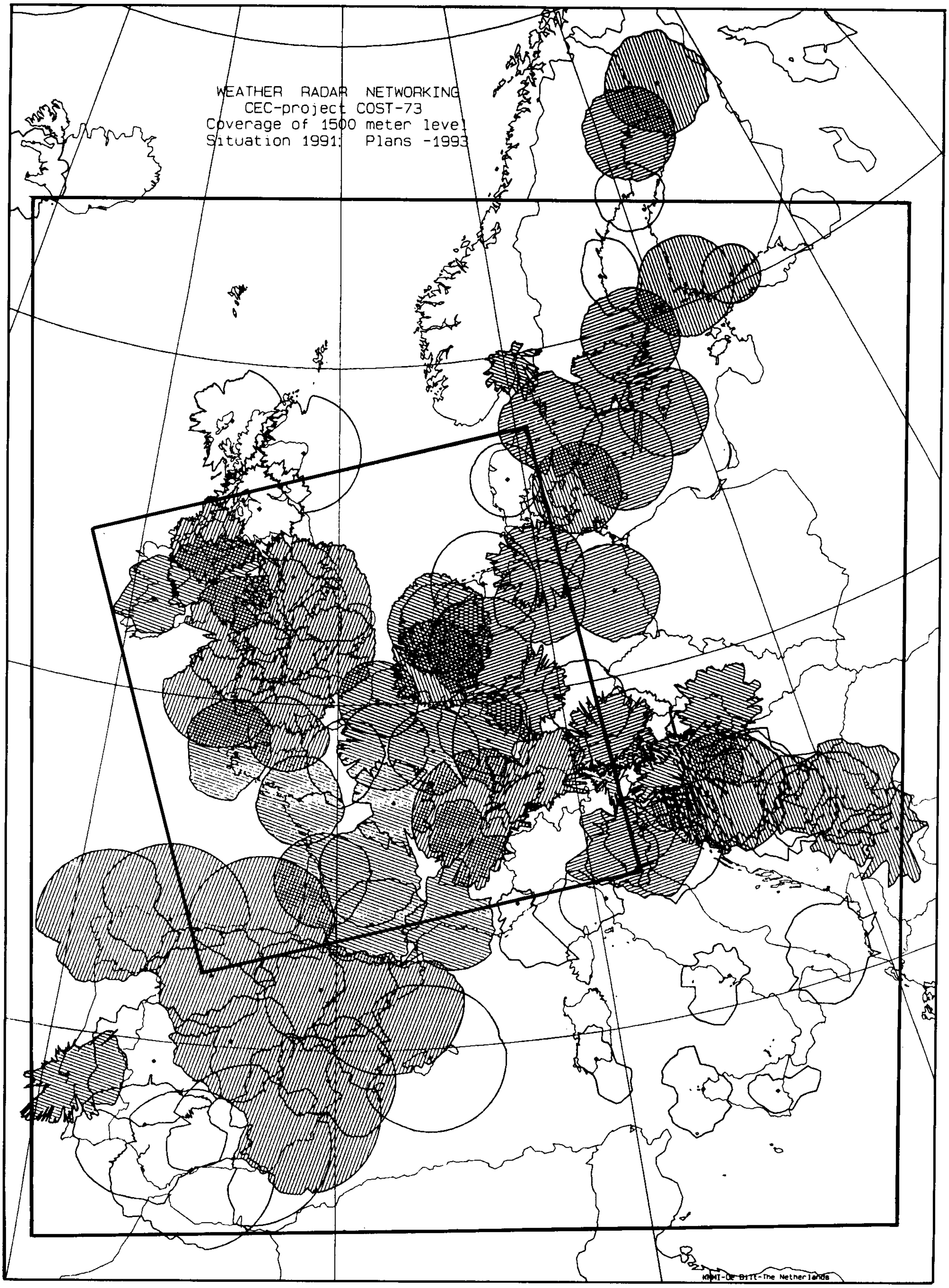

Figure 2. Radar coverage in 1991, with plans to 1993 unshaded.

Figure 3. Radar installation at Hohenpeissenberg, Germany.

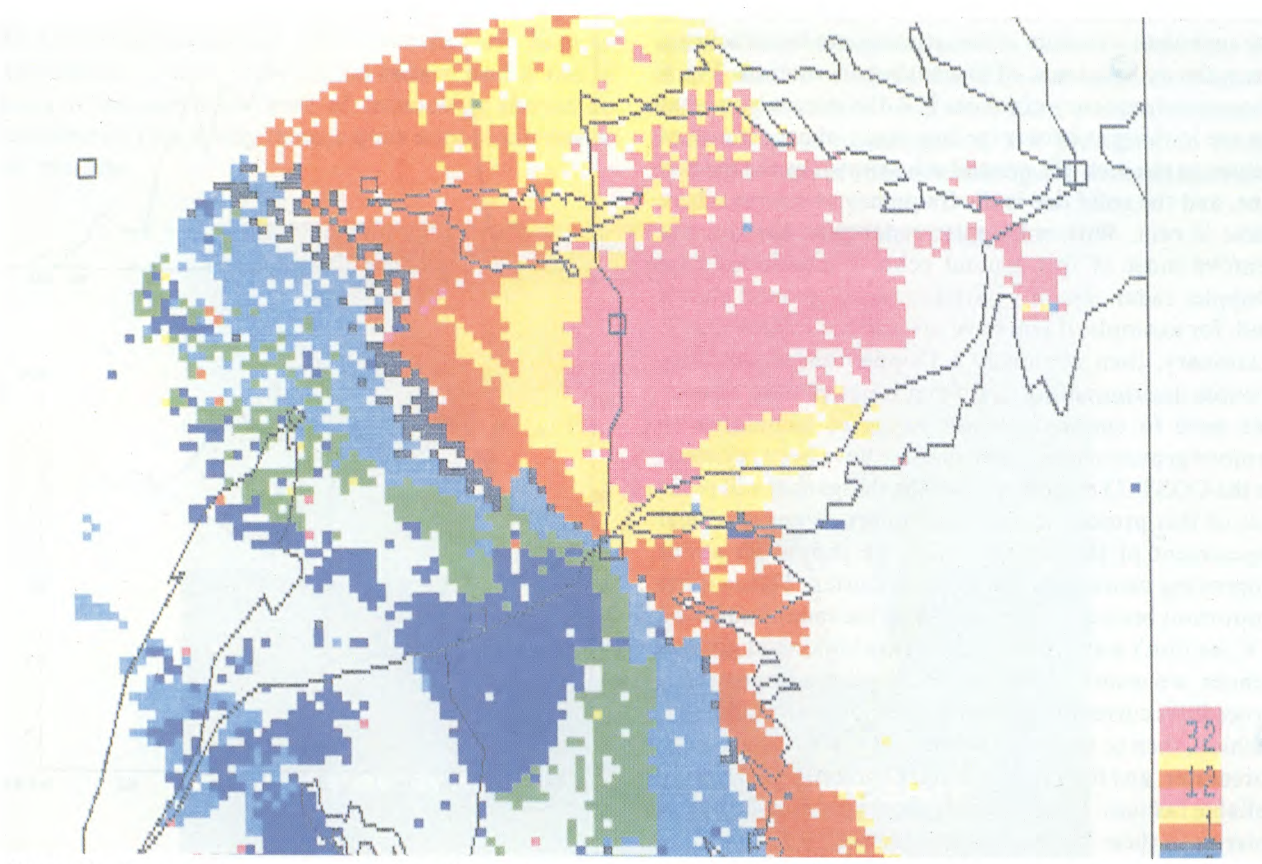

Figure 4. Example of radial motion displayed from a Doppler radar located at Norrköping, Sweden. (Courtesy of Ericsson Radio Ltd.)

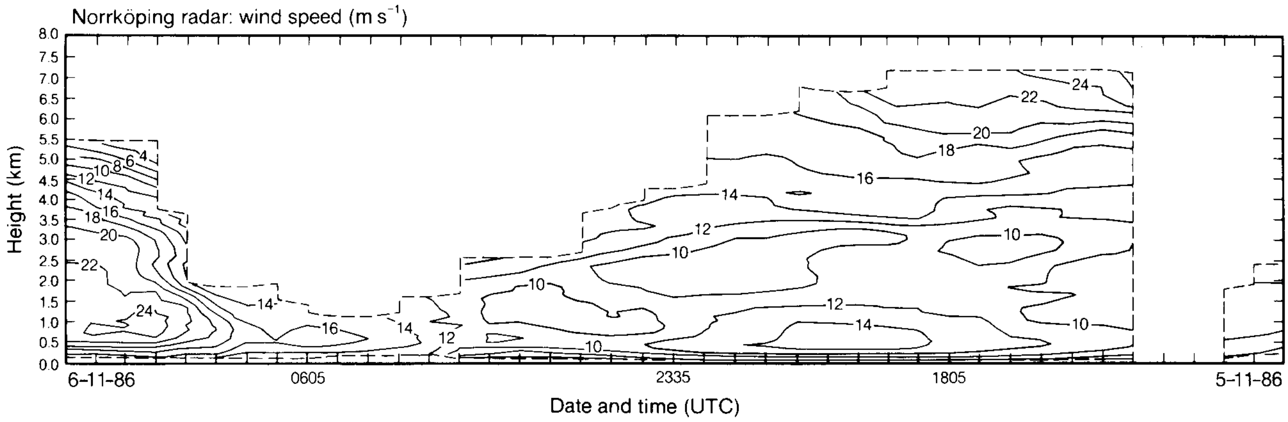

Figure 5. Example of wind data (m s^{-1}) derived from displays such as Fig. 4. (Courtesy of SMHI.)

perhaps we won't be able to detect except at very close range. In the United Kingdom we really need to investigate what we can and can't see with low-power Doppler radars. So what is the benefit of having Doppler radar if you cannot make measurements in clear air? Well I have mentioned the wind measurements where there is precipitation, and you could also use these systems to partially suppress ground clutter. Ground clutter, echoes produced where the radar beam hits the ground, varies only slowly in time, so if you can measure the motion of the echo fields then you can discriminate between moving rain and the not-moving ground echoes. However, it is not quite as easy as I have implied. In addition, Doppler radars also make measurements of the turbulent structure of the atmosphere by measuring the velocity spectrum of the turbulent motion. Fig. 6 shows the frequency of echoes in 2 dbz intervals so what we are looking at here is the frequency of occurrence of echoes in the area of a ground echo shown by the dashed line, and the solid line is the frequency of echoes where there is rain. With a Doppler radar you can actually remove most of this ground echo. I mentioned that Doppler radar can only partially cancel ground clutter and, for example, if you have orographic rainfall that is stationary, then obviously a Doppler radar can have trouble discriminating that from other ground echoes. We need to employ a whole range of techniques to remove ground clutter, and all these have been reviewed in the COST-73 project. One of the things that will come out of this project, in the final report, is some critical assessment of the way in which we should go about improving cancellation of ground clutter. This is quite important because when we look at the radar images on TV, we don't want to be confused by looking at ground echoes, we want to look at rain. If we can improve the procedures currently employed, perhaps in an automated fashion, then so much the better — it takes a load off the forecaster, and hopefully provides corrections in a more reliable fashion. Consequently there is a large degree of interest in these kinds of technique.

Still on the radar systems, there are also newer advanced radar systems. Dual frequency radars exist in eastern Europe, but there are all sorts of other radars,

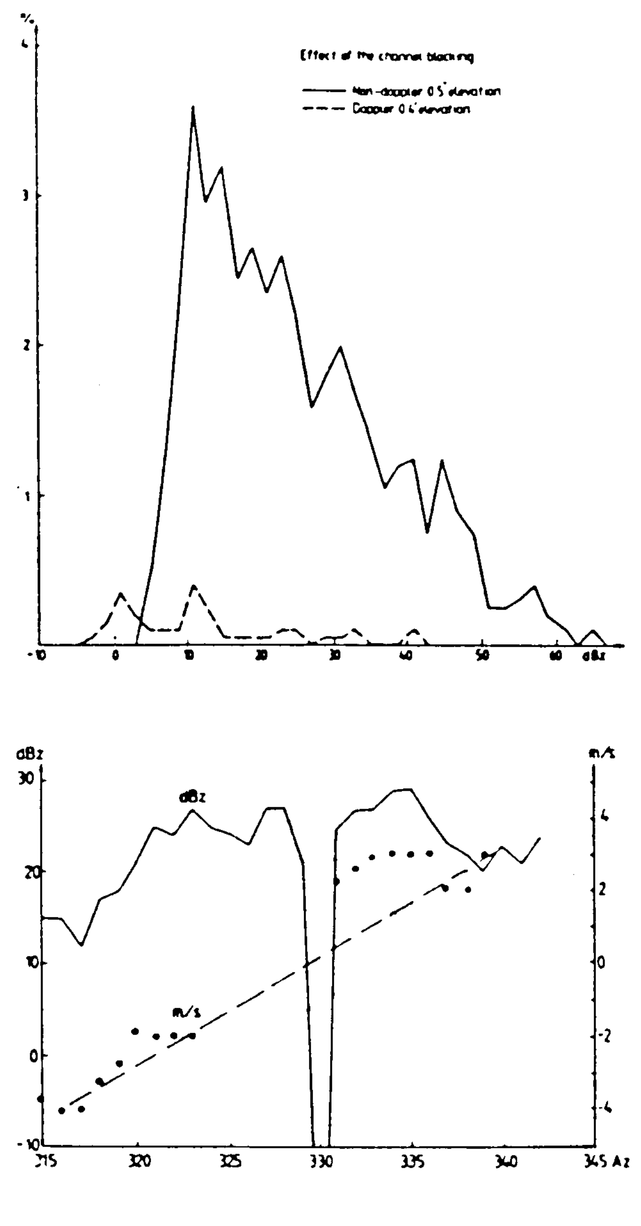

Figure 6. Frequencies of echoes per 2 dBz interval in the vicinity of a ground echo. The area of investigation was azimuth 220–230° with range 30–55 km. The antenna elevation is 0.5°.

including dual polarization radar. You may have heard of the Chilbolton radar which allows measurements to be made of the actual characteristics of the hydrometeors we are looking at, using parameters based upon polarization and phase differences in the radar beam generated by rapid electronic switching between circuitry. Electronic scanning radar is also a possibility where instead of having the conventional metal dish, you actually have a phased electronic array to produce the beam. COST-73 has looked at the range of radar types.

The electronic scanning radar is not brand new technology. Most defence radars are actually electronic scanning radars. Fig. 7 is one such device which detects little metal objects flying at high speeds and low elevation. It is the MESAR radar produced by Siemens Plessey Radar Ltd, and the figure shows the phased array that is normally behind a cover. The whole assembly rotates mechanically around a vertical axis, but scanning in the vertical using phased array technology. This could be adapted for meteorological use, and provide three-dimensional measurements of the atmosphere instantaneously. This is attractive, but the problem is, of course, the development cost. Investigations are beginning with several companies to look in detail as to whether this technology can be transferred to the civil sector at a reasonable cost. Why are we interested in all these fancy radars? Well I mentioned earlier that the technology that we are presently using is 25 years or so old. In another 5 years the United Kingdom and other countries will have to start replacing their older digital radars, and if this is going to happen what kind of technology should be considered? This is why there is quite a lot of interest at the moment.

Moving from the radar sensor itself, COST-73 has been responsible for intercomparing the characteristics of all the radar networks from all western European countries. Table I is an example of the comparisons which have been produced. This example shows the average radar area and the beam size which are used in the radar network for particular countries. In the United Kingdom the area per radar in thousands of square kilometres is the lowest of all the radar networks in western Europe so we have the most dense network. However, you can see that Spain in 1989 has a coverage of 500 000 square kilometres per radar which drops rapidly to 33 000 in the next year or so. There are a whole range of items including comparisons of the measurements of precipitation, who does what and how they do it. All this information is contained in the COST-73 Final Report.

Turning to severe-weather definitions, it is actually amazing how different the definitions of severe weather are in the different countries around Europe. Table II gives a few: Austria, Norway, Spain, and you can see that the one common thread that goes through them all is thunderstorms which perhaps cause the most serious problems: heavy rainfall, hail and so on. Nevertheless there is a whole range of definitions which are used in different countries. In addition, severe weather algorithms for radar have been reviewed. Just to illustrate some of these algorithms, Fig. 8 shows Russian work giving height as a function of the reflectivity measured by the radar. These reflectivity profiles in the vertical may be interpreted in terms of the different types of weather including thunderstorms, very deep precipitation, and small cumulus clouds giving low precipitation rates. Scientists such as Albert Waldvogel in Switzerland have

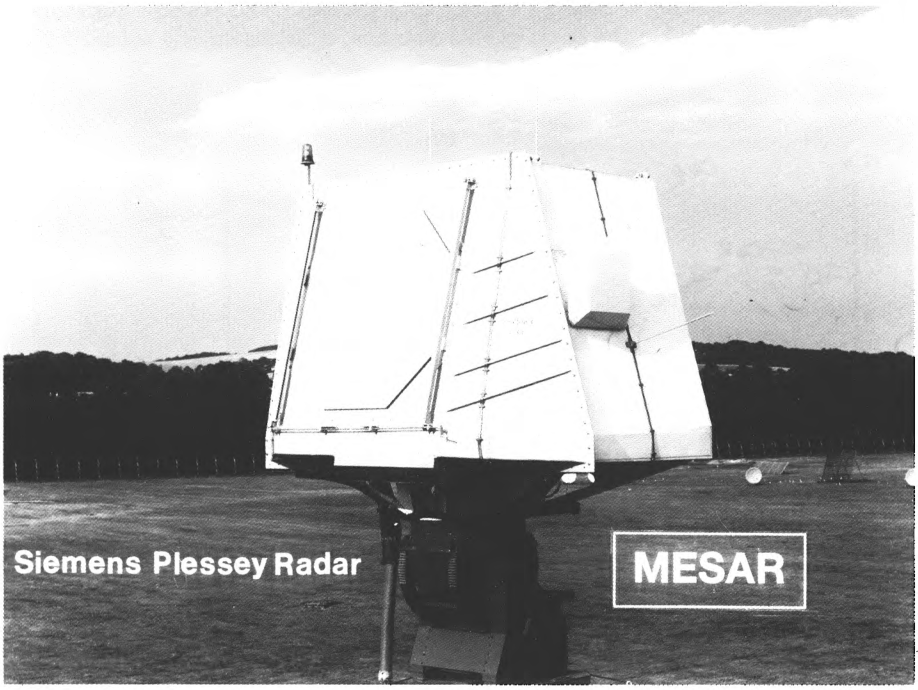

Figure 7. An electronic scanning radar without its cover. (Courtesy of Siemens Plessey Radar Ltd.)

Table I. Answers and calculated results from the questionnaire of COST-73 existing and planned radars

Average Area and Beam Size

Country	No. of radars		Area per radar 1 000 km^2		Average range km		Average beam dia. [3dB] km	
	1989	1993	1989	1993	1989	1993	1989	1993
Austria	3	4	28	22	92	80	1.8	1.5
Belgium	1		50		121		2.1	
Denmark	1		43		113		1.8	
Finland	3		112		83		1.6	
France	11		50		121		3.0	
Germany	3	10	183	25	157	86	3.0	1.7
Ireland	1		70		145		2.5	
Italy	2	15	162	22	217	79	3.2	1.2
Netherlands	2		20		77		1.5	
Norway	1		386		340		5.0	
Portugal	1		93		166		3.2	
Spain	1	15	500	33	387	100	6.1	1.6
Sweden	3		133		200		3.0	
Switzerland	2	3	20	13	77	63	1.5	1.2
United Kingdom	8	13	13	8	61	48	1.1	0.S
Yugoslavia	4	13	64	10	138	100	2.4	1.8*

* 3.5 km for XS band radars

Note:

The table gives the number, area per radar and average distance and horizontal extension of the radar beam for existing and planned radars as reported in COST 73. The average distance from the radar is defined as the true average distance to the closest radar (all radars equally spaced) multiplied by 1.5 because of non-regular spacing of radars (= 0.54 SQRT (Area)). The average horizontal extension of the radar beam is the extension of the beam at this distance, considering the actual 3 dB width of the beam as indicated by each country.

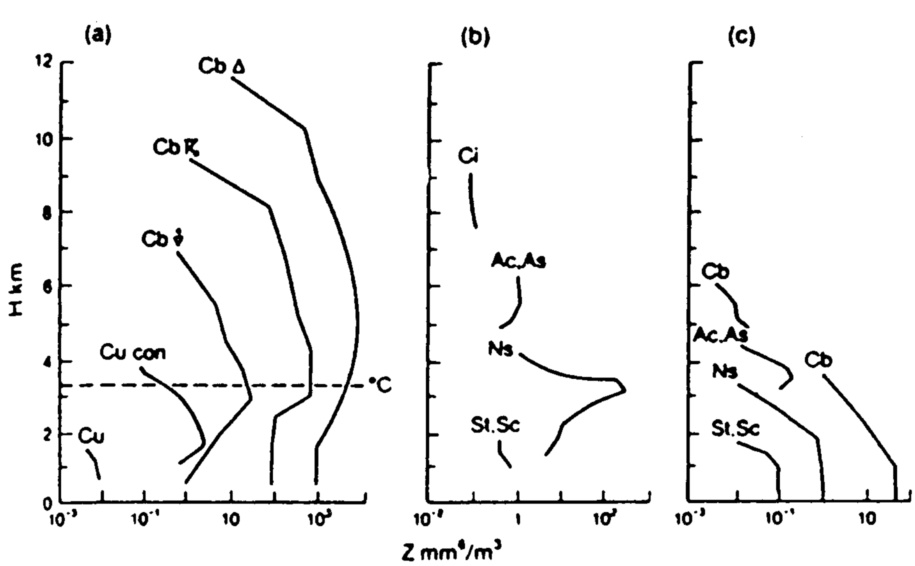

Figure 8. Vertical reflectivity profiles related to severe weather occurrence and cloud type.

Table I. (continued)

Receiver and Range Correction

Country	Receiver lin range dB	Receiver lin toler. dB	Receiver log range dB	Receiver log toler. dB	from km	to km	Range correction log dB/dek	Range correction lin dB/km
Austria			80	+2/-0	5 (s)	230	20	0.017
Belgium	35	0.5	75	0.5	5 (s)	240	20	
Denmark	92	?	?	?	2	240		
Finland			70	?	1	300	20	0.015
France			70	+/-1	5 (hs)	100		
Germany			95	+/-0.5	1 (f)	230	20	0.016
Ireland			64	+/-0.5	4 (s)	200	20	
Italy	45	+/-1	>80	+/-1	1 (s)	400	20	0.015
Netherlands			80	1.5	2 (s)	128	20	0.005
Norway	87	0.4	85	0.4	1 (s)	240	20	0.015
Portugal			80	0.5	4 (s)	200	20	0.015
Spain	86	0.4	86	0.4	1 (s)	240	20	0.016
Sweden	85		85		1 (h)	480		0.016
Switzerland			90	+/-0.5	5 (s)	230	28	0.017
United Kingdom			70	1.0	5 (hs)	210	20	0.017
Yugoslavia	90	1	85	+/-0.5	5 (s)	200	20	0

Note:

Range correction made in software (s), hardware (h) and/or in the firmware (f) (read-only memory).

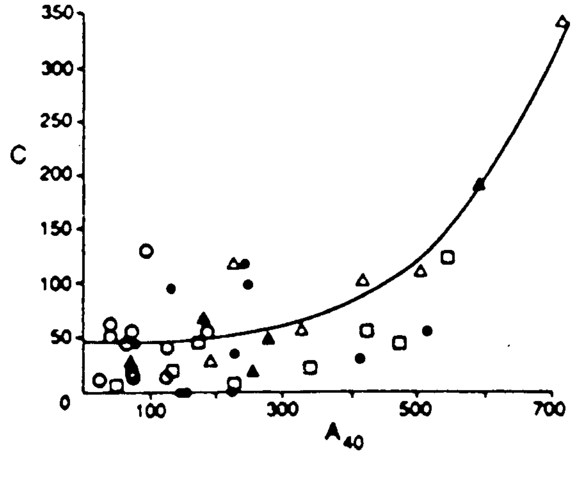

Figure 9. The peak radiated field for five storms as a function of the 40 dbz contour.

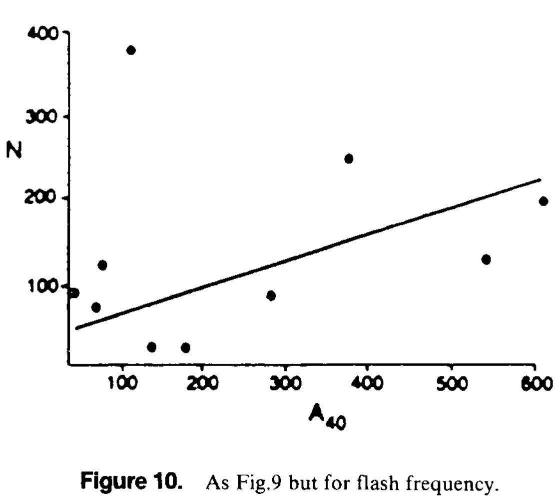

Figure 10. As Fig.9 but for flash frequency.

Table II. Examples of some severe weather definitions

AUSTRIA
- Thundersorms
- Thunderstorms with hail
- Intense snowfall (6–12 hours)

NORWAY
- Precipitation 3–4 mm/10 minutes in north
  7–8 mm/10 minutes in south
  6–11 mm/30 minutes
  Freezing > 0.5 mm h^{-1}
- Heavy snowfall 2 cm h^{-1} (4–5 mm h^{-1})
  First snowfall in autumn — 0.5 cm
- Wind gusts > 25 m s^{-1} inland
  > 28–39 m s^{-1} coastal areas

SPAIN
- Heavy rain $\geqslant 50$ mm in 12 hours or $\geqslant 15$ mm h^{-1}
- Strong winds > 25 kn
- Visibility < 100 m
- Snow
- Mountain waves
- Strong wind shear
- Hail

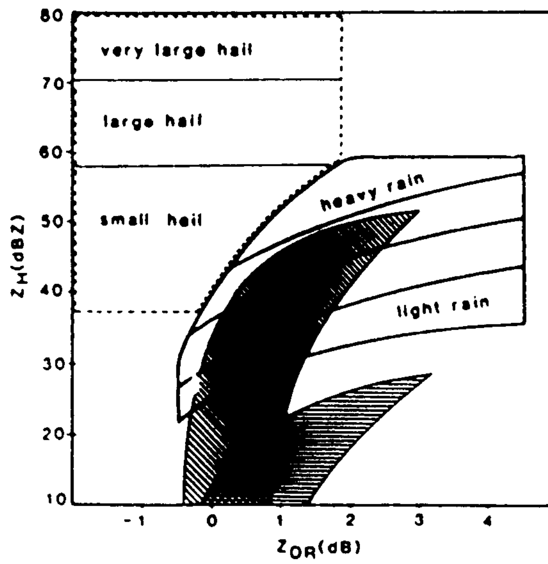

Figure 11. Reflectivity and differential reflectivity fields as measured by the Chilbolton radar.

actually come up with little algorithms relating radar reflectivity to the occurrence of hail. If the 45 dbz contour exceeds the height of 0 °C isotherm by more than 1½ kilometres then there is a high probability that hail occurs. In Figs 9 and 10 is shown another type of algorithm which is beginning to be used to detect lightning from radar information. The peak radiative field of lightning is shown as a function of the area of the 40 db contour. It is evident from the scatter that this relationship is not very reliable, but nevertheless just by looking at the radar image you can get a probability that the particular storm you are looking at is actually producing lightning. We don't use any of these in the Met. Office at the present time, and this is rather a pity considering the quality of the radar pictures we have.

If we move on to Doppler radar, then there are a whole range of new algorithms to look at. A relationship exists between maximum hail size and the divergent flow which you can measure from Doppler radar, and there appears to be a pretty good relationship between these two quantities so that one can say something about hail size. Hail detection is perhaps not a major problem in the United Kingdom, but elsewhere in southern Europe it is. Also, by measuring the low-level flow you can make some statement about whether you are likely to get a tornado or not. A debate at the moment in Europe, particularly in Spain, is whether you can actually make the necessary measurements with these low-power radars that we have in Europe, because much of the published research work has been carried out in the USA with radars which are very powerful. Those in southern Europe in particular, believe they have a serious problem with downbursts, tornadoes and things like that, and they are particularly concerned with these types of system.

Finally, if there is access to a dual polarization radar, it may be possible to say something about the differences in the radar echoes when heavy rain, hail or other severe weather types are present. Fig. 11 shows reflectivity as a function of differential reflectivity, ZDR. We haven't time to go into the definition of ZDR, but with this kind of radar you can say something about precipitation type.

So that is the radar sensor; turning now to the radar network itself. Fig. 12 is an example of a fully configured data network, and I think if you look at the figure you will see that system elements are pretty well backed up. Imagine a radar being located at each of the nodes, then there is dual communication between each site. You can establish a particular network architecture based around a computing system where the network centre is going to be. This is similar to what we have in the Met. Office. We have a local area network, we have various computers hanging off it. In the COST-73 project we have looked at these general architectures for radar networks, and then compared them against the architecture used in practice. Fig. 13 shows an architecture which is increasingly being used by quite a number of countries. You can see that it is somewhat different from the ideal structure shown in Fig. 12. Mostly the telecommunications of the sites are not backed up, cost dictating that there is a single communication link between the radar and the central compositing centre. If for comparison we just look at our own network in the United Kingdom the telecommunications configuration is a star arrangement, very similar to that shown in

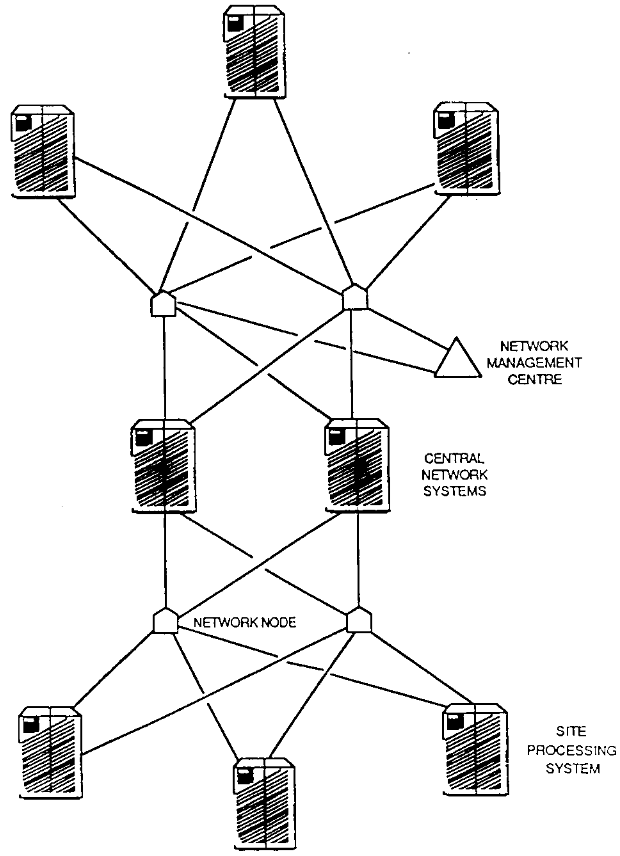

Figure 12. A fully configured data network.

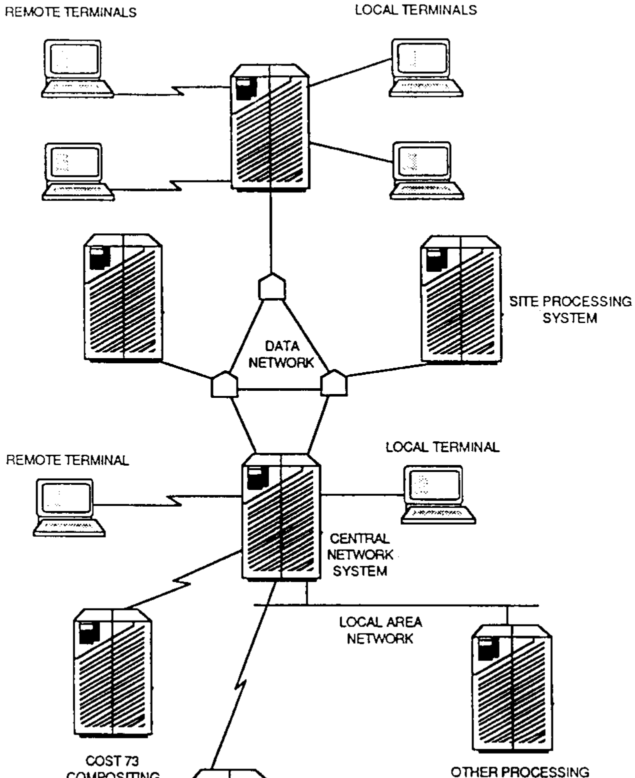

Figure 13. A typical national weather radar network system with international connections.

Fig. 13, with all the radars sending their data to Bracknell. This kind of structure is being reproduced throughout Europe. Germany, for example, has established a network very similar to this. Most countries cannot afford to have duplicate communication links.

So what has COST-73 done for communications in radar networks? A considerable amount of effort, led by a working group chaired by France, has modified WMO FM 94 BUFR code to cope with radar data, and the modifications have been accepted by WMO. We are in a position now to use this standard WMO code to exchange radar data between countries. Although I have mentioned this quickly, this work represents an enormous amount of effort lasting just about most of the 5 years of the COST-73 project.

In order to try to investigate some of the communication problems likely to be encountered in radar networks, the Project utilized the WMO GTS. Experiments were carried out to exchange some data between centres on an experimental basis. Largely through the good offices of the Met. Office Telecommunication Department we were able to use the GTS on an experimental basis using existing codes (ITA5 not BUFR) to transfer data between Bracknell and Finland, Bracknell and Paris, Bracknell and the Netherlands, and Bracknell and Ireland. This led to investigations of data compression techniques. A comparison of various compression algorithms including BUFR, because BUFR code itself produces a degree of compression of the data, has been looked at within the Project. I am bound to tell you that no definite conclusion has been arrived at about which compression algorithm is best, but we do at least have some objective information on performance.

Finally on communications some of you may have noticed that we did all of a sudden have a satellite dish appear on the roof of the Richardson Wing. This is a terminal which in theory would have allowed the transfer of radar data via the Olympus satellite, and between Austria (Graz) and Bracknell on an experimental basis. The equipment was borrowed from RSRE Defford with the help of ESA Estec. Everything was set up all ready to go, but the satellite developed problems on the day of the first full test. Recently (March 1992) the satellite has come back, and tests have resumed.

If we move from the communications to the central compositing. What do meteorologists do when they have data from a number radars? Table III shows an example of the range of central processing carried out at network centres in western Europe. You can see that, for example, 19% of countries send the raw data to the compositing centre then remap them to produce a composite image. Here, remapping is a transformation from polar to Cartesian coordinates, while 81% of the radar installations in Europe carry out remapping at the radar site, 57% of these networks use fixed boundaries like we do in the Met. Office. Use of fixed boundaries means that if a radar is lost, then the boundaries change.

Table III. Combination of data from different radars

(a) Change of grid and projection compared with a single radar

Country	new grid size km	method comb.	project type	method reproj.	before merging?	changed where?	merged where?
Austria	2	=	rectang.	=	=	=	display
Belgium							
Denmark							
Finland	7.1	max: 9	psp	table	during	centre	centre
France	3	=	psp	=	=	=	centre
Germany	4	max: 4	psp 10E	=	after	centre	centre
Ireland							
Italy							
Netherl.	2.4	=	psp	=	=	=	centre
Norway							
Portugal							
Spain	4	av. rain	lambert	=	before	radar	centre
Sweden	4	max: 4	psp 14E	=	during	centre	centre
Switzerl.	2	=	rectang.	=	=	=	centre
U.K.	5	av. rain	trv.merc.	=	before	radar	centre
Yugoslavia	2	=	rectang.	=	=	=	centre

(b) Combination of data from different radars

Country	input data	overlap data choice	boundary choice	other composite products (planned)
Austria	max. vert. col.	max	-	(1)
Belgium				
Denmark				
Finland	max. vert. col.	max	-	high resolution composite
France	low elevation	no	nearest avail.	
Germany	low no clutt.	max	-	
Ireland				
Italy				
Netherl.	low no clutt.	max/swap	avoid clutt.	
Norway				
Portugal				
Spain	3 km CAPPI	max of 4	nearest 4	echotop; hourly rainfall
Sweden	low CAPPI	no	optimum	echotop;max.vert. column
Switzerl.	max.vert.col.	max	-	(1, 2)
U.K.	low no clutt.	no	nearest avail.	
Yugoslavia	low no clutt.	lowest	to be defined	max. vert. column

(= no change; psp = polar stereographic projection, trv. merc. = transverse mercator projection)

(1) The composite includes side and front views.
(2) A full volume (12 layers of 1 km) product with linearly averaged rain-rate data is planned.

43% of countries use the maximum value in the overlap area.

So what do these COST images actually look like? Fig. 14 is one example at 2000 UTC on 7 March 1991, including data from the United Kingdom, France, Ireland, Switzerland and the Netherlands. The blue area is infrared data from the European satellite Meteosat, lighter blue being medium-level cloud and dark blue is high-level cloud, the other colours are radar data. Also shown are the coast of France, the coast of Spain, the Bay of Biscay, the United Kingdom and Ireland, and political boundaries. The limit of the radar coverage is shown as a full or broken line. This kind of image is currently produced every hour. Most of the data are archived.

Work has been done in the project on uses of multinational composites. I am going to look at these uses very quickly, starting with forecasting of rain. So far very little work has been done on how to use these kinds of wide-area radar data as a contribution to data assimilation within numerical forecast models. It is important that this work is done.

First of all the contribution of wide-area radar composites to general forecasting. Fig. 15 is an example showing a thunderstorm moving from off the Cornish coast at 1100 UTC right through France into Germany. The solid shading is the radar data, the lighter shading is the satellite infrared data. It is interesting to note that if you look at the time 1700 UTC in a region where I know there is good radar coverage, you can see the overhanging cirrus from the thunderstorm which certainly does not correspond to the rain area. Clearly, if you have international radar data then you can track systems for a very long way on many occasions. Of course we in the United Kingdom tend to be on the windward side of Europe, but those countries further into Europe have a real need for the data from the United Kingdom.

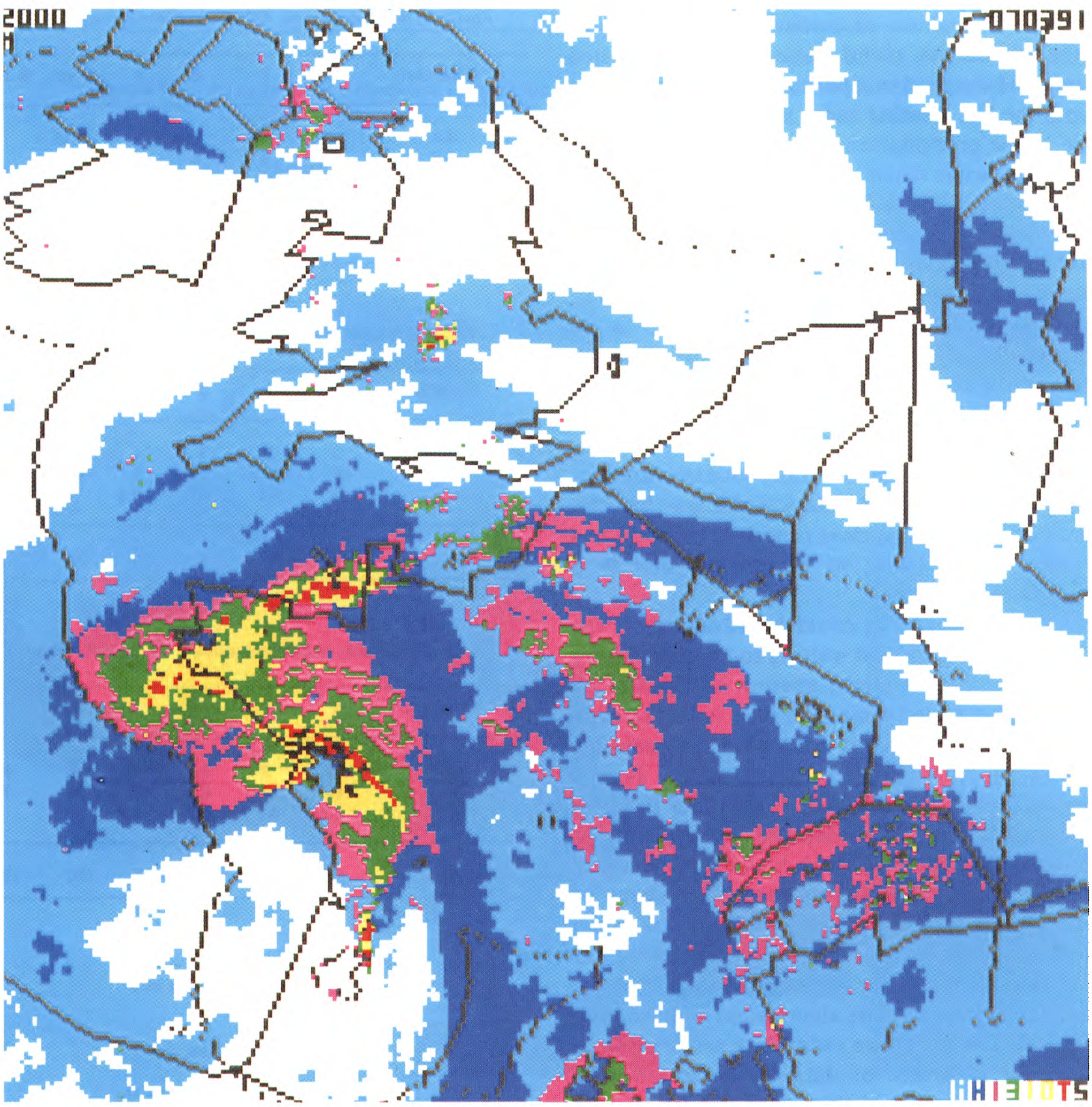

Figure 14. An example of a COST image. See text for full explanation.

Table IV shows the results of the assessment carried out at London Weather Centre, then at Aberdeen when the offshore bench was transferred there, and also in the Netherlands. To assess the utility of COST data for forecasting offshore, we distributed a questionnaire to the forecasters. If you look at the figures in Table IV, code numbers represent the precipitation types, and A, B, and C represent the quality of the guidance. A is good additional guidance, that is additional to the database that already existed, B agrees with other data and C is misleading advice from the COST data. The first thing to notice is that both in the Netherlands and the United Kingdom the results are more or less consistent. In addition, for roughly 36% of occasions the COST image provided good guidance for the forecaster. It is clear that this kind of data has a positive impact for this forecasting application.

Another application is the use of COST data for pollution monitoring. A numerical model developed at Imperial College by Helen ApSimon has been used to simulate the deposition of caesium from Chernobyl when the radioactive cloud passed over the United Kingdom, and she used as input to that model the radar data from the UK weather radar network to provide a measure of the precipitation that washed out caesium from the radioactive cloud. If you compare that model prediction and the actual distribution of caesium, there is good correspondence. From that start David Goddard and Brian Conway have developed a procedure for estimating the best precipitation field using radar, satellite and numerical model data. Fig. 16 is an example of the resultant field, where the different colours on this particular display represent the different types of data. These data are used as one input to the NAME deposition model, developed by a team led by Barry Smith and Roy Maryon. Many countries are now very interested in using radar data in this way because there are rather a lot of nuclear power stations, quite a lot of them very similar to Chernobyl, and it is important to be prepared.

Scientific understanding could be advanced by the COST data set which is just waiting to be used. To try and illustrate what we might attempt to do, Fig. 17 shows a COST image (again, the blue is the satellite data) in which the infrared is not making any sensible measure of the surface precipitation at all. It is a complete mismatch over most of France and the Low Countries. Over south-west England and Ireland the satellite and radar data are much better matched. The Met. Office hosted a multi-national experiment in February and March 1991 aimed at collecting as much satellite data as possible over north-west Europe with as much rain-gauge and radar data as possible, to allow scientists to test their satellite algorithms for estimating precipitation. The European radar data are proving to be a very useful source of data for these kinds of assessment. An example of the use of this imagery in research into the development of mesoscale conceptual models is shown in Fig. 18, an example of a split front; there is clearly a lot of information in these images.

Table IV. Assessments of COST-73 for maritime forecasting — from various users

London Weather Centre;
138 observations November 23 - December 21, 1989

Situation:	0	1	2	3	Total	% 1-3 only
%A	0	3	0	2	5	10
%B	35	38	0	9	81	86
%C	12	2	0	0	14	4
	46	43	0	11	100	100

Aberdeen Weather Centre; 631 observations January 19 - May 6, 1991

Situation:	0	1	2	3	Total	% 1-3 only
%A	7	0.6	6	1	15	31
%B	45	5	8	2	60	62
%C	24	0	1	0.3	25	7
	76	5	15	4	100	100

Schiphol Airport; 1458 observations July 10 1990 - March 9, 1991

Situation:	0	1	2	3	Total	% 1-3 only
%A	4	8	2	4	18	36
%B	55	14	1	9	79	62
%C	2	0.1	0	0.6	3	2
	61	23	3	14	100	100

Hoek van Holland; 1458 observations July 10, 1990 - March 9, 1991

Situation:	0	1	2	3	Total	% 1-3 only
%A	3	7	2	4	16	27
%B	49	17	6	12	83	72
%C	0.1	0.3	0.3	0	1	1
	52	24	8	16	100	100

A = good additional guidance
B = agrees with other data
C = misleading

0 = no precipitation, 1 = front(s), 2 = active front(s), 3 = unstable air mass.

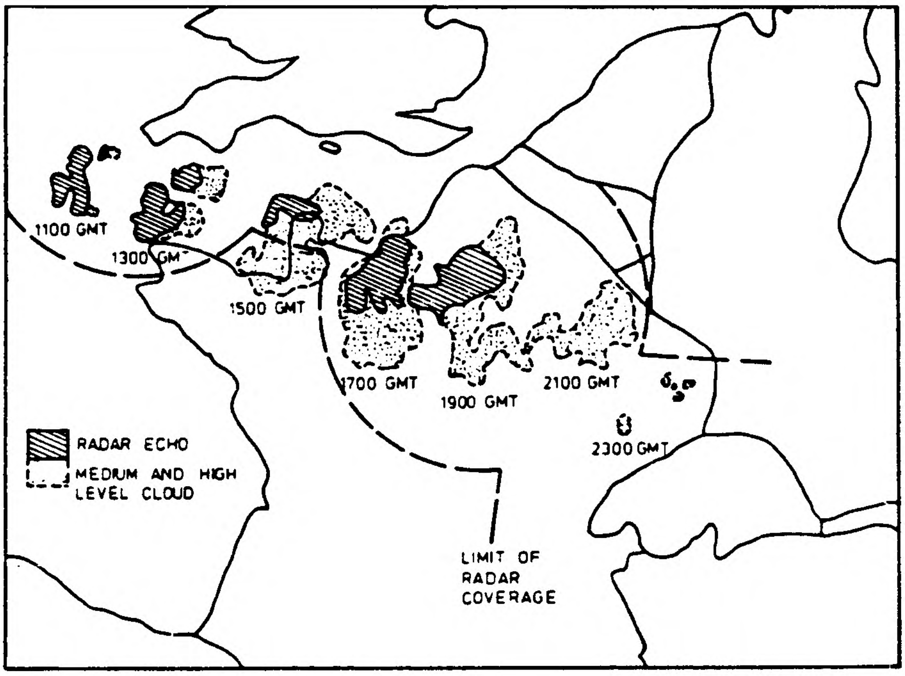

Figure 15. An example of a composite showing the progress of thundery activity across western Europe.

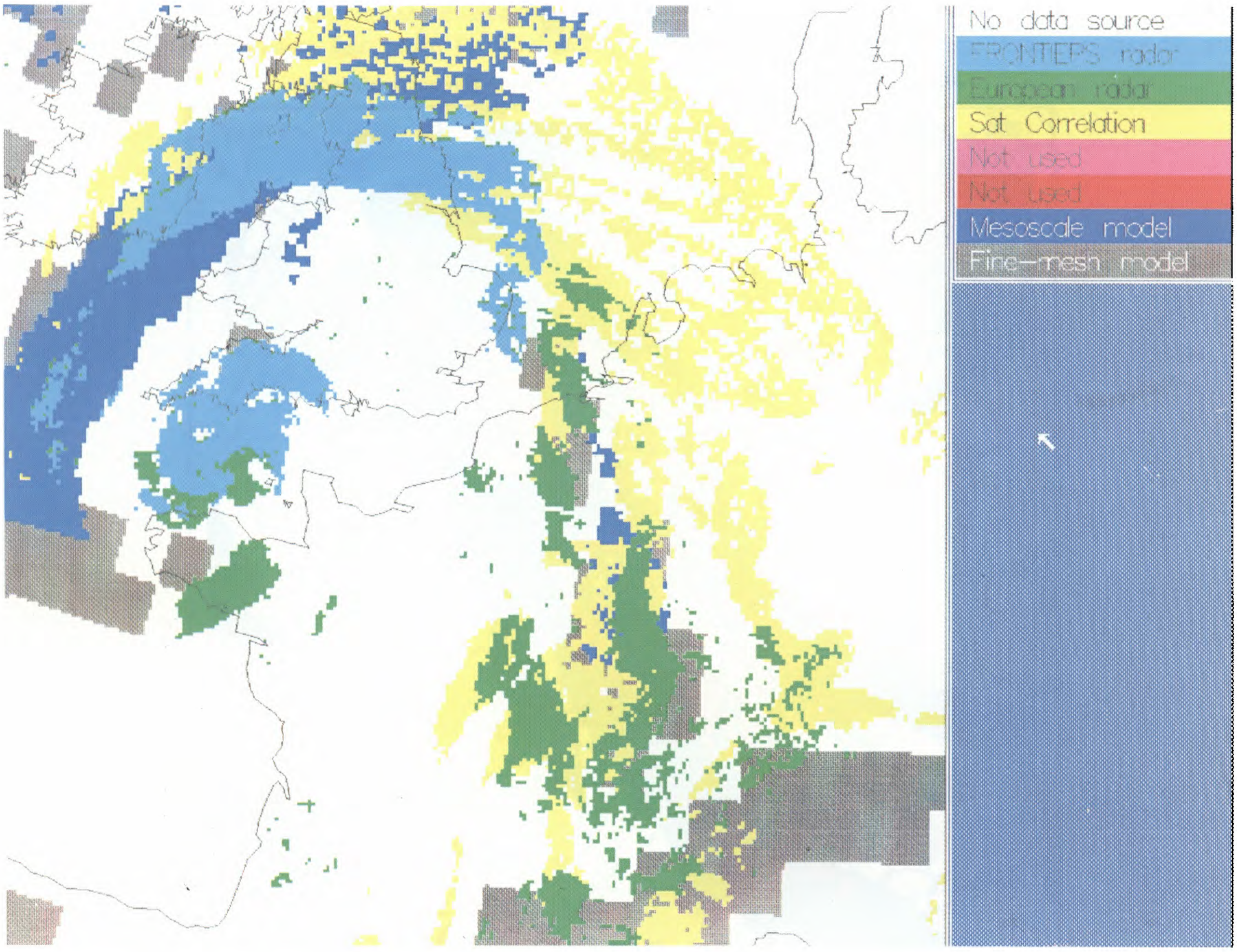

Figure 16. Estimated best-precipitation field from radar, satellite and numerical model data.

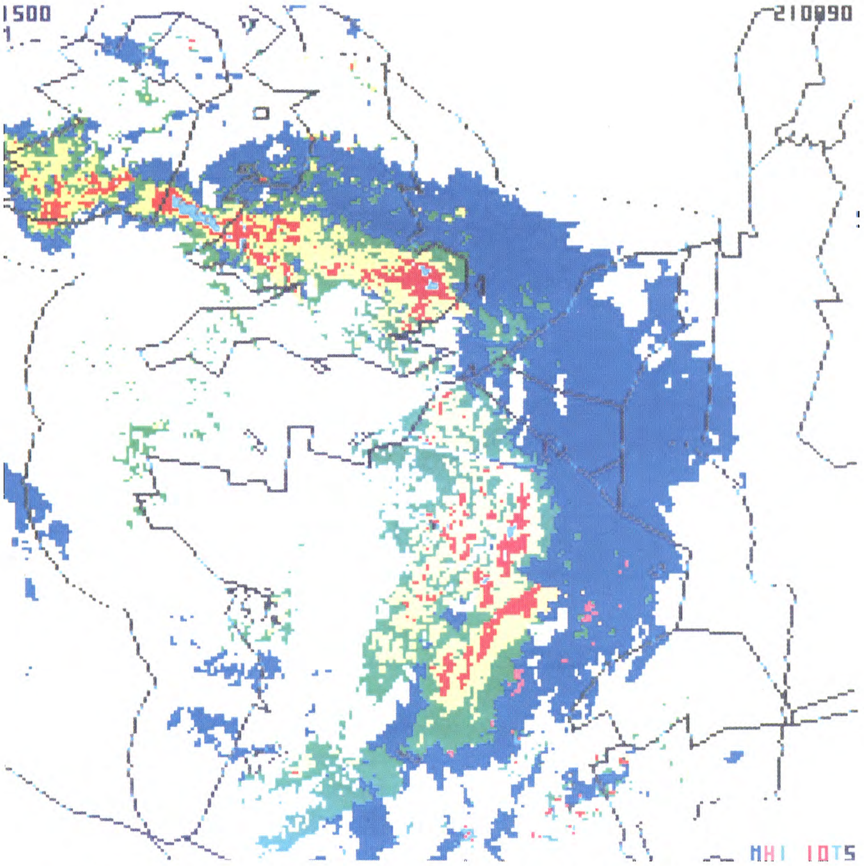

Figure 17. As Fig. 14, but showing a mis-match of radar and satellite data.

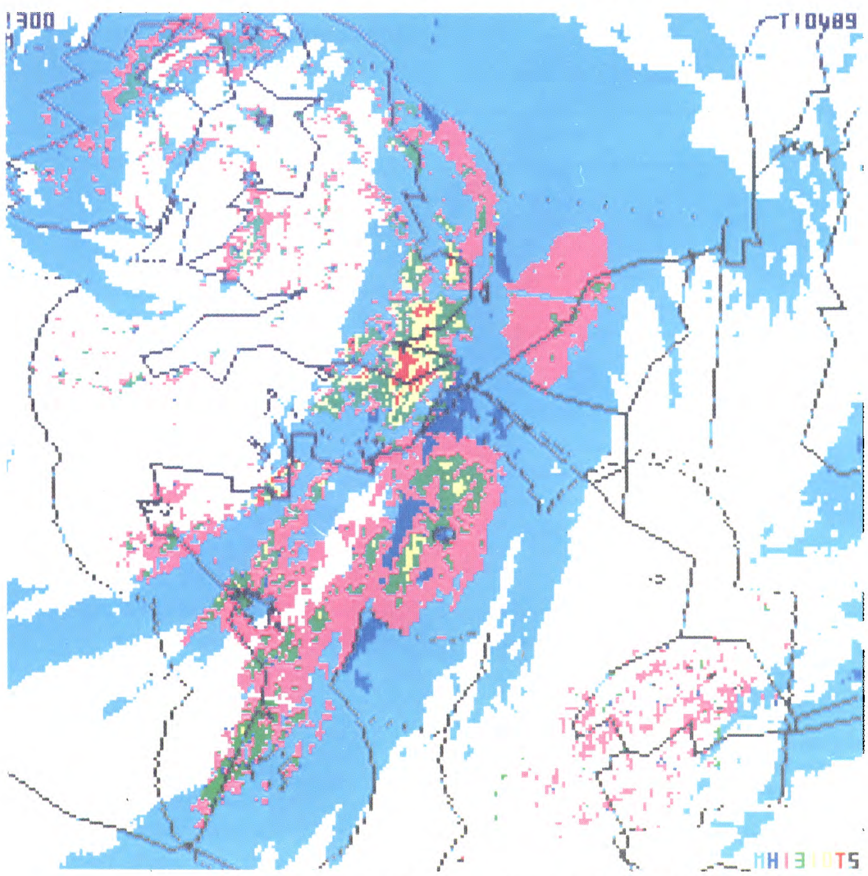

Figure 18. Example of a split front observed using COST data.

A further application of international radar data is as a contribution to continental-scale hydrology — looking at hydrological processes on a continental scale. Fig. 19 shows the international river basins over Europe. The Danube is the most international river in the world. It is bordered by the most countries, and the only way in which one can understand hydrological processes on the scale of the Danube is to use precipitation information on the scale of the entire river basin. That in Europe could mean radar data you can integrate.

Another application of these radar data would be as part of an international river watch. Some of you may recall in the papers some years ago when a company tipped a whole bag of chemicals into the river Rhine in Switzerland, and the pollution travelled all the way down the Rhine killing many fish. Hydrological models of water quality exist and are being developed on the basin scale. They need real-time precipitation input to make them fully operational.

The Met. Office have employed a company to look at possible commercial benefits from the use of COST images. They identified two areas in particular. Fresh food importers, who would like to go to individual farms in Southern Europe to select produce on the basis of whether it rained at a particular farm or not as it makes a difference to the quality of the produce they are going to buy. In addition, European TV Channels expressed particular interest. New types of user will necessitate the development of new products, and some examples have been proposed in the COST-73 project.

So what are the recommendations of COST-73? Table V lists the main recommendations. Of particular importance is operational network continuity. There have been some proposals that work started in COST-73should be continued, and that FM 94 BUFR should be used for international radar transmissions. There is a gap in the radar network coverage over the North Sea. Perhaps one or two Doppler radars could be established on platforms in the North Sea as shown in Fig. 20. Likely costs have been investigated and are not prohibitive, particularly if one recalls that Doppler radar will measure wind speed as well as reflectivity.

The technology of current radars is rather old, and a new COST action has been proposed (now designated COST-75) to look at new forms of radar technology, including electronic scanning and multi-parameter radars, and the algorithms and software needed to process the data from the radars in real time. This could lead to specifications for the next generation of radar in Europe. I am bound to say that there was some interest from scientists at the weather radar conference held in June 1991 in Paris. Scientists from NCAR looked at electronic scanning technology and decided that it was feasible some 5 or 6 years ago. However, they did not

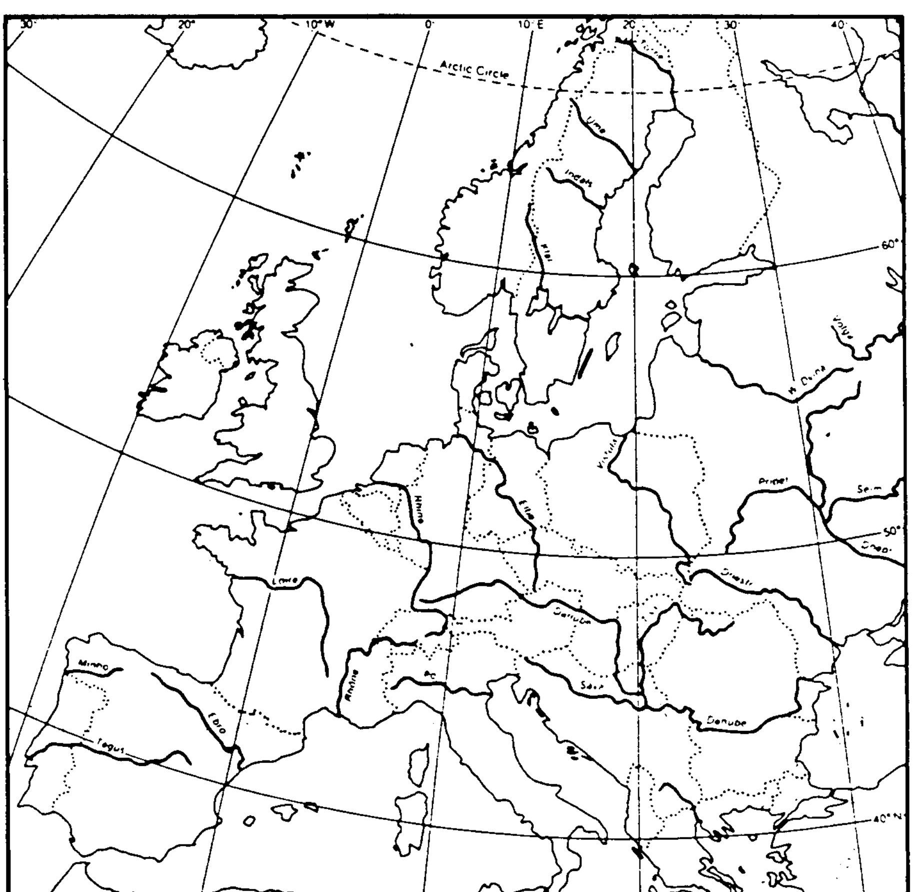

Figure 19. Map of the major river systems of Europe.

Table V. COST-73 recommendations

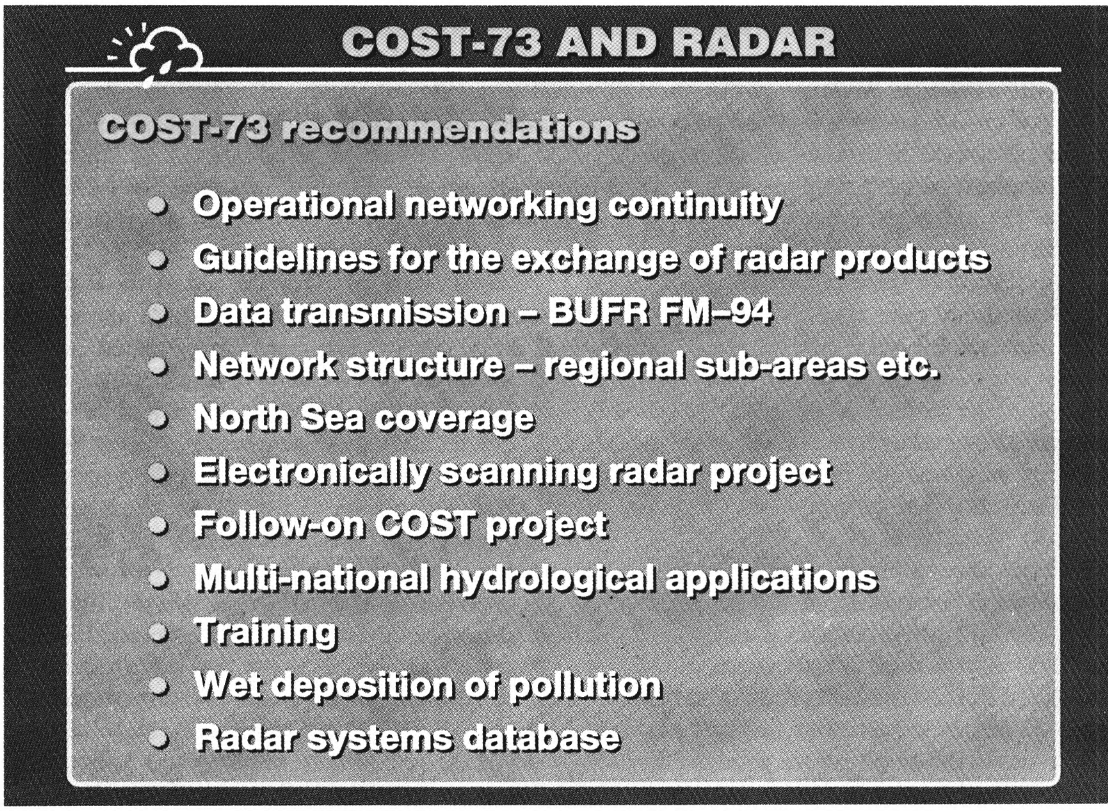

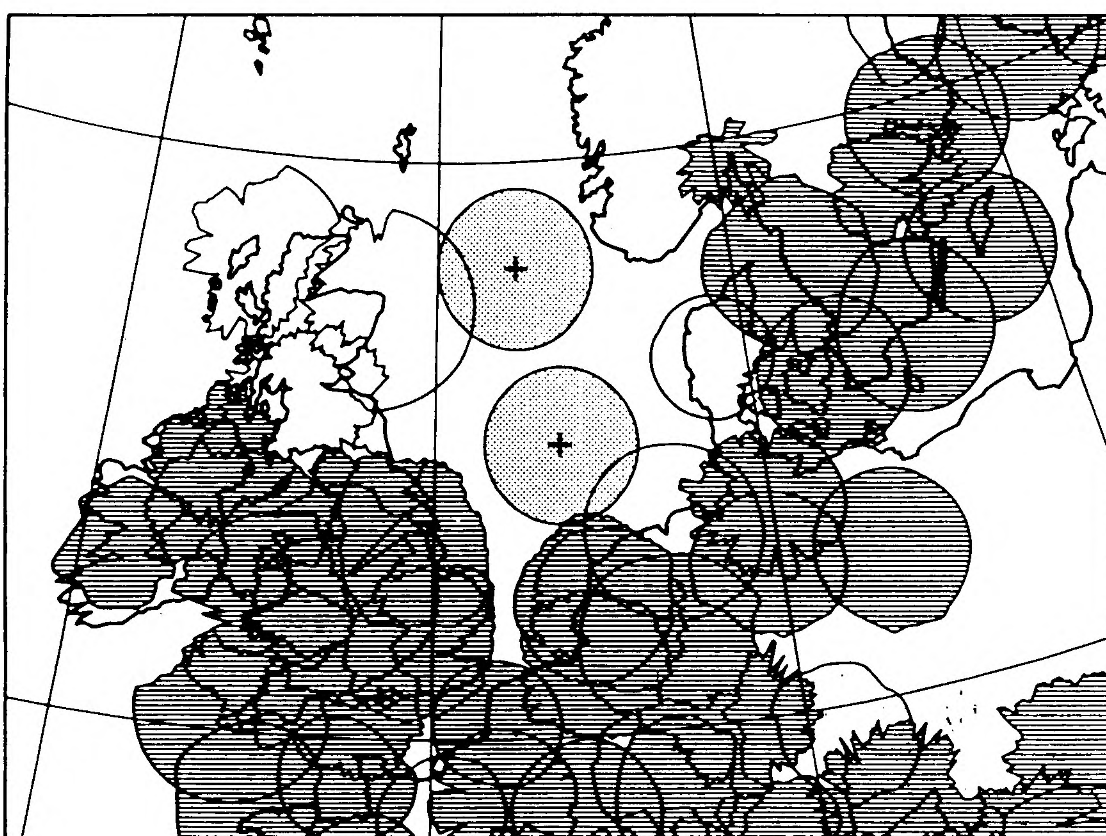

Figure 20. Possible location of North Sea radars.

take this further for surface radars, but instead transferred that technology to an airborne radar. However, when we showed them pictures of this type of radar being used for defence purposes there was some renewed interest from North America, and hopefully this will be pursued through the new project.

The COST-73 Management Committee felt that training in radar meteorology was totally inadequate, and the Committee specified, in some detail, a training curriculum that could be used as a basis for the training of technicians, meteorologists and users.

As the Project finished the Directors of West European Met. Services established a working group to look, in detail, at how work in COST-73 might be taken and transferred into an operational environment. The working group met in Florence in the summer of 1991, the Met. Office being represented by Kirby James and Francis Hayes. A report is due to be presented to the Directors of European Met. Services, and I hope they conclude that there should be a permanent group established to manage the international exchange of radar data around Europe. (Since delivering the lecture this has been agreed.)

I believe that COST-73 was a very successful example of international cooperation. A detailed Final Report has been completed and will be published by the European Commission (DGXII) soon. Without the efforts of many people this achievement would not have been possible. For me as Chairman of the Management Committee it has been marvellous project, and one which I feel very fortunate to have had the opportunity to experience at first hand.

551.553.11:551.515.82

A sea-breeze front seen by radar

T. Andersson and B. Lindgren
Swedish Meteorological and Hydrological Institute, Norrköping, Sweden

Ahead of a cold front on 7 May 1990, there was an exceptionally distinct sea-breeze over parts of the Swedish east coast. The sea-breeze front was clearly depicted by the Norrköping Doppler weather radar. The echoes, which were weak, did not originate from precipitation, but were clear air echoes from insects or sharp gradients in the refractive index of the air. The operative Doppler weather radars of today are sensitive enough to detect those echoes on practically every day in the warmer seasons (in our climate).

Fig. 1 gives a mesoscale analysis of the wind field at anemometer height. The positions of the sea-breeze front at successive times are also given. Fig. 2 is a pseudo-CAPPI

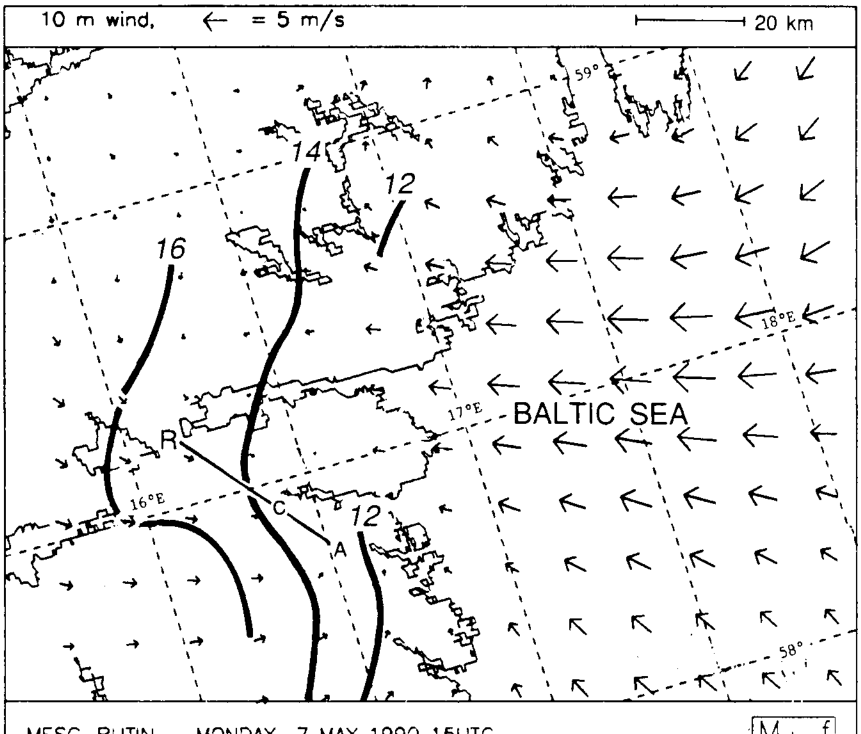

Figure 1. Mesoscale analysis of the wind at anemometer height at 15 UTC on 7 May 1990. Isochrones for the sea-breeze front at 12, 14 and 16 UTC are given. The baseline of the vertical cross-section in Fig. 4 is marked R–A, and R is the position of the radar.

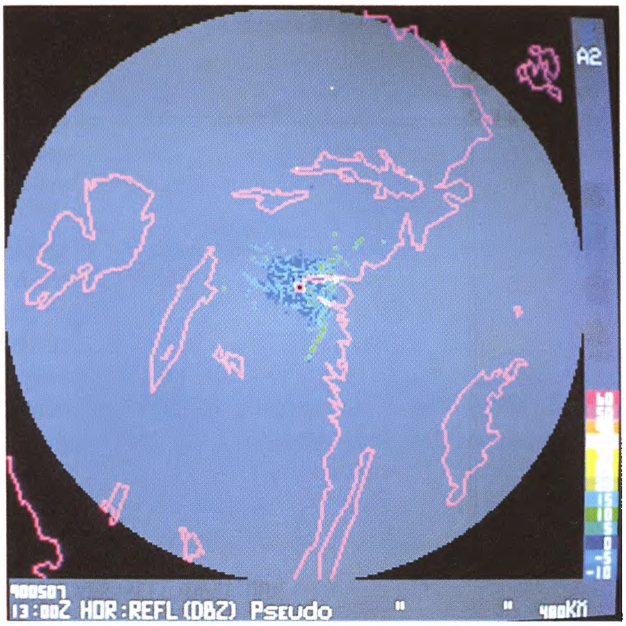

Figure 2. Pseudo-CAPPI of reflectivity at 13 UTC on 7 May 1990. The reflectivity scale is given to the right. The Norrköping Doppler weather radar with a range of 240 km.

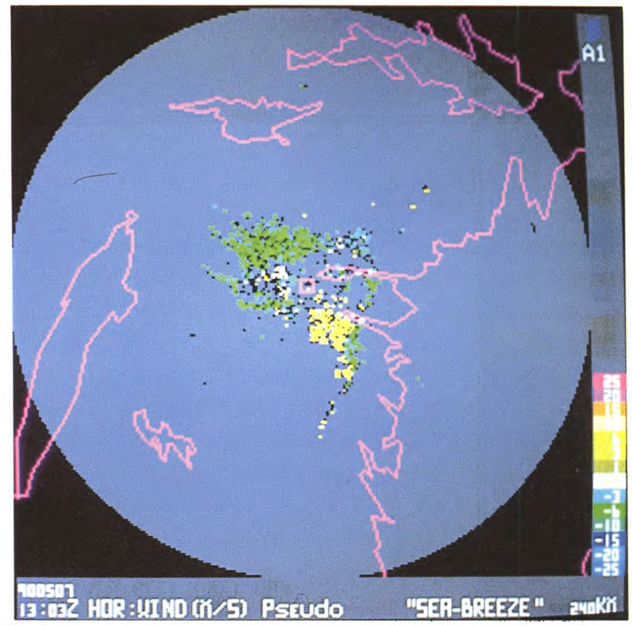

Figure 3. PPI (antenna elevation angle 0.4°) of radial wind at 13 UTC on 7 May 1990. The radial wind scale is given to the right. Positive winds blow out from the Norrköping Doppler weather radar — range 120 km.

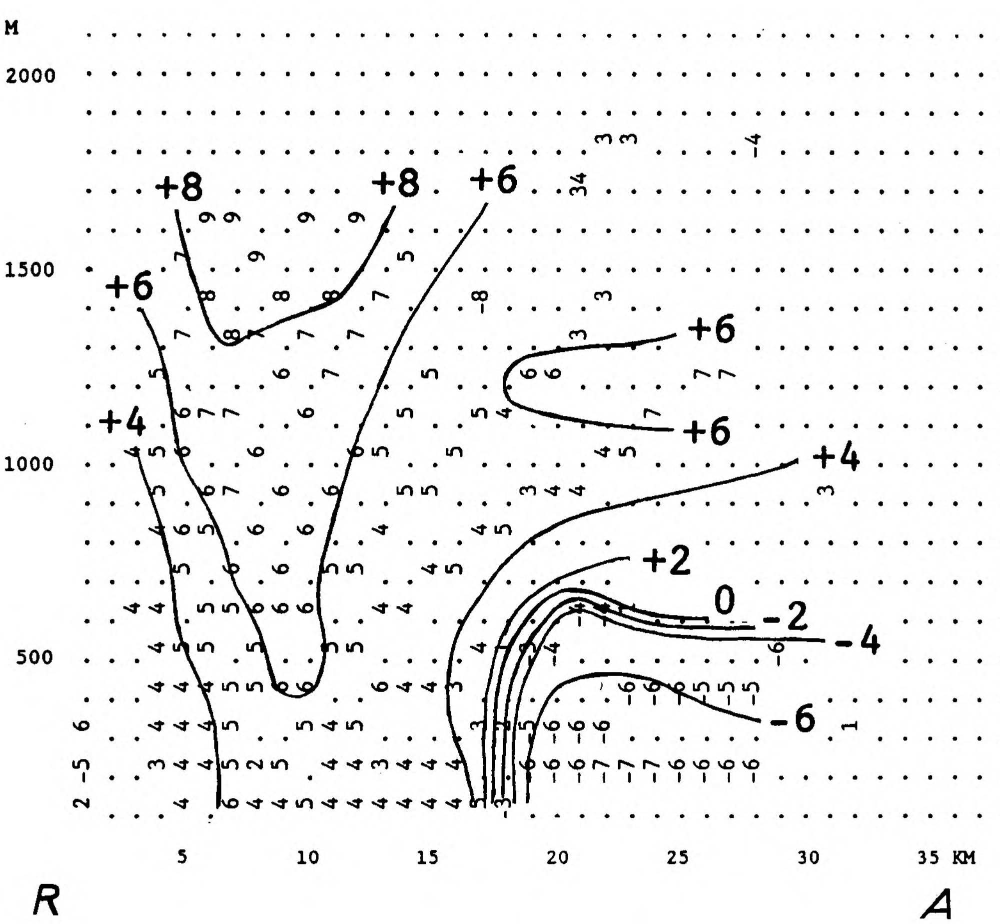

Figure 4. Vertical cross-section of radial winds along the line R–A in Fig. 1 at 14 UTC on 7 May 1990.

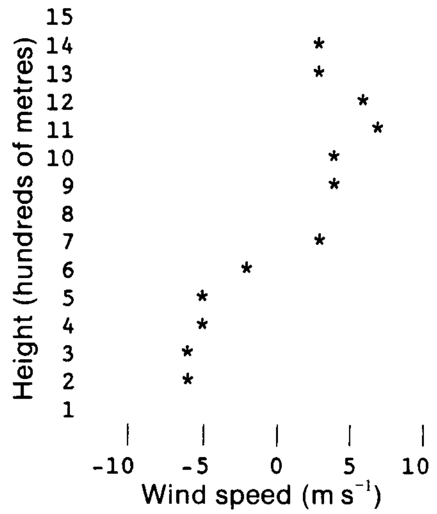

Figure 5. Vertical profile of radial winds at a range of 25 km from the radar, at position C in Fig. 1 at 14 UTC on 7 May 1990.

(Constant Altitude Plan Position Indicators) of reflectivity, where the thin (green) line echo shows the sea-breeze front and the weaker (blue) echoes mostly are other clear-air echoes, which give the radial winds depicted in Fig. 3. The sea-breeze wind shift occurs at the border between the positive (yellow, blowing out from the radar) and negative (green, blowing towards the radar) echoes.

A vertical cross-section in the direction of 140° from the radar lies mainly in, and 180° from, the wind directions and therefore gives a good picture of the real winds. Such a cross-section (along the line R–A in Fig. 1) is given in Fig. 4. The clear-air echoes reached up to about 1600 m, and the winds could thus be depicted up to this altitude. A vertical profile of the radial winds (Fig. 5) at a range of 25 km from the radar in the direction of 140° (at the position marked C in Fig. 1) also shows that this sea-breeze front was very sharp.

Correspondence

Hoar frost deposition

In their useful article about hoar frost deposition on roads (*Meteorol Mag*, **121**, 1–21), T.D. Hewson and N.J. Gait refer to the thickness of hoar frost accumulation that may give rise to a significant ice danger. It seems, however, that they were comparing this with a road surface that would otherwise have been dry. I would suggest that a more appropriate comparison is with a salted road which will rapidly become damp through the hygroscopic effect of the salt. A damp road is not, of course, as slippery as an icy one, but the salty dampness is very much more persistent than early morning hoar frost. In the absence of rain to wash the salt away, the artificial dampening effect can last for many nights and days, mitigated only temporarily each afternoon by partial drying of the salt. The resultant safety penalty from persistent dampness has to be set against any benefit from the original salting.

An informal confirmation can be made by anyone walking to their railway station on a bright winter's morning. The surfaces of roads on the council's salting run can frequently be seen to be damp, or even wet, when unsalted narrow side streets are dry. If, however, the unsalted streets are found to be freshly icy, then there may indeed have been a safety gain from salting, at least as far as that locality was concerned.

R. Mansell

8 Curthwiate Gardens
Enfield
Middlesex EN2 7LN

Reviews

The *New Scientist* guide to chaos, edited by N. Hall. 153 mm × 234 mm, pp. 224, *illus.* London, Penguin Books Ltd, 1992. Price £9.99. ISBN 0 14 014571 0.

A year or two ago, a series of articles appeared in New Scientist on chaos theory and its implications for different branches of science. This book, compiled by the physical sciences editor of that journal comprises the complete series and contains contributions from 18 authors mainly from British universities.

The series begins with a historical review following the development of mathematical physics through the deterministic theories of Newton and Laplace, and the quantum theory of the 1920s with its randomness and unpredictability to the new theory of chaos, unpredictable yet deterministic. This is followed by several chapters illustrating the nature of chaos and designed to give the reader a feel for chaotic behaviour.

For a practical example of chaos, a pendulum seems an unlikely candidate but a spherical pendulum under forced oscillation near its resonant frequency readily shows the symptoms. An easily followed mathematical chapter looks at chaos from a theoretical point of view, and an occasionally light-hearted chapter on visualizing chaos introduces trajectories, attractors, bifurcation, etc. and supports the author's assertion that 'a picture is worth a million numbers'.

Fluid dynamics provided some of the earliest recognized physical manifestations of chaos, particularly turbulent flows. It has also proved one of the most difficult to study. A general chapter on fluids uses simple laboratory systems as examples — real turbulent flows are just too complex.

Chaos is a well-known occupational hazard for weather forecasters. Tim Palmer from ECMWF explains how ensemble forecasting (generating several predictions with slightly different initial conditions) provides information on the reliability of forecasts. In the tropics the influence of sea surface temperature anomalies makes things more complicated — reliable extended-range forecasting of El Niño requires a coupled atmosphere–ocean model. All this is explained in a very readable manner without a single equation.

Subsequent chapters show how chaos has influenced research in many other branches of science. Electric circuits, especially those involving feedback or signal amplification, have always relied on the designer's intuition to avoid non-linearity and spurious response, but chaos is helping to replace art by science. In the life sciences, chaos has applications to population dynamics, genetic variability and neurophysiological disorders.

Several authors point out that interest in chaos stems from the limitations of traditional theoretical techniques based on studies of systems in static or dynamic equilibrium. Applied to systems far from equilibrium or with strong transient forcing, the latter not only fall down in their quantitative predictions but sometimes even fail to predict the type of behaviour experienced. Thus ships capsize in heavy seas, structures fail in gusty winds, and thermodynamic and chemical systems evolve in unexpected ways. A chapter on chemistry dwells largely on a laboratory curiosity, the cyclic Belousov–Zhabotinskii reaction, but also mentions combustion and catalysis, both of great importance in industry.

Some applications are more unexpected. Gravitational effects can cause chaotic behaviour in the orbits of asteroids, and even the earth's orbit may be unpredictable on time-scales of hundreds of millions of years. A surprising discovery is that as the size of physical systems are reduced to the point where quantum theory takes over from classical physics, chaotic behaviour is suppressed. On the stock market, prices are controlled by complicated feedback interactions — conditions in which chaos can thrive. However there are so many external random market forces that it is difficult to detect chaotic behaviour in economic data with any confidence.

Two chapters on fractals (one of them by Benoit Mandelbrot) comprise an introduction to the subject, material which will be familiar to many readers. A chapter on number theory, though interesting, seems a little out of place as it says much about randomness but little about chaos.

The variety of scientific disciplines in which the theory of chaos has found application is perhaps the most lasting impression given. Although only the simplest mathematical systems have been studied so far, the common picture of chaos that emerges is one of exponential error growth stemming from non-linearity resulting either from resonance (where amplitude growth is restricted only by non-linear effects) or from feedback mechanisms. A brief summary chapter to point out these common threads through the book would have made a useful conclusion.

The book is well printed and the black and white figures are supplemented by 16 pages of colour plates, mostly computer generated. On the whole, the similar depth of coverage by each author preserves a good balance with a few references for further reading at the end of each chapter. In spite of the variety of authors, a number of chapters contain references to work described elsewhere in the book thus avoiding unnecessary repetition.

It would be interesting to compare the contents of the present book with that of an updated version published in, say, 10 or 20 years' time. Such is the widespread applicability of chaos and the unpredictable nature of its revelations that the future development of the subject may itself provide yet another example of the theory in action. In the meantime, the present book will provide a useful and comprehensive background for understanding the behaviour of our chaotic world.

B.R. Barwell

Plants and Microclimate: A quantitative approach to environmental plant physiology

(second edition), by H.G. Jones. 150 mm × 227 mm, pp. xxiv+428, *illus.* Cambridge University Press, 1992. Price, £55.00, $100.00 (hardback, ISBN 0 521 41502 0), £19.95, $39.95 (paperback, ISBN 0 521 42524 7).

This second edition is a thorough review of the first, with all aspects of the book improved or brought up to date. For a review of the first edition, see *Meteorological Magazine*, **114**, 62–63. The basic purpose of the book remains to 'provide a soundly based introduction to those features of the atmospheric environment of relevance to plants', and while the basic structure of the first edition remains, changes have been made to the text, tables, figures, references and the sample questions at the end of each chapter.

The book starts with an introductory chapter on modelling and experimentation which now includes a mention of the practical uses of models as well as their scientific contribution. The following three chapters on the physics of radiation, heat, mass and momentum transfer and also evaporation are revised to include further information on indirect methods for determining canopy structure and evaporation from plant communities.

The remaining chapters are organized much as before except that the old chapter 'Environmental Control of Morphogenesis' has become 'Light and Plant Development'. In these chapters are described topics such as plant-water relations, stomata, photosynthesis and respiration, temperature, drought, the effects of wind and altitude, and with a section on the 'greenhouse effect' and the effects of atmospheric pollutants. New topics include chlorophyll fluorescence, carbon isotope discrimination and high temperature injury.

All of this is presented in a thorough, but easy to read style much of which would be useful to meteorologists faced with trying to understand plant–atmosphere interactions. Chapter 3 now includes transfer processes in the canopy (penetration of gusts) and the evaporation section now has the concept of 'coupling to the environment', both of which topics have appeared in the last 10 years. Chapter 9, on plant development, is timely because of the increasing interest in crop simulation models. However, it would have been useful to have had an example, say the AFRC wheat development model, which demonstrates the use of thermal time modified by both photoperiod and vernalization. The section on water-use efficiency is expanded and there is now a section on the 'Crop Water Stress Index' introduced recently as an aid to irrigation management. The new section on the greenhouse effect forms a useful introduction to the topic and concentrates on the effects of carbon dioxide on plants while rightly drawing attention to the errors in prediction of future climates by global climate models.

The book is over 100 pages longer than the first edition. In part this is due to new additions, but also because it has slightly smaller width and length and a slightly larger print size. It is easier to read than the first edition and the use of a system of bolding text when a definition is first used is a great help. The 'Answers to selected problems' contains brief working as well as the final answer, which can be a help if you are not sure how to tackle a problem. All the symbols are explained in a glossary, but users familiar with the first edition will have to be a bit careful at times because the meaning of some symbols has changed, e.g. 'i' in the first edition meant 'inlet', but this changes to 'e' in the new edition. Some minor errors remain, e.g. in Figure 2.1 the '0' should be '10 to the power 0' and on page 204 '17.5 Kg/g' should be '17.5 KJ/g'. However, these are minor complaints about an excellent revision, although some of the new material would not be of great interest to meteorologists.

M.N. Hough.

Books received

The listing of books under this heading does not preclude a review in the Meteorological Magazine at a later date.

Glaciers, by M. Hambrey and J. Alean (Cambridge University Press, 1992. £19.95, $29.95) contains many photographs (mostly colour) of glaciers and their accoutrements from worldwide locations. The text aims to describe and explain glaciers while conveying their beauty and importance. ISBN 0 521 41915 8.

International weather radar networking, edited by C.G. Collier (Dordrecht, Kluwer Academic Publishers Group, 1992. £66.00, $110.00, Dfl.190.00) contains about 40 papers presented at a COST-73 seminar at Ljubljana in June 1991. The wide-ranging contents highlight the many facets involved in creating and combining national and international networks. ISBN 0 7923 1706 8.

Climate change: Science, impacts and policy, edited by J. Jäger and H.L. Ferguson (Cambridge University Press, 1991. £50.00 (hardback), £24.95 (paperback)) contains the proceedings of the Second World Climate Conference held in Geneva in October–November 1990. The papers included cover all aspects of climate, and the book is material evidence of the remarkable cooperation of six international agencies. ISBN 0 521 41631 0, 0 521 42630 8.

Greenhouse earth, by A. Nilsson (Chichester, New York, Brisbane, Toronto, Singapore, John Wiley and Sons, 1992. £9.95) attempts to 'translate' the scientific community's report on the subject for the non-scientific reader. The variety of scenarios painted, caused by the different factors considered, are described. ISBN 0 471 93628 6.

Infrared image of a cloud-head — 27 April 1992 at 1800 UTC

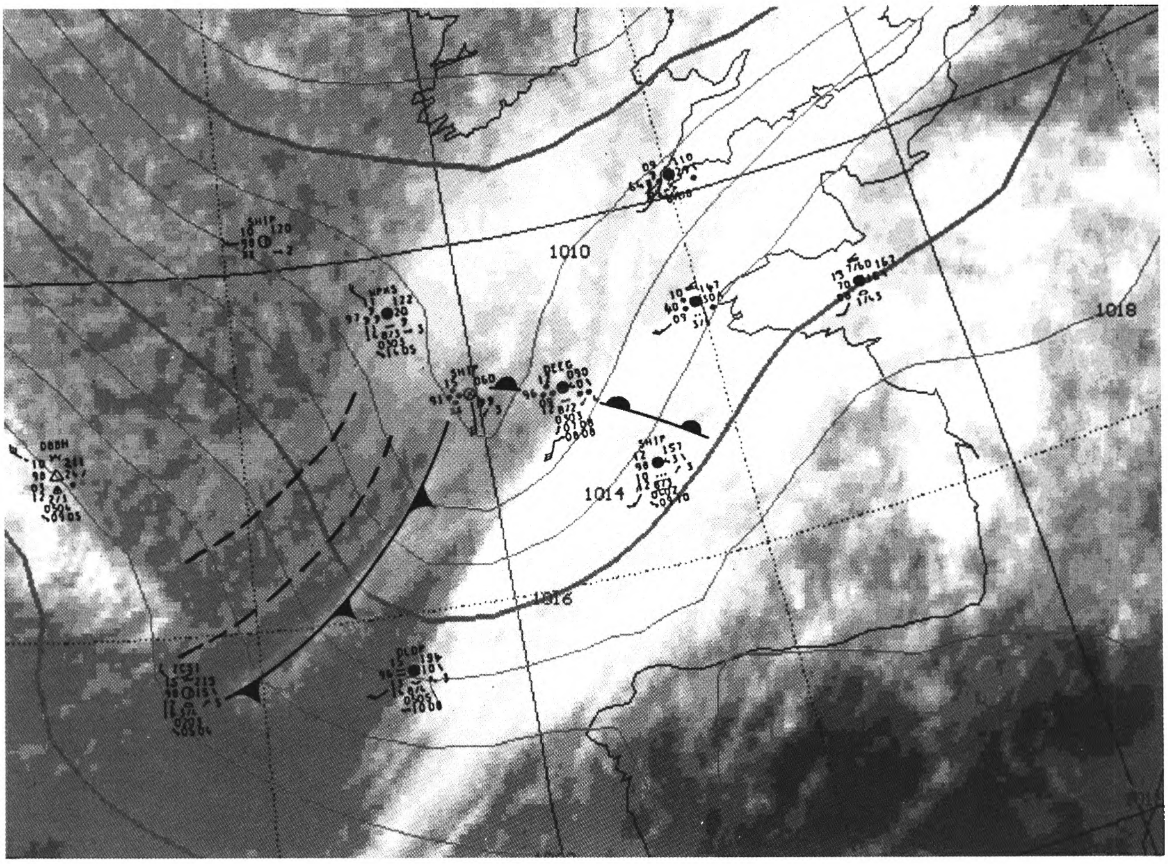

The figure shows a Meteosat infrared image of a cloud-head (see Monk and Bader*) associated with a developing low. Superimposed on this are isobars at 2 mb intervals taken from the 1800 UTC operational analysis of the Meteorological Office unified limited area model (LAM), together with a selection of surface observations. The low subsequently tracked east-north-east, deepened to about 996 mb by 0600 UTC on the 28th, generated 60 m.p.h. gusts over the Channel Islands, and produced 10–20 mm of rain over southern Britain from the northern portion of the cloud-head (i.e. that centred around 50° N, 09° W at 1800 UTC).

During the period 1230 to 2030 UTC on the 27th, 67 dropsondes were released in the vicinity of the low, from the Met. Research Flight's C-130 aircraft, as part of the 'FRONTS '92' project. Preliminary cross-sections derived from the sonde data have indicated the presence of one surface warm front, and up to four surface cold fronts. The most pronounced cold front crosses 45° N, 14° W. The plotted warm and cold front positions are based partly on this cross-section data, and partly on surface observations.

The figure exhibits the following features:

(a) The warm front is not collocated with any particular feature on the imagery. However, the multiple cold fronts are linked to banding in relatively warm, low cloud. The main band of cirrus (through 45° N, 10° W), which might appear to be frontal, does in fact lie well ahead of the main surface cold front. The C-130, flying at 20 000 ft, traversed a region of clear air below this cirrus.

(b) The heaviest precipitation is generally not coincident with the coldest cloud tops — note the two ship observations closest to 48° N, 09° W. This inference is supported by other ship observations (not shown), as well as data from the aircraft radar. It follows that most of the precipitation is probably being generated in the lower troposphere.

(c) The unified LAM pressure field appears to have underestimated the depth of the low. This is partly due to late ship observations having been missed by the data assimilation, but also emphasizes the importance of hand-drawn analyses. Issued forecasts for this low and the associated weather showed a marked improvement on the model guidance.

T.D. Hewson

* Monk, G.A. and Bader, M.J.; Satellite images showing the development of the storm of 15–16 October 1987. *Weather*, **43**, 1988, 130–135.

GUIDE TO AUTHORS

Content

Articles on all aspects of meteorology are welcomed, particularly those which describe results of research in applied meteorology or the development of practical forecasting techniques.

Preparation and submission of articles

Articles, which must be in English, should be typed, double-spaced with wide margins, on one side only of A4-size paper. Tables, references and figure captions should be typed separately. Spelling should conform to the preferred spelling in the *Concise Oxford Dictionary* (latest edition). Articles prepared on floppy disk (IBM-compatible) can be labour-saving, but only a print-out should be submitted in the first instance.

References should be made using the Harvard system (author/date) and full details should be given at the end of the text. If a document is unpublished, details must be given of the library where it may be seen. Documents which are not available to enquirers must not be referred to, except by 'personal communication'.

Tables should be numbered consecutively using roman numerals and provided with headings.

Mathematical notation should be written with extreme care. Particular care should be taken to differentiate between Greek letters and Roman letters for which they could be mistaken. Double subscripts and superscripts should be avoided, as they are difficult to typeset and read. Notation should be kept as simple as possible. Guidance is given in BS 1991: Part 1: 1976, and *Quantities, Units and Symbols* published by the Royal Society. SI units, or units approved by the World Meteorological Organization, should be used.

Articles for publication and all other communications for the Editor should be addressed to: The Chief Executive, Meteorological Office, London Road, Bracknell, Berkshire RG12 2SZ and marked 'For Meteorological Magazine'.

Illustrations

Diagrams must be drawn clearly, preferably in ink, and should not contain any unnecessary or irrelevant details. Explanatory text should not appear on the diagram itself but in the caption. Captions should be typed on a separate sheet of paper and should, as far as possible, explain the meanings of the diagrams without the reader having to refer to the text. The sequential numbering should correspond with the sequential referrals in the text.

Sharp monochrome photographs on glossy paper are preferred; colour prints are acceptable but the use of colour is at the Editor's discretion.

Copyright

Authors should identify the holder of the copyright for their work when they first submit contributions.

Free copies

Three free copies of the magazine (one for a book review) are provided for authors of articles published in it. Separate offprints for each article are not provided.

Contributions: It is requested that all communications to the Editor and books for review be addressed to the Chief Executive, Meteorological Office, London Road, Bracknell, Berkshire RG12 2SZ, and marked 'For *Meteorological Magazine*'. Contributors are asked to comply with the guidelines given in the *Guide to authors* (above). The responsibility for facts and opinions expressed in the signed articles and letters published in *Meteorological Magazine* rests with their respective authors.

Subscriptions: Annual subscription £36.00 including postage; individual copies £3.25 including postage. Applications for postal subscriptions should be made to HMSO, PO Box 276, London SW8 5DT; subscription enquiries 071–873 8499.

Back numbers: Full-size reprints of Vols 1–75 (1866–1940) are available from Johnson Reprint Co. Ltd, 24–28 Oval Road, London NW1 7DX. Complete volumes of *Meteorological Magazine* commencing with volume 54 are available on microfilm from University Microfilms International, 18 Bedford Row, London WC1R 4EJ. Information on microfiche issues is available from Kraus Microfiche, Rte 100, Milwood, NY 10546, USA.

October 1992

Vol. 121
No. 1443

Contents

ISSN 0026–1149

ISBN 0-11-728988-4

Printed in the United Kingdom for HMSO Dd 291241, 10/92, C13, 543, 24503.

The Meteorological Magazine

November 1992

History of MRF
PAMPA flights
Teaching dynamic meteorology
Autumn of 1991

HMSO

Met.O.1004 Vol. 121 No. 1444

First published 1992

HMSO

HMSO publications are availa

HMSO Publications Centre
(Mail, fax and telephone orde
PO Box 276, London, SW8 5I
Telephone orders 071-873 909(
General enquiries 071-873 001
(queuing system in operation i
Fax orders 071-873 8200

HMSO Bookshops
49 High Holborn, London, W
(counter service only)
071-873 0011 Fax 071-873 820(
258 Broad Street, Birminghan
021-643 3740 Fax 021-643 651(
Southey House, 33 Wine Stree
0272 264306 Fax 0272 294515
9-21 Princess Street, Manches
061-834 7201 Fax 061-833 063
16 Arthur Street, Belfast, BT1
0232 238451 Fax 0232 235401
71 Lothian Road, Edinburgh I
031-228 4181 Fax 031-229 273

HMSO's Accredited Agents
(see Yellow Pages)

and through good bookseller

The
Meteorological Magazine

November 1992
Vol. 121 No. 1444

551.5(09):551.507.352

A short history of the Meteorological Research Flight (MRF) 1942–92

W.T. Roach
AD Met O(MRF) 1985–88

Summary

A brief history of meteorological observations in the free atmosphere from the 17th century to the beginning of World War II is followed by an account of the events leading to the formation of MRF. Then follows the main part of the paper which consists of an account of the work (scientific, observational and airborne meteorological sensor development) of MRF during the period 1942–92, how this work was integrated with the research programme of the Meteorological Office, and of national and international collaboration with universities and other research institutions in major field experiments.

1. Before MRF

Reports of the sporadic use of kites and balloons to make meteorological measurements in the free atmosphere appear in the literature back to the mid-eighteenth century. From then until the birth of aviation in the first decade of this century, highlights were:

(a) The first manned balloon flight to measure temperature, humidity and pressure was made by an English gentleman called Jeffries in 1784, who reached an altitude of about 3 km.

(b) About 1862, Glaisher and Coxwell made similar measurements from an open gondola on several balloon flights, once attaining nearly 9 km, and nearly losing their lives in the process.

(c) During the period 1898–1904, the French investigator, Teisserenc de Bort, made nearly 600 unmanned balloon ascents to measure temperature up to 14 km. His painstaking analysis of his measurements led to the discovery of the stratosphere. These flights were the first serious meteorological research, rather than reconnaissance, flights.

As early as 1913, Shaw (then Director of the Meteorological Office) realized the potential of the aircraft as a platform for meteorological measurements and research, and suggested mounting vanes on aircraft to measure vertical air motion, and an accelerometer to measure 'bumpiness', as well as 'other meteorological measurements' including atmospheric electricity. The technology, funds and resources were not available then, or for some time afterwards, to give Shaw's proposals practical effect. Between the wars, limited attempts to fit some basic instruments to a few aircraft were made and, in 1927, a meteorological reconnaissance flight was established at Duxford, but little of meteorological value came from these initiatives.

However, the weather dependence of aviation had, from the beginning, created a demand for meteorological reporting and forecasting services, and resulted in 1920 in the absorption by the Air Ministry of the Meteorological Office. In addition, the rapid technical development of aircraft, forced by the operational demands of two world wars, had soon revealed further weather-related hazards (e.g. airframe icing, visibility of aircraft contrails to enemy aircraft, fog) which created a requirement for applied meteorological research.

During the first two years of World War II, it soon became apparent that the (still) rudimentary state of forecasting science, exacerbated by the lack of observations from the Atlantic Ocean — the source of most of our weather — was inadequate for aircraft operations in war. The need to mitigate this situation led to two initiatives:

(a) The formation of duty meteorological reconnaissance flights at RAF stations all over the United Kingdom. By about 1942, one, two, or three flights were being made daily from up to 40 stations to observe temperature, humidity, winds, cloud amount, base and top height, to heights of up to 6 km. These observations formed an essential supplement to the standard synoptic observation network. Some 20 000 flights were made in all. Recently, this data was put into computer-compatible form and used to assist the helicopter icing problem.

(b) The formation of the Meteorological Research Committee (MRC) in November 1941 with an urgent brief to foster and oversee investigation and research into meteorological science.

One of the first initiatives of the MRC was to arrange (through the Air Ministry) for the deployment of meteorologists, led by Dr A.W. Brewer, to the High Altitude Flight (HAF) at Boscombe Down in August 1942 to investigate the atmospheric conditions favouring the formation of aircraft contrails.

2. Boscombe Down (1942–46)

At Boscombe Down, Brewer's group were initially allocated two Boston and one Spitfire aircraft on which to install their instrumentation. Soon afterwards, Fortress, Mosquito and Hudson aircraft were added. (At that time, aircraft were easier to obtain than staff!) Flying in these early aircraft, often without cabin pressurization or heating, was arduous and tiring. However, the Mosquito was better liked; pilot and meteorological observer sat cosily side-by-side in the aircraft cabin and cooperated very effectively.

The first task was to develop and install aircraft instrumentation for measuring temperature and humidity:

Temperature. A remote reading resistance thermometer was developed for temperature measurements from a Spitfire aircraft. Radiation shielding of the thermometer element, and calibrations to determine the correction required for kinetic heating of the element when exposed to airflows of up to 200 m s^{-1} enabled an accuracy of better than ± 1 °C to be attained. These thermometers were later installed on all MRF aircraft.

Humidity. The frost-point hygrometer for humidity measurements depended on noting the temperature at which frost could first be seen (by a met. observer) forming on a 'thimble' of black glass cooled by liquid nitrogen while exposed to the external airflow. This device was developed by Brewer's group and first flown successfully in a Fortress aircraft late in 1943.

With these basic instruments, it was found that the upper troposphere was quite often supersaturated with respect to ice — conditions which favoured the formation of dense, persistent contrails — and that the stratosphere was extremely dry. These results led to a practical aircraft-contrail forecasting method, but was also a scientific discovery of major importance to studies of the atmospheric general circulation and the related distribution of water vapour as a tracer of atmospheric motion.

3. MRF — The early period (1946–62)

3.1 Move to Farnborough

Following the end of World War II, the practical and scientific success of the meteorological section of the HAF at Boscombe Down led to the establishment in 1946 of the Meteorological Research Flight at the Royal Aircraft Establishment (RAE), Farnborough with the main task of advancing meteorological science, but continuing to provide advice as required on weather-related problems of aircraft design and operation. Although MRF was not so called until 1946, its work was a continuation of HAF work, and so MRF is generally considered to have begun its work in 1942.

MRF commenced with establishment for a larger scientific staff, two Mosquito and two Halifax aircraft and RAF aircrew. Fairly early in the period, these aircraft were replaced by Hastings, Varsity and (in 1952) Canberra aircraft. The Canberra could be 'nursed' to 15 km under favourable conditions, and complemented the lower-level work of the other aircraft. MRF staff and aircrew were accommodated in 'temporary' prefabricated huts near the RAE control tower until 1961, when they moved into a purpose-built brick building on the other side of the airfield.

The aircraft were serviced by the RAE, who also designed the installation of meteorological instrumentation on aircraft to ensure that military safety standards were met, and provided (from various departments) invaluable technical advice on a wide variety of topics. The crucial role played by the RAF aircrew during the whole life of MRF cannot be overstated. A posting to MRF from a 'standard' RAF station was a 'cultural shock' to some aircrew, but they soon entered into the work, and educated the scientists into what flight plans were possible under the increasingly severe navigational constraints imposed by outside military and civil aviation interests.

The daily operational schedule began (subject to aircraft availability) with a briefing meeting at 0830 UTC (often earlier) at which final flight plans for the day were decided on the basis of the meteorological situation provided by the forecasting office based (until recently) at RAE. A flight-liaison officer liaised between scientific users, MRF technical staff, RAF aircrews and several departments of the RAE in relation to flight planning and briefing, and installation and removal of scientific equipment from the aircraft. Finally, he coordinated overseas detachments, where effective liaison with a host airfield staff unfamiliar with the special demands of MRF was essential for the success of a detachment.

This organizational set-up has remained unchanged in fundamentals to this day, though naturally there has been a great increase since 1946 in the sophistication of scientific equipment and data-processing, and also in the lead time required to design and install new equipment on aircraft.

Although aircraft have been used for meteorological research in other countries (particularly in America) since the end of World War II, the MRF facility is unique — as far as the author is aware — in having an aircraft and aircrew dedicated to it full-time.

3.2 Scientific work

The emphasis of 'in house' MRF research was (and still is) on physical rather than dynamical meteorology — i.e. with the structure and behaviour of weather on a fairly local scale, rather than the large-scale atmospheric circulation which carries, and, to some extent creates, weather. Under the active direction of Dr Murgatroyd, three main topics characterized the work of this period: aerosol and cloud physics, radiative transfer and atmospheric tracers.

3.2.1 Aerosol and cloud physics

This was a period of active development of sensors (with considerable assistance from the RAE) to measure the physical properties of clouds — e.g. the distribution of liquid water content, cloud- and rain-drop sizes, and ice particles — and of associated cloud condensation nuclei.

Sensors used then were: impaction on aluminium foil to detect ice particles and drizzle droplets, oiled slides to collect cloud droplets, hot-wire devices to measure cloud water content and a (Pollak) total aerosol counter. Data had to be manually processed which was very slow and time-consuming, but nevertheless produced some valuable studies. The emphasis was on rain-producing clouds, particularly cumulus in various stages of development, but some studies of clouds associated with atmospheric fronts, and also layer clouds were made. This work was to some extent complementary to laboratory studies of cloud microphysics being made at that time under B.J. Mason at Imperial College, and all contributed to a better understanding of the generation of precipitation, and the role of ice particles in this.

3.2.2 Radiative Transfer

Brewer and Houghton (University of Oxford) flew an infrared radiometer from the MRF Mosquito aircraft in 1954 to make some of the earliest measurements of long-wave radiative fluxes and heating rates through the troposphere. So began a long tradition of the use of MRF facilities by Oxford to fly radiometers developed in the Clarendon Laboratory. Later, the installation of photometers and solarimeters on MRF aircraft were used to measure upward and downward solar fluxes in cloud and clear air. The infrared absorption properties of liquid water and water vapour were already known, but MRF flights gave some of the earliest indications of significant additional absorption of solar radiation in clouds and clear air, attributed to the presence of aerosol, particularly downstream of urban areas.

3.2.3 Atmospheric Tracers

During the period covered by this section, first under Dr R. Frith, and then under Dr R.J. Murgatroyd, much further use was made of the frost-point hygrometer and, late in the period, of an ozone detector (also developed by Brewer in the Clarendon Laboratory, University of Oxford) to study the distribution of water vapour and ozone in the upper troposphere and lower stratosphere, particularly through jet streams, and also through a range of latitudes from 10° S to 75° N. A related study was of the incidence of cirrus cloud at high levels, particularly in the easterly jet stream outflow from the Indian monsoon spreading over equatorial Africa during summer.

This topic departed from the mainstream of MRF research in that it was relevant to studies of the stratospheric–tropospheric interchange of air associated with large-scale vertical circulations in temperate and subtropical jet streams in relation to the movement of radioactive products of nuclear tests during the period. The relatively quiescent mid stratosphere was identified as a 'storage tank' for these products.

3.3 Collaborative projects

While the research outlined above was carried out largely 'in-house', it was realized that the exploitation of the data-gathering potential of the aircraft required continued development of airborne sensors and of associated data-processing; of more staff to handle this development; and (perhaps most importantly) the involvement of other research groups. Consequently, collaborative projects became an increasingly important feature of MRF work during this (early) period. Examples were: Observations of the structure of jet streams and fronts in collaboration with the Meteorological Office Forecasting Research Dept., discharge of smoke puffs and radar-reflecting foil for short-period wind investigations at the Meteorological Office radar station, sampling particle plumes for medium-range dispersion studies at the Meteorological Office research outstation at Porton Down in collaboration with the Chemical Defence Experimental Establishment there, carrying radioactive particle samplers, providing solar radiation observations for Kew Observatory, and obtaining samples of airborne pollen for Rothamsted Experimental Station. In addition, links with university research groups were strengthened and many smaller projects undertaken.

The high-altitude work of MRF was interrupted in February 1962 by the loss of the Canberra aircraft (but, miraculously, none of its aircrew) in the sea when approaching to land at Leuchars, Scotland after a long flight to measure water vapour and ozone distribution in the lower Arctic stratosphere. This work was recommenced in the following year with a replacement Canberra with improved instrumentation.

4. The Middle Period (1962–81)

This period marked a transition from the early period with several aircraft, few staff and limited resources to the modern period with advanced technological support and a much larger staff. The work was more integrated within broader research projects.

The rapid advances in microchip and computer technology in this period greatly increased the potential for instrument development on one hand, and for the modelling of atmospheric physical and dynamical processes on the other hand. In particular, the increasing speed and capacity of computers enabled the incorporation of (usually parametrized) physical processes into numerical forecasting and general circulation models, and towards the end of the period, into climate models. MRF therefore had an increasingly significant role to play in providing basic physical data for improving and validating the parametrization of physical processes in models.

In any case, a natural break in MRF work in 1962 was occasioned by the move of MRF to its new building, the loss of the Canberra aircraft and the departure of Dr Murgatroyd. After brief tenures by Mr Zobel and Mr Aanenson, Dr D.G. James became Head of MRF from 1971 to 1982.

External factors shaping the development of the MRF programme during this period were:

(a) Prof B.J. Mason was appointed Director-General of the Meteorological Office in 1965 and, soon afterwards, transferred his Cloud Physics Department at Imperial College with some of its staff to the Meteorological Office under Mr P. Goldsmith. This department has been the principal user of MRF facilities since then.

(b) The Meteorological Research Unit located at the Telecommunications and Radar Research Station, Malvern led (after 1966) by Dr K.A. Browning. This unit was responsible for pioneering the national weather radar network we now have, and its common areas of interest with MRF were frontal dynamics and clear air turbulence.

(c) The Meteorological Research Unit at Cardington, Bedford used the tethered balloon facility there to make measurements of the structure of the atmospheric boundary layer. This unit has collaborated with MRF in studies of boundary-layer flow and turbulence in the vicinity of hills.

(d) Growing concern with atmospheric pollution in general and the acid rain problem in particular during the 1970s led to collaboration with the Central Electricity Research Laboratories (CERL), Leatherhead and the beginning of atmospheric chemistry studies at MRF.

The Hastings and Varsity aircraft were withdrawn from MRF at the end of their design lives during the late 1960s, and replaced by another Varsity and (not until 1974) by the C-130 Hercules aircraft (XV208), or 'Snoopy' as it became known after the installation of its nose probe (Fig. 1).

The case for acquiring the C-130 rested heavily on the invitation for it to participate in the international Global Atlantic Tropical Experiment (GATE) in 1975. This was the first of about a dozen international cooperative experiments (see Annex B) in which the Hercules has participated up to now.

4.1 Instrumental development

Important developments during this middle period were:

On-board data-processing system. At the beginning of this period, aircraft data was recorded manually by observers, or on charts, and the subsequent processing was also largely manual. It had been realized for some time that a radical improvement in aircraft data-process-

Figure 1. A view of the C-130 in flight. Its capacity and endurance make it ideal for atmospheric research.

ing facilities was essential if further scientific progress was to be made. The main concept was to install an on-board computer to record data from meteorological sensors on tape to be processed after the flight by ground-based computer. This computer was installed in an observer's cabin (or van) in the Hercules. This cabin protected observers in it from aircraft noise, provided real-time displays in the van and to the aircraft scientist on the flight deck, while the van itself could be removed bodily from the aircraft during periods of major servicing.

The implementation of this system was given urgency by the planned participation of the Hercules in GATE. Aircraft data had to be transferred to magnetic tape in a prescribed format for transmission to other scientific institutions involved in GATE.

A parallel development was a move away from dependence on the RAE for ground-based computer processing of data with the installation of computer systems in MRF, and virtually complete independence from RAE computing facilities was achieved by about 1980.

Inertial navigation. The installation, first on the Canberra and later on the C-130, of nose probes carrying rapid-response wind vanes linked to inertial platforms centred near the aircraft centre of gravity, made it possible to extract the aircraft position at any time, and also wind and turbulence data from which aircraft motions had been automatically removed. This development was foreseen by Shaw 60 years before.

Dropsondes. One of the first tasks undertaken by the Cloud Physics Department after its move to the Meteorologcal Office was to develop a radiosonde to be released from the Hastings aircraft. The transmitted data would then be received and stored by an on-board computer. This system was used on the Varsity aircraft in Project SCILLONIA (see below) in 1969–70. A radically improved system was then developed for installation on the C-130, and eventually used in a major project in 1987.

Cloud-physics probes. During the first decade of this period, it became possible to collect and process large amounts of cloud microphysical data in a reasonable time using advanced optical-sensing techniques developed in particular by Knollenberg, an American electronics engineer. Some of his optical probes were purchased by the Cloud Physics Dept. and installed on the C-130. They depended mainly on detecting and measuring the intensity of pulses of light scattered from cloud droplets (and later precipitation and ice particles) passing through a sensitive volume exposed to the airflow. An example of the data obtained using these probes is shown in Fig. 2.

A holographic camera was also installed to give the 'instantaneous' location and size of particles in a 0.5 litre air sample 'caught' by a laser pulse a few nanoseconds in duration. Liquid water content was measured by an advanced hot-wire device and compared with liquid water contents derived by summing over drop-size distributions obtained with the Knollenberg probes. There remained, however, considerable difficulties in assessing how representative the measurements were of the structure of cloud volumes large compared with the (very small) sampling volume of the probes.

Chemical sampling. A range of chemical sampling equipment was installed on the C-130 for use by CERL. These enabled both *in situ* measurements to be made,

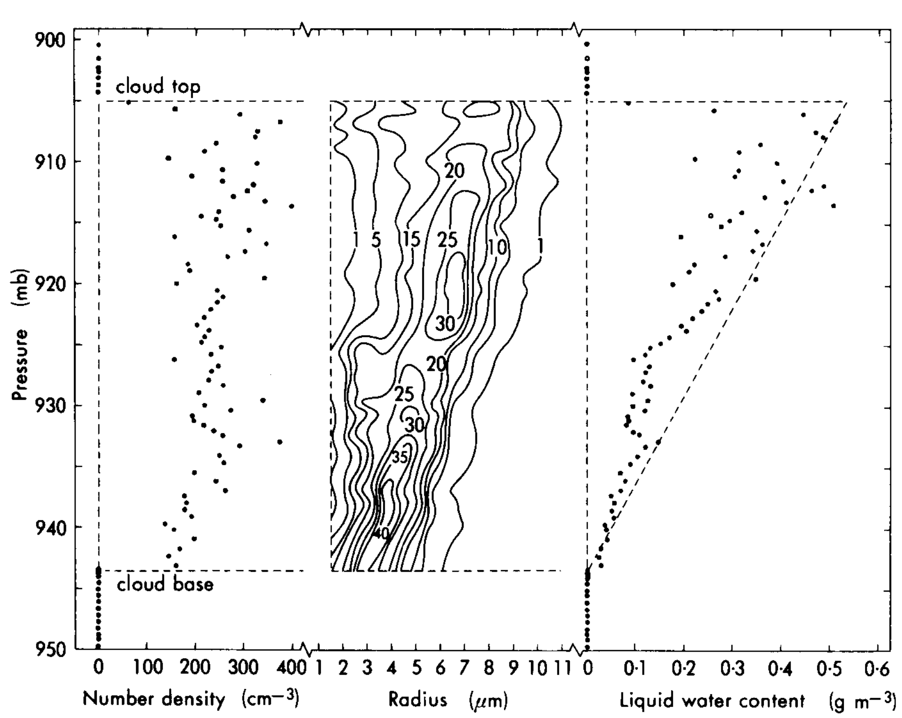

Figure 2. Profiles of the concentration and spectra of cloud droplets, and of the liquid water content through a layer of stratocumulus cloud on 19 November 1976 using an optical probe.

and samples collected for later analysis of several chemical species, particularly nitrogen and sulphur species and ozone.

4.2 Scientific work

Cloud Physics. Early in this period, the main thrust of research in cloud physics was moving away from laboratory studies and towards the interaction of the cloud microphysics with cloud dynamics. This study could only be advanced by the use of research aircraft.

The first major project SCILLONIA (based from the Scilly Isles) used dropsondes released at 5 km from the Varsity aircraft to obtain the mesoscale structure of wind, temperature and humidity within active warm-frontal zones approaching the British Isles from the Atlantic, where the system was (as yet) undisturbed by topography. A major finding of this study was the existence of organized bands of vertical ascent and descent spaced apart by about 100 km and correlated with bands of precipitation. This led to the development of a new dynamical theory of 'conditional symmetric instability' depending for its initiation upon the release of latent heat in air ascending the frontal slope.

Atmospheric turbulence. The installation of the inertial platform on the Canberra and C-130 made possible some important studies of turbulence in various meteorological contexts:

(a) Studies of the structure of the marine boundary were made to check existing marine boundary layer similarity theory and bulk aerodynamic transfer coefficients. As part of this study, the C-130 participated in the Joint Air–Sea Interaction (JASIN) experiment off north-west Scotland in 1978.

(b) In collaboration with MRU Cardington, measurements were made from the C-130 of the flow and turbulence structure around Ailsa Craig, a steep, symmetrically shaped island off south-west Scotland. Measurements were also made with a tethered balloon deployed to Ailsa Craig. This study was used to validate a numerical model of the airflow in order to tackle the very difficult problem of airflow over hilly or mountainous terrain needed urgently to improve parametrization of frictional drag of the earth in forecasting models.

(c) Studies of the structure of high-level clear air turbulence and mountain waves were made using the Canberra aircraft with the objective of improving understanding of the role of internal friction (as distinct from friction with the ground) in modifying the atmospheric circulation. Some clear air turbulence studies were made in collaboration with MRU Malvern, with the aircraft flying over a high-power Doppler radar able to detect clear air turbulence. A detachment of the Canberra aircraft was made to the Colorado mountains in 1973 to measure the vertical transfer of momentum flux by high-level standing gravity waves. This is internal drag due to the 'cog-wheel' effect of distortions of the wave shape.

Atmospheric Chemistry. A series of flights were made over the North Sea in downwind plumes emitted by a major power station to study the dispersion and chemical evolution of plume pollutants. The rate of oxidation of sulphur dioxide to sulphate was found to depend critically on the presence of cloud.

Radiative Transfer. Work in this area was relatively low-key during this period. However, the prototype flight model of the Selective Chopper Radiometer flown on the NASA NIMBUS 5 satellite was installed on the Canberra aircraft, and a study made by the University of Oxford group of the background (continuum) absorption (attributed to water vapour) across the 10–12 micron 'window' in the atmospheric infrared spectrum. The emission associated with this absorption is a significant contributor to the greenhouse effect, but has not had the 'publicity' of carbon dioxide in this regard.

During the late 1970s, the evolution of layer clouds, and particularly their interaction with radiative transfer had begun to attract attention. Fluxes of solar and terrestrial (long-wave infrared) radiation through marine stratocumulus were observed during JASIN with radiometers mounted on the Hercules and other aircraft. In this case, the fluxes observed agreed well with those generated by radiative transfer schemes.

By the end of this middle period, MRF had an international reputation, and the C-130 was in regular demand to participate in international projects.

The Canberra aircraft (WE173) was removed as part of the cuts in Government expenditure in 1981. The ability of the Canberra aircraft to provide observations in the lower stratosphere was limited to the aircraft ceiling of about 15 km. While this had been an advance on the Mosquito aircraft ceiling of about 12 km, 15 km was not adequate for comprehensive observations within most of the ozone layer — probably the most important requirement in modern environmental studies of the stratosphere. Unfortunately, there was no opportunity in 1981 of obtaining a replacement aircraft with a sufficiently high ceiling to make worthwhile advances in many investigations of the stratosphere. Accordingly, the thrust of MRF's work became concentrated on tropospheric studies during the modern period.

5. The modern period (1981–92)

With the withdrawal of the Canberra aircraft in 1981 and the retirement of Dr James in 1982, MRF entered a slightly unsettled period in that Dr Jenkins, the present Head of MRF, became (in 1991) the seventh incumbent of that post since James departed in 1982. Nevertheless, the momentum of MRF progress was not seriously interrupted. The main initiatives taken during this period (in roughly chronological order) were:

(a) By 1981, climate research was increasing in importance. When Dr Readings took over from Dr James in 1982, he was directed to upgrade radiative transfer research at MRF in view of the significance of cloud-radiation interaction to climate research.

(b) The ground-based computer at MRF was becoming obsolescent and had to be replaced to cope with the increasing data-processing, analysis and numerical modelling work being undertaken in MRF. In addition, the capacity of recently established links with the main Meteorological Office computer system at Bracknell needed expanding. The development was successfully completed by 1988.

(c) Upgrading of the airborne data-processing system and the transcription of aircraft data tapes to the ground system had again become necessary. This had achieved an acceptable level of performance by 1989.

(d) Installation of additional sensors on the C-130 continued throughout the period in response to the research requirements detailed below. The aircraft now probably carries a larger range of meteorological sensors (Figs 3 and 4) than any other meteorological research aircraft.

(e) As part of a reorganization of the structure of the Physical Research Directorate of the Meteorological

Figure 3. The operation of the meteorological sensors is coordinated by the Aircraft Scientist from the flight deck where he has a clear view through the aircraft window and can call up a graphical display of the real-time output of any sensor as required.

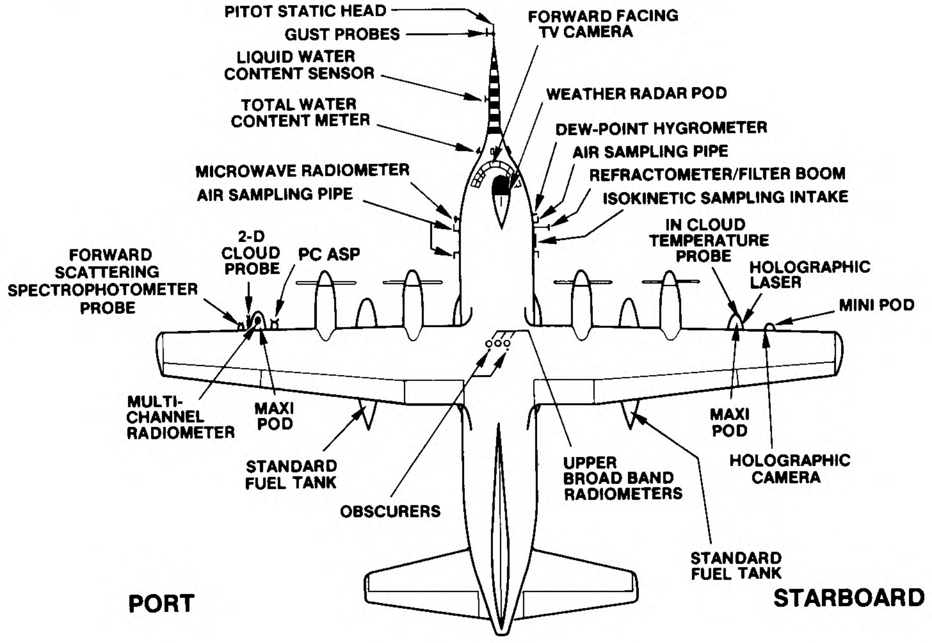

Figure 4. Plan view of the C-130, showing the location of the main meteorological sensors.

Office, the Cloud Physics Department was disbanded, but its two sections using MRF (cloud microphysics and atmospheric chemistry) were brought into the branch, but it was not until 1991 that the latter section moved to Farnborough. In addition, the advanced satellite instrumentation section of the old High Altitude Research Branch was moved to a separate unit located next to MRF, to be known as the Remote Sensing Instrumentation Branch. At the end of these moves the Meteorological Office presence at RAE had expanded from about 25 to about 75. By that time, RAE had become part of the Defence Research Agency (DRA).

Most of the work on the research topics pursued during the middle period (section 4) has continued to the present day, but with some changes of emphasis.

Radiative Transfer. Of central importance to all general circulation and climate modelling is an accurate evaluation of the contribution of radiative transfer to the distribution of heating and cooling in the atmosphere. Accordingly, the principal research objective at MRF was to obtain simultaneous measurements of the optical and physical properties of clouds and aerosol and their environment in order to improve the basis of radiative transfer schemes used in general circulation and climate models. To this end, the first few years of this period were devoted to upgrading the radiometer installations on the C-130 in the following respects:

(a) An updated version of the Oxford Selective Chopper Radiometer (SCR) — previously installed on the Canberra — was installed on the starboard wing of the C-130. This radiometer was designed to sense radiation in 16 channels distributed mainly in the atmospheric window region (10–12 microns) and the near solar infrared spectrum.

(b) Upward- and downward-facing total solar (pyranometers) and terrestrial (pyrgeometers) radiative-flux sensors and their associated data-processing were upgraded.

This equipment was operational by 1987, and the following studies made:

(a) There is a balance of evidence that the observed absorption of solar radiation in layer clouds is generally higher (particularly in the near infrared), and the albedo (reflectivity) of cloud is less than model predictions. In addition, the rate of increase of albedo with fractional cloud cover of broken cloud fields is slower than model predictions. Several theories have been advanced to account for these discrepancies, which remain unresolved. However, the observational base for this study is still inadequate. In this regard, participation of MRF in FIRE (the First International Satellite Cloud and Climatology Regional Experiment) in California in 1987 was an important step.

(b) A long-standing area of uncertainty is the cause and amount of background (continuum) absorption and emission of infrared radiation stretching across the 8–13 micron window, and is attributed to water vapour. This is about 10% in temperate latitudes, but is about 50% in tropical latitudes and is a significant contributor to the greenhouse effect. The SCR was used in a detachment to Dakar, Africa to obtain much-needed observations of the tropical continuum absorption, found to be about 30% higher than existing theoretical models. Further flights have been made around the United Kingdom and over the Mediterranean, and are being analysed.

(c) A start was made on the difficult study of cirrus cloud, limited (at MRF) by the inaccessibility of the higher cirrus cloud by the C-130. MRF participated in a European International Cirrus Experiment in 1989 in parallel with other aircraft with higher ceilings. While some rudimentary knowledge of the gross optical properties of cirrus cloud are beginning to emerge, problems of methods of measurement and their interpretation have still to be resolved, and are likely to absorb most effort in this area for some time to come.

Mesoscale Frontal Dynamics. A major collaborative field study — FRONTS 87 — with French research groups, using ground radar and aircraft deploying dropsondes (Fig. 5) was based at Brest.

The main objective was to obtain an improved dynamical understanding of synoptic — (100–1000 km), mesoscale — (30–100 km) and smaller-scale interactions within systems containing cold fronts. Some principal findings were:

(a) Thermal wind balance along a front is roughly maintained on scales greater than 50 km, but instabilities occur on smaller scales.

(b) Direct evidence of conditional symmetric instability, first thought to be associated with rain bands in warm fronts observed in SCILLONIA.

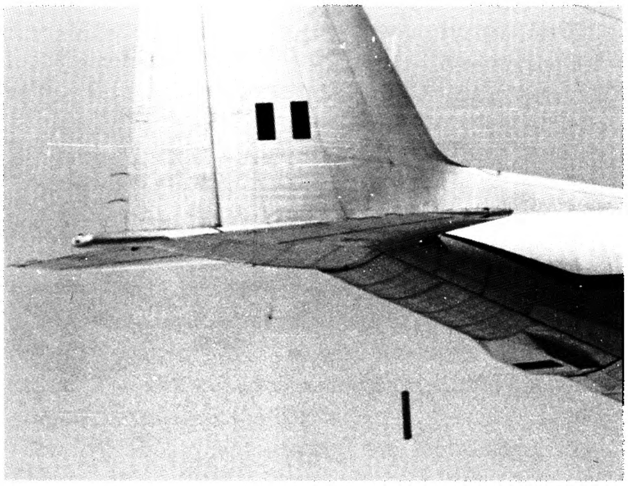

Figure 5. A dropsonde immediately after ejection from the horizontal slot to the right of the sonde. A small parachute is deployed from the sonde a few seconds after release

(c) Frontal development is significantly influenced by regions of condensation and evaporation — particularly of snow and ice particles.
(d) The importance of the role of some conservative dynamic variables (particularly potential vorticity) was clarified.

The data collected during FRONTS 87 (e.g. Fig. 6) has given a fresh impetus to the difficult study of factors controlling the mesoscale structure of fronts, and a successful follow-on study (FRONTS 92) promises to be equally rewarding.

Cloud Physics. Observations and numerical modelling of the water and heat balance of marine stratocumulus was the main theme of this period. Aspects receiving particular attention were: entrainment of dry, relatively warm air into the cloud at cloud top; interaction of the cloud evolution with radiative transfer; and the formation and precipitation of drizzle formed in thicker cloud layers. Successful field-studies were made as contributions to the programmes of FIRE and (recently) ASTEX (Atlantic Stratocumulus Transition Experiment).

A related study of nocturnal stratocumulus was also made from a tethered balloon at Cardington using some of the cloud physics probes normally operated from the C-130. Finally, some case-studies of sea fog forming in early summer off the north-east coast of Scotland were made using the C-130, and the results interpreted as an extension of a numerical model of stratocumulus cloud with its base on the sea surface. Insight into the fog as a self-maintaining, persistent system was gained.

A study was made of the microstructure of ice particles in light precipitating cloud. This involved collaboration of the C-130 with the Rutherford Appleton Laboratory using their dual polarization radar at Chilbolton Observatory. The ratio of horizontally and vertically polarization reflectivity of the cloud observed by radar was related (with some success) to the physical properties of the ice crystals observed from the C-130.

Atmospheric Turbulence. Further projects to investigate the effect of hills on airflow were made over the hills of South Wales using the C-130, tethered balloon and other surface observations. Other international projects were joined to measure the structure of organized convection over the North Sea (KONTUR) and humidity exchange over the sea.

Satellite Meteorology. MRF's involvement in aspects of satellite meteorology have expanded in two main areas; the evaluation of sensors to be installed on satellites, and the provision of ground truth measurements from the aircraft for comparison with satellite measurements at the same time in the same area (known as calibration–validation or 'cal–val' activities).

In the first area, an evaluation has been made of the microwave radiometer (AMSU-B) mounted on the C-130 to measure water-vapour emission in two wavelengths. This radiometer is due to be installed on a NOAA satellite in 1994. The MCR was used during the detachment of the C-130 to Dakar in 1987 to test the principles of the Along Track Scanning Radiometer (ATSR) developed for the ERS-1 satellite.

Cal–val activities have concentrated on the European Space Agency ERS-1 satellite launched in 1991. In September 1991, wind measurements over the sea off the west coast of Norway were made to validate wind algorithms derived from ERS-1 scatterometer data (Fig. 7).

Shortly afterwards, measurements of sea surface temperature (SST) were made from the C-130 in the South Atlantic for comparison with ATSR. (This detachment also provided measurements of the effect of diffuse and direct solar radiation on the dust veil from Mt Pinatubo.)

Atmospheric Chemistry. Although work on 'acid rain' is no longer a major topic (however, sulphur dioxide plumes are still tracked to compare against the

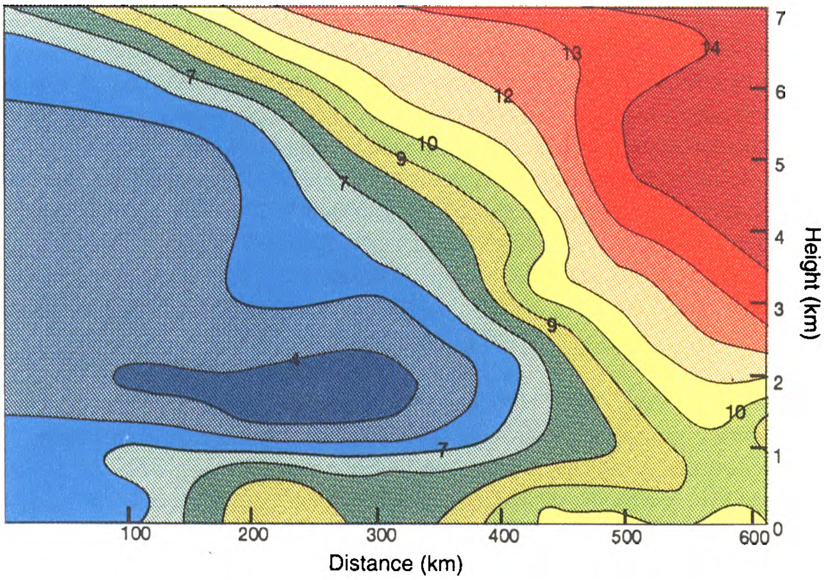

Figure 6. A cross-section of a cold front from FRONTS 87 revealing the fine details of humidity (as wet-bulb potential temperature in °C).

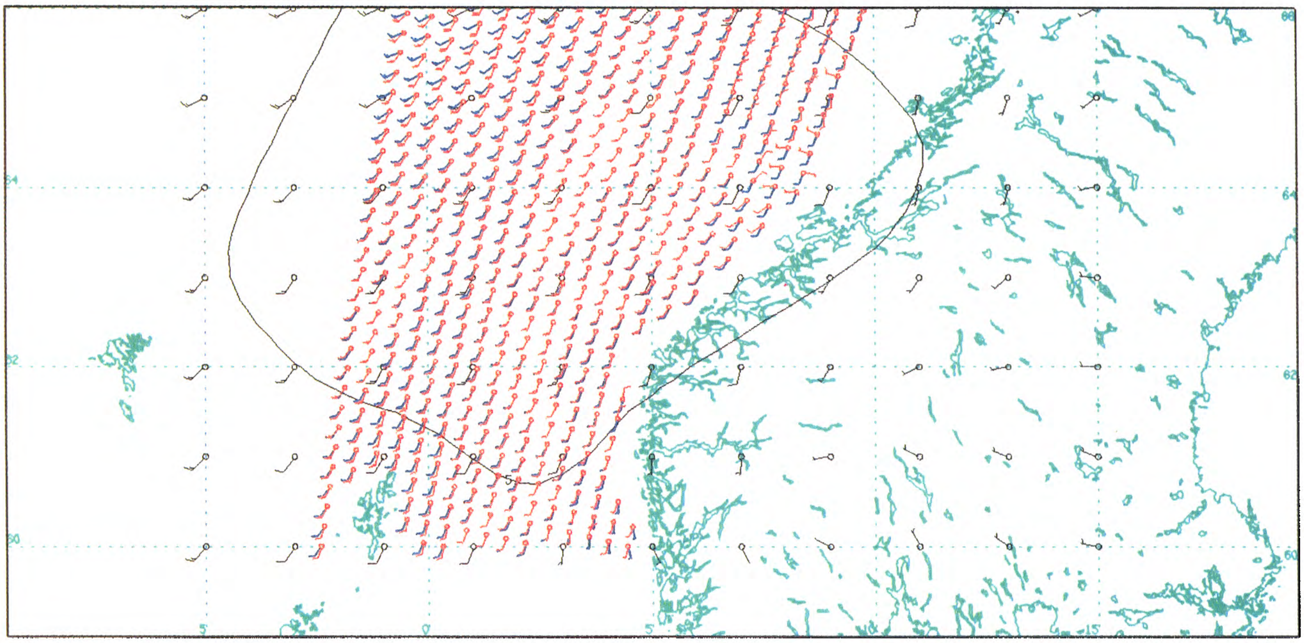

Figure 7. Low-level winds (black vectors) measured from the C-130 off the Norwegian coast are compared with those (red vectors) derived from the scatterometer on the ERS-1 satellite.

predictions of the Met. Office's Nuclear Accident Model), other areas of atmospheric chemistry have expanded. The increasing concentration of ozone in the troposphere, and the realization of its importance as a 'greenhouse' gas has highlighted the need to understand its generation from pollutants such as nitrogen oxides, hydrocarbons and carbon monoxide. The contribution from the stratosphere is also not well known. By 1990, a wide range of chemical samplers had been installed on the C-130 in conjunction with the University of East Anglia and KFA Julich in Germany to tackle this problem.

The chemical instrumentation was brought into use in an unexpected way in March 1991 after the Gulf War had left several hundred oil wells alight in Kuwait. Model calculations that the environmental impact would be locally severe but regionally and globally insignificant were supported by the first airborne measurements made by MRF of chemical and radiative properties of the smoke plume a few weeks after the end of the war. US and German aircraft followed shortly after.

6. The future

Following a major service in 1992, the C-130 has a very full diary for the following two years, with involvement in international programmes in air–sea interaction (TOGA-COARE), atmospheric chemistry (OCTA and NARE) and clouds and radiation (EUCREX). NERC has established a post of Aircraft Officer at MRF in order to enhance the use of the C-130 by the university community in collaborative research programmes with MRF.

There is little doubt that the requirement for a platform for *in situ* measurements of atmospheric processes will continue for the foreseeable future, although the particular emphasis will change. Although weather forecasting and climate prediction models can be improved by greater time and space resolution, this must be accompanied by a better representation of physical processes, many of which are still poorly understood. The main task of MRF continues to be the execution of basic research of atmospheric processes and publication of the results, but with increasing emphasis on the timely incorporation of the results into atmospheric models. In addition, the need for satellite instrumentation development, with the subsequent validation of space-borne measurements, is likely to expand as a greater proportion of global data comes from satellites.

Finally, following the announcement in 1991 that routine military flying will cease from the Farnborough airfield in 1995, hard decisions will have to be made about the future location of MRF. A return to the MRF birthplace at Boscombe Down is one possibility.

Acknowledgements

The author is indebted to Dr G.J. Jenkins, Head of Meteorological Research Flight, for his cooperation, and for contributing sections 5 and 6, photographs and Annexes of this paper. The author also thanks Dr A.W. Brewer and Dr R.J. Murgatroyd for their comments on, and suggested additions to, a draft of this paper.

ANNEX A

Aircraft of the Meteorological Research Flight

2 x Spitfire + Boston (original establishment)	
Hudson	
Flying Fortress	
Mosquito	
Mosquito	VL621
Mosquito	RG248
Halifax	ST817
Halifax	ST796
Hastings	TG618
Hastings	TG619
Canberra B2	WJ582
Varsity	WJ906
Canberra PR7	WE173
Varsity	WF425
Hercules	XV208

Assistant Directors Meteorological Office (Meteorological Research Flight)

1942	Dr A.W. Brewer
1946	Dr R. Erith
1951	Mr H.C. Shelland*
1951	Dr R.J. Murgatroyd
1962	Mr R.F. Zobel
1967	Mr C.J.M. Aanensen
1971	Dr D.G. James
1982	Dr C.J. Readings
1984	Dr R. Pettifer
1985	Dr W.T. Roach
1988	Dr P. Jonas
1989	Dr S. Mattingly
1990	Mr W.D.N. Jackson*
1991	Dr G.J. Jenkins

* Acting Heads between main appointments

Officers Commanding Meteorological Research Flight

1948	Flt Lt Tomlinson
1952	Flt Lt N.C. Thorne
1953	Flt Lt H. Baker
1955	Flt Lt S.F. Thomas
1958	Flt Lt D.A. Cree
1962	Flt Lt A. Abczynski
1966	Flt Lt G.F. Holbrook
1969	Sqn Ldr G.F. Holbrook
1970	Sqn Ldr N. Lamb
1977	Sqn Ldr M.J. Bibby
1980	Sqn Ldr M.K. Allport
1983	Sqn Ldr M.J. Stokes
1985	Sqn Ldr D. Curteis
1988	Sqn Ldr S.R. Roberson
1991	Sqn Ldr M. Lampitt
1992	Sqn Ldr H. Burgoyne

ANNEX B

Aircraft campaigns and detachments

Year	Aircraft	Base	Projects
1952	Canberra	Khartoum	Humidity
1957		Malta	Latitudinal
		Nairobi	variations of temperature
1960		Nairobi	and humidity
1961		Malta	at high levels
1962		Bodø	Ozone also measured after 1959
1965	Canberra	Singapore	Vertical extent of Cb
1970	Canberra	Malta	Sea surface temperture
1970	Varsity	St Mawgan	SCILLONIA: warm fronts
1973	Canberra	Denver	WAMFLEX: mountain waves
1974	Hercules	Dakar	GATE: tropical convection
1975	Canberra	Dakar	Tropical radiation
1978	Hercules	Gibraltar	measurements for satellites
1979		Dakar	and air sampling
1977–80	Canberra	Lossiemouth	Lat/Seasonal humidity cross-sections
1978	Hercules	Machrihanish	JASIN: air–sea interaction
1978		Gibraltar	Meteosat
1979		Dakar	Meteosat
1980		Gibraltar	Mount St Helens volcanic dust sampling
1981		Europe	KONTUR: turbulence over the sea
1983		Bermuda	CAMEX: microwave sounding trials
1983		Machrihanish	NARTHEX: frontal structure
1985		Bodø	PLEXUS: polar lows
1987		Farnborough	HEXOS: humidity over the sea
1987		San Diego	FIRE: marine stratocumulus
1987		Farnborough	FRONTS87: frontal dynamics
1988		Dakar	WATER: water vapour continuum
1989		Farnborough	ICE89: International Cirrus Experiment
1990		Trondheim	ERS-1 instrument development
1990		Oulu	SAAMEX: microwave
1990		Crete	MASTEX: water vapour continuum
1991		Farnborough	TOASTE: strat–trop exchange
1991		Bahrain	GULFEX: Kuwait oil smoke plume
1991		Farnborough	CHEMEX: atmospheric chemistry
1991		Trondheim	RENE1: ERS-1 winds comparison
1991		Ascension Is	FATE: ERS-1 SST comparison
1991		Trondheim	RENE2: ERS-1 winds comparison
1992		Farnborough	FRONTS92: cold front waves
1992		Azores	ASTEX: marine stratocumulus

The PAMPA flights

R.J. Ogden
Silverwood Drive, Camberley

Summary

To mark the 50th Anniversary of the wartime weather reconnaissance missions flown with Mosquito aircraft, these operations and the background to them are described.

1. Introduction

With the aim of improving the standard of weather forecasting, meteorological reconnaissance flights were made regularly during the 1940s to obtain observations from the data-sparse areas of the North Sea and eastern Atlantic. Tracks, schedules and operating procedures for these flights were all standardized and many details have been published (e.g. Air Ministry (AHB) 1954, Kraus 1985, Ogden 1985, Yates 1986, Rackliff 1987). But only passing references (Rackliff 1987, Ratcliffe 1987) have appeared in meteorological publications about a quite different type of weather reconnaissance; this was that made over enemy territory primarily for operational rather than synoptic reasons. Those missions were known as PAMPA (Photographic and Meteorological Photography Aircraft) flights*.

2. The formation of 1409 (Met) Flight in RAF Bomber Command

1401 (Met) Flight based at Mildenhall was responsible for obtaining vertical profiles of temperature and humidity; by mid 1941 it was equipped with Gladiators for the famous THUM (Temperature and HUMidity) flights and with Spitfires for the complementary PRATA (PRessure And Temperature Ascent) flights. During August of that year two additional Spitfires were allocated to the Flight specifically to undertake 'long-range reconnaissance over enemy and enemy-occupied territory. Tracks laid on as required'. (Meteorological Office Archives); this was the new PAMPA role. In late October the Flight moved to Bircham Newton where 1403 (Met) Flight was based to operate the RHOMBUS flights over the North Sea; in January 1942 the two Flights were amalgamated and all the operations were then moved to the satellite airfield at Docking (Bowyer 1979). The PAMPA Spitfires were replaced during the following month by two Mosquito IV aircraft which carried crews of two and had an endurance of about 4.5 hours (Meteorological Office Archives). Operational PAMPA sorties using the Mosquitos probably started in May 1942 (Rackliff 1987). With Gladiators, Spitfires, Hudsons and Mosquitos for the THUM, PRATA, RHOMBUS and PAMPA flights respectively, 1401 (Met) Flight by then had very wide responsibilities and not surprisingly on 1 August 1942 it was upgraded to become 521 (Met) Squadron (Bowyer 1979).

*A new series of so-called PAMPA flights was operated from Waddington between 1946 and 1949 by 61 Squadron, Bomber Command, using Lincoln aircraft; these were not comparable with the wartime missions and are not covered in this article.

To meet the need for more operational weather reconnaissance as the RAF Bomber Command offensive gathered momentum, at the end of September the number of Mosquitos in the Squadron was increased from two to eight (Meteorological Office Archives). Not long before this, the new Pathfinder Force (PFF) had been formed in Bomber Command under Gp Capt (later Air Vice-Marshall) Donald Bennett. He had strong views about the importance of operational weather reconnaissance, especially in relation to PFF tasks, and gently tried to bring the PAMPA Flight under his command (Bennett 1958). That did not formally come about until 1 April 1943 when the eight Mosquitos of 521 (Met) Squadron were hived off to form a new 1409 (Met) Flight based at one of the original PFF airfields of Oakington, near Cambridge (see Fig. 1). After converting to Mosquito IXs, the Flight moved to Wyton in January 1944 and remained there for the rest of the War (Bowyer 1979); one Mk. IX aircraft was retained for low-level sorties, but the others were subsequently exchanged for six Mosquito XVIs, painted in PR (photo-recce) blue and equipped with pressurized cabins. All these later aircraft were fitted with extra fuel tanks, both internally and as drop tanks under each wing; this increased the endurance to nearly 6 hours and the extreme range to 2000 miles or so. But it should never be forgotten that the PAMPA Mosquitos carried no bombs and had no defensive weaponry (Currie 1983).

3. Crew selection

Despite their lack of guns for self-protection, the PAMPA crews were often ordered to penetrate deep into Germany, even in broad daylight with no cloud cover. To minimize the chances of fighter interception they naturally flew high (e.g. 30 000 ft or more) and fast whenever possible, but the Me 262 jet fighter which the Luftwaffe brought into service late in the War could outpace the Mosquito, and only the superior manoeuvrability of the latter, allied to a high degree of pilot skill, could then keep them out of trouble (Bennett 1959).

The role of the navigator was equally vital. He had personally to plan the route (see below), then with the aid of Gee and radar monitor the aircraft's progress, advising the pilot of course changes and computing winds *en*

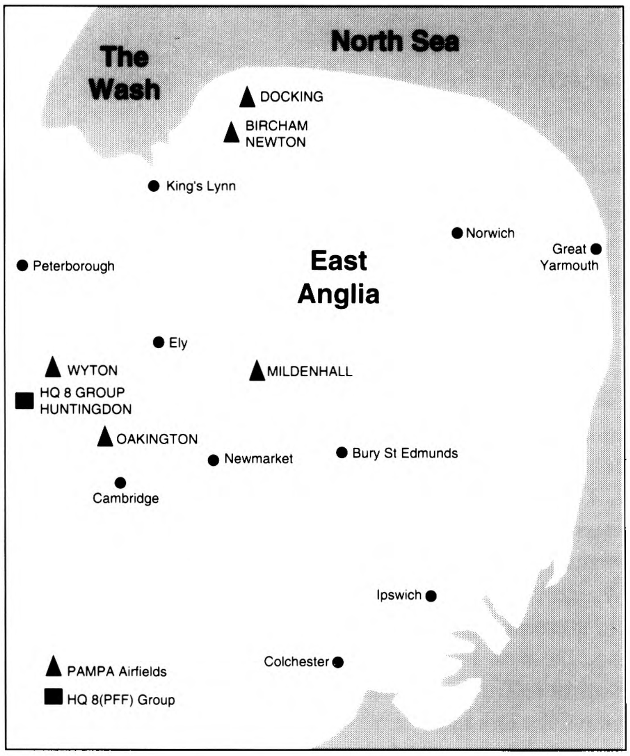

Figure 1. East Anglian locations mentioned in the text.

route; he was also responsible for making the weather observations, a task for which he was specially trained. In these circumstances, it is not surprising that the PAMPA crews were chosen with great care. All the crews in PFF were selected from volunteers, but for 1409 (Met) Flight there were additional constraints; only those who were both commissioned and had been awarded above average ratings at the Mosquito OTUs were considered (Currie 1983).

4. Organization of PAMPA sorties

Having decided on a probable target, and in the light of discussions with his Chief Meteorological Officer (M.T. Spence), the C-in-C of Bomber Command might elect to order a PAMPA flight as an essential preliminary before tactics for PFF and the main force were finalized. In total contrast to the procedures for the regular scheduled meteorological reconnaissance flights, PAMPA sorties might be dispatched at short notice anywhere, at any time, and had to be completed without delay. The required task was detailed to 8 (PFF) Group for action by 1409 (Met) Flight. The navigator of the duty crew then had to prepare his own flight plan to cover the given objectives, avoiding well-defended areas whenever possible and also incorporating sundry changes of course both to mask the specific area of interest and to make it more difficult for fighters to intercept the aircraft. On occasions, the AOC of 8 Group also aranged PAMPA flights to meet specific requests from other Commands or from other services such as the USAAF. On a particular day a single flight might suffice, but as many as four or even more sorties were sometimes mounted within a 24-hour period (Bennett 1958). At full strength 1409 (Met) Flight had 10 crews, and unless formally stood down duty crews had to be ready to carry out any assigned task immediately; moreover, stand-by crews and aircraft were always available so that if an aircraft became unserviceable before or shortly after take-off, a replacement could be airborne very quickly, using the flight plan prepared by the original crew (Currie 1983).

The detailing of the task was strongly influenced by the meteorological input at Bomber Command. Sometimes the objective was to provide a general survey of a broad area which included the target. More usually however, the PAMPA mission was to make detailed appraisals of particular significance for the raid being planned; the emphasis was then primarily on cloud conditions. For example, the zone just behind a cold front is often a very suitable location for clear identification of a target, but it is essential to know whether the front concerned is indeed immediately followed by a significant cloud clearance and if so exactly where the front is, whether it has any waves on it and how steadily it is moving (Ratcliffe 1987).

From late 1943 onwards, the operations of 1409 (Met) Flight and indeed other PFF formations were greatly assisted by the availability of FIDO, the first installation of which was at Graveley, another of the original four PFF airfields. The first landing in fog using FIDO was made there by Bennett himself in July 1943, and other nearby airfields were equipped with FIDO later that year, including Downham Market which became an 8 Group station in March 1944 (Ogden 1988). Knowing that aircraft could be landed safely in fog meant that PAMPA sorties could be dispatched when, without FIDO, they would have been grounded.

5. Meteorological procedures

Having fought hard to bring the PAMPA Flight under his command, AVM Bennett naturally took a keen interest in its work, and he maintained a close liaison with M.J. Thomas, his Group Meteorological Officer. Each sortie was given detailed objectives not only on where to go but also on what to look out for. The making of comprehensive cloud observations was paramount — types, amounts, height of tops and often of bases as well. To assist the navigator he was provided with a hand-held camera which could be used looking forward through the windscreen to photograph interesting cloud features such as cumulonimbus. The aircraft might then deliberately fly into Cb clouds at various levels to determine the degrees of turbulence and airframe icing which might be highly relevant for the forthcoming operation. Although it is normally safer when flying at higher altitudes, the aircraft often made descents in key areas to measure the heights of cloud tops and bases and to obtain vertical temperature profiles (Currie 1983). The computation of winds was a routine procedure and accuracy here clearly depended on the efficiency of the navigation.

Photograph by courtesy of the Royal Air Force Museum

Figure 2. De Havilland Mosquito P.R. XVI

On return to Oakington or Wyton, the navigator reported immediately on a scrambler telephone to the 8 Group Met. Office at Huntingdon who passed on the information to HQ Bomber Command and also prepared a summary report for transmission to ETA (the Met. Comms Centre at Dunstable); this latter text was subsequently disseminated on the meteorological teleprinter broadcast to all the Bomber Command outstations.

Although the majority of PAMPA operations were pre-attack sorties that reported to base before the main force took off, sometime after PFF introduced the procedure whereby a Master Bomber controlled the attack over the target (a practice that started late in 1943). 1409 (Met) Flight also flew additional missions some 30 minutes ahead of the PFF target markers; the PAMPA pilot then gave an up-to-date weather report for the target area directly by radio to the Master Bomber or his Deputy (Currie 1983).

6. Postscript

To forecasters at Bomber Command outstations between 1942 and 1945, the PAMPA.reports on the teleprinter broadcast provided most welcome factual information to clothe the bare bones of the operational forecasts we received and on the basis of which we had to brief the main-force crews. But their primary contribution was at the heart of the operational planning at Group and Command level. The last words should be left to AVM Bennett: '1409 (Met) Flight never hesitated and never failed to do their job with absolute reliability and constancy. The danger was extreme and it was a most nerve-wracking job for the crews, (yet) in the final analysis their losses were extremely low, although not quite as low as in the rest of PFF.'

References

Air Ministry (Air Historical Branch), 1954: The Second World War 1939–1945: Meteorology. (Unpublished copy available in National Meterological Library, Bracknell.)

Bennett, D.C.T., 1958: Pathfinder. Frederick Muller

Bowyer, M.J.F., 1979: Action Stations. Vol. I, Wartime military airfields of East Anglia 1939–1945. Cambridge, Patrick Stephens.

Currie, J., 1983: Mosquito Victory. Goodall Publications.

Kraus, E.B., 1985: How the meteorological reconnaissance flights began. *Meteorol Mag*, **114**, 24–30.

Meteorological Office Archives, ...: History of Meteorological Reconnaissance Flights. (Unpublished, undated papers probably written in the late 1940s.)

Ogden, R.J., 1985: Meteorological Reconnaissance Flights. *Meteorol Mag*, **114**, 108–113.

—,1988: Fog dispersal at airfields, Parts 1 & 2. *Weather*, **43**, 20–25 and 34–38.

Rackliff, P.G., 1987: Meteorological Reconnaissance Flights. Meteorology and World War II, Vol. I, pp. 1–13. Royal Meteorological Society.

Ratcliffe, R.A.S., 1987: Bomber Command Upper Air Unit. Meteorology and World War II, Vol. I, pp. 46–57. Royal Meteorological Society.

Yates, J.B., 1986: Wartime long range meteorological flights. *Weather*, **41**, 61–62.

551.511.3:37

A modern tool for teaching dynamic meteorology

M.J.M. Saraber, T.H. The* and L.J.M. Kroon
Wageningen Agricultural University, The Netherlands

Summary

A problem in teaching dynamic meteorology is that solutions to the dynamic equations of atmospheric motion are not simply obtained. A user-friendly software package has been developed, which makes it possible to construct approximate solutions to the equations in a step-by-step way, which then can be studied and understood. The package runs on Apple Macintosh personal computers.

1. Introduction

One of the fundamentals of modern meteorology and weather forecasting in particular is the understanding of synoptic-scale dynamics of the atmosphere. This understanding is based on the combination of theoretical knowledge and its application to real weather situations. From the educational point of view this can be achieved by constructing solutions of the relevant equations for real weather situations, which then can be studied and understood. It is the construction of realistic solutions which is such a difficult problem. The reason for this lies mainly in the highly complicated nature of atmospheric dynamics. Solving the dynamical equations for a fluid in motion on a rotating sphere is a very difficult task indeed.

There are several ways of approaching the problem. One way is to try and find analytic solutions, which are rather easy to understand. To obtain such solutions, however, one has to simplify the equations rigorously. This results in the so-called textbook solutions, which have almost no link with real weather situations. This approach, therefore, is only useful to a very limited degree.

A different way is to try to construct more-realistic solutions by computational methods and to study these. This is done nowadays and the equations are solved numerically. This has led to the advanced, but complicated, numerical models of the atmosphere, which run on supercomputers every day. The problem is that these models are mathematically complicated and distract the attention from the dynamical (i.e. meteorological) problem towards the numerical (i.e. mathematical) problems one has to solve. Also, from the point of view of the physics of the atmosphere, these models are very complex. They tend to generate only final results of all the complex atmospheric processes together, making it almost impossible to study certain isolated dynamical problems. These models, even the more simple ones of the early days of numerical weather prediction, tend to obscure rather than to increase the understanding of synoptic-scale atmospheric dynamics and therefore are of almost no use for educational purposes. To this must be added the fact that most of these numerical models need large computers to run and are difficult to handle in practice. Therefore it is understandable that using these models as tools in education, mostly results in frustration both with students and teachers.

Particularly in the 1940–60s, however, when almost no computing capacity was available, many manual methods were developed, resulting in approximate but rather realistic solutions of the equations. Even today these methods are of great value for the understanding of synoptic-scale atmospheric dynamics, because the solutions are constructed in a step-by-step way and can be studied and understood quite well. The drawback of these methods, however, still is the amount of work needed to produce practical results. This not only distracts the attention from the meteorological problem, but it makes it almost impossible to obtain these results in a reasonably short time. For these reasons, they are not directly suitable for educational purposes.

2. Looking for a remedy

From the educational point of view the situation sketched above is rather unsatisfying. There is a need for new educational tools, which can help to bridge the gap between teaching theory and application of the theory in real weather situations.

What is needed, is a combination of theory and a transparent step-by-step method to do the necessary calculations, which can be understood and easily handled by the students. If one also could present the results of the calculations graphically and apply the method to real weather situations, one could expect to have made a major step forward in explaining and understanding the dynamics of the atmosphere.

It is at this point that personal computers come into view. These machines nowadays combine calculating power with the possibilities of graphical (and alphanumerical) presentation, both on screen and printer. Add to this the fact that these machines are rather cheap and easy to handle, and it is clear that personal computers have the potential to serve as a tool to close the gap between theory and practice.

* Present affiliation: Royal Netherlands Meteorological Institute (KNMI), de Bilt, The Netherlands.

3. A new tool

For the purpose of teaching dynamic meteorology, a user-friendly software-package has been developed at the Department of Meteorology of Wageningen Agricultural University. At the time the package took approximately a year to develop and runs on Apple Macintosh personal computers, but would probably take less time now. 'User-friendly' means that students do not have to do any programming themselves and that they do not have to bother about computational problems.

The one thing students do have to bother about is how to solve the dynamical (i.e. meteorological) problem in a step-by-step way. In practice they have to work out for themselves which equations should be solved and in what order. The computer then does the calculating work.

The package is mouse-menu driven and the essential part of it is a formula parser, which can be accessed by means of a worksheet, in which the formula one wants to calculate has to be typed in. Essential for solving synoptic-scale dynamical problems of the atmosphere, is the necessity to solve the equations for a large number of points, that is, one needs to calculate fields rather than point values. Besides, one needs to calculate derivatives in space, for which we need values at several locations.

Calculations, therefore, are automatically performed on a grid and the values at the grid-points together represent the field which is required. The grid is polar stereographic, covering Europe and a large part of the North Atlantic Ocean. It contains 30 × 18 grid-points and the grid-point distance is 300 kilometres.

The calculation of derivatives in space is preprogrammed in the package and can be performed easily by using the relevant mathematical symbols, which can be accessed by typing a certain key-combination. To link the calculations to real weather situations, basic fields, such as height of pressure levels, temperature at pressure levels, etc. from the ECMWF atmospheric model are used, but basic fields from other sources could be used instead.

Fig. 1 shows the worksheet, in which the equations one wants to evaluate, can be typed in as algebraic formulas. This done in the 'Equation-window'. Capital letters are used to indicate variables (i.e. fields). Derivatives are indicated by means of their mathematical symbols. These are shown in the left area of the worksheet, together with some much-used symbols in meteorology (u_g and v_g stand for the geostrophic wind components, ζ for vorticity, Φ for geopotential height, f^{-1} for the inverse of the Coriolis parameter and ω is the vertical velocity in pressure coordinates). They can be accessed by simple key-combinations. Some basic variables (like the Coriolis parameter f and the mapfactor m) and constants (like the acceleration of gravity g) are available too.

The equations which are evaluated are also shown in the larger window in the middle of the worksheet. This makes it possible to check on errors in the formulas, made by the students. In the educational process this is an important feature of the program.

In the window in the upper right corner of the worksheet, one has to type in the pressure level at which the calculations have to be performed. One can choose from a number of (standard) pressure levels. The date and time (UTC) of the weather situation which is studied have to be chosen too. By typing in this date and time, ECMWF data for this time become available.

In the bar at the top of the worksheet main-menue options are shown. These options give access to presentation, file-handling, etc.

4. Example

Figs 1–4 show a typical example of how the package can be used. Suppose one is interested in the development of mid-latitude cyclones. From theory it follows that temperature advection and vorticity advection play a dominant part in this process. Thus one is interested in calculating these quantities in a particular situation. For the example the storm of 25 January 1990 was chosen. First of all, and this is essential in the process of teaching and learning, students have to work out, step by step, how these quantities can be calculated from the basic ECMWF fields, in this case from the height of pressure levels. Thus, the problem first has to be analyzed and the relevant equations written down in the correct order.

In the example one starts with calculating the geostrophic wind components (u_g and v_g) from the height of the relevant pressure levels, in this case 500 hPa. This height-field is indicated by the letter 'Z' and linked to the file ZZ0500_900125_12, which contains the ECMWF data. The formulas are typed in and calculated. Next the temperature field is constructed by subtracting the heights of two pressure level, resulting in the thickness of the atmospheric layer, which is proportional to the mean temperature of the layer (this is all basic theory). In this case the thickness of the layer between 500 hPa and 1000 hPa is calculated, indicated by 'T'. The height of the 1000 hPa level is given by the field 'H'. This field is linked to the file ZZ1000_900125_12, containing the ECMWF data. Now thickness (temperature) advection is the internal product of the wind vector and the gradient of the temperature. The thickness-advection, indicated by 'A', can now be calculated.

Similar to the calculation of the temperature and temperature-advection, vorticity and vorticity-advection are calculated.

The calculated equations are visible in the large window, and the formula which has been calculated last is also visible in the 'Equation-window'. The calculated fields can be presented on the screen and then printed. It is possible to present (and print) different fields together. Fig. 2 shows the 500 hPa height-field together with the calculated geostrophic wind vectors. Fig. 3 shows the 1000–500 hPa thickness field together with the calculated thickness (temperature) advection. Fig. 4 finally shows the 500 hPa field, vorticity contours and regions with positive vorticity-advection (these regions are shaded). In principle the whole operation can be done in a rather

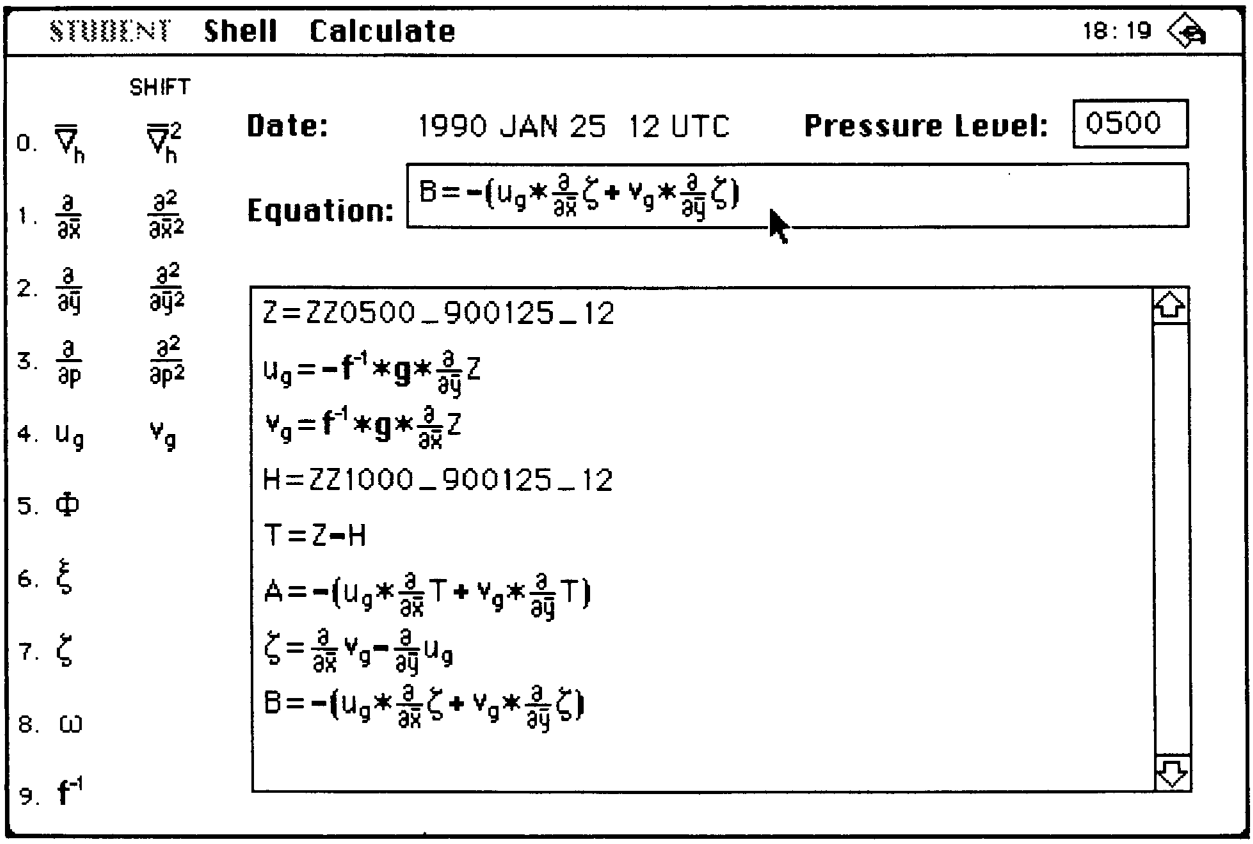

Figure 1. Worksheet, showing the windows for the equations, the pressure level and the large window with the calculated formulas. The mathematical symbols which can be used in the formulas are shown in the left-hand area of the worksheet. In the bar at the top of the sheet, options of the main menu are shown. The equations which had to be calculated to solve the problem of the example are shown in the large window. The last equation which was calculated, is also shown in the 'equation-window'.

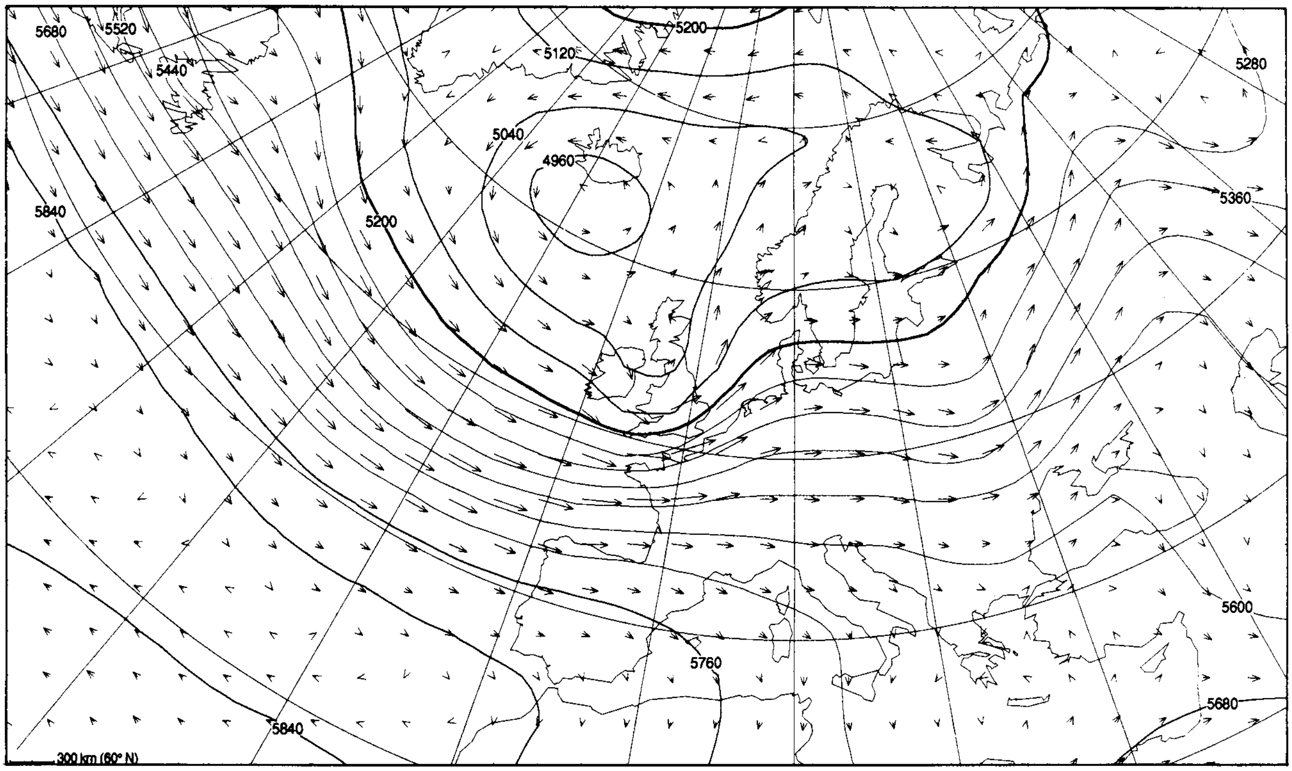

Figure 2. Results of the example, showing the heights (m) of the 500 hPa level together with the geostrophic wind field (arrows). This figure also shows the area covered by the grid.

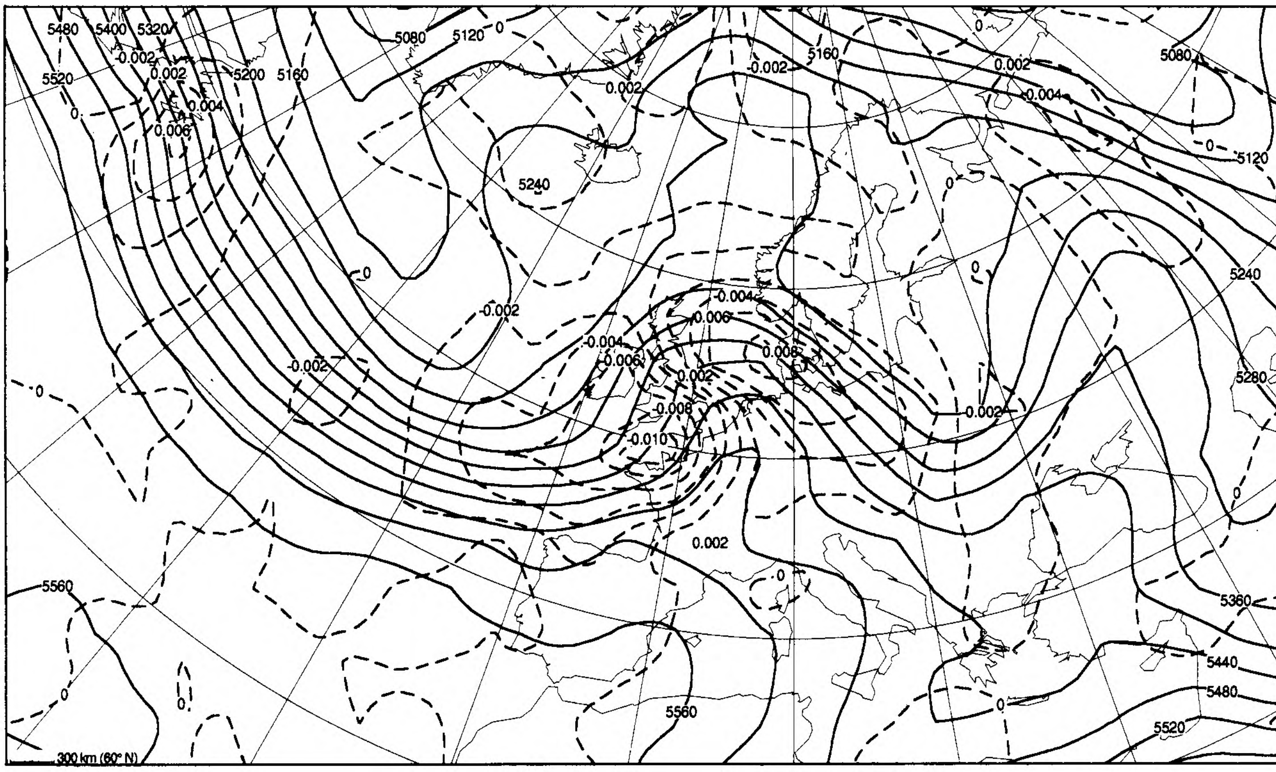

Figure 3. Results of the example, showing the 1000–500 hPa thickness field, together with thickness-advection (m s^{-1}) dashed lines.

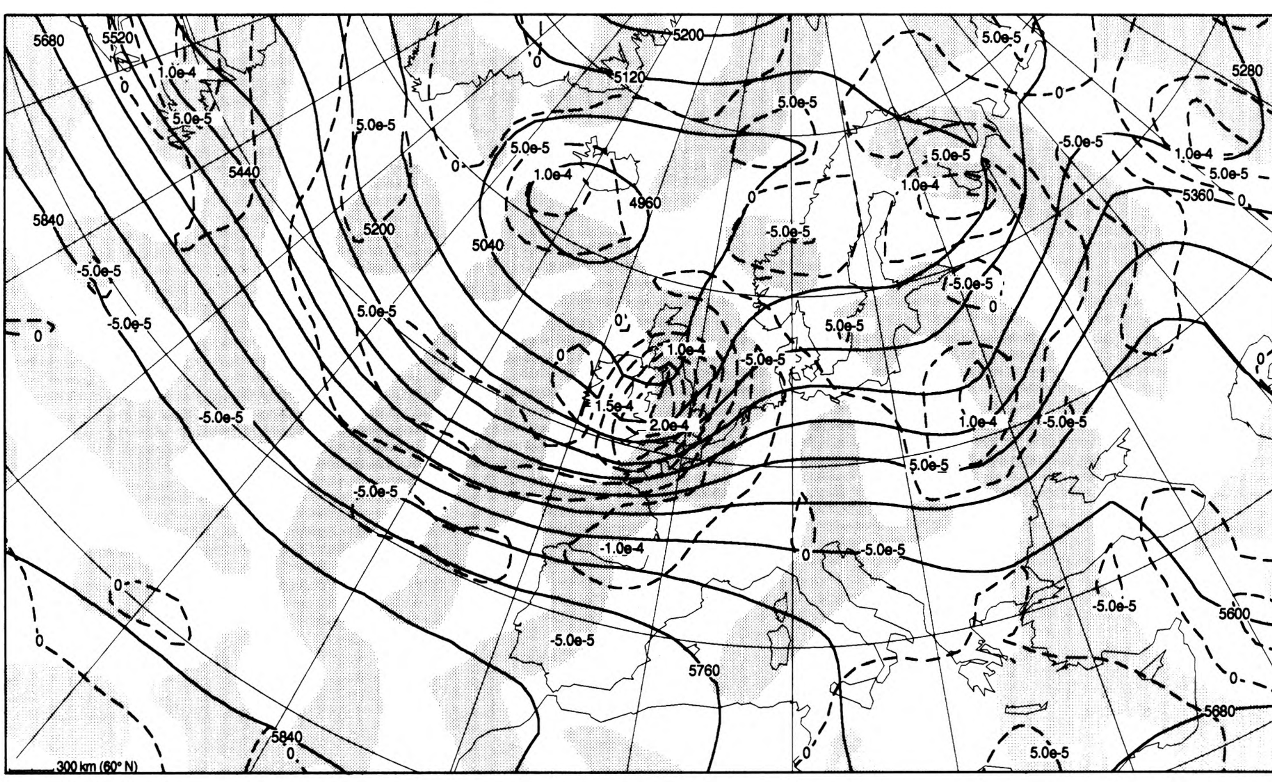

Figure 4. Results of the example, showing the 500 hPa height field (m), together with relative vorticity (s^{-1}) dashed lines and vorticity advection (shaded areas indicate positive vorticity-advection).

short time (calculation of a particular field and preparing the graphical presentation on the screen takes only a few minutes), but depends of course on the skills of the student who has to solve the dynamical problem.

5. Final remarks

Though the above example may be simple, it shows some essential points, namely:

(a) Students can concentrate on solving the dynamical (i.e. meteorological) problem and on the interpretation of the results of the calculations. Students have to think and work out for themselves how to solve the problem.

(b) The computer is a helpful tool — it carries out the laborious calculations and it generates no precooked solutions.

(c) End results and in-between results of the calculations can easily be presented, both on screen and printer.

(d) Students do not have to bother about numerical problems, e.g. how to calculate derivatives on a grid. This is preprogrammed in the package.

At the moment experience has been gathered in the use of the package, but the full potential of it still has to be exploited much further. A further paper is planned to describe the experience of and developments in the system. Developments being considered are a real-time datalink and the writing of a manual for general release. A thorough technical description of the package is required in the first instance.

Although there never are perfect solutions to educational problems, in the opinion of the authors this software package is a major step forward in the way dynamic meteorology can be taught by combining theory and practice.

References

Holton, J.R., 1979: An introduction to dynamic meteorology (Second edition). New York, Academic Press.

Saraber, M.J.M., The, T.H., and Kroon, L.J.M., 'Integrating Theory and practice in teaching Dynamic Meteorology'. Paper presented at the WMO Symposium on Methods of Meteorological Education and Training including the use of new relevant techniques, Toronto, Canada, 19–23 August 1991.

551.506.1(41-4)

The autumn of 1991 in the United Kingdom

G.P. Northcott
Meteorological Office, Bracknell

Summary

Temperatures remained about average over the autumn period generally; the autumn was wet over most of Scotland and north-west England, but generally dry elsewhere, and sunny everywhere excepting north-west Scotland.

1. The autumn as a whole

Seasonal temperatures were near or below normal over much of Scotland and Northern Ireland, but mainly above normal over England and Wales, ranging from 0.9 °C above normal at Penkridge, Staffordshire and Poole, Dorset to 0.4 °C below normal at Glenlee, Dumfries and Galloway. Rainfall amounts were above average over north-west England, part of North Wales, the Bristol Channel area, part of the Midlands and the Norwich area of Norfolk and most of Scotland except for the south-east, and below or near average elsewhere. Values ranged from 141% of normal at Cheltenham, Gloucestershire to 55% of normal at Cawood, North Yorkshire. Sunshine amounts were above average in most parts of the United Kingdom apart from north-west Scotland where it remained dull, and parts of southern and central England where amounts were near average, ranging from 137% of average at Buxton, Derbyshire to only 81% of average at Hadlow College, Kent.

Information about the temperature, rainfall and sunshine during the period from September to November 1991 is given in Fig. 1 and Table I.

2. The individual months

September. Mean monthly temperatures were above normal over England, Wales and Northern Ireland, but below normal generally over Scotland, ranging from 1.9 °C above normal at Penkridge, Staffordshire and Malvern, Hereford and Worcester to 0.4 °C below normal at Camps Reservoir, Strathclyde Region. The highest temperatures occurred during the first week, and it was the warmest September in some places for 30 years. Monthly rainfall totals were generally below normal except in north-western parts of Scotland and parts of southern and eastern England where they were about or above normal, and ranged from 168% at Woburn, Bedfordshire to as little as 26% at Edinburgh,

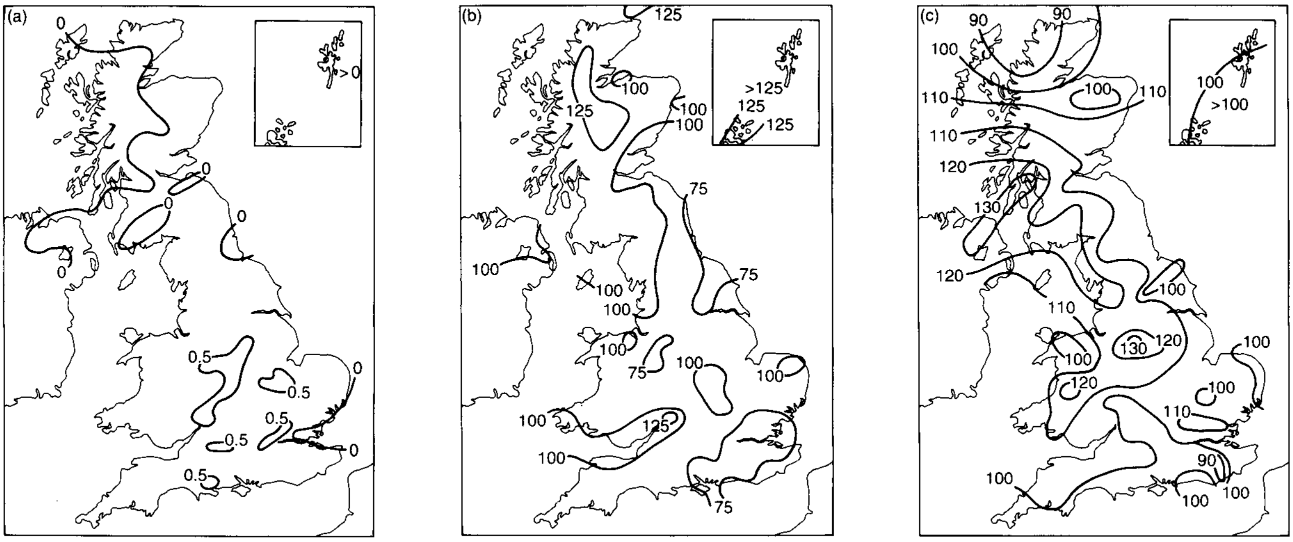

Figure 1. Values of (a) mean temperature difference (°C), (b) rainfall percentage and (c) sunshine percentage for autumn, 1991 (September–November) relative to 1951–80 averages.

Table I. District values for the period September–November 1991, relative to 1951–80 averages

District	Mean temperature (°C)	Rain-days	Rainfall	Sunshine
	Difference from average		Percentage of average	
Northern Scotland	–0.1	+1	127	89
Eastern Scotland	+0.1	0	110	102
Eastern and north-east England	+0.2	–1	91	104
East Anglia	+0.2	–1	83	98
Midland counties	+0.5	–1	86	100
South-east and central southern England	+0.3	–1	75	96
Western Scotland	0.0	0	116	111
North-west England and North Wales	+0.3	0	97	102
South-west England and South Wales	+0.3	0	97	98
Northern Ireland	+0.1	+1	100	118
Scotland	0.0	0	121	101
England and Wales	+0.3	–1	91	100

Highest maximum: 29.7 °C in south-eastern and central southern England in September.
Lowest minimum: –8.4 °C in northern Scotland in November.

Royal Observatory. The rainfall on the 14th was the first rain for 32 days at Charing, Kent. Monthly sunshine totals were above normal nearly everywhere except for one or two places on the coasts of southern and eastern England and ranged from 168% at Camps Reservoir, Strathclyde Region to 98% at Mayflower Park, Southampton.

September was warm, especially in the south, and generally dry, but during the second half of the month it became less settled and cooler, with some areas of heavy rainfall, although southern areas remained warm until the last week. There were thundery outbreaks over eastern Scotland from Aberdeen to Berwick on the 16th. Showers were of sleet at Fair Isle, Shetland on the 22nd and 23rd. Thunder was reported over Somerset and Dorset later on the 25th, and thundery showers, some accompanied by hail, became widespread over central southern and eastern England on the 26th, bringing the first heavy rain of the month to many parts of England, with outbreaks over Lincolnshire and Norfolk, South Wales and across southern England from Cornwall to Kent. On the 26th waterspouts were observed, 26 km south-west of Llanbedr, Gwynedd and off Pendine, Dyfed. Scattered thunderstorms on the 27th gave some prolonged spells of rain, some of it heavy. Thunderstorms occurred over central southern England later on the 28th and into the 29th, and later that day over parts of south-east England and East Anglia.

October. Mean monthly temperatures were below normal nearly everywhere and ranged from 0.4 °C above normal at Penkridge, Staffordshire to 1.6 °C below normal at Castle Archdale, Co. Fermanagh. On the morning of the 21st Bedford recorded its lowest October temperature since its records began in 1957. Monthly rainfall amounts were above normal in the west and north-east, but below normal in central Scotland and central and eastern England, ranging from 166% at Braemar, Grampian Region to as little as 30% at Greenwich, Greater London. Monthly sunshine amounts were below average nearly everywhere except for eastern Kent and parts of the Midlands where sunshine was just above average, and ranged from 106% of average at Keele, Staffordshire to less than 50% at Kinlochewe, Highland Region.

During the afternoon of the 1st a thunderstorm was reported over Manchester. On the 3rd there were reports of hail at Cape Wrath in the Highland Region. On the 4th Orkney and Shetland reported thundery outbreaks. Thundery activity was reported over east Devon on the 8th, 9th and 11th. Hail was reported widely between the 16th and 19th, and thunder in the south-west on the 18th. After a settled period from the 20th to 29th, the weather was unsettled during the last two days, producing the most significant rainfall of the month at some places in south-east England. On the 31st many areas had a wet and windy 24 hours: Winterbourne, West Midlands reported serious local flooding on roads in Birmingham City Centre and Bidston, Merseyside reported torrential rain with flooding on roads. On the 18th Guernsey Airport received an aircraft report of a waterspout at 1658 UTC, 020° 12 miles from Alderney; the cloud base was 2000 ft (600 m) and the weather showery, the showers heavy at times.

November. Mean monthly temperatures were normal over Northern Ireland and above normal over most of the remaining parts of the United Kingdom, ranging from about 1 °C above normal in parts of northern Scotland to 0.5 °C below normal at Lowestoft, Suffolk. Monthly rainfall amounts were generally above normal north of a line from Preston, Lancashire to Scarborough, North Yorkshire, apart from some places around the Firth of Forth, the Firth of Tay, and Tyneside, Tyne and Wear, where rainfall was below normal. South of the line most places except South Wales, the south Midlands, and parts of East Anglia and Kent were generally dry. Amounts ranged from 198% of normal at Prestwick, Strathclyde Region to 56% of normal at Sparsholt, Hampshire. Monthly sunshine amounts were below average nearly everywhere apart from a few locations in southern and eastern Scotland and northern England and ranged from 124% at Dumfries, Dumfries and Galloway and Buxton, Derbyshire to only 50% at Aberporth, Dyfed.

During the first fortnight it was generally unsettled with bands of rain affecting most areas, especially the north. The last two weeks of the month were generally quieter, except for the 19th, with some overnight fog. On the 12th gusts exceeded 60 kn in many places; during the passage of a squally cold front gusts reached 81 kn at Aberporth, Dyfed, 79 kn at Ronaldsway, Isle of Man and 77 kn at Gwennap Head, Cornwall; Botwnnog School, Gwynedd reported extensive structural damage caused by the 'ferocity of the gale'. During the evening of the same day a tornado was reported at Dullingham, Cambridgeshire. Thunder occurred locally on the 1st and was widespread on the 3rd over England and Wales. Thunder was reported over western Scotland on the 11th, and was widespread over Wales and northern and eastern England between the 11th and 14th. Overnight on the 12th/13th violent thunderstorms were reported over Cumbria.

Note from the Editor

In the October 1992 issue, a preamble was accidentally omitted from the start of Mr Collier's article entitled 'International radar networking'. Most readers will have correctly assumed that the article is in fact an edited transcript of a talk. This was given earlier this year to a rapt audience at the Meteorological Office. It has been reproduced in this form because it saved Mr Collier from having to rewrite the whole; more importantly, the form associated with the use of the first person (grammatically) makes for a much easier read. If you would like to comment on this milestone in scientific publishing please write to me.

We much regret that production difficulties in the Meteorological Office have caused this issue to be published very late. The December issue will, we hope, follow this issue quickly. We cannot yet be sure of the January publication date because Christmas complicates matters: but by February everything should be back to normal.

R.M. Blackall

Reviews

Asymptotic modelling of atmospheric flows, by R. Zeytounian. 157 mm × 240 mm, pp. xii+396, *illus.* Berlin, Heidelberg, New York, Springer-Verlag, 1990. Price DM 170.00. ISBN 3 540 19404 5.

This book is based on a series of graduate courses given by the author, however it is very different from the popular texts such as Gill, *Atmosphere Ocean Dynamics* or Holton, *An Introduction to Dynamic Meteorology.* The author treats meteorology as a fluid-mechanics discipline and, in doing so, presents the material in a formal and mathematically detailed manner. However this style is not inappropriate for the subject matter. The main aim of the book is to derive a number of consistent approximations to the Navier–Stokes equations, that are of particular interest to the meteorologist, using expansions in the dimensionless numbers that describe properties of the atmospheric flow. Using jargon from numerical weather prediction, filtered models are obtained as limiting flows when the dimensionless numbers are assumed to be small or large compared to unity. There is an absence of extensive discussion of the dynamics of the solutions, however the presentation is clear and in a logical order. The book achieves its aim.

Following the introduction where about nine dimensionless parameters are mentioned, some of which are not often seen in English literature, the next three chapters are devoted to an overview of material that is familiar to most. In these chapters the term 'filtering' is used in place of the more common expression 'approximation'. The author uses the term filtering when discussing the *model* obtained by approximating the Navier–Stokes equations. The term 'approximation' is reserved for the study of the limiting process using asymptotic methods. In chapter two, the f-plane (in the book the Coriolis parameter is denoted by l) and, β-plane approximations, the Euler equations and the Primitive equations are discussed. Chapter three deals with internal waves and filtering, in particular quasi-static filtering, Boussinesq filtering and Anelastic (referred to as Deep Convection) filtering. Chapter four is devoted to the topic of Rossby waves. This material is followed by a discussion of asymptotic methods: The Matched Asymptotic Expansions Method and Multiple-Scale Method. Chapters six–ten examine in detail the various approximations used in the models discussed in chapter three, by use of asymptotic expansions. Chapters eleven–thirteen are devoted to the quasi-geostrophic and ageostrophic models, the low Mach number models and models for mesoscale flows. An appendix discusses a consistent treatment of the hydrostatic equations and points out that the equations most commonly used in meteorology and numerical weather prediction do not appear to be asymptotically consistent from the point of view adopted in this book.

The author includes 29 references to his own work, covering a period of over 22 years. The majority were published in French or Russian with only about a quarter appearing in English. There is currently much interest in the generation of consistent rather than *ad-hoc* approximations to the Navier–Stokes equations using techniques such as variational principles. The appearance of this self-contained account is timely and complements alternative approaches to the subject .

I would recommend this book to researchers in atmospheric dynamics and numerical weather prediction. I feel that few people will consider it suitable as a textbook for a course in dynamical meteorology, as it employs specialized mathematical techniques and lacks a discussion of the more physical aspects of the results. However, it is worth emphasizing that it deals with issues that are central to an understanding of many problems in numerical weather prediction. To quote from the Preface, 'Much of knowledge, however, is based on simple truths which are exceedingly difficult to put into words.'; therefore, what better language than that of mathematics.

I. Roulstone

The year without a summer?: World climate in 1816, edited by C.R. Harington. 217 mm × 279 mm, pp. iv+576, *illus.* Ottawa, Canadian Museum of Nature, 1992. Price C$42.80. ISBN 0 660 13063 7.

This volume collects together the 39 conference papers given by climatologists, vulcanologists, glaciologists, dendrologists, geographers and historians at an international meeting held at Ottawa during 25–28 June 1988. It can, therefore, be described as a large volume of conference proceedings; with an introduction (by Harington), a summary (by Cynthia Wilson), and a very thoroughly compiled 18-page index, all added at a later date.

Perhaps it is the diversions and 'dead ends' which make this historical investigation so enjoyable to read! No sooner do we establish how very cold 1816 was around the Hudson Bay, when a study of tree-ring growth from the Canadian Rockies points to both 1799 and 1824 as being apparently much colder there (see pp. 275–276 of Luckman & Colenut, an article containing the book's five black and white photographs). In the north-eastern USA, Baron (pp. 124–144) mentions that 1812, 1817 and 1836 had equally low or lower summer temperatures, but that the combination of killing frosts and drought affecting the growing season caused 1816 to gain notoriety as 'eighteen-hundred-and-froze-to-death' in local 'folklore'.

We are looking at a 'milestone volume' rather than a finished production because much of its contents are concerned with 'historial comparison' which will go some way towards enabling the continuing (and more difficult) work of synoptic reconstruction to be done. In this respect, early records of the Hudson's Bay Company have been particularly helpful to researchers Wilson &

Ball. Nearly 200 pages of this volume are devoted to the climate and weather of the period in Canada.

Probably too early in the book, Harington mentions (on p. 7 of the introduction) that "Certainly 'the year without a summer' in 1816 was a regional phenomenon... parts of Western North America, Eastern Europe and Japan seem to have had average or above-average temperatures as opposed to the remarkable cold that characterized much of Eastern North America, Western Europe and China. Incursion of freezing arctic air southward in one region was offset by poleward flow of tropical air in another. " Wilson's conclusion also points to persistent meridional airflows around strongly developed atmospheric 'blocking patterns' as being primarily responsible for these regional climatological anomalies, rather than to effects of the volcanic eruption of Tambora in Indonesia during April 1815 which seems, at most, a possible contributory effect and at least, a complete 'red herring'.

On this basis, it was probably unnecessary to include so much of the 'General' material on volcanism, and the particular concentration on Tambora, which make up much of pp. 12–92; and a future revision might include more synoptic meteorological charts (the reconstruction for 5 June 1816, is not only repeated on p. 179 and p. 192, but is also to be found prepublished in *Weather*, **40**, p. 137...meaning that it is probably 1984 vintage). As yet there appear to be no reconstructions planned for charts covering 18–22 August 1816, which was a particularly cold period in eastern North America. Also, the general notion of severe unseasonal frosts does not live happily with that of a persistent volcanic 'pall', darkening the sky by day, but probably also reducing night-time radiation.

There does not seem to be much pictorial evidence from 1816 that skies (particularly at sunrise or sunset) were unusually coloured, and if there had been, one suspects that Ball (who makes a brief passing reference to paintings on p. 202) would have mentioned this. In the United Kingdom, Constable painted unsettled, showery, cyclonic weather that year (particuarly on his honeymoon in Dorset during October–December. The various versions of'Weymouth Bay', one of which appears on the front cover of *Weather* magazine in September 1968, date from his 'oil sketches', made from nature during this period). In Canada, the cold weather was probably at least partly responsible for the portrait painter, Robert Field, emigrating from Halifax, Nova Scotia, to Kingston, Jamaica, at the end of summer 1816. Such 'artistic clues' to the prevailing weather could have usefully illustrated this work, which otherwise only has a reproduced poem ('Darkness', written by Lord Byron in Geneva, which is, arguably, the biggest 'red herring' ever reproduced as the 'frontispiece' of a scientific volume of literature!?) and a photographed medallion (front cover) which was struck in southern Germany 'in memory of the great famine of 1816–17'. Also, an art historian could have been employed to discuss some of the more-worthy paintings dating from 1816.

Nevertheless, this collection of so many climatological articles from both northern and southern hemispheres make this wide-ranging volume well worth the £20 asking price (current exchange rate approximately C$2. 15 = £1) to those fascinated by historical detective work in progress. The conclusion has not been firmly arrived at as yet, which is probably why the editor decided that a 'question mark' should still appear in the title?

W.S. Pike

Correspondence

Hoar-frost deposition

With reference to the letter of R. Mansell (*Meteorol Mag*, **121**, 241), the purpose of the paper was to elucidate the *meteorological factors* evident in the formation of *hoar-frost* alone. This treatment necessarily excluded ice formation by other means along with the effects of salt concentration, traffic density, road surface type, etc.

We agree that a wet, salty road is more slippery than a dry one, and that the number of hours in a wet, salty state is highly likely to exceed the number of hours in an ice covered state.

Motorists are expected to adjust their driving speed according to ambient conditions. Wet, salty roads are usually extensive due to the nature of salt application and the spreading effect of traffic. The more localized nature of hoar-frost and other forms of ice makes them less obvious, thereby increasing the accident risk. This must be borne in mind when a decision on salting has to be made.

From any viewpoint, a better understanding of hoar-frost deposition and other ice forming processes can lead to nothing but improved road safety *and* fewer wasted saltings.

N. Gait and T. Hewson

GUIDE TO AUTHORS

Content

Articles on all aspects of meteorology are welcomed, particularly those which describe results of research in applied meteorology or the development of practical forecasting techniques.

Preparation and submission of articles

Articles, which must be in English, should be typed, double-spaced with wide margins, on one side only of A4-size paper. Tables, references and figure captions should be typed separately. Spelling should conform to the preferred spelling in the *Concise Oxford Dictionary* (latest edition). Articles prepared on floppy disk (IBM-compatible) can be labour-saving, but only a print-out should be submitted in the first instance.

References should be made using the Harvard system (author/date) and full details should be given at the end of the text. If a document is unpublished, details must be given of the library where it may be seen. Documents which are not available to enquirers must not be referred to, except by 'personal communication'.

Tables should be numbered consecutively using roman numerals and provided with headings.

Mathematical notation should be written with extreme care. Particular care should be taken to differentiate between Greek letters and Roman letters for which they could be mistaken. Double subscripts and superscripts should be avoided, as they are difficult to typeset and read. Notation should be kept as simple as possible. Guidance is given in BS 1991: Part 1: 1976, and *Quantities, Units and Symbols* published by the Royal Society. SI units, or units approved by the World Meteorological Organization, should be used.

Articles for publication and all other communications for the Editor should be addressed to: The Chief Executive, Meteorological Office, London Road, Bracknell, Berkshire RG12 2SZ and marked 'For Meteorological Magazine'.

Illustrations

Diagrams must be drawn clearly, preferably in ink, and should not contain any unnecessary or irrelevant details. Explanatory text should not appear on the diagram itself but in the caption. Captions should be typed on a separate sheet of paper and should, as far as possible, explain the meanings of the diagrams without the reader having to refer to the text. The sequential numbering should correspond with the sequential referrals in the text.

Sharp monochrome photographs on glossy paper are preferred; colour prints are acceptable but the use of colour is at the Editor's discretion.

Copyright

Authors should identify the holder of the copyright for their work when they first submit contributions.

Free copies

Three free copies of the magazine (one for a book review) are provided for authors of articles published in it. Separate offprints for each article are not provided.

Contributions: It is requested that all communications to the Editor and books for review be addressed to the Chief Executive, Meteorological Office, London Road, Bracknell, Berkshire RG12 2SZ, and marked 'For *Meteorological Magazine*'. Contributors are asked to comply with the guidelines given in the *Guide to authors* (above). The responsibility for facts and opinions expressed in the signed articles and letters published in *Meteorological Magazine* rests with their respective authors.

Subscriptions: Annual subscription £36.00 including postage; individual copies £3.25 including postage. Applications for postal subscriptions should be made to HMSO, PO Box 276, London SW8 5DT; subscription enquiries 071–873 8499.

Back numbers: Full-size reprints of Vols 1–75 (1866–1940) are available from Johnson Reprint Co. Ltd, 24–28 Oval Road, London NW1 7DX. Complete volumes of *Meteorological Magazine* commencing with volume 54 are available on microfilm from University Microfilms International, 18 Bedford Row, London WC1R 4EJ. Information on microfiche issues is available from Kraus Microfiche, Rte 100, Milwood, NY 10546, USA.

November 1992

Edited by R.M. Blackall
Editorial Board: R.J. Allam, R. Kershaw, W.H. Moores, J. Gloster, C. Nicholass, G. Lupton

Vol. 121
No. 1444

Contents

ISSN 0026—1149

ISBN 0-11-728989-2

Printed in the United Kingdom for HMSO Dd 291241, 1/93, C13, 543, 24503

The Meteorological Magazine

December 1992

Analysis of intense mid-latitude cyclones
Noctilucent clouds 1991
GCOS Report

HMSO

Met.O.1004 Vol. 121 No. 1445

First published 1992

HMSO

HMSO publications are ava

HMSO Publications Centre
(Mail, fax and telephone or
PO Box 276, London, SW8
Telephone orders 071-873 9C
General enquiries 071-873 0
(queuing system in operatio
Fax orders 071-873 8200

HMSO Bookshops
49 High Holborn, London,
(counter service only)
071-873 0011 Fax 071-873 8
258 Broad Street, Birmingh
021-643 3740 Fax 021-643 6
Southey House, 33 Wine St
0272 264306 Fax 0272 2945
9-21 Princess Street, Manch
061-834 7201 Fax 061-833 0
16 Arthur Street, Belfast, B
0232 238451 Fax 0232 2354
71 Lothian Road, Edinburg
031-228 4181 Fax 031-229 2

HMSO's Accredited Agent
(see Yellow Pages)

and through good booksell

The
Meteorological Magazine

December 1992
Vol. 121 No. 1445

551.515.1:551.509.3

Synoptic and mesoscale analysis of intense mid-latitude cyclones

G.A. Monk
Meteorological Office, Gibraltar

Summary

Surface observations together with radar and satellite imagery are used to identify the subsynoptic-scale air-mass structure of an intense cyclonic storm that crossed the British Isles on 16 October 1987. Comparison of their characteristics with those of a number of more recent intense cyclonic storms indicate a number of common features.

1. Introduction

The intense depression that crossed southern Britain during the early hours of 16 October 1987 will be remembered mostly for the exceptionally strong surface winds and enormous damage to the tree population of the area. However, meteorologically, several other notable events occurred:

(a) A sharp warm front preceded the depression with temperatures rising by up to 10 °C in places during its passage.

(b) Within the warm air, several distinct and sometimes sudden changes of temperature and/or dew-point occurred.

(c) Behind, and on the eastern flank of the low, the transition back to cold air was, in some places, very sharp whilst at other places gradual.

(d) Very large pressure rises were recorded immediately behind the low.

The first part of this paper seeks to explain these events within a synoptic context using surface observations, autographic records and radar rainfall and satellite imagery. Later, important similarities between the structure of this storm and those of more recent storms are identified.

2. The storm prior to arrival over Great Britain

Although this paper is mainly restricted to the weather of 16 October 1987 over the British Isles, clues to the synoptic structure of the storm in the twelve hours or so before its arrival over Britain were gained from satellite imagery supported by surface observations. The surface analysis at 1500 UTC 15 October 1987 (Fig. 1(a)), showing two roughly parallel fronts, has been drawn with considerable weight given to satellite imagery (Fig. 2). Front 'F', associated with a cloud band 'X' had been in existence for upwards of 24 hours, whilst a newly formed front, 'P', has been drawn within low cloud at the forward edge of a cloud area labelled 'Y' in the NOAA infrared image shown in Fig. 2. The centre of the surface low that developed into the storm is located close to front 'P'.

Subsequent movement of front 'P' was determined by tracking the forward edge of cloud area 'Y' using a movie-loop of Meteosat infrared images. This cloud edge became increasingly curved with a tongue of low cloud being drawn round the low to its eastern flank (Fig. 3). By 2200 UTC the cloud pattern had become too ill-defined for further tracking.

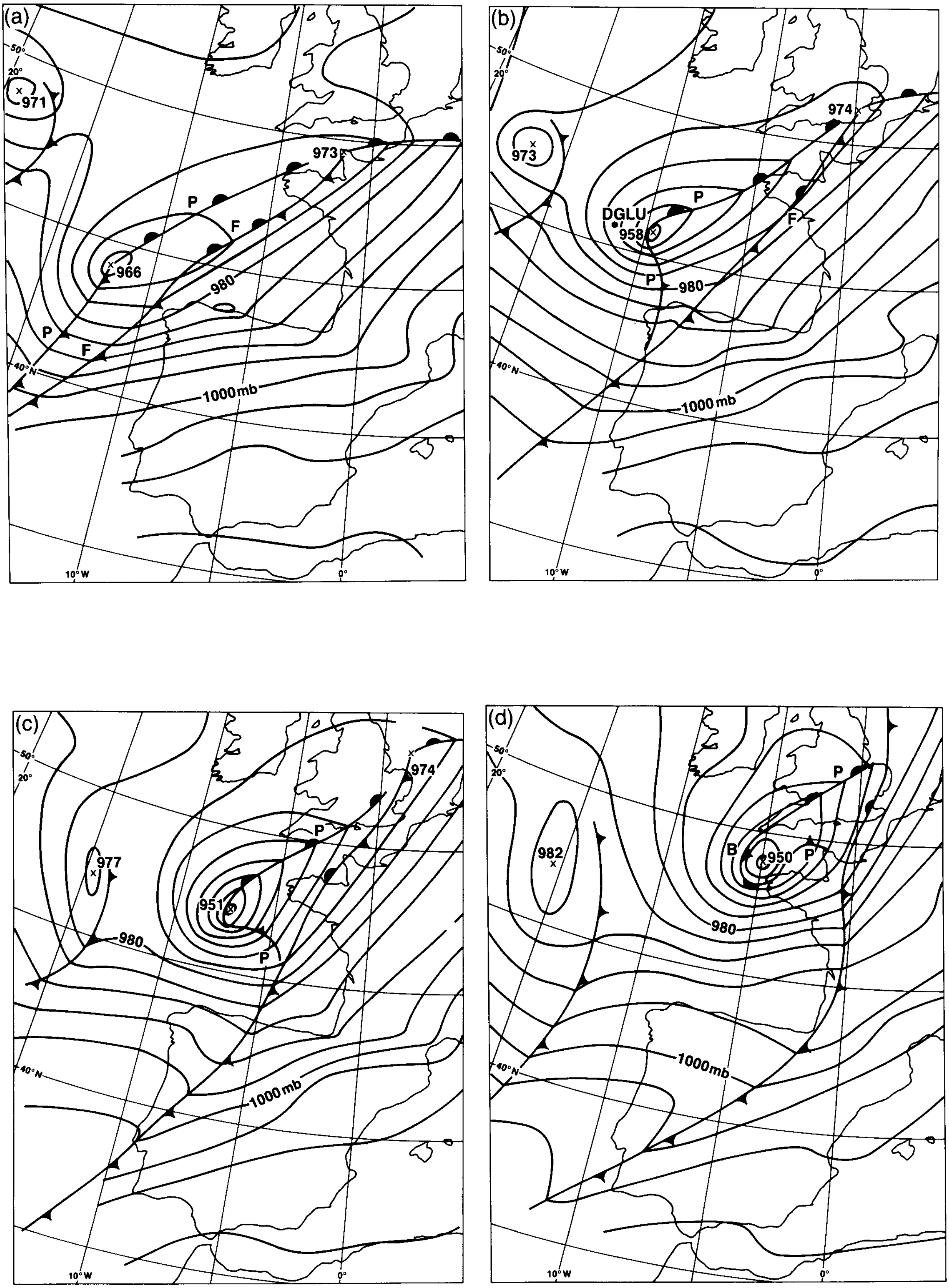

Figure 1. Surface analyses at (a) 1500 UTC on 15 October 1987, (b) 1800 UTC on 15 October 1987, (c) 2100 UTC on 15 October 1987 and (d) 0000 UTC on 16 October 1987. The position of ship DGLU at 1800 UTC is shown in (b).

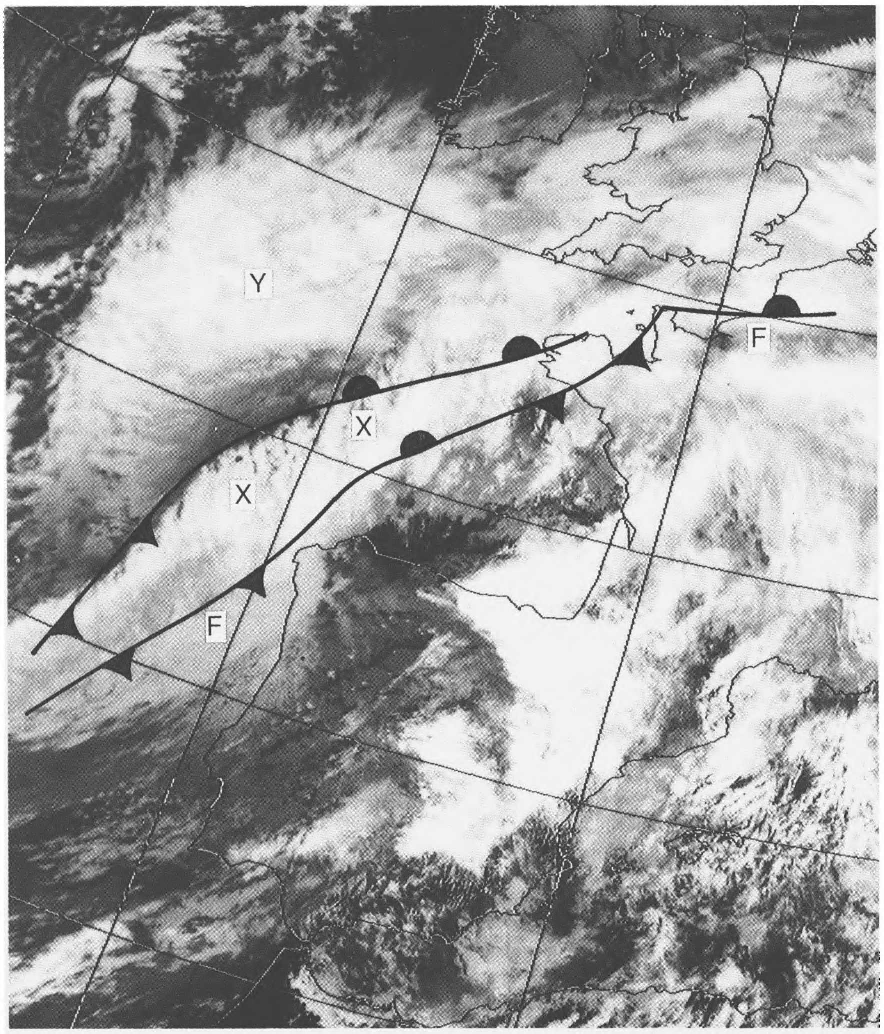

Figure 2. Infrared satellite image at 1450 UTC on 15 October 1987 showing the relation between cloud features and surface fronts. Front 'F' is associated with the cloud band 'X', and front 'P' with cloud area 'Y'.

The movement of the low was also determined using the satellite movie-loop. Its position was estimated as being at the centre of rotation of fragments of low cloud. This placed the track west of the synoptic analyses shown in Woodroffe (1988) who carried out a reanalysis immediately after the storm, but is in close agreement with that of Jerraud *et al.*(1989). Although the low-level rotation centre of low cloud is not necessarily coincident with the isobaric centre (see later text), it was considered a reasonable guide.

The only other evidence of the low position at 18 UTC came from a single nearby ship observation, which unfortunately contained errors. Ship DGLU, (position located in Fig. 1(b)) reported a pressure of 978.5 mb having apparently risen by 9.5 mb in the previous 3 hours. However, the ship's previous observation 6 hours earlier reported a pressure of 988.0 mb, exactly 9.5 mb higher than that observed at 1800 UTC. The 1200 UTC pressure had been flagged as incorrect by the Meteorological Office Central Forecasting Office since it was approximately 10 mb higher than a cluster of adjacent ships. It is assumed that at 1800 UTC, its reported pressure remained 10 mb too high, that in the pressure tendency group the apparently rising pressure should have been falling and the tendency period was between observations, namely six hours, and not the normal three hours. None of these errors are unprecedented in ship observations.

Further deepening of the low occurred during the evening (Fig. 1(c)), and by midnight 16 October (Fig. 1(d)), the low had reached its deepest, 950 mb just off Brittany. Jerraud *et al.* (1988) show the barogram trace from Brest at the western extremity of Brittany, north-west France dipping slightly below 950 mb just before midnight.

3. The storm over Great Britain

The surface low reached southern Britain during the early hours of 16 October. In order to obtain a detailed surface analysis during this period, all surface synoptic reports for southern Britain between 0100 and 0500 UTC inclusive were compiled onto a single map, nominally for

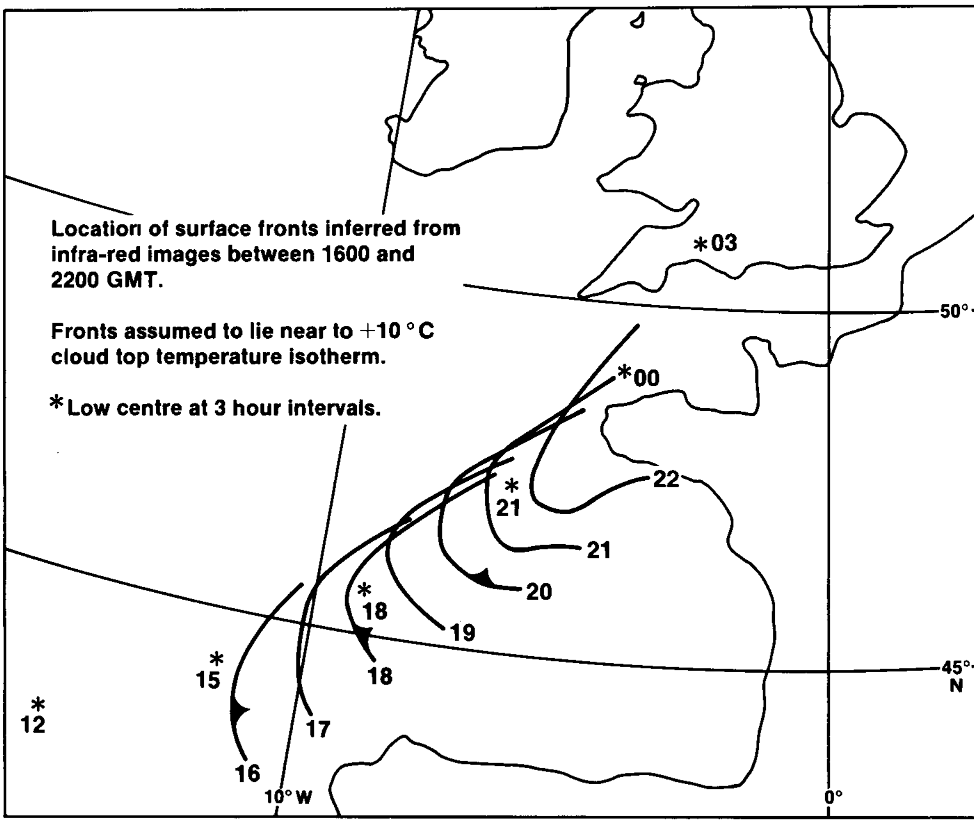

Figure 3. Positions of front 'P' at hourly intervals derived from the movement of a band of low cloud at the leading edge of cloud area 'Y' (see Fig. 2) and, at 3-hourly intervals, the position of the low centre (denoted by asterisks). Positions of the low at 1800 and 2100 UTC are based on imagery.

0300 UTC, by displacing observations recorded before or after 0300 UTC according to the velocity of the low during the period, i.e. 215° 48 kn. The advantage of the method was that in the rapidly changing conditions, 'rogue' observations, taken a few minutes away from nominal observation time were easily identified within the large field of observations. Exposed coastal stations which tended to experience stronger mean winds and higher temperatures also stood apart.

Fig. 4 presents the results, showing in Fig. 4(a) aspects of the surface weather and in Fig. 4(b) the frontal and air-mass analysis. Most air-mass boundaries are seen to be related to a strongly contorted front, shown later to be front 'P'. For ease in the following discussion, air on the cold side of front 'P' (originating west and north of the front) is labelled air mass 1, and that on the warm side air mass 2.

Strongest temperature and dew-point gradients occurred on the northern and western flank of the storm. Ahead of the storm, air mass 2 advanced slowly north, temperatures typically rising around 8 °C within about 30 minutes. On the southern and eastern flanks of the low, the thermal contrast between air masses 1 and 2 progressively decreases, although a marked dew-point discontinuity persists. The analysis also suggests that on the eastern flank, the returning air mass 1 (labelled 1M) has advanced around the low so as to begin to cut-off a 'warm-core seclusion', a region of moist and relatively warm air near the vortex centre (labelled 2S). The term seclusion was first used by Bergeron, but has recently been adopted by Shapiro (1989) in describing warm cores of intense cyclonic storms off the eastern seaboard of the United States.

The eastern and northernmost boundary of air mass 1M has been labelled a cold front although the temperature falls little despite distinct humidity change. Rather, the passage of the front marks the onset of a period of sustained temperature fall. The front was also accompanied by a band of showers which were identified by radar. Fig. 5 shows the 0130 UTC picture, when the showers were near the centre of the radar area. The speed and direction of travel of the shower band derived from a succession of radar images suggested it to be the advancing front 'P' identified approaching Brittany 3 hours earlier using the satellite movie-loop.

Within air mass 1M and also in that part of air mass 2 labelled 2M in Fig. 4(b), certain stations reported particularly dry air, although according to the analysis in Fig. 4(a), its structure was incoherent. However, Meteosat infrared and water vapour imagery at the time (not shown) indicated a tongue where cloud was confined to very low levels, with extremely dry air aloft. Although no radiosonde ascent sampled this air, it is most likely that in the strong low-level winds, patches of dry air

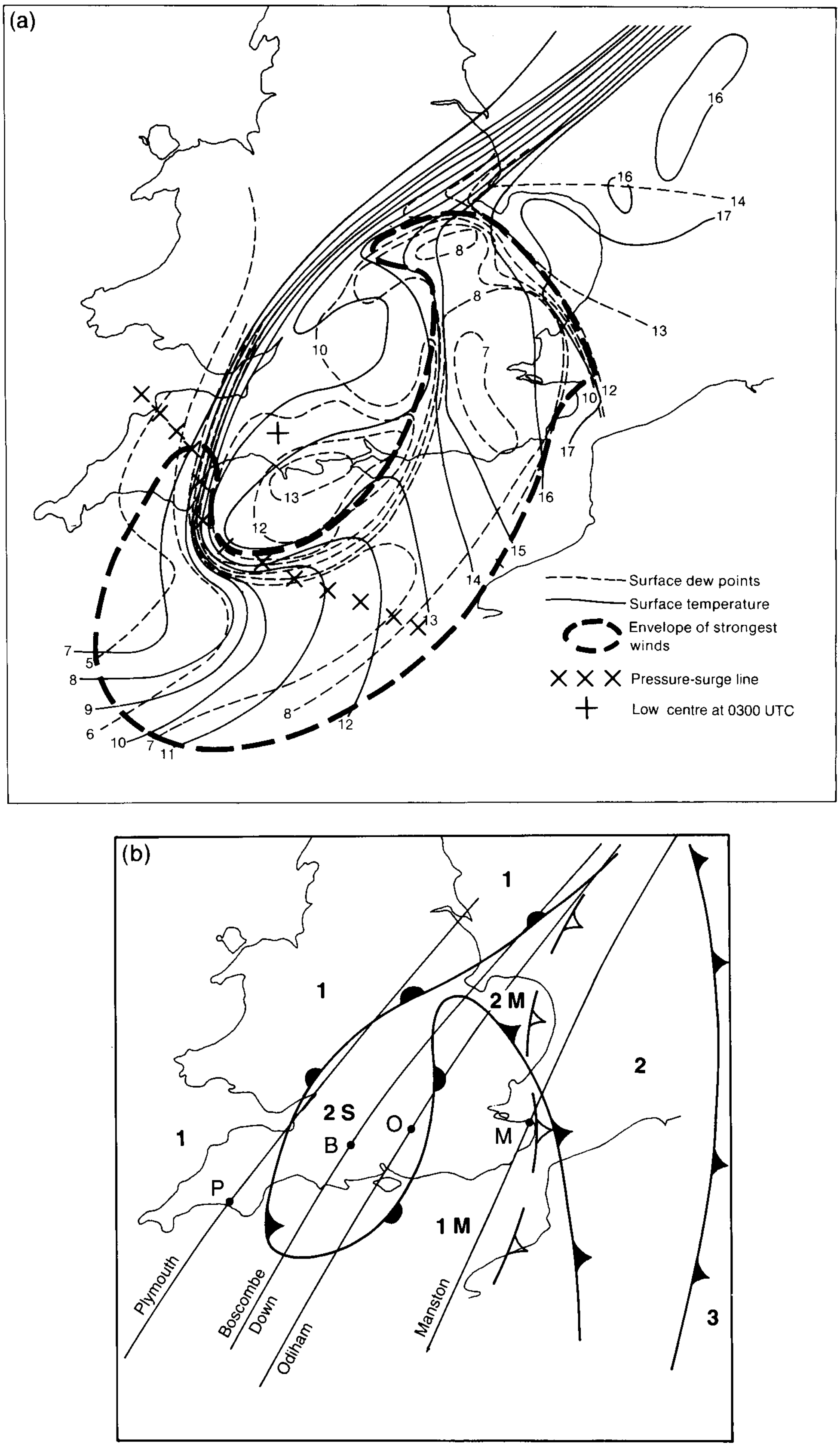

Figure 4. (a) Detailed surface analysis of the storm at 0300 UTC on 16 October 1987, based on all observations between 0100 and 0500 UTC (data before or after 0300 UTC are plotted relative to the 0300 UTC data by moving according to the system velocity of 215° 48 kn). (b) Locations of fronts and air masses derived from the analysis in (a). Air mass 1 refers to the cold air mass, 1M being modified cold air being drawn around the right flank of the low. Air mass 2 is the warm air mass, region 2M has been modified by the presence of very dry air, and 2S is the warm-core seclusion. (c) (overleaf) Surface synoptic and wind analysis derived only from 0300 UTC observations. The centre of cyclonic rotation according to surface winds is indicated by arrows.

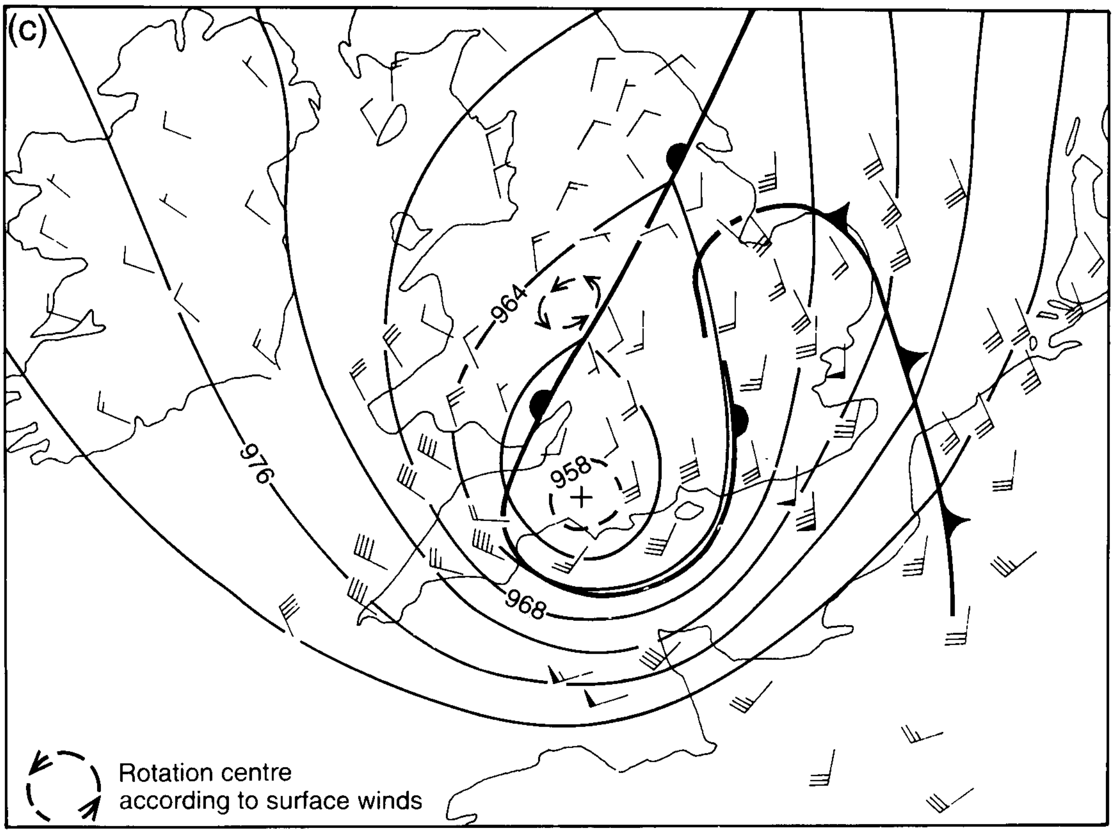

Figure 4. (Continued)

reached the ground, but since the tongue of dry air was moving at a different velocity to that of the low centre, it was not resolved in the analysis.

Reports of strong winds, mean winds of 45 kn or more and gusts of 60 kn or more all fell within a well defined curved envelope lying within air masses 1 and 1M. Another feature of the observations, rapid pressure rises, commenced along the line marked by crosses.

The isobaric analysis together with observed winds at 0300 UTC is shown in Fig. 4(c). The isobaric and wind circulation centres are not coincident, with southerly (ageostrophic) winds in the region of lowest pressure. The tendency for winds in the centre of a fast moving, intense low to blow along its direction of travel has been documented elsewhere. See for example Monk *et al.* (1987). Note that due to different analysis methods, there is a slight difference in the frontal positions shown in Figs 4(b) and 4(c).

Figure 5. Precipitation at 0130 UTC on 16 October 1987 at the cold-frontal boundary separating air mass 2 from the advancing air mass 1M derived from the UK rainfall radar network. Precipitation remote from the front has been excluded

4. Autographic records

Further support for the analysis was obtained from a study of around 60 sets of autographic records of temperature, humidity, wind and barometric pressure obtained from locations within Great Britain. Each record was initially checked for timing errors, this being done independently of this study. Any errors were noted. Records were then scrutinized in order to identify significant meteorological events. A sample from four sets of records, chosen to form a west to east section across southern England are described here.

Fig. 6 shows the thermograph and hygrograph traces for Plymouth, in the west of England (labelled P in Fig. 4(b)). Although lying mostly within the cold air mass 1, for 2 hours this was replaced by the warm core

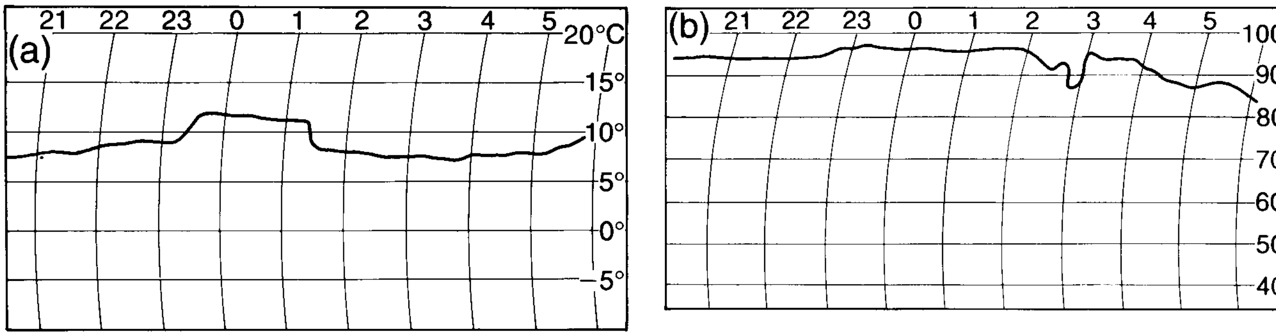

Figure 6. (a) Thermograph and (b) hygrograph records for Plymouth on 15/16 October 1987.

seclusion (air mass 2S), when the temperature increased by 4 °C. At Plymouth, both air masses were nearly saturated.

Boscombe Down (labelled B in Fig. 4(b)), lay very close to the storm track, the isobaric centre passing just to the west. Its records are shown in Fig. 7. As at Plymouth, the arrival and final departure of air mass 2 is marked by sudden temperature rise and fall respectively (observed at 2230 and 0430 UTC in Fig. 7(a), the final temperature falling back to its initial value. However, the relative humidity trace (Fig. 7(b)) shows considerable fluctuation. One hour after arrival of the warm air (air mass 2), the humidity began to drop; the fall commencing with the arrival of the dry air aloft indicated by satellite imagery. The fall in humidity was temporarily halted at 0030 UTC, when the band of showers shown in Fig. 5 passed, and air mass 1M arrived. Between 0130 and 0200 UTC the air at Boscombe Down returned to saturation with some drop in temperature as the warm-core seclusion, air mass 2M, arrived. Following return to the cold air mass 1, the humidity began to drop.

The wind record (Fig. 7(c)) shows two distinct periods of strong winds, occurring just after 0100 and 0430 UTC separated by a lull coinciding with the warm-core seclusion (air mass 2M). Maximum gusts were recorded immediately before and after the lull. The barogram record (Fig. 7(d)), shows a steady and sustained fall of pressure until 0300 UTC. After a short steady period, pressure began to rise extremely rapidly — nearly 25 mb in the next 3 hours. The pressure rise began just before the departure of the warm core, ahead of the pressure-surge line shown in Fig. 4(a), the discrepancy being due to the line in Fig. 4(a) being derived only from hourly ynoptic observations.

Fig. 8 shows the thermogram and hygrogram for Odiham (O in Fig. 4(b)), located just east of Boscombe Down. The temperature rose 8 °C at 2200 UTC, accompanied by a fall in humidity as air mass 2 arrived. A temporary rise in humidity and onset of period of falling temperatures occurred as the shower band passed at about 0100 UTC. A small temperature rise accompanied the arrival of the warm core (0245 UTC), followed by the usual sharp fall to its initial value with the return of air mass 1 at 0430 UTC.

Finally, Fig. 9 shows the thermograph (a) and hygrograph (b) record for Manston. Unfortunately, both records were judged to have timing errors and considerable blotting of the temperature trace occurred during the windiest part of the night. The timing error on the humidity record approached 90 minutes, but the error was known to the local observer who later annotated and reset the chart. For ease of reference, the traces have been redrawn with corrected timing. Once again, the same features were observed, except that Manston never experienced the warm core. Air mass 1M arrived at 0240 UTC accompanied by the familiar temporary rise in humidity and a sustained period of temperature fall.

Earlier in the night, other air-mass changes were shown in the records for Manston that were not observed elsewhere. Although not carefully analysed, they were judged to be related to the advance and retreat of frontal zone F which affected only extreme south-east England.

5. The warm-core seclusion and bent-back warm front

A well organized curved band of cloud and rain, best seen at 0500 UTC (Fig. 10) when the rain was situated near the centre of radar coverage, lay around the periphery of the warm core. Only on the eastern flank of the low were both cloud and rain either absent or disorganized. South of the low centre, middle- and upper-level cloud and general rain terminated abruptly within a sharply curved 'hook-shaped' region. The hook was located within the rearward (western) part of the envelope of strongest surface winds shown in Fig. 4(a). Movie-loops of both satellite and radar data indicated that the cloud/rain system and hook location moved with the system velocity and hence remained tied to the region of strong winds and the warm core. There was also strong indication that cloud and precipitation elements moving from the west into the hook underwent decay, suggesting air-mass descent.

Since the air near the low centre was of warm origin with very marked thermal change north and west of the low, its boundary has been marked in Fig. 4(b) as a warm front (apart from a small part of the front travelling 'the other way' and hence marked as a cold front). The radiosonde ascent for Camborne in south-west England at

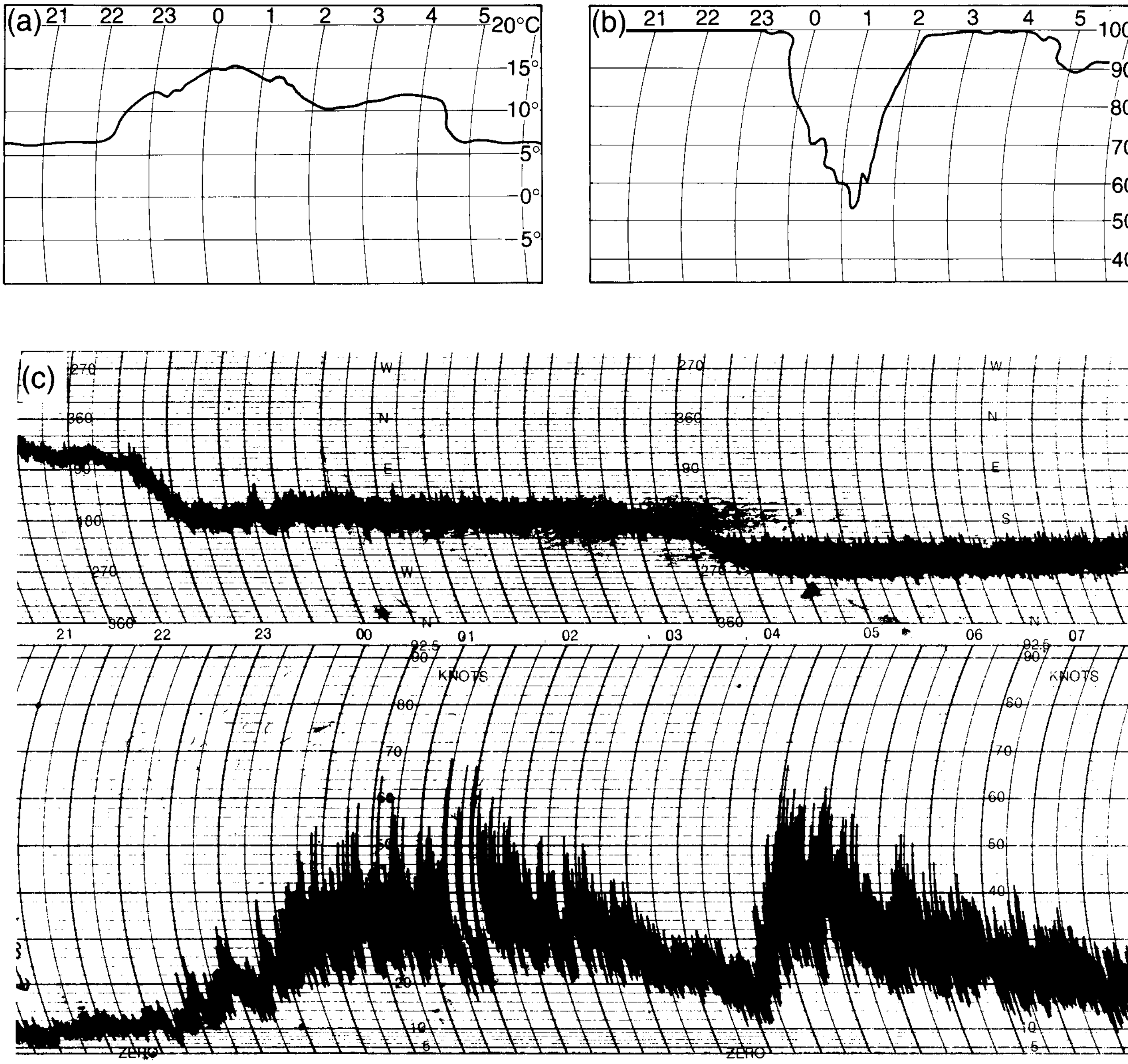

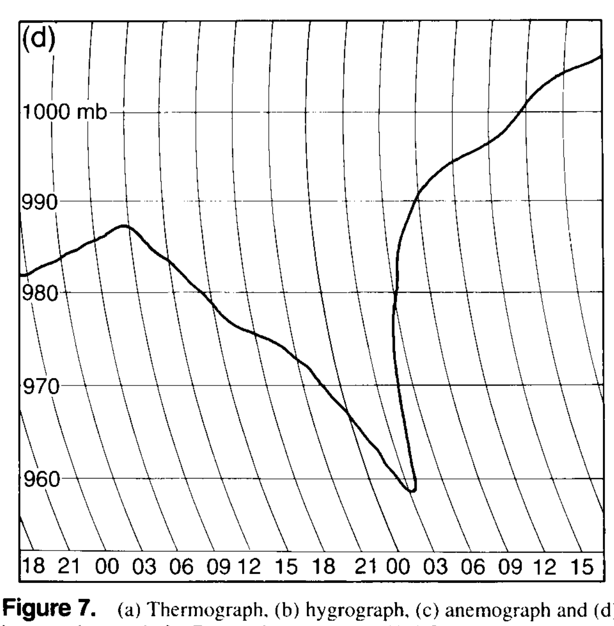

Figure 7. (a) Thermograph, (b) hygrograph, (c) anemograph and (d) barograph records for Boscombe Down on 15/16 October 1987.

0000 UTC on 16 October 1987 sampled low-level air just west of the front, ahead of the warm core (Fig. 11). A sharp frontal inversion is observed at 850 mb, beneath which winds increase rapidly toward the ground indicating a reversed thermal wind gradient confirming the presence of warm air toward the low centre. Since the warm front is curved around the low, it maybe referred to as a 'back-bent warm front' rather than the traditional back-bent occlusion. Shapiro (1989) first refers to back-bent warm fronts in association with intense cyclonic storms.

During the winters that followed the October 1987 storm, a number of intense cyclonic storms either crossed or passed near to Britain. A study of each storm revealed a number of features in common with the October 1987 storm. Their overall weather distribution and frontal structure are summarized in Fig. 12, and three of the cases are discussed briefly in section 6. The key features common to the storms are:

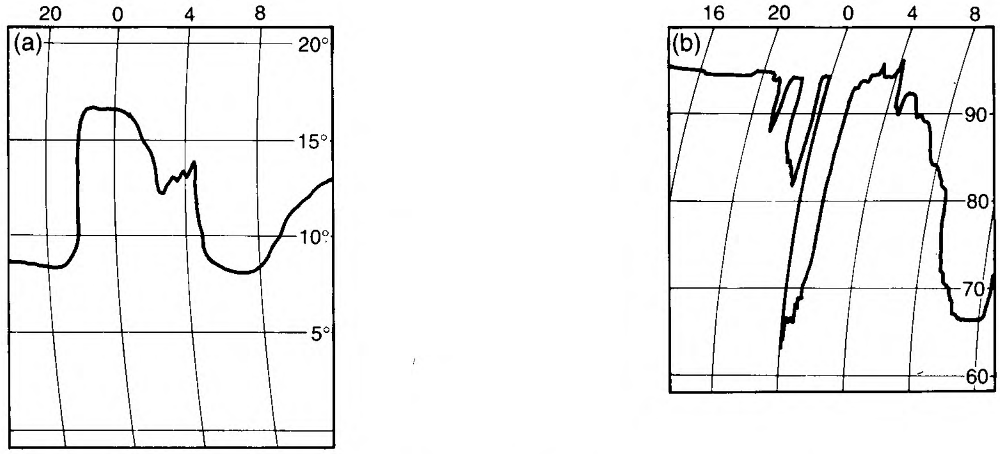

Figure 8. (a) Thermograph and (b) hygrograph records for Odiham on 15/16 October 1987. The hygrograph record is approximately 1 hour slow.

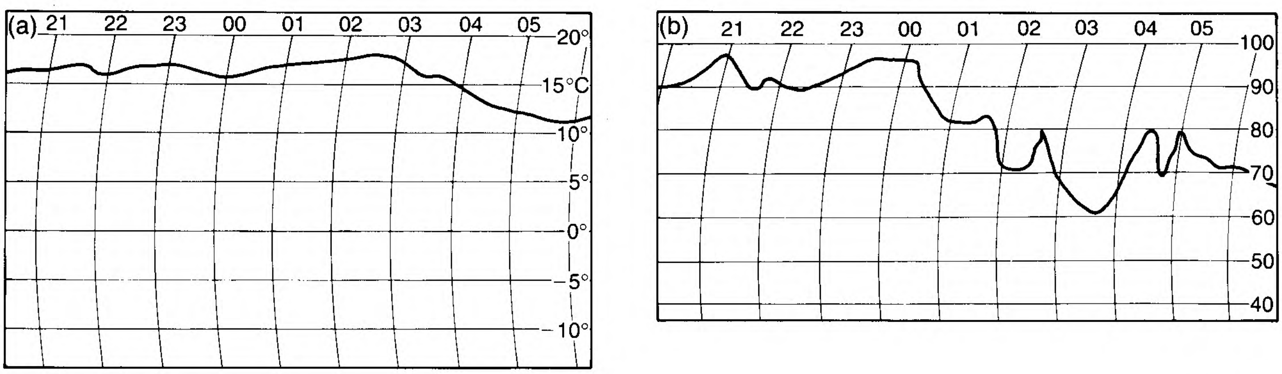

Figure 9. (a) Thermograph and (b) hygrograph records for Manston on 15/16 October 1987. Both records had timing errors and have been redrawn (see text).

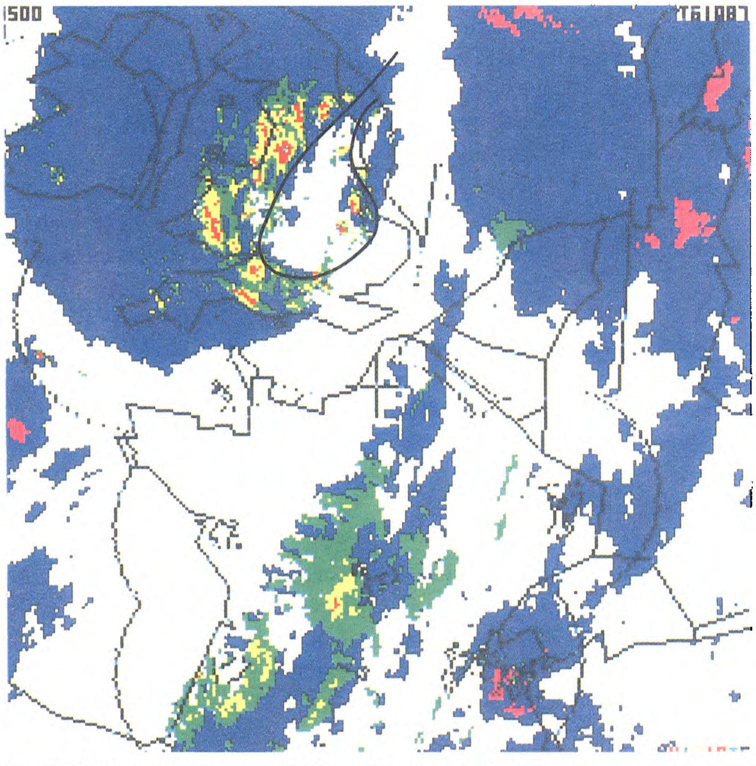

Figure 10. Satellite and radar (COST-73 network) at 0500 UTC on 16 October 1987. The blue and pink areas represent temperature ranges in the infrared, pink representing the coldest cloud tops, whilst the green, yellow, red and blue represent increasingly intense precipitation as measured by weather radar. The location of the back-bent warm front is superimposed.

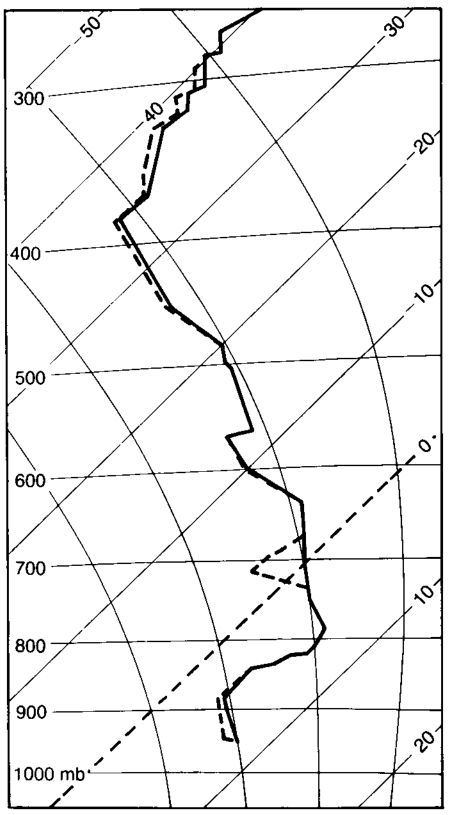

Figure 11. Tephigram for Camborne, south-west England, at 0000 UTC on 16 October 1987.

(a) Each have a warm core.

(b) The warm core is either partly or totally secluded, that is cut off from the main region of warm air.

(c) A sharp temperature contrast exists on the left flank of each low at the boundary of the warm core suggesting a back-bent warm front. North-west of each storm, there is often a region of particularly low temperature in the cold air adjacent to the back-bent warm front.

(d) A curved region of strong winds lies just outside the warm core.

(e) A broad band of thick cloud and rain partly surround each warm core. Thickest cloud and rain usually terminate abruptly within a hook-shaped region on the right flank (usually southern side) of each low, collocated toward the upwind limit of the region of strong winds.

(f) Very rapid rises of pressure set in behind each low.

Generally, there was some evidence of a double frontal zone and, according to water vapour imagery, there was often a tongue of extremely dry air aloft. On more than one occasion the pattern of rainfall at a secondary cold front strongly resembled the convective streets shown in Fig. 5. Very rapid pressure rises set in behind each low, the strongest rises being found in the region of the cloud/precipitation hook. Typically, immediately behind each low, beneath the area of cloud and rain, surface isobars converged, with the tightest isobaric gradient beneath the cloud/precipitation hook.

6. Comparison with other intense cyclonic storms

The major characteristics of intense cyclonic storms at or toward the end of the deepening phase are shown for a small sample of cases using only a single surface synoptic analysis supported by temperature and dew-point observations and imagery. In each case, the weather conforms to the schematic model shown in Fig. 12.

6.1 8 November 1989

This was the least intense storm discussed here, although as the deepening low reached eastern England reported gusts of wind approached 70 kn. The warm core was particularly small, and there had been some evidence of multiple fronts (a second warm front is shown in Fig. 13(a)). Strongest thermal gradient is present at the back-bent warm front on the left flank of the low. The infrared satellite image (Fig. 13(b)) and the UK weather radar image (Fig. 13(c)) clearly show a sharp hook (H), located near the upwind limit of the region of strongest winds and a broad band of cloud and rain associated with the back-bent warm front toward the left flank of the low.

6.2 25 January 1990

On 25 January 1990, a core of hurricane-force winds crossed southern Britain and the near Continent. Severe damage occurred, and news reports suggested that the loss of nearly 100 lives could be attributed to the storm. Gusts of wind exceeded 80 kn over a wide area.

Once again, the moist warm core and back-bent warm front are clearly defined (Fig. 14(a)). West and north-west of the low centre, there was a temperature minimum within the cold air mass, resulting in rain turning to snow. Although not shown, a band of showers similar to those shown in Fig. 5 were observed as the second cold front crossed southern Britain. The convection was deeper than in the October storm, and accompanied by squalls with wind gusts almost as strong as within the main strong wind belt. The hook shown in the infrared image (Fig. 14(b)) is, at this time, not as well marked as in other cases, although it had been more distinct earlier.

6.3 3 February 1990

Although this depression was very shallow (988 mb) in comparison to most intense depressions, surface pressure gradients were very strong and gusts of winds exceeded 80 kn over northern France and later Germany. However, the warm core and back-bent warm front are clearly defined. At 1200 UTC, the bent back front has not penetrated as far round the depression as in the previous cases, and the core of strong winds is centred west of the low centre (Fig. 15(a)). A temperature minimum occurred west and north-west of the low centre, leading as in the previous case, to a temporary change of rain to snow. East of the low, the first cold front is not easy to

Met.O.1004

THE METEOROLOGICAL MAGAZINE

1992 *Volume 121*

The responsibility for facts and opinions expressed in the signed articles and letters published in this magazine rests with their respective authors.

Published for the Meteorological Office by HMSO

INDEX

	Pages		Pages
January	1–28	July	157–172
February	29–56	August	173–196
March	57–88	September	197–220
April	89–112	October	221–244
May	113–132	November	245–268
June	133–156	December	269–288

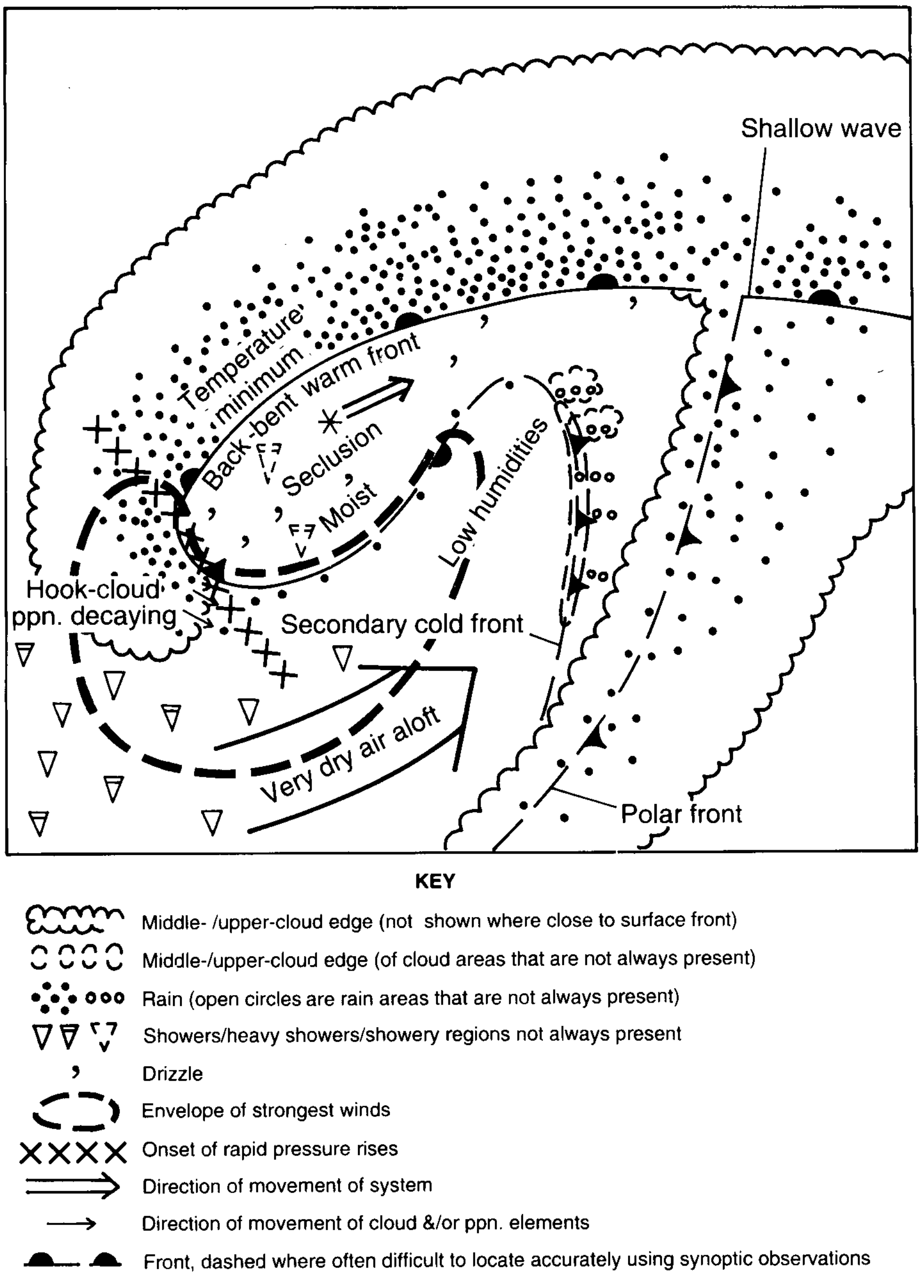

Figure 12. Schematic model showing the air mass and surface weather distribution within an intense mid-latitude cyclone.

locate due to relatively small temperature and dew-point changes. Fig. 15(b), a combined radar and infrared image, shows the broad region of cloud and rain associated with the back-bent warm front, although at this stage, there is relatively little curvature along the front. Cloud and rain terminate suddenly at the southern limit of the band, although a hook is not seen at this time. As in earlier examples, the band of strong winds extends forward from the region of cloud and precipitation decay.

6.4 Storm off the Pacific coast of the United States.

Fig. 16 shows a thermal analysis associated with an intense north Pacific storm investigated by Shapiro (1989) using aircraft measurements. There is remarkable similarity between this and the thermal structure of the October 1987 storm and those referred to above. In particular, strong thermal gradient locates a back-bent warm front west of the warm core.

Routine synoptic analysis and inspection of imagery over the north Atlantic suggests that the formation of back-bent warm fronts are relatively common, sometimes forming within cyclonic circulations that are not as intense as those referred to here. A well documented example is shown in McGinnigle *et al.* (1988). The formation of a hook in the imagery occurs only during development of intense lows. However, whether a cloud hook is or is not present, middle and upper cloud terminates abruptly behind the surface low and strongest surface winds within the low circulation occur beneath

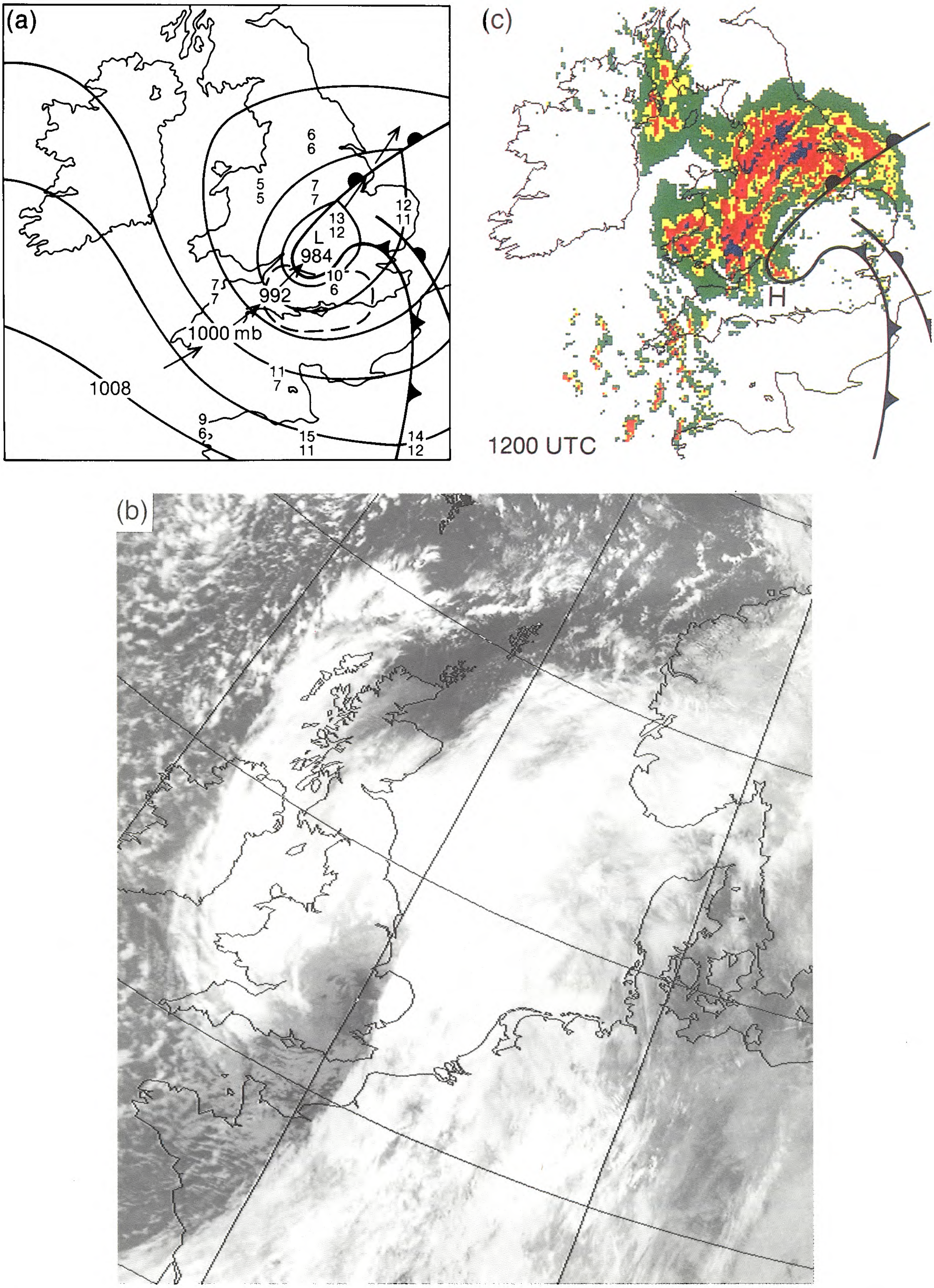

Photograph by courtesy of University of Dundee

Figure 13. (a) Surface analysis, showing dry-bulb temperature (upper figure) and dew-points (lower figure), (b) infrared image and (c) radar (UK network) at 1200 UTC on 8 November 1989.

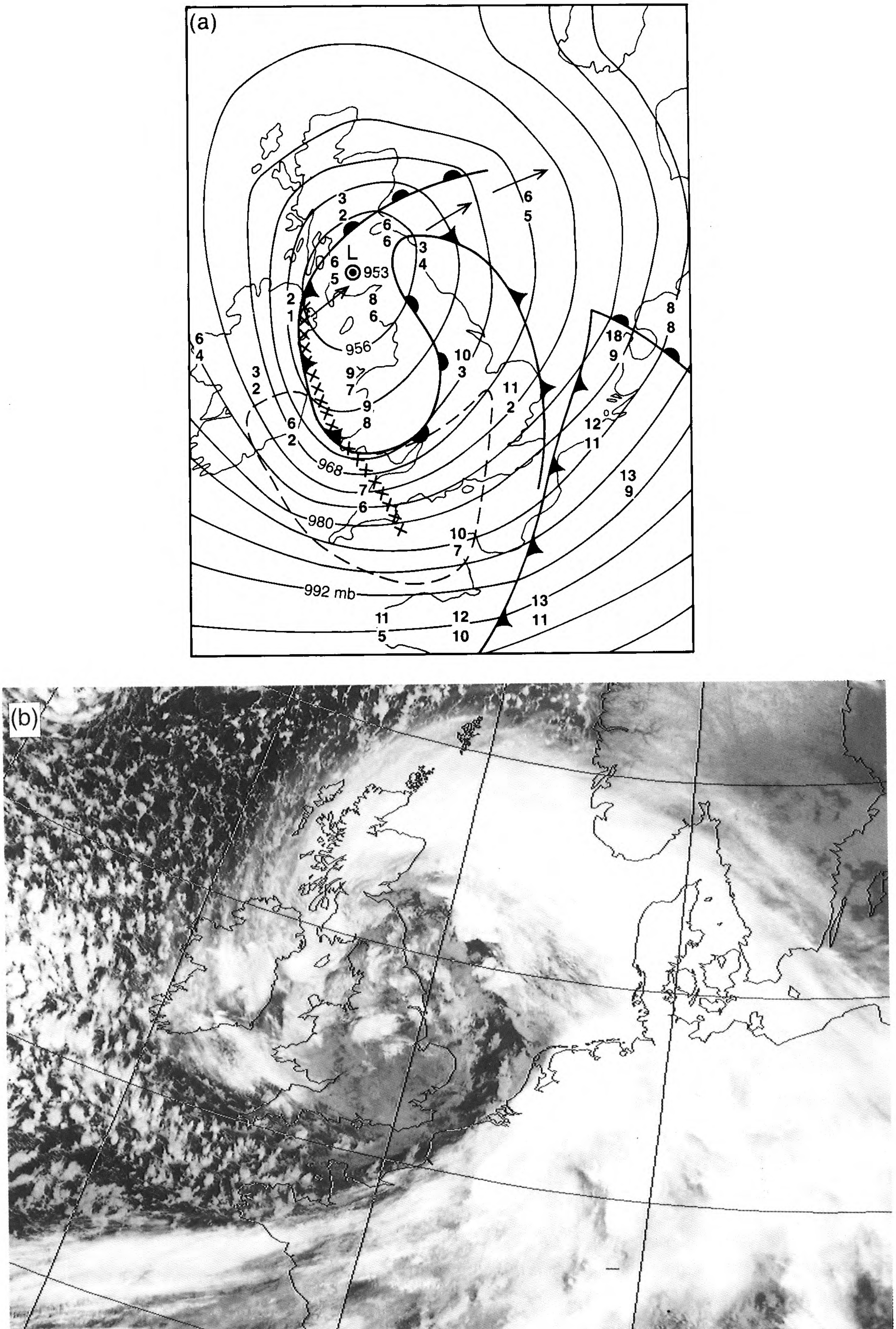

Photograph by courtesy of University of Dundee

Figure 14. (a) Surface analysis at 1200 UTC; and (b) infrared image at 1324 UTC on 25 January 1990.

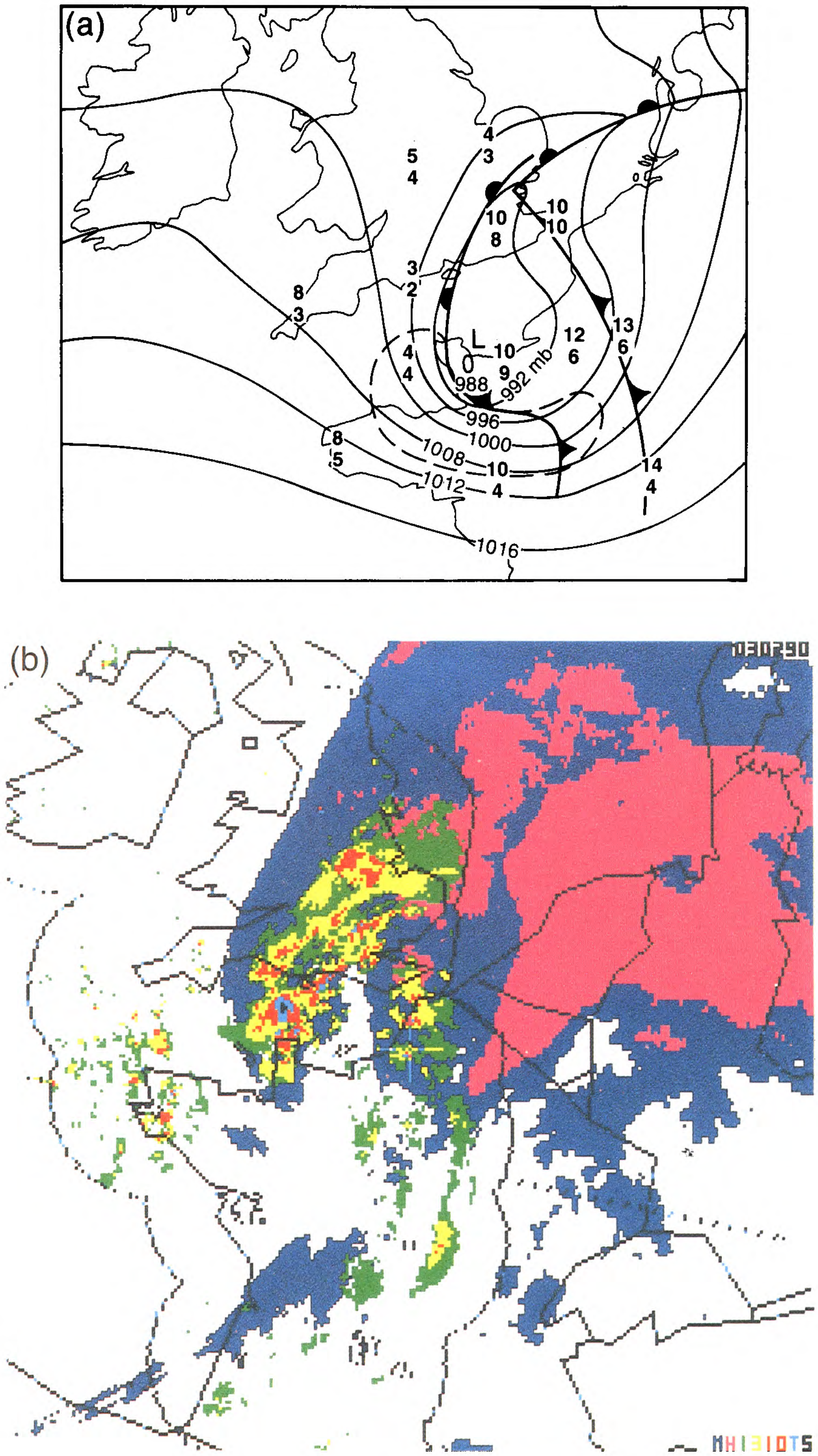

Figure 15. (a) Surface analysis, and (b) satellite and radar (COST-73 network) at 1200 UTC on 3 February 1990. Colours as in Fig. 10

the region of cloud dissipation. The most intense lows are characterized by a very broad cloud area at the back-bent warm front (ahead of, and on the left flank of, the surface low). The broad cloud area constitutes part of a cloud head (Böttger *et al.* 1975, Monk and Bader 1988) which forms during the early stages of cyclogenesis.

7. Conclusion

Back-bent warm fronts, surrounding a warm core and a curved zone of very strong winds are common to many developing and maturing intense mid-latitude oceanic cyclonic storms. These characteristics, including the approximate location of the strongest winds may be iden-

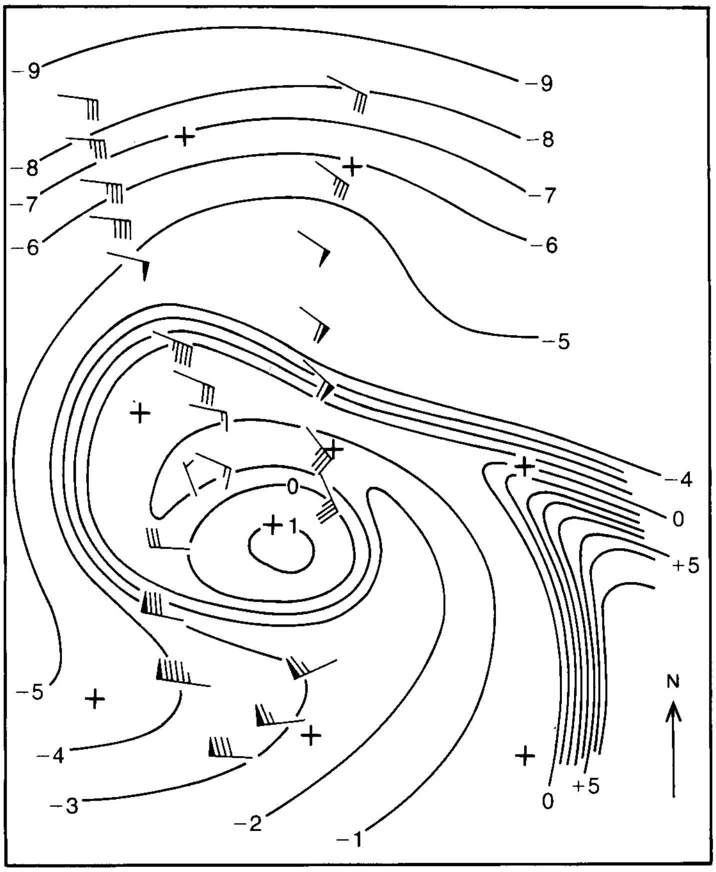

Figure 16. Temperature analysis (°C) at 850 mb of a warm-core seclusion situated in the Gulf of Alaska at 0000 UTC on 10 March 1987. From Shapiro (1989).

tified by synoptic-scale analysis and the use of satellite and/or radar imagery.

An operational forecaster analysing an intense low, may with the application of the model shown in Fig. 12, anticipate the regions of severest weather and make sense of quickly changing surface conditions even though he may not locate all the air-mass boundaries present. Satellite imagery is a particularly powerful tool, since major storms may be identified over the data sparse oceans, and regions of potentially damaging winds located.

The analyses also suggest that the traditional back-bent occlusion, should at least during the development stage of intense lows, be replaced by a warm front.

Acknowledgements

Grateful thanks to Doug Mansfield who painstakingly analysed the autographic records. Also to Glenn Shutts and Terry Davies for discussions regarding the nature of the warm core. Thanks also for the useful comments by Alistair Woodroffe and Martin Young on the draft version.

References

Böttger, H., Eckardt, M. and Katergiannakis, U., 1975: Forecasting extratropical storms with hurricane intensity using satellite information. *J Appl Meteorol*, **14**, 1259–1265.

Jerraud, M., Goas, J. and Deyts, C., 1989: Prediction of an exceptional storm over France and southern England (15–16 October 1987). *Weather and Forecasting*, **4**, 517–536.

McGinnigle, J.B., Young, M.V. and Bader, M.J., 1988: The development of instant occlusions in the North Atlantic. *Meteorol Mag*, **117**, 325-341.

Monk, G.A. and Bader, M.J., 1988: Satellite images showing the development of the storm of 15–16 October 1987. *Weather*, **43**, 130 135.

Monk, G.A., Browning, K.A. and Jonas, P.R., 1987: Forecasting applications of radar-derived precipitation echo velocities in the vicinity of polar lows. *Tellus*, **39a**, 426–433.

Shapiro, M.A. 1989: The mesoscale structure of extratropical marine cyclones. In Fifth scientific assembly of the International Association of Meteorology and Atmospheric Physics, Reading, 31 July to 12 August 1989, Vol. I. Reading, University of Reading.

Woodroffe, A., 1988: Summary of weather pattern developments of the storm of 15/16 October 1987. *Meteorol Mag*, **117**, 99–103.

Noctilucent clouds over western Europe during 1991

D.M. Gavine
29, Coillesdene Crescent, Edinburgh EH15 2JJ

Summary

Noctilucent cloud observations by voluntary and professional observers in the British Isles, Denmark and the Netherlands suggest a low incidence of the phenomenon.

Table I summarizes the noctilucent cloud (NLC) reported to the Aurora Section of the British Astronomical Association (BAA) during 1991. The times (UT) are the reported sightings limits, not necessarily the durations of the displays. 'Negative' nights (Table II) are based on the judgement of two or more experienced observers north of 54° N with clear or nearly clear sky conditions over the period of the night when NLC is likely to occur.

Only 21 definite and 4 suspected NLC displays were reported but the summer of 1991 was beset by a great deal of tropospheric cloud. None of the bright, extensive displays characteristic of the late 1980s was seen, and some were so faint as to be recognizable only in binoculars by experienced and dedicated amateurs. Contributions were received from 19 individual observers and 5 meteorological stations in the British Isles, 2 observers in Denmark (Mr Olesen and Mr Andersen whose reports and photography were again of the highest class), and 3 stations of the Royal Netherlands Meteorological Institute. There is still a lack of response from the rest of western Europe. Details of Finnish–Estonian NLC sightings are published annually in the journal *Ursa Minor* of the URSA Astronomical Association (Laivanvarustajankatu 3, SF-00140, Helsinki 14). Details of individual NLC nights are available from the author, but all NLC data up to 1988 are held in the Balfour Stewart Archive at the University of Aberdeen.

Our thanks to all observers, amateur and professional, and to the following for their support and co-operation: Mr Ron Livesey (BAA Aurora Section Director), Mr Tom McEwan (Junior Astronomical Society Aurora Section Director), Mr Veikko Mäkelä (URSA, Finland), Dr Balthus Zwart (Netherlands), Mr Mark Zalcik (USA–Canada NLC Network) and Dr Michael Gadsden (University of Aberdeen).

Table I. Displays of noctilucent clouds over western Europe during 1991

Date — night of	Times UT	Notes
27/28 May	2300–2310	Silvery-blue billows and patches reported at Beauly, no NLC at Alness 2200.
31/01	0003–0150	Alness — no NLC 0015, 0130 small patches, 0140-0150 faint bands and billows, elev. at St Andrews 20°. Faint bands at Vildbjerg, Denmark, 0003–0045.
1/2 June	2345–0215	Faint bands in tropospheric cloud gaps at Vildbjerg, moderately bright bands and whirls at elev. 15°, Rønne, Denmark; bands and billows elev. 20° Rotterdam 0140–0215.
5/6	2230–0200	Rather faint bands and billows observed and photographed in central Scotland, max. elev. 15°. Faint bands and whirls Vildbjerg; all forms, faint, Rønne.
7/8	0110–0215	Faint diffuse bands at 12°, Glengarnock near Ayr.
10/11	0048–0245	Suspect faint bands at Glengarnock 0048–0100, with aurora 0041–0050. Billows in patches from 0205, elev. 60° Essex.
12/13	0050–0127	Billows and whirls to elev. 30°, Dundee, bands very low at Pensarn, N. Wales, 0127.
13/14		Billows suspected with auroral arc, Upton-on-Severn.
15/16 June	2300–0245	Faint bands elev. 14°, Machrihanish, faint NLC suspected at Petworth, Sussex, from 0200.
16/17	2300–2315	Faint veil and patches suspected at Petworth.
21/22	2345–0015	Veil, bands and billows in trop. cloud breaks, Stirling.
22/23	2250–0300	Moderately bright, all forms, in patchy trop. cloud in Scotland, max. elev. Kinloss 24° at 2250. Extensive faint bands and billows photographed by Mr Peter at Carnoustie. NLC to elev. 15°, Rotterdam.
23/24	2205–2305	Suspected NLC at Appingedam, The Netherlands.
25/26	2300–0130	Moderately bright bands and billows, max. elev. 15°, central Scotland, Pensarn and Ronaldsway (Isle of Man).
26/27	0000–0212	Faint veil and bands at Glengarnock, max. elev. 25°, brighter and sharp 0145. Suspect NLC at Rotterdam 0000.
27/28	0120–0145	Suspect bands in haze, Glengarnock.
28/29	2250–0123	Faint veil, bands and billows at elev. 10°, Glengarnock. Faint veil at Pulborough, Sussex, 2250.

Date — night of	Times UT	Notes
2/3 July	0100	Moderately bright bands in haze, Arisaig.
4/5	2335–0015	Faint bands photographed at Vildbjerg.
7/8	2310–0115	Faint veil and bands, elev. 14°, Vildbjerg.
9/10	2315–0015	Very faint and poorly-defined bands/patches observed in binoculars, Glengarnock and Morpeth.
10/11	2130–0155	Faint veil, bands and whirls in trop. cloud gaps at Morpeth; patch of billow at Stambourne, Essex, 2200; bands and veil in evening twilight, Funen, Denmark; moderately bright bands, billows and whirls at Vildbjerg, max. elev. 44° at 0130, faded 0145.
12/13	0030–0100	Moderately bright whirls in trop. cloud gaps, Sumburgh, Shetland.
13/14 July	0020–0145	No NLC before 0000 Morpeth, then faint veil, bands and billows with auroral ray. Brighter bands, billows and whirls from 0045. At Musselburgh, Lothian, Mr Waldron saw brighter billows in trop. cloud 0100 and photographed auroral arc above faint bands 0111. Bands and billows in trop. cloud gaps, Glengarnock.
15/16	2130	Billows in trop. cloud gaps, Pulborough.
19/20		Dr Reid photographed NLC at Eigg.
20/21	2322–0230	Faint veil, bands, billows, some whirls, at Morpeth; brighter 0145, max. elev. 10°. Similar structures at Glengarnock, brightening 0015.
9/10 Aug.	0020–0115	Faint bands elev. 15°, De Bilt, The Netherlands.

Table II. Negative nights (British Isles) north of latitude 54° N.

May 24/25; 29/30; June 3/4; 4/5; 19/20; 20/21; July 5/6; 11/12; 28/29; 29/30; Aug. 11/12.

Conference Report

Seminar on the United Kingdom contribution to the Global Climate Observing System (GCOS), Houghton Lecture Theatre

The Office's new lecture theatre was officially opened by Sir John Houghton on 7 July 1992. The occasion was marked first by the presentation of the John Houghton Trophy for Weather Forecasting, to the Offshore forecasting team at Aberdeen, and then by a seminar on the UK contribution to GCOS which attracted a distinguished list of speakers and audience members. The theme of the seminar was particularly appropriate in view of the leading role that Sir John has played in initiating GCOS.

He described in his introduction how the recent UN Conference on Environment and Development in Rio had kept to the forefront concern about climate issues. Events such as Mrs Thatcher's celebrated 'green' speech to the Royal Society in 1988 and the setting up of the Intergovernmental Panel on Climate Change soon after, followed by its authoritative reports in 1990 and 1992, had also focused this concern, with the United Kingdom at the forefront of action. However, climate needs to be measured as well as modelled. Thus GCOS was conceived over lunch in Geneva during planning for the Second World Climate Conference (SWCC). Its birth was at SWCC, as a truly international activity. The need now is to put flesh on its bones, to produce a carefully thought out programme which can be convincingly argued and sold to the world's resource providers.

The first session considered GCOS in the context of climate prediction. Paul Mason (Met. Office) provided an overview summarizing why climate data are required. Thus, for monitoring and detecting change he stressed the need for data continuity and accuracy, and careful selection of the key variables. Observations are needed for demonstrating how well climate models can simulate present climate, and their credibility therefore in climate prediction; they are used also for model initialization, for example to describe the cryosphere and distribution of trace gas concentrations, and initial mean ocean state. He distinguished between deterministic predictability (scales ranging from a few days for atmospheric eddies, up to ENSO events) and statistical predictability (for mean climate and its variability). He noted that GCOS will underpin many process studies even though these may not be a central GCOS activity. The demanding requirements of a truly operational system which GCOS has to be were emphasized, for example in instrument technology and data processing.

John Mitchell (Met. Office) reviewed the data requirements for atmospheric models, from the perspectives of initial conditions, boundary conditions, conventional observations and new variables. He showed how substantially different initial temperatures perturb model predictions for only about a decade. The strong influence of ice-sheet extent on climate predictions was demonstrated, and the changes in heating rates over the last two centuries following changes in trace gas and sulphate aerosol concentrations were described. He illustrated the requirement for sub-daily temperature and daily rainfall observations to validate the predictions of different climate models, and to verify model sensitivity to CO_2 concentrations. The sensitivity of models to cloud schemes and their feedbacks was stressed, and the use of satellite data to validate models and help constrain parametrizations of cloud properties was demonstrated. In summary, even though initial meteorological conditions were largely irrevelant, atmospheric data are needed for validation; boundary conditions are clearly required, as are the present conventional meteorological data, but new data requirements are emerging such as cloud water content.

Data needs for ocean modelling were described by Howard Cattle (Met. Office), distinguishing between predictions on century time-scales and seasonal time-scales. Model boundary conditions such as surface fluxes of heat, and their uncertainties, were reviewed. Large-scale or global ocean models reproduce many of the larger-scale features such as western-boundary currents. The use of tracers such as tritium as well as more conventional data (temperature, salinity) to verify models was described. Higher-resolution modelling is required to test whether ocean eddies need to be resolved or can be parametrized in coupled ocean–atmosphere models. The long time-scales of large-scale oceanic structure indicate that initial conditions are important for ocean modelling, unlike for atmospheric climate models. Coupling of models was briefly reviewed, with the possibility of regionally dependent modelling approaches when predictions are on short (e.g. interannual) time-scales. The overall data requirements were for surface fluxes and sea surface temperatures, large-scale ocean structure and variability, tracers, CO_2, nutrients and biology, and ocean eddy structure for key regions.

The second session, on measurement strategy, began with a review of space-based measurements by John Harries (Rutherford Appleton Laboratory). The advantages of space observations — global coverage, good calibration and multiplicity of measurements — are tempered by their limited spatial resolution, obscuration by clouds and precipitation, and cost; nonetheless, they have a major role to play in GCOS. Relevant current space-programmes such as the Upper Atmosphere Research Satellite (UARS), the Earth Resources Satellite (ERS-1) and the Earth Radiation Budget (ERB) were described, with examples shown of H_2O and NO_2 measurements by UARS, and sea surface temperatures from ERS-1. Future directions of the space programmes are under review in NASA and ESA at present. However GCOS requires an ambitious programme in order to monitor satisfactorily the composition, dynamics and energy balance of the atmosphere, and its clouds and precipitation.

Ground-based measurements were then discussed by Chris Folland (Met. Office). He emphasized the important role of radiosonde data in GCOS, and described problems with the existing networks; especially important are the decline in coverage in some regions, and disagreements between different radiosonde types. He showed how discontinuities in data series in recent years have been caused by the introducion of new sensors (e.g. rain-gauges in Finland; thermistor thermometers in USA), and how changes in measuring surface wind at sea had produced a varying bias. The role of mountain glaciers as monitors of climate change was mentioned. He concluded by stressing the vital need for homogeneity of past and future data for climate-change assessment.

The oceans are enormously important in controlling climate, and the more important issues here were presented by John Woods (NERC). Large-scale deep ocean circulations with their long time-scales for change are important for climate predictions decades or more ahead; near-surface circulations have important influences for the carbon cycle. Many of the currents are organized in narrow unstable jets near western boundaries and on the eastern side of bottom topography, and are difficult to measure routinely, or to model, because of the high resolution needed. The seasonal ocean boundary layer strongly influences atmosphere–ocean exchanges. Salinity structure (which cannot be measured from space) may change substantially over a few years in some areas, with consequent density changes. The measurement strategy for GCOS is to resolve the broad features at low resolution but to increase resolution in regions of intense jets and eddies; ship measurements will have to be vastly supplemented by fixed, drifting or motoring ('auto-sub') systems and acoustic remote sensing.

John Pyle (University of Cambridge) reviewed chemical aspects for both the troposphere and stratosphere, with emphasis on ozone, and tropospheric OH (important in controlling methane and HCFCs). Results in the troposphere from some chemical models were compared with observations. Various chemical processes influencing ozone concentrations were described, with emphasis on the lower stratosphere, and wide disagreements between results from different models of these processes were highlighted. Measurement strategies were outlined for the troposphere and lower stratosphere, employing ground- and satellite-based systems.

The third session, on data management, was opened by Andrew Lorenc (Met. Office) who explained the role which methods of data assimilation will have in GCOS. At any one time, observations are always insufficient to determine the state of the atmosphere or ocean. The prediction models provide an evolution with time, allowing data distributed in time to be used with them; assimilation in four dimensions is the process of finding the model representation most consistent with the observations, using these data to modify the model state in a statistically optimal way. He described various uses for assimilation in GCOS, and the ways in which assimilation might be organized, such as in near real-time (when resources might be shared with numerical weather prediction), or in delayed mode (when the penalty of some duplication of effort is compensated for by more time to collect and process observations). Among the advantages of assimilation he listed obtaining a consistent picture from disparate observations, getting more detail than from observations alone, and providing consistent derived fields from the physical understanding incorporated in the models.

Crucial to the success of GCOS is the operational management of the data which it will produce. Peter Ryder (Met. Office) summarized the particular characteristics of its data such as exceptionally large volumes, diversity of types and sources, and large numbers of users, and explained the consequences; for example there will have to be much real-time processing and exchange, building on existing operational facilities, a systematic standardized approach, and significant investment. He sketched the data management components and summarized aspects of the system which GCOS mirrors in many respects and will be largely developed from — the World Weather Watch. He emphasized deficiencies needing to be corrected in this to cope with the substantial increase in throughput, such as under-investment in the satellite ground segment, the gulf between the space industry and users, and incomplete policy for data distribution.

In the penultimate session Alan Apling (DoE) considered the UK response to funding GCOS, from DoE's perspective. That Department is understandably cautious at this stage. There are no problems in drawing DoE in if the key to GCOS is climate change induced by human activities, and potentially controllable; but GCOS is also concerned with climate *per se*, in which many departments have an interest. The case for GCOS must be well substantiated. The key issues are: what are the deliverables? what are the benefits? The setting up of an intergovernmental committee has been an important step in the quest for funding. Very important here is to understand the long-term costs completely — there must be no surprises in a few years time! While many things are going GCOS's way at present, the crucial questions, on deliverables and objectives, need to be answered with great clarity when presenting the case.

The final talk was by Sir John, summarizing the present status of GCOS, and looking at the way forward. GCOS is needed to detect climate change as early as possible, and to validate and improve models. This will require better measurements of temperature, and other parameters. The international organization of GCOS is already well under way, with four sponsoring agencies, a Joint Scientific and Technical Committee (JSTC), and a Joint Planning Office in Geneva. The main functions and tasks of JSTC have been agreed. A good draft of the GCOS plan is required by the end of 1992, with assistance from people involved in WWW, GOOS, GAW (Global Atmospheric Watch), WCRP and CEOS (Committee on Earth Observation Satellites). The challenge is the precise definition of requirements. The core of GCOS is operational, and we have to work as far as possible through existing operational systems as well as research programmes. We have to recognize the world of difference between a research and an operational programme — the effort for the latter is consistently underestimated. Some of the TOGA measurements have to be continued to support GCOS. The problems of dealing with the huge quantities of data from the space component have to be addressed. Resources will have to come from national and international agencies as they do for WWW, from National Meteorological Services and space organizations for example. The intergovernmental meeting in April 1993 has important decisions to make here. Universal support, however modest (e.g. from some developing countries) is needed for GCOS to succeed. In the United Kingdom the key players will be the Met. Office, DoE, BNSC and the Research Councils, and they have to be on stage and working together. The Met. Office will have a key role because of its operational capabilities. DoE's clear interest is very welcome, though the line it is apparently drawing between natural, and human-induced, variability is a bit worrying. The space component is crucial, and the Research councils have a clear role also. One looks for growth in the Research Councils and Universities to undertake the many new studies which GCOS will require.

N. Thompson

NOAA use European satellite data during hurricane Andrew

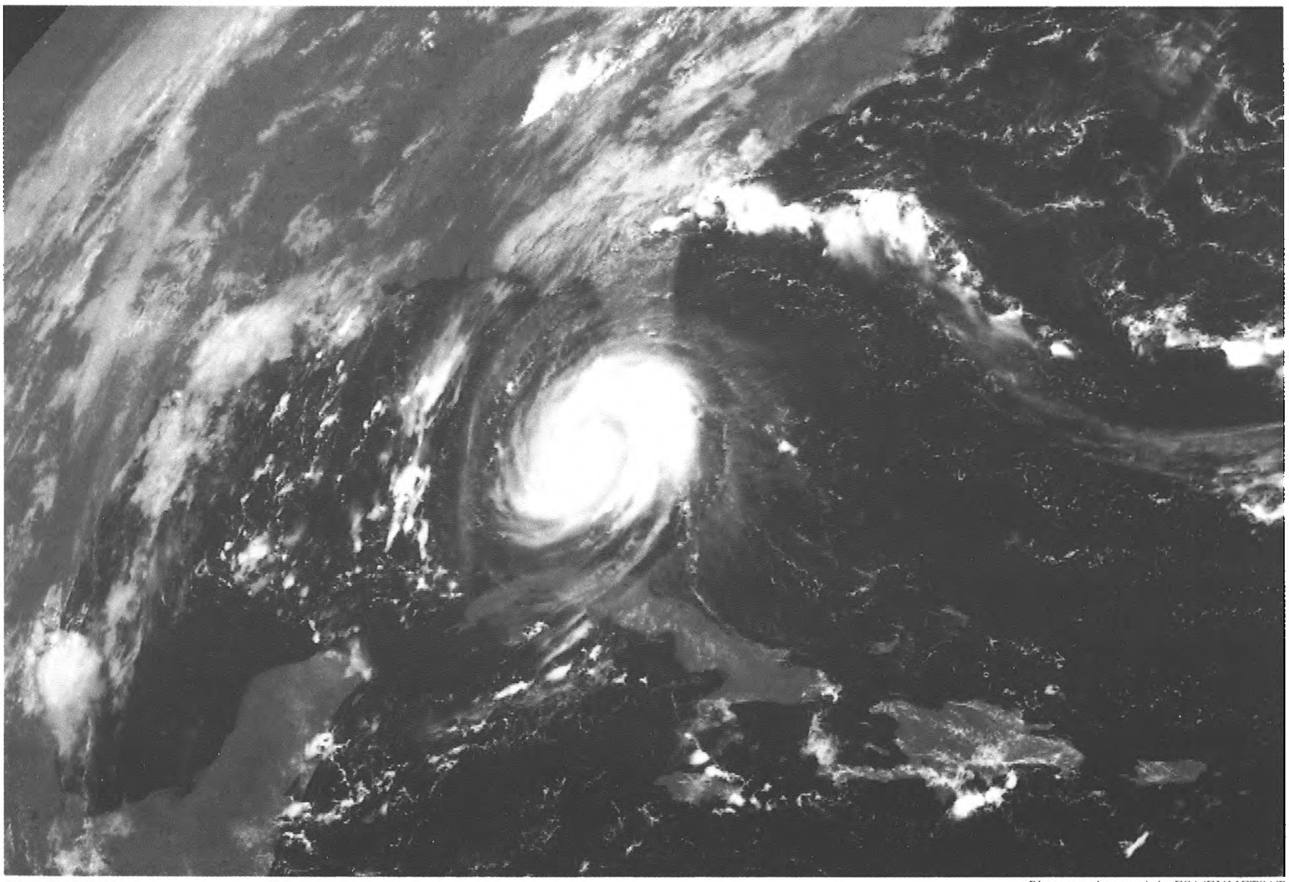

Photograph copyright ESA/EUMETSAT

Meteosat visible image for 1455 UTC on 24 August 1992 as Andrew crosses Florida.

During 'Andrew's' lifetime, a combination of GOES and Meteosat images were used to monitor the cyclone at NOAA's National Hurricane Center (NHC) and Synoptic Analysis Branch (SAB) located in the NOAA National Environmental Satellite, Data, and Information Service (NESDIS). Using visible and infrared satellite imagery, both facilities analyse cloud patterns and overall organization (i.e. spiral bands, central dense overcast, eye pattern, etc.) to determine the location and intensity of tropical cyclones (these location/intensity estimates are termed 'classifications').

From 12 August to 14 August 1992, Andrew was tracked as an incipient disturbance over western Africa and the adjacent coastal waters. Meteosat-4 imagery was used exclusively during this stage.

Beginning on 15 August, the system began organizing over the open Atlantic south of the Cape Verde Islands, near latitude 9° N, longitude 22° W. Based upon Meteosat-3 data, NHC began preparing location and intensity estimates at 15/0000 UTC using infrared imagery; SAB began classifying the system at 15/1200 UTC using visible imagery.

Based exclusively on the systems organization depicted in Meteosat-3 imagery, the National Hurricane Center issued the first advisory for Tropical Depression 3 at 17/0300 UTC near latitude 11° N, longitude 38° W.

The system was upgraded to Tropical Storm Andrew at 17/1500 UTC near latitude 13° N, longitude 43° W, based on satellite classifications using Meteosat-3 visible/infrared imagery. Meteosat-3 water vapour imagery was used to track a strong upper-level cyclonic circulation north of Andrew; NHC forecast a period of 'slow development' based on this imagery and numerical model forecasts. Air Force Reserve reconnaissance aircraft began cyclone penetration on 19 August. Meteosat-3 continued to be the primary source of satellite imagery through 22/0000 UTC.

As Andrew crossed longitude 66° W (on 22/0000 UTC), the system entered the usable GOES-7 field of view (Meteosat-3 became a vital back-up data source). The system was upgraded to hurricane intensity at 22/0900 UTC near latitude 25.8° N, longitude 67.5° W. The hurricane attained sustained winds of at least 130 knots and a minimum central pressure of 922 hPa at 23/1800 UTC (this was at least a strong Category 4 hurricane on the Saffir–Simpson 1 to 5 scale). The hurricane crossed the Florida coast at about 24/0830 UTC and struck Louisiana at about 26/0730 UTC with sustained winds near 120 knots.

M. Phillips

GUIDE TO AUTHORS

Content

Articles on all aspects of meteorology are welcomed, particularly those which describe results of research in applied meteorology or the development of practical forecasting techniques.

Preparation and submission of articles

Articles, which must be in English, should be typed, double-spaced with wide margins, on one side only of A4-size paper. Tables, references and figure captions should be typed separately. Spelling should conform to the preferred spelling in the *Concise Oxford Dictionary* (latest edition). Articles prepared on floppy disk (IBM-compatible) can be labour-saving, but only a print-out should be submitted in the first instance.

References should be made using the Harvard system (author/date) and full details should be given at the end of the text. If a document is unpublished, details must be given of the library where it may be seen. Documents which are not available to enquirers must not be referred to, except by 'personal communication'.

Tables should be numbered consecutively using roman numerals and provided with headings.

Mathematical notation should be written with extreme care. Particular care should be taken to differentiate between Greek letters and Roman letters for which they could be mistaken. Double subscripts and superscripts should be avoided, as they are difficult to typeset and read. Notation should be kept as simple as possible. Guidance is given in BS 1991: Part 1: 1976, and *Quantities, Units and Symbols* published by the Royal Society. SI units, or units approved by the World Meteorological Organization, should be used.

Articles for publication and all other communications for the Editor should be addressed to: The Chief Executive, Meteorological Office, London Road, Bracknell, Berkshire RG12 2SZ and marked 'For Meteorological Magazine'.

Illustrations

Diagrams must be drawn clearly, preferably in ink, and should not contain any unnecessary or irrelevant details. Explanatory text should not appear on the diagram itself but in the caption. Captions should be typed on a separate sheet of paper and should, as far as possible, explain the meanings of the diagrams without the reader having to refer to the text. The sequential numbering should correspond with the sequential referrals in the text.

Sharp monochrome photographs on glossy paper are preferred; colour prints are acceptable but the use of colour is at the Editor's discretion.

Copyright

Authors should identify the holder of the copyright for their work when they first submit contributions.

Free copies

Three free copies of the magazine (one for a book review) are provided for authors of articles published in it. Separate offprints for each article are not provided.

Contributions: It is requested that all communications to the Editor and books for review be addressed to the Chief Executive, Meteorological Office, London Road, Bracknell, Berkshire RG12 2SZ, and marked 'For *Meteorological Magazine*'. Contributors are asked to comply with the guidelines given in the *Guide to authors* (above). The responsibility for facts and opinions expressed in the signed articles and letters published in *Meteorological Magazine* rests with their respective authors.

Subscriptions: Annual subscription £36.00 including postage; individual copies £3.25 including postage. Applications for postal subscriptions should be made to HMSO, PO Box 276, London SW8 5DT; subscription enquiries 071–873 8499.

Back numbers: Full-size reprints of Vols 1–75 (1866–1940) are available from Johnson Reprint Co. Ltd, 24–28 Oval Road, London NW1 7DX. Complete volumes of *Meteorological Magazine* commencing with volume 54 are available on microfilm from University Microfilms International, 18 Bedford Row, London WC1R 4EJ. Information on microfiche issues is available from Kraus Microfiche, Rte 100, Milwood, NY 10546, USA.

December 1992

Edited by R.M. Blackall
Vol. 121
No. 1445

Contents

ISSN 0026—1149

ISBN 0-11-728990-6

9 780117 289901

Printed in the United Kingdom for HMSO Dd 291241, 1/93, C13, 543, 24503